National Library
of Canada

Acquisitions and
Bibliographic Services Branch

395 Wellington Street
Ottawa, Ontario
K1A 0N4

Bibliothèque nationale
du Canada

Direction des acquisitions et
des services bibliographiques

395, rue Wellington
Ottawa (Ontario)
K1A 0N4

Your file   Votre référence

Our file   Notre référence

NOTICE

The quality of this microform is heavily dependent upon the quality of the original thesis submitted for microfilming. Every effort has been made to ensure the highest quality of reproduction possible.

If pages are missing, contact the university which granted the degree.

Some pages may have indistinct print especially if the original pages were typed with a poor typewriter ribbon or if the university sent us an inferior photocopy.

Reproduction in full or in part of this microform is governed by the Canadian Copyright Act, R.S.C. 1970, c. C-30, and subsequent amendments.

AVIS

La qualité de cette microforme dépend grandement de la qualité de la thèse soumise au microfilmage. Nous avons tout fait pour assurer une qualité supérieure de reproduction.

S'il manque des pages, veuillez communiquer avec l'université qui a conféré le grade.

La qualité d'impression de certaines pages peut laisser à désirer, surtout si les pages originales ont été dactylographiées à l'aide d'un ruban usé ou si l'université nous a fait parvenir une photocopie de qualité inférieure.

La reproduction, même partielle, de cette microforme est soumise à la Loi canadienne sur le droit d'auteur, SRC 1970, c. C-30, et ses amendements subséquents.

Canada

UNIVERSITY OF ALBERTA

SEQUENCE STRATIGRAPHY, DIAGENESIS AND HYDROGEOLOGY OF THE LOWER CRETACEOUS CLEARWATER FORMATION, COLD LAKE OIL SANDS DEPOSIT, EAST-CENTRAL ALBERTA, CANADA

BY

LORI MAY MARY WICKERT ©

A THESIS
SUBMITTED TO THE FACULTY OF GRADUATE STUDIES AND RESEARCH
IN PARTIAL FULFILLMENT OF THE REQUIREMENTS FOR THE DEGREE OF
MASTER OF SCIENCE

DEPARTMENT OF GEOLOGY

EDMONTON, ALBERTA

FALL, 1992

National Library of Canada
Bibliothèque nationale du Canada

Canadian Theses Service
Service des thèses canadiennes

Ottawa, Canada
K1A 0N4

The author has granted an irrevocable non-exclusive licence allowing the National Library of Canada to reproduce, loan, distribute or sell copies of his/her thesis by any means and in any form or format, making this thesis available to interested persons.

The author retains ownership of the copyright in his/her thesis. Neither the thesis nor substantial extracts from it may be printed or otherwise reproduced without his/her permission.

L'auteur a accordé une licence irrévocable et non exclusive permettant à la Bibliothèque nationale du Canada de reproduire, prêter, distribuer ou vendre des copies de sa thèse de quelque manière et sous quelque forme que ce soit pour mettre des exemplaires de cette thèse à la disposition des personnes intéressées.

L'auteur conserve la propriété du droit d'auteur qui protège sa thèse. Ni la thèse ni des extraits substantiels de celle-ci ne doivent être imprimés ou autrement reproduits sans son autorisation.

ISBN 0-315-77312-X

Canadä

UNIVERSITY OF ALBERTA

RELEASE FORM

NAME OF AUTHOR: Lori May Mary Wickert

TITLE OF THESIS: Sequence Stratigraphy, Diagenesis and Hydrogeology of the Lower Cretaceous Clearwater Formation, Cold Lake oil sands deposit, east-central Alberta, Canada.

DEGREE: Master of Science

YEAR THIS DEGREE GRANTED: Fall, 1992

PERMISSION IS HEREBY GRANTED TO THE UNIVERSITY OF ALBERTA LIBRARY TO REPRODUCE SINGLE COPIES OF THIS THESIS AND TO LEND OR SELL SUCH COPIES FOR PRIVATE, SCHOLARLY OR SCIENTIFIC RESEARCH PURPOSES ONLY.

THE AUTHOR RESERVES OTHER PUBLICATION RIGHTS, AND NEITHER THE THESIS NOR EXTENSIVE EXTRACTS FROM IT MAY BE PRINTED OR OTHERWISE REPRODUCED WITHOUT THE AUTHOR'S WRITTEN PERMISSION.

(SIGNED) LMWickert

(PERMANENT ADDRESS)

c/o G.H. Wickert
1617 Mallard Drive
Courtenay, B.C. V9N 8L8

Date: October 9, 1992

UNIVERSITY OF ALBERTA

FACULTY OF GRADUATE STUDIES AND RESEARCH

THE UNDERSIGNED CERTIFY THAT THEY HAVE READ, AND RECOMMEND TO THE FACULTY OF GRADUATE STUDIES AND RESEARCH FOR ACCEPTANCE, A THESIS ENTITLED **SEQUENCE STRATIGRAPHY, DIAGENESIS AND HYDROGEOLOGY OF THE LOWER CRETACEOUS CLEARWATER FORMATION, COLD LAKE OIL SANDS DEPOSIT, EAST-CENTRAL ALBERTA, CANADA,** SUBMITTED BY **LORI MAY MARY WICKERT** IN PARTIAL FULFILLMENT OF THE REQUIREMENTS FOR THE DEGREE OF MASTER OF SCIENCE.

....
Dr. S. George Pemberton - Supervisor

Fred Longstaffe
Dr. Fred J. Longstaffe - Supervisor

RA Burwash
Dr. Ron A. Burwash

J. D. Scott
Dr. J. Don Scott

Date: October 2, 1992

DEDICATION

Completion of this thesis would not have been possible without the abiding love and support from my family, both Wickert and Matte. It is dedicated to my husband, Gregory C. P. Matte, and to my parents, Gordon and Nettie Wickert. You have encouraged and nurtured my curiosity, aspirations, and strive for excellence which led to the initiation, and now the culmination of this thesis. Thank you, all of you.

ABSTRACT

The Clearwater Formation contains significant bitumen reserves (6.9 x 10^{10} bbls) within Lower Cretaceous sands of the Cold Lake oil sands deposit in east-central Alberta (A.E.R.C.B., 1985). This thesis reports the findings of an investigation into its diagenesis, and its relationship to sequence stratigraphy and hydrogeology within a study area near Leming (twps. 63–67; rgs. 1–6W4).

Deltaic deposition of the Clearwater Formation was controlled by the relief of the depositional surface, influenced by the structure of the eastern basin margin. Two depositional cycles, S_1 and S_2, containing cycles A–C and A–D, respectively, were recognized. Three flooding surfaces (FS1, FS2, and FS3), were identified, and two sequence boundaries (SB1 and SB2), form the sequence bounding surfaces. Sequence boundary SB1 represents a period of relative sea-level fall, manifested by a basinward shift in facies from more distal deltaic front sedimentation, to the progradation of more proximal thick delta front sands. It is characterized mineralogically and geochemically in the underlying sediments by abundant early (framboidal) pyrite formed by bacterial sulphate reduction. This may represent a diagenetic sequence boundary marker for a deltaic, shallow shelf geologic setting.

Detrital study area mineralogy consists of: volcanic rock fragments, quartz, plagioclase, K feldspar, dolomite, detrital clays, minor sedimentary and metamorphic rock fragments (chert), and trace accessory minerals. Textural relationships, mineral relationships, and the stratigraphic distribution of diagenetic features delineate the paragenetic sequence: 1) glauconite; 2) early (framboidal) pyrite and berthierine; 3) early (Type 1) calcite ($\delta^{18}O \approx 19.1‰$ (SMOW), $\delta^{13}C \approx -0.3‰$ (PDB)), and early (concretionary) siderite; 4) diagenetic illite, illite / smectite and chlorite / smectite; 5) late siderite; 6) feldspar and quartz overgrowths; 7) zeolite (clinoptilolite); 8) late (euhedral) pyrite and late (Type 2 and 3) calcites ($\delta^{18}O \approx 19.2‰$ (SMOW); $\delta^{13}C \approx +4.2‰$ (PDB)); 9) diagenetic kaolinite and iron oxides. Three stages of diagenesis were interpreted: 1) early *shallow* and early burial diagenesis; 2) intermediate to late diagenesis; and 3) uplift and erosion.

Changing porewater compositions, originally brackish–marine, in a local to intermediate groundwater flow system, characterized Stage 1 and early Stage 2 diagenesis. A regional gravity-driven flow system was established during Stage 2, resulting in the migration and emplacement of oil. Reintroduction of a local–intermediate groundwater flow system in Stage 3, with infiltration by meteoric porewaters, led to bitumen biodegradation and present porewater conditions.

ACKNOWLEDGEMENTS

I am indebted to my supervisors, Dr. Fred J. Longstaffe and Dr. S. George Pemberton, for their guidance, encouragement and support throughout the duration of this project. Their comments, criticisms and editorial efforts were much appreciated, and this thesis is far better as a result. I am also beholden to Dr. Jean Doucet of Alcan International Ltd., who has repeatedly granted me time off work in the last three years, during my efforts to complete this project part-time. Merci de m'avoir offert le soutiens personnel et professionnel et la possibilité de réaliser mes objectifs.

The list of others who contributed to the completion of this thesis is long, and distinguished. Acknowledgements are extended to Gordon Bird, from the Alberta Research Council-Cloverbar, for the bitumen extraction of my samples and insights into Clearwater mineralogy; to Dave Taylor and Dave James of Esso Resources, for sharing expertise in sequence stratigraphy and printing of reference maps; and to Daryl Wightman and Rand Harrison of the Alberta Research Council (ARC), for their support and interest in my project.

I am grateful to Diane Caird for her guidance, and assistance in understanding and operating the X-ray diffractometer; and to Paul Middlestead, who taught me how to operate the carbonate isotope line at the University of Western Ontario, answered all my questions, and gave me a place to stay during many of my visits. Technical assistance was also received from Max Baaske (ARC-Millwoods), in the preparation of thin sections; John Forth of the University of Western Ontario for their subsequent staining; and from George Braybook, University of Alberta, and Hélène Dufour, Alcan International Ltd, who provided their invaluable assistance in Scanning Electron Microscopy.

Other technical expertise was furnished by Dr. Josef Tóth, who enthusiastically encouraged my work on hydrogeology; Ron Dean, of Esso Resources, who shared his expertise on the identification of clays within the Clearwater Formation; and Dr. Charles Wu, who helped with the preparation and analysis of my samples by X-ray fluorescence.

My thanks are extended to many friends and fellow graduate students for their encouragement, moral support, and insights, including: Tom Saunders, Rhea Karvonen, Alan Fryar, Dirk Noteboom and Nathalie Lavoie. Special thanks go to Joanne Thompson, Rob Schincariol and Jennifer McKay for their support. Lastly, I would like to acknowledge the considerable support, guidance and encouragement extended by friend and fellow grad student Mike Ranger. Thanks for being there.

Financial support for this thesis was contributed by Natural Science and Engineering Research Council grants to Dr's Longstaffe and Pemberton, a grant from Esso Resources to Dr. Pemberton, an AOSTRA grant to Dr. Longstaffe (#680), and some funding from the Alberta Research Council.

TABLE OF CONTENTS

CHAPTER **PAGE**

DEDICATION iv
ABSTRACT v
ACKNOWLEDGEMENTS vi
LIST OF TABLES xii
LIST OF FIGURES xiii
LIST OF PLATES xvii
LIST OF SYMBOLS, NOMENCLATURE AND ABBREVIATIONS xviii
- 1. INTRODUCTION AND REGIONAL SETTING 1
  - A. INTRODUCTION 1
  - B. PREVIOUS WORK 6
  - C. OBJECTIVES 7
  - D. STUDY AREA 7
  - E. CHAPTER SUMMARY 9
  - F. REFERENCES 10

- 2. CONTROLS ON THE DEPOSITION OF THE CLEARWATER FORMATION, COLD LAKE OIL SANDS DEPOSIT: An application of sequence stratigraphy..13
  - A. INTRODUCTION 13
    - PREVIOUS WORK 14
    - STUDY AREA 16
  - B. REGIONAL SETTING 16
    - STRATIGRAPHY 16
    - REGIONAL GEOLOGY AND PALEOGEOGRAPHY 22
      - Tectonic History 22
      - Structural Influences on Sedimentation 26
      - Cretaceous Paleogeography 27
      - Hydrocarbon Accumulation 34
  - C. APPLICATION OF SEQUENCE STRATIGRAPHY TO THE CLEARWATER FORMATION 36
    - SEQUENCE STRATIGRAPHY 36
      - Basic Concepts 36
      - Factors which influence Eustatic Sea-level 40
      - Important Considerations for Western Interior Basin Deposits....42

CLEARWATER FORMATION DEVELOPMENT 42
  Depositional Setting 44
    Open Marine / Prodelta 47
    Delta Fringe 47
    Lower Delta Front 47
    Middle Delta Front 48
    Upper Delta Front 48
    Wabiskaw Member - Shoreface 49
  Ichnology 50
  Sequence Stratigraphy 53
  Discussion 58
  Regional Implications 63
D. CONCLUSIONS 64
E. REFERENCES 69

3. DIAGENESIS OF THE LOWER CRETACEOUS CLEARWATER FORMATION, AND ITS APPLICATION TO SEQUENCE STRATIGRAPHY NEAR LEMING IN THE COLD LAKE OIL SANDS DEPOSIT, EAST-CENTRAL ALBERTA 82
A. INTRODUCTION 82
  OBJECTIVES 82
  PREVIOUS WORK 83
  STUDY AREA 83
B. GEOLOGICAL BACKGROUND 86
C. ANALYTICAL TECHNIQUES 88
  SAMPLING METHODOLOGY 88
  OPTICAL PETROGRAPHY 93
  SCANNING ELECTRON MICROSCOPY 93
  X-RAY DIFFRACTION 94
  X-RAY FLUORESCENCE 97
  STABLE ISOTOPE ANALYSIS 98
D. RESULTS OF MINERALOGICAL AND GEOCHEMICAL INVESTIGATIONS 99
  MINERALOGY 99
    Petrographic Study – Detrital Minerals 101
      Altered Grains 101
      Rock Fragments 101

- Quartz 102
- Feldspars 103
- Dolomite 104
- Detrital Clays 104
- Accessory Minerals 105

Petrographic Study – Diagenetic Mineralization 106

- Glauconite 106
- Pyrite 106
- Berthierine 107
- Calcite 107
- Authigenic Illite and Mixed-Layer Clays 109
- Siderite 110
- Feldspars 110
- Quartz 111
- Zeolite 111
- Kaolinite 111
- Minor Phases 111

X-ray Diffraction Study 112

- Whole Rock Mineralogy 112
- < 45μm Mineralogy 116
- Clay (< 2μm) Mineralogy 118

Elemental Geochemistry 125

- X-ray Fluorescence Results 125
- SEM Elemental Analyses 129

Stable Isotope Geochemistry 129

- Discussion 130

E. CLEARWATER DIAGENESIS 134

- STUDY AREA PARAGENESIS 134
- DISCUSSION 134
  - Stage 1: Early (Shallow) and Early Burial Diagenesis 134
  - Stage 2: Intermediate to Late Burial Diagenesis 139
  - Stage 3: Uplift and Erosion 142

F. SEQUENCE STRATIGRAPHIC APPLICATION OF DIAGENESIS 143

- SEQUENCE STRATIGRAPHIC BACKGROUND 143
- INVESTIGATION RESULTS 144
  - Mineralogical Results 144

Geochemical Results 153

G. CONCLUSIONS 158

MINERALOGY 158

DIAGENESIS 160

CHARACTERISTICS OF SEQUENCE BOUNDARY SB1 162

H. REFERENCES 165

4. A HYDROGEOLOGICAL STUDY OF THE COLD LAKE OIL SANDS AREA, EAST-CENTRAL ALBERTA: Influence on Clearwater Formation Diagenesis. 200

A. INTRODUCTION 200

B. STUDY AREA 202

PHYSIOGRAPHY 202

CLIMATE 204

C. GEOLOGY 206

WESTERN CANADA SEDIMENTARY BASIN 206

COLD LAKE STUDY AREA 206

Surficial Geology 206

Bedrock Geology 209

D. HYDROGEOLOGY 212

BACKGROUND 212

METHODOLOGY 217

INFLUENCES ON HYDRAULIC HEAD 218

GROUNDWATER FLOW 220

Western Canada Sedimentary Basin 220

Cold Lake Study Area 222

GROUNDWATER CHEMISTRY 230

Western Canada Sedimentary Basin 230

Cold Lake Oil Sands Area 231

E. INFLUENCE OF HYDROGEOLOGY ON DIAGENESIS 243

CLEARWATER MINERALOGY 243

Detrital Minerals 245

Diagenetic Mineralogy 245

DIAGENESIS 247

DISCUSSION 248

F. CONCLUSIONS 251

G. REFERENCES 255

5. GENERAL DISCUSSION AND CONCLUSIONS 259
    A. INTRODUCTION 259
    B. A MODEL OF DEPOSITION AND SEQUENCE STRATIGRAPHY IN THE CLEARWATER FORMATION 260
        DEPOSITIONAL CONTROLS 260
        CLEARWATER DEPOSITIONAL ENVIRONMENTS 261
        SEQUENCE STRATIGRAPHY 264
    C. MINERALOGICAL AND GEOCHEMICAL CHARACTERIZATION OF SEQUENCE BOUNDARY SB1 268
        DISCUSSION 269
    D. MINERALOGY, DIAGENESIS AND HYDROGEOLOGY OF THE CLEARWATER FORMATION 275
        CLEARWATER MINERALOGY AND PARAGENESIS 275
        HYDROGEOLOGY OF THE CLEARWATER FORMATION 277
        A DIAGENETIC / POREWATER MODEL FOR THE LEMING AREA 278
    E. RECOMMENDATIONS 282
    F. REFERENCES 283

APPENDICES:

APPENDIX 1: CORE LOG DATA 285
APPENDIX 2: CROSS-SECTION (A - A') 313
APPENDIX 3: MINERALOGICAL DATA 314
APPENDIX 4: ELEMENTAL DATA 345
APPENDIX 5: HYDROGEOLOGICAL EQUATIONS 353
APPENDIX 6: FLUID DATA AND METHODOLOGY 355

LIST OF TABLES

TABLE **PAGE**

2.1 Classification of Ichnogenera recognized in the Clearwater Formation 51

3.1 Samples Investigated in Study 89
3.2 Average Whole Rock XRD Mineral Abundance Results by Lithology 113
3.3 Average < 45μm XRD Mineral Abundance Results by Lithology 117
3.4 Summary of Clay Mineral Data 119
3.5 Primary XRD Peaks and Characteristic Treatment Responses used in the Identification of Clay Minerals in the Study Area 122
3.6 Summary of Average XRF Major Oxide Elemental Results by Lithology 126
3.7 Summary of Average XRF Trace Element Results by Lithology 127
3.8 Stable Isotope Data for Carbonates 131
3.9 Summary of Average Whole Rock Mineral Abundances for Sequences S_1 and S_2..145

5.1 Characteristics of Clearwater Formation Depositional Environments observed in the Study Area 263
5.2 Ichnological Characteristics of Clearwater Formation Depositional Environments observed in the Study Area 265

LIST OF FIGURES

FIGURE PAGE

1.1 Location of the Cold Lake oil sands deposit within Alberta 2
1.2 Position of the Western Canada Sedimentary Basin and associated basins and structural features in western Canada 4
1.3 Location map of study area within the Cold Lake oil sand deposit 8

2.1 Location of the Cold Lake oil sands deposit within Alberta 17
2.2 Location map of study area and Albertas oil sands deposits 18
2.3 Geologic cross-section of the Western Canada Sedimentary Basin 20
2.4 Lower Cretaceous Stratigraphic Correlation Chart of the Western Canada Sedimentary Basin 21
2.5 Schematic diagram of Precambrian basement features and the position of the Western Canada Sedimentary Basin in western Canada 23
2.6 Schematic cross-section illustrating the structural configuration of the uplifted early Cordilleran orogen to the thick sediment wedge of the Alberta foreland basin during the Cretaceous 24
2.7 Schematic of structural features evolved during tectonism and groundwater flow directions in the Alberta foreland basin from the Paleozoic to present 25
2.8 Structural features that influenced deposition of the Lower and Upper Mannville Group in the Lower Cretaceous 28
2.9 Structure of the pre-Mannville depositional surface 29
2.10 Lower Mannville (lower McMurray Formation) paleogeography in the Early Cretaceous 31
2.11 Lower Mannville (upper McMurray Formation) paleogeography in the Western Canada Sedimentary Basin 32
2.12 Lower Mannville (Wabiskaw Member) paleogeography in the Lower Cretaceous of western Canada 33
2.13 Upper Mannville (Grand Rapids Formation) paleogeography in the Western Canada Sedimentary Basin 35
2.14 Diagram illustrating the position of the lowstand, highstand and transgressive systems tracts and the condensed section in a coastal margin setting 37
2.15 Sequence stratigraphic concepts illustrating depositional systems tracts and surfaces during the formation of Type 1 and Type 2 unconformities 39

2.16 Structure contours on top of Precambrian basement in the Western Canada Sedimentary Basin 43
2.17 Gamma Ray and Density type log of the Clearwater Formation 45
2.18 Position of wells used in study 46
2.19 Sequence Stratigraphic Model of Clearwater Formation deposition in the study area 54

3.1 Location map of study area within the Cold Lake oil sands deposits 84
3.2 Positions of wells used in study and approximate positions of local Pilot Plant sites 85
3.3 Stratigraphic succession in the northern Cold Lake oil sand area 87
3.4 Summary of petrographic classification of samples from the Clearwater Formation by various authors on Folk's Ternary Diagram for Sandstones 100
3.5 Plot of log (Na_2O / K_2O) versus log (SiO_2 / Al_2O_3) from XRF data for various lithologic samples from the study area 128
3.6 Plot of $\delta^{13}C$ versus $\delta^{18}O$ values for detrital dolomite and authigenic calcite from the study area in the Clearwater Formation 132
3.7 Paragenetic sequence of Clearwater Formation diagenetic events in the study area 135
3.8 Distribution of pyrite relative abundance (%) over sequence boundary SB1 in wells during Clearwater deposition 147
3.9 Distribution of siderite relative abundance (%) over sequence boundary SB1 in wells during Clearwater deposition 149
3.10 Detailed clay mineral succession over sequence boundary SB1, well 3-13-65-4W4 150
3.11 Detailed clay mineral succession over sequence boundary SB1, well 16-2-66-3W4 151
3.12 Detailed clay mineral succession over sequence boundary SB1, well 8-19-66-2W4 152
3.13 Distribution of the abundance (%) of various major oxides over sequence boundary SB1 in well 6-31-66-2W4 154
3.14 Distribution of the abundance (%) of various major oxides over sequence boundary SB1 in well 16-2-66-3W4 155
3.15 Distribution of the abundance (ppm) of various trace elements over sequence boundary SB1 in well 6-31-66-2W4 156
3.16 Distribution of the abundance (ppm) of various trace elements over sequence

boundary SB1 in well 16-2-66-3W4 157

4.1 Location map of study area within the Cold Lake oil sands deposit 201
4.2 Physiographic map of the northern Cold Lake oil sands study area 203
4.3 Drainage of the northern Cold Lake oil sands study area 205
4.4 Geologic cross-section of the Western Canada Sedimentary Basin showing the major stratigraphic units and present-day topographic profile 207
4.5 Summary of late Pliocene and Quaternary sediments in the Sand River map area 208
4.6 Stratigraphic succession in the northern Cold Lake oil sand area 210
4.7 Schematic of local, intermediate and regional systems of groundwater flow in a sedimentary basin 214
4.8 The Chebotarev Sequence and flow system types of the chemical evolution of groundwater 216
4.9 Regional paleoflow and hydrocarbon accumulation for the oil sands deposits in Alberta 221
4.10 Conceptual model of gravity-driven groundwater flow and hydrocarbon accumulation on the eastern margin of the Western Canada Sedimentary Basin.221
4.11 Potentiometric surface map of the Upper Mannville Group within the northern Cold Lake oil sands study area 225
4.12 Plot of hydraulic head versus topography in the Upper Mannville Group 226
4.13a Pressure versus depth (P(d) plot) for the Colony Formation 227
4.13b Pressure versus elevation above sea level (datum) (P(z) plot) for the Colony Formation 227
4.14a Pressure versus depth (P(d) plot) for the Grand Rapids Formation 228
4.14b Pressure versus elevation above sea level (datum) (P(z) plot) for the Grand Rapids Formation 228
4.15 Total dissolved solids (TDS) in the Colony Formation 232
4.16 Chloride (Cl^-) concentration in the Colony Formation 233
4.17 Sulphate (SO_4^{2-}) concentration in the Colony Formation 234
4.18 Bicarbonate (HCO_3^-) concentration in the Colony Formation 235
4.19 Total dissolved solids (TDS) in the Grand Rapids Formation 236
4.20 Chloride (Cl^-) concentration in the Grand Rapids Formation 237
4.21 Sulphate (SO_4^{2-}) concentration in the Grand Rapids Formation 238
4.22 Bicarbonate (HCO_3^-) concentration in the Grand Rapids Formation 239
4.23 Structure map of the Devonian surface in the Cold Lake study area 242

4.24 A graphical representation of Ca/Mg, the major anion and total dissolved solids for the study area 244

5.1 Sequence Stratigraphic Model of Clearwater Formation deposition in the study area 267

5.2 Distribution of the abundance (%) of various major oxides over sequence boundary SB1 in well 16-2-66-3W4 270

5.3 Detailed clay mineral succession over sequence boundary SB1, well 16-2-66-3W4 271

5.4 Distribution of the abundance (ppm) of various trace elements over sequence boundary SB1 in well 16-2-66-3W4 273

5.5 Distribution of pyrite relative abundance (%) over sequence boundary SB1 in wells during Clearwater deposition 274

5.6 A model of diagenetic and groundwater flow system history for the Leming study area in the Clearwater formation 279

LIST OF PLATES

PLATE **PAGE**

2.1 Photographs of typical ichnogenera of the Clearwater Formation 75

2.2 Photographs of sequence boundary SB1 in well 3-28-66-2W4 77

2.3 Photographs of core in well 3-13-65-4W4 79

2.4 Photographs illustrating the features of sequence boundary SB1 in various wells within the study area 81

3.1 A–F. General overview, biologic material and altered grains 173

3.2 A–F. Altered grains, volcanic rock fragments 175

3.3 A–F. Chert and detrital quartz 177

3.4 A–F. Detrital quartz, feldspars, dolomite and polycrystalline quartz 179

3.5 A–F. Detrital dolomite and detrital clays 181

3.6 A–F. Detrital clays, detrital accessory minerals and diagenetic glauconite 183

3.7 A–F. Diagenetic glauconite and pyrite 185

3.8 A–F. Diagenetic berthierine 187

3.9 A–F. Diagenetic calcite 189

3.10 A–F. Diagenetic illite, mixed-layer illite / smectite and siderite 191

3.11 A–F. Diagenetic siderite and K feldspar 193

3.12 A–F. Diagenetic K feldspar, plagioclase and quartz 195

3.13 A–F. Diagenetic quartz and zeolite (clinoptilolite) 197

3.14 A–F. Diagenetic kaolinite and minor diagenetic phases 199

LIST OF SYMBOLS, NOMENCLATURE AND ABBREVIATIONS

The abbreviations listed below are used in Tables, Figures, Plates and Text:

UNITS OF MEASUREMENT

Metric

km	kilometre
km^2	square kilometres
km^3	cubic kilometres
m	metre
m^2	square metres
m^3	cubic metres
cm	centimetre
mm	millimetre
µm	micrometre (micron, 1 x 10^{-6} m)
Å	Angstroms (1 x 10^{-10} m)

Imperial

mi	mile
mi^2	square miles
ft	foot
ft^2	square feet

General

API	American Petrol. Institute units
bbls	billion barrels
65°20'	degrees, minutes
°C	degrees Celcius
kV	kilovolts
mA	milliamps

ABBREVIATIONS

a	altered
ac	acidic
A.E.R.C.B.	Alberta Energy Resources Conservation Board
Amp	amphibole
approx.	approximate(ly)
avg.	average
B	bitumen
Be	berthierine
C	Clay
Ca	Calcium (or calcite - plates)
Cal	calcite
carb.	carbonate
cem.	cement(ed)
Ch	chert
char.	characteristic
Chl	chlorite
Cl	Chlorine
Clw.	Clearwater
CO_3	Carbonate
conc.	concentration
concr.	concretion
cross-polars	cross-polarized light
Cruz.	Cruziana
C/S	chlorite / smectite
d	detrital
DC	Distributary Channel
Del.	Delta
DF	Delta Fringe
dist.	distribution / distributary

DMB	Distributary Mouth Bar
Dol or D	dolomite
dst	drill stem test
E.R.C.B.	Energy Resources Conservation Board
Fe	iron
f.g.	fine grained
Fm.	Formation
Fr.	Front
FS	Flooding Surface
G	glauconite
gen.	general(ly)
Gr	grain
GR	Grand Rapids
HCO_3	Bicarbonate
Ichn.	Ichnofacies
Ilm	ilmenite
inc.	increase(s)
I/S	illite / smectite
K	Potassium
KB	kelly bushing
KF	K feldspar
L.	Lower
LDF	Lower Delta Front
lg	large
Lk.	Lake
LS	Lower Shoreface
LSD	legal subdivision
m	monocrystalline
M.	Middle
Mag	magnetite
Mag.:	magnification
mar.	marine
Mbr.	Member
MDF	Middle Delta Front
Mg	Magnesium
m.g.	medium grained
mid.	middle
mod.	moderate
MS	Middle Shoreface
Mth.	Mouth
Mu	muscovite
Na	Sodium
NTS	National Topographic System
occ.	occasional(ly)
om	organic matter
OM	Open Marine
p	polycrystalline
po	porphyritic
Pl	plagioclase
PPL	plane polarized light
press.	pressure
P.R.	pressure recorder
Py	pyrite
Qtz or Q	quartz
R	residual rim
RF	rock fragment(s)
rel.	relative(ly)
rge.	range
RH	relative humidity
S_1	sequence S_1, S_2
sat'd	saturated
SB	Sequence Boundary
SC	smectitic clays / swelling clays
sec.	section or seconds
sed.	sediment(ation)
SEM	Scanning Electron Microscopy
sh.	shale
Si	Silicon / Silica
Sid	siderite
siltst.	siltstone
Skol.	Skolithos

sm	small
SO_4	Sulphate
sp. grav.	specific gravity
sst.	sandstone
strat.	stratified / stratification
TDS	total dissolved solids
temp.	temperature
twp.	township
U.	Upper
UDF	Upper Delta Front
v	volcanic
vert.	vertical
v.f.g.	very fine grained
Wab.	Wabiskaw
W.C.S.B.	Western Canada Sedimentary Basin
W.R.	whole rock
x.	cross
XRD	X-ray Diffraction
XRF	X-ray Fluorescence
Zi	zircon
Zoo.	Zoophycus

CHAPTER 1:

INTRODUCTION AND REGIONAL SETTING

A. INTRODUCTION

Located 300km (187mi) northeast of Edmonton, Alberta, the Cold Lake oil sands deposit contains the second largest abundance of bitumen-saturated sand in Canada. Estimated reserves of $3.5 \times 10^{10}m^3$ (2.2×10^{11}bbls) of high viscosity, 10 to 14°API gravity oil are found within 6500km^2 (2340mi^2) in the Lower Cretaceous Mannville Group (Outtrim and Evans, 1977; A.E.R.C.B., 1985) (Figure 1.1). The Clearwater Formation, the highest bitumen–saturated interval within the deposit, is currently being produced at a number of *pilot plant* facilities by means of *in-situ* cyclic steam injection. As Mannville Group sediments are situated from 300 to 565m (950–1850ft) below the surface, surface mining methods such as those employed in the Athabasca tar sands deposit are not viable in the Cold Lake deposit. Bitumen recovery from steam injection methods is relatively poor in the Clearwater Formation; current estimates are that 20 percent or less of the hydrocarbons are recovered (Shepherd, 1981). Production problems are related to a number of factors associated with the injection of steam, such as fines migration, and the dissolution and the precipitation of mineral phases, resulting in permeability reduction in the reservoir (Kirk *et al.*, 1987). These and other production difficulties in the Cold Lake deposit means that economic development of the reserves will not be a simple task. As development of the extensive reserves of the Cold Lake oil sands deposit is important to the future energy needs of Alberta and Canada, it is imperative that a good understanding of the predevelopment mineralogy and natural diagenesis of the Clearwater Formation is achieved prior to full-scale development of the reserves. One of the objectives of this thesis was the investigation of diagenetic changes which have occurred in Clearwater sediments since deposition, in a selected area of the the Cold Lake oil sands deposit. These results can be used at a later date to better evaluate the potential effects of production on reservoir quality in this area, as well as add to a regional database of information which researchers and developers can utilize in future projects in the Cold Lake deposit.

Diagenetic changes which occur in clastic sediments subsequent to deposition are a function of many factors including; depositional setting, detrital mineralogy, mineral reactivity, changing pore water compositions resulting from fluid movement, diffusion, cation-exchange, compaction and thermal history. Diagenesis in general terms may be

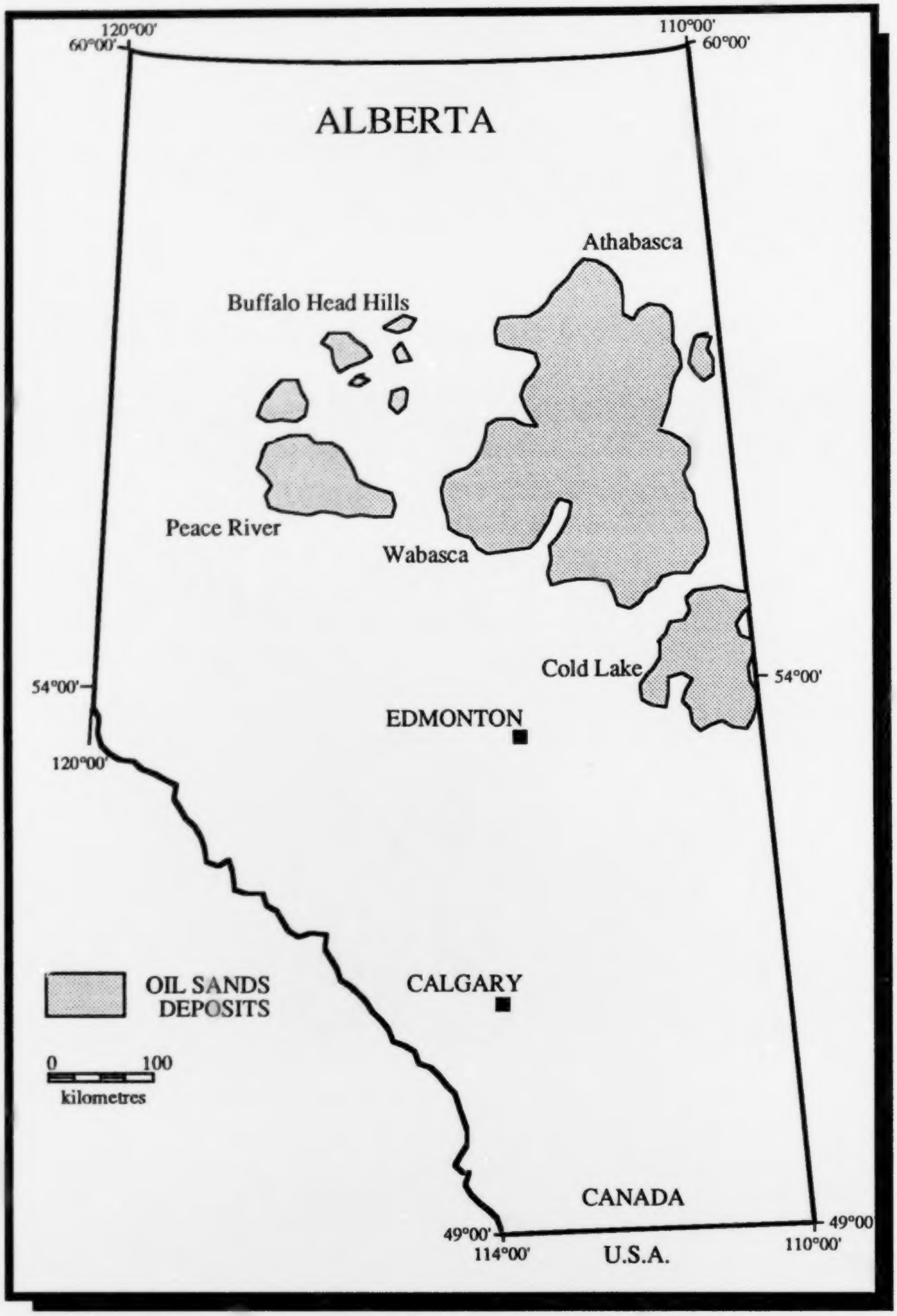
120°00'
60°00'
110°00'
60°00'
ALBERTA
Athabasca
Buffalo Head Hills
Peace River
Wabasca
Cold Lake
54°00'
54°00'
EDMONTON
120°00'
OIL SANDS DEPOSITS
CALGARY
0
100
kilometres
CANADA
49°00'
114°00'
U.S.A.
49°00'
110°00'

Figure 1.1: Location of the Cold Lake oil sands deposit within Alberta .

considered as all the changes that occur after sediment deposition. This can be broken down into a number of regimes which include: early / shallow diagenesis, namely that which occurs during and subsequent to sediment deposition to the onset of compaction; burial diagenesis, which includes all processes in the subsurface from compaction to those which approach metamorphism; and uplift, which comprises late stage surface processes in the shallow subsurface to outcrop. Diagenetic characteristics observed in the Clearwater Formation are all relatively early; the formation was not buried deeply, and very little compaction or lithification has occurred during its burial history.

Mineralogical and geochemical variation within a sedimentary basin is the function of numerous variables in the original depositional system as well as changes resulting from diagenetic processes. Primary factors which influence sedimentation patterns in a marine depositional system are tectonics, sea-level fluctuation, variable sediment supply and subsidence (Weimer, 1983). In the Western Canada Sedimentary Basin, which extends from the western edge of the Cordilleran mountains near the Alberta / British Columbia border, east into northeastern Saskatchewan (Figure 1.2), the influence of these factors in a clastic marine system varies with the site of sediment deposition. Subsidence and tectonic effects resulting from folding and thrusting in the basin are of greater importance in western margin deposits. Sediments such as those near the Cold Lake heavy oil deposit on the shallowly dipping eastern margin of the basin are more apt to be influenced by fluctuations in sea-level and sediment abundance. Provenance also plays an important role as it controls the type of detrital mineralogy carried to the depositional site. The Cordilleran Rocky Mountains and the exposed rocks of the Canadian Shield have been identified as two sources of clastic detritus in the Western Canada Sedimentary Basin during Cretaceous time, although the Cordillera is believed to be the dominant sediment source during Clearwater deposition in the Cold Lake area (Jackson, 1984). Probable controls on sedimentation patterns within the study area have been examined in this thesis, both on a large scale such as thrusting in the Cordillera, and on an areally specific scale, such as salt dissolution on the eastern margin of the basin.

Sequence stratigraphy, the interpretation of sedimentary facies as a series of stacked units bounded by unconformities, is a newer concept in sedimentary stratigraphic interpretation that was used in the interpretation of the Clearwater Formation in this thesis. Successive genetically-related units combine to form *sequences*, which are bounded by sequence boundaries and are composed of systems tracts, linking facies from different depositional systems in a chronostratigraphic framework. The formation was studied

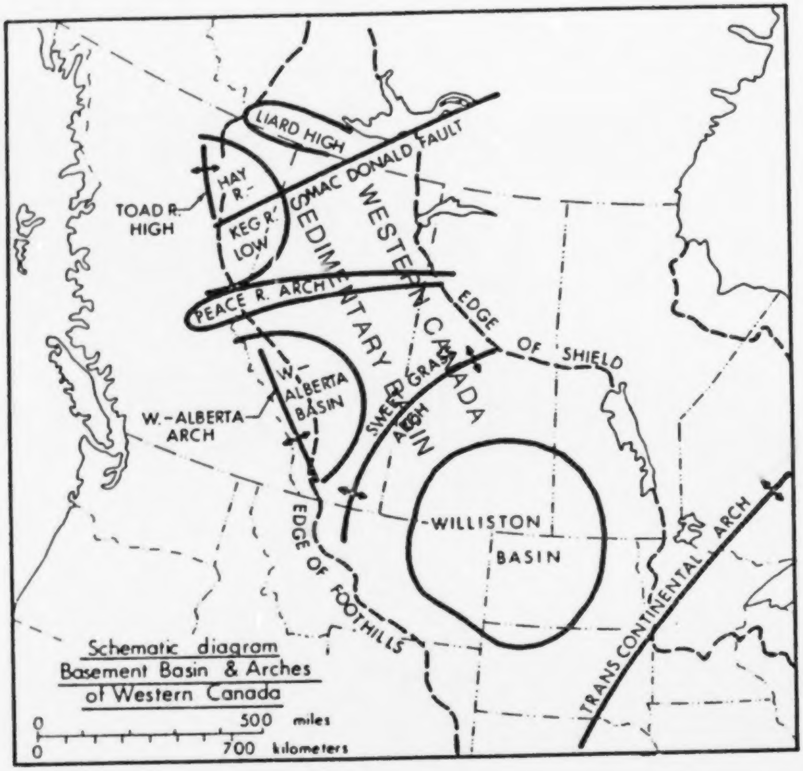
LIARD HIGH
HAY R.
TOAD R. HIGH
KEG R. LOW
MAC DONALD FAULT
WESTERN CANADA
SEDIMENTARY BASIN
PEACE R. ARCH
EDGE OF SHIELD
W.-ALBERTA BASIN
W.-ALBERTA ARCH
SWEET GRASS ARCH
WILLISTON BASIN
EDGE OF FOOTHILLS
TRANS CONTINENTAL ARCH
Schematic diagram
Basement Basin & Arches
of Western Canada
0
500 miles
0
700 kilometers

Figure 1.2: Position of the Western Canada Sedimentary Basin and associated basins and Precambrian basement features in western Canada (modified after Stelck, 1975).

from a genetic standpoint; an interpretation of depositional patterns in the sediments, and their related bounding surfaces in terms of their relationship to relative sea-level rise and fall. This was done in conjunction with a detailed interpretation of formation facies and their depositional environments. Overall, this led to the development of a model that embraces the depositional characteristics of the formation in the study area with its genetic, cyclic stratigraphy. Inherent characteristics of the formation are often related to its cyclic stratigraphic history. For example, change in the environment of deposition may result in accompanying changes in detritus, organic debris, ichnogeneric habitation, and later diagenenetic characteristics. As changes in the sequence stratigraphy are most often associated with its bounding surfaces, namely sequence boundaries, they should in theory show evidence of these changes internally. A hypothesis put forth at the onset of this study was that such sequence boundaries should have detectable features which mark its environmental changes, such as a characteristic mineralogy or geochemical variability. The objective of this thesis was to test this hypothesis, which if true, would provide results that could be used in the recognition and confirmation of other, perhaps more difficult to identify sequence boundaries in other positions.

The asymmetrical configuration of the Western Canada basin has played a major role in basin diagenesis as it has greatly controlled the direction of fluid movement within the basin (Hitchon, 1969a). In terms of overall basin hydrology, fluids recharge on the western portion of the basin, move down and flow laterally in the midline region and up to where they discharge on the eastern margin (Hitchon, 1969a). This provides ample opportunity for fluids to interact with the basin rock framework, altering lithologic characteristics and the chemistry of the moving fluids. Shallower hydrologic systems react to basin morphology in a similar way, although they are more affected by local topography, and thereby spend much less time in the subsurface. Therefore, one aspect of undertaking a diagenetic study in the Cold Lake area should be concerned with understanding the relationship between basin and study area hydrogeology, and basin hydrogeologic features that may or may not have influenced diagenetic trends. As variation in subsurface mineralogy occurs primarily through reactions between framework grains and pore-filling fluids (Curtis, 1978), an effort has been made to investigate the nature of fluid movement and chemistry in the study area in order to apply this knowledge to variations in diagenetic mineralogy that were observed within the Clearwater Formation.

B. PREVIOUS WORK

The paleogeography of the Western Canada Sedimentary Basin in relation to Mannville Group sedimentation in the Lower Cretaceous has been studied by many individuals. Early studies include: Badgley, 1952; Carrigy, 1959; Glaister, 1959; Williams, 1963; Rudkin, 1964; and Mellon, 1967. More recent studies are contained within: Stelck, 1975; Williams and Stelck, 1975; and Jackson, 1984. The overall conclusion of these researchers is that Mannville Group deposition occurred during a period of significant sea-level fluctuation in western Canada at the time of encroachment of the Boreal sea during Aptian to Albian time. Additional detailed studies of the Clearwater Formation have generally concluded that sediments were deposited in a shallow marine environment as a series of prograding deltaic lobes that extended northeastward into the shallow seaway (Harrison *et al.*, 1981; Wightman and Berezniuk, 1986; Maher, 1989). The Cretaceous is believed to have been a time of great sea-level fluctuation worldwide, and although disagreement exists in the literature as to whether tectonism or eustatic variation was the primary control on sedimentation, sea-level change is believed to have played a significant role in controlling the configuration of Cretaceous sediments in the Western Interior Basin (Kauffman, 1969; Weimer, 1983; Stott, 1984).

The presence of diagenetic mineralization within the Clearwater Formation has been known for some time, although the detailed mineralogy and natural diagenesis has not been widely reported. Previous public domain reports on the mineralogy of the Clearwater Formation include: Mellon, 1967; Schooley, 1975; Bayliss and Levinson, 1976; Harrison *et al.*, 1981; Putnam and Pedskalny, 1983; Kirk *et al.*, 1987; Prentice and Wightman, 1987; Wickert *et al.*, 1988; Abercrombie, 1989; Abercrombie *et al.*, 1989; Hutcheon *et al.*, 1989; Longstaffe *et al.*, 1989a, 1989b, 1989c; Racki *et al.*, 1989; Wickert *et al.*, 1989; Longstaffe *et al.*, 1990; Racki, 1991; and Longstaffe *et al.*, 1992. For the most part the older studies focus on general mineralogical variations and provenance studies in the Clearwater Formation, although Kirk *et al.* (1987), Abercrombie (1989) and Abercrombie *et al.* (1989) are concerned with post-production mineralogy. The more recent studies are focused on diagenesis and stable isotope studies of Clearwater sediments in various parts of the Cold Lake oil sands deposit.

The hydrogeological setting of the Cold Lake oil sands area has not been extensively studied in the past. Most studies, such as Yoon, 1977, Ozoray *et al.*, 1980 and a number of confidential reports are concerned with surficial geology and the quantity of water resources in the area. Hitchon, 1969a, 1969b; Bachu, 1985 and Garven, 1989, briefly discuss fluid flow in the Cold Lake area, but focus primarily on the associated topics of hydrocarbon migration and subsurface temperature gradients. Two types of data were collected in this study from available sources in the Cold Lake area, undisturbed formation pressures and fluid analyses. The investigation of present fluid conditions in the subsurface can often be utilized in the interpretation of paleo fluid flow patterns, rates and chemistry, all of which may help to explain diagenetic relationships within the formation.

C. OBJECTIVES

This study of the Clearwater Formation has three primary objectives:

1) to develop a model of the depositional history of the Clearwater Formation, based on sedimentologic and sequence stratigraphic features observed and inferred in the study area;
2) to utilize stratigraphic, geochemical and mineralogical data in the characterization of an unconformity / sequence boundary identified within the study area; and
3) to develop a basic understanding of diagenesis within the Clearwater Formation in the study area, including mineralogical variations, paragenetic trends, and their controls within the formation.

Secondary objectives are: to develop a good understanding of factors which influenced the deposition of Clearwater sediments and led to their ensued sedimentologic, ichnologic and mineralogic characteristics; and to determine local fluid flow and groundwater chemistry for the study area and its influence on diagenesis.

Analytical methods utilized in the thesis include: core, well-log, map and cross-sectional interpretations, optical (thin section) petrography, scanning electron microscopy, x-ray diffraction, x-ray fluorescence spectroscopy, stable isotope geochemistry, and analyses of groundwater flow and fluid chemistry data.

D. STUDY AREA

The study area for this project is located in the National Topographic System (NTS) Sand River area in east-central Alberta, contained within townships 63 to 67, ranges 1 to 6 west of the fourth meridian (Figure 1.3). All of the fluid data collected for the hydrogeological section of the thesis are contained within this area in the Lower Cretaceous Mannville Group. A smaller area, located within the study area and situated

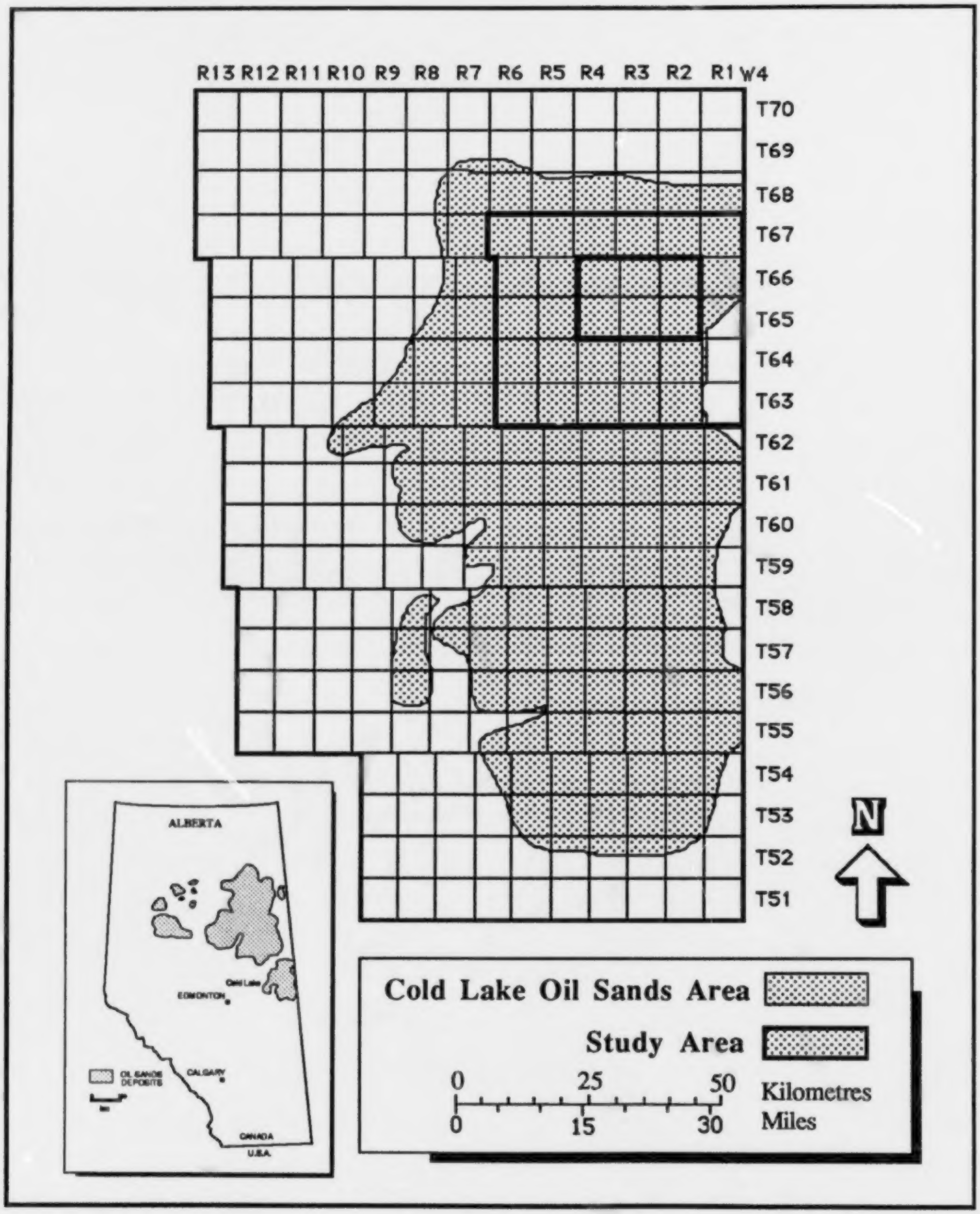
R13 R12 R11 R10 R9 R8 R7 R6 R5 R4 R3 R2 R1 W4
T70
T69
T68
T67
T66
T65
T64
T63
T62
T61
T60
T59
T58
T57
T56
T55
T54
T53
T52
T51
N
Cold Lake Oil Sands Area
Study Area
0
25
50
Kilometres
0
15
30
Miles
ALBERTA
Cold Lake
EDMONTON
CALGARY
OIL SANDS DEPOSITS
CANADA
U.S.A.

Figure 1.3: Location map of study area and Alberta oil sands deposits.

for the most part within the Esso Lease in the Cold Lake oil sands deposit, contains all of the wells and core examined and sampled for stratigraphic and diagenetic features in the thesis. It is located in townships 65 and 66, ranges 2 through 4 west of the fourth meridian (Figure 1.3).

E. CHAPTER SUMMARY:

Results from this thesis are presented in four chapters, as follows:

Chapter 2: Sequence stratigraphic and sedimentologic aspects of the Clearwater Formation within a defined study area in the Esso Lease of the Cold Lake oil sands deposit, are presented. Concepts of sequence stratigraphy are discussed and applied, along with facies and environmental interpretations, to a model of the depositional history of the Clearwater Formation in the study area.

Chapter 3: Geochemical and mineralogical changes identified within the Esso Lease study area in the Clearwater Formation, are reported, with emphasis on those associated with a sequence boundary (SB1) identified by stratigraphic interpretation in Chapter 2. Results of diagenetic investigations of the Clearwater Formation are presented, focusing on mineralogic data from x-ray diffraction, scanning electron microscopy and thin section studies, and also including stable isotopic data from carbonate cemented intervals.

Chapter 4: A report on the hydrogeological setting of the Cold Lake oil sands area, incorporating all available data in the study area from all Mannville Group formations, is presented. Present groundwater flow patterns and fluid chemistry data, are reported, and an attempt is made to relate observed changes in known fluid flow patterns and water chemistry on a regional scale in the Western Canada Sedimentary Basin. An attempt is made to relate the effect of moving groundwater on diagenetic features observed in the Clearwater Formation.

Chapter 5: The results and conclusions from all previous chapters are summarized. A depositional model of sequence stratigraphy for the Clearwater Formation, is presented. Diagenetic processes interpreted in this study are reviewed, and a paragenetic sequence for the Clearwater Formation is presented, based on data from the Esso Lease study area.

F. REFERENCES

Abercrombie, H.J. 1989. Water-rock interaction during diagenesis and thermal recovery, Cold Lake Alberta. Ph.D. thesis, University of Calgary, Calgary, Alberta.

Abercrombie, H.J., Shevalier, M., and Hutcheon, I.E. 1989. Natural diagenesis during steam-assisted recovery of heavy oil, Cold Lake, Alberta, Canada. *In:* Miles, D.L., ed., Proceeding of the Sixth International Symposium on Water-Rock Interaction, p. 1-4.

Alberta Energy Resources Conservation Board. 1985. Atlas of Alberta's crude bitumen reserves. Alberta Energy Resources Conservation Board Reserve Report Series 38, 37pp.

Bachu, S. 1985. Influence of lithology and fluid flow on the temperature distribution in a sedimentary basin: A case study from the Cold Lake area, Alberta, Canada. Tectonophysics, 120, p. 257-284.

Badgley, P.C. 1952. Notes on the subsurface stratigraphy and oil and gas geology of the Lower Cretaceous series in central Alberta, Canada. Geological Survey Paper 52-11, 12pp.

Bayliss, P., and Levinson, A.A. 1976. Mineralogical review of the Alberta oil sand deposits (Lower Cretaceous Mannville Group). Bulletin of Canadian Petroleum Geology, v. 24, p. 211-224.

Carrigy, M.A. 1959. Geology of the McMurray Formation, Pt. III. General geology of the McMurray area. Alberta Research Council, Geology Division, Memoir 1, 130pp.

Curtis, C.D. 1978. Possible links between sandstone diagenesis and depth-related geochemical reactions occurring in enclosing mudstones. Journal of the Geological Society of London, v. 135, p. 107-117.

Garven, G. 1989. A hydrogeological model for the formation of the giant oil sands deposits of the Western Canada Sedimentary Basin. American Journal of Science, v. 289, p. 105-166.

Glaister, R.P. 1959. Lower Cretaceous of southern Alberta and adjoining areas. American Association of Petroleum Geologists, v. 43, p. 590-640.

Harrison, D.B., Glaister, R.P. and Nelson, H.W. 1981. Reservoir description of the Clearwater oil sand, Cold Lake, Alberta, Canada. *In:* Meyer, R.F. and Steele, C.T., eds., The Future of Heavy Crude and Tar Sands, Unitar, McGraw Hill, New York, ch. 30, p. 264-279.

Hitchon, B. 1969a. Fluid flow in the Western Canada Sedimentary Basin. 1. Effect of topography. Water Resources Research, v. 5, no. 1, p. 186-195.

Hitchon, B. 1969b. Fluid flow in the Western Canada Sedimentary Basin. 2. Effect of geology. Water Resources Research, v. 5, no. 2, p. 460-469.

Hutcheon, I., Abercrombie, H., Putnam, P., Gardner, R. and Krouse, R. 1989. Diagenesis and sedimentology of the Clearwater Formation at Tucker Lake. Bulletin of Canadian Petroleum Geology, v. 37, no. 1, p. 83-97.

Jackson, P.C. 1984. Paleogeography of the Lower Cretaceous Mannville Group of western Canada. *In:* Masters, J.A., ed., Elmworth–Case Study of a Deep Basin Gas Field, American Association of Petroleum Geologists Memoir 38, p. 49-77.

Kauffman, E.G. 1969. Cretaceous marine cycles of the Western Interior. Mountain Geologist, v. 6, no. 4, p. 227-245.

Kirk, J.S., Bird, G.W. and Longstaffe, F.J. 1987. Laboratory study of the effects of steam-condensate flooding in the Clearwater Formation: High temperature flow experiments. Bulletin of Canadian Petroleum Geology, v. 35, no. 1, p. 34-47.

Longstaffe, F.J., Ayalon, A. and Racki, M.A. 1989a. Oxygen and carbon isotope studies of diagenesis in heavy oil deposits of the Clearwater Formation, northeastern Alberta. Geological Association of Canada / Mineralogical Association of Canada Annual Meeting, May 15-17, Program with Abstracts, v. 14, p. A85.

Longstaffe, F.J., Ayalon, A. and Racki, M.A. 1989b. Natural diagenesis of Clearwater Formation reservoirs in the Cold Lake area, Alberta. Part I: Mineralogical studies. Exploration Update '89, Calgary, C.S.P.G. Program and Abstracts, p. 130.

Longstaffe, F.J., Ayalon, A., Racki, M.A., and Bird. G.W. 1989c. Natural diagenesis of Clearwater Formation reservoirs in the Cold Lake area, Alberta. Part II: Stable isotope studies of water / mineral interaction. Exploration Update '89, Calgary, C.S.P.G. Annual Meeting, Program and Abstracts, p. 142.

Longstaffe, F.J., Ayalon, A., Racki, M., Wickert, L.M., Wightman, D.M., and Bird, G.W. 1990. Water-mineral-organic matter interactions during clastic diagenesis of Cretaceous heavy oil reservoirs, Cold Lake area, Alberta. American Association of Petroleum Geologists Bulletin, v. 74, p. 1306-1307.

Longstaffe, F.J., Ayalon, A., and Racki, M.A. 1992. Stable isotope studies of diagenesis in berthierine-bearing oil sands, Clearwater Formation, Alberta. *In:* Kharaka and Maest, eds., Proceedings of the Seventh International Symposium on Water-Rock Interaction. Balkema, Rotterdam, p. 955-958.

Maher, J.B. 1989. Geometry and reservoir characteristics Leismer Clearwater 'B' gas field, northeast Alberta. Case Studies in Canadian Petroleum Geology. Bulletin of Canadian Petroleum Geology, v.37, no. 2, p. 236-240.

Mellon, G.B. 1967. Stratigraphy and petrology of the Lower Cretaceous Blairmore and Mannville groups, Alberta Foothills, and Plains. Research Council of Alberta Geological Division, Bulletin 21, 270pp.

Outtrim, C.P. and Evans, R.G. 1977. Alberta's oil sands reserves and their evaluation. *In:* Redford, D.A. and Winestock, A.G. eds., The Oil Sands of Canada-Venezuela, Canadian Institute of Mining and Metallurgy, Special Volume 17, p. 36-69.

Ozoray, G., Wallick, E.I. and Lytviak, A.T. 1980. Hydrogeology of the Sand River area, Alberta. Alberta Research Council Earth Sciences Report 79-1, 11pp.

Prentice, M.E. and Wightman, D.M. 1987. Mineralogy of the Clearwater Formation, Cold Lake oil sands area: Implications for enhanced oil recovery. Alberta Geological Survey Report, 41pp.

Putnam, P.E. and Pedskalny, M.A. 1983. Provenance of Clearwater Formation reservoir sandstones, Cold Lake, Alberta, with comments on feldspar composition. Bulletin of Canadian Petroleum Geology, v. 31, p. 148-160.

Racki, M.A., Ayalon, A. and Longstaffe, F.J. 1989. Mineralogical Studies of Diagenesis in heavy oil deposits of the Clearwater Formation, northeastern Alberta. Geological Association of Canada / Mineralogical Association of Canada Annual Meeting, May 15-17, Program with Abstracts, v. 14, p. A85.

Racki M. 1991. Diagenesis of the Lower Cretaceous Clearwater Formation, Cold Lake, Alberta. M.Sc. thesis, University of Western Ontario, 250pp.

Rudkin, R.A. 1964. Lower Cretaceous. *In:* McCrossan, R.G. and Glaister, R.P., eds., Geological History of Western Canada. Alberta Society of Petroleum Geologists, Ch. 11, p. 156-168.

Schooley, J.V. 1975. A study of the mineralogy of Lower Cretaceous Mannville Group oil sand deposits, Alberta and west Saskatchewan. Unpublished M.Sc. thesis, The University of Calgary, Calgary, Alberta, 134pp.

Shepherd, D.W. 1981. Steam stimulation recovery of Cold Lake bitumen. *In:* Meyer, R.F. and Steele, C.T., eds., The Future of Heavy Crude and Tar Sands, Unitar, McGraw Hill, New York, p. 349-360.

Stelck, C.R. 1975. Basement control of Cretaceous sand sequences in western Canada. The Geological Association of Canada Special Paper Number 13, p. 427-440.

Stott, D.F. 1984. Cretaceous sequences of the foothills of the Canadian Rocky Mountains. *In:* Stott, D.F. and Glass, D.J., eds., The Mesozoic of Middle North America. Canadian Society of Petroleum Geologists Memoir 9, p. 85-107.

Weimer, R.J. 1983. Relation of unconformities, tectonics, and sea level changes, Cretaceous of the Denver Basin and adjacent areas. *In:* Mesozoic Paleogeography of the west-central United States: Rocky Mountain Section. Society of Economic Paleontologists and Mineralogists, Rocky Mountain Paleogeography Symposium 2, p. 359-376.

Wickert, L.M., Pemberton, S.G. and Longstaffe, F.J. 1988. An application of sequence stratigraphy to depth-related clastic diagenesis in the Cold Lake oil sands, east-central Alberta (abst.). *In:* James, D.P. and Leckie, D.B., eds., Sequences, Stratigraphy, Sedimentology: Surface and Subsurface. Canadian Society of Petroleum Geology, Memoir 15, p. 585.

Wickert, L.M., Longstaffe, F.J., and Pemberton, S.G., 1989. A diagenetic investigation of sequence stratigraphy in the Lower Cretaceous Clearwater Formation, Cold Lake oil sands, east-central Alberta. Geological Association of Canada / Mineralogical Association of Canada Annual Meeting, May 15-17, Program with Abstracts, v. 14, p. A86.

Wightman, D.M., and Berezniuk, T. 1986. Resource characterization and depositional modelling of the Clearwater Formation, Cold Lake oil sands deposit, east-central Alberta. *In:* Westhoff, J.D., and Marchant, L.C. eds., Proceedings of the 1986 Tar Sands Symposium, ARC Contribution No. 1452, Jackson, Wyoming, July 7-10, p. 20-45.

Williams, G.D. 1963. The Mannville Group (Lower Cretaceous) of central Alberta. Bulletin of Canadian Petroleum Geology, v. 2, p. 350-368.

Williams, G.D. and Stelck, C.R. 1975. Speculation on the Cretaceous Paleogeography of North America. The Geological Association of Canada Special Paper Number 13, p. 1-20.

Yoon, T.N., Goble, K.A. and Carlson, V.A. 1977. Groundwater resources in the Cold Lake oil sands area. *In:* Redford, D.A. and Winestock, A.G., eds., The Oil Sands of Canada-Venezuela, Canadian Instittiute of Mining Special Volume 17, p. 133-138.

CHAPTER 2:

CONTROLS ON THE DEPOSITION OF THE CLEARWATER FORMATION, COLD LAKE OIL SANDS DEPOSIT:

An application of sequence stratigraphy

A. INTRODUCTION

Shallow marine clastic sequences have been the focus of abundant research in past decades, commonly because of their frequent association with hydrocarbon accumulations. Clastic sedimentary studies centre on the examination of vertical facies changes as they apply to depositional variations of local significance. Classifications such as *fining upward sequence*, *coarsening upward sequence* and *Bouma sequence* are prevalent in the older literature (Bergman and Walker, 1988). A new approach to the study of sedimentologic sequences has evolved in recent years. Concepts of sequence stratigraphy have provided a framework that focuses on the relationship between adjacent depositional systems as a function of sea-level variation. In many ways it is a revolutionary new way of viewing depositional systems as it forces the investigator to understand *the big picture*, sedimentologically speaking. It is now necessary to be able to identify all the major variables affecting sedimentation on a more regional scale, and conceptualize how the interplay of these variables will be transmitted to the depositional pattern in the area of study. Sequence stratigraphy has been applied successfully to the study of both ancient and modern depositional systems with successful results (Plint *et al.*, 1988; Boyd *et al.*, 1988).

The Clearwater Formation is an important bitumen-saturated interval within the Cold Lake oil sand deposit on the eastern margin of the Alberta Foreland basin. It contains the richest bitumen-saturated interval within the Cold Lake deposit, with reserves of 1.1 x 10^{10}m^3 (6.9 x 10^{10}bbls) of heavy oil at relatively shallow depths (A.E.R.C.B., 1985). The depth of overburden and unlithified nature of the deposit disqualifies open-pit mining as a production strategy, and proposed *pilot plant* production methods include cyclic steam injection and *in-situ* combustion (Nicholls and Luhning, 1977). Bitumen is generally found within the thicker, coarser-grained sands, which have been identified as delta front distributary mouth-bar and channel sands that formed during deposition of the formation in a shallow marine environment (Harrison *et al.*, 1981). Prediction of the position of the richest and most economic areas of the deposit is therefore dependent on an understanding of the depositional setting of the deposit, as well as the factors which may have influenced its sedimentation during the Lower Cretaceous.

The purpose of this study is to provide detailed stratigraphic and sedimentologic information from the Clearwater Formation in the Cold Lake oil sands deposit, and to utilize this information in the interpretation of an overall sequence stratigraphic model and its associated depositional characteristics in the study area. Concepts of sequence stratigraphy have been applied in this study to the analysis of regional and local controls on depositional patterns, particularly with respect to interpreting positions of relative sea-level change within the study area. This type of local to limited-regional paleogeographic analysis provides the basic framework for interpreting the controls on local stratigraphic and mineralogical variations within the study area in subsequent chapters of this thesis.

PREVIOUS WORK

Many sea-level fluctuations throughout geologic history have been found to be global or eustatic in extent. Sedimentation on the margins of continents and in intercratonic basins responding to changing sea-level has produced a stratigraphic record of genetically related sedimentary packages bounded by unconformities. Each unconformity bounded sediment package is considered to be a stratigraphic sequence. This concept of sequence stratigraphy, first presented at the Annual Meeting of the Geological Society of America in 1948 by L.L. Sloss (1949), has grown considerably since its introduction.

Seismic stratigraphy, the direct precursor of sequence stratigraphy as it is applied today, was defined by Peter R. Vail and his co-workers (Vail *et al.*, 1977), as a method of interpreting sedimentary sequences using seismic reflection. Sequence stratigraphy, derived from the application of seismic concepts to the rock record, is now becoming widely used as a means of correlating and subdividing data obtained from outcrop, core, well logs and seismic reflection. In many respects sequence stratigraphy is a subdivision of geology, overflowing with its own terminology, definitions and acronyms. A number of recent publications have been addressed to the clarification of sequence stratigraphic concepts, including, Haq *et al.*, 1987, Van Wagoner *et al.*, 1987, Posamentier and Vail, 1988, and Posamentier *et al.*, 1988.

Concepts of sequence stratigraphy as defined by Vail and his co-workers consider the major control on the deposition of cyclic sequences to be eustatic sea-level fluctuation. Coastal onlap (or eustatic sea-level) curves, based on comparisons of seismic and stratigraphic sections with paleontological control, have now been created for many periods of geologic time, including the Cretaceous (Haq *et al.*, 1987). Eustatic sea-level variation is a controversial issue however, as cycles of sea-level change observed in stratigraphic sections are not always global in scale. Although sea-level is essentially the same everywhere at one geologic time, the height of the land is determined by local geologic conditions and varies from place to place (Vail and Hardenbol, 1979). In the attempt to prove or disprove this new method of viewing vertical facies relationships, a number of investigators have concentrated some of their research on understanding the mechanisms controlling eustatic sea-level. Menard (1964), Hays and Pitman (1973), Pitman (1978), and Donovan and Jones (1979), have identified glacial retreats and advances as only one of the mechanisms which could account for the large scale global variations in sea-level which have been identified in the rock record. This poses some problems at certain times in the geologic past however, as eustatic sea-level variations have been documented during periods of geologic time when glacial events were not thought to have occurred (Donovan and Jones, 1979; Vail and Hardenbol, 1979). As a result, a number of researchers have questioned the definitions set out by Vail and others, in favor of the belief that tectonism played a greater role on cyclic deposition. Bergman and Walker (1988), and Embry and Podruski (1988), are two examples from recent publications. Future research on the application of sequence stratigraphic concepts in settings throughout the world should help refine the role that factors such as eustacy and tectonism played in ancient depositional systems.

The Western Canada Sedimentary Basin was the depositional site of numerous clastic sequences in the Mesozoic. Progressive encroachment of the Boreal sea into this intercratonic basin eventually resulted in an epicontinental seaway that extended from Arctic Canada to the Gulf of Mexico in the Late Cenomanian to Early Turonian (Kauffman, 1977). Extensive research has been carried out on Cretaceous deposition during this time, especially with regard to the relationship between sea-level fluctuation and patterns of sediment deposition. Selected references from the Western Interior Basin are: Kauffman, 1969; Scott, 1970; Kauffman, 1977; Ryer, 1977; Stott, 1984; and Weimer, 1984. Studies on Cretaceous clastic deposits within the Western Canada Sedimentary Basin include: Cant, 1984; Cant and Hein, 1986; and numerous references from the recent C.S.P.G. Memoir 15 on sequence stratigraphy, including: Carmichael, 1988; Eyles and Walker, 1988; MacDonald *et al.*, 1988; Plint *et al.*, 1988; and Strobl, 1988.

The Clearwater Formation is a relatively thick, largely marine clastic sequence deposited during Aptian to Albian time on the eastern margin of the Western Canada Sedimentary Basin (Williams and Stelck, 1975; Harrison *et al.*, 1981). It is one of three formations within the Mannville Group of east-central Alberta which constitute the bitumen-rich reserves of the Cold Lake oil sands deposit. Figure 2.1 illustrates the position of the Cold Lake oil sands deposit within eastern Alberta. As Canada's second largest heavy oil deposit, the Cold Lake oil sands have been the focus of abundant and diverse research in the past decade. Paleogeographic studies of the Western Canada Sedimentary Basin which discuss factors that affected Mannville Group deposition include: Badgley, 1952; Carrigy, 1959; Glaister, 1959; Rudkin, 1964; Stelck, 1975; Williams and Stelck, 1975; and Jackson, 1984. Studies by: Williams, 1963; Vigrass, 1965; Mellon, 1967; Gallup, 1974; Jardine, 1974; Mossop *et al.*, 1981 and Wightman *et al.*, 1991; are also quite regional in nature and focus on Mannville Group sedimentation within Alberta's Cretaceous oil sands deposits. A number of studies have also been concerned with sedimentological and other characteristics of the Clearwater Formation within the Cold Lake oil sands deposit. These include: Minken, 1974; Harrison *et al.*, 1981; Putman and Pedskalny, 1983; Wightman and Berezniuk, 1986; and Prentice and Wightman, 1987.

STUDY AREA

Clearwater Formation core and corresponding well logs examined in this study are contained within townships 65 and 66, ranges 2 through 4 west of the fourth meridian in east-central Alberta. This relatively small area is for the most part entirely within the Leming pilot area of the Esso Lease in the northern part of the Cold Lake oil sands deposit. Well logs from 11 other wells were examined in surrounding parts of the Cold Lake oil sands deposit. This entire area encompasses a larger study area contained within townships 63 to 67, ranges 1 through 6 in east-central Alberta. Figure 2.2 shows the position of these two study boundaries within the Cold Lake oil sands deposit.

B. REGIONAL SETTING

STRATIGRAPHY

The Western Canada Sedimentary Basin is composed of thick sequences of Paleozoic to Tertiary strata which unconformably overlie the folded and faulted crystalline

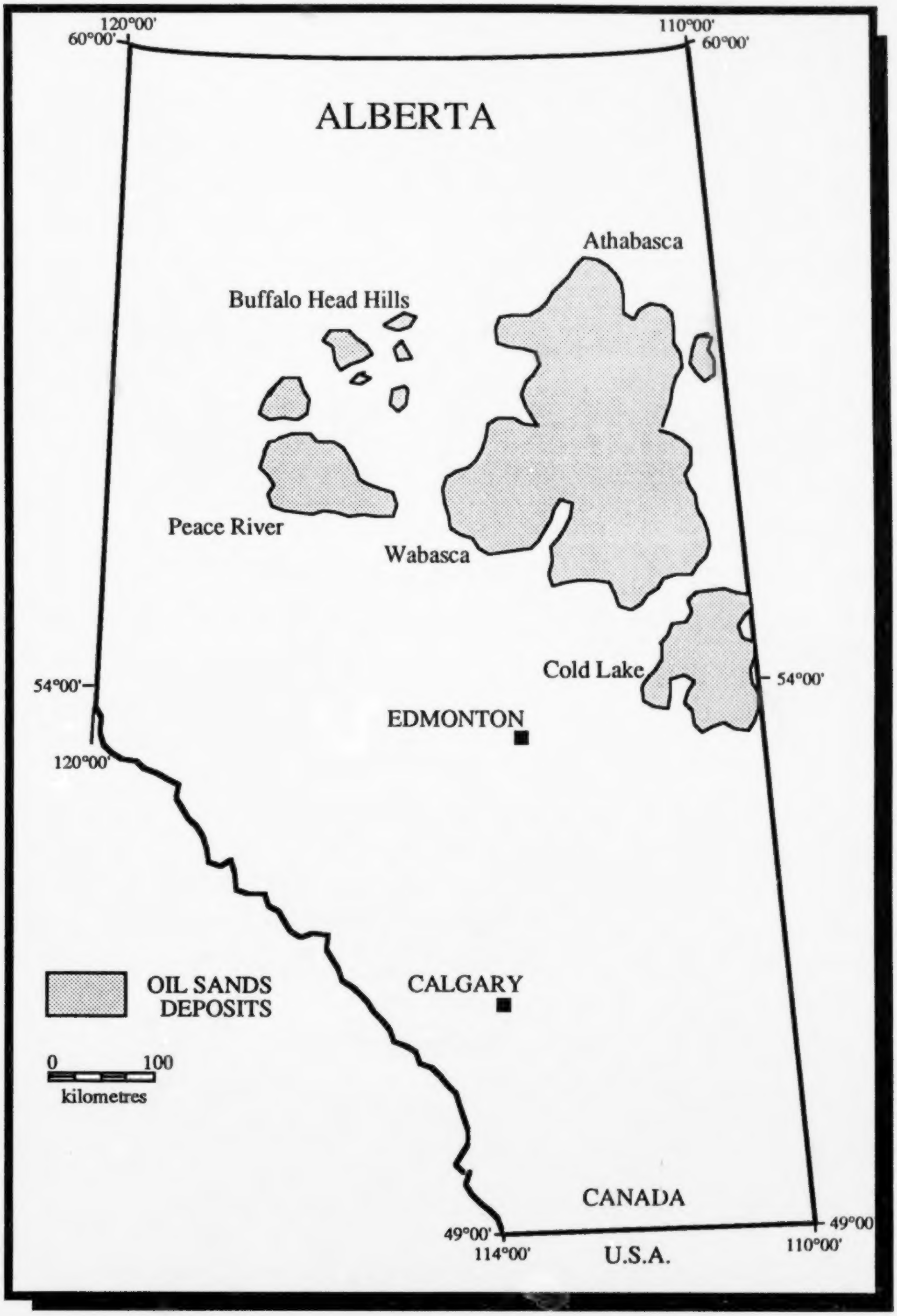
ALBERTA
120°00'
60°00'
110°00'
60°00'
Athabasca
Buffalo Head Hills
Peace River
Wabasca
Cold Lake
54°00'
54°00'
EDMONTON
120°00'
CALGARY
OIL SANDS DEPOSITS
0
100
kilometres
CANADA
U.S.A.
49°00'
114°00'
49°00'
110°00'

Figure 2.1: Location of the Cold Lake oil sands deposit within Alberta .

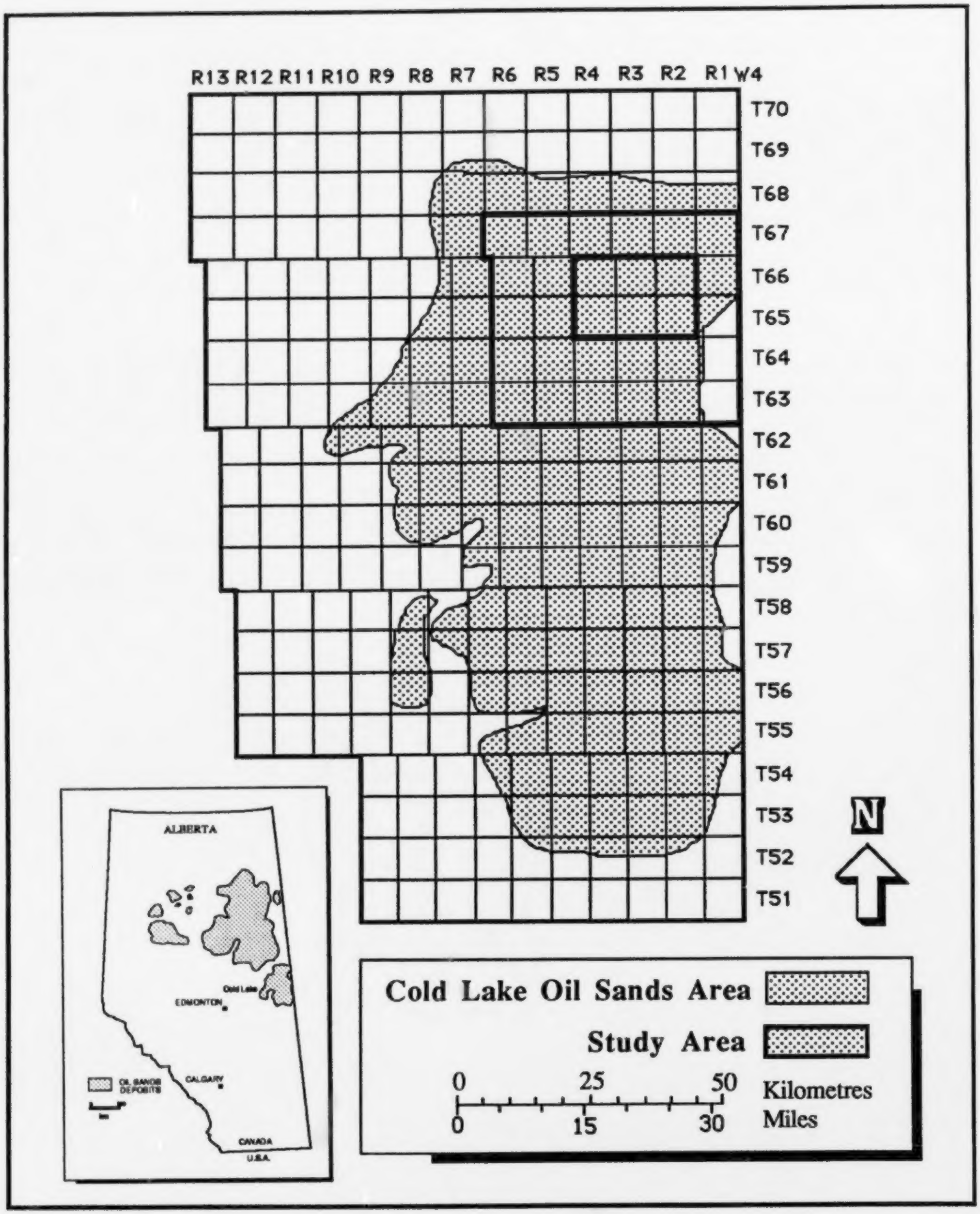
R13
R12
R11
R10
R9
R8
R7
R6
R5
R4
R3
R2
R1
W4
T70
T69
T68
T67
T66
T65
T64
T63
T62
T61
T60
T59
T58
T57
T56
T55
T54
T53
T52
T51
N
Cold Lake Oil Sands Area
Study Area
0
25
50
Kilometres
0
15
30
Miles
ALBERTA
Cold Lake
EDMONTON
CALGARY
OIL SANDS DEPOSITS
CANADA
U.S.A.

Figure 2.2: Location map of study area and Alberta oil sands deposits.

rocks of the Precambrian basement. Paleozoic sequences are predominantly calcareous with isolated intervals of evaporites and fine-grained clastic rocks. Cretaceous sequences in the Alberta basin are mainly clastic and generally lie unconformably on Jurassic clastic and Paleozoic carbonate rocks. The Mannville Group directly overlies the pre-Cretaceous unconformity in the Cold Lake study area. Figure 2.3 illustrates the major lithologies and their position within the Western Canada Sedimentary Basin.

The McMurray, Clearwater and Grand Rapids formations were originally defined as part of the Fort St. John Group in the lower Athabasca River section by McLearn (1932), and remained in this classification even after a revision of Lower Cretaceous stratigraphy by McLearn (1944). The Mannville Group was first named, 'The Mannville Formation,' by A.W. Nauss (1945) from the Vermilion area of east-central Alberta. This original definition included all beds lying between the lower eroded surface of the Devonian Winterburn and Woodbend Groups and the overlying Colorado Group (Williams, 1963). These sediments were correlated with the McMurray, Clearwater, and Grand Rapids formations of the lower Athabasca River valley, and were raised to group status by Badgley (1952). Badgley (1952) also correlated the Mannville Group with the upper part of the Bullhead Group, the Bluesky and the Spirit River formations, and part of the Peace River Formation. Glaister (1959) divided the Mannville Group into Upper and Lower intervals, and correlated the beds with the Blairmore Group of the southern and central foothills. Mellon and Wall (1961) refined correlations between the Mannville Group and the Blairmore Group of the foothills, and Williams (1963) further subdivided the McMurray Formation into members in the lower Athabasca River valley and Edmonton areas.

In current definitions, the Mannville Group of east-central Alberta is divided into three formations, each of which is distinct from the other in environment and resulting facies. Furthermore, the group is often divided into Lower and Upper intervals; with the Grand Rapids and Clearwater Formations constituting the Upper Mannville Group; and the McMurray Formation constituting the Lower Mannville Group (Figure 2.4). In east-central Alberta, the Clearwater Formation is overlain by the Grand Rapids Formation, which is commonly subdivided into a Lower and Upper Formation within the Cold Lake area. The Grand Rapids Formation extends south into the Lloydminster area where it has been further subdivided into formations of different facies (McLean and Putnam, 1983). Correlation of these facies into the Cold Lake area is difficult because of extensive lateral facies changes; this is the subject of study by B.M. Beynon and others (1988). The Grand Rapids Formation extends north into the Athabasca area, and is laterally equivalent

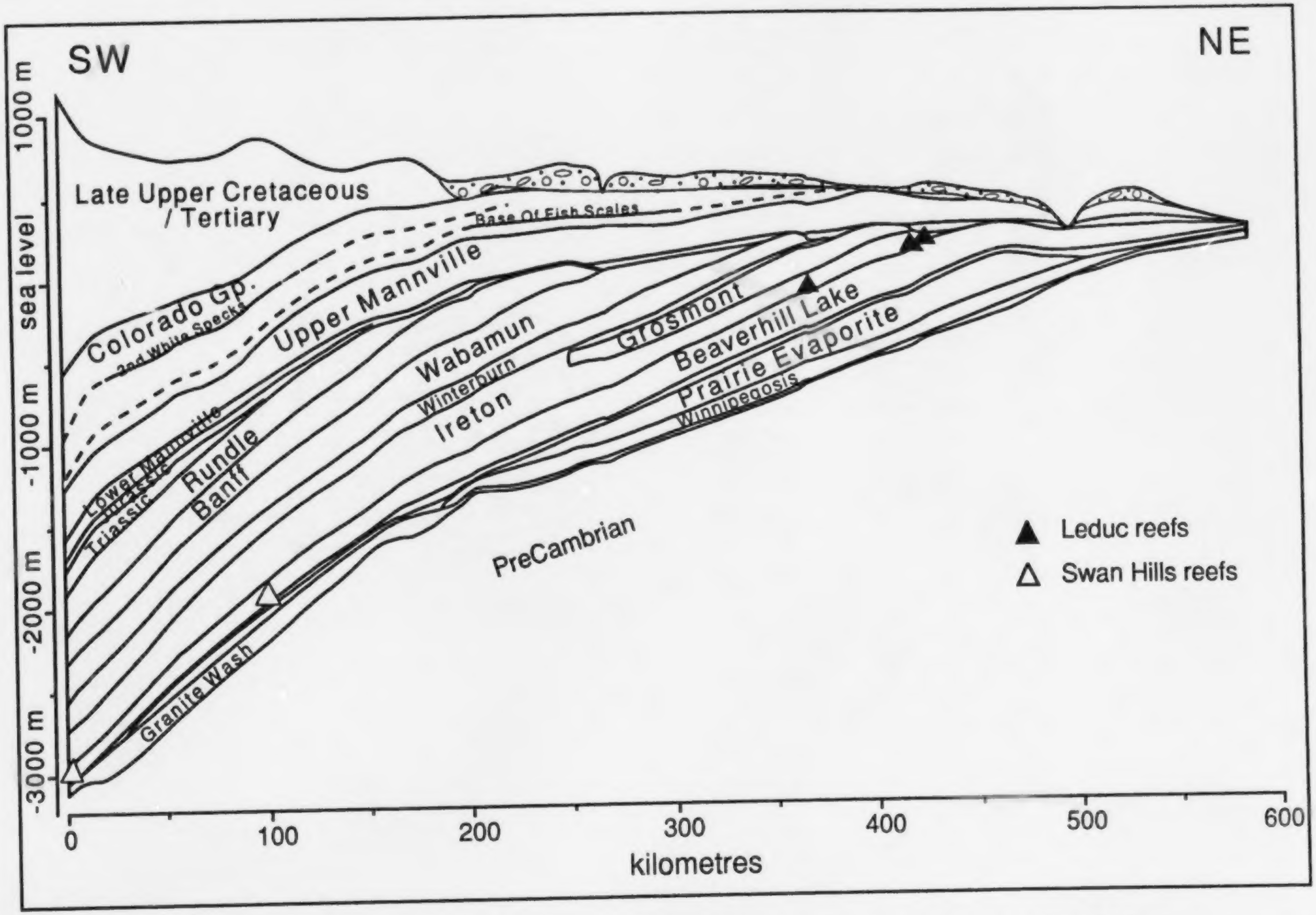
SW
NE
1000 m
sea level
-1000 m
-2000 m
-3000 m
Late Upper Cretaceous / Tertiary
Base Of Fish Scales
Colorado Gp.
2nd White Specks
Upper Mannville
Lower Mannville
Jurassic
Triassic
Rundle
Banff
Wabamun
Winterburn
Ireton
Grosmont
Beaverhill Lake
Prairie Evaporite
Winnipegosis
Granite Wash
PreCambrian
▲ Leduc reefs
△ Swan Hills reefs
0
100
200
300
400
500
600
kilometres

Figure 2.3: Geologic cross-section of the Western Canada Sedimentary Basin showing the major stratigraphic units and their position (modified from Ranger and Pemberton, 1992).

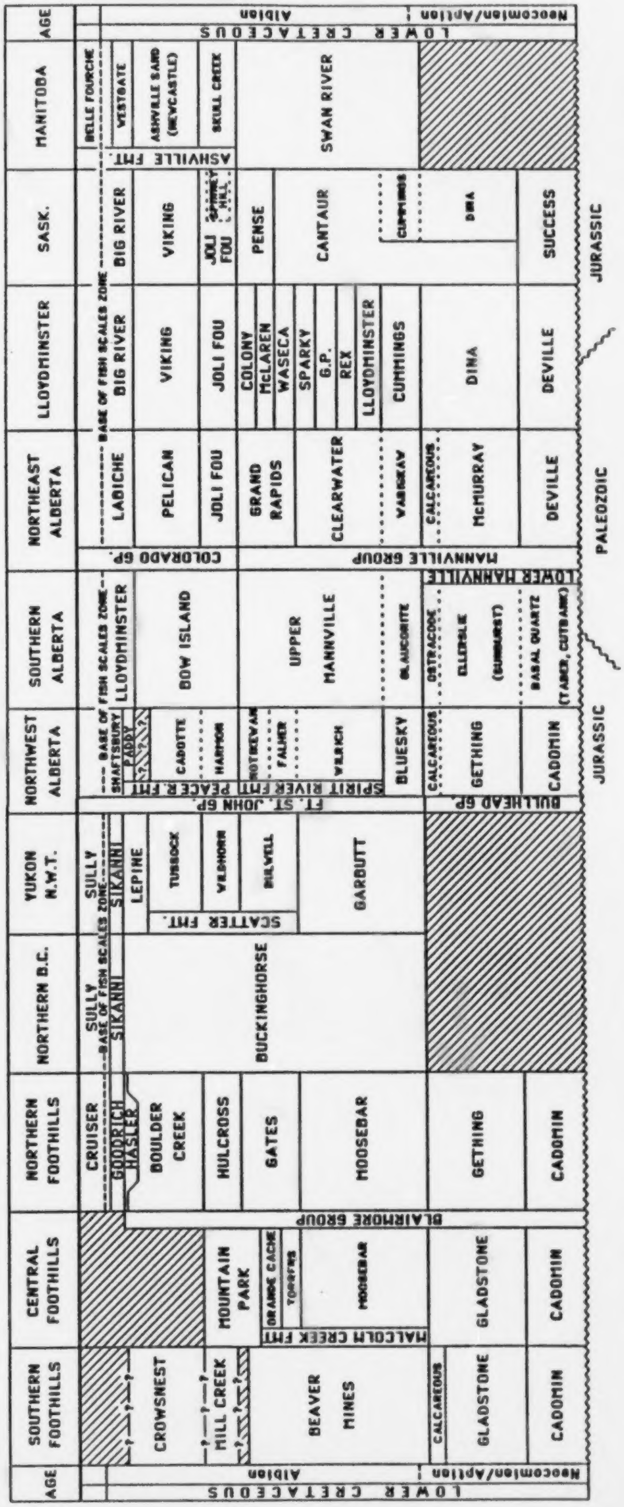
AGE
SOUTHERN FOOTHILLS
CENTRAL FOOTHILLS
NORTHERN FOOTHILLS
NORTHERN B.C.
YUKON N.W.T.
NORTHWEST ALBERTA
SOUTHERN ALBERTA
NORTHEAST ALBERTA
LLOYDMINSTER
SASK.
MANITOBA
LOWER CRETACEOUS
Albian
Neocomian/Aptian
CROWSNEST
HILL CREEK
BEAVER MINES
CALCAREOUS
GLADSTONE
CADOMIN
MOUNTAIN PARK
GRANDE CACHE
TORRENS
MOOSEBAR
MALCOLM CREEK FMT
BLAIRMORE GROUP
CRUISER
GOODRICH
HASLER
BOULDER CREEK
HULCROSS
GATES
GETHING
SULLY
BASE OF FISH SCALES ZONE
SIKANNI
BUCKINGHORSE
LEPINE
TUSSOCK
WILDHORN
BULWELL
SCATTER FMT.
GARBUTT
SHAFTSBURY
PADDY
CADOTTE
HARMON
NOTIKEWAN
FALHER
WILRICH
PEACE R. FMT
SPIRIT RIVER FMT
FT. ST. JOHN GP.
BLUESKY
BULLHEAD GP.
JURASSIC
LLOYDMINSTER
BOW ISLAND
UPPER MANNVILLE
GLAUCONITE
OSTRACODE
ELLERSLIE
(SUNBURST)
BASAL QUARTZ
(TABER, CUTBANK)
LOWER MANNVILLE
LABICHE
PELICAN
JOLI FOU
GRAND RAPIDS
CLEARWATER
WABISKAW
McMURRAY
DEVILLE
COLORADO GP.
MANNVILLE GROUP
PALEOZOIC
BIG RIVER
VIKING
COLONY
McLAREN
WASECA
SPARKY
G.P.
REX
CUMMINGS
DINA
SPINNEY HILL
PENSE
CANTAUR
SUCCESS
BELLE FOURCHE
WESTGATE
ASHVILLE SAND (NEWCASTLE)
SKULL CREEK
ASHVILLE FMT.
SWAN RIVER

Figure 2.4: Lower Cretaceous Stratigraphic Correlation Chart of the Western Canada Sedimentary Basin.

to the Notikewan and Falher Members of the Spirit River Formation in the Peace River area (Mossop *et al.*, 1981). The Clearwater Formation is underlain by the sands and shales of the McMurray Formation, which extend north to where they constitute the richest bitumen-saturated interval in the Athabasca oil sands deposit. The McMurray Formation is laterally equivalent to the Dina Formation in the Lloydminster area, the Ellerslie interval of the Lower Mannville in southern Alberta, and the Gething Member of the Bullhead Group in the Peace River area (Mossop *et al.*, 1981). The Wabiskaw Member is a glauconite-rich, interval which occurs at or near the base of the Clearwater Formation in the Cold Lake area. It is laterally equivalent to the Glauconitic Member of southern Alberta, the Cummings Formation in the Lloydminster area, the Bluesky Formation in the Peace River area and extends north into the Athabasca area (Ranger *et al.*, 1988).

REGIONAL GEOLOGY AND PALEOGEOGRAPHY

The Western Canada Sedimentary Basin is bounded on the west by the Rockies of the Canadian Cordillera, on the east by the emergent Canadian Shield, and is separated from the Williston Basin to the southeast by the Sweetgrass Arch (Figure 2.5). The present configuration of this foreland basin is an asymmetrical syncline, the result of major tectonism of the Cordilleran in the west, combined with downwarping (subsidence) of sediments accumulating on the frontal ranges of the Rockies (foredeep) (Jackson, 1984) (Figure 2.6). This onloading of sediment and resulting subsidence in the foredeep resulted in the formation of the Deep Basin with sediment thicknesses in excess of 16 km (10 mi) (Hitchon, 1969).

Tectonic History

Paleozoic carbonates, evaporites, shales and other Cambrian to Mississippian clastic rocks within the Western Canada Sedimentary Basin were deposited during a relatively passive tectonic period (Spencer, 1974), as illustrated in Figure 2.7a. In the early to mid-Triassic, deformational pulses, regional metamorphism, and the emplacement of granitic plutons in the Eastern Cordillera, which constitute the Tahltanian orogeny (Spencer, 1974), likely resulted in erosion of any Upper Pennsylvanian to Permian rocks present within the basin. This formed a pre-Jurassic / Early Cretaceous depositional surface of subdued, cuesta-like relief (Jackson, 1984). The Early Jurassic

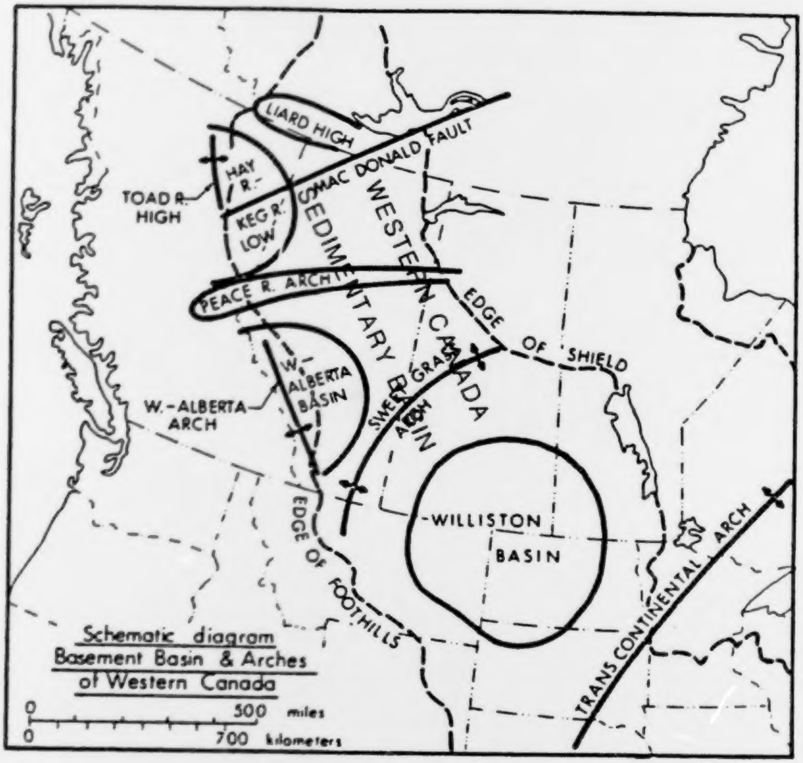
LIARD HIGH
MAC DONALD FAULT
HAY R.
TOAD R. HIGH
KEG R. LOW
WESTERN CANADA
SEDIMENTARY BASIN
PEACE R. ARCH
EDGE OF SHIELD
W. ALBERTA BASIN
W.-ALBERTA ARCH
SWEET GRASS ARCH
WILLISTON BASIN
EDGE OF FOOTHILLS
TRANS CONTINENTAL ARCH
Schematic diagram
Basement Basin & Arches
of Western Canada
0 500 miles
0 700 kilometers

Figure 2.5: Schematic diagram of Precambrian basement features and the position of the Western Canada Sedimentary Basin in western Canada (modified from Stelck, 1975).

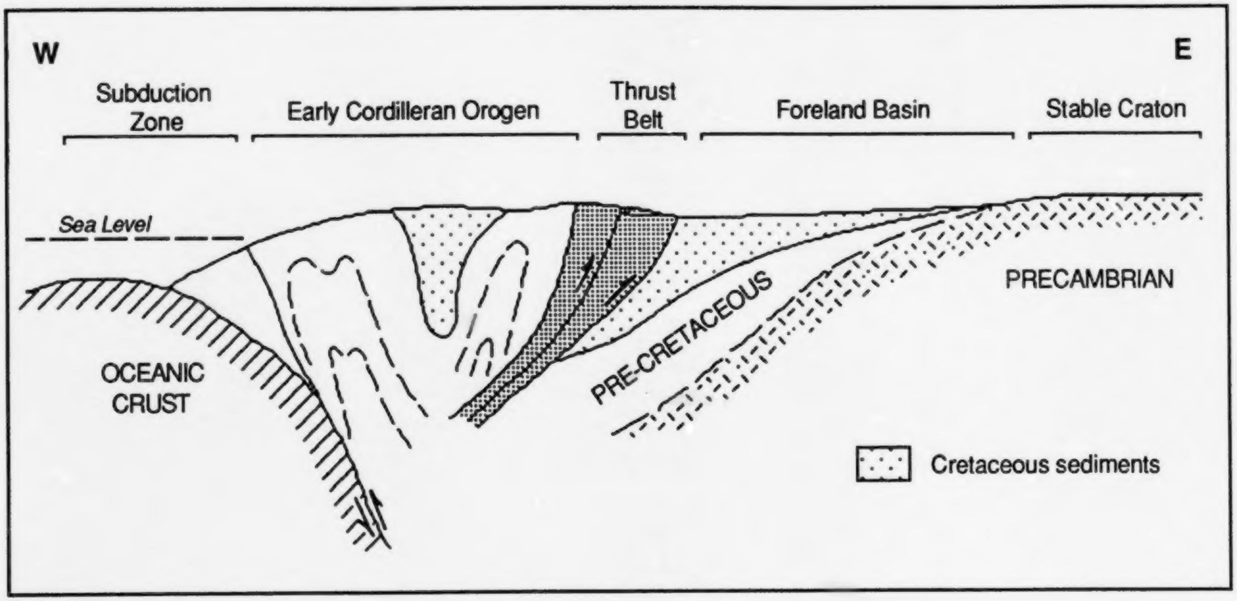
W
E
Subduction Zone
Early Cordilleran Orogen
Thrust Belt
Foreland Basin
Stable Craton
Sea Level
OCEANIC CRUST
PRE-CRETACEOUS
PRECAMBRIAN
Cretaceous sediments

Figure 2.6: Schematic cross-section illustrating the structural configuration of the uplifted early Cordilleran orogen to the thick sediment wedge of the Alberta foreland basin during the Cretaceous (modified after Jackson, 1984).

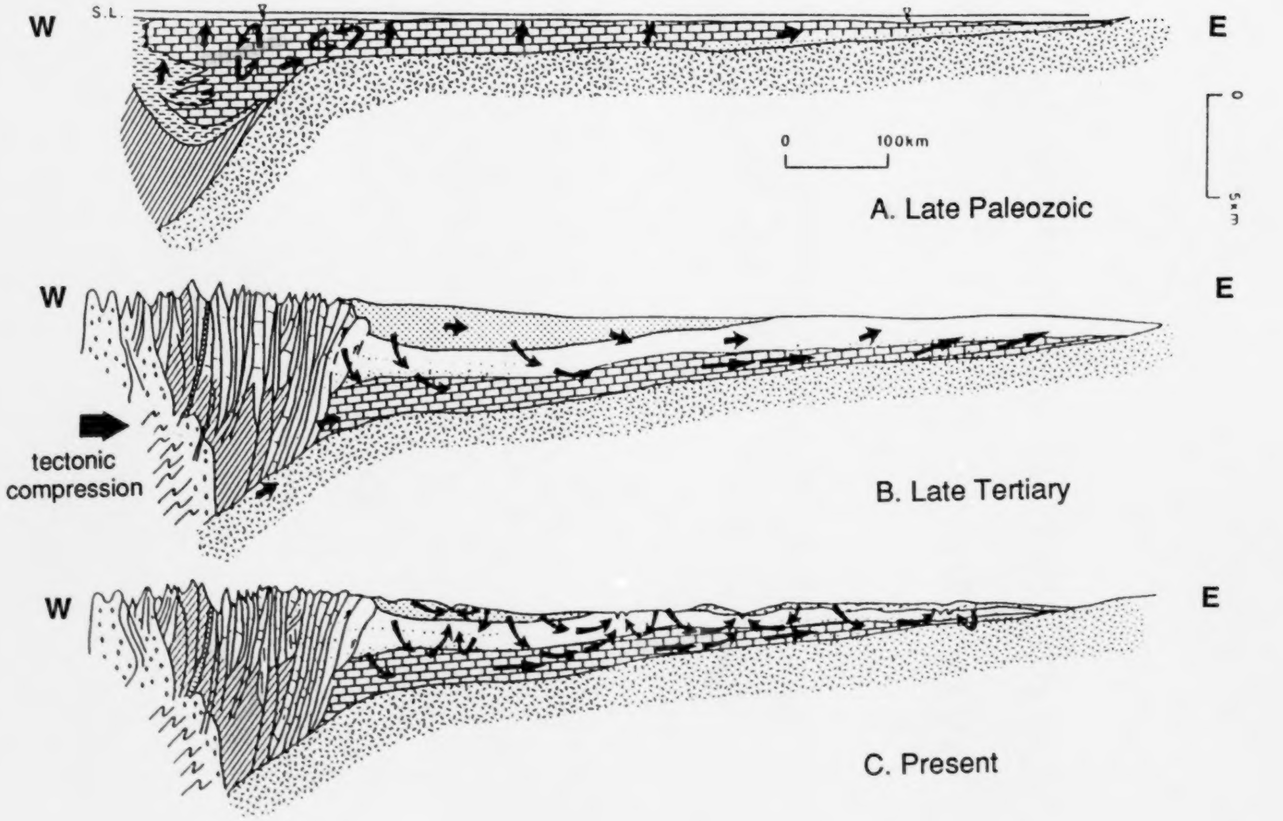
W
S.L.
E
0
100km
0
5km
A. Late Paleozoic
W
E
tectonic
compression
B. Late Tertiary
W
E
C. Present

Figure 2.7: Schematic of structural features evolved during tectonism and groundwater flow directions in the Alberta foreland basin from the Paleozoic to present. (a). Late Paleozoic stage - passive margin. (b). Late Tertiary stage - soon after tectonic compression and flexural uplift. (c). Present day structure and topography (modified from Garven, 1989).

was marked by a renewed uplift in the Eastern Cordillera that shed abundant sediment east down into the basin (Spencer, 1974).

The Columbian orogeny began in the mid-Jurassic (Bathonian) in the Omineca Batholiths located in the southern part of the Rocky Mountains (Spencer, 1974). Major thrusting and associated folding of the thrust sheets in the Rockies resulted in substantial crustal shortening along a zone of décollement about 190 km (119 mi) relative to the craton (Spencer, 1974). The uplift associated with the Columbian orogeny shed abundant clastic debris east into the western margin of the Alberta basin. Crustal shortening and downwarping resulting from the heavy sediment load led to the formation of the large clastic sediment wedge present in the western margin of the basin (Figure 2.6). Continued uplift and deformation throughout the Cretaceous resulted in the eastward migration of depositional clastics with time, with the greatest episode of uplift in the late Aptian / early Albian. Subsidence continued throughout the Laramide orogeny, which began in the Late Cretaceous, and continued until the Early Cenozoic (Kauffman, 1977). Figures 2.7b and 2.7c illustrate the overall structure of the Western Canada Sedimentary Basin in the Late Tertiary and at the present time. The southwest margin of the Western Canada Sedimentary Basin was the zone of greatest subsidence. The asymmetrical downwarping of the basin in this area reflects primary tectonic control and subsidence resulting from the heavy sediment load, but may also have been influenced by plate tectonism, the possible drag effect of the Pacific plate underriding Middle North America (Kauffman, 1977). It is not known to what degree these factors affected the present day basin configuration, but they led to the development of structures critical to Mannville Group sedimentation (Jackson, 1984).

Structural Influences on Sedimentation

An analysis by Jackson (1984), of structural features which affected Mannville Group paleogeography determined that all of the following features significantly influenced Mannville Group sedimentation:

1) the foredeep trough with a distinct hingeline on its eastern flank;
2) an axial high region (Athabasca anticline) in the eastern portion of the Western Canada Sedimentary Basin; and
3) an eastern regional low.

The axial trend which extended from northeastern British Columbia to the Swift Current Platform in southwestern Saskatchewan developed as a result of the formation of the foredeep trough to the southwest (Jackson, 1984), and the regional low from salt dissolution of Middle Devonian evaporites (Jardine, 1974; Wightman and Berezniuk, 1986). Dominant structural features which influenced Cretaceous sedimentation in the Western Canada Sedimentary Basin are illustrated in Figure 2.8.

Devonian carbonates of the BeaverHill Lake and Woodbend (Cooking Lake Formation) groups formed the Mannville depositional surface in the Early Cretaceous in east-central Alberta (Figure 2.9). Topography of this surface was influenced by a number of factors, namely:

1) variable erosion of Upper Devonian carbonates;
2) salt dissolution of underlying Middle Devonian evaporites; and
3) structural deformation associated with the axial high (Jackson, 1984) (Figure 2.9).

The axial high (Athabasca anticline) is believed to have directed early Mannville drainage to previously present structural lows during deposition of the McMurray Formation, resulting in valley incision over one hundred feet in depth in some areas (Jackson, 1984; Wightman *et al.*, 1991). It is also believed to have separated the transgressing Boreal sea in a marine phase of Lower Mannville sedimentation. Dissolution of salt leading to the collapse of Middle Devonian evaporites is thought to have continued to affect sedimentation in the study area throughout deposition of the Lower Cretaceous and is likely still continuing at the present time (Jardine, 1974; Maher, 1989; M. Ranger[1], per. comm.).

Cretaceous Paleogeography

Two principal stages of marine sedimentation governed Cretaceous paleogeography in the Western Canada Sedimentary Basin. There was an initial Early Cretaceous transgression of the Boreal sea and a later major transgression of maximum onlap in the Late Cretaceous (Kauffman, 1977). Deposition of the Mannville Group in east-central Alberta occurred prior to and during the initial stage of marine sedimentation, the result of the inundation of the Boreal sea into northern Canada (Kauffman, 1977).

The Lower Mannville was characterized primarily by continental sedimentation in east-central Alberta and elsewhere in the basin. Sediments which constitute the lower McMurray Formation were eroded from the Eastern Cordillera and were carried by rivers draining northwest into east-central Alberta via a number of major channel systems

---

[1] Department of Geology, University of Alberta, Edmonton, Alberta, Canada.

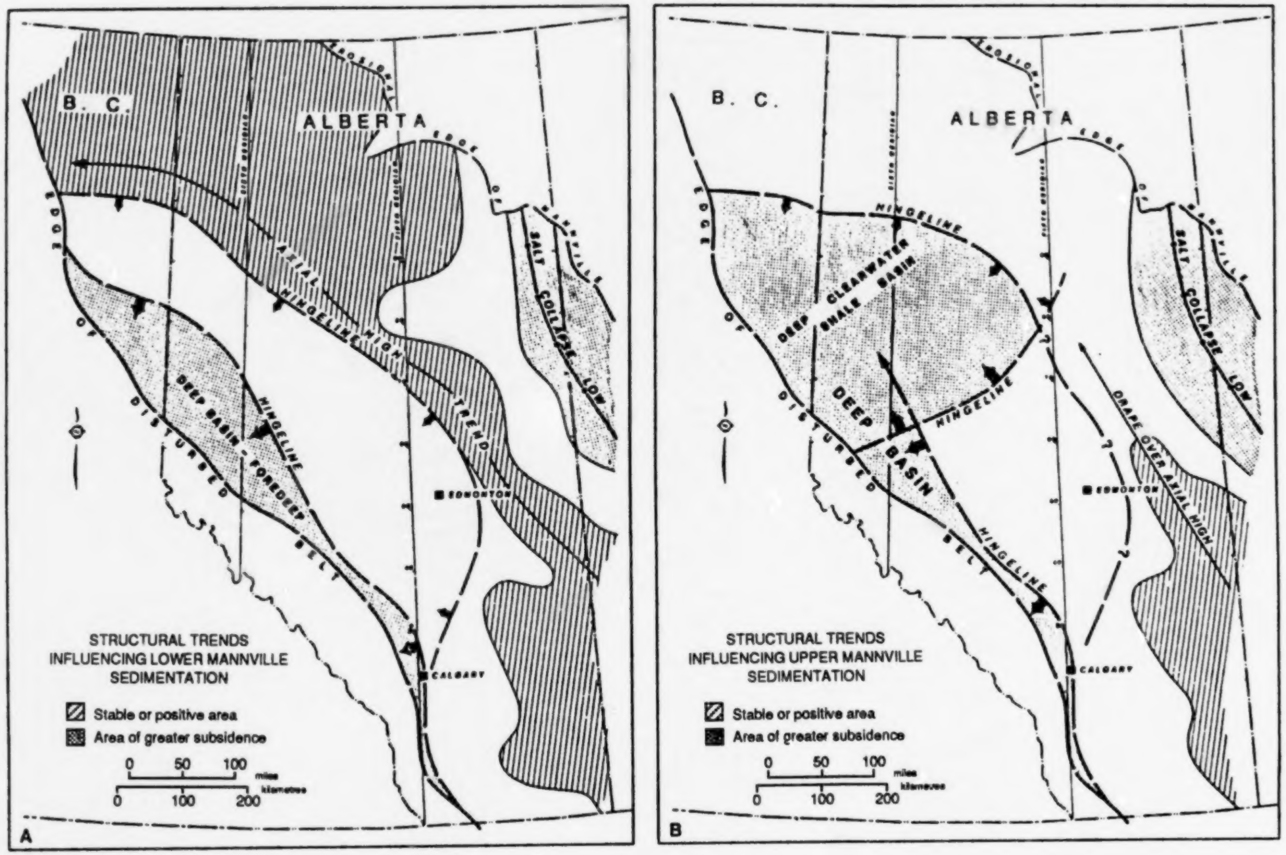
A
B. C.
ALBERTA
EROSIONAL EDGE OF MANNVILLE
SALT COLLAPSE LOW
AXIAL HIGH TREND
HINGELINE
DEEP BASIN - FOREDEEP
EDGE OF DISTURBED BELT
EDMONTON
CALGARY
STRUCTURAL TRENDS INFLUENCING LOWER MANNVILLE SEDIMENTATION
▨ Stable or positive area
▩ Area of greater subsidence
0 50 100 miles
0 100 200 kilometres
B
B. C.
ALBERTA
EROSIONAL EDGE OF MANNVILLE
SALT COLLAPSE LOW
HINGELINE
DEEP CLEARWATER SHALE BASIN
DEEP BASIN
DRAPE OVER AXIAL HIGH
EDGE OF DISTURBED BELT
EDMONTON
CALGARY
?
STRUCTURAL TRENDS INFLUENCING UPPER MANNVILLE SEDIMENTATION
▨ Stable or positive area
▩ Area of greater subsidence
0 50 100 miles
0 100 200 kilometres

Figure 2.8: Structural features that influenced deposition of the Lower (A) and Upper (B) Mannville Group in the Lower Cretaceous (modified from Jackson, 1984).

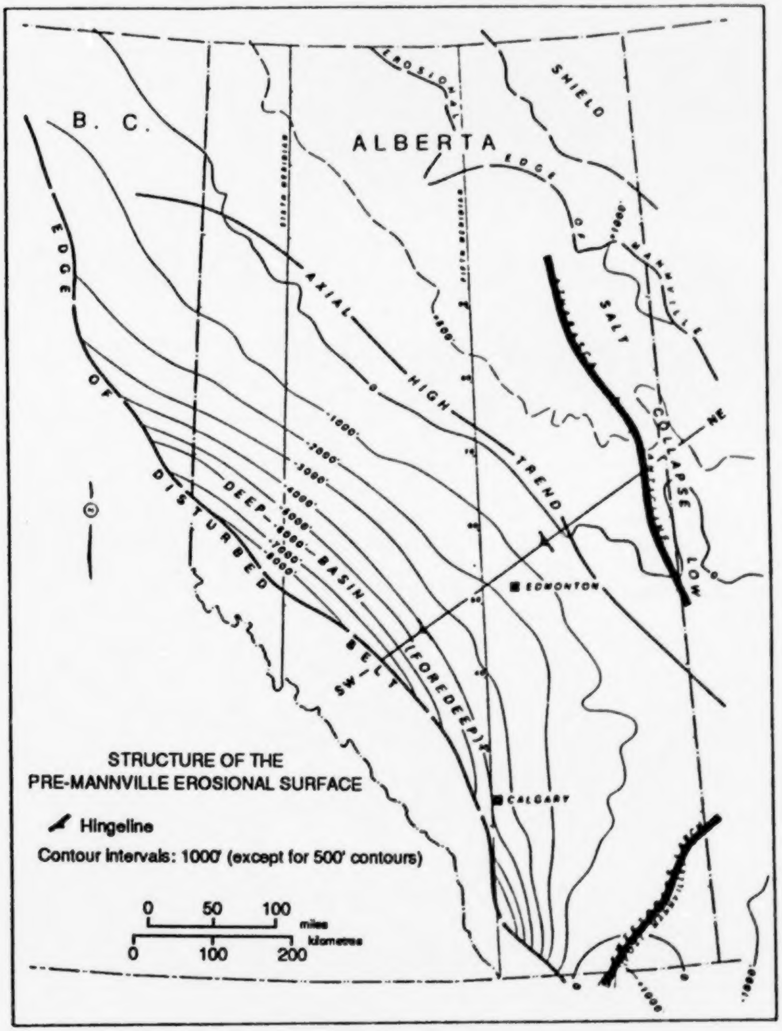
B. C.
ALBERTA
EROSIONAL EDGE OF MANNVILLE
SHIELD
EDGE OF DISTURBED BELT
AXIAL HIGH TREND
DEEP BASIN (FOREDEEP)
SALT COLLAPSE LOW
NE
SW
EDMONTON
CALGARY
0
-500'
-1000'
-2000'
-3000'
-4000'
-5000'
-6000'
-7000'
-8000'
STRUCTURE OF THE
PRE-MANNVILLE EROSIONAL SURFACE
Hingeline
Contour intervals: 1000' (except for 500' contours)
0
50
100
miles
0
100
200
kilometres

Figure 2.9: Structure of the pre-Mannville depositional surface (modified after Jackson, 1984).

(Jackson, 1984; Wightman *et al.*, 1991). The St. Paul Channel system on the east side of the axial high was the main means of sediment conveyance of the lower McMurray Formation. McMurray sediments may have also been supplied by erosion of the axial high (Jackson, 1984), or some debris may have been contributed from the emergent Canadian Shield (Harrison *et al.*, 1981). Figure 2.10 is a map of Lower Mannville paleogeography which illustrates the positions of the fluvial systems in the first phase of Mannville Group deposition.

The Boreal sea had transgressed into northeastern Alberta by the mid-Aptian and began to influence Mannville sedimentation by the time of Upper McMurray deposition (Jackson, 1984). The Lower Mannville in east-central Alberta is believed to have been deposited as a series of tidal channels in a brackish / marginal marine environment (Harrison *et al.*, 1981; Jackson, 1984) (Figure 2.11).

Further transgression of the Boreal sea from the northeast led to the deposition of the Wabiskaw Member of the Clearwater Formation in east-central Alberta. It is generally agreed that Wabiskaw sediments developed in an offshore, shallow marine environment (Outtrim and Evans, 1977; Ranger *et al.*, 1988; Wightman *et al.*, 1991). Wabiskaw sands have been identified by some researchers as transgressive lags or regressive pulses (Outtrim and Evans, 1977), deposited in a shallow marine setting as offshore bars in a continued transgression of the Boreal sea (Bayliss and Levinson, 1976; Jackson, 1984) (Figure 2.12), but in other studies have been identified as a progradational units (Ranger *et al.*, 1988; Strobl, 1988).

Continued deposition of the Clearwater Formation in the Aptian to Albian in east-central Alberta marks the beginning of an increase in the supply of clastic debris to the Western Canada Sedimentary Basin. This is likely the result of a phase of more pronounced tectonism and uplift in the Eastern Cordillera. The large influx of detritus overcame basin subsidence and eustatic sea-level rise and deposited the Clearwater Formation as a series of progradational pulses into a shallow marine deltaic setting at the edge of the Boreal sea.

Continued progradation into east-central Alberta during the Albian resulted in the deposition of the Upper and Lower Grand Rapids Formations. Clastic debris shed from the Cordilleran and perhaps some contribution from the Canadian Shield were deposited in numerous tidal and fluvial channels in brackish-water conditions (Jackson, 1984; Wightman *et al.*, 1987; Beynon *et al.*, 1988). Repeated transgressions during a period of overall regression caused an overall shallowing of nearshore marine conditions during

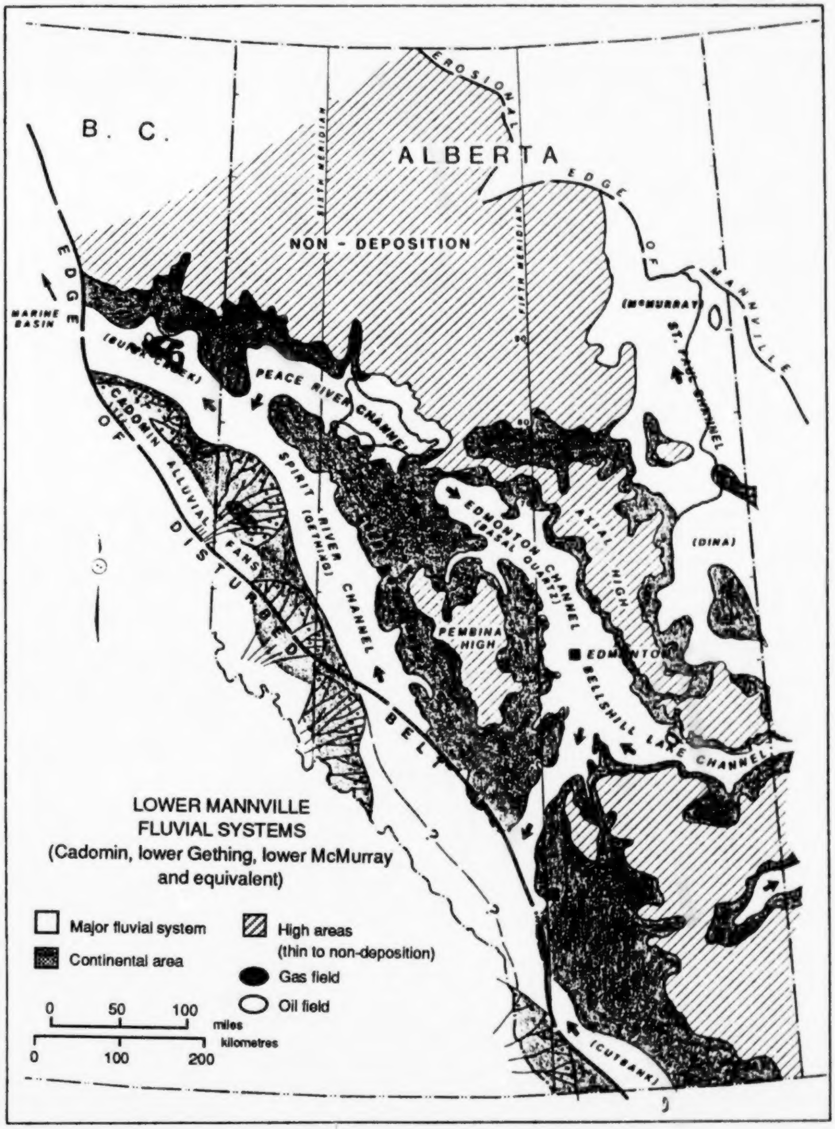
B. C.
ALBERTA
EROSIONAL EDGE
EDGE OF MANNVILLE
NON - DEPOSITION
5TH MERIDIAN
6TH MERIDIAN
EDGE
MARINE BASIN
(BUICK CREEK)
PEACE RIVER CHANNEL
CADOMIN
ALLUVIAL FANS
EDGE OF DISTURBED BELT
SPIRIT RIVER CHANNEL
(GETHING)
EDMONTON CHANNEL
(BASAL QUARTZ)
PEMBINA HIGH
AXIAL HIGH
(McMURRAY)
ST. PAUL CHANNEL
(DINA)
EDMONTON
BELLSHILL LAKE CHANNEL
(CUTBANK)
LOWER MANNVILLE
FLUVIAL SYSTEMS
(Cadomin, lower Gething, lower McMurray
and equivalent)
Major fluvial system
Continental area
High areas
(thin to non-deposition)
Gas field
Oil field
0
50
100
miles
kilometres
0
100
200

Figure 2.10: Lower Mannville (lower McMurray Formation) paleogeography in the Early Cretaceous (modified from Jackson, 1984).

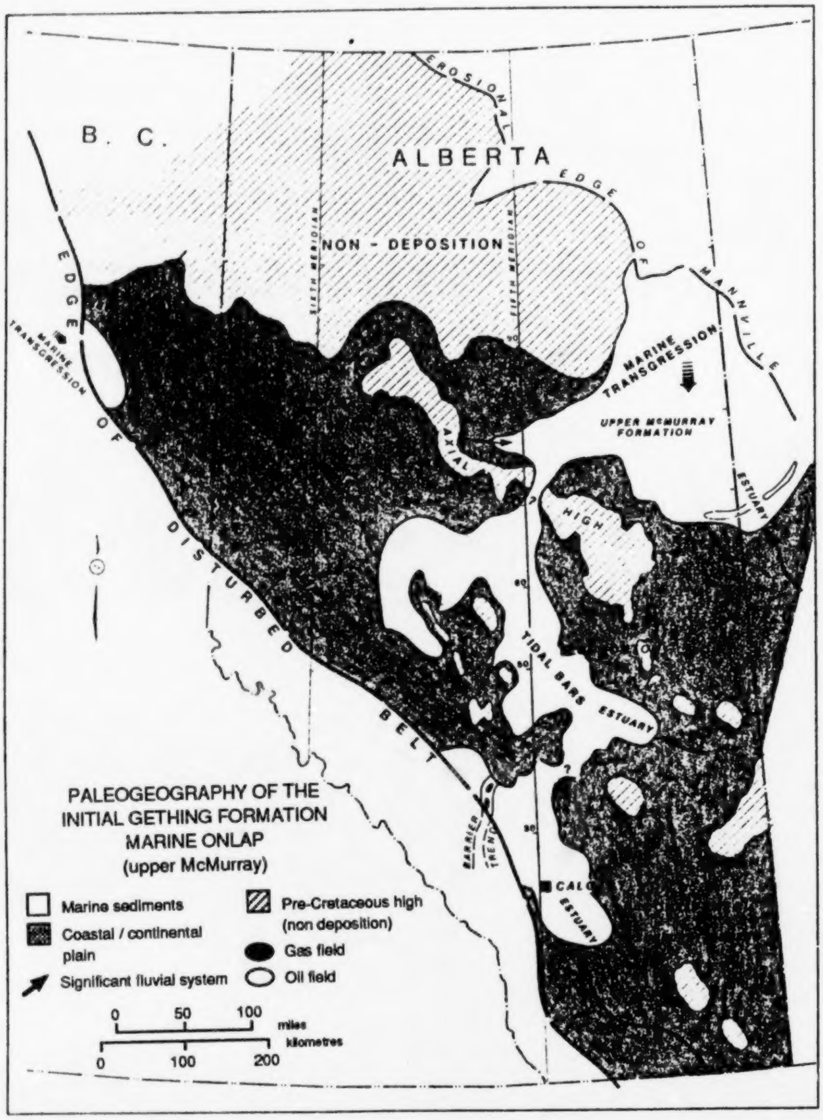
B. C.
ALBERTA
EROSIONAL
EDGE OF MANNVILLE
NON - DEPOSITION
SIXTH MERIDIAN
FIFTH MERIDIAN
EDGE OF DISTURBED BELT
MARINE TRANSGRESSION
MARINE TRANSGRESSION
UPPER McMURRAY FORMATION
AXIAL
HIGH
ESTUARY
TIDAL BARS ESTUARY
BARRIER
TREND
CALG
ESTUARY
?
?
PALEOGEOGRAPHY OF THE
INITIAL GETHING FORMATION
MARINE ONLAP
(upper McMurray)
☐ Marine sediments
▩ Coastal / continental plain
↗ Significant fluvial system
▨ Pre-Cretaceous high (non deposition)
● Gas field
○ Oil field
0 50 100 miles
0 100 200 kilometres

Figure 2.11: Lower Mannville (upper McMurray Formation) paleogeography in the Western Canada Sedimentary Basin (modified from Jackson, 1984).

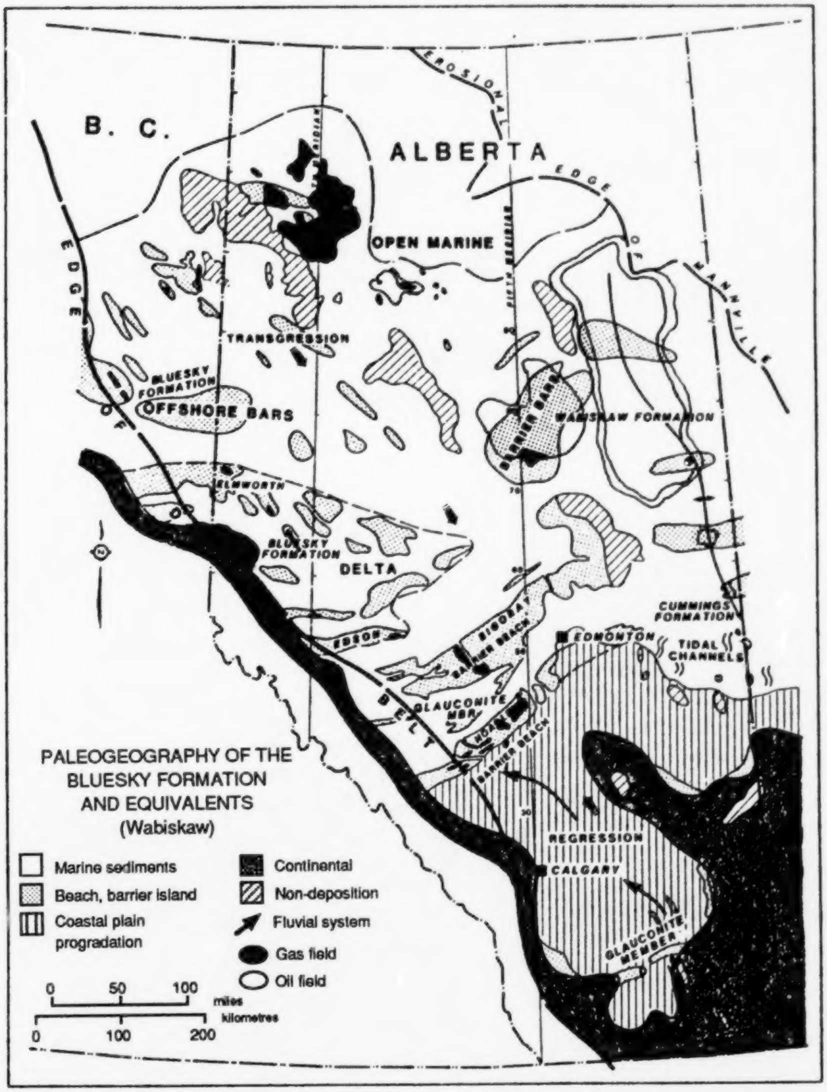
B. C.
ALBERTA
EROSIONAL
EDGE
OF
MANNVILLE
EDGE
OF
OPEN MARINE
TRANSGRESSION
BLUESKY FORMATION
OFFSHORE BARS
ELMWORTH
BLUESKY FORMATION
DELTA
EDSON
BELT
BIGORAY BARRIER BEACH
GLAUCONITE MBR.
HOADLEY BARRIER BEACH
BARRIER BARS
WABISKAW FORMATION
CUMMINGS FORMATION
EDMONTON
TIDAL CHANNELS
REGRESSION
CALGARY
GLAUCONITE MEMBER
PALEOGEOGRAPHY OF THE BLUESKY FORMATION AND EQUIVALENTS (Wabiskaw)
Marine sediments
Beach, barrier island
Coastal plain progradation
Continental
Non-deposition
Fluvial system
Gas field
Oil field
0
50
100
miles
kilometres
0
100
200

Figure 2.12: Lower Mannville (Wabiskaw Member) paleogeography in the Lower Cretaceous of western Canada (modified from Jackson, 1984).

Grand Rapids deposition (Jackson, 1984). Figure 2.13 is a paleogeographic map that depicts depositional conditions during the latter part of Upper Mannville deposition.

Deposition of the Grand Rapids Formation was followed by a second major transgression of the Boreal sea, matched by a southern advance of the Gulfian Sea into the southern United States from the Gulf of Mexico. These two embayments finally met up in the Late Cretaceous at a time of maximum flooding in the basin, creating the Western Interior Seaway of North America, and resulting in the deposition of the marine shales of the Colorado Group over the Mannville Group sediments in the study area (Kauffman, 1977; Jackson, 1984).

Hydrocarbon Accumulation

Mannville Group formations in eastern Alberta contain the majority of Alberta's heavy oil deposits. The timing of oil accumulation into these formations has been the subject of controversy, and recent studies suggest oil emplacement occurred shortly after deposition (Harrison *et al.*, 1981; Garven, 1989). Mannville source rocks are believed to be Jurassic to Cretaceous organic-rich shales situated downdip and west in the syncline of the Alberta Basin (J. Allan[2] and S. Creany[2], per. comm.). Oil migrated from downdip in the basin and was trapped both stratigraphically and structurally in the highly porous and permeable sands within the broad, gently dipping flanks of the Athabasca anticline. Migration of the oil is believed to have taken place to a large degree through the Devonian carbonates which underlie the Mannville sediments in the study area (Garven, 1989). Although substantial controversy still surrounds theories of major migration mechanisms, most researchers believe that paleo-groundwater flow directions represent past migration pathways, as oil travelled either as a dissolved phase or as small micelles within the water phase (Hitchon, 1969; Garven, 1989). Paleo-groundwater flow directions proposed by Garven (1989), are shown with respect to geologic time in Figures 2.7a to 2.7c. Shallower Mannville oil deposits on the eastern side of this axial high, including the Cold Lake oil sands and Athabasca oil sands deposits, were subsequently biodegraded into their present state as viscous, low gravity bitumen (Brooks *et al.*, 1988; Garven, 1989).

---

[2] Esso Resources Ltd., Calgary, Alberta, Canada.

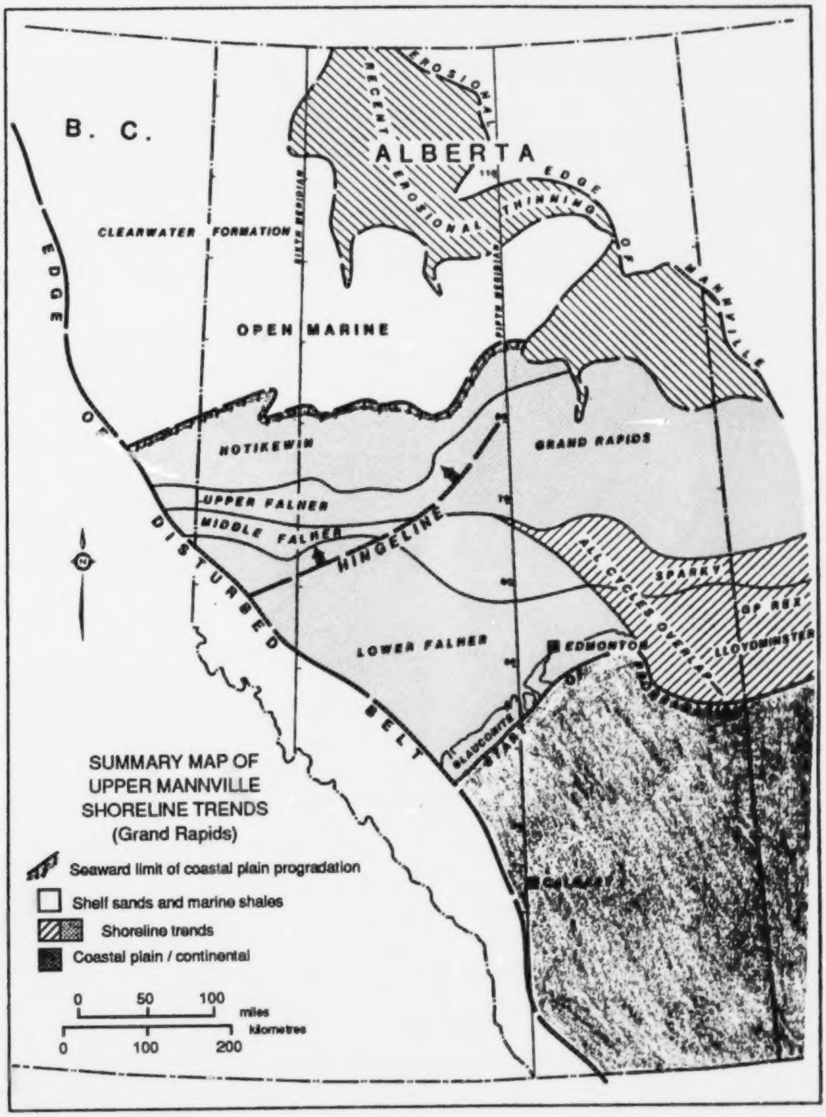
B. C.
ALBERTA
RECENT EROSIONAL EDGE
EROSIONAL EDGE
EDGE OF MANNVILLE
THINNING
CLEARWATER FORMATION
SIXTH MERIDIAN
FIFTH MERIDIAN
OPEN MARINE
EDGE OF DISTURBED BELT
NOTIKEWIN
GRAND RAPIDS
UPPER FALHER
MIDDLE FALHER
HINGELINE
ALL CYCLES OVERLAP
SPARKY
OF REX
LLOYDMINSTER
LOWER FALHER
EDMONTON
GLAUCONITE
CALGARY
N
SUMMARY MAP OF
UPPER MANNVILLE
SHORELINE TRENDS
(Grand Rapids)
Seaward limit of coastal plain progradation
Shelf sands and marine shales
Shoreline trends
Coastal plain / continental
0
50
100
miles
kilometres
0
100
200

Figure 2.13: Upper Mannville (Grand Rapids Formation) paleogeography in the Western Canada Sedimentary Basin (modified from Jackson, 1984).

C. APPLICATION OF SEQUENCE STRATIGRAPHY TO THE CLEARWATER FORMATION

SEQUENCE STRATIGRAPHY

Basic Concepts

Concepts of sequence stratigraphy are applied in the analysis of sea-level changes in order to link together sedimentological events in adjacent depositional systems. The fundamental unit of sequence stratigraphy is the *sequence*, defined by Mitchum *et al.* (1977), as, 'a stratigraphic unit composed of a relatively conformable succession of genetically related strata and bounded at its top and base by unconformities or their correlative conformities'. Eustatic changes in sea-level result in a succession of systems tracts that combine to form sequences deposited between eustatic fall inflection points (Posamentier *et al.*, 1988). Two major types of sequences have been recognized:

1) a Type 1 sequence, which contains lowstand deposits at its base, and transgressive and / or highstand systems tracts; and
2) a Type 2 sequence, which has no lowstand deposits, only transgressive, highstand and shelf margin wedge systems tracts (Posamentier and Vail, 1988).

Systems tracts are composed of stacked parasequences bounded by marine flooding surfaces (Van Wagoner *et al.*, 1987).

The development of such depositional models have largely been applied to continental margin sedimentation patterns, with four main components: the coastal plain; shelf; slope; and rise (Weimer, 1984). Figure 2.14 illustrates the position of the highstand, transgressive and lowstand systems tracts and the condensed section in a continental margin setting. Highstand deposits such as delta front sediments are the regressive deposits that prograde off the shelf during sea-level highstands. The sea-level is generally high up on the shelf, and the depocentre is generally that of the deltaic system (Weimer, 1984). The lowstand systems tract includes deposits such as submarine fans and levée-channel deposits which form basinward of the shelf margin during periods of sea-level lowstand (at the edge of the continental shelf) (Boyd *et al.*, 1988). The transgressive systems tract includes non-marine to transitional deposits formed on the shelf and shoreline during periods of rapid sea-level rise (Posamentier and Vail, 1988). The condensed interval forms during maximum sea-level rise when the major depocentre is shifted landward and the outer shelf is sedimentologically starved (Haq *et al.*, 1987).

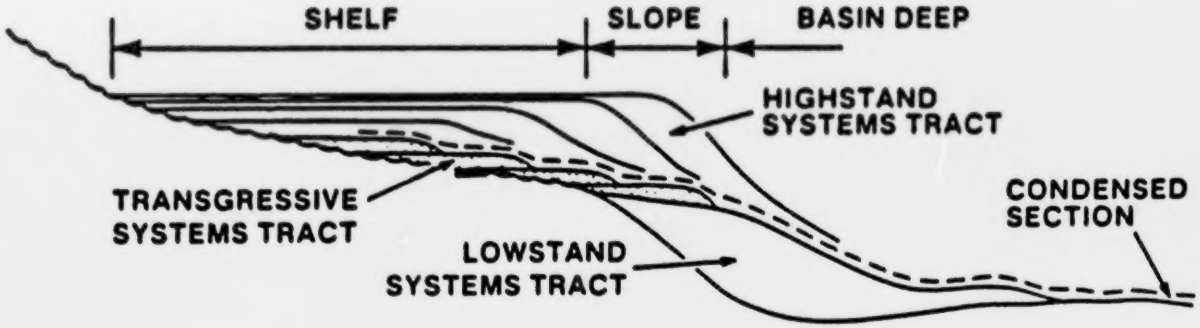
SHELF
SLOPE
BASIN DEEP
HIGHSTAND SYSTEMS TRACT
TRANSGRESSIVE SYSTEMS TRACT
CONDENSED SECTION
LOWSTAND SYSTEMS TRACT

Figure 2.14: Diagram illustrating the position of the lowstand, highstand and transgressive systems tracts and the consensed section in a coastal margin setting (modified from Carmichael *et al.*, 1988).

It occurs largely within the transgressive and distal highstand systems tracts and is characterized by very little deposition (Figure 2.14). Another depositional package, the shelf margin wedge systems tract, develops in place of the lowstand systems tract when the rate of sea-level fall is slow, and the submarine fan and levée-channel deposits do not form (Posamentier *et al.*, 1988). In such a case, shelf margin facies prograde directly over the shelf edge and onto the slope (Figure 2.15).

Depositional sequences are separated by sequence boundaries or unconformities and their correlative conformities. Two types of sequence boundaries, Type 1 and Type 2, have been identified in the literature, each of which characterize the lower boundary of depositional sequences which can be distinguished by their different rates of sea-level fall (Haq *et al.*, 1987). The position of the two types of sequence boundaries is shown in Figure 2.15. Each type of sequence boundary (or unconformity) extends from a subaerial to submarine position and is associated with a period of nondeposition and / or erosion. A Type 1 sequence boundary marks a position of relatively rapid sea-level fall on the coastal margin (Posamentier *et al.*, 1988). This results in a basinward shift in depositional facies, and may result in exposure (and incision) of the shelf. The sequence boundary may therefore be conformable to the transgressive surface in a shoreward position, and the top of the highstand systems tract deeper into the basin. The Type 1 sequence boundary is followed by a Type 1 sequence and is bounded at the top by either a Type 1 or Type 2 unconformity. Type 2 sequence boundaries result from a relatively slow rate of sea-level fall (Haq *et al.*, 1987). They are not as prominent as Type 1 sequence boundaries and the entire shelf is not generally exposed or associated with incision. The Type 2 sequence boundary is followed by a Type 2 sequence which is bounded at the top by either a Type 1 or Type 2 unconformity.

The principal concept behind sequence stratigraphy is the interplay between eustatic sea-level, subsidence and sediment supply, which results in the overall pattern of sediment deposition. Variation in one or more of these variables while the other(s) are held constant will result in the rise or fall of *relative* sea level. Sediment supply and subsidence are partially related to the amount and degree of tectonism in the source area, in addition to lithologic durability and the degree of physical and chemical weathering. Eustacy and subsidence combine to make the space (accommodation) available for the sediment fill (Posamentier *et al.*, 1988). Changes in accommodation are therefore controlled by changes in relative sea-level. For example, during conditions of eustatic sea-level rise, constant subsidence, and low, constant sediment supply, a transgression

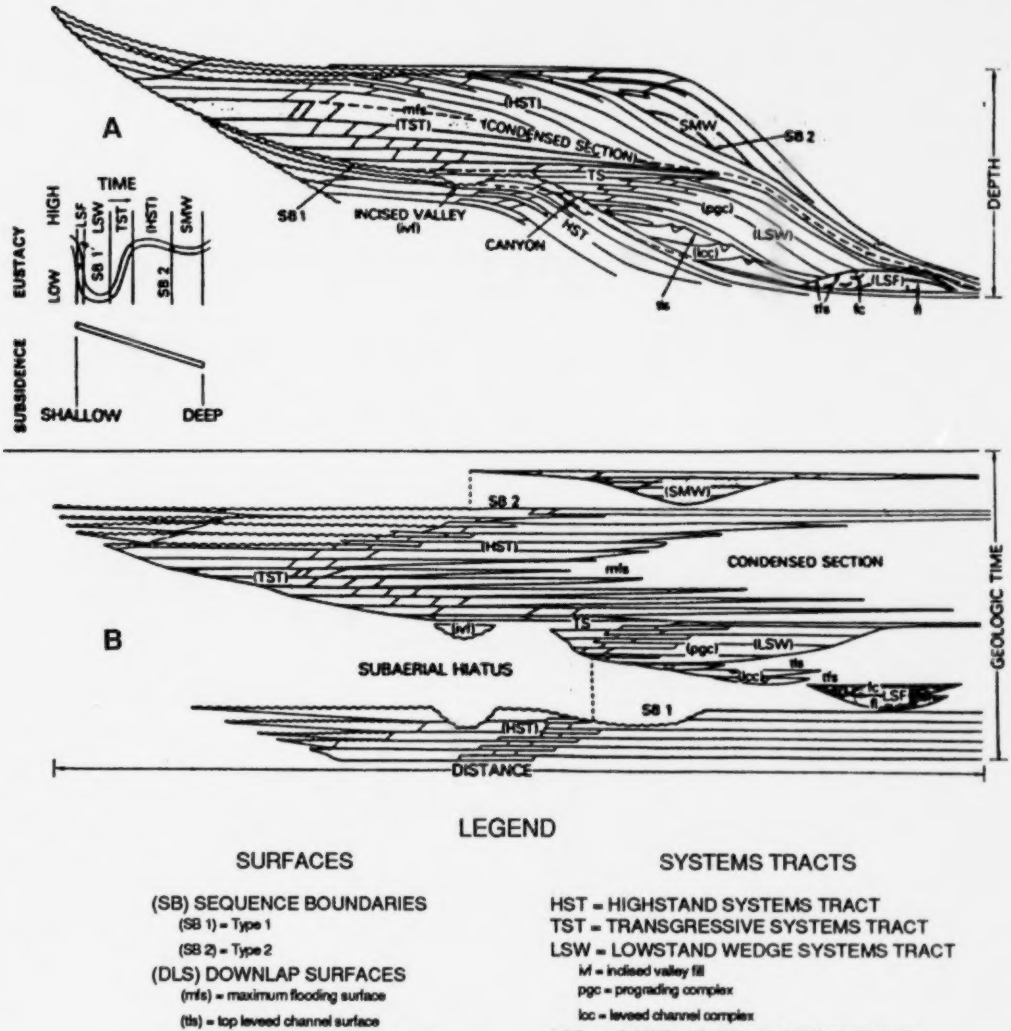
A
TIME
HIGH
LOW
EUSTACY
LSF
LSW
TST
(HST)
SMW
SB 1'
SB 2
SUBSIDENCE
SHALLOW
DEEP
mfs
(HST)
(TST)
(CONDENSED SECTION)
SMW
SB 2
TS
SB 1
INCISED VALLEY (ivf)
CANYON
HST
(pgc)
(LSW)
(lcc)
tls
tfs
fc
fl
(LSF)
DEPTH
B
SB 2
(SMW)
(HST)
mfs
CONDENSED SECTION
(TST)
(ivf)
TS
(pgc)
(LSW)
(lcc)
tls
tfs
fc
fl
LSF
SUBAERIAL HIATUS
SB 1
(HST)
DISTANCE
GEOLOGIC TIME

LEGEND

SURFACES

(SB) SEQUENCE BOUNDARIES
- (SB 1) = Type 1
- (SB 2) = Type 2

(DLS) DOWNLAP SURFACES
- (mfs) = maximum flooding surface
- (tls) = top leveed channel surface

(TS) TRANSGRESSIVE SURFACE
(first flooding surface above maximum regression)

SYSTEMS TRACTS

HST = HIGHSTAND SYSTEMS TRACT
TST = TRANSGRESSIVE SYSTEMS TRACT
LSW = LOWSTAND WEDGE SYSTEMS TRACT
- ivf = incised valley fill
- pgc = prograding complex
- lcc = leveed channel complex

LSF = LOWSTAND FAN SYSTEMS TRACT
- fc = fan channels
- fl = fan lobes

SMW = SHELF MARGIN SYSTEMS TRACT

Figure 2.15: Sequence stratigraphic concepts illustrating depositional systems tracts and surfaces during the formation of Type 1 and Type 2 unconformities.
(a) systems tracts in relation to depth,
(b) the same features plotted against geologic time.
(modified from Haq *et al.*, 1987).

would occur on the shelf resulting from an overall relative sea-level rise. However, an increase in sediment supply under the same conditions of constant subsidence and eustatic rise may result in a regression, and the progradation of sediment onto the slope. In this situation the increase in sediment supply would decrease the effective accommodation, thereby resulting in progradation. Again, if basin subsidence was not constant and was very rapid, it would tend to balance out the controlling factor of abundant sediment input into the system, and may result in decreased progradation, a stillstand or a transgression depending on the magnitude of the subsidence. Therefore, overall changes in relative sea-level produce transgressions or regressions which shift the sediment depocentre between the deep sea floor (lowstand systems tract) and alluvial plain / continental shelf (highstand systems tract), with several intermediate positions occupied by transgressive and shelf margin wedge systems tracts (Boyd *et al.*, 1988).

Factors which influence Eustatic Sea-level

The most commonly used definitions of sequence stratigraphy (as defined by Vail *et al.*, 1977), consider eustatic sea-level fluctuation to be the major control on sedimentation patterns in most depositional systems. Variations in sediment supply resulting from tectonic events are thought to be only locally important. Eustatic changes in sea-level have been attributed to a variety of processes. The two major factors which affect eustatic sea-level are changes in the volume of land ice (from glacial advances and retreats), and changes in the volume of ocean basins by spreading at ocean ridges, although the former is greater than the latter by a number of magnitudes (Pitman, 1978; Donovan and Jones, 1979). Second-order factors are sediment accumulation in the ocean basins and desiccation of isolated basins (Pitman, 1978). A few other processes, namely an increase in the volume of ocean water resulting from the generation of juvenile water at mid-oceanic ridge axes and island arcs, or changes in the capacity of the ocean basins as a function of continuing differentiation between continental and oceanic lithosphere are long term, slow changes (Donovan and Jones, 1979). Changes in mean oceanic temperature may also have an effect on the volume of ocean water. The occurrence of warmer water faunas at the high latitudes of the Western Interior Seaway are thought to reflect global warming, although the presence of only two distinct paleobiogeographic units reflects broad and diffuse temperature gradients (Kauffman, 1977). The effect of thermal expansion or contraction has been shown to be relatively small, likely to be masked by other processes, and in fact sea-level fluctuations induced by temperature change are considered to be an order of magnitude smaller than those induced by glaciation (Donovan and Jones, 1979).

Significant sea-level changes can be caused by variations in the amount of water incorporated as land-based ice sheets. For example, it has been calculated that the total melting of all the land ice existing today would lead to a rise in eustatic sea-level of 40 to 50m (130–165ft) (Donovan and Jones, 1979). The rate of formation and dissipation of ice sheets has been found to be rapid. The general accepted curve for postglacial rise, totally accounted for by ice-sheet melting was 5000 km^3/year, leading to an average sea-level rise of about 1 cm/year (Donovan and Jones, 1979). The time required for changes in eustatic variation to come to equilibrium has been calculated to be 8000 years (Donovan and Jones, 1979); therefore sea-level lowstands, especially those of short duration, cannot be correlated directly with specific glacial advances.

The volume of the world ridge system ($1.6 \times 10^8 km^3$) is a significant proportion of the total volume of ocean water ($1.35 \times 10^9 km^3$) (Menard, 1964). Changes in the volume of the ocean basin are the result of changes in the length of spreading axes, and changes in the spreading rate (Donovan and Jones, 1979). Hays and Pitman (1973) were able to show quantitatively that the transgression in the Late Cretaceous and regression in the Cenozoic could have been caused by expansion and contraction of the mid-Atlantic ridge system. Plate tectonics and the creation of spreading centres resulting from continental breakup is believed to have caused world-wide transgressions, for example the progressive splitting of Pangea in the Mesozoic (Donovan and Jones, 1979). The analysis made by Hays and Pitman (1973) showed that sudden alterations in spreading rates can produce changes in sea-level on the order of 1 cm every 1000 years.

Short-term variations in eustatic sea-level, such as those documented by Vail *et al.* (1977) for the Jurassic, could theoretically have resulted from glacial ice melting, leading to a eustatic sea-level rise of a few hundred metres over a period of approximately 15,000 years. A major problem with glacio-eustacy is that there has not been any evidence proving the presence of large ice caps in the Jurassic, Cretaceous and most of the Tertiary which could have resulted in large variations in eustatic sea-level (Donovan and Jones, 1979). Although it has been shown that selected transgressive and regressive phases since the Mesozoic may have resulted from changes in the volume of ocean basins, the rate of eustatic sea-level fluctuation due to such tectonism is substantially slower than that of glacial-eustacy, the changes are for a longer duration, and do not fit with sea-level curves such as those produced by Vail *et al.* (1977) (Donovan and Jones, 1979). Rapid subsidence is the only other mechanism that is known to cause fast, although not long-term, variations in eustatic sea-level, but the height of sea-level fluctuation produced by this mechanism is not thought to have reached the magnitude predicted by Vail *et al.* (1977) (Donovan and Jones, 1979).

Important Considerations for Western Interior Basin Deposits

The Western Interior Basin of North America is an intercratonic basin formed by the transgression of the northern Arctic sea and the southern Gulfian sea onto north America in the Late Cretaceous. The Western Canada Sedimentary Basin, the northern sector of the Western Interior Basin, is characterized by a shelf / slope profile that differs substantially from the continental margin model generally employed in standard sequence stratigraphic definitions. The present overall slope of the Western Canada Sedimentary Basin eastern margin is very gentle and ramp-like, approximately 1.5 m/km, calculated from structure contours on the Precambrian basement (Hitchon, 1969) (Figure 2.16). This slope figure has been altered slightly since deposition because of subsidence, and is not representative for the entire basin, but is likely close to the overall slope of the eastern margin at the time of deposition. (The western margin of the basin would have had much more relief as the result of nearby thrusting and folding in the Cordilleran.) This is well illustrated in Figure 2.9a, which depicts the Western Canada Sedimentary Basin at the beginning of Mannville deposition. The position of the shoreline would have therefore varied greatly during deposition of the numerous Cretaceous deposits, especially when it was located on the eastern margin of the basin. A small change in relative sea-level could therefore have led to a large lateral variation in the position and hence nature of the resulting depositional facies. Although the fluctuation in the shoreline position would have likely been controlled by the overall regional dip, variations in local paleogeography, the result of numerous structural (topographic) features in the Cretaceous, would have controlled the morphology of the deposit in any one area within the basin.

CLEARWATER FORMATION DEVELOPMENT

Within the study area the Clearwater Formation is composed of very fine to medium grained sands, interbedded sands and muds, and silts and shales up to 65m (215ft) thick. The primary composition of Clearwater sediments has been identified as feldspathic litharenites and litharenites, along with abundant organic detritus (Putnam and Pedskalny, 1983; Prentice and Wightman, 1986; Maher, 1989). It is cemented

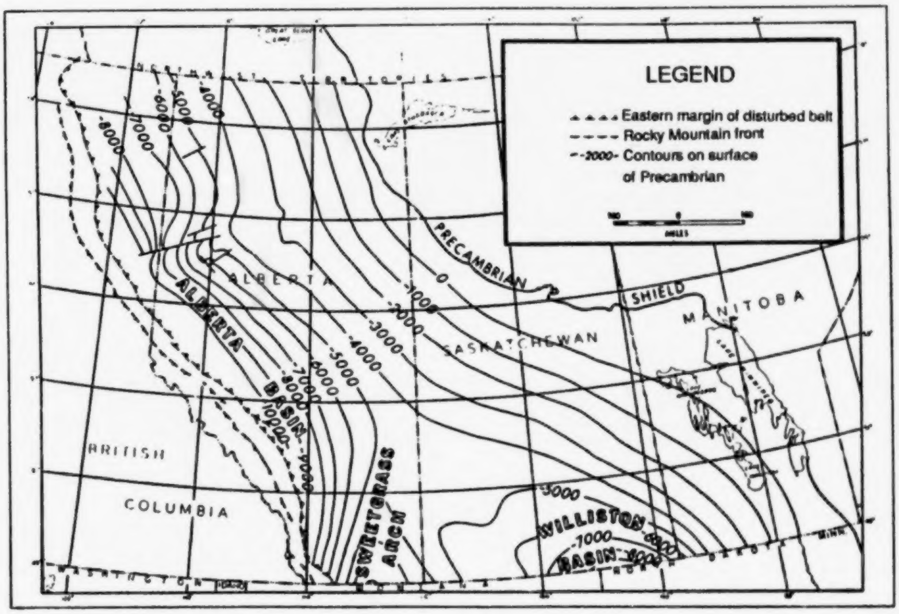
LEGEND
Eastern margin of disturbed belt
Rocky Mountain front
-2000- Contours on surface of Precambrian
MILES
ALBERTA
ALBERTA BASIN
BRITISH COLUMBIA
SASKATCHEWAN
MANITOBA
PRECAMBRIAN SHIELD
SWEETGRASS ARCH
WILLISTON BASIN
0
-1000
-2000
-3000
-4000
-5000
-6000
-7000
-8000
-9000
-10000
-7000
-3000

Figure 2.16: Structure contours on top of Precambrian basement in the Western Canada Sedimentary Basin (modified from Hitchon, 1969).

concretions . Bitumen saturation ranges from moderate to very high in the upper, sandier units, and diminishes to moderate or water-saturated in the generally silt to shale-rich lower units.

For the purposes of this study, the Clearwater Formation has been defined as the sediment interval which lies between the lower boundary of the marine shale which separates the Wabiskaw Member from the underlying McMurray Formation; and the lower boundary of the marine shale which lies above the uppermost sand of the Clearwater Formation. This appeared to be the most consistent definition in the literature, and is the one used most commonly by the Alberta Research Council and the Alberta Energy Resources Conservation Board in the past (AERCB, 1973; Wightman and Berezniuk, 1986; Prentice and Wightman, 1988). Figure 2.17 is a type log of the Clearwater Formation indicating the position of these boundaries in well 3-28-66-2W4.

Depositional Setting

In this study, a total of 10 wells with core and well logs from the smaller study area (Figure 2.18), were analyzed in detail to interpret vertical and lateral stratigraphic relationships in the Clearwater Formation. A number of other well logs located in the larger study area were also investigated to determine the regional extent of stratigraphic interpretations in the northern part of the deposit. Features observed from each of the cores were logged graphically, and are contained within Appendix 1. Most cores were available from the ERCB Core Research Centre in Calgary, Alberta, but a number were donated by Esso Resources for this project. One core, 13-20-65-3W4, was made available for viewing by Esso Resources in their core storage facility. Cores from the ERCB coreshed had been opened and exposed to the air for some time, but the donated cores were obtained from cold storage, and had to be unwrapped and carefully handled to avoid disruption of the finer sedimentary features, and skin burns from the more volatile hydrocarbons. Features documented included gross lithology, grain-size variability, sedimentary structures, ichnofossil type and abundance, organic remains, bitumen saturation and diagenetic characteristics.

The principal environments and facies recognized in the study area are open marine to prodelta marine muds, delta fringe marine muds and sands, lower delta front interbedded sands and muds, middle delta front sands, and upper delta front sands originating in distributary mouth-bar, channel and interdistributary bay facies. Within

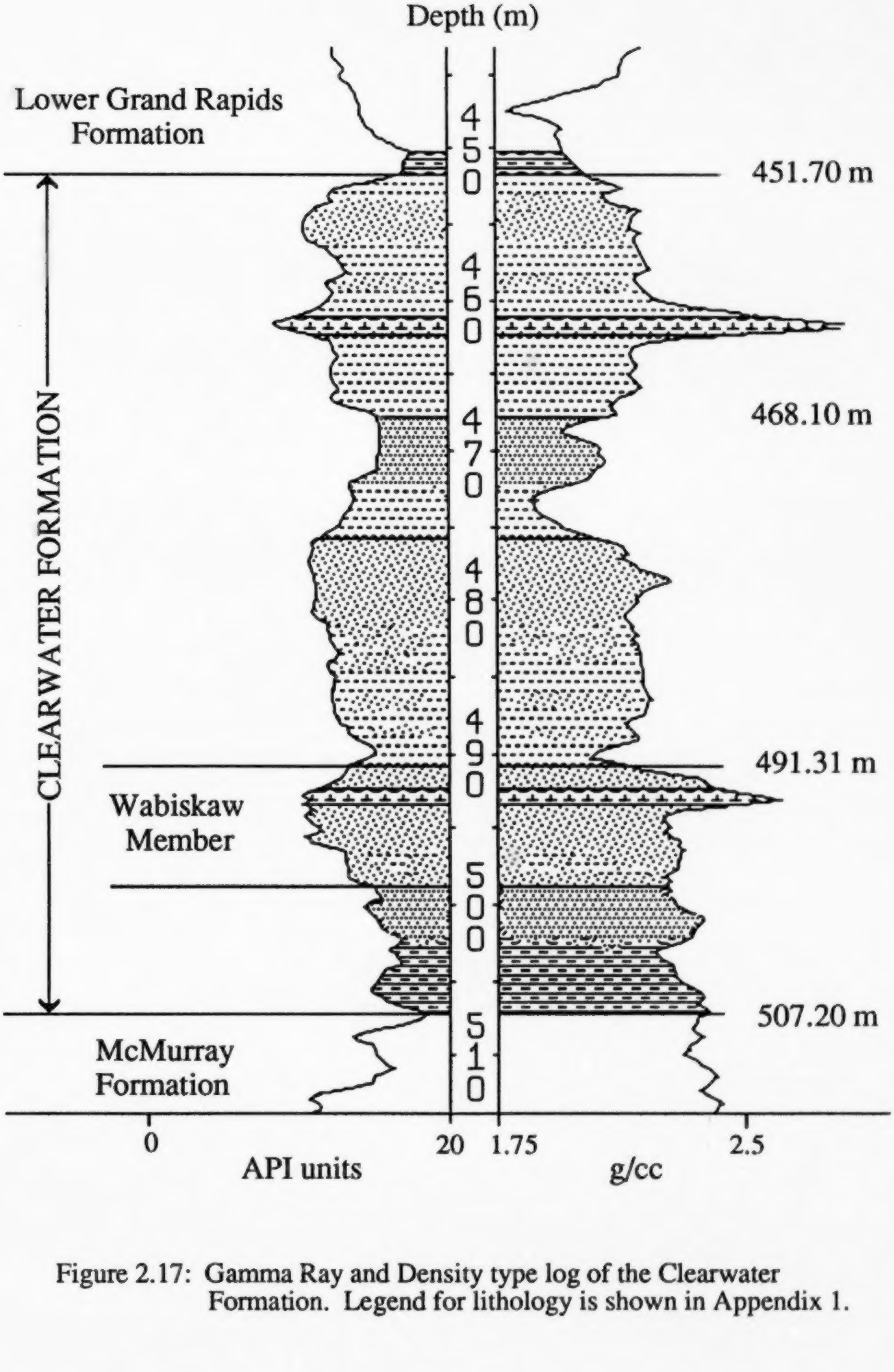

Figure 2.17: Gamma Ray and Density type log of the Clearwater Formation. Legend for lithology is shown in Appendix 1.

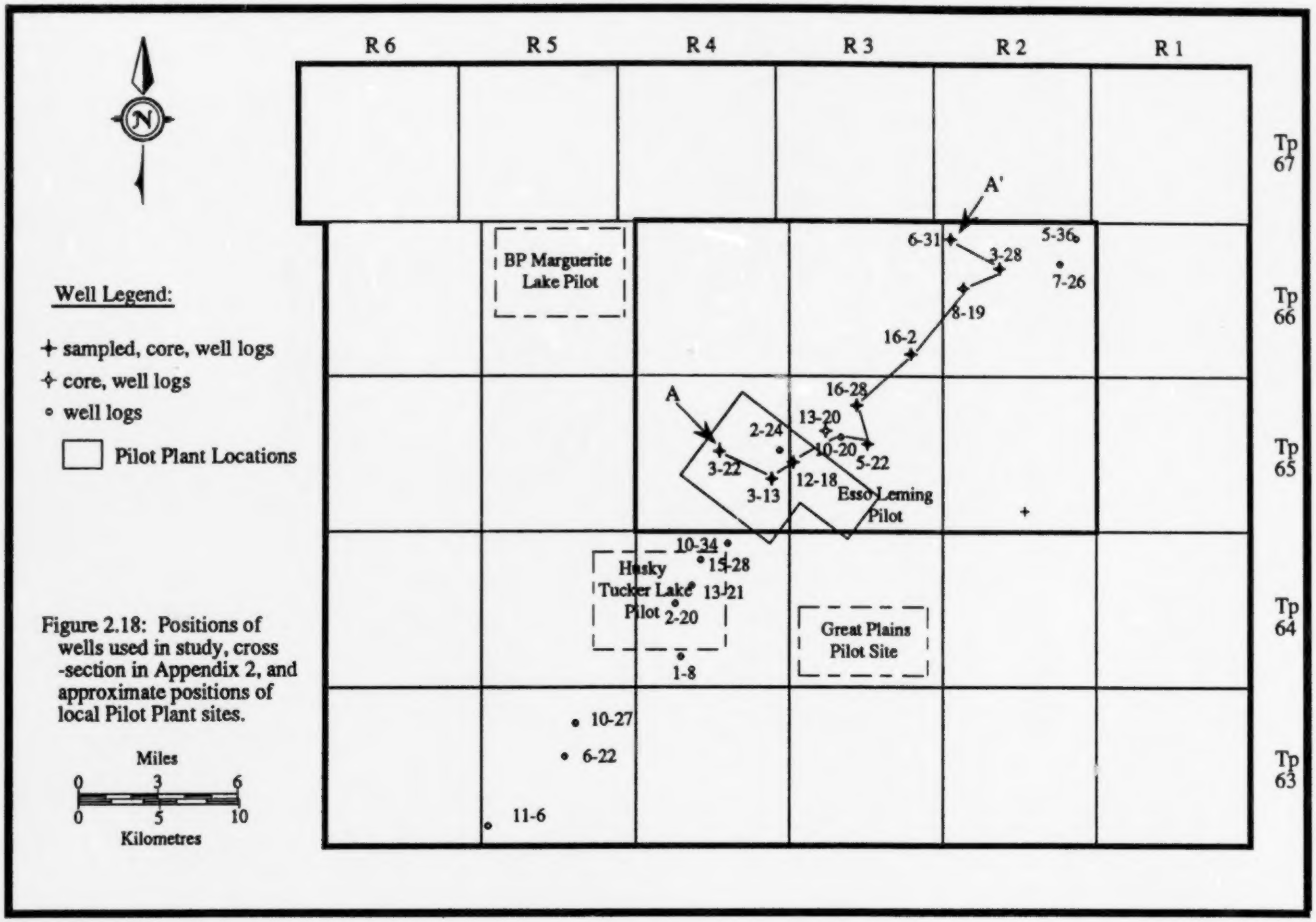
N
R 6
R 5
R 4
R 3
R 2
R 1
Tp 67
Tp 66
Tp 65
Tp 64
Tp 63
Well Legend:
✦ sampled, core, well logs
✧ core, well logs
∘ well logs
☐ Pilot Plant Locations
BP Marguerite Lake Pilot
Esso Leming Pilot
Husky Tucker Lake Pilot
Great Plains Pilot Site
A
A'
6-31
3-28
5-36
7-26
8-19
16-2
16-28
13-20
10-20
5-22
2-24
3-22
3-13
12-18
10-34
15-28
13-21
2-20
1-8
10-27
6-22
11-6
Miles
0
3
6
0
5
10
Kilometres

Figure 2.18: Positions of wells used in study, cross -section in Appendix 2, and approximate positions of local Pilot Plant sites.

many cores the facies are often intergradational, and sharp contacts are relatively rare. In the associated well logs these environments tend to show characteristic gamma-ray and density (or SP, Resistivity, etc.) log signatures, such as the serrated shape of lower delta front interbedded sands and muds, the coarsening upward characteristics of the progradational middle to upper delta front sands and distributary mouth-bar deposits, and the more cylindrical shape of distributary channel sands. In the following descriptions, proximal refers to a position relatively close to the position of the shoreline during Clearwater position (nearshore), whereas distal refers to a position further offshore.

Open Marine / Prodelta

Open marine / prodelta muds occur at the base of the Clearwater succession, as well as in the first Lower Grand Rapids sediments which overly the uppermost Clearwater sands. Bedding is planar to wavy with low angle inclinations, and some herringbone cross-stratification and soft sediment deformation features are observed. Biogenic activity is variable from low to high, and typically a low diversity of ichnogenera is noted, although the abundance and diversity is found to increase in more nearshore wells. Bitumen saturation is very low to nonexistent, and some iron staining and siderite is observed.

Delta Fringe

Thinly interbedded silts and shales, occasionally with thin beds of interstratified sand, were interpreted as facies typical of a delta fringe environment. Units are typically coarsening up, supporting their interpretation as progradational. Bedding tends to be planar to low cross-stratified, especially in the more distal cores, although wavy and herringbone stratification is also observed. This facies often contains soft sediment deformation and faulting features, small vertical fractures, and rarely mud clasts. It overall has a moderate biogenic diversity, the highest level within deltaic sediments at any one position in the formation, and the highest overall level of bioturbation, often containing bedding so burrowed it appears churned. Organic remains are abundant and consist of shell and coal fragments. Bitumen saturation is typically poor, from low to water-saturated, and diagenetic features include occasional carbonate beds and lenses (some bitumen saturated), and iron staining and pyrite.

Lower Delta Front

Lower delta front sediments within the study area are fine to very fine grained marine sands and with interbedded muds (silts and/or shales). Bedding is often observed to be periodic or cyclic, with the spacing increasing towards the top of the unit. Distal settings tend to contain more shaly intervals, and more proximal settings have a higher concentration of silty beds. Sedimentary features consist of planar, wavy, and low to moderate angle bedding, as well as some indications of soft sediment deformation, faulting, mud flasers and vertical fractures. Some instances of herringbone, trough and ripple stratification are observed, and shale clasts are often abundant, especially near the bottom of the unit. Bioturbation and biogenic diversity is extremely variable, with the shaliest and most organic-rich intervals receiving the most intense burrowing activity and containing the greatest ichnofaunal diversity. Bioturbation levels range from low to moderate. Organic remains consist of coal fragments and occasionally shells or shell fragments. Water sands are common in the lowermost units, and bitumen saturation in uppermost units may be as high as moderate, with high levels in the sandier interbeds. Carbonate cemented zones and lenses are relatively common, and appear to be randomly situated. Other diagenetic features include the presence of clays, siderite, iron staining, and occasionally traces of glauconite in the bottom of the lowermost intervals where they grade into the Wabiskaw sands.

Middle Delta Front

Middle delta front sands are transitional facies, situated between the more mud-rich sands of the lower delta front, and the thick sand units of the upper delta front. They often contain thin interbeds of shale and / or silt, the sand tends to be slightly coarser grained than that found in the lower delta front, and most units exhibit a coarsening up trend. Bedding is variable and may be planar, wavy, lenticular, contain low to moderate angles of cross-stratification (i.e. 10°), or ripples. Sedimentary features such as those of soft sediment deformation are rare, and mud clasts and lenses are common. Biogenic activity is rather limited, ranging from no burrowing activity in more proximal settings to low in distal areas, and ichnofaunal diversity is rather low. Coal and wood fragments are found in cores from this facies, and bitumen saturation is quite good, ranging from low to nonexistent in the most silty interbeds to moderate and even high in the sandiest zones. Carbonate cemented zones and concretions are randomly situated throughout the formation. Other diagenetic features include clays, and the presence of siderite.

Upper Delta Front

Upper delta front facies include sands from both distributary mouth-bar and distributary channel settings. Both are composed primarily of fine to medium grained sand, with little to no silt or shale interbeds, except in between successive stacked mouth-bar or channel units which have been interpreted as interdistributary bays. Upper delta front facies are contained primarily only in the most proximal (southwest) cores in the study area, or in the upper units of adjacent cores. This facies contains the thickest units in the study area, consisting of stacked or amalgamated sands with only small changes in grain size and bitumen saturation the major indications of cyclic differences in core. Bedding orientation may be planar to wavy, contain low to moderate (10°) angled stratification, or trough or herringbone cross-stratified. The highest angles are generally found in the coarsest sands. Soft sediment deformation features are noted in the finer grained intervals, and in interdistributary bays. Shale clasts, which may even appear armored with a coating of mud and may be quite large, are very common, especially in the bottom of the interval where upper delta front facies contact finer grained facies. Very little biogenic activity has occurred in this facies. Only a few ichnogenera were noted in the siltier interbeds in the dirtiest sands. The diversity and abundance of ichnogenera in the interdistributary bay environment are equivalent to that of the lower delta front sands and muds. As in other facies, organic debris consists of coal and shell fragments. Bitumen saturation is the highest in this facies, and the thick coarsest sands are essentially completely saturated. Saturation drops slightly in siltier intervals, but remains moderate to high overall, with the greatest bitumen saturation generally in the top of the interval. Bitumen saturation may drop to low or moderate in the interdistributary bays. Diagenetic features consist of carbonate cemented lenses and concretions, most of which are located in the bottom part of the facies, as well as iron staining and siderite.

Wabiskaw Member - Shoreface

The Wabiskaw Member is located at the base of the Clearwater Formation, and directly overlies the marine muds which separate the Clearwater from the McMurray Formation throughout the study area. Wabiskaw sediments in the study area are primarily fine to medium-grained sands, containing variable amounts of mud. They tend to be better sorted than comparable overlying Clearwater sands, and have been interpreted as a marine-bar facies deposited in a shoreface environment. The grain size variability in the member appears to be somewhat associated with the distal–proximal nearshore relationship observed in the overlying sediments, suggesting that the position of the shoreline was in a comparable position during its deposition. Bedding in the interval is planar, wavy or has low-angle inclination, and rarely exhibits characteristics of herringbone-type cross-stratification. Evidence of soft sediment deformation is observed, and mud clasts are occasionally present. Substantial bioturbation has occurred in this interval, even in very sandy units. There is a significant increase in the ichnofaunal abundance and diversity in this facies in comparison to facies of equal grain size in the overlying Clearwater sediments. Biogenic activity typically ranges from low to moderate / high, may be churned, and is only rarely absent (in the cleanest sands). Organic remains consist only of coal fragments. This interval is often water-saturated, although in some areas low to moderate bitumen saturation has been observed. The Wabiskaw Member can be differentiated from overlying sediments by the relatively abrupt presence of substantial authigenic glauconite, often resulting in greenish-colored sands. Diagenetic alteration features consist of siderite and iron staining, as well as occasional carbonate cemented lenses.

Ichnology

A varied ichnofossil assemblage was observed in core in the study area, representing 13 ichnogenera, including; *Asterosoma, Arenicolites, Bergaueria, Chondrites, Cylindrichnus, Diplocraterion, Palaeophycus, Planolites, Rhizocorallium, Rosselia, Skolithos, Teichichnus, Thalassinoides* and *Zoophycos*, as well as a few escape structures. In a number of cores particular facies exhibited bedding which has been intensely bioturbated, or churned, to the point where recognition of a particular species was difficult. Typically, each ichnogenus can be associated with a particular type of behavior (ethological classification), method of feeding (trophic group), and probable group of organism (Table 2.1). Particular assemblages of trace fossils have been defined in the literature, based on the above classifications and their association with specific niches or depositional sites in the rock record (Ekdale *et al.*, 1984). An effort has been made to associate these accepted ichnofacies assemblages for shallow-marine environments with the depositional facies observed in the study area. The interpretation has been recorded on each of the core logs contained in Appendix 1, and can be generalized as follows. It is important to note that these generalizations do not apply strictly to all settings in all cores because of the transitional nature of the facies.

Open marine to prodelta facies have been interpreted as belonging to a mixed Cruziana / Zoophycos Ichnofacies. This is indicated by the presence of *Chondrites* and *Planolites* in the most distal position, with the addition of *Asterosoma* in more nearshore wells, with all ichnogenera deposit-feeders. The interpretation is extended to that of the Zoophycos Ichnofacies because of the quiet water conditions that were likely present during deposition, despite the actual presence of the *Zoophycos* tracemaker.

Table 2.1: Classification of Ichnogenera recognized in the Clearwater Formation.

ICHNOGENUS	ETHOLOGICAL CLASSIFICATION	TROPHIC GROUP	PROBABLE PRODUCER
Asterosoma	fodinichnia	deposit-feeder	annelid
Arenicolites	domichnia	suspension feeder	annelid
Bergaueria	cubichnia/domichnia	carnivore	anemone
Chondrites	fodinichnia	deposit-feeder	sipunculid/annelid
Cylindrichnus	fodinichnia/domichnia	deposit-feeder	annelid
Diplocraterion	domichnia	suspension-feeder	crustacean
Palaeophycus	domichnia	carnivore	annelid
Planolites	fodinichnia	deposit-feeder	annelid
Rhizocorallium	fodinichnia	deposit-feeder	crustacean
Rosselia	fodinichnia	deposit-feeder	annelid
Skolithos	domichnia	suspension-feeder	annelid
Teichichnus	fodinichnia	deposit-feeder	annelid
Thalassinoides	domichnia	deposit-feeder	crustacean
Zoophycos	pascichnia	deposit-feeder	sipunculid/annelid

Members of 6 ichnogenera were identified in the delta fringe environment, including; *Chondrites, Palaeophycus, Zoophycos, Asterosoma, Skolithos*, and *Planolites*. Most ichnogenera are deposit feeders, with the exception of *Palaeophycus*, a carnivore, and *Skolithos*, a suspension-feeder. Despite the presence of *Zoophycos*, this association has been interpreted as belonging to the Cruziana Ichnofacies. Both biogenic diversity and abundance are quite high, and *Zoophycos* and *Skolithos* are interpreted as evidence of opportunistic behavior by their particular organisms. *Zoophycos* is generally only found in the most offshore settings.

In the lower delta front environment the following ichnogenera were observed; *Chondrites, Palaeophycus, Planolites, Bergaueria, Asterosoma, Cylindrichnus, Rosselia, Skolithos, Teichichnus*, and rarely *Thalassinoides, Diplocraterion, and Arenicolites*. Because of the overall domination of deposit-feeders this facies has been interpreted as characterized by the Cruziana Ichnofacies. The presence of *Skolithos and Diplocraterion*, both suspension-feeders, is viewed as opportunistic. These tracefossils are only typically associated with the sandiest units, and concentrated in the more proximal wells, which suggests a slight shift in this local setting to that of the Skolithos Ichnofacies.

The biogenic diversity is slightly diminished in the middle delta front setting, with *Palaeophycus, Chondrites, Planolites, Asterosoma, Teichichnus, Skolithos, Rosselia* and *Bergaueria* ichnogenera observed, although generally only a few ichnogenera are present at any one place. This assemblage has been interpreted as also belonging to the Cruziana Ichnofacies, although the greater abundance of *Skolithos* suggests that depositional conditions more typical of the Skolithos Ichnofacies tracemakers are becoming more prominent locally in more proximal settings.

The upper delta front environment contains the lowest abundance and biogenic diversity in the formation. Ichnogenera are limited to *Teichichnus, Palaeophycus, Asterosoma, Rosselia, Planolites, Chondrites* and *Skolithos*, most of which are found only in the silty areas, or in interdistributary bays. There are very few tracefossils in the thick sands typical of this setting. Although most ichnogenera are deposit-feeders, the prominence of the Skolithos tracemaker leads to the interpretation of a mixed Cruziana / Skolithos Ichnofacies. Tracefossils from the Cruziana Ichnofacies are the most dominant in the interdistributary bays, and those of the Skolithos Ichnofacies in the thick sands and interbedded silts. There is evidence of opportunistic behavior from members of both trophic groups, deposit and suspension-feeders.

The Wabiskaw Member is characterized by an ichnofaunal assemblage belonging to a mixed Cruziana / Skolithos Ichnofacies, with members from 11 ichnogenera, including: ***Planolites, Chondrites, Asterosoma, Palaeophycus, Zoophycos, Bergaueria, Teichichnus, Skolithos, Rhizocorallium, Rosselia*** and ***Diplocraterion.*** ***Zoophycos*** is associated with organic-rich facies in more distal, offshore wells, and ***Skolithos, Diplocraterion, and Rhizocorallium*** are found in sandier units situated more proximal to the paleo-shoreline. As mentioned previously, this facies exhibits a higher biogenic diversity than comparable grain-sized units in the remaining Clearwater sediments. Plate 2.1 contains photographs of a number of ichnofossils characteristic of the Clearwater Formation in the study area.

Sequence Stratigraphy

Within the study area, the Clearwater Formation has been subdivided based on accepted sequence stratigraphic principles into two primary sequences S_1 and S_2, bounded by sequence boundaries SB1 and SB2. Three flooding surfaces have also been identified, FS1, FS2 and FS3. Figure 2.19 contains a schematic representation of the these sequences and their various bounding surfaces and internal breakdown within the Clearwater Formation. The formation was correlated in the study area based on these stratigraphic principles, and a cross-section (A to A') (position indicated in Figure 2.18), illustrating these relationships from a nearshore to offshore is included in Appendix 2. It is possible that the sequences referred to here are actually sub-sequences when examined in terms of strict sequence stratigraphic definitions. This was impossible to confirm within the confines of this study however, as a much greater regional examination of the formation would be required, and therefore the terminology of sequence has been upheld.

The top of sequence S_1 is marked within the Clearwater Formation by flooding surface FS1, which is the contact between the uppermost Clearwater sands and muds and the first marine muds of the Lower Grand Rapid Formation. This surface marks a position of relative sea-level rise, or deepening of the water during sediment deposition. In many positions this contact is somewhat gradational. The base of the sequence is manifested by the presence of sequence boundary SB1; identified throughout the study area, both in core and well logs. The characteristics associated with SB1 vary depending on its relative position within the deposit, specifically with respect to its position relative to the paleo-shoreline. It is most prominent in a distal setting, in the northeastern position of the study area, distinguished by a relatively abrupt shallowing of overlying facies. In a more proximal, nearshore setting in the southwestern part of the study area the degree of

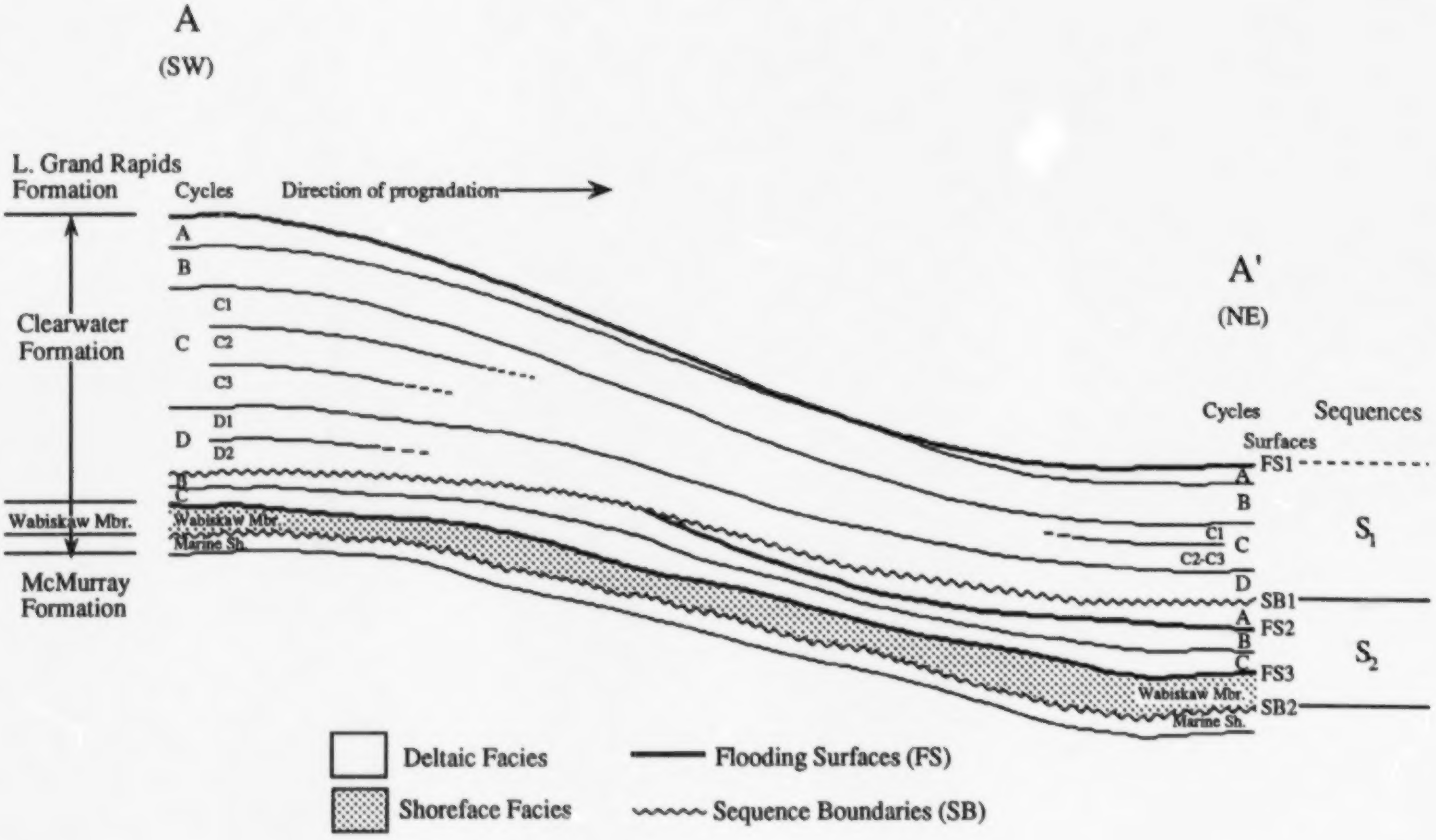
A
(SW)
L. Grand Rapids Formation
Clearwater Formation
Wabiskaw Mbr.
McMurray Formation
Cycles
Direction of progradation
A
B
C
C1
C2
C3
D
D1
D2
D
C
Wabiskaw Mbr.
Marine Sh.
A'
(NE)
Cycles
Surfaces
Sequences
FS1
A
B
C1
C
C2-C3
D
SB1
A
FS2
B
C
FS3
Wabiskaw Mbr.
SB2
Marine Sh.
S1
S2
Deltaic Facies
Shoreface Facies
Flooding Surfaces (FS)
Sequence Boundaries (SB)

Figure 2.19: Sequence Stratigraphic Model of Clearwater Formation deposition in the study area.

shallowing is generally less evident, although other features, such as the presence of abundant mud clasts may be distinctive. Sequence boundary SB1 is underlain by lower to middle delta front marine sands in a proximal position with respect to the paleo-shoreline, grading to delta fringe muds and sands more offshore. Sequence S_1 has also been subdivided into a number of genetic units or cycles, labelled A to D (Figure 2.19, Appendix 2). Each cycle is believed to represent a successive event during Clearwater deposition. A further division of these cycles has been done where possible, generally in the thickest sands, representing successive individual progradational events such as the stacking of distributary mouth-bar and channel sands within a central lobe of the deltaic complex. These sub-cycles are less discernible beyond the upper delta front environment. Within each cycle, A to D, there is a gradual deepening of facies from a proximal to distal position with respect to the paleo-shoreline, a trend represented by the shift from an upper delta front environment to a lower delta front setting.

The second sequence interpreted in the study area, S_2, is topped by SB1, and contains SB2 at its base. Sequence boundary SB2 is quite distinct throughout the study area, and is manifested by a shallowing or relative sea-level fall associated with the facies boundary between the base of the Wabiskaw Member and the top of its underlying marine silts and shales, which separate the Clearwater from the McMurray Formation. This sequence boundary was distinguished primarily by well logs, as it was only available for physical examination within a few cores. SB2 is characterized throughout the study area by a relatively abrupt shallowing of facies, and the marine muds exhibit little variability, which indicates that deposition of the underlying muds was a much more widespread event, and likely deeper water than that of the facies which underlies SB1.

Two flooding surfaces were identified within sequence S_2. The first, FS2, is believed to be quite local in extent because it is only well discernible in a more offshore setting. It is recognizable as the relative deepening associated with the facies change from underlying lower to middle delta front marine sands and muds, to the delta fringe muds and lower delta front sands and muds which directly underlie SB1. Although this could also represent a facies transition, the change in facies is rather abrupt and has been interpreted as that of a relative sea-level rise. In more proximal wells, the position of this transgressive surface becomes equivalent to that of the overlying sequence boundary SB1. This can be interpreted as a function of erosion or because evidence of the surface cannot be distinguished in the sandier facies associated with the more nearshore environments.

The second flooding surface, FS3, marks a transgressive period between the end of deposition of the Wabiskaw Member and the return to the more deltaic-marine conditions which dominated during deposition of the overlying Clearwater sediments in sequence S_2. It is generally, but not always characterized by a relative deepening from underlying to overlying facies and may be somewhat gradational. This indirect trend has been attributed to the dominance of marine conditions during Wabiskaw deposition, with sediment sorting more a function of such processes as wave action, rather than the relative position with respect to the paleo-shoreline as in the remainder of the formation.

Sequence S_2 has also been subdivided into a number of cycles, labelled A to C as well as the Wabiskaw Member. As with sequence S_1, each cycle represents a successive genetic event during formational deposition. Cycle A is present below SB1 and FS2, and eventually grades out in a proximal position, along with the disappearance of FS2. Cycles B and C are present throughout the study area between FS2 and the top of the Wabiskaw Member FS3. These cycles are thought to have been generated during a period of time dominated by progradation, following the deepening associated with flooding surface FS3.

In order to better illustrate the characteristics of the Clearwater Formation within a sequence stratigraphic context, descriptions of the features of two cores have been included; each at different relative positions within the study area.

Appendix 2 contains the logged features of a type core, 3-28-66-2W4, located in the northeastern portion of the smaller study boundary, in an area believed to be in a distal position with respect to the paleo-shoreline. The lower part of the Clearwater Formation in this core contains open marine–delta fringe marine silts and shales which separate the formation from the underlying McMurray Formation. These are overlain by the glauconite-rich, muddy sands of the Wabiskaw Member, separated by SB2. Wabiskaw sands also contain a calcite cemented interval within this well. The shallow marine environment of the Wabiskaw Member is indicated by its abundant ichnogenera (Cruziana Ichnofacies); *Chondrites, Planolites, Asterosoma, Palaeophycus, Teichichnus, Bergaueria* and *Zoophycos* in addition to the presence of abundant glauconite. Wabiskaw sands are differentiated from the overlying Clearwater sediments by flooding surface FS3, manifested by a decrease in glauconite abundance, sorting, and grain-size. Lower Clearwater sediments which overly the Wabiskaw Member consist of coarsening-upward planar to wavy or rippled sands with abundant mud, occasional mud clasts, and mud drapes characteristic of a lower delta front environment. *Asterosoma, Chondrites, Planolites, Bergaueria, Palaeophycus* and *Cylindrichnus* ichnofauna can be found in this moderately organic-rich environment. This interval is separated from the overlying facies by flooding surface FS2, and overlain by deeper-water planar muds interbedded with some sand. They contain an abundant ichnofossil assemblage of *Asterosoma, Chondrites, Skolithos, Palaeophycus* and *Zoophycos* (Cruziana Ichnofacies), characteristic of a delta fringe environment. Although in a deeper-water setting, this interval also coarsens upward in grain size, typical of progradational deltaic deposits. These deeper water facies are topped by sequence boundary SB1, manifested by an abrupt shallowing of facies in overlying deposits, a decrease in the abundance of iron minerals found in higher abundance below the sequence boundary, an abrupt decrease in ichnofauna and an increase in bitumen saturation (associated with the change in grain size). Plate 2.2 contains photographs of core 3-28-66-2W4, illustrating the position of sequence boundary SB1 and its features in a distal setting. Sequence boundary SB1 is overlain by fine grained planar to wavy sands and muds that are moderate to highly bitumen saturated with occasional calcite cemented zones. It is an interval of lower delta front deposits containing a smaller ichnofaunal assemblage of *Skolithos, Planolites, Asterosoma, Bergaueria, Teichichnus* and *Rosselia.* A number of mud drapes occur throughout the interval. The top of the interval, characterized by siltier sand and abundant shale rip-up clasts, are coarser lower delta front sediments, which are overlain by the open marine to prodelta muds of the Lower Grand Rapids Formation.

The log of a typical proximal core within the study area, 3-13-65-4W4, is contained within Appendix 2. The contact between the McMurray and Clearwater Formation, or SB2, were not present in the core, and the first identifiable facies are the shallow marine deposits of the Wabiskaw Member. They consist of planar, fine to very fine grained glauconite-rich sands and muds characterized by *Asterosoma, Diplocraterion, Planolites* and *Rhizocorallium* ichnofauna (Cruziana / Skolithos Ichnofacies). Flooding surface FS3 occurs at the top of the Wabiskaw Member, although in this instance its presence is not manifested by a decrease in grain-size. The difference between the two facies at this surface is typified more by the change in environment, highlighted by the abrupt disappearance of glauconite in the overlying sands. The overlying middle delta-front sands are fine to medium grained, planar to cross-bedded and highly bitumen saturated, and contain occasional muddy intervals, mud clasts, and a calcite cemented zone. This interval is separated by overlying sediments by sequence boundary SB1. Note that at this position on the shelf there are no lower delta front or delta fringe sediments below the sequence boundary, and flooding surface FS1 does not appear to be present. The sequence boundary is characterized by an abrupt change from sand containing thinly bedded mud intervals to one congested with abundant mud clasts. Many of these clasts are armored by clay as the result of transportation in a relatively high energy environment, perhaps as fragments of landward-situated interdistributary deposits or levées. Although there does not appear to be a significant visual change in grain-size of the sand, a small increase in bitumen saturation is associated with the sequence boundary, likely because of the lack of silts in the overlying sands. The thick sediments which overly the sequence boundary consist of fine to medium grained sands deposited in an upper delta front environment that shifted from distributary mouth-bar to channel sands with continued progradation. These thick upper shelf deposits, which compose the remainder of the core in this well, are among the coarsest, most highly bitumen-saturated sands in the deposit, those which are currently being produced by in-situ steam injection methods. Plate 2.3 contains core photographs of the sequence boundary in well 3-13-65-4W4.

Discussion

Clearwater sediments were deposited in the shallow Boreal sea during a period of overall eustatic sea-level rise according to sea-level chronology by Haq *et al.*, 1987. The tectonism-induced increased sediment supply during this period was of sufficient magnitude to overcome the effect of rising sea-level and resulted in cyclic periods of relative sea-level fall, regression of the shoreline, and progradational deposition of deltaic sediments in the study area. Detailed examination of Clearwater sediments in the Cold Lake oils sands deposit by previous researchers led to the identification of the Clearwater Formation as a progradational, deltaic shallow marine complex, consistent with the larger paleogeographic interpretations by others such as Hitchon (1969), and Jackson (1984) (Harrison *et al.*, 1981; Wightman and Berezniuk, 1986). Progradation is believed to have occurred toward the north and northeast as detritus was supplied from rivers draining from the south and southwest. The approximate position of the shoreline during the main deltaic phase of Clearwater deposition southwest of the study area is believed to have been in approximately an east to west / northwest to southeast orientation (Maher, 1989). It is not known how far away the shoreline was during deposition as there in no evidence of subaerial erosion in any core within the study area, although such evidence has been suggested by other researchers (H. Abercrombie[3], per. comm.). The shoreline is believed to have wrapped around the axial high in the study area, and joined up with the remainder of the Clearwater sea to the northwest (Jackson, 1984). The position of the Esso lease is believed to be the approximate centre of this deltaic complex at one depositional period, with lobe switching during progradation resulting in stacked sequences of thick, fine-grained sand in the thickest parts of the deposit.

---

[3] Institute of Sedimentary Petroleum Geology, Calgary, Alberta, Canada.

Within the study area, the thickest sands have been identified as upper delta front distributary mouth-bar and channel sands, and are gradational through middle delta front sands and silts to the more distal lower delta front sands and muds. These deposits are typical of the facies found within sequence S_1. Sequence S_2 contains middle to lower delta front sands and muds in the most shoreline-proximal wells, with delta fringe muds and sands and open marine to prodelta muds located even further offshore. The presence of more distal shoreline facies in sequence S_2 in the same well as more proximal facies in overlying S_1 supports the proposal that the shoreline during Clearwater deltaic-marine deposition was closer to the study area during the deposition of S_1, indicating an overall progradational depositional pattern for the formation. As well, the absence of rootlets or other indicators of exposure suggests that the Clearwater Formation was entirely submerged in the study area during deposition.

Mineralogically, the Clearwater Formation is composed mainly of detrital quartz, potassic and plagioclase feldspars, abundant lithic (mainly volcanic) rock fragments, chert, and dolomite. Detrital clays are present throughout the formation, although concentrated mainly in silts and shales, and include chlorite, illite, smectite, trace amounts of muscovite, biotite and kaolinite. Trace abundances of accessory minerals are present as amphibole, ilmenite and heavy minerals. The Clearwater Formation has a complex diagenetic mineral assemblage consisting predominantly of glauconite, berthierine, illite, smectite, kaolinite and mixed-layer clays. Overgrowths of quartz and potassium feldspar are present to a limited extent. Two to three generations of calcite are present as a pervasive cement resulting in the carbonate cemented zones and concretions, and minor to trace amounts of other phases, including siderite, pyrite and zeolites (clinoptilolite) are present. The low abundance of detrital kaolinite in the sediments suggests little to no contribution from adjacent Precambrian rocks of the Canadian Shield in the study area. The compositional immaturity, and specifically the abundant lithic fragments and feldspars, are indicative of a Cordilleran source of detritus (McLean and Putnam, 1983).

The Wabiskaw Member of the Clearwater Formation has been interpreted by previous researchers as a short transgressive interval in the late Aptian at a relatively shallow position on the shelf (Outtrim and Evans, 1977), deposited as offshore bars in a continued transgression of the Boreal sea (Bayliss and Levinson, 1976; Jackson, 1984). To the north in the Primrose area it has been suggested that the Wabiskaw sands are estuarine deposits within incised valleys resulting from underlying evaporite dissolution (Wightman *et al.*, 1991). The Wabiskaw Member has also been interpreted as a progradational shoreface-attached marine bar complex in the Athabasca area (Ranger *et al.*, 1988). A study of the laterally equivalent Glauconite Member in central Alberta by Strobl (1988), found this interval to be composed of a thicker sequence of overall progradational deposits composed of cycles of early sediments resulting from sea-level rise and later sediments resulting from sea-level fall. Another study, by Rosenthal (1988), also identified a number of periods of transgression and regression associated with the deposition of the Glauconite Formation in west-central Alberta. Again, sediments are interpreted as cyclic representatives of sea-level rise and fall during the early Cretaceous. The Glauconite units in central and west-central Alberta are much thicker than the glauconite-rich Wabiskaw Member of Cold Lake, which in the study area has an average thickness of about 8m (26ft).

Observation from core and well logs indicate that deposition of the Wabiskaw sands in the study area was influenced by fluctuation in relative sea-level, in that it was associated with the change from the deltaic-marine setting of the offshore marine muds deposited at the end of McMurray and beginning of Clearwater time, to a marine-dominated shoreface setting during Wabiskaw time. The base of this interval is sequence boundary SB2, which marks a period of overall shallowing and relative sea-level fall. The initial relative fall would have brought the sand-rich facies of the Wabiskaw Member into a more proximal shoreline setting than that of the underlying prodelta silts and shales. But it is also associated with a shift in the position of distributaries supplying detritus to the underlying deltaic complex to another, likely adjacent position during Wabiskaw deposition. This may have resulted in the prominence of marine-dominated shoreface conditions during Wabiskaw deposition in the study area. As with other Clearwater sediments, variability in the sediment pattern would have been affected by more localized affects such as salt dissolution. The change in environmental conditions is supported by the presence of glauconite throughout the Wabiskaw member in the study area, which is generally interpreted as characteristic of fully marine conditions (Odin and Matter, 1981). Internally, the Wabiskaw Member exhibits characteristics of a marine bar, which in more distal bar areas may be quite muddy. Log signatures and cores support progradational deposition rather than deposition during a transgressive phase. Therefore, the depositional conditions identified in a study area to the north by Ranger *et al.* (1988), and that of Rosenthal (1988), in west-central Alberta, and Strobl (1988), in central Alberta are thought to extend into the study area examined here. The end of Wabiskaw deposition is manifested by flooding surface FS3, indicative of a relative sea-level rise, and most importantly a return to former deltaic-marine conditions within the study area.

Mineralogically, the Wabiskaw Member is composed of detritus corresponding to primarily a Cordilleran sediment source. Grains tend to be slightly to moderately rounded, and generally more sorted than overlying Clearwater sediments which fits well with their deposition in a higher energy, shallow marine bar environment. Deposition was likely controlled by relief on the pre-Cretaceous unconformity, with deposits accumulating in depositional lows still present subsequent to McMurray deposition.

The two sequence boundaries, SB1 and SB2, identified in the study area are the most important in terms of sequence stratigraphy because by definition they separate different depositional sequences or periods, and thereby different patterns of Clearwater Formation. Both are associated with periods of relative sea-level fall. SB1 was initially identified in marine facies in a core located at a distal position on the shelf (with respect to the shoreline), and is believed to have formed at a relatively early time during Clearwater depositional history. It was traced landward into more proximal facies in the study area, towards the position of Esso's pilot plants, and the thickest, richest sands in the area. SB2 marks a major change from the deltaic-system dominated conditions of deposition present at the end of McMurray time, to the shoreface marine-dominated conditions of Wabiskaw deposition. In general the two sequence boundaries are characterized in core and well logs by a number of features, which vary depending on the depth of the water at the time, in essence a function of their position with respect to the shoreline in deltaic-marine conditions. Characteristics observed in the study area change from the underlying to overlying sediments, and are more prominent in some settings than others. They can be summarized as:

1) a relatively abrupt shallowing of facies (distal settings);
2) the presence of ripped up and armored mud clasts (proximal settings);
3) a decrease in the presence of iron-rich minerals (distal facies);
4) an abrupt decrease in ichnofaunal abundance; and
5) a small increase in bitumen saturation (associated with changes in grain-size).

Not all of these features characterize each sequence boundary; generally, a combination of one or more features could be distinguished at any one position in the study area. A certain amount of erosion is believed to have been associated with deposition of the Clearwater Formation, especially in the formation of early upper to middle delta front deposits in the period of sea-level fall at the time of formation of SB1. Little to no erosion would be expected in the lower energy environments in the lower delta front / delta fringe positions and in the basinward prodelta deposits. Plate 2.4 contains a number of photographs illustrating the features of sequence boundary SB1 in wells located between the most proximal and distal positions in the study area.

A relatively abundant assemblage of ichnofauna characterize the Clearwater Formation in the study area. The general association of the ichnofauna identified in core are those which tend to be located in abundance in marine facies. Certain types of trace fossils can be related to their position on the shelf in a particular depositional environment depending on their feeding behavior (trophic group). An example of this is the presence of *Zoophycos*, a deposit feeding trace found in the more distal wells. This tracemaker belongs to the ethological classification pascichnia, in which the organism exhibits deposit-feeding or grazing behavior that allows it to ingest as much food as possible with the least amount of movement (Table 2.1, Ekdale *et al.*, 1984). Its presence may also be characteristic of an oxygen-low marine environment, and is therefore a good indicator of deeper water conditions on the shelf (Ekdale *et al.*, 1984). The size and number of tracemaking organisms can also be an important indicator of depositional environment. In general, fewer and smaller trace fossils tend to occur in the higher energy environment of the upper shelf, and more plentiful fossils tend to be found in the quieter water environments of the lower shelf. Therefore, the change in abundance and type of ichnogenera species from distal to proximal cores is an indicator of an increase in environment energy and a decrease in the availability of food (organic content). Such trends are commonly associated with an increase in proximity to nearshore environments. The absence of ichnofauna in the coarser grained facies of well 3-13-65-4W4 is likely associated with higher water energy, higher turbidity, and a lower organic content at this position, resulting in an inhabitable environment for most trace-making organisms. In terms of environmental conditions, the input of freshwater into the higher salinity seawater in the delta during sediment influx results in the development of brackish-water conditions, with a salinity gradient extending from the point of input out onto the delta plain. Brackish-water environments are more physiologically stressful on organisms than freshwater or fully marine conditions, and as a result are generally characterized by fewer species, an increase in the depth to which organisms may survive, and often a decrease in their size (Ekdale *et al.*, 1984). The higher diversity in the ichnofossil assemblage found in the Wabiskaw Member, in comparison to comparable grain-sized sediments in the Clearwater Formation, has been interpreted to be the result of the higher salinity marine conditions present during Wabiskaw deposition, in contrast to the deltaic, somewhat brackish-water conditions present during deposition of the remaining Clearwater sediments.

Cross-section A to A' illustrates the variation in position and internal characteristics of the various genetic units within the study area (Appendix 2). The cross-section is located in a southwest to northeast trend, which is fairly representative of the direction of progradation during Clearwater deposition in the study area. Constant well spacing was used in the cross-section, as a representative scale would not allow effective correlation between close wells. The datum for the cross-section is the top of the Mannville Group. Although this surface would not have been totally flat as depicted, it results in a relatively good representation of topographic variation in the underlying sediments. There are visible changes in the position of the sequence boundaries, flooding surfaces, and relative thickness of depositional cycles throughout the study area. This has been attributed to local variation in the underlying depositional surface, and the variable position of sediment input into the basin. Sediments may develop depositional thicks in pre-depositional lows because of favorable sediment influx, then at a later time, under different depositional conditions, appear to accumulate relatively thin deposits, where in relatively nearby areas depositional thicks are forming. This would greatly affect the vertical position of bounding surfaces, such as sequence boundaries and flooding surfaces, but would not change the sequence of genetic units within various sequences. This is well illustrated in cross-section A to A'. In idealized models, the thickness of various genetic units thickens slightly at the shelf slope margin, but is otherwise essentially uniform. Within inter-continental basins, such as that of Clearwater deposition, the scenario is very different, especially if deposition is affected by much more than eustatic sea-level fluctuation.

Regional Implications

The sequences and their bounding surfaces were identified throughout the small study area within townships 65 and 66, ranges 2 through 4, but their extent beyond these boundaries was not known. Therefore, well logs outside of the smaller study area were observed in a cursory fashion. Characteristics observed in the smaller study area appeared to be continuous and transferable into the surrounding wells, allowing the sequences to be extended to this area. This supports the hypothesis that the sequence stratigraphic interpretation inferred from the small study area has greater than local extent, and that it may in fact extend entirely throughout the depositionally similar northern sector of the Cold Lake deposit.

D. CONCLUSIONS

The purpose of this chapter was to gather sufficient information regarding detailed stratigraphic and sedimentologic characteristics of the Lower Cretaceous Clearwater Formation in order to be able to understand the relationship between its internal stratigraphy and depositional environment. This included an analysis of both regional and local factors that influenced Clearwater deposition in the study area, detailed information on the sediments, their features, internal characteristics and ichnofossil assemblages. A sequence stratigraphic and depositional model for the study area was developed from this collected information, providing a working hypothesis on which future studies in the interpretation of associated formational characteristics can be based.

An analysis of all available data derived from core, well logs, maps, and cross-sections has determined that deposition was influenced by two primary factors, the relief of the Clearwater depositional surface, and numerous fluctuations in relative sea-level. Variations in the depositional surface resulted from:

1) the low (ramp-like) and variable slope of the eastern margin of the developing Alberta Foreland basin;
2) erosion and channel downcutting into earlier Cretaceous McMurray and Wabiskaw sediments which overlie the pre-Cretaceous unconformity;
3) the structure of the pre-Cretaceous unconformity, which is itself a function of differences in carbonate formation in the Devonian,
4) erosion of the pre-Cretaceous unconformity prior to Cretaceous deposition; and
5) pre-, syn- and post-Devonian dissolution of underlying Paleozoic evaporite deposits.

Fluctuation in relative sea-level during the Cretaceous resulted from a number of interrelated factors. The effect of periodic dynamic tectonism of the western Cordilleran belt is thought to have been significant, as it led to episodic high sediment fluxes conveyed into the study area by rivers draining from the west and southwest. Variation in eustatic sea-level may also have influenced deposition, but subsidence is not believed to have been important, as subsidence rates on the eastern margin of the basin would have been quite low, and not of a magnitude to significantly affect accommodation in the study area. Studies of eustatic sea-level fluctuation by other researchers have suggested that the Aptian to Albian was a period of overall eustatic sea-level rise during the early Cretaceous (Haq *et al.*, 1987). The findings of this study are that the Clearwater Formation formed during the early Cretaceous in an overall period of rising relative sea-level in the basin, with deposition occurring in regressive pulses primarily because of fluctuations in sediment supply or tectonism from the western basin margin. It is not known if global fluctuations in sea-level contributed to Clearwater Formation depositional patterns, or if so, to what extent, although the significant tectonism during this period suggests that it would have been minor in influence.

Eustatic fluctuations in sea-level have been suggested by many researchers to have resulted from relatively few mechanisms, with limitations primarily associated with the large magnitude of the required process. The most significant of these processes are:

1) changes in the volume of land ice;
2) changes in the volume of ocean basins by spreading at ocean ridges; and
3) rapid subsidence.

Although glacial-eustacy appears to be the most likely process in terms of magnitude, there has not been any evidence attesting to the presence of any Jurassic to Early Tertiary ice caps that could have resulted in the large scale fluctuations documented in the literature for this period (Donovan and Jones, 1979; Haq *et al.*, 1987). Ocean ridge spreading is not thought to have been sufficient in magnitude to have resulted in the documented fluctuations. Rapid subsidence is known to cause fast, short-term variations in eustatic sea-level, but the height of the fluctuation produced this way is probably too small to have caused global fluctuations (Donovan and Jones, 1979). Therefore, although it is quite possible that eustatic fluctuations in sea-level may have affected Clearwater Formation depositional patterns, continued research into the factors which affect eustatic fluctuation are necessary before its effects can be correctly determined.

Detailed examination of core and well logs, including an analysis of gross lithology, detailed sedimentary structures, grain-size relationships, diagenetic characteristics and ichnofaunal distributions aided in the interpretation of Clearwater depositional environments within the study area.

Overall, the Clearwater Formation is dominated by very fine to medium-grained sands with varying degrees of interbedded silt and shale. Muds and shales occur as thin, 0.1 to 3 cm thick beds or lenses or as rounded mud clasts which are often elongated or armored with finer grained mud. Coal chips or lenses, fine-grained organic detritus and wood and shell fragments are all found in the formation, especially in the finer grained sediments. Clearwater sediments are characterized by low to high angle stratification, herringbone and trough cross-bedding, wavy bedding, occasional rippled bedding, and soft sediment deformation or faulting. They are typically well bitumen saturated and form good reservoir rocks, especially in the sandiest units, and may contain thin randomly positioned carbonate cemented zones and concretions, as well as other diagenetic features as clay, siderite, glauconite or iron staining.

The majority of Clearwater sediments were deposited in a shallow marine deltaic environment, in a proximal position relative to the paleo-shoreline. Upper delta front distributary channel and mouth-bar facies were deposited in a relatively high energy setting, forming thick intervals of stacked fine to medium-grained sand in various delta lobes. Marine sands and silts are associated with a more distal middle delta front setting, and are gradational with lower delta front sands and interbedded muds. Marine silts, shales and fine sands are found in further offshore, quieter-water settings of the delta fringe, followed by the thinly interbedded marine silts and shales of the prodelta to open marine environment. The thick glauconite-rich sands of the Wabiskaw member were deposited in a more marine dominated interval during Clearwater deposition, and are characteristic of marine-bar sands with their associated muds in a shoreface setting.

In sequence stratigraphic terms the Clearwater Formation is composed of two sequences, in this study labelled S_1 and S_2, and a number of bounding surfaces, namely two sequence boundaries, SB1 and SB2, and three flooding surfaces, FS1, FS2, and FS3. Each sequence contains successive units of genetically related strata separated by the sequence boundaries, which represent periods of relative sea-level fall. The flooding surfaces are contained within the sequences and delineate periods of relative sea-level rise. Each sequence has been subdivided into a number of genetic units or cycles, designated A to D in S_1, and A to C and the Wabiskaw Member in S_2. Each cycle exhibits a lateral shift in depositional facies from a proximal to distal position relative to the paleo-shoreline.

Progradational conditions dominated during the formation of both sequences, with internal transgressional events manifested by the position of flooding surfaces, and small scale relative sea-level fluctuations associated with each genetic cycle. Sequence S_1 appears to have had depositional conditions in which the paleo-shoreline was closer, resulting in the thick deltaic lobe deposits associated with the upper levels of the Clearwater Formation. Sequence S_2 contains more transgressive flooding surfaces, and contains Wabiskaw sediments, indicative of a shift in dominant environmental factors from deltaic to open marine and back during deposition in the study area.

The two sequence boundaries are of primary importance in the formation as they are the foundation upon which the stratigraphic breakdown and interpretation of relative sea-level fluctuation are based. In theory they are time-stratigraphic, representing a period in time just prior to the onset of a relative sea-level fall, and are identifiable by a number of characteristics associated with the underlying sediments, as well as the variable facies which onlap subsequent to shallowing. The characteristics observed in the study area for sequence boundaries SB1 and SB2 have been summarized as follows:

1) evidence of a relative sea-level fall manifested by a shallowing of facies (more pronounced in distal positions);
2) evidence of erosion, as indicated features such as downcutting and mud clasts (more likely in nearshore environments);
3) changes in the depositional characteristics, specifically in organic content, bioturbation, biogenic diversity and ichnofossil assemblage;
4) changes in diagenetic features, such as the abundance of iron-bearing species, perhaps indicating a relationship between formation of the sequence boundary and early diagenesis; and
5) changes in bitumen saturation, useful as an aid in evaluating changes in grain-size and internal mineralization.

The two sequence boundaries are believed to have formed in response to relative sea-level drops on the shelf in the early Albian. In each case this situation likely resulted from a period of relatively low sediment input into the basin, such as a sea-level highstand, followed by a period of significant sediment input, resulting in the erosion of nearshore deposits and deposition of coarser grained deposits over the finer grained sediments in the study area. The initial period of low sediment input would have been a time of low to non-deposition in offshore environments with sediment reworking and minor erosion occurring at shallow nearshore positions. The drop in relative sea-level associated with the formation of the sequence boundary would have been followed by a subsequent slow rise in relative sea-level once the initial large sediment flux began to diminish, resulting in the formation of progradational deposits. It is difficult to determine if the rate of sea-level drop resulting in the formation of the sequence boundaries was fast or slow because of the limited lateral extent of the study area. Deposition occurred during a period of overall eustatic sea-level rise, and sediment input was sufficient to cause progrdation which suggests a Type 2 sequence boundary, but deposition appears to have been relatively quick, with evidence of erosion. In addition, the delta front sequences overlying SB1 are highstand deposits characteristic of a Type 1 sequence. Therefore overall, characteristics suggest a Type 1 sequence boundary. Investigations into the lateral extent of these boundaries and their accompanying sequences indicates that they extend throughout the the larger study area and perhaps further into the northern part of the deposit. The area covered by this study is quite small on a regional scale however, and future investigation is required to determine if this hypothesis is indeed true.

The conditions manifested by the sequence boundary in shelf or ramp-like shelf shallow-marine environments are of special interest because they represent a time of flux and change of depositional conditions in the basin. Large variations in relative sea-level may result in the stratification of sequences from vastly different environments. Although not present in this study area, this could result in the subaerial exposure of former offshore submarine sediments, resulting in the onset of oxidizing conditions with their accompanying diagenetic effects, and the exposure of the organic-rich substrate for habitation by a new group of opportunistic ichnofauna. The evidence of this change may be conserved in the rock record. In an offshore setting the non-depositional period associated with the relative sea-level fall of the sequence boundary may result in more reducing conditions in the sediment, and the onset of sulphate-reduction processes with their associated mineralogic markers. Conversely, another approach could be used, in which recognition of characteristics from studies of such occurrences and other less extreme variations may help in the easier identification of sequence boundaries in other positions, and hence the interpretation of their associated stratigraphic sequences. The sequence stratigraphic interpretation provided by this study, with its accompanying depositional model, provides the necessary infrastructure for future research into these areas in the Clearwater Formation.

E. REFERENCES

Alberta Energy Resources Conservation Board. 1973. Geology and proved in place reserves of the Cold Lake oil sands deposits. Alberta Energy Resources Conservation Board Report 70-L-Geol, September, 23pp.

Alberta Energy Resources Conservation Board. 1985. Atlas of Alberta's crude bitumen reserves. Alberta Energy Resources Conservation Board Reserve Report Series 38, 37pp.

Badgley, P.C. 1952. Notes on the subsurface stratigraphy and oil and gas geology of the Lower Cretaceous series in central Alberta, Canada. Geological Survey Paper 52-11, 12pp.

Bayliss, P., and Levinson, A.A. 1976. Mineralogical review of the Alberta oil sand deposits (Lower Cretaceous Mannville Group). Bulletin of Canadian Petroleum Geology, v.24, p. 211-224.

Bergman, K.M. and Walker, R.G. 1988. Formation of Cardium erosion surface E5, and associated deposition of conglomerate: Carrot Creek field, Cretaceous Western Interior Seaway, Alberta. *In:* James, D.P. and Leckie, D.A., eds., Sequences, Stratigraphy, Sedimentology: Surface and Subsurface. Canadian Society of Petroleum Geologists, Memoir 15, p. 15-24.

Beynon, B.M., Pemberton, S.G., Bell, D.D. and Logan, C.A. 1988. Environmental Implications of Ichnofossils from the Lower Cretaceous Grand Rapids Formation, Cold Lake oil sands deposit. *In:* James, D.P. and Leckie, D.A., eds., Sequences, Stratigraphy, Sedimentology: Surface and Subsurface. Canadian Society of Petroleum Geologists, Memoir 15, p. 275-289.

Boyd, R., Suter, S. and Penland, S. 1988. Implications of modern sedimentary environments for sequence stratigraphy. *In:* James, D.P. and Leckie, D.A., eds., Sequences, Stratigraphy, Sedimentology: Surface and Subsurface. Canadian Society of Petroleum Geologists, Memoir 15, p. 33-36.

Brooks, P.W., Fowler, M.G., MacQueen, R.W. and Mathison, J.E. 1988. Use of biomarker geochemistry to identify variable biodegradation trends, Cold Lake oil sands (Fort Kent area), Alberta. *In:* James, D.P. and Leckie, D.A., eds., Sequences, Stratigraphy, Sedimentology: Surface and Subsurface. Canadian Society of Petroleum Geologists, Memoir 15, p. 529-535.

Cant, D.J. 1984. Development of shoreline-shelf sand bodies in a Cretaceous epeiric sea deposit. Journal of Sedimentary Petrology, v. 54, no. 2., p. 541-556.

Cant, D.J. and Hein, F.J. 1986. Depositional sequences in ancient shelf sediments: Some constraints in style. *In:* Knight, R.J. and McLean, J.R., eds., Shelf Sands and Sandstones, Canadian Society of Petroleum Geologists, Memoir II, p. 303-312.

Capeling, R.R. and Peggs, J.K. 1981. Experimental steamflood. Cold Lake oil sands. *In:* Meyer, R.F. and Steele, C.T., eds., The Future of Heavy Crude and Tar Sands, McGraw Hill, New York, p. 361-368.

Carmichael, S.M.M. 1988. Linear estuarine conglomerate bodies formed during a mid-Albian marine transgression; Upper Gates Formation, Rocky Mountain Foothills of northeastern British Colunbia. *In:* James, D.P. and Leckie, D.A., eds., Sequences, Stratigraphy, Sedimentology: Surface and Subsurface. Canadian Society of Petroleum Geologists, Memoir 15, p. 49-62.

Carrigy, M.A. 1959. Geology of the McMurray Formation, Pt. III. General Geology of the McMurray area. Alberta Research Council, Geology Division, Memoir 1, 130pp.

Donovan, D.T. and Jones, E.J.W. 1979. Causes of world-wide changes in sea-level. Journal of the Geological Society of London, v. 136, p. 187-192.

Ekdale, A.A., Bromley, R.G. and Pemberton, S.G. 1984. Ichnology. The use of trace fossils in sedimentology and stratigraphy. Society of Economic Paleontologists and Mineralogists, 317pp.

Embry, A.F. and Podruski, J.A. 1988. Third-order depositional sequences of the Mesozoic succession of Sverdrup Basin. *In:* James, D.P. and Leckie, D.A., eds., Sequences, Stratigraphy, Sedimentology: Surface and Subsurface. Canadian Society of Petroleum Geologists, Memoir 15, p. 73-84.

Eyles, C.H. and Walker, R.G. 1988. Geometry and facies characteristic of stacked shallow marine sandier-upward sequences in the Cardium Formation at Willesden Green, Alberta. *In:* James, D.P. and Leckie, D.A., eds., Sequences, Stratigraphy, Sedimentology: Surface and Subsurface. Canadian Society of Petroleum Geologists, Memoir 15, p. 85-95

Gallup, W.B. 1974. The geological history of McMurray-Clearwater deposition in the Athabasca oil sands area. *In:* Hills, L.W., ed., Oil Sands, Fuel of the Future. Canadian Society of Petroleum Geologists, Memoir 3, p. 100-114.

Garven, G. 1989. A hydrogeological model for the formation of the giant oil sands deposits of the Western Canada Sedimentary Basin. American Journal of Science, v. 289, p. 105-166.

Glaister, R.P. 1959. Lower Cretaceous of southern Alberta and adjoining areas. American Association of Petroleum Geologists, v. 43, p. 590-640.

Haq, B.U., Hardenbol, J. and Vail, P.R. 1987. Chronology of fluctuating sea-levels since the Triassic. Science, v. 235, p. 1156-1167.

Harrison, D.B., Glaister, R.P. and Nelson, H.W. 1981. Reservoir description of the Clearwater oil sand, Cold Lake, Alberta, Canada. *In:* Meyer, R.F. and Steele, C.T., eds., The Future of Heavy Crude and Tar Sands, McGraw Hill, New York, ch. 30, p. 264-279.

Hays, J.D. and Pitman, W.C. III. 1973. Lithospheric plate motion, sea level changes and climatic and ecological consequences. Nature, London, v. 246, p. 16-22.

Hitchon, B. 1969. Fluid flow in the Western Canada Sedimentary Basin. 1. Effect of topography. Water Resources Research, v. 5, no. 1, p. 186-195.

Jackson, P.C. 1984. Paleogeography of the Lower Cretaceous Mannville Group of western Canada. *In:* Masters, J.A., ed., Elmworth–Case Study of a Deep Basin Gas Field, American Association of Petroleum Geologists Memoir 38, p. 49-77.

Jardine, D. 1974. Cretaceous oil sands of western Canada. *In:* Hills, L.W., ed., Oil Sands, Fuel of the Future. Canadian Society of Petroleum Geologists, Memoir 3, p. 50-67.

Kauffman, E.G. 1969. Cretaceous marine cycles of the Western Interior. Mountain Geologist, v. 6, no. 4, p. 227-245.

Kauffman, E.G. 1977. Geological and biological overview: Western Interior Cretaceous Basin. Mountain Geologist, v. 14, nos. 3-4, p. 75-99.

MacDonald, D.E., Langenberg, C.W. and Strobl, R.S. 1988. Cyclic marine sedimentation in the Lower Cretaceous Luscar Group and Spirit River Formation of the Alberta Foothills and Deep Basin. *In:* James, D.P. and Leckie, D.A., eds., Sequences, Stratigraphy, Sedimentology: Surface and Subsurface. Canadian Society of Petroleum Geologists, Memoir 15, p. 143-153.

Maher, J.B. 1989. Geometry and reservoir characteristics Leismer Clearwater 'B' gas field, northeast Alberta. Case Studies in Canadian Petroleum Geology. Bulletin of Canadian Petroleum Geology, v.37, no. 2, p. 236-240.

McLean, J.R. and Putnam, O.E. 1983. Comparison of heavy oil reservoirs: the Lloydminster Formation; Lloydminster area, and the Clearwater Formation, Cold Lake area. *In:* McLean, J.R. and Reinson, G.E., eds., Sedimentology of Selected Mesozoic Clastic Sequences. Proceedings of Corexpo '83, Calgary. Canadian Society of Petroleum Geologists, p. 81-93.

McLearn, F.H. 1932. Problems of the Lower Cretaceous of the Canadian Interior. Transactions of the Royal Society of Canada, 3rd series, v. XXVI, sec. IV, p. 37-43.

McLearn, F.H. 1944. Revision of the Lower Cretaceous of the Western Interior of Canada. Geological Survey of Canada, Department of Mines and Resources, Paper 44-17, 9pp.

Mellon, G.B. 1967. Stratigraphy and petrology of the Lower Cretaceous Blairmore and Mannville groups, Alberta Foothills and Plains. Research Council of Alberta Geoligical Division, Bulletin 21, 270pp.

Mellon, G.B. and Wall, J.H. 1961. Correlation of the Blairmore Group and equivalent strata. Edmonton Geological Society Quarterly, v. 5, no. 1.

Menard, H.W. 1964. Marine geology of the Pacific. McGraw-Hill, New York, 271pp.

Minken, D.F. 1974. The Cold Lake oil sands: Geology and a reserves estimate. *In:* Hills, L.W., ed., Oil Sands, Fuel of the Future. Canadian Society of Petroleum Geologists, Memoir 3, p. 84-99.

Mitchum, R.M., Vail, P.R. and Thompson, S. 1977. Seismic stratigraphy and global changes of sea-level, Part 2: The depositional sequence as a basic unit for stratigraphic analysis. *In:* Payton, C.E., ed., Seismic Stratigraphy–Applications to Hydrocarbon Exploration. American Association of Petroleum Geologists Memoir 26, p. 53-62.

Mossop, G.D., Kramers, J.W., Flach, P.D. and Rottenfusser, B.A. 1981. Geology of Alberta's oil sands and heavy oil deposits. *In:* Meyer, R.F. and Steele, C.T., eds., The Future of Heavy Crude Oils and Tar Sands, Unitar, McGraw Hill, New York, p. 197-207.

Nauss, A.W. 1945. Cretaceous stratigraphy of the Vermilion area, Alberta, Canada. American Association of Petroleum Geol. Bull., v. 29, no. 11, p. 1605-1629.

Nicholls, J.H. and Luhning, R.W. 1977. Heavy oil sand *in-situ* pilot plants in Alberta (past and present). *In:* Redford, D.A. and Winestock, A.G., eds., The Oil Sands of Canada-Venezuela. Canadian Institute of Mining and Metallurgy, Special Volume 17, p. 36-69.

Odin, G.S. and Matter, A. 1981. De glauconiarum originae. Sedimentology, v. 28, p. 611-641.

Outtrim, C.P. and Evans, R.G. 1977. Alberta's oil sands reserves and their evaluation. *In:* Redford, D.A. and Winestock, A.G., eds., The Oil Sands of Canada-Venezuela. Canadian Institute of Mining and Metallurgy, Special Volume 17, p. 36-69.

Pitman, W.C. III. 1978. Relationship between eustacy and stratigraphic sequences of passive margins. Geological Society of America Bulletin, v. 89, p. 1389-1403.

Plint, A.G., Walker. R.G. and Duke, W.L. 1988. An outcrop to subsurface correlation of the Cardium Formation in Alberta. *In:* James, D.P. and Leckie, D.A., eds., Sequences, Stratigraphy, Sedimentology: Surface and Subsurface. Canadian Society of Petroleum Geologists, Memoir 15, p. 167-183.

Posamentier, H.W. and Vail, P.R. 1988. Eustatic controls on clastic deposition II–Sequence and systems tract models. *In:* Wilgus, C.K. *et al.*, eds., Society of Economic Paleontologists and Mineralogists, Special Pub. 42, p. 125-154.

Posamentier, H.W., Jervey, M.T. and Vail, P.R. 1988. Eustatic controls on clastic deposition I–Conceptual framework. *In:* Wilgus, C.E. *et al.*, eds., Society of Economic Paleontologists and Mineralogists, Special Publication 42, p. 109-124.

Prentice, M.E. and Wightman, D.M. 1987. Mineralogy of the Clearwater Formation, Cold Lake oil sands area: Implications for enhanced oil recovery. Alberta Geological Survey Report, 41pp.

Putnam, P.E. and Pedskalny, M.A. 1983. Provenance of Clearwater Formation reservoir sandstones, Cold Lake, Alberta, with comments on feldspar composition. Bulletin of Canadian Petroleum Geology, v. 31, no. 3, p. 148-160.

Ranger, M.J., and Pemberton, S.G. 1992. Trapping mechanism and Time of oil migration in the Athabasca oil sands deposit. Presented at American Association of Petroleum Geologists Annual Convention, Calgary, Alberta, Canada, 20-24 June 1992, abstract, p. 108.

Ranger, M.J. Pemberton, S.G. and Sharpe, R.J. 1988. Lower Cretaceous example of a shoreface-attached marine bar complex: The Wabiskaw 'C' sand of northeastern Alberta. *In:* James, D.P. and Leckie, D.A., eds., Sequences, Stratigraphy, Sedimentology: Surface and Subsurface. Canadian Society of Petroleum Geolgoists, Memoir 15, p. 439-450.

Rosenthal, L. 1988. Wave dominated shorelines and incised channel trends: Lower Cretaceous Glauconite Formation, west-central Alberta. *In:* James, D.P. and Leckie, D.A., eds., Sequences, Stratigraphy, Sedimentology: Surface and Subsurface. Canadian Society of Petroleum Geologists, Mem.15, p. 207-220.

Rudkin, R.A. 1964. Lower Cretaceous. *In:* McCrossan, R.G. and Glaister, R.P., eds., Geological History of Western Canada. Alberta Society of Petroleum Geologists, p. 156-168.

Ryer, T.A. 1977. Patterns of Cretaceous shallow-marine sedimentation, Coalville and Rockport areas, Utah. Geological Society of America Bulletin, v. 88, p. 177-188.

Scott, R.W., 1970. Stratigraphy and sedimentary environments of Lower Cretaceous rocks, southern Western Interior. American Association of Petroleum Geologists Bulletin, v. 54, p. 1225-1244.

Sloss, L.L., Drumbein, W.C. and Dapples, E.C. 1949. Integrated facies analysis. *In:* Longwell, C.R., Chairman, Sedimentary facies in geologic history. Geologic Society of America Memoir 39, 171pp.

Spencer, A.M. (ed.). 1974. Mesozoic-Cenozoic orogenic belts: Data for orogenic studies. The Geological Society of London, Special Publication No. 4, p. 600-603.

Stelck, C.R. 1975. Basement control of Cretaceous sand sequences in western Canada. The Geological Association of Canada Special Paper Number 13, p.427-440.

Stott, D.F. 1984. Cretaceous sequences of the foothills of the Canadian Rocky Mountains. *In:* Stott, D.F. and Glass, D.J., eds., The Mesozoic of Middle North America. Canadian Society of Petroleum Geologists Memoir 9, p. 85-107.

Strobl, R.S. 1988. The effects of sea-level fluctuations on prograding shorelines and estuarine valley-fill sequences in the Glauconitic Member, Medicine River field and adjacent areas. *In:* James, D.P. and Leckie, D.A., eds., Sequences, Stratigraphy, Sedimentology: Surface and Subsurface. Canadian Society of Petroleum Geologists, Memoir 15, p. 221-236.

Vail, P.R. and Hardenbol, J. 1979. Sea-level changes during the Tertiary. Oceanus, v. 22, p. 71-79.

Vail, P.R., Mitchum, R.M. Jr., Todd, R.G., Widmier, J.M., Thompson, S. III, Sangree, J.B., Bubb, J.N. and Hatlelid, W.G. 1977. Seismic stratigraphy and global changes of sea-level, Parts 1-6. *In:* Payton, C.E., ed., Seismic Stratigraphy–Applications to Hydrocarbon Exploration. American Association of Petroleum Geologists, Memoir 26, p. 49-212.

Van Wagoner, J.C., Mitchum, R.M. Jr., Posamentier, H.W. and Vail, P.R. 1987. Key definitions of sequence stratigraphy. *In:* Bally, A.W., ed., American Association of Petroleum Geologists, Studies in Geology, 27, p. 11-14

Vigrass, L.W. 1965. General geology of Lower Cretaceous heavy oil accumulations in western Canada. The Journal of Canadian Petroleum Technology, Oct.-Nov., p. 168-175.

Weimer, R.J. 1984. Relation of unconformities, tectonics and sea-level changes, Cretaceous of Western Interior, U.S.A. *In:* Schlee, J.S., ed., Interregional Unconformities and Hydrocarbon Accumulations. American Association of Petroleum Geologists, Memoir 36, p. 7-35.

Wightman, D.M. and Berezniuk, T. 1986. Resource characterization and depositional modelling of the Clearwater Formation, Cold Lake oil sands deposit, east-central Alberta. *In:* Westhoff, J.D. and Marchart, L.C., eds., Proceedings of the 1986 Tar Sands Symposium, Jackson, Wyoming, July 7-10, p. 20-45.

Wightman, D.M., Pemberton, S.G. and Singh. 1987. Depositional modelling of the Upper Mannville (Lower Cretaceous), east-central Alberta: Implications for the recognition of brackish-water deposits. Reservoir Sedimentology, Society of Economic Paleontologists and Mineralogists Special Publication No. 40, p. 189-220.

Wightman, D.M., MacGillivray, J.R., McPhee, D., Berhane, H. and Berezniuk, T. 1991. McMurray Formation and Wabiskaw Member (Clearwater Formation): Regional perspectives derived from the North Primrose area, Alberta, Canada, Fifth Unitar / UNDP International Conference on Heavy Crude & Tar Sands, p. 1-36.

Williams, G.D. 1963. The Mannville Group (Lower Cretaceous) of central Alberta. Bulletin of Canadian Petroleum Geology, v. 11, p. 350-368.

Williams, G.D. and Stelck, C.R. 1975. Speculation on the Cretaceous paleogeography of North America. The Geological Association of Canada Special Paper Number 13, p. 1-20.

PLATE 2.1:

Photographs of typical ichnogenera of the Clearwater Formation:

(a) Large *Arenicolites* burrow at 459.05 m (1506.2 ft) in well 3-28-66-2W4. Core 4, box 2 of 5, 1506–1510 ft. Magnification (Mag): 0.46X.

(b) *Zoophycos* burrow at 411.0 m (1545.3 ft) in well 3-28-66-2W4. Core 6, box 1 of 5, 1541–1545 ft. Mag: 0.74X.

(c) *Palaeophycus* burrow at 501.02 m (1643.9 ft) in well 6-31-66-2W4. Core 2, box 5 of 7, 499.95–501.35 m. Mag: 0.24X.

(d) *Rosselia* burrow at 449.56 m (1475.0 ft) in well 5-22-65-3W4. Core 7, box 4 of 4, 1474–1479 ft. Mag: 0.33X.

(e) *Palaeophycus* (Pa) and *Chondrites* (Ch) burrows in well 16-2-66-3W4. Core 5, box 3 of 4, 1525–1530 ft. Mag: 0.34X.

(f) Large escape structure, perhaps from a bivalve? in well 8-19-66-2W4. Core 11, box 6 of 6, 486.25–487.75 m. Mag: 0.33X.

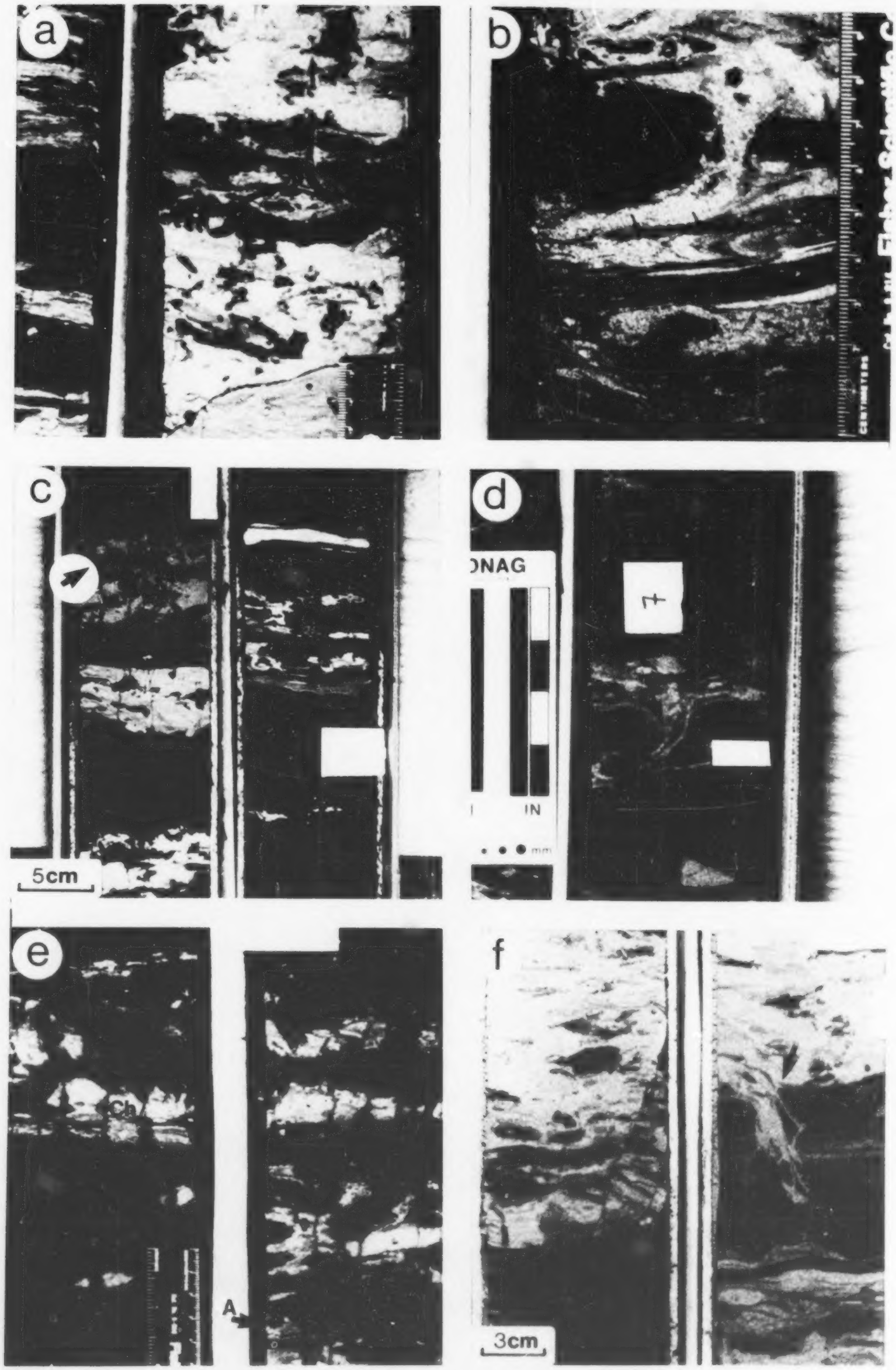
a
b
CENTIMETERS
c
5cm
d
ONAG
IN
mm
7
e
Ch
A
f
3cm

PLATE 2.2:

Photographs of sequence boundary SB1 in well 3-28-66-2W4, located at a distal position on the shelf with respect to the paleo-shoreline, in the northeastern part of the study area.

(a) an overview of the core illustrating the facies transition at sequence boundary SB1 (468.61m, 1537.5 ft) from the underlying delta fringe marine muds and sands to the overlying lower delta front marine sands and muds. Core 5, boxes 3 and 4 of 5, 1533–1541 ft. Mag: 0.20X.

(b) a close-up of SB1 and its features; underlain by a coal lense, numerous coal chips and shell fragments. Core 5, box 4 of 5, 1537–1541 ft. Mag: 0.76X.

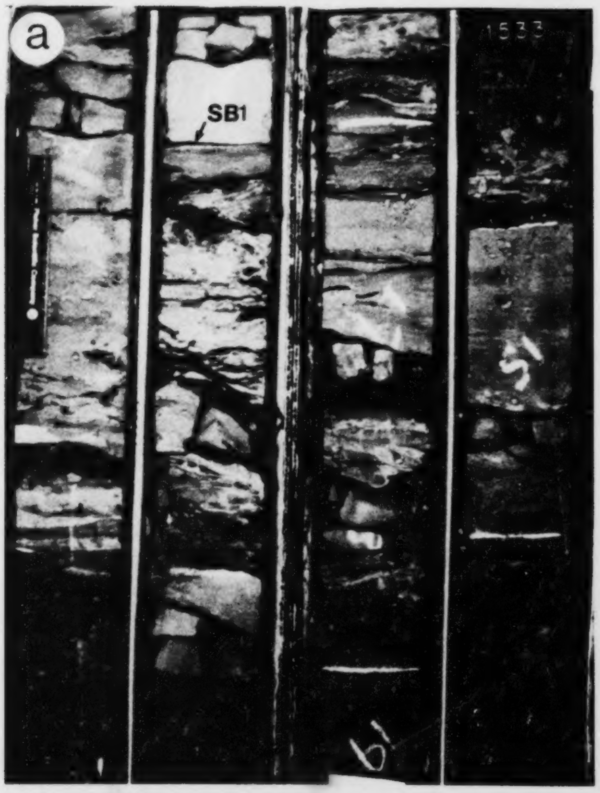
a
SB1
1533

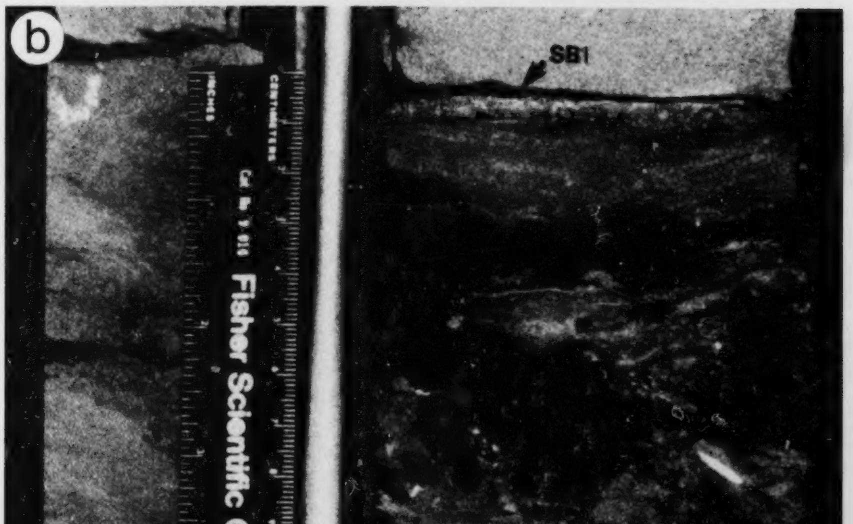
b
INCHES
CENTIMETERS
Fisher Scientific Company
SB1

PLATE 2.3:

Photographs of core in well 3-13-65-4W4, illustrating the features of sequence boundary SB1 located at a proximal position with respect to the paleo-shoreline in the southwestern part of the study area.

(a) and (b) illustrate the clast-rich environment of the upper delta front sands overlying sequence boundary SB1 in this well. Many clasts are quite large, and some are armored, indicative of the relatively high energy environment present during deposition. (a) Core 5, box 1 of 4, 478.0–479.30 m, (b) Core 5, box 2 of 4, 479.30–480.85 m. Mag: 0.37X.

(c) an overview of SB1 illustrating the facies transition from the underlying lower to middle delta front marine sands and muds, to the overlying upper delta front, distributary mouth-bar sands. The sequence boundary is characterized at this position in the deltaic complex by the abundance of clasts in the overlying facies. Core 5, box 3 of 4, 480.85–482.30 m. Mag: 0.37X.

(d) photograph of thick sands with mud interbeds in the lower to middle delta front sands which underly sequence boundary SB1. Many of the units have been disturbed as a result of coring. Core 5, box 4 of 4, 482.30–483.80 m. Mag: 0.37X.

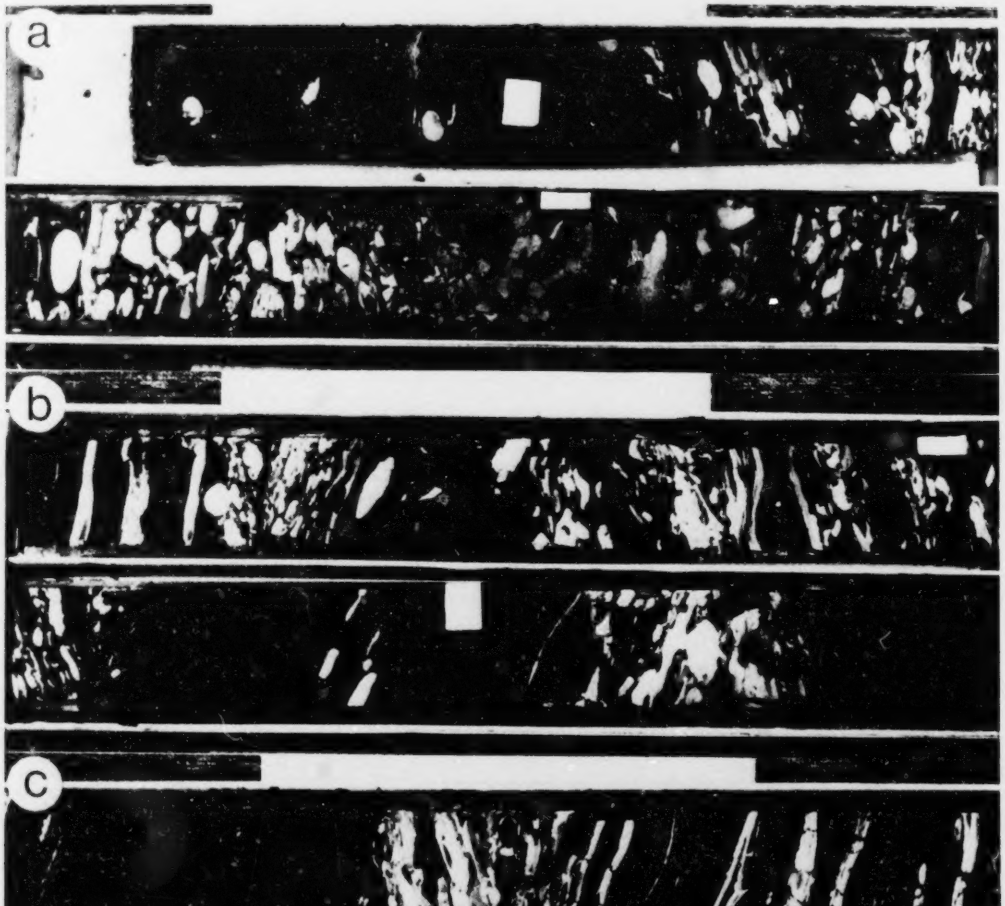
a
b
c
d
10 cm

PLATE 2.4:

Photographs illustrating the features of sequence boundary SB1 in various wells within the study area. Refer to Figure 2.18 for the relative positions of each of the wells.

(a) SB1 in well 8-19-66-2W4 at a middle to distal position with respect to the paleo-shoreline. Characterized by the facies transition from underlying delta fringe marine muds (which are very thin in this well), to the overlying lower delta front marine sands and muds. Delta fringe sediments contain abundant *Chondrites* and *Planolites* ichnofossils, and the lower delta front sands tend to contain more *Skolithos, Bergaueria* and *Diplocraterion*. A distinct change bitumen saturation is associated with SB1. Note the presence of flooding surface FS2. Core 10, box 4 of 6, 474.30–475.88 m. Mag: 0.35X.

(b) SB1 in core of well 6-31-66-2W4, at a distal position with respect to the paleo-shoreline. Illustrates the facies transition from underlying delta fringe marine muds with abundant tracefossils (mainly *Chondrites*), to the overlying middle delta front distibutary mouth-bar sands. Note the clasts in the overlying sands, and the increase in bitumen saturation associated with the coarser facies. Core 3, box 5 of 6, 510.12–511.62 m. Mag: 0.37X.

(c) SB1 in well 16-2-66-2W4, at a midpoint in the deltaic complex in the study area. The photograph illustrates the transition from underlying delta fringe facies, marine muds and sands, to the marine sands and muds of the lower delta front environment. The delta fringe sediments are well bioturbated—could be described as churned, by *Chondrites, Planolites* and *Paleophycus* ichnogenera. They also contain coal fragments, and a thin carbonate cemented interval. The overlying sands contain very few ichnofauna. As in other wells, there is an evident change in the bitumen saturation accompanying the facies transition. Core 5, box 2 of 4, 1520–1524 ft. Mag: 0.42X.

(d) Photograph of well 12-18-65-3W4, revealing the missing core over the interval which has been interpreted to have contained sequence boundary SB1. This well is located at a relatively proximal position with respect to the paleo-shoreline in the study area, towards the edge of the thick delta front accumulation in the southwest. SB1 was inferred to have been in this position by the slight variation in facies over this interval; the marked reduction in interbedded silt and shale rich beds in the overlying lower delta front sands, and the substantial increase in mud and shale clasts. There is also a disappearance of tracefossils, with *Planolites* and *Chondrites* ichnofauna present in the underlying delta fringe–lower delta front sands and muds, and no ichnofossils in the overlying sands. Core 7, boxes 1 and 2 of 4, 1523–1533 ft. Mag: 0.17X.

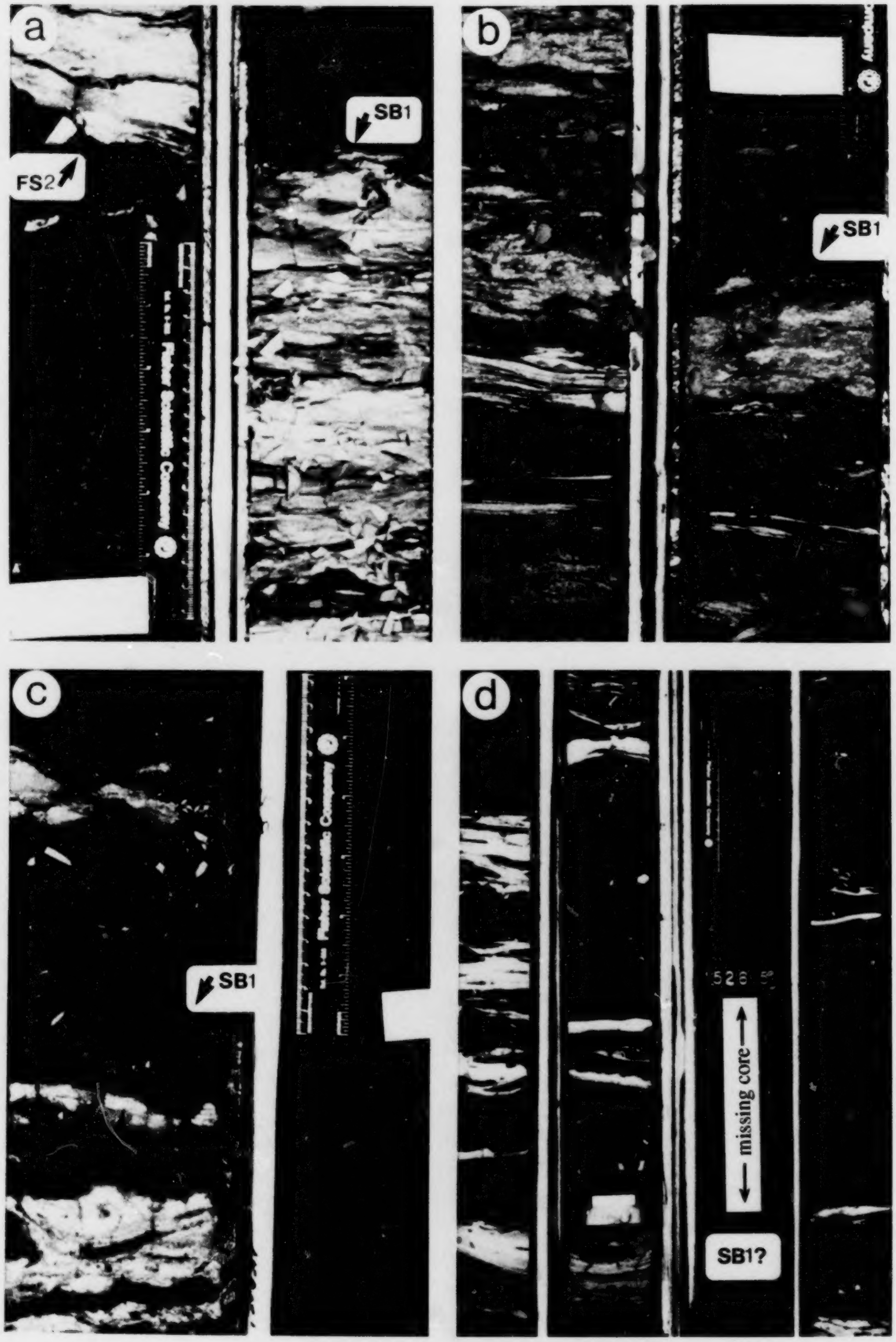
a
FS2
SB1
Fisher Scientific Company
b
SB1
c
SB1
Fisher Scientific Company
d
1526.5
missing core
SB1?

CHAPTER 3:

DIAGENESIS OF THE LOWER CRETACEOUS CLEARWATER FORMATION, AND ITS APPLICATION TO SEQUENCE STRATIGRAPHY NEAR LEMING IN THE COLD LAKE OIL SANDS DEPOSIT, EAST-CENTRAL ALBERTA

A. INTRODUCTION

The Clearwater Formation is a heavy oil bearing formation in the Cold Lake oil sands deposit, located northeast of Edmonton on the Alberta / Saskatchewan border. The deposit is currently being exploited on a pilot plant scale by means of *in-situ* cyclic steam injection, at depths of greater than 300m (950ft). Estimated reserves for the Clearwater Formation are on the order of 1.1 x 10^{10}m^3 (6.9 x 10^{10}bbls), with additional reserves in the deposit in the overlying Grand Rapids Formation and underlying McMurray Formation (A.E.R.C.B., 1985).

Production of the bitumen saturated sands of Cold Lake deposit, and specifically the Clearwater Formation, poses some serious challenges. Pilot plant tests and laboratory work has shown that injection of high temperature steam, used to raise the formation temperature, promotes 'thermal' cracking, reduces bitumen viscosity and results in a significant reduction in reservoir porosity and permeability because of reservoir sensitivity to *in-situ* injection fluids (Sedimentology Research Group, 1981; Boon and Hitchon, 1983a). The reduction in reservoir quality ensues from the reaction of grain coating, pore lining and pore filling minerals, and exposed surfaces of framework grains with relatively freshwater injection fluids, leading to the precipitation of new pore-filling minerals (Sedimentology Research Group, 1981; Boon and Hitchon, 1983b; Kirk *et al.*, 1987). Certain minerals appear to be more reactive than others; hence knowledge of the distribution of natural diagenetic and detrital mineralization in the formation is essential to the planning of future production strategies.

OBJECTIVES

The objectives of this chapter are twofold: 1) to investigate the detrital and diagenetic mineralization of the Clearwater Formation within a small portion of the Cold Lake deposit, and 2) to mineralogically and geochemically characterize systematic variations associated with a sequence boundary (SB1) that was identified in Chapter 2, and interpreted as a position of local sea-level fall. The purpose of such characterization is to determine whether this sedimentological event had any effect on the resulting diagenetic mineralization, and if geochemical and mineralogical variations can be used to identify and / or confirm the presence of sequence boundaries. A detailed listing of mineralogical and elemental data to be added to the growing database for the Clearwater Formation (i.e. Longstaffe *et al.*, 1991a, 1991b, 1992a, 1992b) is included in Appendices 3 and 4.

PREVIOUS WORK

Diagenetic research on the Clearwater Formation has been gaining momentum in recent years, with works such as: Prentice and Wightman, 1987; Wickert *et al.*, 1988; Abercrombie, 1989; Abercrombie *et al.*, 1989; Hutcheon *et al.*, 1989; Longstaffe *et al.*, 1989a, 1989b, 1989c; Racki *et al.*, 1989; Wickert *et al.*, 1989; Longstaffe *et al.*, 1990; Racki, 1991; and Longstaffe *et al.*, 1992a, 1992b, now published. Earlier mineralogy work and provenance studies include: Mellon, 1967; Schooley, 1975; Bayliss and Levinson, 1976; Harrison *et al.*, 1981; and Putnam and Pedskalny, 1983. Diagenetic studies which address post-production mineralogy on the Clearwater Formation include Hebner *et al.*, (1986), Kirk *et al.* (1987), Abercrombie (1989), and Abercrombie *et al.* (1989). Many other published reports address development and production strategies for use in the Cold Lake oil sands deposit, with reference to the Clearwater Formation. It is evident that the importance of understanding the natural suite of diagenetic minerals on production has been recognized for some time. Such reports include: Kendall, 1977; Nicholls and Luhning, 1977; Towson, 1977; Capeling and Peggs, 1981; Grabowski and Rubin, 1981; Sedimentology Research Group, 1981; Shepherd, 1981; Boon and Hitchon, 1983a, 1983b; and Boon *et al.*, 1983.

STUDY AREA

The study area examined is located within townships 65 and 66, ranges 2 through 4 west of the fourth meridian in the northern Cold Lake oil sands deposit (Figure 3.1). It is for the most part entirely contained within the Esso lease in the Leming area of the Cold Lake oil sands deposit, and situated adjacent to Esso's Leming megaproject *in-situ* pilot plant test site (Figure 3.2).

Eight wells were examined and sampled for mineralogical and geochemical analyses. Most were available from the Energy Resources Conservation Board Core

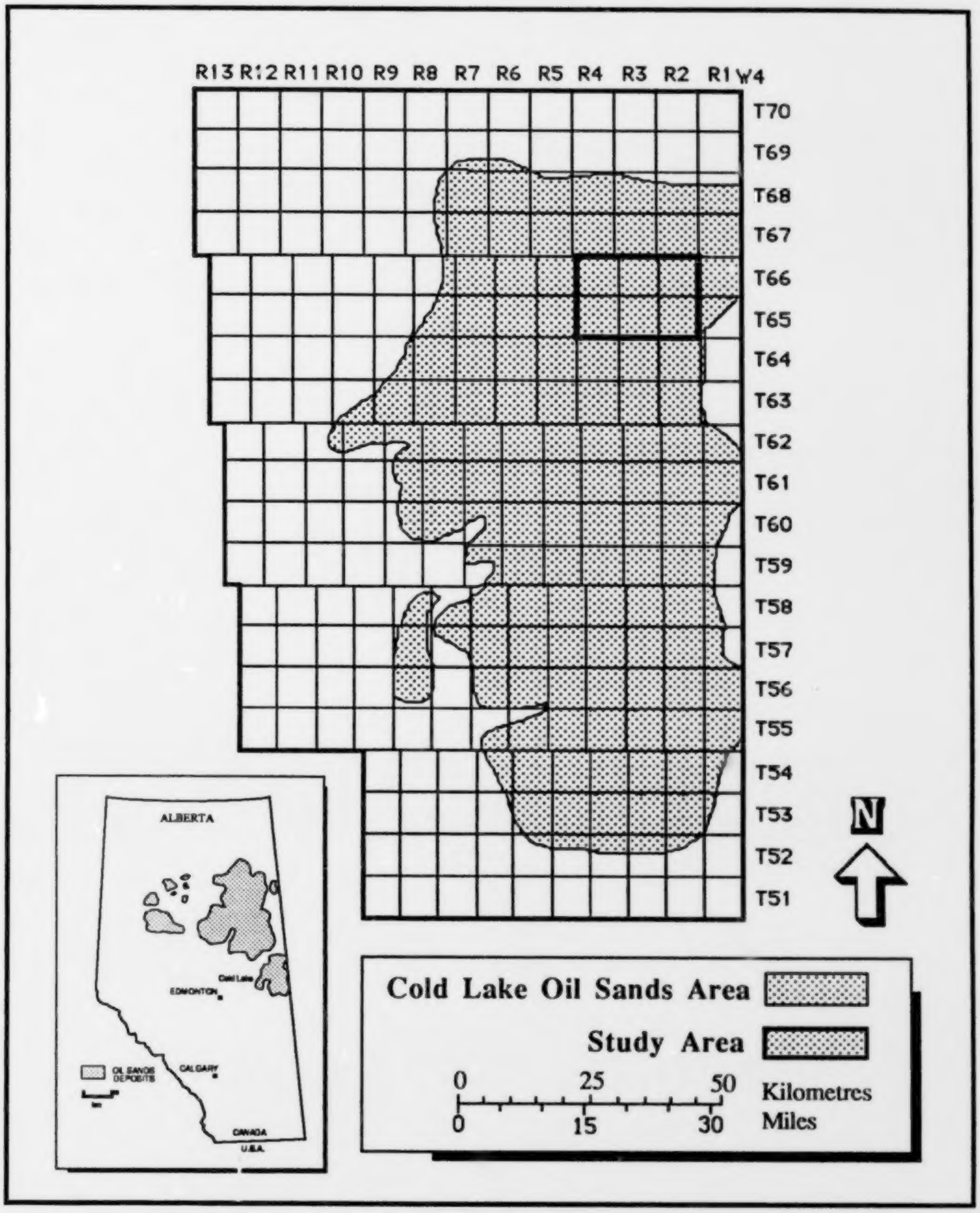
R13 R12 R11 R10 R9 R8 R7 R6 R5 R4 R3 R2 R1 W4
T70
T69
T68
T67
T66
T65
T64
T63
T62
T61
T60
T59
T58
T57
T56
T55
T54
T53
T52
T51
N
Cold Lake Oil Sands Area
Study Area
0
25
50
Kilometres
0
15
30
Miles
ALBERTA
Cold Lake
EDMONTON
CALGARY
OIL SANDS DEPOSITS
CANADA
U.S.A.

Figure 3.1: Location map of study area within the Cold Lake oil sands deposit.

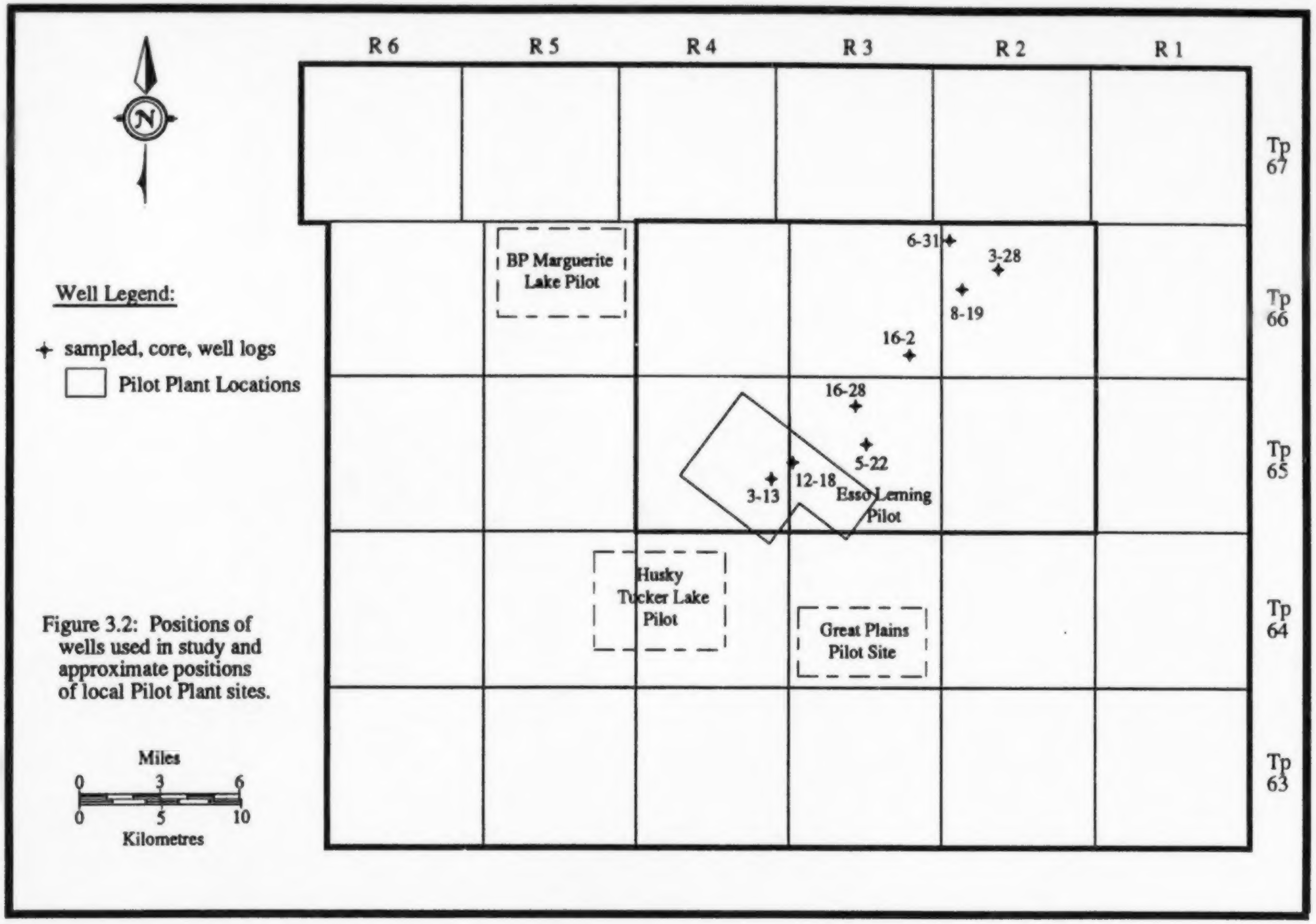

N
Well Legend:
+ sampled, core, well logs
Pilot Plant Locations
Miles
0
3
6
0
5
10
Kilometres
R 6
R 5
R 4
R 3
R 2
R 1
Tp 67
Tp 66
Tp 65
Tp 64
Tp 63
BP Marguerite Lake Pilot
6-31
3-28
8-19
16-2
16-28
5-22
12-18
3-13
Esso Leming Pilot
Husky Tucker Lake Pilot
Great Plains Pilot Site

Figure 3.2: Positions of wells used in study and approximate positions of local Pilot Plant sites.

Research Facility, although a number of cores were donated by Esso Resources for the study.

B. GEOLOGICAL BACKGROUND

The Cold Lake deposit contains bitumen in three Lower Cretaceous formations of the Mannville Group. These are positioned stratigraphically with the McMurray Formation at the base, overlain by the Clearwater Formation, which contains the Wabiskaw member in its lower extent, all of which is overlain by the Upper and Lower Grand Rapids formations (Figure 3.3).

Clearwater Formation sediments are located at depths approximately 400 to 520m (1315 to 1700ft) below surface, with a regional dip of approximately 1.3–1.5m/km (0.13°) to the southwest (Hitchon, 1969; Wightman and Berezniuk, 1987). The formation varies in thickness in various highs and lows which were previously developed on the pre-Cretaceous unconformity, ranging in thickness from greater than 65m (215ft) in the northeast to a thin of 6m (20ft) in the southwest (Minken, 1974).

The Clearwater Formation was deposited during late Aptian to Albian time during a period of shallow marine sedimentation, associated with the inundation of the northern Boreal sea into eastern Alberta (Williams and Stelck, 1975; Jackson, 1984). Deposition of Wabiskaw and Clearwater sediments took place during a number of transgressive and regressive events, believed to be associated with episodes of pronounced tectonism in the Eastern Cordillera during the Columbian Orogeny. Fluvial systems brought detritus derived from the western Rockies towards the east, and dumped it into a deltaic system at the eastern edge of the Western Canada Sedimentary Basin in the study area.

Local depositional controls during Clearwater deposition have been assessed (Chapter 2), and determined to be primarily the variable slope of the eastern basin margin and the relief of earlier McMurray Formation sediments, which themselves were eroded and affected by the relief of the underlying pre-Cretaceous unconformity.

The paleogeographic factors which affected Clearwater morphology include the presence of a nearby axial high, which is believed to have influenced the position of the Boreal shoreline on the eastern margin of the basin, and the amount of sediment input and subsidence during deposition. The thickest Clearwater sands are believed to have formed during a main progradational period during the Albian, which resulted in the deposition of

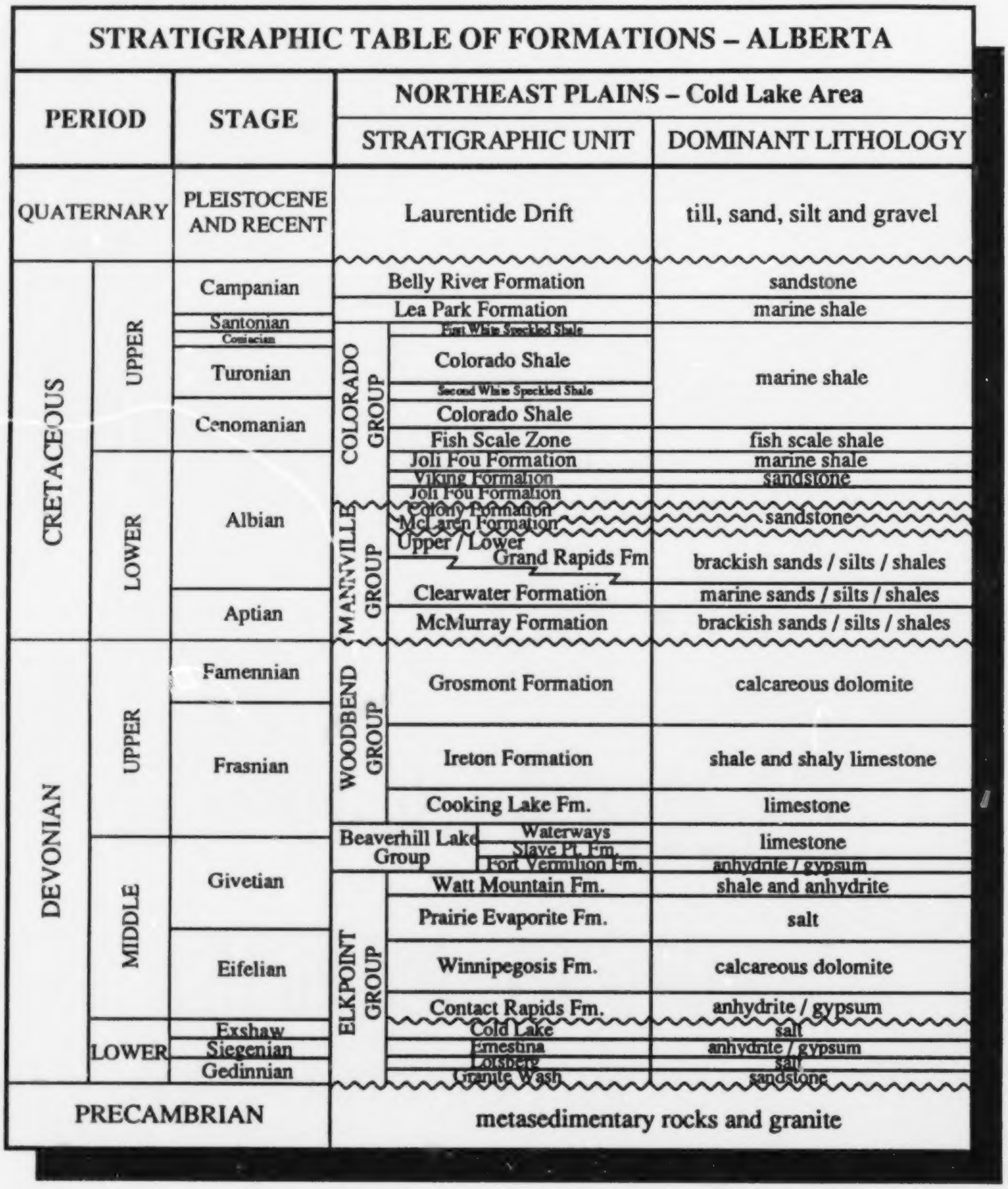

STRATIGRAPHIC TABLE OF FORMATIONS – ALBERTA

PERIOD		STAGE	NORTHEAST PLAINS – Cold Lake Area		
			STRATIGRAPHIC UNIT		DOMINANT LITHOLOGY
QUATERNARY		PLEISTOCENE AND RECENT		Laurentide Drift	till, sand, silt and gravel
CRETACEOUS	UPPER	Campanian		Belly River Formation	sandstone
		Santonian		Lea Park Formation	marine shale
		Coniacian	COLORADO GROUP	First White Speckled Shale	marine shale
		Turonian		Colorado Shale	
				Second White Speckled Shale	
		Cenomanian		Colorado Shale	
				Fish Scale Zone	fish scale shale
	LOWER	Albian		Joli Fou Formation	marine shale
				Viking Formation	sandstone
				Joli Fou Formation	
			MANNVILLE GROUP	Colony Formation	sandstone
				McLaren Formation	
				Upper / Lower Grand Rapids Fm	brackish sands / silts / shales
		Aptian		Clearwater Formation	marine sands / silts / shales
				McMurray Formation	brackish sands / silts / shales
DEVONIAN	UPPER	Famennian	WOODBEND GROUP	Grosmont Formation	calcareous dolomite
		Frasnian		Ireton Formation	shale and shaly limestone
				Cooking Lake Fm.	limestone
			Beaverhill Lake Group	Waterways	limestone
				Slave Pt. Fm.	
	MIDDLE	Givetian		Fort Vermilion Fm.	anhydrite / gypsum
			ELKPOINT GROUP	Watt Mountain Fm.	shale and anhydrite
				Prairie Evaporite Fm.	salt
		Eifelian		Winnipegosis Fm.	calcareous dolomite
				Contact Rapids Fm.	anhydrite / gypsum
	LOWER	Exshaw		Cold Lake	salt
		Siegenian		Ernestina	anhydrite / gypsum
		Gedinnian		Lotsberg	salt
				Granite Wash	sandstone
PRECAMBRIAN				metasedimentary rocks and granite	

Figure 3.3: Stratigraphic succession in the northern Cold Lake oil sand area (modified from Mossop *et al.*, 1981; Western Atlas Int., 1988).

thick, stacked sands in the study area, now bitumen saturated and of good reservoir quality.

The shoreline is believed to have been located to the west / southwest of the study area during Clearwater deposition, in approximately a north / northwest to south / southeast orientation, with progradation and sediment deposition occurring towards the east / northeast (Mahar, 1989).

Depositional environments and facies interpreted for the study area include: fine to medium grained upper delta front sands in distributary channel and distributary mouth-bar deposits, with fine grained sands in muds in associated interdistributary bays in the southwestern part of the study area; which trend to middle delta front fine to medium grained sands and occasional muds; fine sands and interbedded muds from lower delta front deposits; delta fringe interstratified silts and shales with occasional sands; and prodelta to open marine silts and shales in the northeastern corner of the study area.

The Wabiskaw Member was deposited early in Clearwater depositional history. It has been interpreted in the study area as fine to medium grained marine bar sands with varying degrees of interstratified mud. It is commonly better sorted than the overlying Clearwater sediments, and is believed to have been exposed to more open marine conditions in a shoreface setting during deposition, as evidenced by the presence of extensive glauconite (Odin and Matter, 1981).

C. ANALYTICAL TECHNIQUES

SAMPLING METHODOLOGY

The Clearwater Formation wells chosen for examination are located on a trend believed to be approximately parallel to the primary progradation direction of sediments in this area (Figure 3.2). This direction should be approximately perpendicular to the paleo-shoreline during the deposition of the Clearwater Formation in the Aptian to Albian, with proximal sediments located to the southwest.

Eight cores were logged and 91 samples were collected, and include sands, silts, shales, carbonate cemented sands and concretions. Most are concentrated within the stratigraphic interval in each core containing sequence boundary SB1. Sample details and accompanying analyses are given in Table 3.1. Sampling positions are indicated in well graphic core logs in Appendix 2. One sample of drilling mud was also analyzed. Samples were examined using optical light microscopy, scanning electron microscopy (SEM)

Table 3.1: Samples Investigated in Study

SAMPLE NUMBER	LITHOLOGY	BITUMEN SATURATION	DEPTH (metres)	THIN SECTION	SEM	SIZE-FRACTION FOR XRD			ELEMENTAL ANALYSIS¥	ISOTOPIC ANALYSIS†
						< 2 µm	<45 µm	Whole Rock		
Well 3-28-66-2W4 Imp. 77 O.V.										
LW3-90	si,f.g.sst,m	low-trace	457.03	X	X		X	X		
LW3-20	f.g.sst,m,c	trace	463.27	X	X		X	X		X
LW3-36	f.g.sst,si	water	468.24	X	X		X	X		
LW-87-CW-58	f.g.sst,si	low-trace	468.51	X			X	X		
LW-87-CW-59	f.g.sst,si	low-trace	468.61	X			X	X		
LW-87-CW-60	si,f.g.sst,m	water	468.73				X			
LW3-38	f.g.sst,si,m,c	water	468.76	X	X		X	X		X
LW3-39	f.g.sst,si	water	468.91	X	X		X	X		
LW3-66	sh,tr.sst,si	water	477.14		X		X	X		
LW3-73	f.g.sst	high*	479.27	X	X		X	X		
LW3-13	sh,tr.sst,si	low-trace	491.62	X	X		X	X		
LW3-21	f.g.sst,si,c	water	494.15	X	X		X	X		X
Well 6-31-66-2W4 Esso 86 Cold Lake O.V.										
LW-87-CW-10	f.g.sst,tr.sh	mod*	509.60				X	X	X	X
LW-87-CW-11	f.g.sst,si	mod*	510.10	X			X	X	X	
LW-87-CW-12	f.g.sst,tr.sh	mod*	510.30		X		X	X	X	
LW-87-CW-13	f.g.sst,tr.sh	mod*	510.40	X			X	X	X	
LW-87-CW-14	f.g.sst,tr.sh	mod*	510.50	X			X	X	X	
LW-87-CW-15	f.g.sst,tr.sh	mod*	510.60	X			X	X	X	
LW-87-CW-16	f.g.sst,si	low-mod*	510.70	X			X	X	X	
LW-87-CW-17	sh,tr.sst,si	trace	510.80		X		X	X	X	X
LW-87-CW-18	sh,tr.sst,si	water	510.90				X	X	X	
LW-87-CW-19	sh,tr.sst,si	water	511.00				X	X	X	
LW-87-CW-20	v.f.g.sst,si,sh	water	511.20		X		X	X	X	
LW-87-CW-21	v.f.g.sst,tr.sh	water	511.40				X	X	X	X
LW-87-CW-22	v.f.g.sst,si,sh	water	511.65	X			X	X	X	
LW-87-CW-23	v.f.g.sst,tr.sh	water	511.80	X	X		X	X	X	
LW-87-CW-24	v.f.g.sst,sh	water	512.10		X		X	X	X	

Table 3.1 (cont'd): Samples Investigated in Study

SAMPLE NUMBER	LITHOLOGY	BITUMEN SATURATION	DEPTH (metres)	THIN SECTION	SEM	SIZE-FRACTION FOR XRD			ELEMENTAL ANALYSIS¥	ISOTOPIC ANALYSIS†
						< 2 µm	<45 µm	Whole Rock		
LW-87-CW-25	sh,tr.si,sst	water	512.60		X		X	X	X	
LW-87-CW-26	f.g.sst	water	513.55		X		X	X		
LW-87-CW-27	f.g.sst	water	519.40		X					
Well 3-13-65-4W4 Esso 84 (C1-12) Cold Lk.										
LW-87-CW-28	f.-m.g.sst	mod-high*	470.25	X	X	X	X	X		
LW-87-CW-29	f.-m.g.sst	mod-high*	480.20			X	X	X		
LW-87-CW-30	f.g.sst,tr.m	mod-high*	480.50				X	X		
LW-87-CW-31	f.-m.g.sst	mod-high*	480.80			X	X	X		
LW-87-CW-32	f.g.sst	mod*	481.00			X	X	X		
LW-87-CW-33	sh,sst,si	mod*	481.10	X	X	X	X	X		
LW-87-CW-34	f.g.sst,m	mod*	481.20	X	X	X	X	X		
LW-87-CW-35	f.g.sst,tr.sh	mod*	481.30	X	X	X	X	X		
LW-87-CW-36	f.g.sst	mod*	481.40	X		X	X	X		
LW-87-CW-37	f.g.sst,m	mod*	481.60			X	X	X		
LW-87-CW-38	f.g.sst	mod*	481.80	X			X	X		
LW-87-CW-39	f.g.sst,si	low-mod*	482.20			X	X	X		
LW-87-CW-40	f.g.sst	mod*	483.20	X		X	X	X		
LW-87-CW-41	f.g.sst	mod*	491.20	X		X	X**	X		
LW-87-CC-01	concretion	none	481.00					X		
Well 8-19-66-2W4 Esso 86 Marie O.V.										
LW-87-CW-42	si,f.g.sst	low-trace	473.40	X			X	X		
LW-87-CW-43	f.g.sst,m	low-mod*	473.70			X	X	X		
LW-87-CW-44	f.g.sst	low-mod*	474.00			X	X	X		
LW-87-CW-45	f.-m.g.sst,sh	low-mod*	474.20	X			X	X		
LW-87-CW-46	f.g.sst,si	low-trace	474.30	X		X	X	X		
LW-87-CW-47	si,sh	water	474.40	X	X	X	X	X		
LW-87-CW-48	sh,si	water	474.50	X	X	X	X	X		
LW-87-CW-49	f.g.sst,sh	trace	474.60			X	X	X		

Table 3.1 (cont'd): Samples Investigated in Study

SAMPLE NUMBER	LITHOLOGY	BITUMEN SATURATION	DEPTH (metres)	THIN SECTION	SEM	SIZE-FRACTION FOR XRD			ELEMENTAL ANALYSIS¥	ISOTOPIC ANALYSIS†
						< 2 µm	<45 µm	Whole Rock		
LW-87-CW-50	sh,si	water	474.80			X	X	X		
LW-87-CW-51	sh,f.g.sst	low-trace	475.00	X		X	X	X		
LW-87-CW-52	f.g.sst	mod*	475.20							
LW-87-CW-53	f.g.sst	mod*	475.40	X						
LW-87-CW-54	f.g.sst,si	low-mod*	475.90			X	X	X		
LW-87-CW-55	f.g.sst,sh	low-mod*	476.40	X			X	X		
LW-87-CW-56	sh,si,c	water	477.40			X	X	X		X
LW-87-CW-57	f.g.sst,si	low-trace	487.53				X	X		
Well 16-2-66-3W4 Imp. 77 Medley O.V.										
LW-87-CW-92	si,f.g.sst,c	water	453.57		X			X		X
LW-87-CW-61	f.g.sst	mod*	463.60				X	X	X	
LW-87-CW-62	f.g.sst,si	low-mod*	464.24		X	X	X	X	X	
LW-87-CW-63	f.g.sst	mod*	464.44	X	X	X	X	X	X	
LW-87-CW-64	f.g.sst,sh	low-mod*	464.68	X			X	X	X	
LW-87-CW-65	f.g.sst,si	low-mod*	464.75	X			X	X	X	
LW-87-CW-66	f.g.sst,sh,c	water	464.84	X		X	X	X	X	X
LW-87-CW-67	f.g.sst	low-mod*	465.03		X	X	X	X	X	
LW-87-CW-68	f.g.sst,si	low*	465.43	X			X	X	X	
LW-87-CW-69	f.g.sst,si	low*	465.85			X	X	X	X	
LW-87-CW-70	f.g.sst,si,sh	low-trace	466.45			X	X	X	X	
LW-87-CW-71	f.g.sst	low*	467.07			X	X	X		
LW-87-CW-72	f.g.sst,sh	low*	467.64	X			X	X		
LW-87-CW-73	f.g.sst,sh	low-trace	473.94				X	X		
Well 12-18-65-3W4 Imp. 77 Medley O.V.										
LW-87-CW-74	f.g.sst,d.m.?	mod-high*	462.47				X			
LW-87-CW-75	f.g.sst	mod-high*	464.64	X			X	X		
LW-87-CW-76	f.g.sst	mod-high*	465.05				X	X		
LW-87-CW-77	f.g.sst	mod-high*	465.27	X			X	X		

Table 3.1 (cont'd): Samples Investigated in Study

SAMPLE NUMBER	LITHOLOGY	BITUMEN SATURATION	DEPTH (metres)	THIN SECTION	SEM	SIZE-FRACTION FOR XRD			ELEMENTAL ANALYSIS¥	ISOTOPIC ANALYSIS†
						< 2 µm	<45 µm	Whole Rock		
LW-87-CW-78	f.g.sst	mod-high*	465.74	X						
CW-87-CW-79	f.g.sst	mod*	465.94	X						
LW-87-CW-80	f.g.sst	mod*	466.32				X	X		
LW-87-CW-81	f.g.sst,sh	mod*	466.93				X	X		
LW-87-CW-82	f.g.sst,sh	mod*	467.88	X			X	X		
Well 5-22-65-3W4 Imp. Marie O.V.										
LW-87-CW-93	f.g.sst,sh,c	water	430.97					X		X
LW-87-CW-83	f.g.sst	high*	433.40	X			X	X		
LW-87-CW-84	f.g.sst,si,sh	mod*	440.75	X			X	X		
LW-87-CW-85	f.g.sst	high*	441.69	X			X	X		
Well 16-28-66-3W4 Imp. 77 Marie O.V.										
LW-87-CW-91	f.g.sst,si,c	water	415.26					X		X
LW-87-CW-90	f.g.sst,si,sh,c	water	425.58		X			X		X
LW-87-CW-94	drilling mud	none	408.20					X		

¥ – Elemental analysis was carried out by X-ray Fluorescence (XRF);
† – Isotopic analysis includes C & O values for calcite or dolomite;
sst=sand, si=silt, sh=shale, m=mud, c=carbonate cemented, d.m.=drilling mud;
v.f.g=very fine grained, f.g.=fine grained, m.g.=medium grained;
*=bitumen was extracted by cold process at ARC Cloverbar, oil sand;
**=both < and > 45µm analyses were completed.

including energy dispersive microanalysis (EDX), X-ray diffraction (XRD), X-ray fluorescence (XRF), and light stable isotope analysis (for carbonate cemented intervals).

OPTICAL PETROGRAPHY

Forty-nine samples were chosen for petrological study. The nature, abundance and characteristics of detrital and authigenic minerals was observed. All samples were impregnated with blue epoxy to enhance porosity, glued to a glass plate, and polished dry to a thickness of 30µm in order to prevent any changes, such as swelling of clays, that polishing with water could have produced. Bitumen was not removed prior to epoxy impregnation. This is a special technique for producing representative thin sections of clay-rich bitumen saturated samples developed by M. Baaske, at the Alberta Research Councils Millwoods Laboratories, who produced all the thin sections for this study. Some of the sections were later stained (using standard techniques) by J. Forth, at the University of Western Ontario (Dickson, 1966). Sodium cobaltinitrite was used to stain potassium feldspars yellow, and rhodizonate acid disodium salt was used to stain plagioclase feldspars pinkish-red. Alizarin red and potassium ferricyanide stains were used to distinguish ferroan-rich and poor carbonates, as blue and pink respectively.

SCANNING ELECTRON MICROSCOPY

Twenty-eight Clearwater samples were examined using Scanning Electron Microscopy (SEM), in order to observe morphological and textural characteristics of framework grains, and grain-coating, pore-filling and pore-lining minerals. Grain to grain relationships, diagenetic characteristics such as the degree of mineral dissolution and alteration, and paragenetic relationships were also determined using this method.

Small fractured samples were mounted on SEM stubs using conductive silver paint, and sputter-coated with either gold or a mixture of gold and palladium in order to produce a conductive surface. Bitumen saturated samples were washed alternatively with benzene and toluene to remove much of the bitumen and to expose mineral surfaces, as described by Kramers and Rottenfusser (1980). Samples were examined using either the Cambridge Stereo Scan 250 SEM, equipped with a Kevex (EDX) energy dispersive spectrometer, or a JEOL 850SL SEM equipped with a Kevex, energy dispersive (EDX) spectrometer with electron backscatter capability. The EDX spectrometers made possible semi-quantitative elemental analysis in conjunction with morphological study of the samples.

X-RAY DIFFRACTION

An extensive mineralogical investigation of Clearwater sediments was carried out by XRD. Whole rock, < 45µm and < 2µm fractions were examined to distinguish the identity of various Clearwater minerals in different size distributions, and to better evaluate trends in mineralogy.

Prior to XRD analyses, bitumen was removed from saturated samples by a cold extraction / centrifugation method at the Alberta Research Council Clover Bar Research Laboratory. Samples were then manually crushed to a fine powder using a mortar and pestle, and backpacked into aluminum sample holders to randomly orient the grains for whole rock XRD analysis. XRD analysis was carried out on a Rigaku XRD at the University of Alberta, equipped with a cobalt (Co K_α) radiation source and a graphite monochromator. Standard settings used for XRD analysis were: 1 degree 2θ/min or 2 degrees 2θ/min (with chart speeds of 10mm/min and 20mm/min, respectively), at 1×10^3 to 1×10^4 counts/sec, a time constant of 0.5, a one degree divergent slit, power settings of 50kV and 20mA , and a scan range from 2 to 75 degrees 2θ. Whole rock samples were also screened at 325 mesh (45µm) and the minus fraction collected and backpacked for < 45µm XRD analysis from 2 to 75 degrees 2θ.

Mineralogical results for whole rock and < 45µm fractions were expressed semi-quantitatively by measuring the intensity of the most prominent peaks for each of the mineral phases present, then adjusting by use of a form factor. Results were then normalized to represent relative mineral abundances (not weight percents). Form factors (multipication factors) of 2 and 4 were used to adjust the sensitivity of selected clay minerals (7Å and 10Å respectively), and a form factor of 1 was used for all other mineral phases. Determination of a peak height for quartz that was relatively representative of its abundance in the sample posed somewhat of a problem because of the sensitivity of its peak height to variability in the abundance and random orientation of the mineral in the backpack holder. A decision was made to use the (100) 4.26Å (35 I/I_1) peak in replacement for the most prominent (101) 3.343Å (100 I/I_1) quartz peak. Quartz appears to have no contribution from other mineral species at the 4.26Å position for Clearwater samples. Peak intensities were adjusted to their theoretical intensity for the 3.343Å peak (x 100 / 35), and these values were used in the calculations of relative abundance.

Unless the XRD sensitivity of a particular mineral is high, or has prominent peaks in regions not occupied by other species, minerals with abundances below 2% (and potentially up to 5%) will normally not be detected by XRD. The error associated with such an analysis can be fairly high, influenced to a large degree by the homogeneity and degree of fineness of the sample grind, as well as the degree of random orientation during sample preparation. The reproducibility of the analyses is about ± 15% of the abundance measured (Tilley, 1988). X-ray diffraction can also only be used to identify the relatively well crystallized portions of a sample. Amorphous phases (i.e. amorphous SiO_2, TiO_2 or Fe_2O_3), with a poorly developed crystalline structure will not be identified, and will contribute to the XRD scan background level.

In conjunction with the whole rock and < 45μm study, twenty-nine samples from three cores were used to investigate the clay mineralogy of the Clearwater Formation. These samples were dispersed ultrasonically from whole rock samples already treated to remove bitumen (where required), and the < 2μm fraction separated by standard sedimentation techniques. Residual organic matter was removed by treating the < 2μm material with a 3% solution sodium hypochlorite for a minimum of 24 hours at 60°C. Samples were then thoroughly washed by high speed centrifugation.

The clay (< 2μm) fraction was split into two groups (each of at least 50mg): the first was saturated with a 2 molar solution of Ca^{2+}; and the second with a 2 molar solution of K^+. Remaining sample was left with cation exchange sites saturated with Na^+ from the sodium hypochlorite. Saturated samples were thoroughly washed and freeze-dried. Once dry, each of the Ca^{2+} and K^+ portions were prepared as preferred (basal) oriented samples by deposition of approximately 50mg of the sample by suction onto a ceramic disc. Remaining Na^+ samples were used to prepare a randomly oriented backpack samples for examination of (060) diffractions.

XRD analysis of the < 2μm fraction was performed under specific conditions and humidity. Samples (generally K^+ saturated) run at 0% humidity were kept in a desiccator after removal from the oven (105°C) or furnace (300 or 550°C), prior to being analyzed by XRD, and nitrogen gas was used to maintain 0% relative humidity in the XRD sample chamber. Humidity was controlled at 54% passing air passing through a $MgNO_3$ bubbler into the sample chamber (mostly Ca^{2+} samples). All of the information collected as a result of these treatments was used to identify the various clay species. The following X-ray diffraction patterns were produced:

1) Ca-saturated disc at 54% relative humidity, XRD from 2 to 37 degrees 2θ;
2) Ca-saturated disc, solvated with ethylene glycol, XRD from 2 to 82 degrees 2θ;
3) Ca-saturated disc, solvated with glycerol, XRD from 2 to 16 degrees 2θ (only selected samples);

4) K-saturated disc, at 0% relative humidity, XRD from 2 to 37 degrees 2θ;
5) K-saturated disc, at 54% relative humidity, XRD from 2 to 37 degrees 2θ;
6) K-saturated disc, heated at 300°C for 3 hours, XRD from 2 to 23 degrees 2θ;
7) K-saturated disc, at 550°C for 2 hours, XRD from 2 to 23 degrees 2θ; and
8) Na-saturated sample, backpacked into an aluminum sample holder, XRD from 2 to 82 degrees 2θ (only selected samples).

The Ca^{2+} disc is first scanned at 54% relative humidity to expand swelling clays to a standard thickness of two layers of molecular water in interlayer sites. Further expansion of the structure with ethylene glycol is used to differentiate smectitic clays, and glycerol treatment is used to differentiate between tetrahedrally substituted and octahedrally substituted smectites.

Treatment of the K^+ disc at 0 and 54% humidity allows differentiation of swelling clays by their collapse to their minimum d-spacing, and may indicate the presence of inorganic hydroxy-compounds (x-ray amorphous) as revealed by a low-angle hump or shoulder on the 10Å peak (Burtch, 1986). Further treatments at 300° and 550°C permit the identification of chlorite, 1:1 layer silicates such as kaolinite and berthierine, and confirmation of trioctahedral properties of some swelling clays.

Random orientation of available Na^+ saturated < 2μm fractions were analyzed to determine whether clays in the Clearwater are dioctahedral or trioctahedral 2:1 layer silicates, and to help differentiate the 7Å clays by examination of their characteristic (060) peaks.

The relative abundance of each of the clay minerals was estimated semi-quantitatively by use of a modified version of the method by Biscaye (1964). Clay minerals interpreted for each < 2μm fraction were expressed as a member of a clay family, and a selected peak intensity (minus the background intensity) was measured for each. Specifically, the (001) peak was measured for the 14Å clay (chlorite) from the 550°C K-saturated sample, and the (001) diffractions for the 10Å clay (predominantly illite), 7Å clays (kaolinite and berthierine), and 17Å clays (smectite and mixed-layer smectites) were measured from the ethylene glycol solvated samples. Measured peak intensities were then converted to relative abundances by the use of form factors, related to the relative sensitivity of each of the clays in comparison to their peak intensity. Form factors used in this study were suggested by F.J. Longstaffe (pers. comm.[1]), based on his studies on the Clearwater Formation, and previous work by Biscaye (1964), and were as follows: a form factor of 1 for the 14Å clay and 17Å clay; 4 for 10Å clay; and 2 for 7Å clays. A correction was made for the overlap of the (002) 14Å clay peak over the (001) 7Å clay peaks by subtracting the adjusted peak intensity for 14Å clay from that of the 7Å clays. All adjusted peak heights were then normalized to obtain relative mineral abundances.

---

[1] University of Western Ontario, London, Ontario, Canada.

X-RAY FLUORESCENCE

Elemental analyses by x-ray fluorescence spectroscopy were carried out on selected samples across sequence boundary SB1. Samples were chosen from wells 16-2-66-3W4 and 6-31-66-2W4, which represent 'proximal' and 'distal' positions with respect to the paleo-shoreline during Clearwater deposition.

Twenty-six bulk rock (whole rock) samples were analyzed for both major and minor oxides, and include sands, silts, shales (those both originally bitumen saturated, and those water-bearing), and one carbonate cemented sample. The sequence of sample preparation steps carried out were: sample grinding; determination of loss on ignition (L.O.I.); preparation of a pressed powder pellet for trace element analysis; and preparation of a fusion disc for major oxide analysis.

All samples were finely ground (to less than 200 mesh) by use of a shatterbox, followed by remixing of the sample to ensure homogeneity. L.O.I. results were obtained by baking 1.000 g ± 0.001 g of sample in a 1000°C furnace for a period of two hours. Samples were then loaded into a desiccator, and their weight loss due to volatiles was measured by difference. Weight loss typically stems from the loss of water and gases such as sulphur. A small weight gain also typically occurs on ignition resulting from the conversion of FeO to Fe_2O_3. This gain must be adjusted for to obtain the correct L.O.I. (Wu, 1986).

Pressed powdered pellets (briquets) are used because they are cheaper and simpler than fused discs, and for trace element analysis result in less elemental dilution than fusion discs. Use of briquets leads to a greater analytical error than does use of fused discs because of elemental matrix effects, and the effect of sample versus standard mineralogical variability. A briquet is formed by combining and briefly grinding a 2.00g powdered sample with 0.2g of Somar (a binder). This mix is then loaded into the pellet pressing apparatus and hand pressure is applied to hold the powder together. Borax acid powder is then added to form a support for the powdered sample. The sample is compressed using a hydraulic press, and the surface of the briquet, once removed from the press, is lightly filed (Wu, 1986).

Preparation of fused pellets for major oxide analysis entails collecting all the material remaining after the L.O.I. analysis is complete, and mixing with 5.000 ± 0.0005g of flux and 0.050 ± 0.005g of NH_4NO_3. After homogenization, the mix is melted in a platinum crucible over a blast furnace, a few grams of NH_4I are added as a wetting agent, and all is poured into a platinum mold, which when cooled to room temperature is ready for analysis. A Phillips PW-1450 automatic sequential X-ray spectrometer from the University of Western Ontario was used for the analyses.

STABLE ISOTOPE ANALYSES

Carbonate cemented sands and samples with abundant dolomite were selected for stable isotope analysis of carbonate minerals ($\delta^{13}C$, $\delta^{18}O$). XRD analyses of bulk rock rock samples were examined for the type and proportion of the carbonate phase present to determine which samples should be analyzed. Selected whole rock samples (crushed to < 45µm) were first reacted with 100% phosphoric acid for 1 hour at 25°C to obtain the CO_2 released from calcite following the method by McCrea (1950). The CO_2 was collected under vacuum by use of a carbonate stable isotope line. If the sample also contained dolomite, it was left under vacuum for a period of 3 hours prior to being returned to the 25°C bath. This sample was left in the bath for a total of 10 days to allow further reaction to take place along with other samples in which only dolomite was extracted using phosphoric acid, following the procedure as suggested by Walters *et al.* (1972) to prevent cross-contamination of CO_2 from calcite and dolomite. The CO_2 generated by dolomite for all samples was then collected and purified under vacuum by use of a stable isotope line, as was done for the calcite samples.

The extracted CO_2 evolved from calcite and dolomite were compared with CO_2 derived from standard samples of calcite using a mass spectrometer. Isotopic ratios relative to standard calcite were adjusted to the usual δ-notation relative to Standard Mean Ocean water (SMOW) for oxygen (Craig, 1961), and the *Belemnitella americana* from the Peedee Formation (PDB) for carbon (Craig, 1957). $\delta^{18}O$ values were also reported relative to the PDB notation.

D. RESULTS OF MINERALOGICAL AND GEOCHEMICAL INVESTIGATIONS

MINERALOGY

The Clearwater Formation consists of compositionally immature sandstones which originated primarily from igneous source rocks in the west and southwest (Putnam and Pedskalny, 1983). Its mineral assemblage has been studied by many researchers, with the overall conclusion that Clearwater sands can be classified as feldspathic litharenites according to Folk's (1974) definition of clastic rocks (Harrison *et al.*, 1981; Putnam and Pedskalny, 1983; Wightman and Berezniuk, 1986; Kirk *et al.*, 1987; Prentice and Wightman, 1987; Maher, 1989) (Figure 3.4). Dolomite-rich zones situated randomly throughout the formation tend to be less feldspar-rich and are typically identified as litharenites (Prentice and Wightman, 1987). The application of Folk's sandstone classification scheme is appropriate for Clearwater sands, as by definition lithic arenites are composed primarily of framework grains, contain little matrix materials and have an essentially open pore system (Pettijohn *et al.*, 1987) (Plate 3.1a).

The petrography of Clearwater sediments within the study area can be subdivided into three categories, framework grains, cement and diagenetic material, and porosity. Bitumen is the primary cement holding the clastic sediments together; calcite-rich zones, and shaly intervals are the only real 'lithified' portions of the formation. Porosity is variable, but in the coarsest sands may be very high, and has been reported as averaging near 35% in various locations (Jardine, 1974; Mahar, 1989). Framework grains consist of rock fragments, quartz, feldspars, dolomite, and detrital clays. There are also abundant altered grains, many of which whose original composition is difficult to ascertain. Diagenetic minerals consist primarily of glauconite, pyrite, berthierine, various clays, siderite, calcite, zeolites, and quartz and feldspar overgrowths. A number of minor detrital and diagenetic phases have also been identified. Remains of biologic materials, mainly from plants, have also been observed (Plate 3.1c).

Five main lithologies have been identified within the study area: 1) fine to medium grained 'clean' sands; 2) fine to very fine 'muddy' sands with interbedded silts and / or shales; 3) silts and / or shales with interbedded sands; 4) interstratified silts and shales; and 5) carbonate cemented equivalents of any of the above.

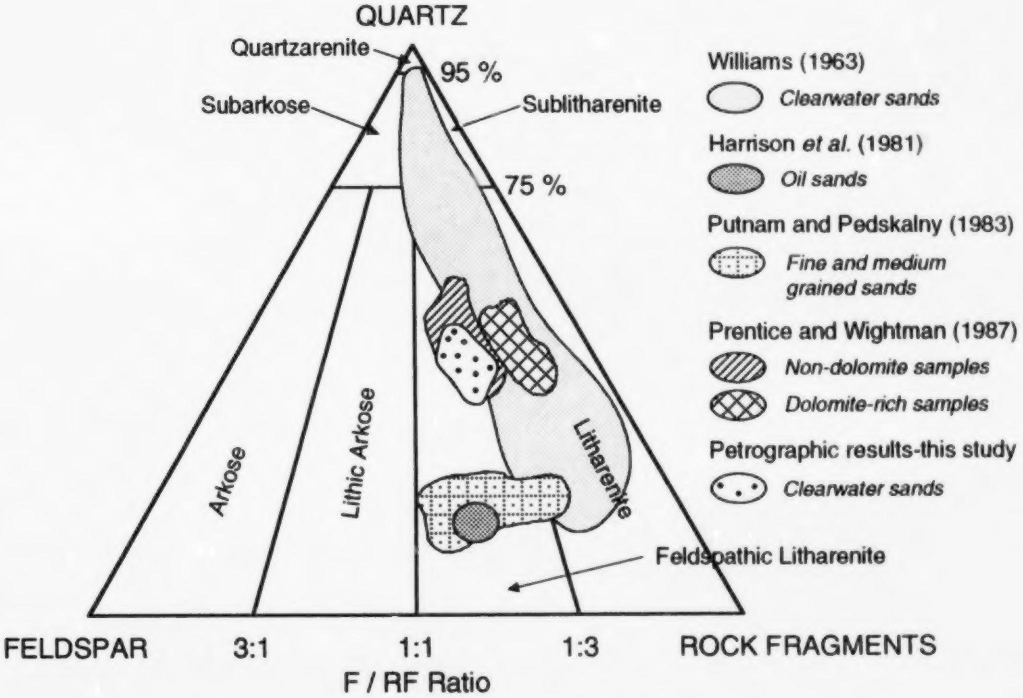

Figure 3.4: Summary of petrographic classification of samples from the Clearwater Formation from this study and by various other authors on Folk's Ternary Diagram for Sandstones.

Petrographic Study – Detrital Minerals

In terms of their detrital assemblage, fine to medium-grained Clearwater sands are dominated by rock fragments, quartz and feldspars, and contain minor amounts of dolomite, and trace levels of detrital clays and accessory minerals. The majority of the clays in sands are authigenic. Detrital framework grains (~220µm; coarsest ~350µm) range in morphology from anhedral to euhedral, although most are rounded or show some evidence of transport. Silt and shale rich clasts are also often present. Sands with interbedded silts contain the same mineral assemblage as the coarser-grained sands, but have fewer and smaller framework grains (~185µm), and more detrital clays in periodic thinly layered, fine-grained, and often organic-rich muddy interbeds (Plate 3.1b). Sandy silt or shale units also contain a fairly large proportion of framework grains, although they are smaller in size than those contained in the sand-rich units (~100µm). Interstratified silts and sands also contain moderate levels of smaller framework grains (~20µm) although they are dominated by highest proportion of detrital clays in organic-rich bedding, and do not contain bitumen. Carbonate cemented zones typically occur in sand facies, although they have also been noted in siltier units, and their highly cemented nature typically excludes bitumen in the study area.

Altered Grains

Many framework grains have been extensively altered, especially rock fragments (mainly of volcanic origin), K feldspars, plagioclase or dolomite. However, it is often difficult to identify the primary grain composition because of the extensive alteration. In such cases the grain is merely referred to as *altered* (Plates 3.1d, 3.1e, 3.1f, 3.2a, 3.8a, 3.8b, 3.10f, 3.11a, 3.11b).

Rock Fragments

Rock fragments are among the most common grains in the formation. Three types have been identified: volcanic, sedimentary, and metamorphic. Volcanic rock fragments are the most abundant, and occur as mottled greenish–brown and white grains (Plate 3.1e, 3.1f, 3.2a, 3.2b, 3.6e, 3.6f). Two main varieties have been noted (Plates 3.2c–f, 3.3a, 3.3b). The most prominent are light brown to greenish in color and generally contain laths of plagioclase feldspar. The less prominent variety are quite dark and fine grained; it is difficult to discern internal features except under higher magnification. These two varieties of volcanic fragments have been labelled as porphyritic and acidic by Putnam and Pedskalny (1983), and Prentice and Wightman (1987). Most volcanic rock fragments are fairly rounded, suggesting that they have been transported some distance, and are generally altered. Alteration may range from a fine layer of clays on the surface commonly coated with bitumen, to near complete obliteration of the original character of the grain.

Sedimentary rock fragments are the second most abundant rock fragments observed in the formation and consist of chert, and pelitic fragments of former siltstones and shales. Chert can be easily confused with volcanic rock fragments as the individual crystals of quartz are often very fine, and the grain may appear somewhat cloudy or brownish under plane polarized light (PPL) (resulting from incorporated organic matter). Differentiation can generally be made by the presence of feldspar within the volcanic fragments (lath-shaped or sometimes exhibiting albite twinning), especially at higher magnification, along with the presence of larger, dark-colored fragments under PPL. In contrast, the crystals within chert are nearly all quartz and generally of uniform size (Plates 3.3a, 3.3b, 3.4a, 3.4d). Pelitic fragments are mainly present as framework grains and are rich in detrital clays. They are often foliated and in such cases could just as easily be labelled metamorphic rock fragments. Unfoliated fragments have been classified as detrital clays in this study.

Metamorphic rock fragments are minor in proportion to volcanic rock fragments and are generally limited to grains of polycrystalline quartz, although a few other grains which may have had a metamorphic origin were noted, namely grains of deformed foliated rocks. Polycrystalline quartz can be differentiated from chert by the presence of internal sutures between grains under cross polarized light (x-polars), and grains are commonly larger than those of chert and nonuniform (Plates 3.4e, 3.4f, 3.5c, 3.5d, 3.13a).

Quartz

Quartz is the single most common mineral phase in the Clearwater Formation within all the different rock types, with the exception of a few isolated carbonate cemented samples which contain calcite as the dominate phase. It is most prominent as monocrystalline grains of volcanic origin, although detrital quartz is present in minor proportions in all types of rock fragments. Volcanic quartz is characterized by its anhedral to euhedral grain boundaries, straight extinction, absence of internal inclusions, and relatively fresh and unaltered appearance (Plates 3.1e, 3.1f, 3.2c, 3.2d, 3.4a, 3.4e, 3.4f). Alteration is limited to coatings of authigenic clay, quartz overgrowths, and dissolution and pitting in zones of pervasive carbonate cement (Plates 3.3c, 3.3d, 3.3e, 3.3f). Quartz is the most stable mineral in the formation, and therefore the most resistant to extensive dissolution within calcite cemented sands. Because of the method of thin section preparation utilized in this study, it was difficult to clearly differentiate fluid inclusions from cloudy coatings or scratches on the surface of the grain except with detailed observation at high magnification. Other forms of quartz in the study area are typically rounder (anhedral to subhedral), and may contain internal inclusions or exhibit undulose extinction (Plates 3.1e, 3.1f, 3.5c, 3.5d, 3.6e, 3.6f, 3.11f). This type of quartz has commonly been exposed to some degree of strain, and may originate from plutonic to low-grade metamorphic environments (Putnam and Pedskalny, 1983; Pettijohn *et al.*, 1987).

Feldspars

Feldspars are the second most abundant singular phase in the Clearwater Formation, leading to its classification as a feldspathic litharenite. Both plagioclase and potassium-rich feldspars are present. Anhedral grains of plagioclase feldspars generally exhibit characteristic albite twinning, although they may also be untwinned, and may be differentiated by their pink stain in thin section (Plates 3.2e, 3.2f, 3.4d, 3.6c, 3.8a, 3.8c, 3.13a). Myrmekite, a relatively unusual form of plagioclase intergrown with quartz was also observed, and likely originated from igneous rocks (Plates 3.11e, 3.11f). Its most likely source is that of the Canadian Shield, which indicates that there was some contribution of clastics from the east during Clearwater deposition. Plagioclase grains were often significantly altered, occasionally to the degree that they are difficult to differentiate from other grains. The types of alteration range from coatings of clay, partial dissolution and replacement by other phases (Plate 3.4c), to nearly complete dissolution with only a shell or rim of the original grain. The abundance of plagioclase feldspars, along with other grains, was reduced significantly in carbonate cemented zones within sand facies, resulting from partial to complete dissolution prior to cementation.

Potassium-rich feldspars (K feldspar) are generally less prominent than plagioclase in most facies, although in isolated samples were the most prominent feldspar phase. Detrital K feldspar occurs as anhedral to subhedral rounded framework grains of variable size, depending on the facies. Twinning is uncommon; grains were generally differentiated from quartz and untwinned plagioclase by the yellow stain in thin sections. Orthoclase was identified as the prominent potassium feldspar by optical petrography (Plates 3.1e, 3.1f, 3.4a, 3.5a), but grains of microcline were also observed in thin section, characterized by their *cross-hatched* or *plaid* twinning (Plate 3.4b). Most grains of potassium feldspar exhibited some alteration, including minor dissolution associated with grain coating clays, especially in sand-rich facies. K feldspar overgrowths and various degrees of dissolution were also associated with later siderite and calcite precipitation. Dissolution generally occurs along cleavage and twin lamellae planes.

Dolomite

Anhedral to subhedral grains of detrital dolomite are present within most facies, in many cases at levels (< 2%) not differentiated by XRD. Dolomite-rich zones are generally associated with sand-rich facies, and typically show a vertical gradation in dolomite abundance over a stratigraphic interval (Appendix 3, W.R. and < 45µm XRD results for well 6-31-66-2W4). Dolomite grains are generally about the same size as the accompanying framework grains in a particular sample, although they may also be smaller and broken up, filling up pore space. Grains are distinctive because of their high order white birefringence, typical rhombohedral cleavage, rounded and broken looking grain boundaries, and slight yellowish color under PPL (Plates 3.2a, 3.2b, 3.2c, 3.2d, 3.4a, 3.4e, 3.4f, 3.5c, 3.5d, 3.6c). Under SEM examination, grain terminations which appear broken under thin section are shown to also be rounded, supporting their detrital origin (Plates 3.5a, 3.5b). The origin of detrital dolomite has been attributed to the mechanical weathering and erosion of nearby Paleozoic carbonates (Prentice and Wightman, 1987). Erosion of nearby carbonates is a typical origin of detrital carbonate grains in sedimentary rocks (Pettijohn *et al.*, 1987). Dolomite in a particular sample did not appear to be related in terms of XRD abundance with the presence of any other particular mineral phase, including calcite, but in thin section the presence of dolomite was commonly associated with the presence of siderite or calcite.

Detrital Clays

The differentiation of detrital and authigenic clays in silt and clay-rich facies of the Clearwater Formation is difficult because of their fine grain size, and compositional and morphological variability. Pelitic particles containing detrital clays are characterized by their fairly large grain size (similar to that of framework grains; 100–500µm), elongate shape, and an internal composition dominated by clays. They may be difficult to impossible to distinguish from clay-rich metamorphic rock fragments as both grains are fairly soft and often flattened against the outer edge of an adjacent grain. Both may contain more than one type of clay. Occasionally a detrital clay-rich grain exhibits characteristics that suggest it is composed predominantly of one phase (i.e. chlorite), but generally detrital clays in sedimentary fragments are individually indistinguishable.

Chlorite is believed to be present only as a detrital phase within the formation, although it is volumetrically minor in abundance (authigenic forms were not observed by SEM). It can be identified in thin section by its greenish color in PPL, and by its characteristic moderate bluish-green / gray birefringence (Plate 3.2a, 3.2b). Detrital clays are present in sand facies primarily in pelitic fragments, although they may also be in fine grained organic-rich partings, or as solitary grains (Plates 3.5f, 3.6e, 3.6f, 3.11e, 3.13a).

Other detrital clays in the formation consist of clays from both mica and smectite-group assemblages. Detrital crystals of mica have been identified by thin section as framework grains in the study area. They are characterized by their elongate morphology (165–540μm), and moderate birefringence. The birefringence appears to be more characteristic of muscovite, but the crystals vary in color in PPL from a light to a darker brown, suggesting that the composition may extend towards that of phlogophite or biotite (Plates 3.3c, 3.3d, 3.5e, 3.13b). Its composition could not be differentiated from that of other 10Å clays in XRD. For the most part, most 10Å clays are thought to belong to the illitic, or hydrated-mica group of clays. The proportion of framework mica grains in proportion to the overall abundance of 10Å clays in the formation is volumetrically minor. Moderate proportions of detrital illitic clays are present in the finest facies, commonly in association with smectite group clays (this association appears to be very strong by XRD). Examination and analysis of detrital clays by SEM / EDX must be done in conjunction with XRD analyses to conclusively identify the clay phase. Detrital clays generally appear quite flattened and generally as part of fragments, not grain coats. Illite and mixed-layer illite / smectite have been identified by XRD as the prominent clay minerals in interstratified silts and shales (presumably mostly detrital). Detrital clays identified as mixed layer illite / smectites have an intermeshed, compacted, webby morphology by SEM, with little to no space between adjacent crystals (Plate 3.6a, 3.6b). Occurrences of detrital non-mixed illitic or smectitic clays were not observed by SEM, although detrital illitic clays appear to be present in silt and shale samples when analyzed by XRD.

Accessory Minerals

Detrital accessory minerals in the study area occur only in trace quantities (generally less than 1%, occasionally 2–4%), and include amphiboles, ilmenite and magnetite, as identitied by XRD. Additional accessory phases observed only in thin section tentatively include olivine (second-order birefringence and typical fractured internal morphology) (Plate 3.6c), and zircon (very high relief and second order birefringence colors) (Plate 3.6d).

Petrographic Study – Diagenetic Mineralization

Despite its shallow depth of burial (Hitchon, 1984) and minor compaction, an extensive suite of diagenetic minerals is present within Clearwater sediments in the study area . Cementation is relatively minor. It is most abundant in certain zones rich in carbonate cement; weak cementation by other diagenetic minerals is present elsewhere. The richest, most bitumen saturated sands exhibit the lowest degree of diagenetic mineralization and are cemented by viscous bitumen. Finer silt and shale-rich facies are generally more lithified because of compaction. Authigenic minerals typically occur as grain coating, pore-lining or pore-filling material, and are most abundant in silty and water saturated intervals. This suggests that the migration of hydrocarbons into the formation, and their accumulation in the sandier facies, has for the most part resulted in the attenuation of subsequent diagenetic activity in bitumen-rich units.

Glauconite

Glauconite pellets are the earliest diagenetic phase observed in the study area, and are believed to have formed during early (shallow) diagenesis. They are a prominent, although volumetrically minor phase in Clearwater sediments, present as rounded grains or pellets, composed predominantly of clays, likely of illitic (10Å) composition. Grains range in shape from nearly perfectly round to oval and somewhat kidney-shaped, and in color from olive to bright yellowish-green with a bright green to brownish-colored birefringence under cross-polars (Plates 3.1e, 3.1f, 3.2e, 3.2f, 3.3a, 3.3b, 3.3c, 3.3d, 3.4e, 3.4f, 3.6e, 3.6f, 3.7a). Glauconite grains are commonly altered and then tend to be darker and more of a brownish color, and may also be partly dissolved or broken. They are more prominent in sand-rich facies, but smaller grains have also been observed in silt and mud-rich units.

Pyrite

Pyrite is a common although volumetrically minor phase exhibiting a variety of morphologies in the study area. It is most common as well-developed spherical framboids (5–30μm), which are aggregates of small octahedrally shaped individual pyrite crystallites (up to ~1μm in size) (Plates 3.7b, 3.7c). This early pore-filling material developed at the onset of burial diagenesis, and can be coated by later diagenetic clays. Pyrite also occurs as accumulations of larger singular euhedral crystals (<1 to 10μm), or as a concentration of pore-filling octahedrons in knobbly framboids or as an aggregate with no particular morphology (Plates 3.7d, 3.7e, 3.7f). This pyrite formed relatively late in diagenesis, but prior to bitumen emplacement. Pyrite has been identified in all facies, although it appears to be preferentially concentrated in finer, mud-rich facies. Presence of the two morphologies is a clear indication that conditions favouring pyrite precipitation were present at least twice during the burial history of the formation, with the characteristic framboids being the earliest phase, developed during the onset of reducing conditions (Raiswell 1982).

Berthierine

Berthierine is an Fe-rich (and occasionally Mg-rich) trioctahedral 7Å clay with a (1:1) layer type structure typical of the serpentine-kaolin group (Brindley and Brown, 1980; Wiewióra, 1990). It has been given various names in earlier publications, such as chamosite (also a 14Å chlorite), 7Å chlorite and septechlorite (Brindley and Brown, 1980; Dean and Nahnybida, 1985).

Berthierine was identified by SEM as a grain coating and pore-lining clay, present preferentially within the thickest, most bitumen-saturated sands. They are the most prominent authigenic clays in the study area, and are volumetrically significant in sand-rich facies. They are less important in finer facies dominated by smectite group authigenic clays. The presence of berthierine was confirmed by XRD and and EDX analyses to be Fe-rich (Appendix 4). Individual crystallites of berthierine are lath-shaped with slightly ragged and crenulated edges, and and range from < 1 to 6μm in length. Individual laths can be intertwined, forming a web-like, wormy-looking mass (~6μm thick) on the surface of many framework grains (Plates 3.8b, 3.8d, 3.8e, 3.8f). It is present as grain coating material on all types of framework grains, although where it is less abundant it is generally associated more with feldspars and volcanic rock fragments than other phases such as quartz. It occurs as a characteristic green coating of grains in thin section, and has a birefringence similar to that of chlorite (anomalous bluish-green / gray) (Plates 3.2a, 3.2b, 3.2e, 3.4d, 3.4e, 3.4f, 3.8a, 3.8c). It does not appear to coat any other authigenic clays in the study area, suggesting it is of early diagenetic origin.

Calcite

Calcite is a relatively common in these sediments, and in particular is abundant as a diagenetic cement in carbonate cemented zones throughout the study area. These zones occur as relatively widespread, thin, concretion-like beds that follow the orientation of bedding. The cemented zones appear to be concentrated in sandier facies, although no other control on their positioning was observed. At least three different types of calcite cement were observed in the study area, in terms of name and paragenesis. Type 1 is an Fe-poor form (pink stain in thin section) of fibrous, somewhat *leaf-like* cement within which nearly all former framework grains and other material has been dissolved (Plates 3.9a, 3.9b). Replacement textures are not evident, and subhedral to euhedral crystals are fairly large (~100μm). This suggests that the cementing fluids were quite *caustic* and of sufficient strength (i.e. of significantly different pH), to dissolve even the most stable phases, such as quartz. Remnants of the former mineralogic assemblage include residual organic matter, and altered remains of former grains, including quartz.

Type 2 calcite is a very fine grained, pervasive calcite characterized by dissolution and replacement of detrital grains, resulting in an interlocking crystalline mosaic of calcite crystals with 'floating' remains of detrital grains, mainly quartz. Most of the more unstable phases, such as volcanic rock fragments and feldspars, have been dissolved or replaced (Plates 3.3c, 3.3d, 3.9c, 3.9d, 3.9e). Type 2 calcite cement is Fe-rich (blue stain in thin section), and very fine grained (< 10μm), especially in former fine grained organic-rich silty or shaly partings in which the replacement cement is dark in colour, very nearly micritic (<<1μm), and contains residual organic matter. The calcite cement is lighter in colour in sandier areas, and is coarser grained within the dissolved boundaries of former framework grains.

Two different generations of Type 3 calcite cement were observed; both occur as relatively coarse vein fillings that cross-cut cemented areas of Type 2 calcite. The first generation of Type 3 calcite infiltrated the former cement and dissolved all in its path, including remaining detrital material. Precipitation of sparry calcite (~180μm crystals) in the vein was initially Fe-rich (blue stain), but changed in composition over time with the last calcite precipitated being depleted in Fe (hence stained pink). Sparry euhedral to anhedral crystals within the veins are oriented initially perpendicular to the vein walls, but form a mosaic at the vein centres. The second generation of Type 3 calcite cement occurs as veinlets cross-cutting both Type 2 cement and the first generation of Type 3 cement. It has a finer crystal size in proportion to the size of the veinlets (~10μm), and also shows a progressive change from Fe-rich to Fe-poor calcite in composition.

Calcite formed at various times in the diagenetic history of the formation. Based on hand specimen and thin section examination, all three cement types reported here are believed to pre-date bitumen emplacement. The paragenetic relationship of the cements was determined texturally by optical petrography and by isotopic studies.

Authigenic Illitic and Mixed-Layer Clays

Authigenic smectite group clay minerals in the study area consist predominantly of randomly interstratified illite / smectite (I/S) and chlorite / smectite clays (C/S), and are volumetrically significant only in the finer facies. They are present as grain coating, pore-lining and pore-filling clays. Identification of these clay types was carried out solely by use of SEM and XRD as the fine size of individual crystals makes thin section identification impossible. Differentiation between the two (ie. I/S versus C/S), is not reliable based solely on SEM observations of morphology or EDX analyses, and must be done in conjunction with XRD results for a particular sample. Diagenetic illite / smectite clays phases typically occur as webby, slightly crenulated crystals (1–2μm), which are linked together, and positioned perpendicular to the surface of the associated framework grain (Plates 3.10d, 3.10e). Flakes may have somewhat wispy, or ragged looking edges, and are characterized by the presence of both K and Ca, along with Si, Al, and Mg (Appendix 4). Chlorite / smectite was not abundant in the study area, was not observed by SEM. That detected was found to be generally associated with sandier facies by XRD.

Authigenic illite was also observed in the study area. It occurs as a grain-coating and pore-filling clay, very similar in morphology to that of berthierine. It forms intertwined laths (~ 1μm thick) with characteristic wispy or fuzzy, serrated edges. They can be differentiated from berthierine by XRD analysis of the clay mineral suite in the sample, and by EDX analysis, which exhibits the presence of abundant K in illitic clays (Appendix 4). Samples were also observed that contained smectitic clays mixed with authigenic illite or berthierine. In terms of paragenetic relationships, authigenic clays minerals other than berthierine appear to have formed subsequent to berthierine and pyrite, and prior to or about the same time as authigenic quartz, feldspars and zeolites. Instances of one phase occurring both paragenetically prior to and subsequent to these authigenic clays is common. Based on their paragenetic relationships with other phases, illite / smectite, chlorite / smectite and authigenic illite are believed to have formed at a midpoint during the diagenetic burial history of the sediments. The abundance of these clays is very low in the sandiest bitumen saturated facies; however, their presence in bitumen-rich intervals within silty facies suggests that they formed prior to bitumen emplacement.

Siderite

Siderite is a relatively common phase of trace to minor abundance, ad identified using XRD, but was very difficult to distinguish petrographically. This is mainly the result of its occurrence as relatively small (20–50μm) well-developed rhombs that are very difficult to distinguish in thin section except at high magnification. Siderite rhombs may be present singularly or as aggregated pore-filling masses, and commonly occur as replacement minerals adjacent to or within the former space of dissolved feldspars or volcanic rock fragments (Plates 3.2a, 3.2b, 3.6e, 3.6f, 3.8a, 3.8b, 3.10f, 3.11a, 3.11b). Siderite appears to be associated with sandier facies (XRD), although it is still present to a lesser degree in sandy mud-rich facies, likely because of its occurrence as a replacement mineral. Siderite was also found to be a very prominent phase in many mud-rich clasts or concretions in the study area, and is present in both bitumen and water saturated sands. From its paragenetic relationships, concretionary siderite is thought to be an early phase, and replacement rhomb siderite a middle to later diagenetic phase, associated with the main dissolution of framework grains.

Feldspars

Crystals of authigenic potassium feldspar are relatively common in the formation, although volumetrically minor, and are present predominantly in water saturated sands and silty sands, although they have also been observed in bitumen saturated sands. They occur as pore-lining and pore-filling pseudorhombic blocks on the surface of framework grains, and are most commonly present as syntaxial overgrowths on grains of partially dissolved K feldspar. They have also been observed as epitaxial overgrowths on other grain types (Plates 3.7e, 3.8b, 3.11c, 3.11d, 3.11e, 3.11f, 3.12a, 3.12b, 3.12c, 3.14e). They are typically associated with other diagenetic phases, are paragenetically later than most diagenetic clays (berthierine as well as other clays), and intermixed with euhedral pyrite, zeolites and occasionally minor diagenetic phases of what is thought to be apatite.

Blocky crystals of what have been identified as diagenetic plagioclase have also been observed in the study area. They are quite rare (present at volumetrically trace levels). Plagioclase is differentiated from K feldspar and zeolites by its blocky, step-like cleavage, and Ca-rich composition (Plates 3.10e, 3.12d).

Quartz

Authigenic quartz is a trace to minor phase in the study area rocks and is present predominantly as grain coating syntaxial to epitaxial overgrowths of detrital quartz in siltier water saturated facies. Crystals generally exhibit a well developed prismatic form and are often doubly terminated, suggesting that they crystallized as open space fillings (Pettijohn *et al.*, 1987) (Plates 3.12e, 3.12f, 3.13a, 3.13b). Quartz overgrowths are believed to have formed relatively late in the diagenetic history, and are generally associated paragenetically with diagenetic illite or smectite group clays.

Zeolite

Tabular, blocky, rectangular, lath and coffin-shaped crystals of diagenetic zeolite are common, although volumetrically at trace levels (Plates 3.13c, 3.13d, 3.13e, 3.13f). They vary in size (crystals ranging from 5 to 30μm were observed), are most commonly found in water saturated sands or silts, and are present as a pore-filling cement. They have been tentatively identified as clinoptilolite by their morphology, typical monolithic symmetry, blocky habit and negative relief. They have also been found to be rich in Ca and Na by EDX analyses (Appendix 4). They may in fact be various members of a clinoptilolite-heulandite series, rather than pure clinoptilolite, which occurs as a solid-solution in many sedimentary rocks (Smyth *et al.*, 1990). Many crystals of clinoptilolite exhibit evidence of dissolution, suggesting that it is highly susceptible to alteration. The pitting suggests porewater conditions in the sediment have changed substantially from conditions under which the crystals formed. Clinoptilolite is commonly associated with grains of K feldspar, and is believed to have formed relatively late in diagenesis, generally after most but not all of the diagenetic clays, and at about the same time as authigenic feldspars and quartz.

Kaolinite

Kaolinite is a trace mineral within the Clearwater Formation in the study area. Although the 7Å peak is prominent in XRD charts for samples from the study area and more than one peak is present at approximately 3.56Å, only a few examples of the typical book-like morphology of kaolinite crystals were observed by SEM (~7–15μm) (Plates 4.14c, 3.14d). This limited abundance of kaolinite is unusual and unique to the study area, as abundant kaolinite has been reported for nearby locations in the formation (Hutcheon *et al.*, 1989; Longstaffe *et al.*, 1991). It may be that kaolinite occurs only within lithoclasts in the study area, and does not occur as a discrete phase in the pore-filling clay assemblage, as reported for a small well located within this study area investigated by the Sedimentology Research Group (1981). It was not possible to determine any paragenetic relationships for kaolinite from this study area. Kaolinite in a nearby location was reported as having a late diagenetic origin (Hutcheon *et al.*, 1989).

Minor Phases

Minor phases (< 1%) identified in the study area include: distinctive elongate crystals identified by EDX analyses to be rich in Ca, Si and P, which are suspected to be authigenic apatite (~4–25μm) (Plates 3.14d, 3.14e, 3.14f), and distinctive crystals rich in Na and Cl (EDX) with a distinctive 'melted pound of butter' morphology thought to be halite (~7–12μm) (Plates 3.14c, 3.14e). Grains are smooth on the surface as if they have been dissolved by flowing water.

X-Ray Diffraction Study

Summary tables of semi-quantitative data obtained from peak heights of characteristic XRD diffractions from whole rock, < 45μm and clay (< 2μm) fractions are given in Appendix 3. Mineral abundances obtained from peak heights are *relative* and *semi-quantitative*, and should not be interpreted as weight percents. The following mineral assemblage was identified by XRD: quartz, plagioclase, potassium feldspar, calcite, dolomite, siderite, pyrite, amphibole, ilmenite, magnetite and various clays, including 14Å chlorite, swelling clays (~12Å), those from the mica / illite group (10Å), and 7Å clays kaolinite and berthierine. Zeolites, specifically clinoptilolite, was also tentatively identified, but not included in the semi-quantitative study because its presence could not be unequivocally identified by XRD.

Whole Rock Mineralogy

Whole rock XRD results indicate that quartz and plagioclase are the most abundant phases within all lithologies in the study area with the exception of calcite-rich cemented intervals (Table 3.2). The ranges in mineral abundance for each lithologic type are given in Appendix 3. For each lithology, the proportion of the various phases, and its trends relative to the presence of authigenic cements and bitumen provide information on the diagenetic history of the formation. Fine to medium grained sands exhibit the least evidence of dissolution and diagenesis. These sands contain a high proportion of quartz (avg. of 53%, Table 3.2), and the highest abundance of both plagioclase and potassic feldspars. The relatively small proportions of clays suggests that few diagenetic changes

Table 3.2: Average Whole Rock XRD Mineral Abundance Results by Lithology.

LITHOLOGY / BITUMEN SATURATION	XRD RELATIVE ABUNDANCE (%)*														
	Qtz	Pl	KF	Chl	SC	10Å	7Å	Cal	Dol	Sid	Py	Amp	Ilm	Mag	Total
Fine to Medium Grained Sands															
Oil (Bitumen) Sands	52.8	23.4	7.9	1.1	0.6	4.5	4.0	0.0	0.7	3.1	0.4	0.1	0.3	1.0	100
Water Sands	54.2	23.3	3.1	1.5	0.5	4.8	6.7	0.0	0.0	3.5	0.2	0.4	1.8	0.0	100
Average:	52.9	23.4	7.5	1.2	0.6	4.5	4.2	0.0	0.7	3.1	0.4	0.2	0.4	0.9	100
Very Fine to Fine Grained Sands with Silt or Shale															
Oil (Bitumen) Sands	52.9	19.3	6.5	1.5	2.4	7.3	5.0	0.1	2.2	1.0	0.7	0.4	0.0	0.6	100
Water Sands	54.9	13.8	4.6	1.9	4.3	8.5	4.3	0.0	5.5	0.3	0.9	1.0	0.0	0.0	100
Average:	53.3	18.3	6.2	1.5	2.8	7.5	4.9	0.1	2.8	0.9	0.7	0.5	0.0	0.5	100
Sandy Silts or Shales															
Oil (Bitumen) Samples	50.5	15.4	3.6	1.6	5.9	11.4	4.1	0.7	1.9	3.0	0.9	0.7	0.0	0.3	100
Water Saturated Samples	47.8	7.5	6.1	3.6	11.4	13.7	2.8	0.0	2.5	2.6	1.3	0.7	0.0	0.0	100
Average:	49.4	12.2	4.6	2.4	8.1	12.3	3.6	0.4	2.2	2.8	1.1	0.7	0.0	0.2	100
Silts and Shales															
Average, Water Samples:	56.5	10.6	3.6	2.0	8.7	10.9	6.3	0.0	0.0	0.0	1.2	0.2	0.0	0.0	100
Calcite Cemented Zones															
Average:	25.9	9.0	4.2	0.9	0.6	5.3	2.3	45.9	2.1	2.2	0.7	0.7	0.0	0.2	100
Recalculated to 0% calcite basis:	47.8	16.5	7.8	1.7	1.2	9.8	4.2	0.0	3.9	4.1	1.4	1.2	0.0	0.4	100

* Results expressed as normalized relative abundances based on peak heights, not weight percent;
Qtz=quartz, Pl=plagioclase, KF=K feldspar, Chl=14Å chlorite, SC=swelling clays (~12Å), 10Å=mica / illite group clays;
7Å=kaolinite and / or berthierine clays, Cal=calcite, Dol=dolomite, Sid=siderite, Py=pyrite, Amp=amphiboles, Ilm=ilmenite, Mag=magnetite.

have taken place in these sediments. This trend is most prominent for oil-rich (bitumen saturated) sands. Water sands have a higher component of 7Å clays, and a slightly greater proportion of 10Å clays. This again suggests that some attenuation of diagenesis was associated with bitumen emplacement.

Results for fine to medium grained sands (Appendix 3) indicate that bitumen-rich sands occur in all sand-rich depositional environments, but are most abundant in the coarser, more proximal upper and middle delta front settings. Only two samples were available for water saturated sands, both from lower delta front environments, located stratigraphically within the lower section of the formation.

A number of other trends are also evident from the data in Appendix 3. The proportion of quartz, plagioclase and chlorite are all relatively stable, indicating either a constant supply from the source areas during deposition, little diagenesis, or both. The proportion of K feldspar, in contrast, is much less stable, suggesting that this phase was more susceptible to dissolution. Indeed, samples containing the higher proportions of 7 and 10Å clays are generally those with the lower K feldspar abundances. The highest values for swelling clays are generally associated with lowest plagioclase abundances, although interpretation of such trends are difficult because of the normalization of the results.

In general, the coarsest grained bitumen saturated sands such as sample LW-87-CW-28 contain a high proportion of framework grains coated by berthierine type 7Å clays, and show few other diagenetic effects. In this sample, only diagenetic K feldspar was observed an additional phase (Plate 3.8a). Water saturated sands such as LW-87-CW-26, however, contain many authigenic phases, including berthierine, pyrite, K feldspar and quartz overgrowths, zeolite and kaolinite and salt. Many of these phases are extremely susceptible to dissolution by steam, and along with dissolution of detrital phases may contribute to subsequent precipitation of pore-filling and blocking phases such as smectite, calcite and analcime (Kirk *et al*., 1987).

Whole rock XRD abundances for very fine to fine grained muddy sands also indicate that diagenetic clays (swelling clays, 7Å clays and some 10Å clays) tend to be more prominent in water saturated sands (Table 3.2). This strongly supports the hypothesis that bitumen emplacement limited subsequent diagenetic effects. These sediments also contain on average less plagioclase, 10Å clays and siderite than the cleaner sands, and more dolomite. For plagioclase, dolomite and to some degree 10Å clays, this difference probably results from variation in provenance. Other differences are probably diagenetic in origin.

Relative to the sandier units, sandy silts or shales contain less plagioclase, slightly more chlorite, more swelling clays, more 10Å clays, less 7Å clays, more pyrite, more amphiboles and less magnetite (Table 3.2). Greater proportions of detrital clays are likely associated with the mainly lower delta front and delta fringe environments of these samples (Appendix 3). Bitumen saturation tends to be very low or absent. In general, samples from this lithology are characterized by diagenetic pyrite, illite, K feldspar, plagioclase and quartz overgrowths, zeolites and minor diagenetic phases (LW3-13, LW-87-CW-17 and LW-87-CW-33; Plates 3.10a, 3.10b, 3.13e, 3.12f). Pyrite is more prominent in the water saturated samples, perhaps because these units are finer grained and may contain more organic matter. In terms of mineral associations, higher levels of siderite appear to be associated with high 10Å clay contents and lower plagioclase (± K feldspar). The one sample from the Wabiskaw Member contains more quartz and chlorite and less plagioclase than other Clearwater samples.

Three silt and shale samples from delta fringe environments were useful in interpreting the mineralogy of the detrital clays (Appendix 3). These samples are rich in quartz, poor in plagioclase and K feldspar. They also have a high proportion of 10Å clays, chlorite, swelling clays, 7Å clays and pyrite (Table 3.2). The pyrite is thought to have formed authigenically. Detailed analysis of the 7Å clays was not carried out in this study, although many of them are suspected to be detrital kaolinites. Authigenic berthierines and kaolinites were not observed by SEM. The other minerals are all thought to be of detrital origin.

Calcite cemented intervals within the study area contain on average 46% calcite; 7Å clays, pyrite, and siderite are also present in addition to detrital quartz and feldspar (Table 3.2). Higher than average proportions of clays in calcite cemented intervals are commonly associated with shale-rich samples or lower concentrations of calcite, which suggests that this clay is of detrital origin.

The average composition of calcite cemented intervals from the study area was recalculated without calcite (renormalized to a calcite free basis, Ca = 0%), to permit the comparison of the abundance of its other mineral phases with other non-cemented lithologies (Table 3.2). The samples contain a fairly high proportion of quartz, plagioclase and K feldspar, similar in fact to the very fine to fine grained silty or shaly sands which are the typical host lithologies for these cemented intervals. However, there are less swelling clays, more 10Å clays, more siderite and more pyrite in the cemented intervals. This behavior may suggest that the bulk of the authigenic swelling clays formed subsequent to the main phase of calcite cementation, and that siderite, pyrite and some 10Å clays (likely glauconite type) formed prior to this cementation.

Only limited generalizations were possible from examination of the XRD characteristics of whole rock samples rich in dolomite and siderite allows only limited generalizations (Appendix 3). Dolomite-rich zones are concentrated within sandy units, but typically units containing a certain proportion of mud (very fine to fine grained sands with silts or shales, or sandy silts or shales). Lower delta front and delta fringe are the most prevalent depositional environments, although dolomite is also present in middle and upper delta front environments within the study area. This translates to the presence of more and thicker dolomite zones in transitional delta front environments in an area extending from relatively proximal to the most distal offshore environments.

Siderite-rich zones are present within all lithologies in the study area, but are clearly concentrated in the sandiest facies. They are the most prevalent in 'clean' sands, only a few silty or shaly siderite-rich samples were observed, excluding siderite in mud clasts. Authigenic siderite is likely concentrated in these environments because of its dominant presence as a replacement for altered framework grains.

< 45μm Mineralogy

As expected, the < 45μm fraction of the samples examined by XRD tends to contain fewer detrital framework grain components than the whole rock fraction, more diagenetic minerals and clays. The ranges in mineral abundance for each lithologic type are listed in Appendix 3, and summarized in Table 3.3. Within the < 45μm fraction, fine to medium grained sands contain the highest proportion of 7Å clays. A large quantity of 10Å clays and siderite is also present in this facies, with water saturated sands being the most enriched. The greater proportion of 10Å clays is somewhat as surprising the bulk of the contribution of 10Å clays from glauconite pellets would be expected to remain in the > 45μm fraction. This behavior suggests that authigenic 10Å clays such as illite are present, as a large proportion of detrital 10Å clays would not be expected in such clean sands. The alternative is that the glauconite was broken up during preparation of the sample. The increase in the proportion of siderite in the < 45μm fraction reflects its fine crystallite size.

Very fine to fine-grained sands with silt or shale on average exhibit an increased fraction of 7 and 10Å clays in the < 45μm fraction, in addition to siderite, pyrite, chlorite

Table 3.3: Average < 45μm XRD Mineral Abundance Results by Lithology.

LITHOLOGY / BITUMEN SATURATION	XRD RELATIVE ABUNDANCE (%)* Qtz	Pl	KF	Chl	SC	10Å	7Å	Cal	Dol	Sid	Py	Amp	Ilm	Mag	Total
Fine to Medium Grained Sands															
Oil (Bitumen) Sands	41.0	23.7	4.0	2.0	2.7	5.8	9.2	0.1	1.3	7.1	1.1	0.3	0.0	1.7	100
Water Sands	37.8	17.6	4.3	2.4	1.3	10.1	12.7	0.0	0.0	9.7	1.3	0.3	2.5	0.0	100
Average:	40.7	23.2	4.0	2.0	2.6	6.2	9.5	0.1	1.2	7.4	1.1	0.3	0.2	1.6	100
Very Fine to Fine Grained Sands with Silt or Shale															
Oil (Bitumen) Sands	47.5	16.7	4.5	2.3	4.0	9.9	6.9	0.0	2.0	3.4	1.3	0.6	0.0	0.8	100
Water Sands	52.5	10.5	4.6	2.0	5.3	9.1	5.9	0.0	6.6	1.0	1.5	1.0	0.0	0.0	100
Average:	48.4	15.6	4.5	2.2	4.2	9.8	6.7	0.0	2.8	3.0	1.3	0.7	0.0	0.7	100
Sandy Silts or Shales															
Oil (Bitumen) Samples	50.7	10.2	3.0	2.3	7.3	13.3	4.9	0.8	2.4	3.1	1.1	0.9	0.0	0.0	100
Water Saturated Samples	49.5	8.3	4.8	2.5	9.5	10.6	4.4	1.7	3.2	2.2	2.0	0.9	0.3	0.0	100
Average:	50.1	9.4	3.9	2.4	8.3	12.1	4.6	1.2	2.8	2.6	1.5	0.9	0.1	0.0	100
Silts and Shales															
Average, Water Samples:	59.9	7.6	4.1	1.8	8.9	10.0	4.5	0.0	0.8	0.0	1.7	0.7	0.0	0.0	100
Calcite Cemented Zones															
Average:	23.6	4.6	1.5	1.3	0.9	5.8	2.4	49.4	2.8	4.3	2.6	0.7	0.0	0.0	100
Recalculated to 0% calcite basis:	46.7	9.1	3.0	2.5	1.8	11.5	4.8	0.0	5.5	8.5	5.1	1.4	0.0	0.0	100

* Results expressed as normalized relative abundances based on peak heights, not weight percent;
Qtz=quartz, Pl=plagioclase, KF=K feldspar, Chl=14Å chlorite, SC=swelling clays (~12Å), 10Å=mica / illite group clays;
7Å=kaolinite and / or berthierine clays, Cal=calcite, Dol=dolomite, Sid=siderite, Py=pyrite, Amp=amphiboles, Ilm=ilmenite, Mag=magnetite.

and swelling clays (Table 3.3). The proportions of quartz, plagioclase, and K feldspar are decreased relative to whole rock samples, and there is a smaller difference between the bitumen saturated and water saturated samples from this facies. As with the clean sands, siderite and pyrite are concentrated in the < 45µm fraction. High abundances of 10Å and 7 Å clay are commonly associated, probably because of the preferential formation of authigenic 7Å berthierine and 10Å clays, including glauconite, in sandier environments.

The < 45µm fraction of the sandy silts or shales contains more clays and dolomite, siderite and pyrite than the whole rock fraction (Table 3.3). One significant difference is that the proportion of 10Å and swelling clays in the water saturated sands actually decreased in the < 45µm fraction (relative to the W.R. fraction). This may be the result of these clays adhering to the framework grains during separation. The increase in dolomite abundance from an average of 2.2 to 2.8% is not significant, but suggests that there are many dolomite grains smaller than < 45µm; this observation is important, because dolomite is highly reactive during steam injection, and the finer its grain size, the faster dissolution will occur.

There is very little change in the average composition of silts and shales from the < 45µm to whole rock fractions (Table 3.3). The average composition of the calcite cemented intervals (recalculated to a 0% calcite basis) exhibits similar trends to that of very fine to fine-grained 'muddy' sands which are its predominant host lithology (Table 3.3). As with other lithologies, the proportion of framework grains decreased, and clays and authigenic minerals increased in the < 45µm fraction.

Clay (< 2µm) Mineralogy

The results of XRD analysis of clay minerals (< 2µm) from three wells are given in Table 3.4, and can be summarized as follows:

1) A primary assemblage of mainly detrital dioctahedral mixed-layer illite / smectite (I/S) (47–67%), and 10Å illitic clays (22–43%), with minor 14Å chlorites (1–8%), and a small fraction of diagenetic 7Å kaolinite ± berthierine? clays (2–9%). This assemblage occurs prominently in silts and shales, as well as sandy facies containing abundant shales and shale fragments.
2) A mixed detrital / diagenetic assemblage of dioctahedral mixed-layer illite smectites (I/S) (20–58%), 10Å illite / mica group clays (24–52%), diagenetic 7 Å clays (14–49), and minor detrital 14Å chlorite (1–7%). This assemblage occurs primarily in silt or shale-rich 'muddy' sands and sandy silts.

Table 3.4: Summary of Clay Mineral Data.

SAMPLE NUMBER	DEPTH (metres)	DEPOSITIONAL CHARACTERISTICS			CLAY ABUNDANCE (XRD)*					ASSM.	COMMENTS
		Lithology	Environment	Sequence	SC¥	Chl	10Å	7Å	% Sm		
Well 3-13-65-4W4 Esso 84 (C1-12) Cold Lk.											
LW-87-CW-28	470.25	f.-m.g.sst	UDF-DC	S1, C3	11	7	7	76	79†	3	SC=dioct. I/S (octa.sub.)±C/S; 7Å=Be
LW-87-CW-29	480.20	f.-m.g.sst	UDF-DMB	S1, D2	12	6	19	63	61†	3	SC=dioct. I/S ± C/S; 7Å=Be
LW-87-CW-31	480.80	f.-m.g.sst	UDF-DMB	S1, D2	19	3	10	68	60	3	SC=I/S; 7Å=Be ± Ka
LW-87-CW-32	481.00	f.g.sst	UDF-DMB	S1, D2	15	5	2	77	55	3	SC=dioct. I/S; 7Å=Be
LW-87-CW-33	481.10	sh,sst,si	UDF-DMB	S1, D2	24	1	52	23	72†	2	SC=I/S; 7Å=Be
LW-87-CW-34	481.20	f.g.sst,m	L/MDF	S2, B	34	4	41	22	69	2	SC=I/S; 7Å=Be
LW-87-CW-35	481.30	f.g.sst,tr.sh	L/MDF	S2, B	25	5	38	32	61†	2	SC=dioct. (octa.sub.) I/S; 7Å=Be
LW-87-CW-36	481.40	f.g.sst	L/MDF	S2, B	20	7	24	49	57	2	SC=I/S; 7Å=Be ± Ka
LW-87-CW-37	481.60	f.g.sst,m	L/MDF	S2, B	23	3	25	49	58	2	SC=I/S; 7Å=Be ± Ka
LW-87-CW-39	482.20	f.g.sst,si	L/MDF	S2, B	29	4	32	36	62†	2	SC=I/S; 7Å=Be ± Ka
LW-87-CW-40	483.20	f.g.sst	L/MDF	S2, B	12	6	26	56	53	3	SC=dioct. I/S ± C/S; 7Å=Be ± Ka
LW-87-CW-41	491.20	f.g.sst	UDF-DMB	S2, C	17	10	24	49	61†	3	SC=I/S ± C/S; 7Å=Be ± Ka
Well 8-19-66-2W4 Esso 86 Marie O.V.											
LW-87-CW-43	473.70	f.g.sst,m	LDF	S1, D	39	4	38	19	75	2	SC=I/S; 7Å=Be ± Ka
LW-87-CW-44	474.00	f.g.sst	LDF	S1, D	12	6	16	66	73	3	SC=dioct. (octa.sub.) I/S; 7Å=Be
LW-87-CW-46	474.30	f.g.sst,si	LDF	S1, D	35	3	31	31	62	2	SC=I/S; 7Å=Be ± Ka
LW-87-CW-47	474.40	si,sh	DF	S2, A	52	3	43	2	80†	1	SC=I/S; 7Å=Be ± Ka
LW-87-CW-48	474.50	sh,si	DF	S2, A	47	1	43	8	76†	1	SC=I/S; 7Å=Be ± Ka
LW-87-CW-49	474.60	f.g.sst,sh	DF	S2, A	66	1	28	5	70	1	SC=I/S; 7Å=Be ± Ka
LW-87-CW-50	474.80	sh,si	DF	S2, A	64	2	31	3	69	1	SC=I/S; 7Å=Be ± Ka
LW-87-CW-51	475.00	sh,f.g.sst	DF	S2, A	63	3	32	2	76†	1	SC=I/S; 7Å=Be ± Ka
LW-87-CW-54	475.90	f.g.sst,si	LDF	S2, B	39	5	32	25	71†	2	SC=I/S; 7Å=Be ± Ka
LW-87-CW-56	477.40	sh,si,c	LDF	S2, B	52	7	38	3	58	3?°	SC=C/S ± Sm; 7Å=Be ± Ka

Table 3.4 (cont'd): Summary of Clay Mineral Data.

SAMPLE	DEPTH	DEPOSITIONAL CHARACTERISTICS			CLAY ABUNDANCE (XRD)*					ASSM.	
NUMBER	(metres)	Lithology	Environment	Sequence	SC¥	14Å	10Å	7Å	% Sm		COMMENTS
Well 16-2-66-3W4 Imp. 77 Medley O.V.											
LW-87-CW-62	464.24	f.g.sst,si	LDF	S1, D	25	7	17	51	61	3	SC=Trioct. C/S ± dioct. I/S; 7Å=Be
LW-87-CW-63	464.44	f.g.sst	LDF	S1, D	21	4	20	54	56	3	SC=Trioct.C/S ± dioct.I/S; 7Å=Be±Ka
LW-87-CW-66	464.84	f.g.sst,sh,c	DF	S2, A	48	8	40	5	56	1	SC=C/S ± I/S; 7Å=Be ± Ka
LW-87-CW-67	465.03	f.g.sst	DF	S2, A	40	7	31	22	78	2	SC=Dioct. I/S ± C/S; 7Å=Be
LW-87-CW-69	465.85	f.g.sst,si	DF	S2, A	58	4	24	14	78†	2	SC=I/S; 7Å=Be ± Ka
LW-87-CW-70	466.65	f.g.sst,si,sh	DF	S2, A	63	2	26	9	69†	1	SC=I/S; 7Å=Be ± Ka
LW-87-CW-71	467.07	f.g.sst	DF	S2, A	67	3	22	8	66	1	SC=I/S; 7Å=Be ± Ka
Averages for assemblages:											
Assemblage 1: *mainly detrital clays*					59	3	33	5	65		
Minimum Value					47	1	22	2	56		
Maximum Value					67	8	43	9	70		
Assemblage 2: *mixed detrital and diagenetic clays*					33	4	33	29	67		
Minimum Value					20	1	24	14	57		
Maximum Value					58	7	52	49	78		
Assemblage 3: *mainly diagenetic clays*					16	6	16	62	60		
Minimum Value					11	3	2	49	53		
Maximum Value					25	10	26	77	73		

* Results expressed as normalized relative abundances based on peak heights, not weight percent; ASSM.=Assemblage;
Chl=chlorite, 10Å=illite / mica and other 10Å clays, Be=berthierine, Ka=kaolinite;
¥ SC = smectitic clay; including smectite, and mixed layer illite/smectite (I/S) or chlorite/smectite (C/S);
trioct.=trioctahedral, dioct.=dioctahedral, octa.sub.=octahedrally substituted;
† questionable value; due to poor form of saddle on Ca glycol chart; ° not included in statistics calculations for assemblages;
sst=sand, si=silt, sh=shale, m=mud, c=carbonate cemented, d.m.=drilling mud; v.f.g=very fine grained, f.g.=fine grained, m.g.=medium grained;
UDF=Upper Delta Front, MDF=Middle Delta Front, LDF=Lower Delta Front; Dist.Chl.=Distributary Channel, Dist.MB=Distributary Mouth Bar;
DF=Delta Fringe, S1=Sequence S1, S2=Sequence S2, A1–D4=respective cycle designations (see Appendix 1).

3) A mainly diagenetic assemblage consisting of a large fraction of diagenetic 7Å berthierine-type clays (49–77%), 10Å illite group clays (2–26%), and a mix of dioctahedral illite / smectite (I/S), trioctahedral chlorite / smectite (C/S) mixed-layer clays (11–25%), and minor detrital 14Å chlorite (3–10%). This assemblage occurs primarily in fine to medium grained 'clean' sands or slightly silty sands.

The identity of the 7Å clays from assemblage 1 could not be differentiated because an examination of (060) peaks was not carried out for these samples. The composition of the detrital phases in this assemblage are assumed to be representative of detrital clays in assemblages 2 and 3. Therefore, the detrital assemblage within assemblage 2 likely contains some detrital mixed-layer illite / smectites and the 10Å illitic clays, but this alone probably cannot account for their high abundance in these sand-rich samples. Within assemblage 3, the mix of smectite group clays was dominated by either chlorite / smectite (C/S) or illite / smectite (I/S), depending on the sample. Overall, when it was possible to confirm the identity of the 7Å clay in a sample it was always berthierine. Kaolinite was not unequivocally identified as the 7Å clay in any sample in the study area studied by XRD (more 060 scans would be required).

One anomalous sample was also examined that did not fit within any of these assemblages. It is a sample of calcite cemented silt and shale contained within the lower sampled interval of well 8-19-66-2W4. It is composed primarily of mixed-layer chlorite / smectite clays ± smectite (52%), 10Å illitic clays (32%), and minor components of 14Å and 7Å clays (7 and 3%, respectively).

A strong correlation was observed between the presence of bitumen in the samples and the associated clay mineral assemblage (comparison of Tables 3.1 and 3.4): Samples containing significant bitumen (moderate–high), assemblage 3; those of low to moderate bitumen saturation, assemblage 2; and water saturated samples or those with only a trace presence of bitumen, assemblage 1.

The various clay minerals were identified by their characteristic responses to the treatments applied prior to and during XRD study. A summary of the responses used to differentiate between clay minerals in the study area is given in Table 3.5. In general, the presence of chlorite can be confirmed by its prominent 14Å (001) peak on various charts, primarily the K^+ 0% RH and 300°C charts where it is not hidden by the presence of swelling clays. Illite and mica group clays, including the mineral glauconite if present, is identified by its prominent 10Å (001) spacing. Kaolinite, a dioctahedral clay, and

Table 3.5: **Primary XRD Peaks and Characteristic Treatment Responses used in the Identification of Clay Minerals in the Study Area***

SAMPLE TREATMENT	CHLORITE	ILLITE	KAOLINITE	BERTHIERINE	SMECTITE	MIXED - LAYER SMECTITES™	
						Illite / Smectite	Chlorite / Smectite
Random Oriented Mounts (Backpacks)							
WHOLE ROCK¥ or < 45µm peaks	14.0–14.5 (001)	9.9–10.3 (001)	7.08–7.24 (001) 3.58–3.56(002)†	7.08–7.24 (001) 3.52–3.54(002)†	14.2–15.4†	12.2–13.7 (001)	14.3–14.4 (001)
Na+ saturated (060) clay peaks	1.50-Dioct.† 1.54-Trioct.†	1.49–1.50†	1.489†	1.563† (1.54–1.56)	1.49–1.50-Dioct.† ~1.54-Trioct.†	1.49–1.52-Dioct. 1.53–1.54-Tioct.	var.~1.50-Dioct. var.~1.54-Trioct.
Basal Oriented Mounts (Ceramic Discs)							
Ca2+ saturated 54 % RH	no change	if symmetrical no change	no change	no change	expansion to ~15.4 (001)†	expansion to 15.1–16.1§(001)	expansion to 14.8–16.0 (001)
Ca2+ saturated Glycol saturated	no change	may become asymmetrical	no change	no change	expansion to ~17.2 (001)†	expansion to 17.0–17.7∞(001)	expansion to 16.3–17.8∞(001)
Ca2+ saturated Glycerol saturated	no change	may become asymmetrical	no change	no change	expansion to 17–17.8 (001)†	~15.0-Tetra.sub.† ~17.8-Octa.sub.	~15.0-Tetra.sub.† ~17.8-Octa.sub.
K+ saturated 0 % RH	no change	no change to slight sharp.	no change	no change	collapse to ~10 (001)†	collapse to ~10 (001)	collapse towards 10 (001) (broad)
K+ saturated 54 % RH	no change	no change	no change	no change	expansion to ~12.5 (001)†	expansion to 12.5–13.9§(001)	expansion to 12.6–15.4 (001)
K+ saturated 300 °C	no change	no change	no change	no change	collapse to ~10 (001)†	collapse to 10 (001)	collapse towards 10 (001)
K+ saturated 550 °C	slight inc. and shift in (001)	no change	destroyed-peaks disappear	destroyed-peaks disappear	complete collapse to ~10 (001)	complete collapse to 10 (001)	collapse to 10 (001)

* all peak values reported in Angstroms (Å); ¥ values are those actually observed in study area; † theoretical values; inc.=increase, var.=variable; Dioct.=dioctahedral, Trioct.=trioctahedral, Tetra.sub.=tetrahedrally substituted, Octa.sub.=octahedrally substituted;
§ value higher than theoretical, may be due to presence of some C/S; for Ca2+ 54% avg. is ~15.3; for K+ 54% avg. is ~12.2–12.6;
∞ value is higher than normal for treatment; may have occurred if glycol on surface of sample; ™ randomly interstratified.

berthierine, a trioctahedral clay, both have their most prominent (001) basal diffraction at approximately 7Å. The second most prominent diffraction (002), in theory can be used to differentiate between kaolinite and berthierine, but did not prove to be very useful in the study. Differentiation of the two species is best accomplished by examination of their (060) diffractions (Table 3.5).

For the samples analyzed in this study, differentiation of smectite and smectite group mixed-layer swelling clays can only be accomplished by controlling humidity and the composition and thickness of interlayer components as indicated in Table 3.5. Smectite and illite / smectite expand to approximately 15.4Å with one interstitial water layer (Ca^{2+}, 54% RH), and to approximately 17Å when interlayer sites are saturated with ethylene glycol, although this may vary with the percentage of smectite layers in the interlayer (F. Longstaffe, per. comm.[2]). Chlorite / smectite may also expand with interlayer water, but the degree of expansion is much less predictable, and is generally dependent upon the amount of smectite in the mixed-layer. Upon glycolation, chlorite / smectite again has a wider range of potential expansion positions. In the study area, this ranged from 16.3 to 17.8Å (Table 3.5). The expansion associated with glycolated samples for both mixed-layer species extended in many cases beyond the theoretical 17.2–17.4Å predicted in the literature. The reason for this is not known, although presence of excess glycol on the surface of the sample may have resulted during saturation, despite the fact that normal techniques were closely followed. The percentage of smectite in mixed-layer smectite species was also estimated by measuring the height of the low angle saddle resulting from the mixed-layer at $\sim 4°2\theta$ on the Ca^{2+} glycol diffractogram (Table 3.5). The technique followed was that of Inoue *et al.* (1989). Presence of this saddle is characteristic of randomly interstratified mixed-layer smectites (Inoue *et al.*, 1989), typical of those in the study area . A few samples were also saturated with glycerol in order to differentiate between tetrahedral isomorphous ion substitution in a smectite (such as beidellite), versus octahedral isomorphous substitution (such as in mortmorillonite) (Thorez, 1976; Brindley and Brown, 1980). In all samples examined, smectite group clays were found to be octahedrally substituted. Examination of characteristic (060) peaks also allowed differentiation of the dioctahedral or trioctahedral character of smectite group clays (i.e. how many octahedral sites were occupied). In all samples examined, illite / smectite clays were found to be dioctahedral, and chlorite / smectite clays trioctahedral.

---

[2] University of Western Ontario, London, Ontario, Canada.

Berthierine is the most prominent in samples from well 3-13-65-4W4, located in the southwestern corner of the study area within thick, bitumen saturated upper and middle delta front sands (Table 3.4). The 10Å clays are the next most abundant, and are primarily illitic, with (001) peaks that have an asymmetry typical of hydrated micas. Presumably, minor contribution of 10Å primary micas are also included within this diffraction, plus any glauconite resulting from the small or broken glauconite pellets. Smectitic clays are also abundant in the samples from this well, and consist primarily of dioctahedral I/S, with minor components of trioctahedral C/S, mainly in the coarsest grained sands in the upper and lowest sampling positions in the well in distributary channel and mouth-bar deposits. The proportion of 14Å chlorite clay is fairly steady within the sampled interval, suggesting that it is of detrital origin.

The < 2μm clays from well 16-2-66-3W4 consist of relatively constant amounts of chlorite and illitic clays, but the proportions of smectitic and 7Å clays are highly variable and dependent on grain size and hence depositional environment (Table 3.4). Sand facies from lower delta front environments typically contain high proportions of 7Å clays, and the smectitic clays consist mostly of trioctahedral chlorite / smectite and dioctahedral illite / smectite. Sands from delta fringe environments consist primarily of mixed-layer dioctahedral illite / smectite, with a minor component of berthierine ± kaolinite.

The < 2μm fractions of samples from well 8-19-66-2W4 consist primarily of illite and smectite group clays, but 7Å clays are also abundant in fine grained sands (Table 3.4). The 7Å clays within delta fringe samples from this well are identified as berthierine ± kaolinite and the abundance of 14Å chlorite is minor and relatively stable. Overall, in the two depositional settings (lower delta front and delta fringe; Table 3.4), there is an inverse relationship between the proportion of 7Å clays and smectitic clays. High abundances of smectitic clays are associated with minor amounts of 7Å clays and vise versa. This can be an indication of the predominant environments for the formation of these two clays, whereby (detrital ± authigenic) smectitic clays are associated more with fine grained, lower porosity environments in the study area, and 7Å clays (specifically berthierine) are typically found in the higher porosity sands. Overall, the percentage of smectite in mixed-layer clays does vary greatly, ranging between 53 and 80%, and there is a slight diminishment in % smectite with depth, with less smectite in C/S clays than I/S.

Elemental Geochemistry

X-Ray Fluorescence Results

Average geochemical variations for major oxides and trace elements have been calculated for Clearwater lithologies and are summarized in Tables 3.6 and 3.7. Very fine to fine grained sands with interstratified silt or shale were broken down into silty sands,shaly sands, and silty and shaly sands. Only a limited number of samples is present in each lithology; therefore the results are likely not representative, although they do represent a sample of this lithology within the study area.

Shales and sandy shales exhibit the highest loss on ignition (L.O.I.), likely because of abundant organic matter, and higher sulphur compositions (as pyrite), and clays. The highest major oxide contents in shaly facies are Al_2O_3, Fe_2O_3, and K_2O. Fine to medium grained clean sands contain the highest values of SiO_2, Na_2O, and CaO. Major element compositions for silty samples (silty sands and silty and shaly sands) lie between these two end members, whereas other oxides, namely K_2O, TiO_2 and P_2O_5 show little variability. Calcite cemented intervals are distinct from the other lithologies, and are characterized (as expected) by low values of SiO_2, Al_2O_3, K_2O and TiO_2, and high values of CaO, MgO, and MnO.

The high Al_2O_3, Fe_2O_3, and K_2O values in shaly rocks are likely the result of their concentration in aluminosilicates, mainly clays, with minor iron also present within pyrite. The prominence of SiO_2, Na_2O and CaO in sands is attributable to the large abundance of silicate such as quartz and chert, in addition to other aluminosilicates. Na and Ca are likely concentrated in rock fragments, feldspars, minor clays and zeolites.

It is possible to characterize the maturity of a sandstone based on its chemical compositional by using a plot of log (Na_2O / K_2O) versus log (SiO_2 / Al_2O_3) (Pettijohn *et al.*, 1987). Comparable to the modal analysis in the petrographic study, samples from the study area plot predominantly as litharenites, although they are approaching the classification of graywacke because of the high abundance of alkali metals in rock fragments (Figure 3.5).

In terms of their trace element composition, the fine to medium grained sands contain abundant Sr and Ba (more than the other lithologies), shale-rich rocks contain more Nb, Y, Rb, Ga, Cu and V, and silty facies contain the most Zr, Pb and Cr. Sulphur is equally abundant in silty and shaly sands, and low in 'clean' sands. The calcite cemented sample is depleted in Nb, Zr, Rb, Ba, La, Cu, Ni, Cr, V and S, and enriched in Sr and Zn.

Table 3.6: Summary of Average XRF Major Oxide Elemental Results by Lithology.

LITHOLOGY	No. of samples	XRF ELEMENTAL ANALYSIS (%) – Raw Data											
		LOI	SiO2	Al2O3	Fe2O3	Na2O	K2O	CaO	MgO	TiO2	P2O5	MnO	Total
Fine to Medium Grained Sands													
Average:	3	4.5	70.6	12.1	4.25	2.33	2.11	1.56	1.62	0.42	0.14	0.04	99.7
Very Fine to Fine Grained Sands with Silt or Shale													
Silty Sands	6	8.0	65.5	13.4	4.85	2.24	2.12	1.32	2.00	0.55	0.14	0.03	100.2
Shaly Sands	9	6.8	68.1	13.2	4.19	2.04	2.13	1.25	1.71	0.50	0.13	0.03	100.1
Silty and Shaly Sands	3	7.8	66.7	13.5	4.02	2.11	2.03	1.13	1.94	0.55	0.13	0.03	99.9
Average:	18	7.4	67.0	13.3	4.38	2.12	2.11	1.25	1.85	0.53	0.13	0.03	100.1
Sandy Silts or Shales													
Average:	4	12.9	58.2	16.0	5.66	1.59	2.12	0.55	2.25	0.64	0.08	0.03	100.0
Calcite Cemented Samples													
Average:	1	34.2	16.1	3.4	2.49	0.00	0.51	41.13	1.30	0.19	0.10	0.91	100.3

Table 3.7: Summary of Average XRF Trace Element Results by Lithology.

LITHOLOGY	No. of	XRF ELEMENTAL ANALYSIS (ppm) – Raw Data															
	samples	Nb	Zr	Y	Sr	Rb	Ba	Ga	La	Pb	Zn	Cu	Ni	Co	Cr	V	S
Fine to Medium Grained Sands																	
Average:	3	5	89	19	327	55	632	10	23	12	66	9	24	158	77	111	2910
Very Fine to Fine Grained Sands with Silt or Shale																	
Silty Sands	6	8	144	22	299	71	506	17	22	15	69	15	25	76	93	146	4732
Shaly Sands	9	8	127	23	290	75	521	15	25	23	71	17	23	55	63	136	2593
Silty and Shaly Sands	3	8	200	24	294	75	471	18	21	17	70	16	23	64	98	139	3688
Average:	18	8	145	23	294	74	508	16	23	20	70	16	23	64	79	140	3488
Sandy Silts or Shales																	
Average:	4	11	183	24	247	105	261	26	24	19	65	24	22	26	56	155	4835
Calcite Cemented Samples																	
Average:	1	3	27	29	650	19	162	<1	12	11	40	10	17	44	14	43	2637

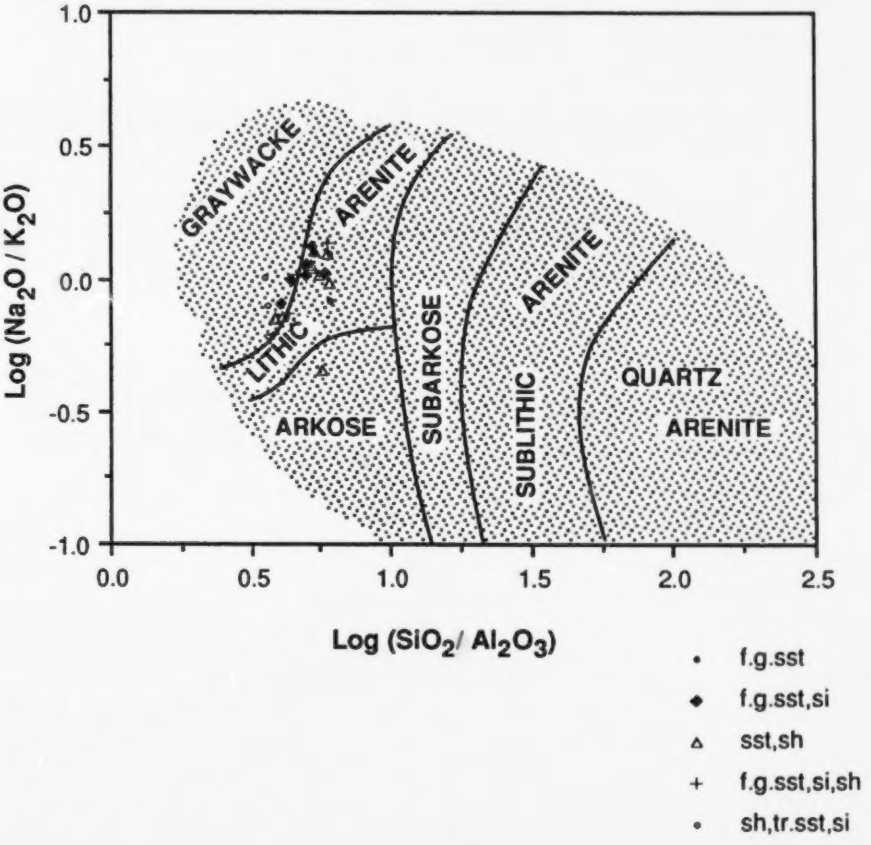

Figure 3.5: Plot of log (Na_2O / K_2O) versus log (SiO_2/ Al_2O_3) from XRF data for various lithologic samples from the study area. This represents the ratio of alkalai metal-rich to alkalai metal-poor components, essentially the maturity index comparable to Folk's modal classification defined in chemical compositional terms (graph after Pettijohn *et al.*, 1987).

The abundance of Sr and Ba within the fine to medium grained 'clean' sands in the study area likely reflects their high content of feldspars and rock fragments. The concentration of trace elements in the shaly rocks is most likely linked to clays in this facies, especially for Y, Rb, Cu and V (Day, 1963; Prudêncio *et al.*, 1989). Zircons are relatively small in Clearwater sediments (< 50μm), which explains the prominence of Zr in silty facies. Sulphur is common in all silty facies resulting from its prominence as pyrite in finer, more organic-rich rocks.

SEM Elemental Analyses

Elemental analysis by a Kevex energy dispersive spectrometer (EDX) was used extensively as an aid in identifying minerals by scanning electron microscopy. Although results are only semi-quantitative, and proportions of the various elements are greatly affected by such factors as smoothness of the sample surface, a few characteristic analyses have been included for reference within Appendix 4. EDX analyses have been included for the following diagenetic minerals: pyrite, berthierine, illite, illite / smectite, zeolite (clinoptilolite), and kaolinite.

Stable Isotope Geochemistry

Stable isotopes of oxygen and carbon are commonly used in studies of carbonate and silicate rocks formed in low temperature settings. The isotopic ratio, or relative difference between the amount of isotopes, i.e. ^{18}O to ^{16}O relative to SMOW or PDB standards for oxygen, are generally characteristic of the waters with which they have interacted during formation, provided that later isotopic exchange did not occur (Craig, 1961). The oxygen isotope composition of a mineral formed during lithification or diagenesis is also a function of its temperature of formation, and the mass balance of oxygen between fluids and rock in the system (Longstaffe, 1983). Carbon isotope ratios, $^{13}C / ^{12}C$, are typically used in the characterization of the source of carbon involved in the formation of a particular mineral, and may also be useful in interpreting the generation, migration or alteration of hydrocarbons (Fuex, 1977; Longstaffe, 1983).

Stable isotope values in this study are reported in the δ-notation in parts per thousand (permill, ‰). The δ-value is defined as:

$$\delta(‰) = \frac{\text{R (sample) - R (standard)}}{\text{R (standard)}} \times 1000 \qquad (1)$$

where R = $^{18}O / ^{16}O$, or $^{13}C / ^{12}C$, relative to SMOW or PDB standards. The partitioning of an isotope between two phases, A and B, is given by:

$$\Delta_{A\text{-}B} = 10^3 \ln\alpha_{A\text{-}B} = \delta_A - \delta_B \quad (2)$$

where α is the oxygen isotope fractionation factor between A and B.

Oxygen and carbon stable isotope values ($\delta^{18}O$ and $\delta^{13}C$) were obtained for twelve carbonate cemented samples. Two samples, LW3-20 and LW3-21, contained both calcite and dolomite, but poor results for dolomite were obtained and subsequently discarded. The dolomite result for sample LW-87-CW-17 was also of poor quality and discarded.

The $\delta^{18}O$ values for calcite range from 18.6 to 19.8‰, and average 19.4‰ (SMOW); $\delta^{13}C$ values vary from -1.3 to 4.5‰, and average +1.9‰ (PDB) (Table 3.8; Figure 3.6). Dolomite $\delta^{18}O$ values are slightly more enriched in ^{18}O relative to calcite at values of 21.5 and 24.1 ‰,(SMOW); $\delta^{13}C$ values(0.6, 2.5‰, PDB) are comparable to calcite.

Discussion

Calcite and dolomite have very different origins in the study area. Calcite is present as a diagenetic cement, whereas dolomite grains are present as detrital grains.

Diagenetic carbonate minerals formed directly from ocean water would be expected to have oxygen isotope values that reflect crystallization from such a source (SMOW). Somewhat lower values might be expected if the inland seaway at this time was somewhat brackish, or if crystallization occurred below the sediment / water interface in a quasi-closed system.

The $\delta^{18}O$ values of meteoric waters (fresh waters) are ≤ 0‰, but highly variable depending on their geographic location. Values range from approximately 0‰ at the equator to -55‰ at the poles (Craig, 1961; Hoefs, 1987).

The oxygen isotopic composition of calcite from the study area (avg.= 19.3‰) is sufficiently low to suggest that a sizeable fraction of meteoric water was involved in its formation. An influx of meteoric waters into the formation is therefore a part of its diagenetic history. Mixing of meteoric and ^{18}O richer formation waters (i.e. seawater) led to the composition of fluids from which calcite precipitated.

The $\delta^{18}O$ and $\delta^{13}C$ values obtained for detrital dolomites in the formation are typical of platform carbonates (Land, 1980). The $\delta^{13}C$ values in particular suggest a marine carbon source. Similar results for detrital dolomite have been reported for other

Table 3.8: Stable Isotope Data for Carbonates

SAMPLE NUMBER	DEPTH (metres)	BITUMEN SATURATION Sample	Zone	C °/oo (PDB)	O °/oo (SMOW)	O °/oo (PDB)	CARBONATE MINERAL
Well 3-28-66-2W4 Imp. 77 O.V.							
LW3-20	463.27	trace	moderate	3.9	18.6	-11.9	Calcite
LW3-38	468.76	water	low	4.5	19.9	-10.7	Calcite
LW3-21	494.15	water	water	4.3	19.2	-11.4	Calcite
Well 8-19-66-2W4 Esso 86 Marie O.V.							
LW-87-CW-56	477.40	water	moderate	3.0	19.1	-11.5	Calcite
Well 16-2-66-3W4 Imp. 77 Medley O.V.							
LW-87-CW-92	453.57	water	moderate	3.2	19.5	-11.0	Calcite
LW-87-CW-66	464.84	water	low	-0.3	19.1	-11.4	Calcite
Well 5-22-65-3W4 Imp. Marie O.V.							
LW-87-CW-93	430.97	water	moderate	-1.3	19.8	-10.8	Calcite
Well 16-28-66-3W4 Imp. 77 Marie O.V.							
LW-87-CW-91	415.26	water	low	-0.6	19.3	-11.3	Calcite
LW-87-CW-90	425.58	water	moderate	1.0	19.8	-10.7	Calcite
Average:				1.9	19.4	-11.2	
Well 6-31-66-2W4 Esso 86 Cold Lake O.V.							
LW-87-CW-10	509.60	mod	moderate	2.5	21.5	-9.1	Dolomite
LW-87-CW-21	511.40	water	water	0.6	24.1	-6.6	Dolomite
Average:				1.5	22.8	-7.9	

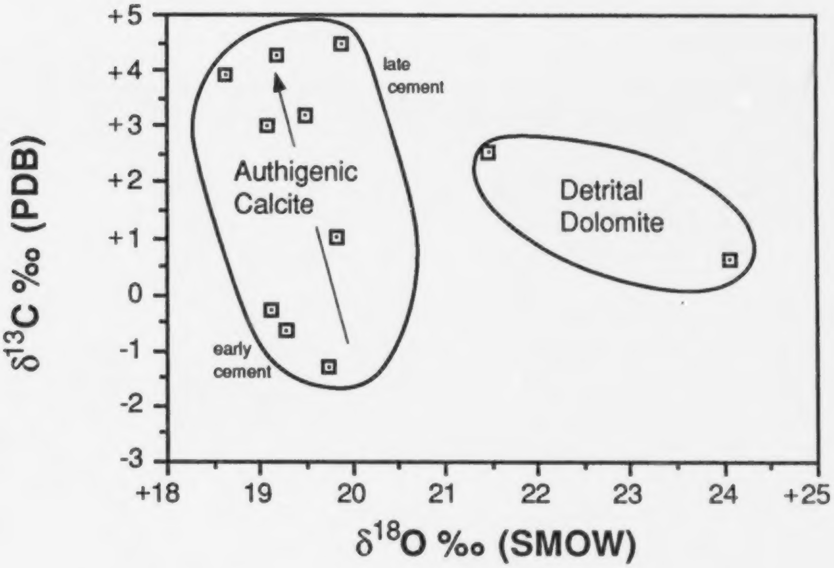

Figure 3.6: Plot of $\delta_{13}C$ versus $\delta_{18}O$ values for detrital dolomite and authigenic calcite from the study area in the Clearwater Formation. Arrow illustrates general trend in isotopic composition of authigenic calcite cements during burial diagenesis for the samples analyzed in the study area. Data from Table 3.8.

stratigraphic intervals in the Western Canada Sedimentary Basin (Longstaffe, 1984; Longstaffe and Ayalon, 1987; and Ayalon and Longstaffe, 1988).

The average of $\delta^{13}C$ values for calcite (+1.9‰ PDB) suggests that the CO_2 involved in its formation was mainly of inorganic origin, and was derived from a marine source ($\delta^{13}C \approx 0$‰) (Fuex, 1977; Hudson, 1977) (Table 3.8). The range of values however, -1.3 to +4.5‰ (PDB), is greater than the standard 0‰ ± 2 that is commonly used in the interpretation of an inorganically derived CO_2, suggesting that other processes may be involved.

Two of the common processes during which calcite cements are formed during burial diagenesis in marine sediments are sulphate reduction and bacterial fermentation (methanogenesis). Depth-related diagenetic reactions for calcite precipitation have been identified which correspond to various zones, including those of sulphate reduction and microbial CO_2 reduction, each of which has a characteristic $\delta^{13}C$ composition (Curtis, 1978). Within the zone of sulphate reduction, CO_2 is generated by the reduction of organic matter by sulphate reducing bacteria. This results in the production of isotopically light ($\delta^{13}C \approx -25$‰) bicarbonate, which precipitates under conditions of supersaturation as calcite, to an estimated depth of approximately 10 metres (Curtis, 1978). Fermentation of organic matter begins below the zone of sulphate reduction to an approximate depth of 1 km, and produces both methane and isotopically heavy CO_2 ($\delta^{13}C \approx +15$‰) (Curtis, 1978). Continued fermentation can lead to a residue of CO_2.

Carbon isotope values obtained for calcites within the study area can generally be separated into two groups; those with $\delta^{13}C \approx 0$‰ (derived from inorganically produced CO_2) and those slightly enriched in ^{13}C ($\delta^{13}C \geq 3$‰), which appear to have been influenced to some degree by the presence of bacterially mediated CO_2. Inorganically derived CO_2 likely originated from the dissolution of detrital carbonate (i.e. dolomite) within the study area, with calcite precipitation occurring in local areas when supersaturation conditions were reached. The ^{13}C enriched calcite likely formed somewhat later, when burial diagenesis processes progressed to those associated with the zone of microbial fermentation. Some ^{13}C rich CO_2 would then have been added to the system. The trend to lower $\delta^{18}O$ values with higher $\delta^{13}C$ values reflects increasing burial temperatures as diagenesis progressed.

E. CLEARWATER DIAGENESIS

STUDY AREA PARAGENESIS

A generalized paragenetic sequence for the Clearwater Formation for the study area near Leming is given in Figure 3.7. It was constructed based on observations from: the petrographic study (as summarized in Plates 3.1 to 3.14); generalizations for different lithologies based on XRF, whole rock, < 45µm and < 2µm XRD data; and from limited isotopic analyses of carbonates. The paragenetic sequence can be summarized from early to late diagenesis as: glauconite; early pyrite, calcite and siderite; authigenic illite, illite / smectite (I/S) and chlorite / smectite (C/S); late siderite and pyrite; feldspar and quartz overgrowths; late calcite; zeolite (clinoptilolite); kaolinite; and Fe oxides.

DISCUSSION

The diagenetic history of the study area extends from early or *shallow* diagenesis, through burial to a relatively late diagenesis which corresponds with uplift and erosion of the eastern margin of the basin (or early, intermediate and late). Over this diagenetic history it is possible to recognize three successive stages, characterized by mineral assemblages which correspond to distinct chemical environments (Figure 3.7). In addition, the diagenetic history of the various lithologies observed in the study area are different, and generally only a portion of the authigenic assemblage is present in any one lithology.

Stage 1: Early *Shallow* Diagenesis and Early Burial Diagenesis

Early or *shallow* diagenesis refers to syn-depositional diagenetic processes, such as the formation of glauconite pellets. Glauconite is the first diagenetic phase observed in the formation, and is present in all lithologies containing framework 'sand' grains. It is the most abundant in the coarsest offshore sand-bearing facies, and within the Wabiskaw Member. Glauconite pellets typically form in semi-confined settings with a connection to open marine sea-water at water depths of 50 to 500m (Odin and Matter, 1981). Glauconization is achieved by the authigenic growth of auto-morphous crystallites in the pores of a parent substrate, and is accompanied by progressive alteration and replacement of this substrate, eventually leading to a bulbous-shaped and often cracked glauconite grains (Odin and Matter, 1981). The parent material may be carbonate particles, argillaceous (kaolinitic) faecal pellets, infillings of foraminiferal tests, various mineral

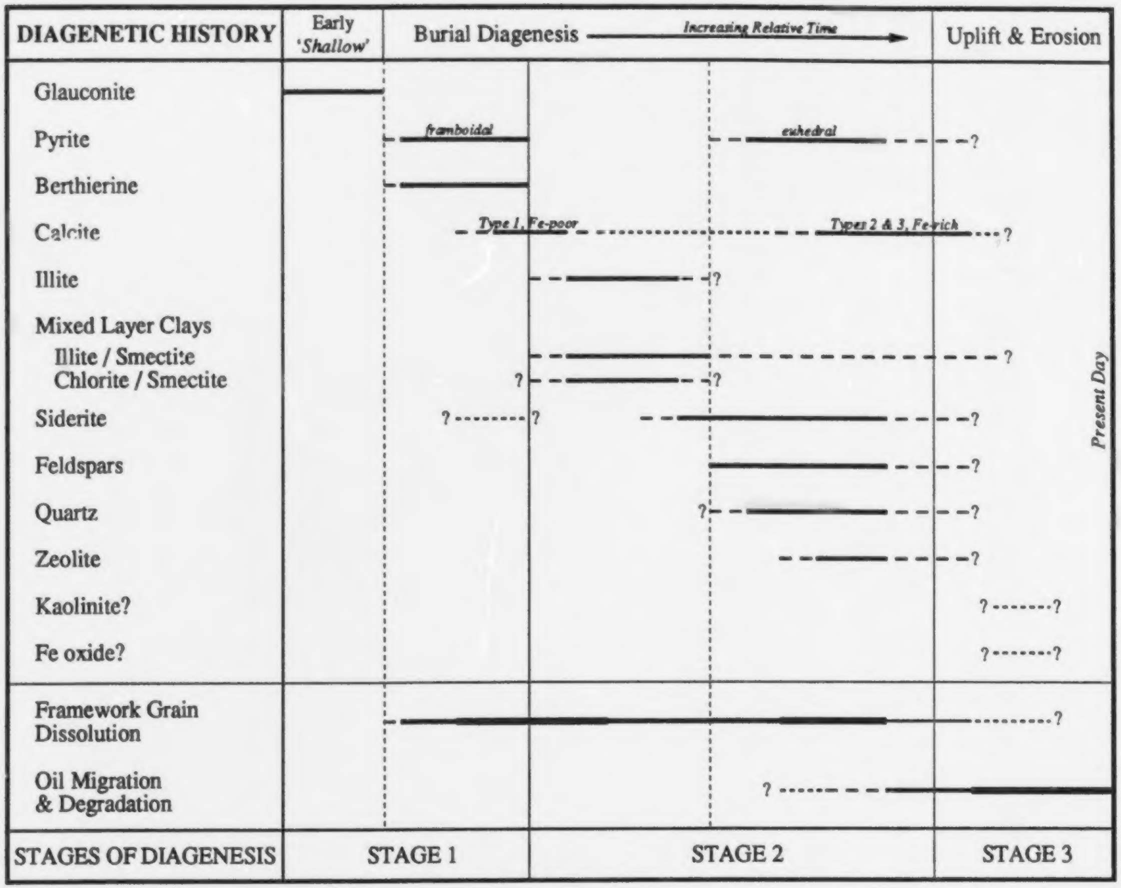
DIAGENETIC HISTORY
Early 'Shallow'
Burial Diagenesis
Increasing Relative Time
Uplift & Erosion
Glauconite
Pyrite
framboidal
euhedral
Berthierine
Calcite
Type 1, Fe-poor
Types 2 & 3, Fe-rich
Illite
Mixed Layer Clays
Illite / Smectite
Chlorite / Smectite
Siderite
Feldspars
Quartz
Zeolite
Kaolinite?
Fe oxide?
Framework Grain Dissolution
Oil Migration & Degradation
Present Day
STAGES OF DIAGENESIS
STAGE 1
STAGE 2
STAGE 3

Figure 3.7: Paragenetic sequence of Clearwater Formation diagenetic events in the study area.

grains and rock fragments (McRae, 1972; Odin and Matter, 1981). The authigenic mineral is generally an iron-rich and potassium-poor glauconitic smectite, although variable potassium is associated with other authigenic phases, notably the mineral glauconite (10Å), Fe-rich illite / smectite, and rarely, mixed-layer chlorite / smectite (celadonite) (Odin and Matter, 1981; Amouric and Parron, 1985). Berthierine has even been identified as the source of the green coloration of 'glauconite-like' grains from more tropical marine environments, and may in fact compose many previously identified glauconite facies identified in the literature (Odin and Matter, 1981). Much of such authigenic material is relatively amorphous, and not detectable by XRD.

Formation of glauconite pellets is governed by the availability of iron and potassium and the balance between the influx of detrital matter and winnowing during sediment deposition (McRae, 1972; Odin and Matter, 1981). Low sedimentation rates with long exposures to an open marine environment, such as during a marine transgression, result in the best developed glauconite facies. The local geochemical conditions are those of a slightly alkaline setting (pH ~7–8) with limited oxygenation, typical of the sediment / water interface beyond the zone of fluvial influence (therefore characteristic of open marine) (Odin and Matter, 1981). The mineralogical composition of glauconite from the study area was not examined in this investigation, and it is possible that some of the glauconite pellets reported for this area are actually berthierine-rich. 'Glauconite-type' berthierine is reported to form at shallow depths in marginal marine, shoaling upward settings in warmer, tropical seas; such conditions commonly associated with river mouths and delta environments (Odin and Matter, 1981; Bhattacharyya, 1983), similar to that of the study area during deposition. The composition of glauconite in the Clearwater Formation should be investigated in future studies, despite the fact that the formation of berthierine and glauconite have been deemed mutually exclusive (Bhattacharyya, 1983).

Minerals typical of early burial diagenesis include framboidal pyrite, berthierine, Type 1 Fe-poor calcite and early concretionary siderite. Framework grain dissolution began at this time and played a big role in supplying ionic species for further porewater interactions. Framboidal pyrite is a characteristic phase of anaerobic bacterial sulphate reduction processes, and in the study area it appears to correspond to such an origin. It is one of the first diagenetic phases in the sediment, and is concentrated in the finest, most organic-rich facies. The zone of sulphate reduction typically extends from just below the sediment / water interface (beyond the extent of oxygenated sediment) to shallow depths (Curtis, 1978). The formation of pyrite is a two-step process; the first of which is the simultaneous oxidation of organic matter and reduction of interstitial dissolved sulphate to hydrogen sulphide by heterotropic bacteria in the sediment (Berner, 1978):

$$2CH_2O + SO_4^{2-} \rightarrow 2HCO_3^- + HS^- + H^+ \qquad (3)$$

This results in an increased net acidity in the sediments, and may contribute to the dissolution of mineral carbonates in the sediment, such as detrital dolomite (Curtis, 1980). In the second step, hydrogen sulphides are converted to pyrite in the presence of unstable ferrous iron (Berner, 1970):

$$Fe^{2+} + HS^- \rightarrow FeS + H^+, \; FeS + H_2S \rightarrow FeS_2 + 2H^+ \qquad (4)$$

The lower limit of this zone is regulated by the extent of sulphate diffusion from depositional waters at sufficient levels to support bacterial growth (Curtis, 1978). In a nearshore setting, in which the composition of the porewaters may have been sufficiently influenced by the presence of fresh waters to limit the diffusion of sulphate into the sediment, the zone of sulphate reduction may have been very small to nonexistent. In deeper water settings, with local concentrations of organic matter and a greater influence of more saline marine waters, the potential for the presence of the zone of sulphate reduction would have been greater, albeit controlled locally by the concentration of organic matter and availability of sulphate. The concentration of pyrite in small patches and in finer, more distal facies is typical of that observed in the study area.

The source of the iron is likely a mixture, consisting of iron present within the porewaters during deposition (small amount), the dissolution of fine grained and amorphous Fe-rich constituents (ferric hydroxides) deposited with the organic matter in the sediment, and relatively unstable detrital mineral phases, such as volcanic rock fragments (Curtis, 1978). Deposition of iron hydroxides with sediment are common in estuarine or nearshore marine environments (Pettijohn *et al.*, 1987). Initial supersaturation with respect to iron sulphides is generally associated with the framboidal texture of the early pyrite (Raiswell, 1982).

Trioctahedral 7Å berthierine clay minerals also formed early in the depositional history of the formation. The berthierine identified within the sand facies in the study area is an early diagenetic grain-coating phase, not the 'glauconite-type' of berthierine reported by Odin and Matter (1981). The formation of diagenetic berthierine is typically associated with burial diagenesis of shallow environments, and has been reported interstratified with 14Å chlorite into which it is thought to be transformed with increased burial (Ahn and

Peacor, 1985; Jahren and Aagaard, 1989). Berthierine is believed to form at low temperatures, and has been shown in the laboratory to form by the diagenetic transformation (neoformation) of detrital kaolinite, in the presence of abundant ferrous iron (Bhattacharyya, 1983). The actual chemical process of berthierine formation in the study area is not known, but based on conditions from published studies, it appears likely that berthierine formed subsequent to the dissolution of some detrital Fe-rich components in the study area, and in the presence of brackish porewaters likely present in the formation during initial burial (Bhattacharyya, 1983; Longstaffe *et al.*, 1989a, 1989b, 1991a, 1992b). It is concentrated within the most sand-rich facies containing the greatest abundance of volcanic rock fragments. The high porosity in these sands results in a large proportion of water in relation to rock in the sediments, and likely leads to increased dissolution (hence greater production of dissolved species). As with pyrite, the source of iron is from poorly crystalline and Fe-rich material (ferric hydroxides) trapped in the sediment, as well as dissolution of unstable Fe-rich phases such as volcanic rock fragments. Pyrite and berthierine are believed to have formed simultaneously in the study area, upon the initiation of dissolution and development of reducing conditions, as petrographic evidence did not indicate that one phase formed prior to the other. As with pyrite, the formation of berthierine is dependent on the development of reducing conditions, although not on the diffusion of sulphate, or presence of sulphate reducing conditions. In fact, it is possible that berthierine was forming under conditions of microbial fermentation within sands in nearshore areas as pyrite was forming in localized areas of sulphate reduction in more organic-rich facies. Some of the thickest sand facies in the study area contain thick grain coats of berthierine; much thicker than in their siltier sand counterparts. The absence of many other diagenetic facies in these units suggests that the formation of berthierine continued beyond Stage 1 diagenesis, perhaps until the emplacement of oil into the study area. Longstaffe *et al.* (1992) used oxygen isotope data for berthierine in the Clearwater Formation and arrived at a similar conclusion.

Two other phases, calcite and siderite, are believed to have formed in this stage of diagenesis. Isotopic evidence suggests that Type 1, Fe-poor calcite formed primarily from the dissolution of detrital carbonate (dolomite) (or at least inorganic carbonate) within the study area, perhaps influenced by slightly more acidic conditions developed during early burial diagenesis. It did not form as a result of bicarbonate produced during the processes of bacterial sulphate reduction, although it is possible that its isotopic composition was influenced by this process in some positions (isotopically poor, $\delta^{13}C \approx$ -25‰, calcite is typical) (Curtis, 1978). Petrographic evidence suggests that this Fe-poor calcite formed relatively early, perhaps subsequent to at least some of the berthierine, but prior to the formation of many of the later diagenetic phases in the formation. Its Fe-poor composition suggests that it must have formed when the abundant iron released into solution during dissolution of framework grains (such as volcanic rock fragments), was being effectively taken up by the precipitation of other Fe-rich phases (in this case pyrite and berthierine). The early calcite has a fibrous texture, with large elongate anhedral crystals, similar to the early calcite cement reported by Bloch (1990), for the Albian within the Harmon Member of the Peace River Formation. Precipitation of calcite likely continued on a smaller scale throughout burial diagenesis, perhaps associated with local dissolution of detrital dolomite.

Evidence for early diagenetic siderite is limited to siderite-rich mud clasts (concretions?), which are typical of early formed siderites (Mozley, 1989; Bloch, 1990). Clasts contained significantly more siderite than in other lithologies in the study area (i.e. LW-87-CC-01, > 26% siderite in whole rock), distinguishing it from later siderite. Concretionary siderites are more typical of fermentation conditions in marine sediments, but may be found in within the sulphate reducing zone in sediments containing meteoric water (Curtis, 1978; Irwin, 1977).

Stage 2: Intermediate to Late Burial Diagenesis

Extensive authigenic activity is associated with this stage of diagenesis, including the formation of many clay minerals and siderite, and at greater depths the growth of authigenic feldspars, quartz, zeolite and calcite. Diagenetic activity also included continued grain dissolution and compaction, resulting in a reduction in the fluid / rock ratio. Conditions are primarily those of methanogenesis, extending from shallow depths to maximum burial. Significant compaction did not occur (grain to grain contacts are not extensive), thereby limiting burial to a depth of approximately 1 to 1.5 km (Pettijohn *et al.*, 1987), similar to that projected for the eastern margin of the basin by Hitchon (1984).

The formation of clay minerals in the intermediate stage of burial diagenesis likely resulted from the increased concentration and eventual supersaturation of various species in the porewaters at greater depths, with the composition of the precipitating phase controlled by the dominant cations and increased levels of silica in solution (Pettijohn *et al.*, 1987). Authigenic grain-coating illite was observed in siltier units, and was generally the first grain coating clay present. It may have formed as the result of increased concentrations of K^+ ions in solution, resulting from the dissolution of volcanic rock fragments and feldspars (Nadeau and Bain, 1986). Experiments have shown that authigenic illite formation in sands is dependent on the fluid / rock ratio, and may result from high levels of feldspar (albite) dissolution (related to high concentrations of Al), under relatively neutral conditions (Huang *et al.*, 1986).

The formation of smectitic clays may have resulted from increased concentrations of Fe^{2+}, Mg^{2+}, Na^{+} and Ca^{2+} cations, with silica originating from feldspar and rock fragment dissolution. Interstratified or mixed-layer smectitic clays commonly form because of the result of differential alteration of parent minerals, such as detrital grains or pre-existing clays (Sudo and Shimoda, 1977). Trioctahedral C/S is present only in the coarsest sands and may in fact be intergrown with berthierine; it may form as an alteration of early (trioctahedral) berthierine. Increased values of Fe and Mg resulting from dissolution of framework grains within sand-rich facies may have favoured the formation of C/S (Pettijohn *et al.*, 1987). The formation of mixed-layer I/S has been attributed to the alteration of volcanic-rich materials (often volcanic glasses). The following diagenetic sequence has been attributed to the formation of illite / smectite with increased burial: volcanic glass → smectite (montmorillonite) → interstratified I/S → illite (Sudo and Shimoda, 1977). The abundance of volcanic-derived material in the Clearwater Formation may have favoured such formation, with I/S forming as an alteration of detrital smectite. Dioctahedral mixed-layer I/S and C/S clays are more abundant in finer facies and appeared to have formed at various times, interspersed with the formation of other authigenic phases during intermediate to late diagenesis. Its formational history is therefore relatively long compared to many other phases, and is thought to extend to the end of Stage 2 diagenesis, and may even overlap into Stage 3.

Formation of late diagenetic siderite is related petrographically to the increased dissolution of framework grains, with siderite commonly forming within the secondary pore space or on the rim of a former grain. This replacement texture of siderite highly suggests that the Fe for its formation was largely supplied by the dissolved grain. CO_2 or bicarbonate may have originated from several of sources (i.e. dissolution of detrital dolomite, or as by-product of methanogenesis).

Ongoing burial and higher temperatures likely contributed to increased diagenetic activity in the latter part of stage 2, resulting in dissolution of some quartz, chert accompanied by greater attack of other grain types. Increased relative concentration of ionic species at these higher temperatures likely led to the precipitation of authigenic feldspars, which tend to require silica levels somewhat higher than required for clay authigenesis (Pettijohn *et al.*, 1987). In localized areas in which silica dissolution was extensive (predominantly finer, water-saturated quartz-rich sediments), supersaturation with respect to silica likely resulted in the precipitation of quartz overgrowths (as a by-product of clay and feldspar precipitation). Zeolite formation is also associated (paragenetically slightly later) with the formation of feldspar and quartz overgrowths. It is generally characteristic of increased silica concentrations from higher pH, and higher temperature waters, and is a common diagenetic mineral in volcaniclastic-rich rocks (Pettijohn *et al.*, 1987; Bowers *et al.*, 1990). Formation of zeolite (clinoptilolite) within the Clearwater formation therefore likely occurred at or near maximum burial conditions.

Methanogenic conditions likely developed early in burial diagenesis, either when the supply of sulphate from the formation waters was exhausted, or in areas of little to no sulphate diffusion and reducing conditions. Degradation of any organic matter progressed on a local scale by anaerobic means (CO_2 reduction). A large quantity of organic matter is not present within porous deltaic sands, but significant organic matter would have been present in fine-grained interdistributary facies, and in interstratified siltier and sandier units in shoreline distal environments. This is supported by the presence of many ichnofossils in the study area (Chapter 2). Breakdown of organic matter by bacterial fermentation results in the generation of methane and bicarbonate by-products (Curtis, 1978):

$$2CH_2O \rightarrow CH_4 + HCO_3^- + H^+ \qquad (5)$$

The increased bicarbonate concentration results in the precipitation of isotopically heavy calcite (Curtis, 1978). Reduction of iron compounds continues in this setting, but the absence of sulphide species allows dissolved ferrous iron concentrations to build up. This contributes to Fe-enrichment in clays and to the formation of siderite. It also results in the formation of Fe-rich calcites (Types 2 and 3). Their isotopic composition was likely slightly affected by the presence of biogenically mediated CO_2, but the overwhelming influence of dolomite dissolution resulted in $\delta^{13}C$ values significantly lower than +15‰ (Curtis, 1978). Precipitation of calcite cement is concretionary and generally along bedding planes.

Authigenesis of the relatively large crystals of late euhedral pyrite is characteristic of slow crystal growth under conditions of low supersaturation with respect to iron sulphates in porewaters (Raiswell, 1982). Ferrous iron, as with other authigenic phases in burial diagenesis, was supplied by the dissolution of detrital phases. The source of the dissolved sulphate is more difficult to deduce, as any sulphate within formation waters would have been depleted early in diagenesis (Stage 1). This suggests that an external source of sulphate must have been involved. A potential source is sulphate-rich waters upwelling from depth by gravity-driven groundwater flow through the pre-Cretaceous unconformity. Dissolution of underlying Devonian Elkpoint Group evaporites has been suggested to have been occurring prior to the deposition of Clearwater sediments (Wightman *et al.*, 1991), and gravity-driven flow has been reported to have developed in the basin subsequent to the Tertiary (Garven, 1989).

The migration of bitumen into the study area is believed to have occurred during the latter part of Stage 2 diagenesis, at a time approaching maximum burial of the sediments. Oil migration has been reported to have been a very long process, taking upwards of 50 million years (Garven, 1989). Oil emplacement was therefore likely sporatic and heterogeneous with oil moving progressively into the area as a function of gravity-driven groundwater flow. Migration of the oil into the formation appears to have greatly attenuated most diagenetic processes in the now highly bitumen concentrated facies. A lesser effect is observed with siltier and shalier facies water saturated facies.

Stage 3: Uplift and Erosion

Uplift of the sediment in the study area resulted in a change in the hydrologic system present at depth within the Clearwater Formation, with more near-surface conditions resulting in the infiltration of meteoric waters. This led to the bacterial biodegradation of the oil into its present state as bitumen (Dimitrakopoulos and Muehlenbachs, 1987; Garven, 1989). Continued precipitation of calcite cements were affected isotopically by the presence of bacterially mediated CO_2 from biodegradation processes (Hutcheon *et al.*, 1989; Longstaffe *et al.*, 1989a, 1989b, 1991a, 1992a).

Other diagenetic processes associated with meteoric input include the formation of kaolinite (although not prominent in the study area), and the precipitation of late iron hydroxides. The formation of kaolinite is typically associated with the presence of relatively fresh waters (Pettijohn *et al.*, 1987). Only limited petrographic evidence for kaolinite is available within the study area. Iron oxides were observed as a localized late coating on clay minerals in the study area. Typically the formation of iron oxides is related to oxygenated conditions (ferric iron), which could only have been present subsequent to uplift with the influx of meteoric waters.

F. SEQUENCE STRATIGRAPHIC APPLICATION OF DIAGENESIS

SEQUENCE STRATIGRAPHY BACKGROUND

Sequence stratigraphy is a concept of viewing stratigraphic records as a series of stacked, genetically related sequences bounded by unconformities or their equivalent conformities (Mitchum *et al.*, 1977). Subdivision of sequences is done based on interpretations of relative sea-level rise and fall in the stratigraphic record, correlated with observations made from geophysical logs, core and outcrop (where available).

Sequence stratigraphic concepts, as discussed by Haq *et al.* (1987), Van Wagoner *et al.* (1987), Posamentier and Vail (1988), and Posamentier *et al.* (1988), although based on relative sea-level fall, affirm that eustatic sea-level fluctuation is the greatest factor controlling sediment deposition and configuration. Other researchers, such as Bergman and Walker (1988), and Embry and Podruski (1988), believe that local tectonism plays a greater role in influencing the pattern of sediment deposition. In fact, it is the interplay between eustatic sea-level, subsidence and sediment supply (influenced by tectonism) that affect deposition. Sequences are composed of genetically related cycles, bounded above and below by sequence boundaries. By definition, a sequence boundary is a surface separating younger and older strata which marks a position of relative sea-level fall (Posamentier *et al.*, 1988). Sequence boundaries are therefore time stratigraphic, and depending on their position in the basin and the basin geometry may be associated with periods of non-deposition and / or erosion (even subaerial exposure). They are therefore surfaces at which fluctuations in sediment depositional patterns can be observed, and surfaces which may be associated with concurrent or subsequent change (i.e. diagenesis), during their depositional and burial history.

Investigation into the paleogeography and controls which influenced Clearwater deposition in the study area has indicated that it was deposited in a predominantly progradational period characterized by abundant sediment supply in a time of overall eustatic sea-level rise (Haq *et al.*, 1987), with little to no effect of subsidence (Chapter 2). Onset of progradation following a relative drop in sea-level initiated the main phase of sediment deposition, and resulted in the development of sequence boundary SB1. A number of other surfaces were also identified in the study area: flooding surfaces FS1, FS2 and FS3, and sequence boundary SB2. SB1 is stratigraphically located between FS1 and FS2, with FS3 located at the upper boundary and SB2 at the lower boundary of the Wabiskaw Member. Sequence boundary SB1 is characterized in the study area by:

1) evidence of a relative sea-level fall manifested by a shallowing of facies, (more pronounced in distal positions);
2) evidence of erosion, as indicated by features such as downcutting and mud clasts, (more prominent in nearshore environments);
3) changes in depositional characteristics, specifically in organic content, bioturbation, biogenic diversity and the ichnofossil assemblage;
4) changes in diagenetic features, such as the abundance of iron-bearing species, perhaps indicating a relationship between formation of the sequence boundary and early diagenesis; and
5) changes in bitumen saturation, useful as an aid in evaluating changes in grain-size and internal mineralization.

It is the diagenetic aspect of these observations which have been examined in more detail here. The primary objective was to document the mineralogic and geochemical trends observed at the sequence boundary in the study area. The secondary aim was to propose explanations for the trends observed, and comment on their significance beyond the study area.

INVESTIGATION RESULTS

Results from six wells were used in this investigation: 3-13-65-4W4; 12-18-65-3W4; 16-2-66-3W4; 8-19-66-2W4; 3-28-66-2W4; and 6-31-66-2W4. Wells are located on a trend from SW to NE in the study area, comparable to the primary direction of progradation during sediment deposition (Figure 3.3).

Mineralogical Results

Whole rock mineral abundances determined by XRD are contained within Appendix 3. Average mineralogical analyses for sequences S_1 and S_2 have been summarized for each well and provide a first guide to mineralogical trends (Table 3.9). Trends in abundance are inconsistent for many minerals below and above SB1. Consistent trends were exhibited by K feldspar and plagioclase which are more abundant in sequence S_1 overlying SB1, and for chlorite and pyrite, which are more concentrated in S_2, underlying SB1.

One additional method of looking at trends in mineral composition over the sequence boundary was employed. The average composition for samples of each lithology were computed for each of sequence S_1 and S_2, and results were also separated

Table 3.9: Summary of Average Whole Rock Mineral Abundances for Sequences S1 and S2.

SEQUENCE	ENVIRONMENT	XRD RELATIVE ABUNDANCE (%)														
		Qtz	Pl	KF	Chl	SC	10Å	7Å	Cal	Dol	Sid	Py	Amp	Ilm	Mag	Total
Well 3-13-65-4W4 Esso 84 (C1-12) Cold Lk.																
Average S1:	UDF	50.0	24.6	8.2	1.2	1.0	6.5	4.0	0.0	0.6	2.5	0.2	0.2	0.1	0.7	100
Average S2:	L/MDF	55.2	21.1	6.1	1.4	0.9	6.1	4.9	0.0	0.3	2.6	0.5	0.2	0.0	0.8	100
Well 12-18-65-3W4 Imp. 77 Medley O.V.																
Average S1:	MDF	60.3	17.6	8.1	1.1	0.0	3.5	3.4	0.0	0.0	2.8	0.8	0.0	0.2	2.1	100
Average S2:	DF/LDF	51.3	21.3	2.1	1.4	2.7	8.0	5.3	0.0	1.5	3.2	1.4	0.3	0.0	1.3	100
Well 16-2-66-3W4 Imp. 77 Medley O.V.																
Average S1:	LDF	44.3	22.4	7.4	0.9	0.5	3.1	2.4	16.3	1.2	1.2	0.1	0.1	0.0	0.0	100
Average S2:	DF/MS	47.2	19.5	6.4	1.2	2.0	4.9	3.8	5.0	4.7	2.6	1.1	0.3	0.5	0.8	100
Well 8-19-66-2W4 Esso 86 Marie O.V.																
Average S1:	LDF	53.2	16.9	6.5	1.5	2.0	8.5	6.3	0.0	3.0	0.4	0.0	0.5	0.0	1.1	100
Average S2:	DF	50.3	14.7	4.2	1.7	6.0	7.2	4.4	9.3	0.7	0.6	0.5	0.2	0.0	0.2	100
Well 3-28-66-2W4 Imp. 77 O.V.																
Average S1:	LDF	38.6	21.6	5.6	0.8	2.2	7.6	3.7	11.3	2.1	4.4	0.5	1.8	0.0	0.0	100
Average S2:	DF/LDF/LS	47.3	13.9	4.9	2.7	2.7	9.0	3.7	5.2	4.9	3.9	1.4	0.4	0.0	0.0	100
Well 6-31-66-2W4 Esso 86 Cold Lake O.V.																
Average S1:	MDF	54.0	17.2	7.4	1.4	0.9	11.2	5.4	0.0	0.8	0.2	0.3	0.5	0.0	0.5	100
Average S2:	DF/LDF	54.7	12.6	4.8	1.9	6.8	9.2	4.6	0.0	2.7	0.5	1.1	0.8	0.3	0.0	100

* Results expressed as normalized relative abundances based on peak heights, not weight percent;
Qtz=quartz, Pl=plagioclase, KF=K feldspar, Chl=14Å chlorite, SC=swelling clays (~12Å), 10Å=mica / illite group clays;
7Å=kaolinite and / or berthierine clays, Cal=calcite, Dol=dolomite, Sid=siderite, Py=pyrite, Amp=amphiboles, Ilm=ilmenite, Mag=Magnetite

by bitumen saturation (Appendix 3). The objective was to observe general trends in lithologic composition in relation to sequence boundary SB1. The following general observations were made:

1) slightly more quartz was observed in most lithologies in sequence S_2;
2) random fluctuations in plagioclase and K feldspar abundance were noted, although overall both were in greater abundance in sequence S_1;
3) variable trends were found for swelling clays, 10Å clays and 7Å clays, although generally more swelling clays were present below SB1, and more 10Å and 7Å clays above;
4) a slight tendency for more calcite and dolomite within lower sequences was noted;
5) there is a variable trend in siderite abundance, with a tendency for more in S_2; and
6) a strong consistent trend of greater pyrite abundance was noted for lithologies located below sequence boundary SB1.

The trends for siderite, pyrite and the clay minerals were noted as the most prominent and were examined in greater detail.

Trends in pyrite composition for all six wells have been plotted relative to depth in Figure 3.8. A consistent trend of increased pyrite abundance below sequence boundary SB1 was observed. There seems to be an influence of lithology on the trend, with more pyrite present in distal wells, which contain finer, organic-rich sediments. The positions of flooding surfaces FS2 and FS3 help to illustrate positions of major fluctuations in facies composition. The consistent trend in pyrite composition may have resulted from differences in the diagenetic history associated with the two sequences bounding SB1. The siltier sediments which occur in the more offshore facies of sequence S_2 may have been more likely to develop a zone of sulphate reduction in distal settings than those of sequence S_1 during early diagenesis because of higher levels of organic components. However, higher levels of pyrite have also been observed for well 3-13-65-4W4, which has thick bitumen saturated sand both above and below the sequence boundary and less of a facies distinction than the other wells. These higher levels of pyrite may reflect an increased probability of sulphate reduction associated with the development of sequence boundary SB1. A break in deposition (hiatus) associated with the development of the sequence boundary may have led to a longer period over which sulphate could diffusion into the underlying sediment, leading to sulphate reduction and the formation of higher abundances of pyrite. There are no apparent differences in the amount of available iron

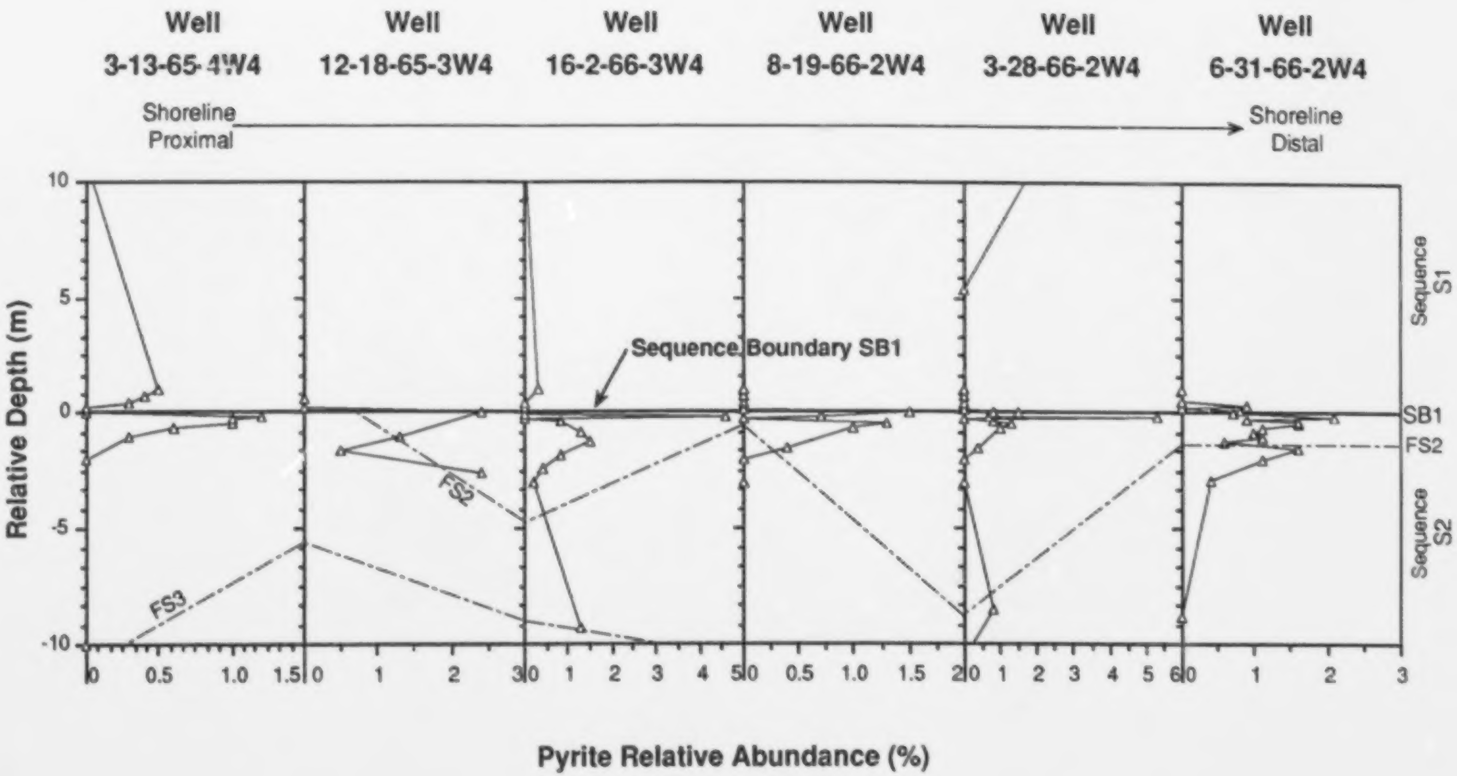

Figure 3.8: Distribution of pyrite relative abundance (%) over sequence boundary SB1 in wells located from proximal to distal positions relative to the paleo-shoreline during Clearwater deposition. Refer to Figure 3.3 for relative positions of wells in study area.

between the two sequences in well 3-13-65-4W4, and it is unlikely that there was a significant difference in the amount of organic matter between the two lithologies. This is supported by the apparent lack of ichnogenera both above and below the boundary in this well (Appendix 2).

Trends in siderite composition relative to depth were also examined (Figure 3.9). In contrast to pyrite, no distinct trends were observed. There is a trend to be more siderite in proximal wells and little to none in distal wells, but there does not appear to be a relationship between siderite abundance and the position of SB1 however. The most likely interpretation is that the abundance of siderite is independent from the development of SB1, consistent with its generally late, replacement texture. The precipitation of siderite is likely related to the presence of more freshwater in proximal sediments.

The clay mineralogy of the three wells (by XRD), 3-13-65-4W4, 16-2-66-3W4, and 8-19-66-2W4, has also been plotted relative to the position of SB1 (Figures 3.10, 3.11 and 3.12). Relative ratios of clays are also shown; the calculated values are also given within Appendix 3. The following observations can be made:

1) the abundance of 7Å clays is relatively low in the underlying facies and increases above SB1;
2) the abundance of smectitic clays is highest in the underlying facies and decreases above SB1;
3) I/S clays are generally present below SB1;
4) the abundance of chlorite is very stable;
5) the abundance of illite tends be higher below and at SB1, and lower in the facies overlying SB1;
6) the ratio of 7Å clays / chlorite and 7Å clays / swelling + 10Å clays are both relatively low in underlying facies and increase above SB1;
7) there is generally a change (decrease) in the %Sm in mixed-layer swelling clays over SB1;
8) there is a strong inverse relationship between the amount of 7Å clay and smectitic clay in each well.

The trends highlight the tendency for grain-coating berthierine 7Å clays to be the dominant clay mineral in the thicker sands overlying the sequence boundary in all three wells. Smectitic and illitic clays are more common in the shale-rich delta fringe sediments below SB1, which suggests they are primarily of detrital origin in this setting. The ratio of 7Å clays to swelling clays + 10Å clays illustrates this relationship. Chlorite / smectite

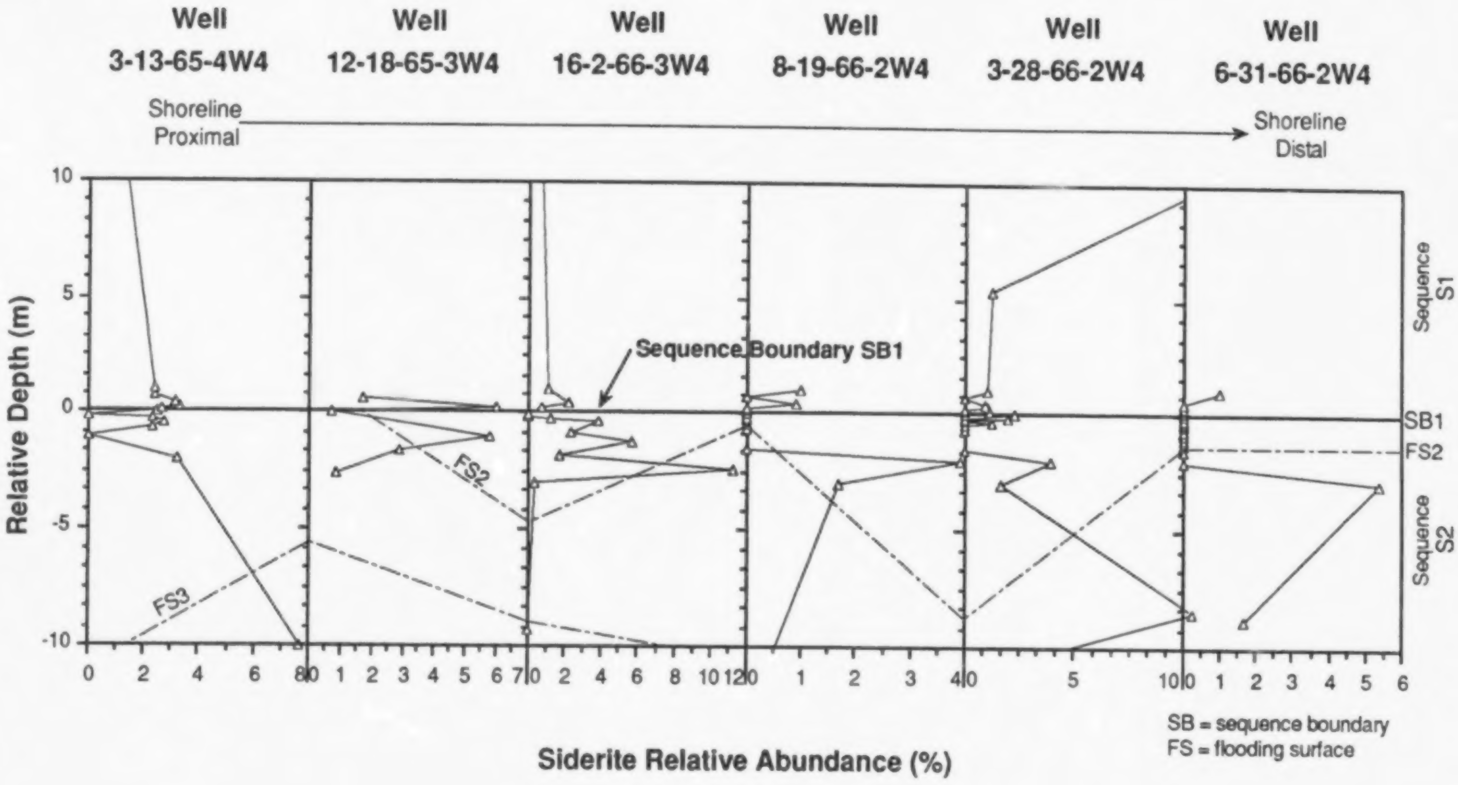

Figure 3.9: Distribution of siderite relative abundance (%) over sequence boundary SB1 in wells located from proximal to distal positions relative to the paleo-shoreline during Clearwater deposition. Refer to Figure 3.3 for relative positions of wells in study area.

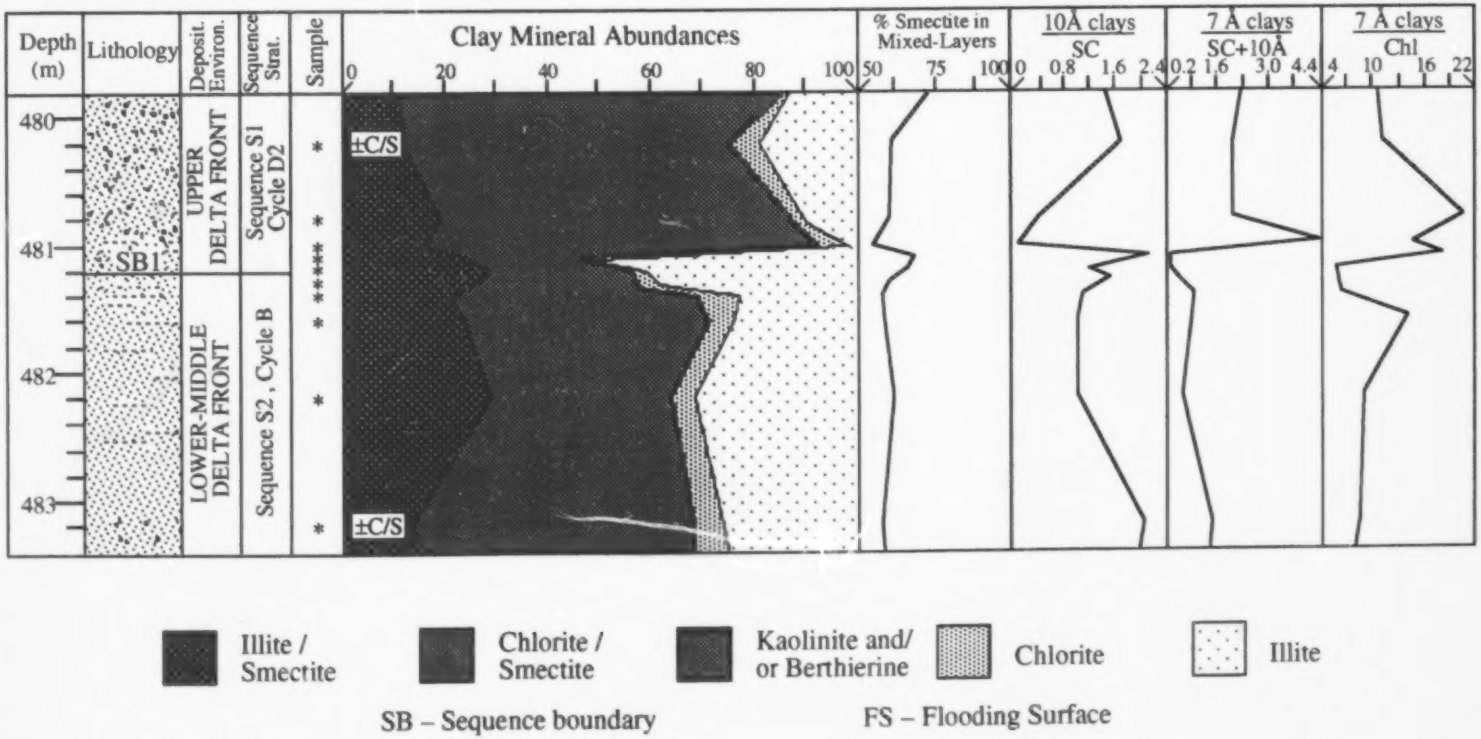

Figure 3.10 : Detailed clay mineral succession over sequence boundary SB1, including details regarding sampling, lithology and depositional environment; Clearwater Formation, well 3-13-65-4W4 (legend for lithology as in Appendix 1).

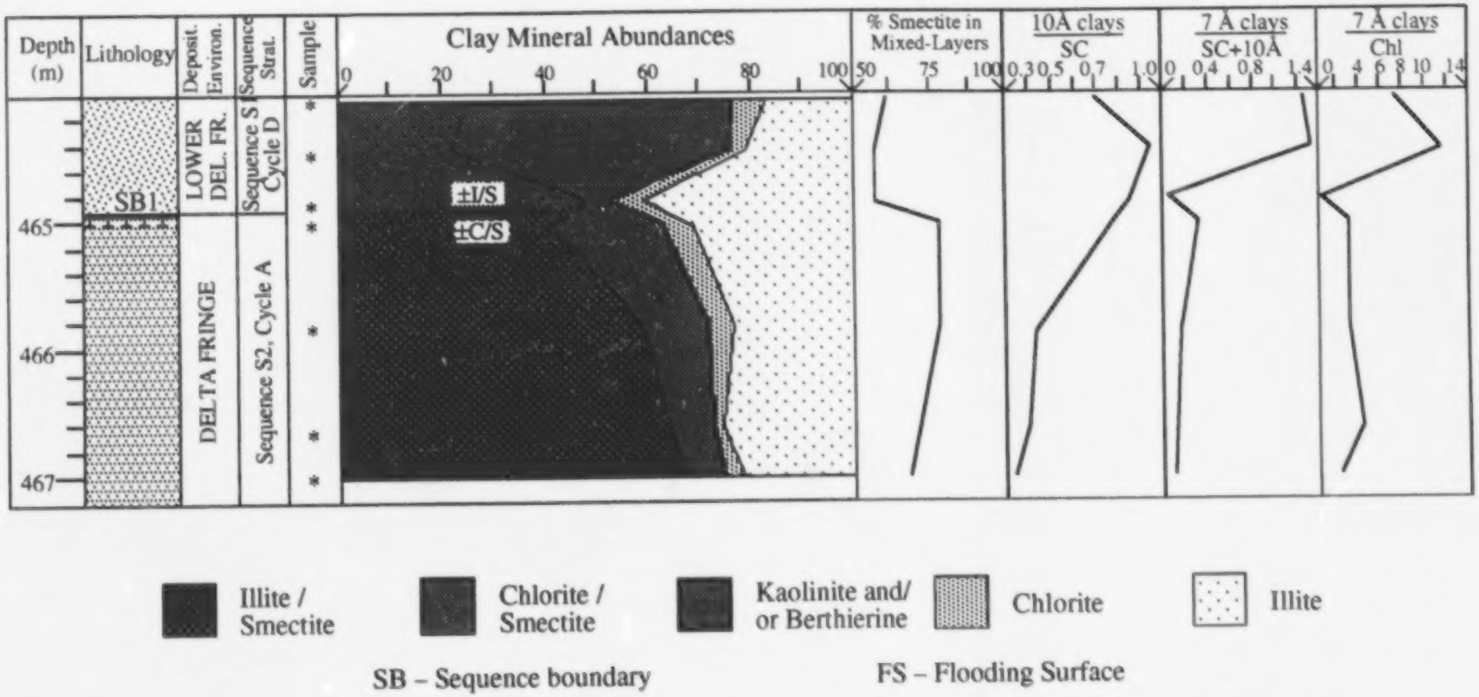

Figure 3.11: Detailed clay mineral succession over sequence boundary SB1, including details regarding sampling, lithology and depositional environment; Clearwater Formation, well 16-2-66-3W4 (legend for lithology as in Appendix 1).

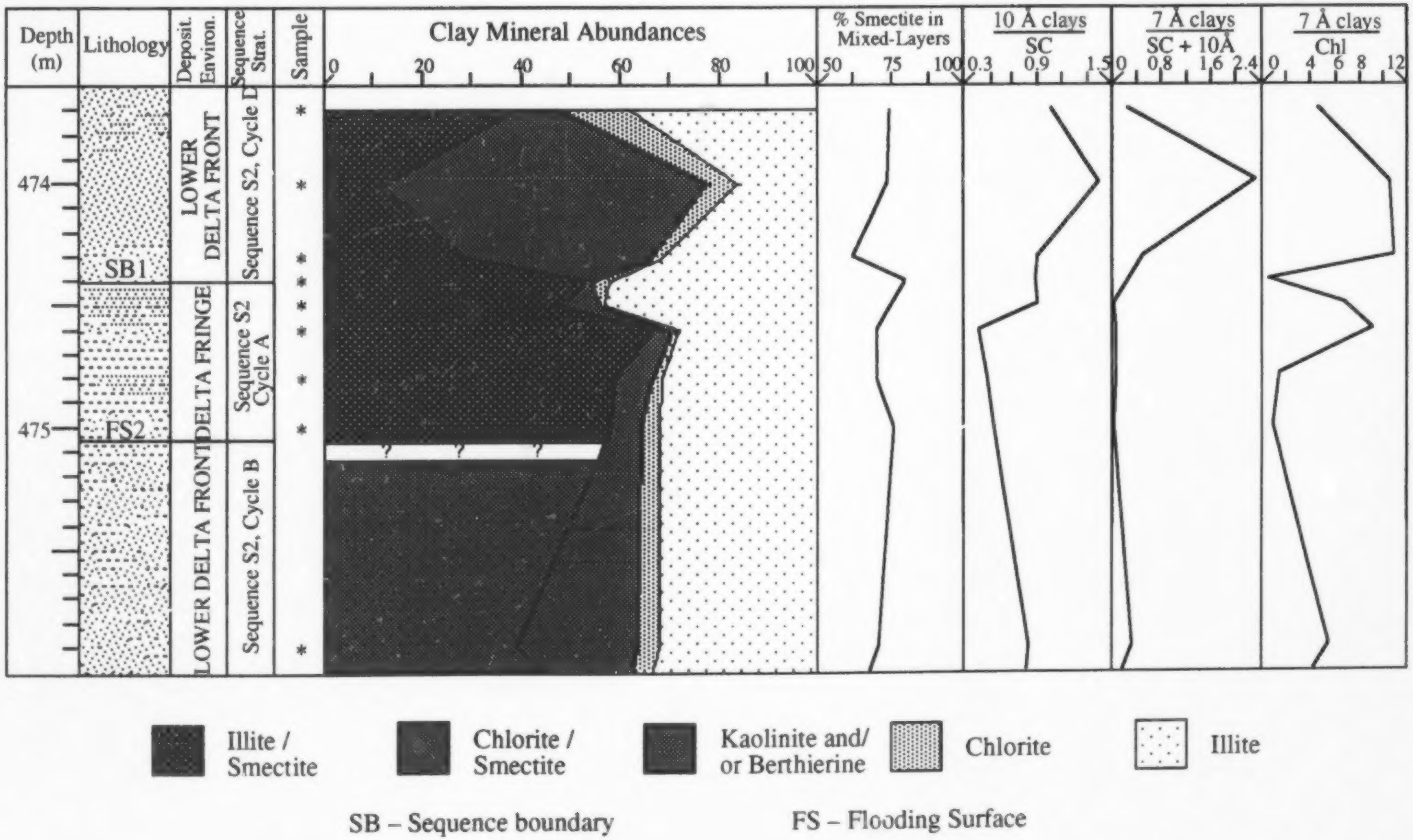

Figure 3.12: Detailed clay mineral succession over sequence boundary SB1, including details regarding sampling, lithology and depositional environment; Clearwater Formation, well 8-19-66-2W4 (legend for lithology as in Appendix 1).

clays are more prominent in coarser sediments which suggests that they are primarily authigenic, but their abundance is independent of SB1. The relationship of 7Å clay to chlorite represents the ratio of diagenetic to detrital clays in a well. The ratio of 10Å clay to smectitic clay is inconsistent between the three wells. It is comparable between wells 16-2-66-3W4 and 8-19-66-2W4, both of which are located in transitional delta front environments with delta fringe facies below the sequence boundary, but is distinct in well 3-13-65-4W4. This clearly suggests that its abundance is related to the lithology / depositional environment of the sample.

Geochemical Results

Trends in major oxide and trace element composition were examined for two wells within the study area, 6-31-66-2W4 and 16-2-66-3W4, to see if there was any relationship between these trends and SB1 (Appendix 4). In terms of major oxide composition, the consistent trends observed from sequence S_2 to sequence S_1 in both wells are as follows (Figures 3.13 and 3.14):

1) an decrease in L.O.I. in facies from S_1 which overlie SB1;
2) a slight decrease in Fe_2O_3, TiO_2 and MgO contents in S_1 relative to S_2; and
3) a slight increase in SiO_2 in sequence S_1 in comparison to S_2.

The decrease in L.O.I. is quite pronounced in well 6-31-66-2W4, and likely results from the higher levels of organic matter in distal delta fringe facies below SB1 versus those of the overlying lower delta front sands. This trend is less well developed in well 16-2-66-3W4. These same trends, although less pronounced, are exhibited for Fe_2O_3, MgO and TiO_2 in both wells, which suggests that they are related to decreased clay contents in delta front facies from S_1. Trends for these components in well 16-2-66-3W4 they are somewhat parallel to the trend in swelling clay abundance. The shift in this trend is likely from the presence of sand lenses. The slight decrease in SiO_2 for both wells (opposite from the trend in quartz) suggests that it is related to the increase in framework grain composition within sands in S_1.

Consistent trends in trace element composition for wells 6-31-66-2W4 and 16-2-66-3W4 over sequence boundary SB1 from S_2 to S_1 (Figures 3.15 and 3.16) can be summarized as:

1) a substantial decrease in S in S_1;
2) a moderate decrease in Zr ;
3) a moderate–low increase in Ba; and

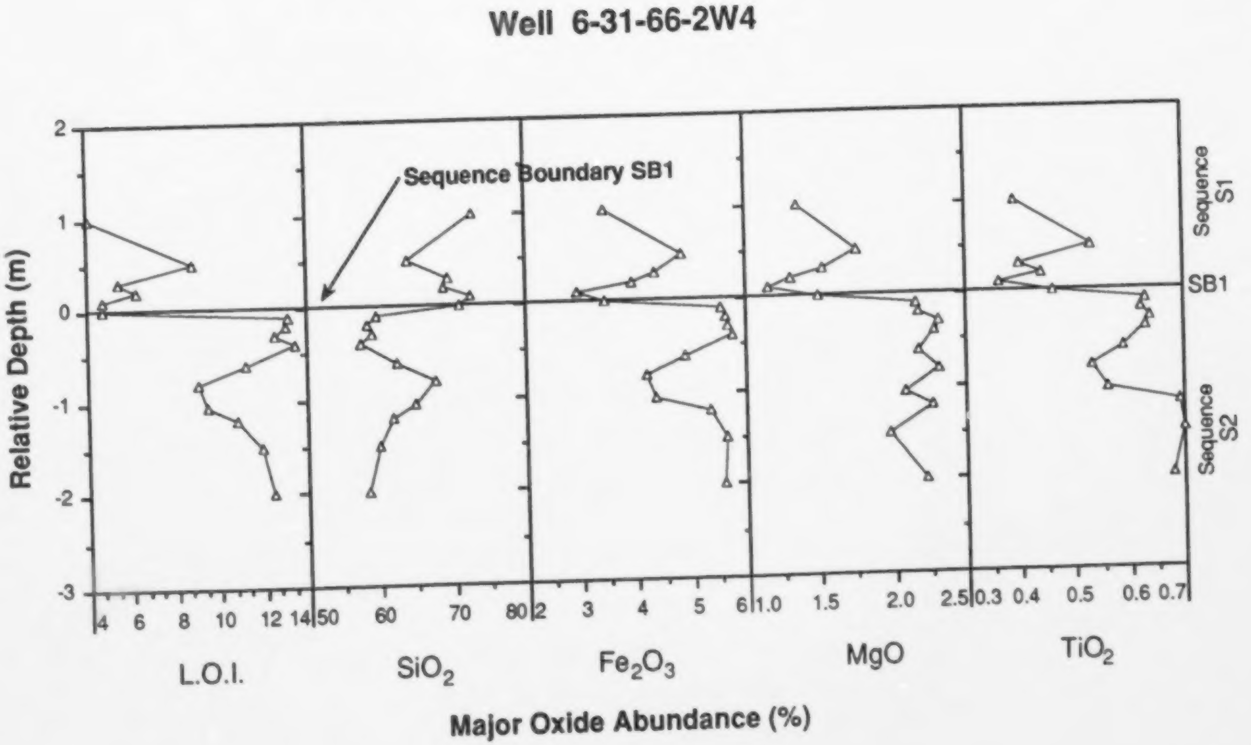

Figure 3.13: Distribution of the abundance (%) of various major oxides over sequence boundary SB1 in Well 6-31-66-2W4.

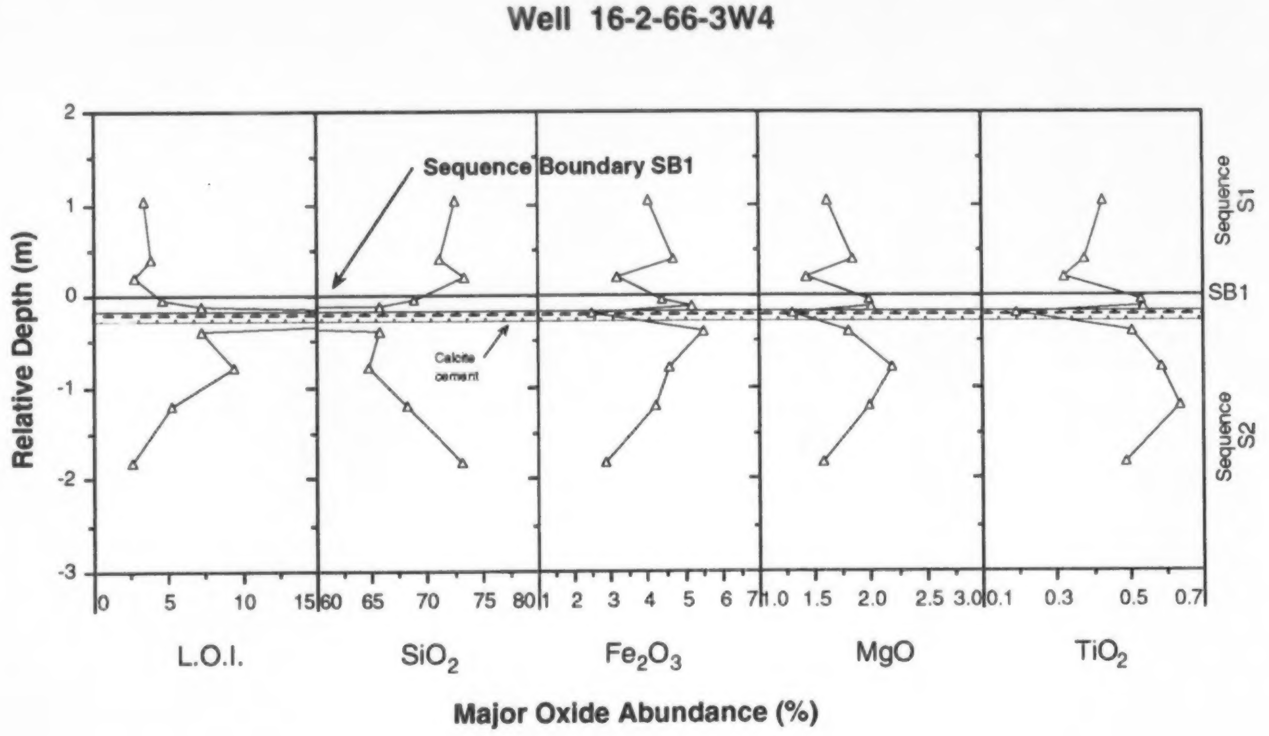

Figure 3.14: Distribution of the abundance (%) of various major oxides over sequence boundary SB1 in Well 16-2-66-3W4.

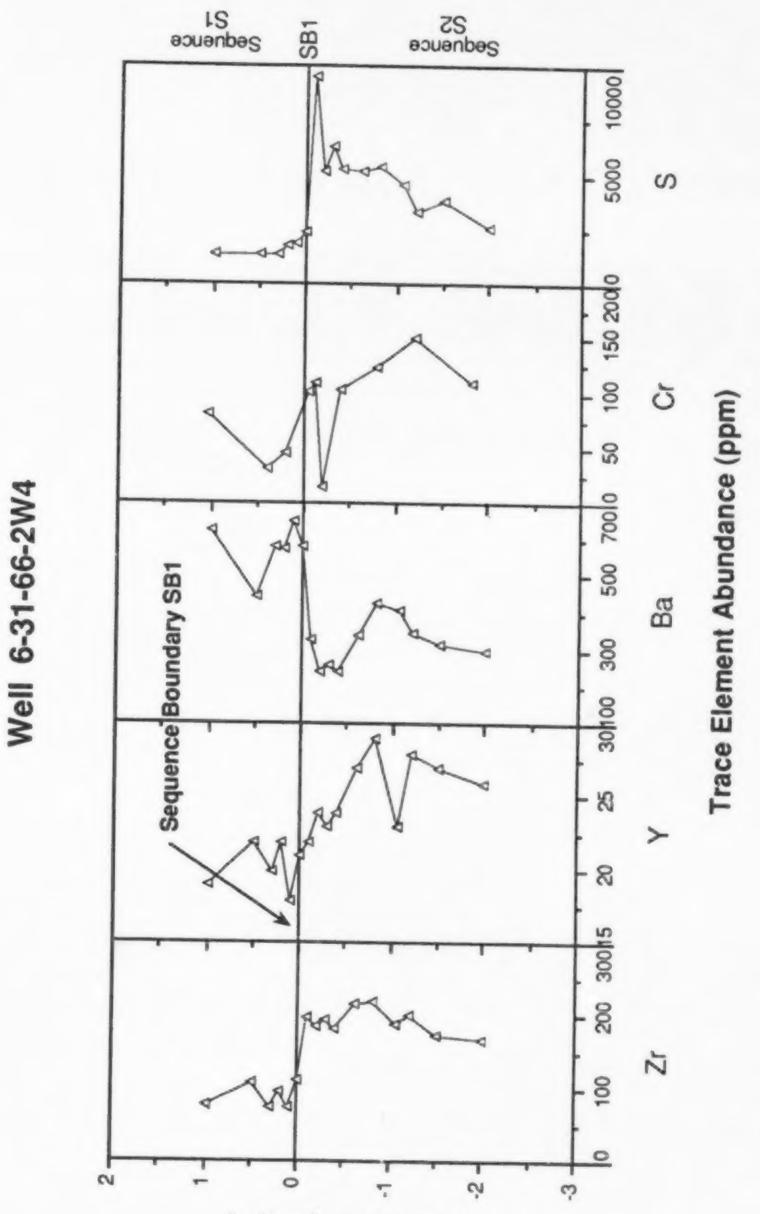

Figure 3.15: Distribution of the abundance (ppm) of various trace elements over sequence boundary SB1 in Well 6-31-66-2W4.

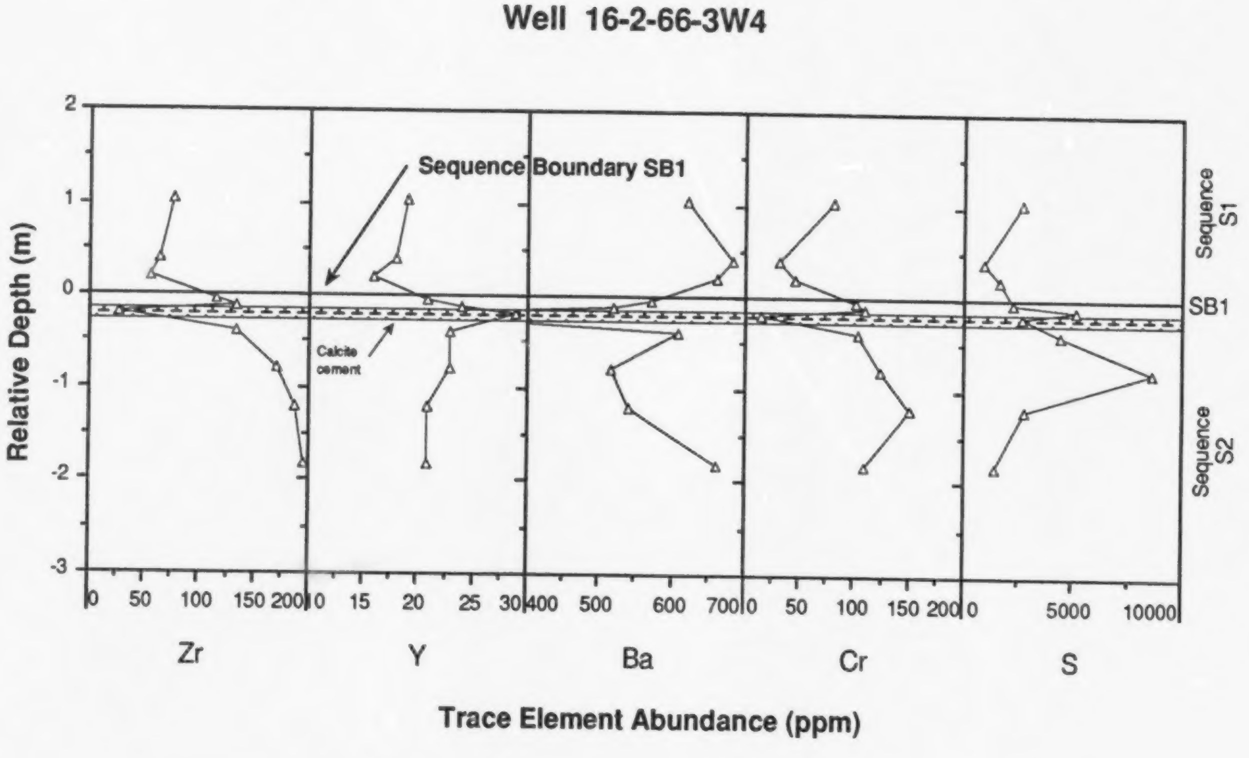

Figure 3.16: Distribution of the abundance (ppm) of various trace elements over sequence boundary SB1 in Well 16-2-65-3W4.

4) a slight decrease in Cr and Y.

The decrease in S in S_1 is a trend comparable to the trend in pyrite content for both wells. The decrease in Zr is likely related to the lower abundance of zircon in sequence S_1. Zircon crystals noted by petrography in the study area were found to be quite small; therefore they would likely be more prominent in the finer grained facies of S_2. Ba occurs typically as a substitution within feldspars, which tend to be more abundant within the sand-rich facies of S_1 (Pettijohn *et al.*, 1987). Cr and Y occur most often in small amounts in clays. Their abundance would likely be higher, as observed, within the fine grained facies of S_2. which likely explains the slight decrease in their abundancies in S_1.

G. CONCLUSIONS

MINERALOGY

Clearwater sediments are compositionally immature sandstones which can be classified as litharenites to feldspathic litharenites. Sands are composed primarily of framework grains, with little matrix or cement (except in calcite cemented sands), and have a high porosity. Their detrital composition represents sediment derived primarily from igneous rocks supplied from a western / southwestern source, and mechanical weathering of nearby exposed carbonates (likely those from the underlying Devonian Grosmont Formation). Some contribution from the rocks of the Canadian Shield is also likely.

Detrital phases consist primarily of volcanic rock fragments, quartz and feldspars, with minor dolomite, sedimentary and metamorphic rock fragments, detrital clays and zircon, amphiboles, ilmenite, magnetite and olivine accessory minerals. Altered grains are also present.

Diagenetic minerals occur as a minor cementing agents and include: glauconite; early and late pyrite; berthierine; early and late calcite; illite; mixed-layer illite / smectite and chlorite / smectite clays; early and late siderite; feldspar and quartz overgrowths; zeolite (clinoptilolite); and trace levels of kaolinite, Fe oxides and minor diagenetic phases (halite and apatite?).

Clearwater sediments can be classified by their lithologies as: fine to medium grained 'clean' sands; fine to very fine 'muddy' sands with interstratified silt or shale; sandy silts or shales; interstratified silts and shales; and carbonate cemented (calcite-rich) sands.

Fine to medium grained 'clean' sands have a relatively stable composition, and contain the largest fraction of quartz, plagioclase, K feldspars, and diagenetic siderite. Sands have a low overall clay content, most of which is diagenetic. They contain the highest abundance of berthierine (7Å) clays, with minor levels of authigenic 10Å clays. Trioctahedral mixed-layer chlorite / smectite is the most prominent mixed-layer clay in the coarsest sands, although dioctahedral mixed-layer illite / smectite is also present along with low levels of detrital 14Å chlorite. Low abundances of K feldspar are somewhat associated with higher values of 7Å and 10Å clays, suggesting a diagenetic relationship between these phases. Most samples are highly bitumen saturated, but water sands located stratigraphically lower in the formation contain a higher proportion of clays (all types).

Fine to very fine grained 'muddy' sands interstratified with silt or shale have the same framework grain composition as 'clean' sands, but with less plagioclase and siderite, and more dolomite and clays. The clay assemblage contains both diagenetic and detrital phases, mainly dioctahedral illite / smectites and 10Å clays, with minor 7Å clays and minor 14Å chlorite. The amount of 7Å clay is comparable to 'clean' sands, but more 10Å and swelling clays are associated with lower abundances of feldspars. Most samples are bitumen saturated, although water saturated samples are more abundant than in fine to medium grained facies.

Sandy silts or shales contain less plagioclase and K feldspar than 'clean' or 'muddy' sands, and more pyrite and clays. The clay assemblage consists of both mixed detrital and diagenetic phases, similar to 'muddy' sands, but with a greater percentage of swelling clays. An increased abundance of pyrite, siderite and 10Å clays is associated with diminished feldspars content. Bitumen saturation is generally poor, and many samples are water saturated.

Interstratified silts and shales contain the highest overall abundance of quartz (avg. 57%) and pyrite (avg. 1.2%), and the lowest content of feldspars. They also contain the greatest abundance of detrital clays, predominantly dioctahedral illite / smectite, with lower levels of 10Å clays, minor amounts of 7Å clays (diagenetic?), and minor chlorites (detrital). All interstratified silts and shales in the study area were water saturated.

Calcite cemented samples have high calcite contents (avg. 46%), and the lowest abundances of framework grains, likely the result of grain dissolution during cementation. Varied amounts of many other phases is also evident, including dolomite, chlorite and swelling clays. High abundances of 7Å and 10Å clays, pyrite and siderite, suggests that in general these phases formed prior to cementation. All samples were water saturated, although a few were coated with bitumen.

Dolomite-rich zones were also examined and found to be concentrated in sandy units, but most commonly in 'muddy' rather than 'clean' sands. This is thought to be related to the average size of the dolomite fragments, which are finer-grained than the fine to medium grained sands in the study area. Siderite-rich samples in contrast are typically located in 'clean' sands, likely because of their habit as replacement minerals in the formation. Only trace amounts of siderite were observed in silt and shale-rich facies.

DIAGENESIS

The depositional environment present during Clearwater deposition in the study area was one of deltaic sedimentation in brackish to marine waters at the edge of a shallow epeiric sea inundating from the north (Jackson, 1984; Chapter 2). Restricted circulation in the sea may have resulted in the development of slightly anoxic conditions in deeper water, as suggested by Stelck and Leckie (1988), which would have led to the development of reducing conditions at shallower depths than normal in the most shoreline-distal facies. In contrast, sediment-laden fresh waters originating from the west would have influenced composition of the water in the seaway, likely resulting in more brackish conditions in nearshore settings.

Fluctuation in relative sea-level subsequent to deposition may have also influenced the initial burial porewater composition in the basin by causing a subsurface incursion of meteoric water into the basin. It has been suggested that this could have resulted in a lateral migration of the mixing zone between fresh and basin waters because of head differences (Bloch, 1990). The result is the presence of an early burial porewater composition influenced to some degree by the presence of meteoric water (brackish). Furthermore, oxygen isotope values for calcite suggest that meteoric water influenced porewater composition throughout their formational history. Carbon isotope results indicate that diagenetically early calcite cements with carbon isotope values near 0‰ formed prior to bitumen emplacement, with CO_2 originating from an inorganic reservoir (perhaps from the dissolution of detrital carbonate). Samples with higher $\delta^{13}C$ values likely incorporated some bacterially mediated CO_2 from methanogenic processes.

Three stages of diagenesis have been recognized: 1) early or *shallow* diagenesis; 2) intermediate to late burial diagenesis; followed by 3) uplift and erosion. The Clearwater Formation was buried only to shallow depths relative to sediments on the western margin of the basin, and maximum burial was reached prior to marked compaction. The characteristics of each of the three stages of diagenesis as observed in the study area are summarized as:

Stage 1: Early *Shallow* Diagenesis & Early Burial Diagenesis

1) formation of syn-depositional glauconite-rich pellets in oxygenated conditions above the sediment / water interface;
2) establishment of local to widespread reducing conditions below the sediment / water interface;
3) initiation of framework grain dissolution;
4) precipitation of framboidal pyrite by local processes of bacterial sulphate reduction;
5) development (neoformation) of Fe-rich berthierine and development of methanogenic conditions in the sediment;
6) precipitation of Fe-poor, Type 1 calcite; and
7) precipitation of concretionary siderite.

Stage 2: Intermediate to Late Burial Diagenesis

1) continued grain dissolution under reducing conditions;
2) formation of authigenic illite;
3) development of mixed-layer smectite clays:
    - chlorite / smectite (C/S) in coarse sands (alteration of early berthierine?);
    - illite smectite (I/S) in finer silt and shale-rich facies (alteration of detrital smectite?);
4) precipitation of pore-filling and rhombic siderite;
5) more pronounced grain dissolution with increased burial temperatures;
6) precipitation of K feldspar overgrowths (with minor plagioclase);
7) precipitation of quartz overgrowths;
8) slow growth of euhedral pyrite in pore spaces;
9) precipitation of pore-filling zeolites;
10) precipitation of pore-filling, Fe-rich, Type 2 calcite;
11) precipitation of vein-filling, Fe-rich to Fe-poor, Type 3 calcite;
12) migration of hydrocarbons into Clearwater sediments (near maximum burial conditions); and

13) infiltration of higher salinity waters from underlying formations along with migrated hydrocarbons (sulphate-rich)?

Stage 3: Uplift and Erosion (maximum burial to present; ~400 m depth)

1) gradual uplift and erosion of overlying basin sediments;
2) continued growth / precipitation of calcite, pyrite, illite / smectite and other late diagenetic minerals for a period of time (water saturated intervals);
3) infiltration of local meteoric water as the result of a change in basin hydrologic conditions associated with uplift;
4) water washing and degradation of oil to form bitumen by bacterial oxidation;
5) precipitation of kaolinite (mainly in water saturated sediments outside of this study area); and
6) late precipitation of Fe-oxides under oxygenated conditions.

CHARACTERISTICS OF SEQUENCE BOUNDARY SB1

In the northeastern part of the study area, sequence boundary SB1 is characterized by a change from underlying delta fringe silts and shales to overlying lower delta front sands in distal facies. Shoreline proximal facies are located within the thick delta front sands in the southwestern part of the study area, and the change in facies over SB1 is much less pronounced, typically from lower–middle delta front sands to upper delta front distributary mouth bar or channel sands. In general, facies present below the sequence boundary are therefore finer in grain size and contain less sand, more clay and more organic carbon that the facies which overly it. This characteristic is related to the definition of a sequence boundary as a surface representing a period of relative sea-level fall. The drop in sea-level results in a basinward shift in depositional facies, and typically results in the presence of coarser facies in the overlying strata. The difference in lithology between the two facies at any one point is a function of the depositional environment, slope of the shelf, amount of sea-level fall, and its relative position within the basin.

The following characteristics / trends of sequence boundary SB1 are associated with the charge from the underlying facies of sequence S_2 into the overlying facies of sequence S_1:

1) a strong decrease in the amount of pyrite in S_1;
2) a strong decrease in the amount of sulphur (S);
3) a marked decrease in the amount of L.O.I.;

4) a moderate decrease in zirconium (Zr) content;
5) a slight decrease in quartz abundance;
6) a slight increase in SiO_2 content;
7) a minor increase in Ba content;
8) a slight decrease in the abundance of Fe_2O_3, MgO and TiO_2;
9) a substantial decrease in the proportion of smectitic mixed-layer clays;
10) a slight decrease in Cr, and Y;
11) a substantial increase in the proportion of 7Å clays within the clay assemblage.

The overall detrital mineral composition of all of the facies observed within the study area is comparable, which supports the belief that there was no large change in the source areas during deposition.

All of these trends, whether related to the composition of detrital or diagenetic minerals, are present because subsequent diagenetic events were controlled by the original detrital composition. For example, the trends for higher levels of S and L.O.I. in sequence S_2, underlying sequence boundary SB1, are likely related to the higher levels of pyrite. Pyrite is a diagenetic mineral which is thought to have formed primarily as the result of bacterial sulphate reduction. The process is dependent on the amount of organic matter and supply of ferrous iron in the sediment (and therefore is controlled somewhat by detrital composition) (Curtis, 1978). It also requires the presence of an increased and continued supply of sulphate in formational waters (Curtis, 1978).

The prominent abundance of pyrite in all environments below the sequence boundary suggests that the conditions favorable for the precipitation of pyrite were present for a longer time during the deposition of sequence S_2 than S_1, perhaps as the result of a hiatus, manifested by the presence of sequence boundary SB1. This is most evident in proximal settings which display fewer facies differences above and below the sequence boundary. This trend suggests that the formational history of the sediments above and below sequence boundary SB1 were different, resulting from differences in detrital mineralogy, environmental factors and diagenetic history. The characteristic presence of pyrite may therefore be suitable as a diagenetic sequence boundary marker.

The final question refers to the hypothesis that the observed trends can be used as a tool to identify and confirm the presence of sequence boundaries in other study areas. The dependence of most trends observed in this study area on detrital mineralogy and depositional setting suggest that they are not useful as universal markers of sequence boundaries in the stratigraphic record. They are however, characteristic of nearshore deltaic marine facies, and could very likely be used as a guide to interpreting characteristics of a sequence boundary in a comparable setting. The best potential for a diagenetic sequence boundary marker lies in the characteristic presence and disproportionate abundance of pyrite in the finer sediments which typically underly most sequence boundaries. It should be present in the sediments underlying a sequence boundary in another setting provided conditions during deposition and early diagenesis were comparable. However, its potential as a diagenetic sequence boundary marker has yet to be tested elsewhere.

H. REFERENCES

Abercrombie, H.J. 1989. Water-rock interaction during diagenesis and thermal recovery, Cold Lake Alberta. Ph.D. Thesis, University of Calgary, Calgary, Alberta.

Abercrombie, H.J., Shevalier, M., and Hutcheon, I.E. 1989. Natural diagenesis during steam-assisted recovery of heavy oil, Cold Lake, Alberta, Canada. *In:* Miles, D.L., ed., Proceeding of the Sixth International Symposium on Water-Rock Interaction, p. 1-4.

Alberta Energy Resources Conservation Board. 1985. Atlas of Alberta's crude bitumen reserves. Alberta Energy Resources Conservation Board Reserve Report Series 38, 37pp.

Ahn, J.H., and Peacor, D.R. 1985. Transmission electron microscopic study of diagenetic chlorite in gulf coast argillaceous sediments. Clays and Clay Minerals, v. 33, no. 3, p. 228-236.

Amouric, M., Parron, C. 1985. Structure and growth mechanism of glauconite as seen by high-resolution transmission electron microscopy. Clays and Clay Minerals, v. 33, no. 6, p. 473-482.

Ayalon, A., and Longstaffe, F.J. 1988. Oxygen isotope studies of diagenesis and pore-water evolution in the Western Canada Sedimentary Basin: Evidence from the Upper Cretaceous basal Belly River sandstone, Alberta. Journal of Sedimentary Petrology, v. 58, no. 3, p. 489-505.

Bayliss, P., and Levinson, A.A. 1976. Mineralogical review of the Alberta oil sand deposits (Lower Cretaceous Mannville Group). Bulletin of Canadian Petroleum Geology, v. 24, p. 211-224.

Bergman, K.M. and Walker, R.G. 1988. Formation of Cardium erosion surface E5, and associated deposition of conglomerate: Carrot Creek field, Cretaceous Western Interior Seaway, Alberta. *In:* James, D.P. and Leckie, D.A., eds., Sequences, Stratigraphy, Sedimentology: Surface and Subsurface. Canadian Society of Petroleum Geologists, Memoir 15, p. 15-24.

Berner, R.A. 1970. Sedimentary pyrite formation. American Journal of Science, v. 268, p. 1-23.

Berner, R.A. 1978. Sulphate reduction and the rate of deposition of marine sediments. Earth and Planetary Science Letters, 37, p. 492-498.

Bhattacharyya, D.P. 1983. Origin of berthierine in ironstones. Clays and Clay Minerals, v. 31, no. 3, p. 173-182.

Biscaye, P.E. 1964. Distinction between kaolinite and chlorite in recent sediments by X-ray diffraction. The American Mineralogist, v. 49, p. 1281-1289.

Bloch, J. 1990. Stable isotope composition of authigenic carbonates from the Albian Harmon Member (Peace River Formation): evidence of early diagenetic processes. Bulletin of Canadian Petroleum Geology, v. 38, no. 1, p. 39-52.

Boon, J.A. and Hitchon, B. 1983a. Application of fluid-rock reaction studies to *in situ* recovery from oil sand deposits, Alberta, Canada –I. Aqueous phase results for an experimental-statistical study of water-bitumen-shale reactions. Geochimica et Cosmochimica Acta, v. 47, p. 235-248.

Boon, J.A. and Hitchon, B. 1983b. Application of fluid-rock reaction studies to *in situ* recovery from oil sand deposits, Alberta, Canada –II. Mineral transformations during an experimental-statistical study of water-bitumen-shale reactions. Geochimica et Cosmochimica Acta, v. 47, p. 249-257.

Boon, J.A., Hamilton, T., Holloway, L., and Wiwchar, B. 1983. Reaction between rock matrix and injected fluids in Cold Lake oil sands–potential for formation damage. Journal of Canadian Petroleum Technology, May-August, p. 55-66.

Bowers, T.S. and Burns, R.G. 1990. Activity diagrams for clinoptilolite: susceptibility of this zeolite to further diagenetic reactions. American Mineralogist, v. 75, p. 601-619.

Brindley, G.W., and Brown, G. 1980. Crystal Structures of Clay Minerals and their X-ray Identification. Mineralogical Society Monograph no. 5, Mineralogical Society, London, England, 495pp.

Burtch, S.D. 1986. Diagenesis of fine-grained Upper Cretaceous and Tertiary Clastic Rocks from the Nova Scotia shelf and slope. M.Sc. Thesis, University of Alberta, Edmonton, Alberta, 118pp.

Capeling, R.R. and Peggs, J.K. 1981. Experimental steamflood. Cold Lake oil sands. *In:* Meyer, R.F. and Steele, C.T., eds., The Future of Heavy Crude and Tar Sands, Unitar, McGraw Hill, New York, p. 361-368.

Craig, H. 1957. Isotopic standards for carbon and oxygen and correction factors for mass-spectrometric analysis of carbon dioxide. Geochimica et Cosmochimica Acta, v. 12, p. 133-149.

Craig, H. 1961. Standard for reporting concentrations of deuterium and oxygen-18 in natural waters. Science, v. 133, p. 1833-1834.

Curtis, D.D. 1978. Possible links between sandstone diagenesis and depth-related geochemical reactions occurring in enclosing mudstones, Journal of the Geological Society of London, v. 135, p. 107-117.

Day, F.H. 1963. The Chemical Elements in Nature. George G. Harrap & Co. Ltd., London, Great Britain, 353pp.

Dean, R.S. and Nahnybida, C. 1985. Authigenic trioctahedral clay minerals coating Clearwater Formation sand grains in Cold Lake, Alberta (extended abstract). Applied Clay Science, v. 1, p. 237-238.

Dickson, J.A.D. 1966. Carbonate identification and genesis as revealed by staining. Journal Sedimentary Petrology, v. 36, no. 2, p. 491-505.

Dimitrakopoulos, R. and Muehlenbachs, K. 1987. Biodegradation of petroleum as a source of ^{13}C-enriched carbon dioxide in the formation of carbonate cement. Chemical Geology, v. 65, p. 283-291.

Embry, A.F. and Podruski, J.A. 1988. Third-order depositional sequences of the Mesozoic succession of Sverdrup Basin. *In:* James, D.P. and Leckie, D.A., eds., Sequences, Stratigraphy, Sedimentology: Surface and Subsurface. Canadian Society of Petroleum Geologists, Memoir 15, p. 73-84.

Folk, R.L. 1974. Petrology of Sedimentary Rocks. Hemphill Publishing Co., Austin, Texas, 182pp.

Fuex, A.N. 1977. The use of stable carbon isotopes in hydrocarbon exploration. Journal of Geochemical Exploration. v. 7, p. 155-188.

Garven, G. 1989. A hydrogeologic model for the formation of the giant oil sands deposits of the Western Canada Sedimentary Basin. American Journal of Science, v. 289, p. 105-166.

Grabowski, J.W. and Rubin, B. 1981. A preliminary numerical simulation study of *in-situ* combustion in a Cold Lake oil sands reservoir. Journal of Canadian Petroleum Technology, April-June, p. 79-89.

Haq, B.U., Hardenbol, J. and Vail, P.R. 1987. Chronology of fluctuating sea-levels since the Triassic. Science, v. 235, p. 1156-1167.

Harrison, D.B., Glaister, R.P. and Nelson, H.W. 1981. Reservoir description of the Clearwater oil sand, Cold Lake, Alberta, Canada. *In:* Meyer, R.F. and Steele, C.T., eds., The Future of Heavy Crude and Tar Sands, Unitar, McGraw Hill, New York, ch. 30, p. 264-279.

Hebner, B.A., Bird, G.W. and Longstaffe, F.J. 1986. Fluid/pore-mineral transformation during simulated steam injection: Implications for reduced premeability damage. Canadian Journal of Petroleum Technology, v. 25, p. 68-73.

Hitchon, B. 1969. Fluid flow in the Western Canada Sedimentary Basin. 2. Effect of geology. Water Resources Research, v. 5, no. 2, p. 460-469.

Hitchon, B. 1984. Geothermal gradients, hydrodynamics, and hydrocarbon occurrences, Alberta, Canada. American Association of Petroleum Geologists, v. 68, p. 713-743.

Hoefs, J. 1987. Stable Isotope Geochemistry. Minerals, Rocks and Inorganic Materials, no. 9, Springer-Verlag, Heidelberg, 241pp.

Hudson, J.D. 1977. Stable isotopes and limestone lithification. Journal of the Geological Society of London, v. 133, p. 637-660.

Huang, W.L., Bishop, A.M., and Brown, R.W. 1986. The effect of fluid / rock ratio on feldspar dissolution and illite formation under reservoir conditions. Clay Minerals, v. 21, p. 585-601.

Hutcheon, I., Abercrombie, H., Putnam, P., Gardner, R. and Krouse, R. 1989. Diagenesis and sedimentology of the Clearwater Formation at Tucker Lake. Bulletin of Canadian Petroleum Geology, v. 37, no. 1, p. 83-97.

Inoue, A., Bouchet, A., Velde, B., and Meunier, A. 1989. Convenient technique for estimating smectite layer percentage in randomly interstratified illite / smectite minerals. Clays and Clay Minerals, v. 37, no. 3, p. 227-234.

Irwin, H., Curtis, C., and Coleman, M. 1977. Isotopic evidence for source of diagenetic carbonates formed during burial of organic-rich sediments. Nature, v. 269, p. 209-213.

Jackson, P.C. 1984. Paleogeography of the Lower Cretaceous Mannville Group of western Canada. *In:* Masters, J.C., ed., Elmworth–Case Study of a Deep Basin Gas Field. American Association of Petroleum Geologists Memoir 38, p. 49-77.

Jahren, J.S. and Aagaard. P. 1989. Compositional variations in diagenetic chlorites and illites, and relationships with formation-water chemistry. Clay Minerals, v. 24, p. 157-170.

Jardine, D. 1974. Cretaceous oil sands of western Canada. *In:* Hills, L.W., ed., Oil Sands, Fuel of the Future. Canadian Society of Petroleum Geologists, Memoir 3, p. 50-67.

Kendall, G.H. 1977. Importance of reservoir description in evaluating *in situ* recovery methods for Cold Lake heavy oil. Part I–Reservoir description. Bulletin of Canadian Petroleum Geology, v. 25, no. 2, p. 314-327.

Kirk, J.S., Bird, G.W. and Longstaffe, F.J. 1987. Laboratory study of the effects of steam-condensate flooding in the Clearwater Formation: High temperature flow experiments. Bulletin of Canadian Petroleum Geology, v. 35, no. 1, p. 34-47.

Kramers, J.W. and Rottenfusser, B.A. 1980. Techniques for SEM and EDS characterization of oil sands. Scanning Electron Microscopy, IV, SEM Inc., AMF O'Hare, Ill. Alberta Research Council Contribution No. 1034. p. 97-102.

Land, L.S. 1980. The isotopic and trace element geochemistry of dolomite: the state of the art. *In:* Zenger, D.H., Dunham, J.B., and Ethington, R.A., eds., Concepts and Models of Dolomitization. Society of Economic Paleontologist and Mineralogists, Special Paper 28, p. 87-110.

Longstaffe, F.J. 1983. Diagenesis 4. Stable isotope studies of diagenesis in clastic rocks. Geoscience Canada, v. 10, p. 43-58.

Longstaffe, F.J. 1984. The role of meteoric water in diagenesis of shallow sandstones: Stable isotope studies of the Milk River aquifer and gas pool, southeastern Alberta. *In:* McDonald, D.S., and Surdam, R.C., eds., Clastic Diagenesis, AAPG Memoir 37, p. 81-98.

Longstaffe, F.J. and Ayalon, A. 1987. Oxygen-isotope studies of clastic diagenesis in the Lower Cretaceous Viking Formation, Alberta: implications for the role of meteoric water. *In:*Marshall, J.D., ed., Diagenesis of Sedimentary Sequences, Geological Society Special Publication No. 36, p. 277-296.

Longstaffe, F.J. and Ayalon, A. 1988. Oxygen isotope studies of diagenesis and pore-water evolution in the Western Canada Sedimentary Basin: evidence from the Upper Cretaceous Basal Belly River Sandstone, Alberta. Journal of Sedimentary Petrology, v. 58, no. 3, p. 489-505.

Longstaffe, F.J., Ayalon, A. and Racki, M.A. 1989a. Oxygen and carbon isotope studies of diagenesis in heavy oil deposits of the Clearwater Formation, northeastern Alberta. Geological Association of Canada, Program with Abstracts, v. 14, p. 485.

Longstaffe, F.J., Ayalon, A. and Racki, M.A. 1989b. Natural diagenesis of Clearwater Formation reservoirs in the Cold Lake area, Alberta. Part I: Mineralogical studies. Exploration Update '89, Calgary, C.S.P.G. Program and Abstracts, p. 130.

Longstaffe, F.J., Ayalon, A., Racki, M.A., and Bird. G.W. 1989c. Natural diagenesis of Clearwater Formation reservoirs in the Cold Lake area, Alberta. Part II: Stable isotope studies of water / mineral interaction. Exploration Update '89, Calgary, C.S.P.G. Annual Meeting, Program and Abstracts, p. 142.

Longstaffe, F.J., Racki, M.A., Ayalon, A., Wickert, L.M., Wightman, D.M. and Bird, G.W. 1990. Water-mineral organic matter interactions during clastic diagenesis of Cretaceous heavy oil reservoirs, Cold Lake area, Alberta. American Association of Petroleum Geologists Bulletin, v. 74, p. 1306-1307.

Longstaffe, F.J., Racki, M.A. and Ayalon, A. 1991a. Diagenesis of Clearwater Formation Reservoirs in the Cold Lake Area, Alberta. AOSTRA-University Agreement #680, Final Report, AOSTRA, 223pp.

Longstaffe, F.J., McKay, J. and Shier, W. 1991b. Regional mineralogical controls on reservoir performance in bitumen-saturated sands, northeastern Alberta. AOSTRA-University Agreement #868, Report #2 of 6 (July 1991), 156pp.

Longstaffe, F.J., McKay, J., Shier, W. and Colquhoun, I.M. 1992a. Regional mineralogical controls on reservoir performance in bitumen-saturated sands, northeastern Alberta. AOSTRA-Univeristy Agreement #868, Report #3 of 6 (January 1992), 86pp.

Longstaffe, F.J., Ayalon, A., and Racki, M.A. 1992b. Stable isotope studies of diagenesis in berthierine-bearing oil sands, Clearwater Formation, Alberta. *In:* Kharaka and Maest, eds., Proceedings of the Seventh International Symposium on Water-Rock Interaction. Balkema, Rotterdam, p. 955-958.

Mahar, J.B. 1989. Geometry and reservoir characteristics Leismer Clearwater 'B' gas field, northeast Alberta. Case Studies in Canadian Petroleum Geology. Bulletin of Canadian Petroleum Geology, v. 37, no. 2, p. 236-240.

McCrea, J.M. 1950. On the isotopic chemistry of carbonates and a paleotemperature scale. Journal of Chemical Physics, v. 18, p. 849-857.

McRae, S.G. 1972. Glauconite. Earth-Science Reviews, no. 8, p. 397-440.

Mellon, G.B. 1967. Stratigraphy and petrology of the Lower Cretaceous Blairmore and Mannville groups, Alberta Foothills, and Plains. Research Council of Alberta Geological Division, Bulletin 21, 270pp.

Minken, D.F. 1974. The Cold Lake oil sands: geology and a reserves estimate. *In:* Hills, L.W., ed., Oil Sands, Fuel of the Future. Canadian Society of Petroleum Geologists, Memoir 3, p. 84-99.

Mitchum, R.M., Vail, P.R. and Thompson, S. 1977. Seismic stratigraphy and global changes of sea-level, Part 2: The depositional sequence as a basic unit for stratigraphic analysis. American Association of Petroleum Geologists Memoir 26, p. 53-62.

Mozley, P.S. 1989. Complex compositional zonation in concretionary siderite: implications for geochemical studies. Journal of Sedimentary Petrology, v. 59, no. 5, p. 815-818.

Nadeau, P.H. and Bain, D.C. 1986. Composition of some smectites and diagenetic illitic clays and implications for their origin. Clays and Clay minerals, v. 34, no. 4, p. 455-464.

Nicholls, J.H. and Luhning, R.W. 1977. Heavy oil sand *in-situ* pilot plants in Alberta (past and present). *In:* Redford, D.A. and Winestock, A.G., eds., The Oil Sands of Canada-Venezuela. Canadian Institute of Mining and Metallurgy, Special Volume 17, p. 36-69.

Odin, G.S. and Matter, A. 1981. De glauconiarum originae. Sedimentology, v. 28, p. 611-641.

Pettijohn, F.J., Potter, P.E., and Siever, R. 1987. Sand and Sandstone. Springer-Verlag, New York, N.Y., 553pp.

Posamentier, H.W. and Vail, P.R. 1988. Eustatic controls on clastic deposition II–Sequence and systems tract models. *In:* Wilgus, C.K. *et al.*, eds., Society of Economic Paleontologists and Mineralogists, Special Publication 42, p. 125-154.

Posamentier, H.W., Jervey, M.T. and Vail P.R. 1988. Eustatic controls on clastic deposition I–Conceptual framework. *In:* Wilgus, C.E. *et al.*, eds., Society of Economic Paleontologists and Mineralogists, Special Publication 42, p. 109-124.

Prentice, M.E. and Wightman, D.M. 1987. Mineralogy of the Clearwater Formation, Cold Lake oil sands area: Implications for enhanced oil recovery. Alberta Geological Survey Report, 41pp.

Prudêncio, M.I., Figueiredo, M.O., and Cabral, J.M.P. 1989. Rare earth distribution and its correlation with clay mineralogy in the clay-sized fraction of Cretaceous and Pliocene sediments (central Portugal). Clay Minerals, v. 24, p. 67-74.

Putnam, P.E. and Pedskalny, M.A. 1983. Provenance of Clearwater Formation reservoir sandstones, Cold Lake, Alberta, with comments on feldspar composition. Bulletin of Canadian Petroleum Geology, v. 31, p. 148-160.

Racki, M.A., Ayalon, A. and Longstaffe, F.J. 1989. Mineralogical studies of diagenesis in heavy oil deposits of the Clearwater Formation, northeastern Alberta. Geological Association of Canada / Mineralogical Association of Canada Annual Meeting, May 15-17, Program with Abstracts, v. 14, p. A85.

Raiswell, R. 1982. Pyrite texture, isotopic composition and the availability of iron. American Journal of Science, v. 282, p. 1244-1263.

Schooley, J.V. 1975. A study of the mineralogy of Lower Cretaceous Mannville Group oil sand deposits, Alberta and west Saskatchewan. M.Sc. Thesis, The University of Calgary, Calgary, Alberta 134pp.

Sedimentology Research Group. 1981. The effects of *in-situ* steam injection on Cold Lake oil sands. Bulletin of Canadian Petroleum Geology, v. 29, no. 4, p. 447-478.

Shepherd, D.W. 1981. Steam stimulation recovery of Cold Lake bitumen. *In:* Meyer, R.F. and Steele, C.T., eds., The Future of Heavy Crude and Tar Sands, Unitar, McGraw Hill, New York, p. 349-360.

Smyth, J.R., Spaid, A.T., Bish, D.L. 1990. Crystal structures of a natural and a Cs-exchanged clinoptilolite. American Mineralogist, v. 75, p. 522-528.

Stelck, C.R. and Leckie, D. 1988. Foraminiferal inventory and lithologic description of the Lower Cretaceous (Albian) Hulcross Shale, Monkman area, northeastern British Columbia. Canadian Journal of Earth Science, v. 25, p. 793-798.

Sudo, T. and Shimoda, S. 1977. Interstratified clay minerals – mode of occurrence and origin. Minerals Science Engineering, v. 9, no. 1, p. 3-24.

Thorez, J. 1976. Practical identification of clay minerals. A handbook for teachers and students in clay mineralogy. SPRL. Imprimerie G. Lelotte, Dison, Beligum, 90pp.

Tilley, B. 1988. Diagenesis and porewater evolution in Cretaceous sedimentary rocks of the Alberta Deep Basin. Ph.D Thesis, University of Alberta, Edmonton, Alberta, 205pp.

Towson, D.E. 1977. Importance of reservoir description in evaluating *in situ* recovery methods for Cold Lake heavy oil . Part II–*In situ* application. Bulletin of Canadian Petroleum Geology, v. 25, no. 2, p. 328-340.

Van Wagoner, J.C., Mitchum, R.M.Jr., Posamentier, H.W. and Vail, P.R. 1987. Key definitions of sequence stratigraphy. *In:* Bally, A.W., ed., American Association of Petroleum Geologists, Studies in Geology, 27, p. 11-14.

Walters, L.J. Jr., Claypool, G.E. and Choquette, P.W. 1972. Reaction rates and δO^{18} variation for the carbonate-phosphoric acid preparation method. Geochimica et Cosmochimica Acta, v. 56, p. 129-140.

Western Atlas International. 1988. Stratigraphic correlation chart of the Western Canada Sedimentary Basin. Western Atlas Canada Ltd., Calgary, Alberta.

Wickert, L.M., Pemberton, S.G. and Longstaffe, F.J. 1988. An application of sequence stratigraphy to depth-related clastic diagenesis in the Cold Lake oil sands, east-central Alberta (abst.). *In:* James, D.P. and Leckie, D.B., eds., Sequences, Stratigraphy, Sedimentology: Surface and Subsurface. Canadian Society of Petroleum Geology, Memoir 15, p. 585.

Wickert, L.M., Longstaffe, F.J., and Pemberton, S.G., 1989. A diagenetic investigation of sequence stratigraphy in the Lower Cretaceous Clearwater Formation, Cold Lake oil sands, east-central Alberta. Geological Association of Canada / Mineralogical Association of Canada Annual Meeting, May 15-17, Program with Abstracts, v. 14, p. A86.

Wiewióra, A. 1990. Crystallochemical classifications of phyllosilicates based on the unified system of projection of chemical composition: III. The serpentine-kaolin group. Clay Minerals, v. 25, p. 93-98.

Wightman, D.M. and Berezniuk, T. 1986. Resource characterization and depositional modelling of the Clearwater Formation, Cold Lake oil sands deposit, east-central Alberta. *In:* Westhoff, J.D., and Marchant, L.C. eds., Proceedings of the 1986 Tar Sands Symposium, ARC Contribution No. 1452, Jackson, Wyoming, July 7-10, p. 20-45.

Williams, G.D. and Stelck, C.R. 1973. Speculations on the Cretaceous paleogeography of North America. Geological Association of Canada Special Paper Number 13, p. 1-54.

Wu, C.T-W. 1986. Operation manual for X-ray fluorescence analysis. Department of Geology, University of Western Ontario, London, Ontario, 9pp.

PLATE 3.1:

(a) LW3-36, silty f.g. sand, water saturated. Thin section photomicrograph illustrating the overall characteristics of Clearwater sands in the study area. Note the angular grains, compositional immaturity, high abundance of quartz (Q), and high porosity (pores filled with blue epoxy). Mag: 46X, PPL, scale bar = 0.24mm. (3-28-66-2W4).

(b) LW3-36, silty f.g. sand, water saturated. Thin section photomicrograph of framework grains adjacent to organic-rich partings. Note presence of twinned plagioclase (Pl) and green glauconite grains (G). Mag: 25X, cross-polarized light (cross-polars), scale bar = 0.1mm. (3-28-66-2W4).

(c) LW3-66, sandy silt / shale, water saturated. SEM photomicrograph of cast of biological material (large cells). Mag: 675X. (3-28-66-2W4).

(d) LW-87-CW-26, water sand. SEM photomicrograph of altered rock fragment (aRF) adjacent to framework grains of quartz (Q) and plagioclase (Pl). Mag: 325X. (6-31-66-2W4).

(e) LW3-36, silty f.g. sand, water saturated. Thin section photomicrograph exhibiting extremely altered grain with residual rim (R), altered glauconite (aG), quartz (Q), volcanic rock fragment (vRF), K feldspar (KF), and chert (Ch). Although a water sand, sample contains residual bitumen (B) around grain boundaries, highlighting presence of diagenetic grain coating clays. Mag: 202X, PPL, scale bar = 49.5μm. (3-28-66-2W4).

(f) as Plate 3.1e, cross-polars.

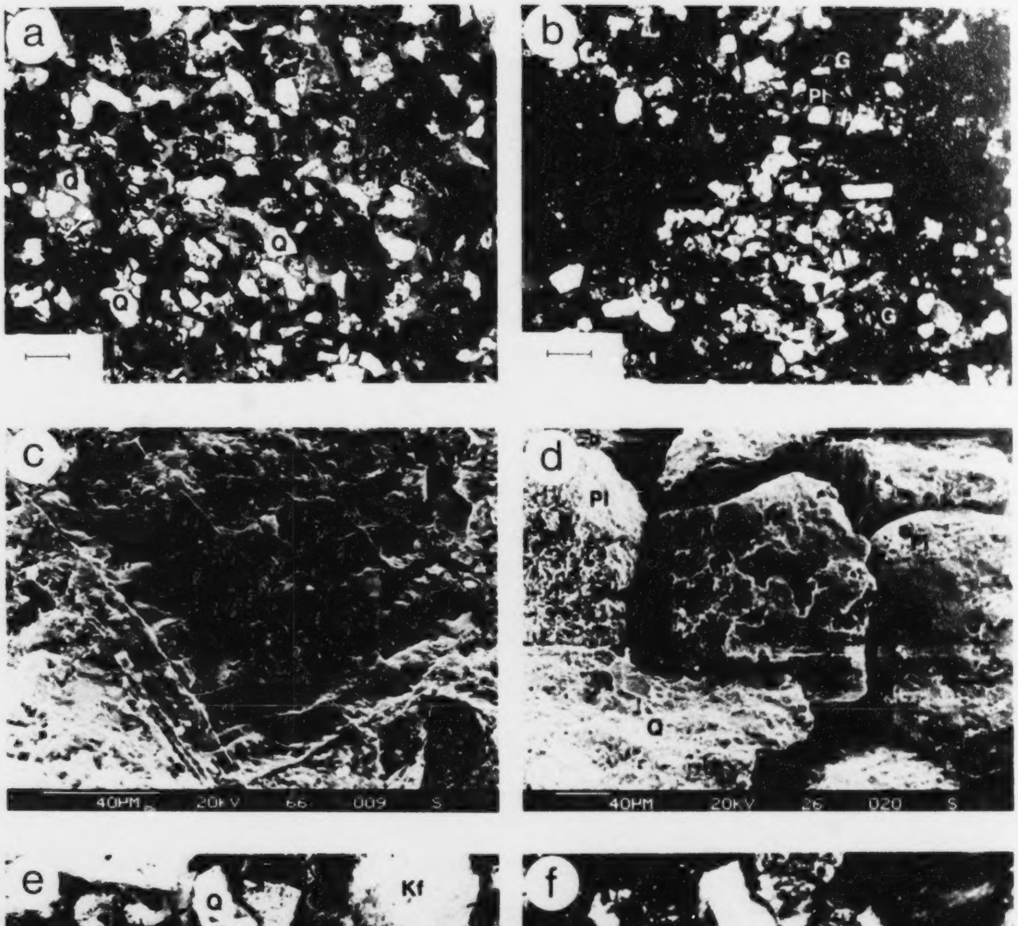
a
Q
Q
Q
b
G
Pl
G
c
40PM 20KV 66 009 S
d
Pl
Pl
Q
40PM 20KV 26 020 S
e
Q
Kf
aG
Q
Q
f

PLATE 3.2:

(a) LW3-36, silty f.g. sand, water saturated. Thin section photomicrograph exhibiting remnants of altered grains (aGr), one of which has been replaced by authigenic siderite (S). Sample also contains grains of dolomite (D), an elongate grain of detrital clay (chlorite?) (dC), and numerous rock fragments (RF) covered by light green grain coating clays, likely berthierine, which are present in this sample. Note residual bitumen coating edges of quartz (Q), highlighting presence of clays. Blue epoxy in open pores. Mag: 202X, PPL, scale bar = 49.5μm. (3-28-66-2W4).

(b) as per Plate 3.2a, cross-polars. Note greyish-blue birefringence of detrital clay (dC), and albite twinning of plagioclase grain (Pl).

(c) LW3-36, silty f.g. sand, water saturated. Thin section photomicrograph illustrating different types of volcanic rock fragments, porphyritic (poRF), and acidic (acRF). Also present are numerous grains of detrital dolomite (D), and euhedral quartz (Q), one of which is covered by a greenish coating of diagenetic clays (C). Mag: 255X, PPL, scale bar = 39μm. (3-28-66-2W4).

(d) as per Plate 3.2c, cross-polars. Note dark colours of acidic rock fragments (acRF). Individual characteristics of porphyritic fragments are difficult to distinguish because of grain coating clays. Dolomite (D) has characteristic high order birefringence.

(e) LW3-38, partially calcite cemented f.g. silty sand containing abundant volcanic rock fragments (acidic (acRF) and porphyritic (pRF)), quartz (Q), chert (Ch), plagioclase (Pl), and green grain coating clays, likely berthierine, which are abundant in this sample (7Å clays compose 5.9% of WR analysis by XRD). Also note altered glauconite grain (aG). Mag: 130X, PPL, scale bar = 77μm. (3-28-66-2W4).

(f) as per Plate 3.2e. Note bright yellowish-green birefringence colours (retardation + natural mineral) of altered early diagenetic glauconite (aG), albite twins of plagioclase (Pl), and individual crystallites of chert (Ch).

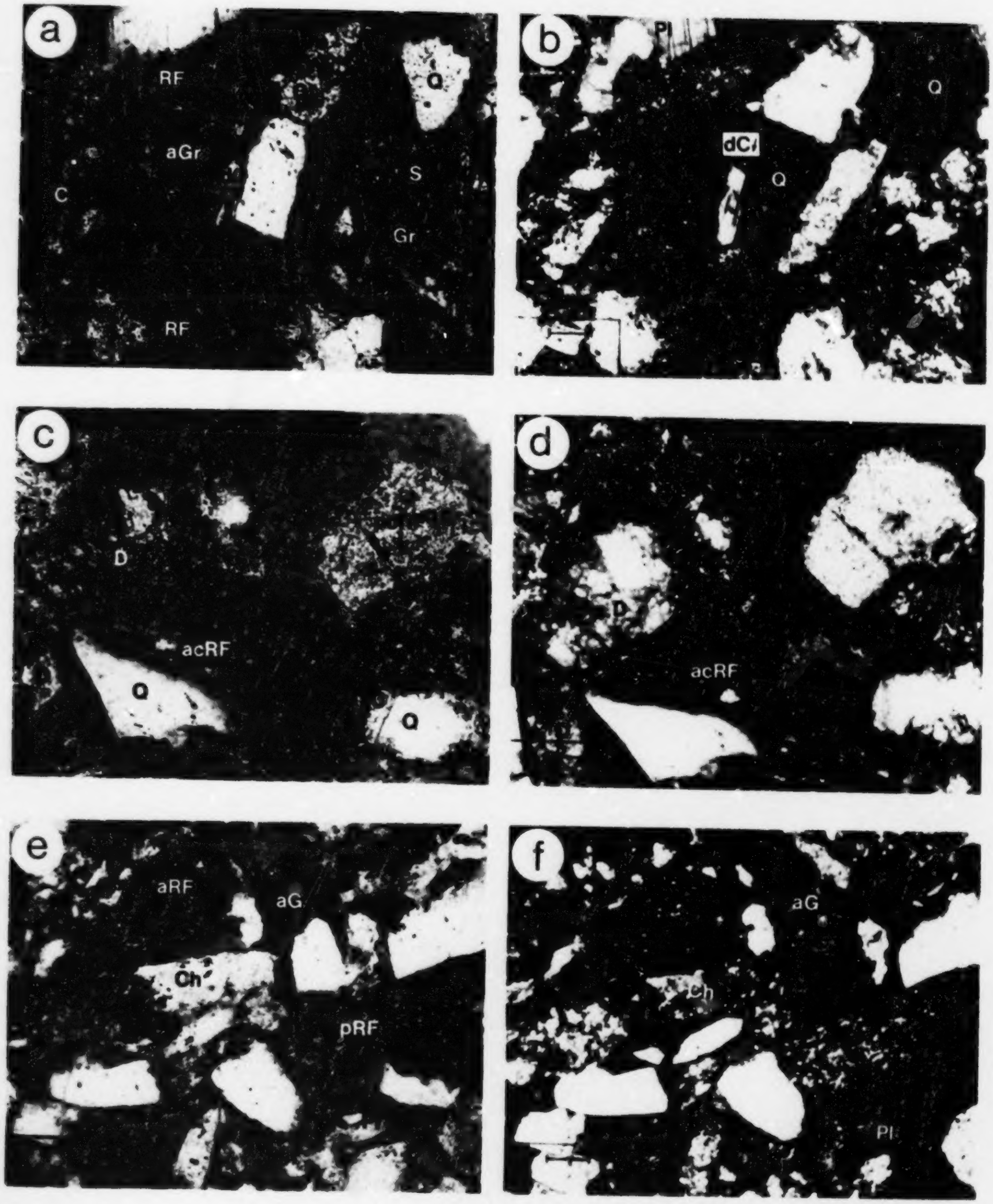
a
RF
Q
aGr
C
S
Gr
RF
b
Pl
Q
dCl
Q
c
D
acRF
Q
Q
d
D
acRF
e
aRF
aG
Ch
pRF
f
aG
Ch
Pl

PLATE 3.3:

(a) LW3-36, f.g. silty sand, water saturated. Thin section photomicrograph of chert (Ch), porphyritic volcanic rock fragments (poRF), quartz (Q), dolomite (D), and slightly altered glauconite (aG) in section. Blue epoxy in pore spaces. Mag: 202X, PPL, scale bar = 49.5μm. (3-28-66-2W4).

(b) as per Plate 3.3a, cross-polars. Note fine-grained uniform quartz crystals characteristic of chert (Ch), and bright birefringence colours of glauconite grains (aG).

(c) LW3-20, calcite cemented muddy f.g. sand. Thin section photomicrograph of quartz (Q), detrital clay (dC), muscovite (M), and altered glauconite grains (aG) within pore filling calcite cement. Note that outer edges of quartz are only marginally dissolved, only remnants remain of other grains (see Plate 3.2d). Mag: 165X, PPL, scale bar = 61μm. (3-28-66-2W4).

(d) as per Plate 3.3c, cross-polars. Note characteristic birefringence of detrital clay (dC) (chlorite-rich?), quartz (Q) and early diagenetic glauconite (aG), despite the presence of abundant calcite cement. Also note the second order birefringence colours of detrital grain of muscovite (M).

(e) LW3-20, calcite cemented muddy f.g. sand. SEM photomicrograph of quartz grain (Q) embedded in fine calcite cement (Ca), which partially dissolved along cleavage planes (not normally visible). Quartz grain in behind exhibits conchoidal fracture on broken grain surface. Mag: 600X. (3-28-66-2W4).

(f) Magnification of partially dissolved quartz grain within box in Plate 3.3f. Illustrates dissolution and pitting of crystal surface. Mag: 9000X.

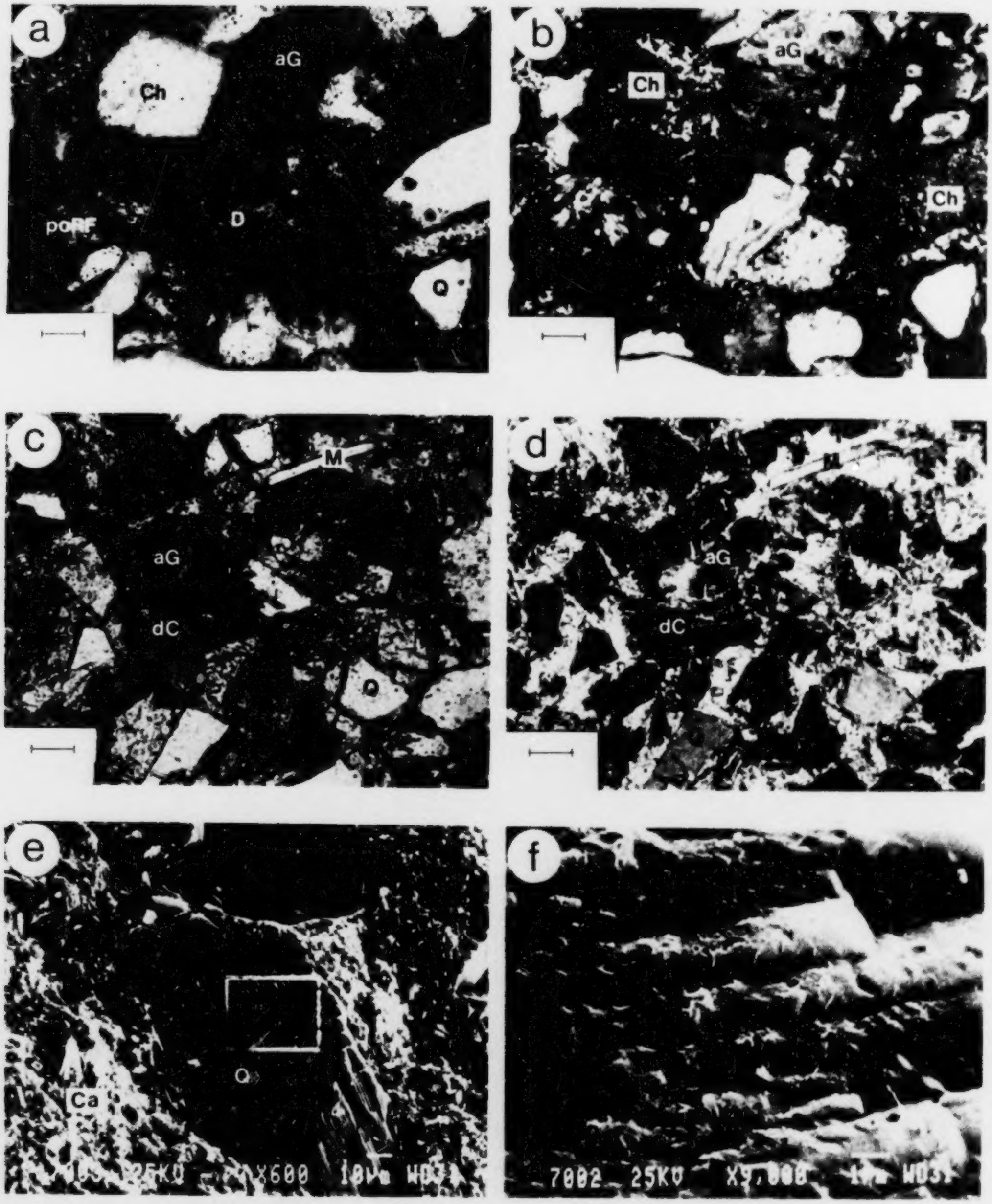
a
Ch
aG
poRF
D
Q
b
aG
Ch
Ch
c
M
aG
dC
Q
d
M
aG
dC
e
Ca
Q
25KV X600 10μm
f
7002 25KV X9,000 1μm WD31

PLATE 3.4:

(a) LW3-38, partially calcite cemented f.g. silty sand. Thin section photomicrograph exhibiting euhedral shape of volcanic quartz grain (vQ), K feldspar with authigenic overgrowths (KF) (boundary shown by arrows), and chert (Ch) amongst abundant rock fragments (RF) and dolomite (D). Mag: 202X, cross-polars, scale bar = 49.5μm. (3-28-66-2W4).

(b) LW3-36, f.g. silty sand, water saturated. Thin section photomicrograph exhibiting typical cross-hatched or 'plaid' twinning of microcline K feldspar (KF), and sutured contacts of polycrystalline quartz (pQ) a metamorphic rock fragment in the sample. Grains of quartz (Q) and volcanic rock fragments (vRF) also present. Mag: 202X, cross-polars, scale bar = 49.5μm. (3-28-66-2W4).

(c) LW-87-CW-33, silty / sandy shale, moderately bitumen saturated. SEM photomicrograph of altered grain of former plagioclase feldspar, replaced by authigenic clays (C), likely illitic (52% of clays in sample). Abundant small framboids of diagenetic pyrite also present (Py). Authigenic crystals of late forming K feldspar (KF) at rear of photograph. Mag: 650X. (3-13-65-4W4).

(d) LW-87-CW-11, f.g. silty bitumen saturated sand. Thin section photomicrograph exhibiting characteristic albite twinning of plagioclase feldspar (Pl) amongst grains of quartz (Q), chert (Ch) and altered volcanic rock fragments (aRF) coated with greenish berthierine type clays. Note abundant bitumen along edges of grains (arrows). Mag: 103X, cross-polars, scale bar = 97μm. (6-31-66-2W4).

(e) LW3-36, f.g. silty sand, water saturated. Thin section photomicrograph of rhomb-shaped dolomite (D) with rounded edges indicative of its detrital origin. Section also contains abundant rock fragments coated with light green diagenetic berthierine-type clays (Be), and detrital polycrystalline quartz (pQ), monocrystalline quartz (Q) and a dark, altered grain of early diagenetic glauconite (aG). Mag: 103X, PPL, scale bar = 97μm. (3-28-66-2W4).

(f) as per Plate 3.4e, cross-polars. Note the variable size and sutured grain boundaries of polycrystalline quartz (pQ), typical birefringence of glauconite (G), and multiple orders of birefringence colours at edge of dolomite grain (D).

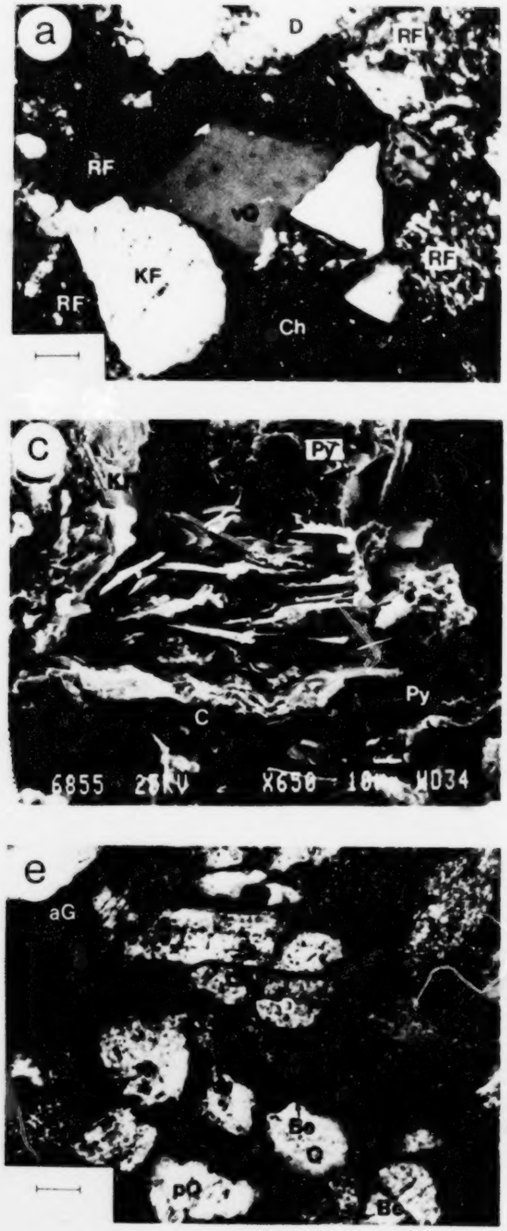
a
D
RF
RF
vQ
KF
RF
RF
Ch
b
vRF
pQ
Q
KF
c
K
Py
Py
C
6855 25KV X650 10µm WD34
d
Pl
Ch
Pl
aRF
Q
e
aG
Be
Q
pQ
Be
f
G
D
pQ

PLATE 3.5:

(a) LW3-36, silty f.g. sand, water saturated. Thin section photomicrograph of detrital dolomite (D) with 'stepped' edges broken along cleavages exhibiting multiple order birefringence colours. Adjacent grains include detrital quartz (Q), K feldspar (KF) and volcanic rock fragments (vRF). Mag: 323X, cross-polars, scale bar = 31μm. (3-28-66-2W4).

(b) LW-87-CW-17, shale with trace of silt and bitumen. SEM photomicrograph of detrital dolomite grain with similar morphology to that of Plate 3.5a. Illustrates rounded ends of dolomite cleavage terminations, as well as some pitting resulting from dissolution (arrows). Mag: 2500X. (6-31-66-2W4).

(c) LW3-36, silty f.g. sand, water saturated. Thin section photomicrograph with abundant detrital dolomite (D), euhedral quartz (Q), volcanic rock fragments (vRF), and dark coloured and foliated metamorphic rock fragments (meRF) containing abundant detrital clays (see Plate 3.5d). Mag: 202X, PPL, scale bar = 49.5μm. (3-28-66-2W4).

(d) as per Plate 3.5c, cross polars. Note sutured internal grain boundaries of polycrystalline quartz (pQ), high order birefringence of detrital dolomite (D), and bluish grey birefringence of detrital clays in the metamorphic rock fragment (meRF), likely from chlorite.

(e) LW3-36, silty f.g. sand, water saturated. Thin section photomicrograph of large elongate grain of detrital mica, likely muscovite, with characteristic second-order birefringence colours. Also present is a second mica grain (M), detrital clay-rich grains (dG) and volcanic rock fragments (vRF) exhibiting internal plagioclase laths. Mag: 130X, cross-polars, scale bar = 77μm. (3-28-66-2W4).

(f) LW-87-CS-27, water saturated f.g. sand. SEM photomicrograph of detrital clay-rich grain (dC), altered at surface to wispy illitic clays (small arrows) abundant in this sample (4.8% of WR fraction). Also note diagenetic pore-bridging illite (I) on adjacent rounded grain (glauconite?), abundant authigenic K feldspars (KF) on surface and within crack of broken grain, and early framboidal pyrite (Py). Mag: 200X. (6-31-66-2W4).

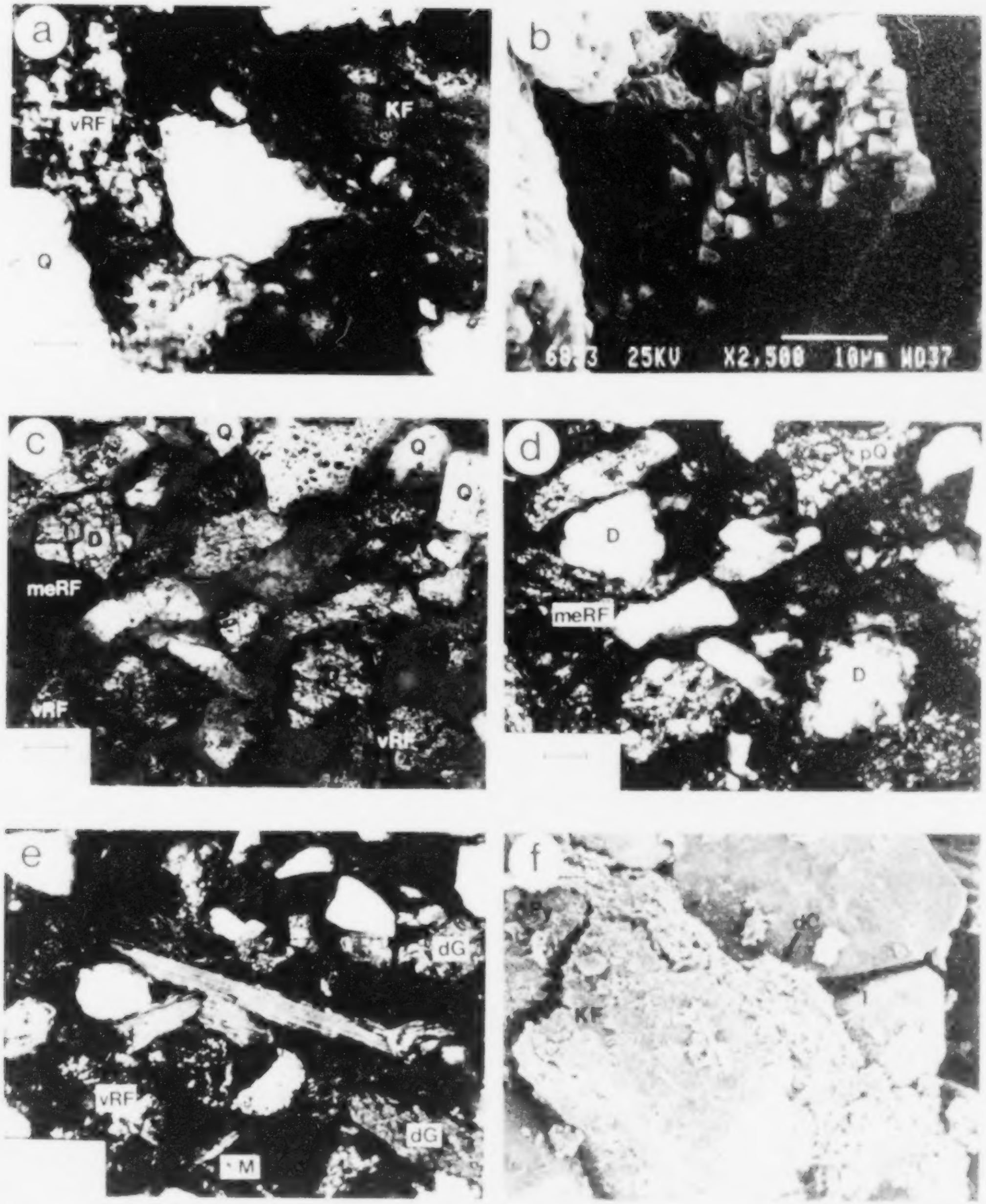
a
vRF
KF
Q
b
25KV
X2,500
10µm
WD37
c
Q
Q
Q
D
meRF
vRF
vRF
d
pQ
D
meRF
D
e
dG
vRF
dG
M
f
KF
dC

PLATE 3.6:

(a) LW-87-CW-33, silty / sandy shale, water saturated. SEM photomicrograph of detrital illite / smectite (I/S) clays, with typical Si, Al, Fe, K, Ca & Mg composition by EDX analysis (as indicated in Appendix 4). I/S comprises 24% of clays in sample. Mag: 3925X. (3-13-65-4W4).

(b) LW-87-CW-47, water saturated silt and shale. SEM photomicrograph of typical flattened, 'webby' morphology of detrital illite / smectite clays in the study area (52% I/S in this sample). Note small blocky lath of diagenetic zeolite (Z), often associated with shales. Mag: 2500X. (8-19-66-2W4).

(c) LW-87-CW-11, f.g. silty bitumen saturated sand. Thin section photomicrograph of accessory mineral which exhibits an uneven fracture and second order birefringence characteristic of olivine (O). Shown in association with detrital dolomite (D), albite twinned plagioclase (Pl), quartz (Q) and volcanic rock fragments (vRF). Mag: 200X, cross-polars, scale bar = 50µm. (6-31-66-2W4).

(d) LW-87-CW-40, f.g. bitumen saturated sand. Thin section photomicrographs of accessory minerals – zircons (Zi), characterized by high relief (under PPL, left photo), and high order birefringence (cross-polars, right photo). Note presence of abundant bitumen (orangish colours in PPL and cross-polars) at the edges of and between grains. Mag: 255X, PPL / cross-polars, scale bar = 39µm. (3-13-65-4W4).

(e) LW3-36, silty f.g. sand, water saturated. Thin section photomicrograph of early diagenetic glauconite (G), and detrital clays (dC) many of which appear foliated and may be classified as metamorphic rock fragments. Section also contains abundant volcanic rock fragments (vRF), and some dolomite (D), and quartz (Q). Mag: 165X, PPL scale bar = 61µm. (3-28-66-2W4).

(f) as per Plate 3.6e, cross-polars. Note typical bright yellow-green birefringence (retardation colours + colour of natural mineral) and 'kidney-like' shape of glauconite pellets.

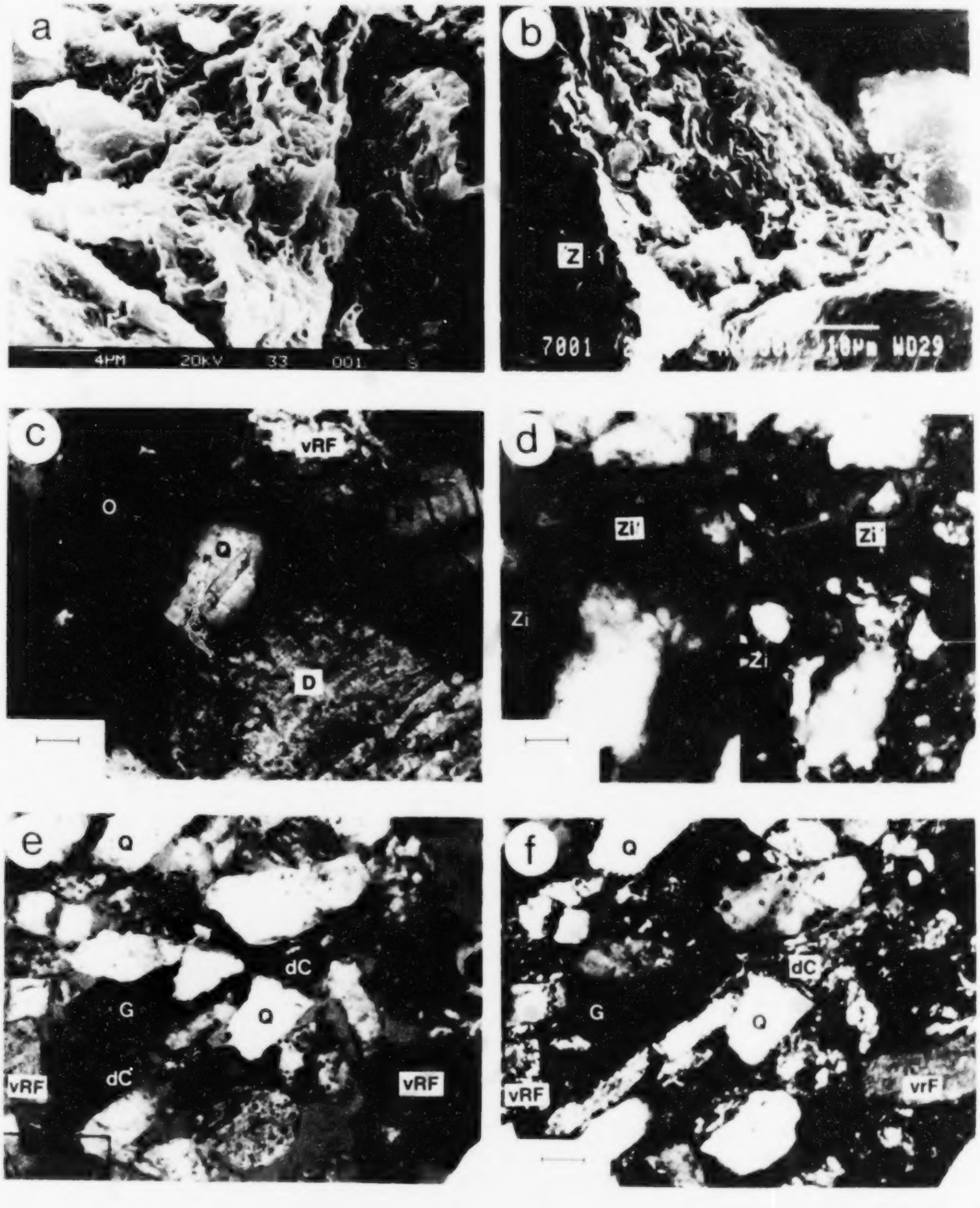
a
4PM 20KV 33 001 S
b
Z
7001
10Pm WD29
c
vRF
O
Q
D
d
Zi'
Zi'
Zi
Zi
e
Q
dC
G
Q
dC
vRF
vRF
f
Q
dC
G
Q
vRF
vrF

PLATE 3.7:

(a) LW-87-CW-27, f.g. water sand. SEM photomicrograph of undeformed glauconite pellet (G), with its outer later of grain coating of authigenic clays, likely illitic (arrows), projecting from the surface (10Å clays compose 3.5% of WR fraction). Adjacent framework grains are often dissolved and similarly altered. Crystals of K feldspar (KF) formed later than the clays (no clay coating). Mag: 300X. (6-31-66-2W4).

(b) LW-87-CW-25, shale containing silt and sand, water saturated. SEM photomicrograph of early pore-filling framboidal pyrite in fine grained sediments (Py). Smooth surfaces are positions of attachment to framework grains now missing. Singular (later?) pyrite crystals are also present (arrow). Late authigenic clays (smectitic?) (Sm) attached to pyrite. (Smectitic clays from 9.5% of WR fraction). Also note prominent grain dissolution (di). Mag: 2000X. (6-31-66-2W4).

(c) LW-87-CW-26, f.g. water sand. SEM photomicrograph of typical early pore-filling sphere-shaped framboidal pyrite, locally abundant in study area. Individual pyrite crystallites are small and do not exhibit a well defined morphology. Pyrite framboids are covered by a thin film, likely of diagenetic clays. Mag: 2700X. (6-31-66-2W4).

(d) LW-87-CW-17, shale containing silt and sand, trace levels of bitumen. SEM photomicrograph exhibits typical octahedrons of late pore-filling pyrite. Crystals occur as knobby framboids and as single crystals. Note positions with shale where crystals are now missing (black arrows). Surrounding shales lightly covered by bitumen (B). Mag: 6000X. (6-31-66-2W4).

(e) LW3-38, f.g. muddy sand, water sand, partially calcite cemented. SEM photomicrograph of octahedral crystals of late pore-filling pyrite (Py) surrounded by other diagenetic phases. Paragenetic relationships are: 1) intergrown clay laths (C) and K feldspar (KF), 2) authigenic pyrite (Py), 3) later authigenic clay on K feldspar and pyrite, intergrown with zeolite plates (Z). Mag: 430X. (3-28-66-2W4).

(f) LW-87-CW-17, shale containing silt and sand, trace of bitumen. SEM photomicrograph exhibits typical pore-filling nature and octahedral form of late pyrite. Singular grains here are small (<< 1 to ~2μm) in size, and some are missing, similar to that described in Plate 3.7d. Surrounding clay-rich shaly rocks are lightly covered by bitumen (B), although pyrite is not, except near edges. Mag: 900X. (6-31-66-2W4).

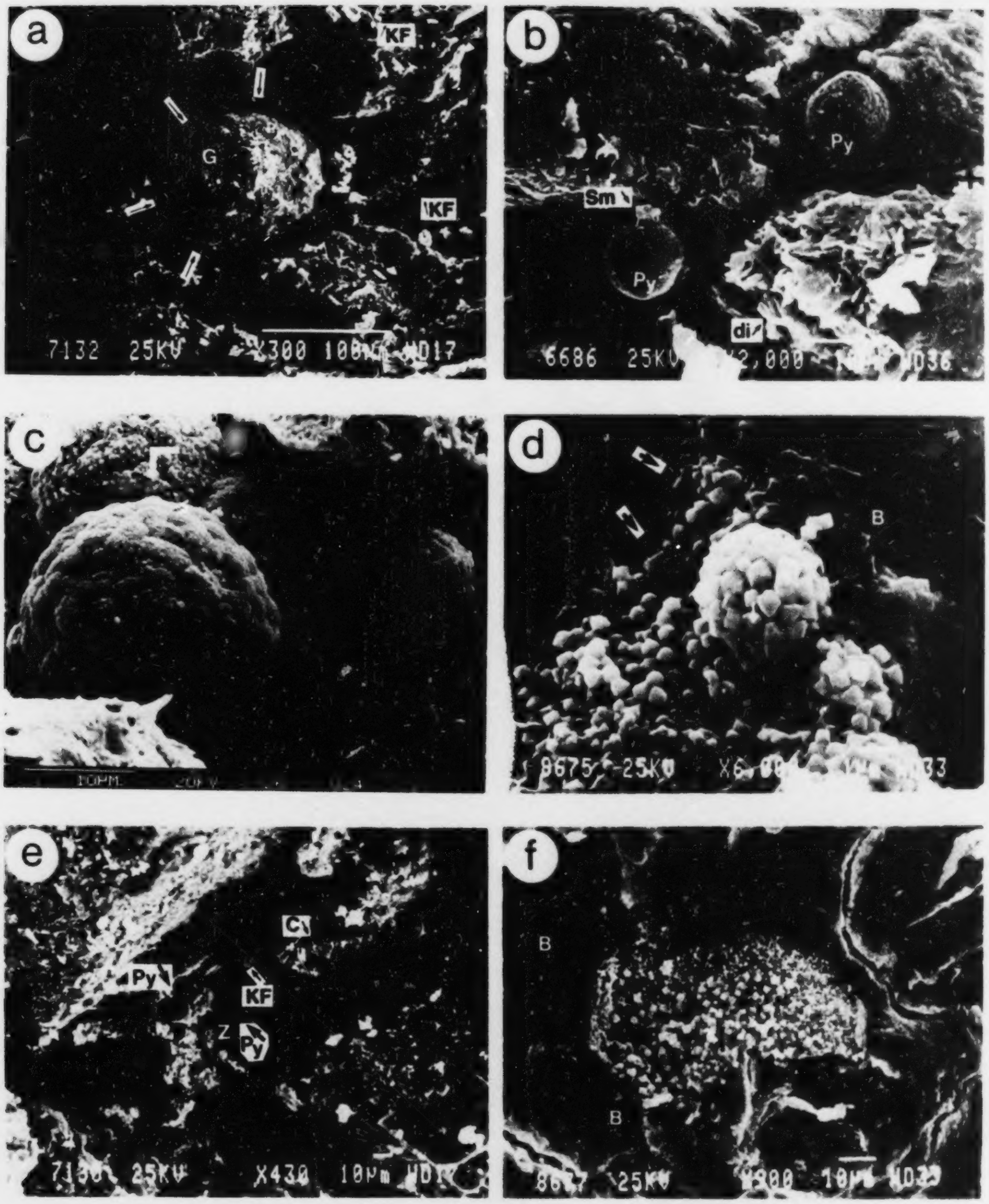
a
KF
G
KF
7132 25KV X300 100Vm WD17
b
Py
Sm
Py
di
6686 25KV
WD36
c
10PM 20KV
d
B
25KV
e
C
Py
KF
Z
Py
25KV X430 10Pm
f
B
B
25KV 10Pm

PLATE 3.8:

(a) LW3-36, silty sand, water saturated. Thin section photomicrograph shows typical green color and nature of abundant grain coating berthierine clays (Be) on surface of altered grain (volcanic?). Adjacent altered grains are filled with authigenic siderite crystal(s). Residual bitumen (B) on surface of nearby volcanic rock fragments (vRF) and quartz (Q). Mag: 202X, PPL, scale bar = 49.5μm. (3-28-66-2W4).

(b) LW-87-CW-28, fine to medium grained bitumen saturated sand. SEM photomicrograph shows typical nature and prevalence of 7Å grain coating berthierine clays in bitumen saturated sands. Missing patches are mainly the points of contact with now missing grains (arrows). Authigenic K feldspars formed after berthierine (non clay coated). Sample is from the thickest reservoir sands in the study area. Note larger size of grains in this locality (~200μm). Mag: 200X. (3-13-66-2W4).

(c) as per Plate 3.8a, cross-polars. Note anomalous blue/green birefringence of diagenetic berthierine (Be), a mix of retardation colours and the natural colour of the mineral. Plagioclase (Pl) shows typical albite twinning. Mica within foliated metamorphic rock fragment exhibits typical high order birefringence (meRF).

(d) Enlargement of boxed area in Plate 3.8b. Grain coating berthierine (Be) is approximately 6μm thick in this sample and very dense. Pore-bridging character of berthierine also evident (arrows). Absence of abundant associated authigenic minerals is characteristic of bitumen-rich sands in study area. Mag: 700X.

(e) LW-87-CW-62, silty sand, bitumen saturated. SEM photomicrograph of typical webby laths of well developed abundant grain-coating berthierine. Edges of laths are slightly crenulated, commonly with small projections, and are quite large in this sample, with an average width of ~6μm. Mag: 750X. (16-2-66-3W4).

(f) Close-up of berthierine laths from Plate 3.8d. As in Plate 3.8e laths are elongate with slightly crenulated edges and small projections, although they are much smaller in this sample (~1μm thick). Berthierine clays compose 76% of the clay in this sample (XRD relative abundance < 2μm fraction). Arrow indicates position of EDX analysis for berthierine in Appendix 4. Mag: 5000X.

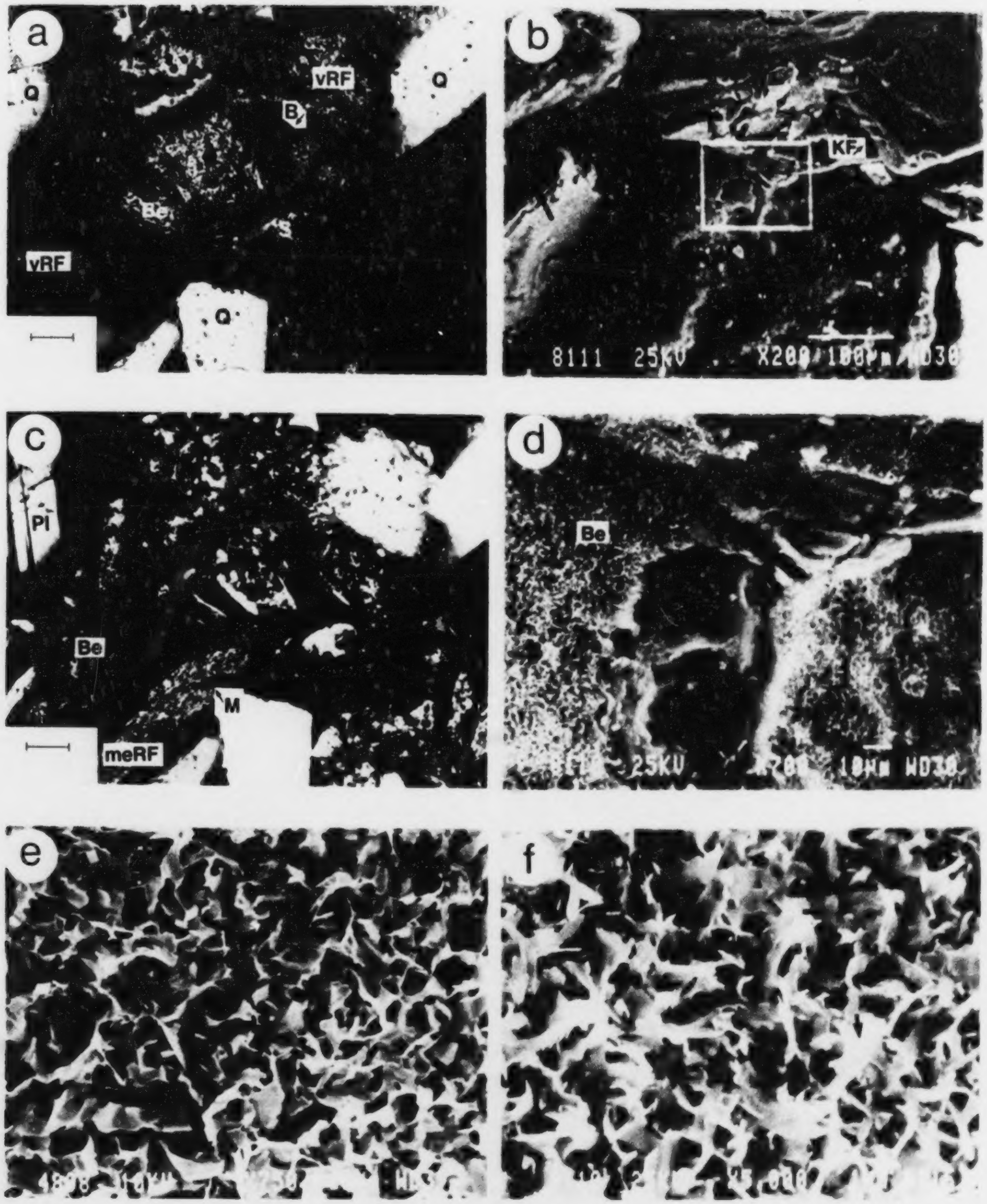
a
Q
vRF
Q
B
Be
S
vRF
Q
b
KF
8111 25KV X200 100µm WD30
c
Pl
Be
M
meRF
d
Be
25KV X200 10µm WD30
e
f

PLATE 3.9:

(a) LW-87-CW-66, calcite cemented shaly sand, bitumen-free. Thin section micrograph of fibrous, Fe-poor (pink stain) calcite cement (47% calcite by XRD). This was identified as Type 1 calcite cement. The fluids which brought it into the formation were very pervasive, dissolving nearly all in its path. Black material is from residual grains and organic matter (om). Mag: 200X, PPL, scale bar = 50μm. (16-2-66-3W4).

(b) LW-87-CW-66, calcite cemented shaly sand, bitumen free. Thin section photograph exhibits near *leaf-like* form of fibrous Type 1 calcite, which occurs as a replacement cement in the sample. Cracks are the result of desiccation of the sample subsequent to staining; blue from epoxy. Mag: 200X, PPL, scale bar = 50μm. (16-2-66-3W4).

(c) LW3-20, calcite cemented muddy sand, trace of bitumen present on surface. Calcite (Fe-rich) cementation of silty / sand and shaly layers (pelitic partings) results in the different characteristics of this Type 2 calcite cement in the study area. Typical nature of this pore-filling cement is shown in Plates 3.3c, 3.3d, 3.3e. Residual organic matter from shaly partings (sp) remains as reddish brown stringers (om). Mag: 25X, cross-polars, scale bar = 0.4mm. (3-28-66-2W4).

(d) LW3-20, calcite cemented muddy sand. Magnified view of characteristics of residual grains within shaly partings of this sand (3.9c). The outer margins of all grains are attacked (arrows), and many grains have been completely dissolved. Quartz grains (Q) were the most resistant. 'Matrix' cement is nearly micritic, extremely fine grained with residual organic matter (om). Coarser-grained calcite cement precipitated in voids left by dissolved grains, forming a layer of coarser grained calcite around crystals. Mag: 165X, cross-polars, scale bar = 61μm. (3-28-66-2W4).

(e) LW3-20, calcite cemented muddy sand. Thin section photomicrograph exhibiting contact between Type 2, Fe-rich (blue stain) f.g. cement in shaly partings and later Type 3, vein-filling calcite cement. Both stained and unstained area shown in photo. Type 3 vein-filling calcite crosscut and dissolved former Type 2 cement (as shown in Plate 3.9d), then reprecipitated as coarse grained interlocking calcite crystals in vein. Type 3 fluids were initially Fe-rich, progressing to Fe-poor as last crystals formed in the vein (pink stain). Mag: 103X, partially crossed-polars, scale bar = 97μm. (3-28-66-2W4).

(f) LW3-20, calcite cemented muddy sand. Thin section photograph exhibiting second generation of Type 3 vein-filling calcite cement crosscut by second calcite-rich veinlet (v). "Sparry" crystals perpendicular to edge are evident in larger vein (which has desiccated slightly subsequent to staining). As in Plate 3.9e, fluids of both generations of Type 3 cement progressed from Fe-rich to Fe-poor (blue–pink) during precipitation. Mag: 103X, cross-polars, scale bar = 97μm. (3-28-66-2W4).

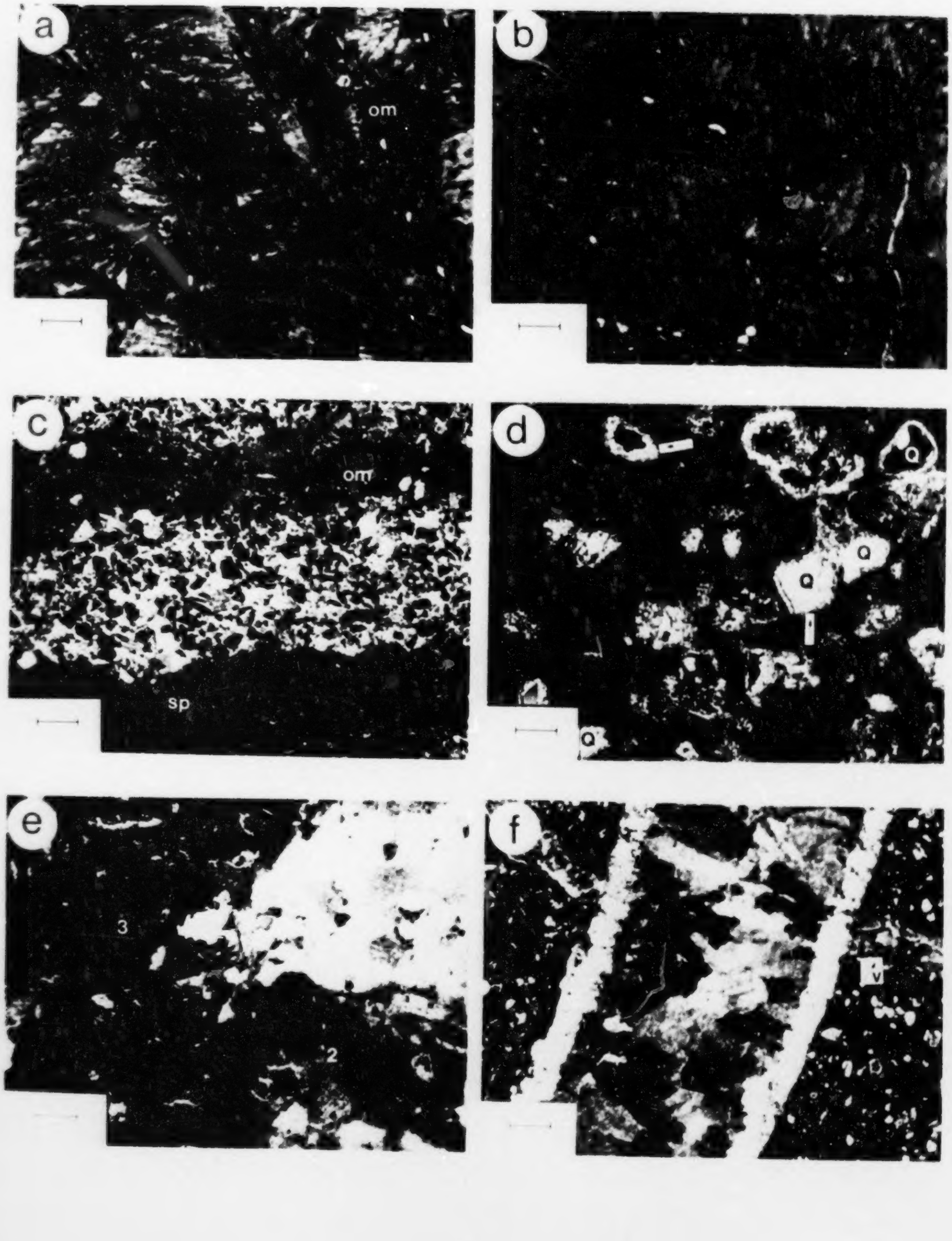
a
om
b
c
om
sp
d
Q
Q
Q
Q
Q
e
3
2
f
v

PLATE 3.10:

(a) LW3-13, silty and sandy shale, containing a trace of bitumen. SEM photomicrograph illustrating typical grain coating and pore-bridging nature of authigenic clays - illite–illite / smectite. EDX analysis indicates clays contain Si, Al, Fe and K, with minor Mg, Ca and Ti (9% illite and ~4% smectitic clays in W.R. XRD analysis). Mag: 205X. (3-28-66-2W4).

(b) LW-87-CW-33, silty / sandy shale, bitumen saturated. SEM photomicrograph of intertwined laths with prominent fuzzy edges which by EDX analysis (arrow) are composed of Si, Al, K and Fe, with minor Mg (Appendix 4). Morphology and composition suggests clay is authigenic and illitic. Illitic (10Å) clays are the most abundant in this sample (52% of < 2μm fraction). Mag: 7000X. (6-31-66-2W4)

(c) LW-87-CW-17, silty / sandy shale, trace of bitumen. SEM photomicrograph exhibiting 'fuzzy' intertwined lath morphology of authigenic illite (12% of W.R. XRD fraction) in this sample. Prominent, 'fuzzy', non-crenulated edges and EDX and XRD analyses help to differentiate this clay from berthierine, which has a similar morphology and habit. Mag: 4000X. (6-31-66-2W4)

(d) LW3-38, muddy f.g. water sand, SEM photomicrograph of mixed authigenic grain coating clays. Webby, somewhat crenulated clays (┌) are composed of Si, Al, Mg, Ca and K with abundant Fe. They have been interpreted as illite / smectites. Other morphologies include laths, many with illite-like wispy projections (I), and plates (p) more typical of chlorite. The presence of iron may be the result of late fine-grained iron oxides (Fe). Mag: 3375X. (3-28-66-2W4).

(e) LW3-38, muddy fine-grained water sand. SEM photomicrograph of authigenic clays exhibiting webby, slightly crenulated morphology. Form is typical of smectitic clays (<1% o,f W.R. fraction by XRD). Authigenic feldspars (aF) formed after clays and have a blocky morphology and cleavage typical of plagioclase. Mag: 4500X. (3-28-66-2W4).

(f) LW3-36, silty f.g. water sand. Thin section photomicrograph of relatively abundant pore-filling siderite rhombs (S). This is a typical occurrence for siderite, as a replacement of altered grains (the source of the Fe is likely from the altered grain—local replacement). Note the small crystals of siderite (arrows) concentrated around the altered grain areas. Mag: 323X, PPL, scale bar = 31μm. (3-28-66-2W4).

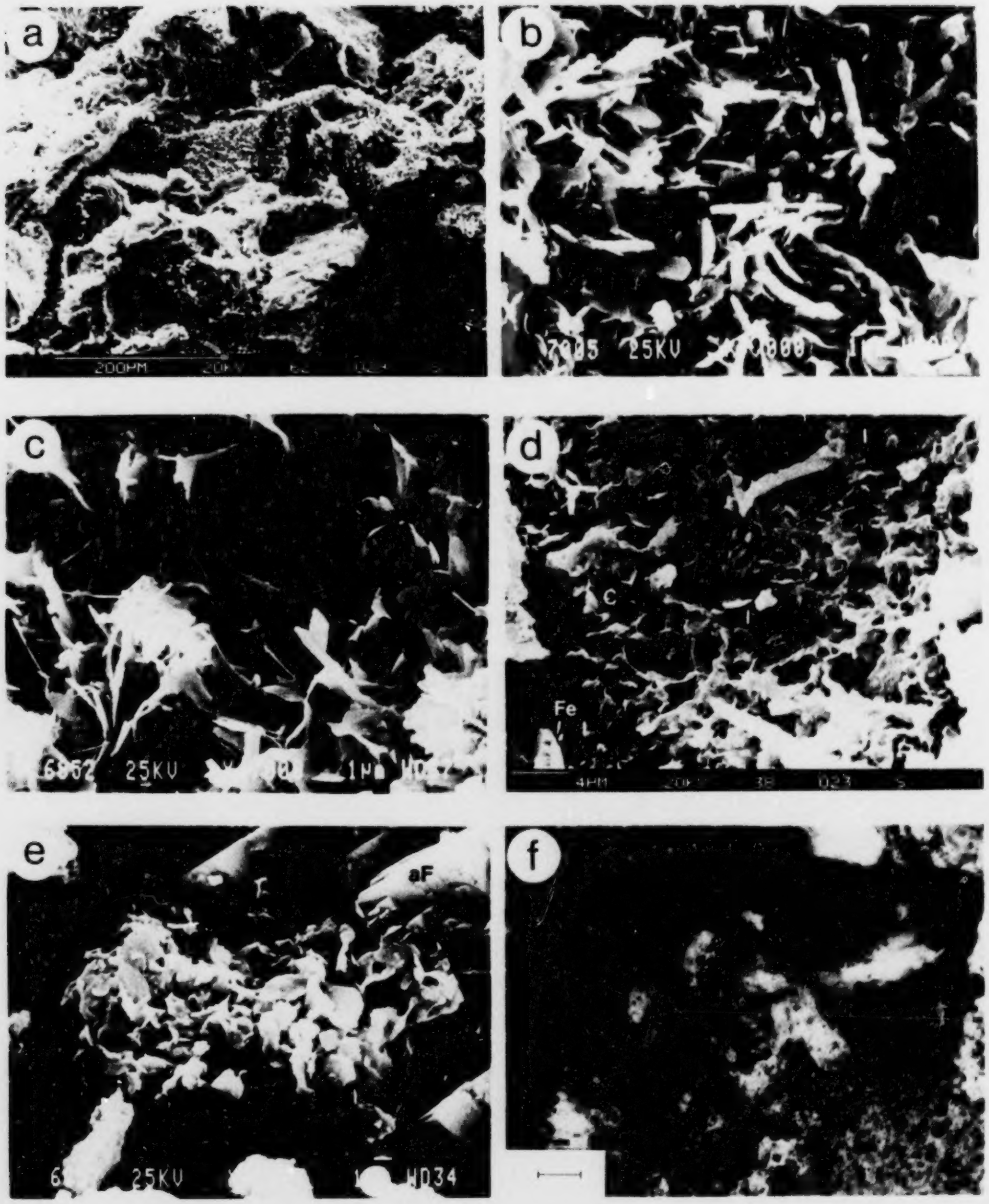
a
200PM 20KV
b
25KV
c
25KV
d
c
l
Fe
L
4PM 20KV 38 023 5
e
aF
25KV
WD34
f

PLATE 3.11:

(a) LW3-36, silty f.g. water sand. Singles and aggregates of rhomb shaped pore-filling siderite (S) replacing an altered grain, adjacent to a grain covered with residual bitumen (B). Siderite exhibits typical yellowish colour under PPL and high relief. Voids filled with blue epoxy. Thin section micrograph. Mag: 323X, PPL, scale bar = 31μm. (3-28-66-2W4).

(b) as per Plate 3.11a, cross-polars. Thin section micrograph shows high order white birefringence of siderite rhombs (S). Second order colours are from micas in grain containing detrital clay (dC).

(c) LW-87-CW-27, f.g. water sand. SEM photomicrograph of typical morphology of abundant diagenetic pore-filling K feldspar (aKF) which grew as an overgrowth on the remains of an altered grain (aG), and after authigenic clays (C). Flat areas areas on K feldspar are former points of contact with other grains (arrows). Platy crystals of authigenic zeolite, likely clinoptilolite (Z) appear to have formed subsequent to K feldspar. Mag: 200X. (6-31-66-2W4).

(d) LW-87-CW-26, f.g. water sand. Characteristic crystals of authigenic K feldspar (aKF) coating framework grain and minor authigenic clays. Cleavage and grain growth typical of K feldspar throughout the study area. It is most prominent in water sands in the study area. Clays (C) on adjacent grain exhibit 'webby' morphology typical of smectites. Mag: 1000X. (6-31-66-2W4).

(e) LW-87-CW-11, silty, f.g. bitumen saturated sand. Thin section photomicrograph exhibiting abundant red stained plagioclase (Pl), quartz (Q), rock fragments (RF) and glauconite (G) next to organic-rich parting. Edge of plagioclase has a yellow-stained overgrowth of authigenic K feldspar, stained yellow. Mag: 103X, PPL, scale bar = 97μm. (6-31-66-2W4).

(f) Magnification of centre grain from Plate 3.11e. Grain of prominently plagioclase composition has a multiple history, resulting in a 'zebra-like' look: 1) original grain composition is believed to be myrmekite - a plagioclase / quartz intergrowth, resulting in the prominent bluish grey / white stripes of grain under cross-polars; 2) an albite overgrowth, characterized by prominent albite twining - has overprinted / engulfed the entire grain; and 3) formation of a K feldspar overgrowth which is bright yellow from staining. Thin section photomicrograph. Mag: 103X, PPL, scale bar = 39μm.

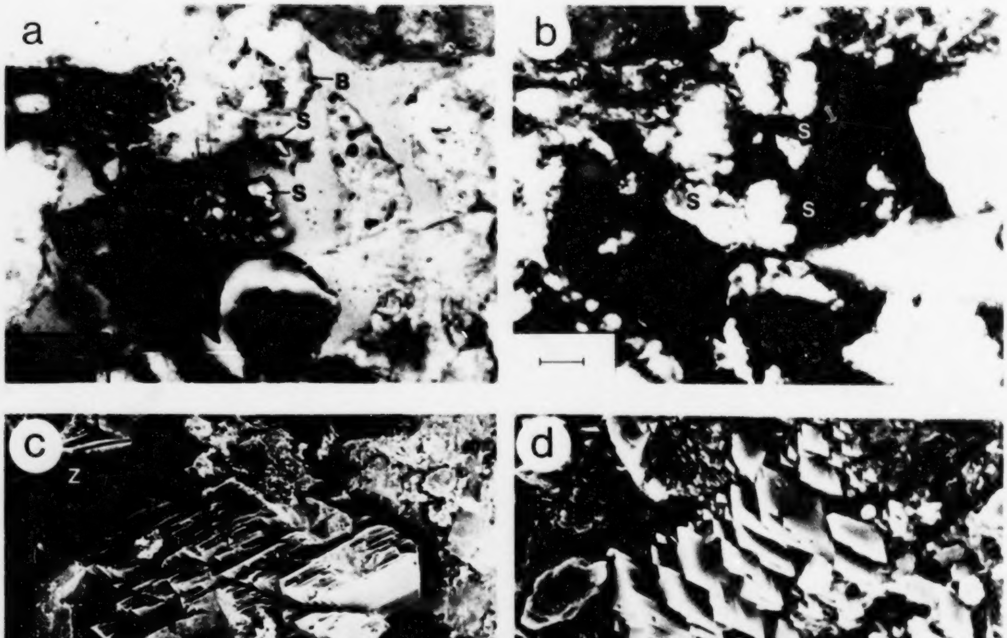
a
B
S
S
b
S
S
S
c
Z
C
aG
4810
d
4812
10µm
e
G
Q
Pl
Pl
Q
f

PLATE 3.12:

(a) LW3-36, silty f.g. water sand. Thin section photomicrograph exhibiting characteristic form and paragenetic order of grain coating diagenetic clays (C) (bladed morphology) overgrown by pore-filling K feldspar (KF). Mag: 1150X. (3-28-66-2W4).

(b) LW-87-CW-17, silty / sandy sample with some shale, trace of bitumen. SEM photomicrograph of intergrown crystals of abundant pore-filling diagenetic K feldspar, partially covered with diagenetic clays (C). Mag: 4500X. (6-31-66-2W4).

(c) LW-87-CW-25, shale with trace of silt and sand, water saturated. SEM photomicrograph of magnified view of crystal of pore-filling diagenetic K feldspar (aKF). Mag: 7000X. (6-31-66-2W4).

(d) LW-87-CW-17, silty / sandy shale, trace of bitumen. SEM photomicrograph of typical blocky morphology of diagenetic feldspar; believed to be plagioclase (Pl). Relatively rare within the study area. It is characterized by an Al, Si, Na, and minor Ca composition by EDX analysis. Crystal developed on diagenetic grain coating clays. Mag: 1200X. (6-31-66-2W4).

(e) LW-87-CW-17, silty / sandy shale, trace of bitumen. SEM photomicrograph of quartz overgrowths (Q) with prismatic terminations intergrown with crenulated 'smectitic-type' and relatively large (~10µm) flakes of pore-filling platy clay (C). Growth appears to be somewhat synonymous, with quartz forming slightly later. Mag: 1800X. (6-31-66-2W4).

(f) LW-87-CW-17, silty / sandy shale, trace of bitumen. SEM photomicrograph of authigenic quartz overgrowths (Q) exhibiting development of doubly terminated prismatic ends, characteristic of open space precipitation. Overgrowths have commonly incorporated earlier clays (C). Mag: 3500X. (6-31-66-2W4).

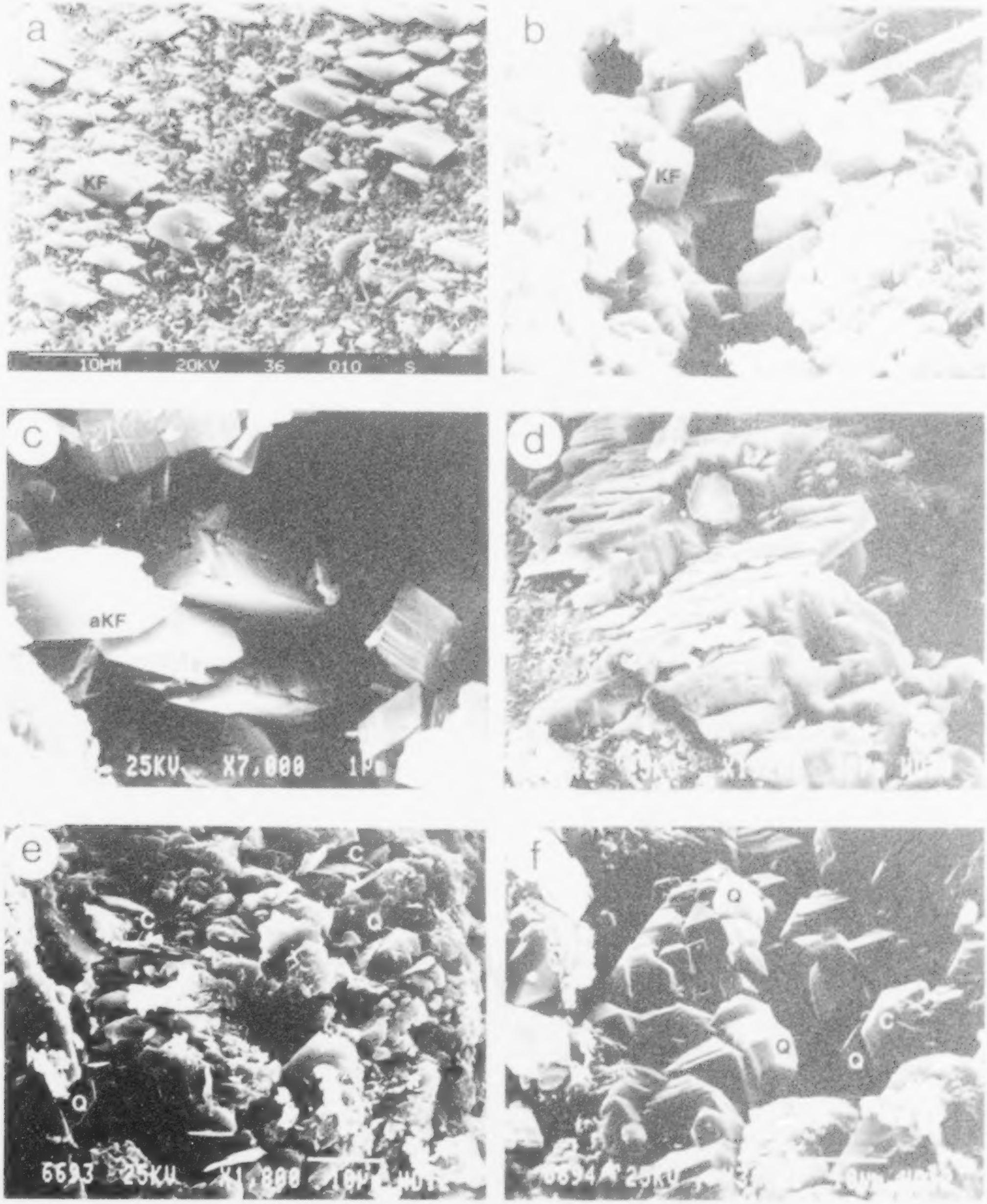
a
KF
10MM 20KV 36 010 S
b
C
KF
c
aKF
25KV X7,000 1P
d
e
C
C
Q
Q
6693 25KV X1,800
f
Q
Q
C
Q
6694 25KV

PLATE 3.13:

(a) LW-87-CW-11, silty, f.g. bitumen saturated sand. Thin section photomicrograph of grain of polycrystalline (sutured) quartz (pQ) next to subhedral volcanic quartz, with an overgrowth of a different extinction (arrow). Note albite twinned plagioclase (Pl), and retardation colours of bitumen on silty parting (B). Mag: 130X, cross-polars, scale bar = 77μm. (6-31-66-2W4).

(b) LW3-38, muddy f.g. water sand. Thin section micrograph of a grain of quartz (Q) with multiple quartz overgrowths (o). Also evident are grains of plagioclase (Pl), dolomite (D) and a detrital grain of muscovite (M). Mag: 165X, cross-polars, scale bar = 61μm. (3-28-66-2W4).

(c) LW3-38, muddy, f.g. water sand. SEM photomicrograph of a cluster of platy (p), lath-shaped (l) and coffin-shaped (c) crystals of diagenetic zeolite, believed to be clinoptilolite. Mag: 2500X. (3-28-66-2W4).

(d) LW-87-CW-27, f.g. water sand. Accumulation of typical pore-filling crystals of zeolite - clinoptilolite which have a minor abundance in the study area, but are concentrated locally within the sands. Crystals forms include rectangular blocks (b), laths (l), platy forms (p) and coffin-shapes (c). Crystals have been partially dissolved subsequent to precipitation, as evidenced by pitting (arrows). SEM photomicrograph. Mag: 700X. (6-31-66-2W4).

(e) LW-87-CW-17, silty/ sandy shale, trace of bitumen. SEM photomicrograph of blocky and rectangular-shaped crystals of diagenetic zeolite, likely clinoptilolite (Z). Former has prismatic termination (pr) at one end. EDX analysis indicates a composition of Si, Al, O, Ca, Na and minor K and Fe (arrow) (Appendix 4). Mag: 3500X. (6-31-66-2W4).

(f) LW3-36, silty f.g. water sand. SEM photomicrograph of platy (p), blocky (b), coffin-shaped (c) and lath-shaped (l) crystals of zeolite - clinoptilolite which exhibit characteristic pitting of subsequent dissolution (arrows). Mag: 2600X. (3-28-66-2W4).

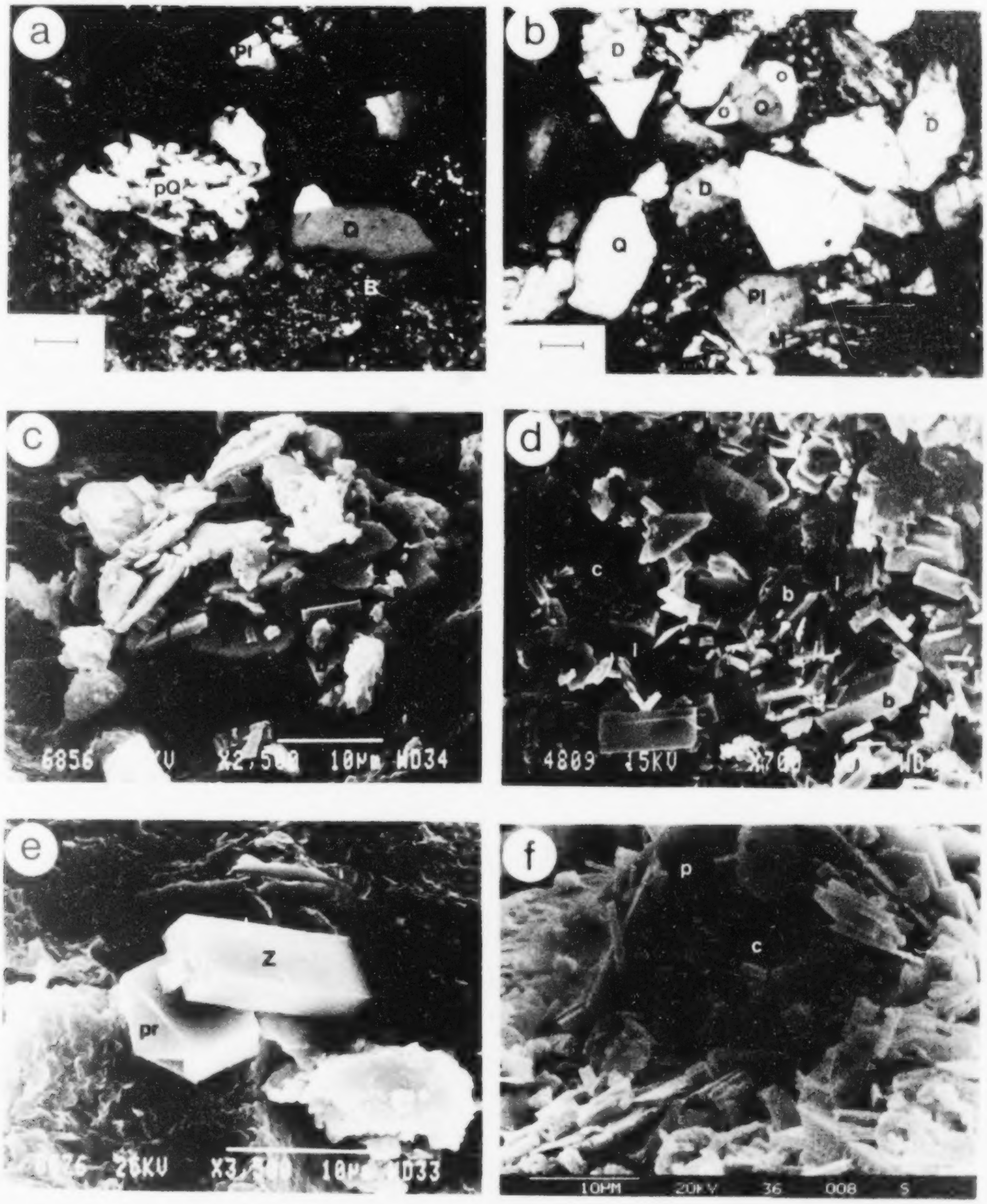
a
Pl
pQ
Q
B
b
D
Q
Q
D
b
Q
Pl
c
6856 KV X2,500 10Pm WD34
d
c
b
l
l
b
4809 15KV X700 WD
e
Z
pr
20KV X3,300 10Pm WD33
f
p
c
10PM 20KV 36 008 S

PLATE 3.14:

(a) LW-87-CW-26, f.g. water sand. SEM photomicrograph of stacked plates of diagenetic clay with 'book-like' morphology, typical of kaolinite. EDX (⌐) indicates Al and Si, with moderate Fe and Ca and minor Mg. Pristine (rhombic?) crystal behind clay is believed to be siderite (S), likely accounting for the abundant Fe. Mag: 1500X. (6-31-66-2W4).

(b) LW-87-CW-26, f.g. water sand. SEM photomicrograph of stacked plates of clay with an EDX composition of Al and Si, with minor Fe (⌐). Morphology is similar to that of Plate 3.14a. May suggest kaolinite is a late diagenetic alteration of former clays? Mag: 6000X. (6-31-66-2W4).

(c) LW-87-CW-26, f.g. water sand. SEM photomicrograph of crystal exhibiting 'melted pound of butter' morphology, rich in Na and Cl by EDX analysis (⌐), believed to be halite. Present only in trace quantities within the study area. Crystal exhibits evidence of dissolution (pitting) on surface (arrows). Mag: 3225X. (6-31-66-2W4).

(d) LW-87-CW-23, v.f.g. water sand, trace shale. SEM photomicrograph of blocky 'melted' form of rectangular crystal of halite?, rich in Na (H). Adjacent rod-shaped authigenic crystal (r) is rich in Ca, P and Si - apatite? Mag: 6250X. (6-31-66-2W4).

(e) LW-87-CW-33, silty sand with some shale, bitumen saturated. SEM photomicrograph of a number of prominent rod-shaped crystals (r) with a curved 'dishy' shape at base. EDX analysis indicated crystals are rich in Ca, Si and P. Authigenic clays (C) with fuzzy edges (illitic?) and later K feldspars (aKF) are also prominent in sample. Mag: 3300X. (3-13-65-4W4).

(f) LW-87-CW-33, silty sand with some shale, bitumen saturated. SEM photomicrograph of abundant 'dishy' rod-shaped crystals (d). Elongate crystals appears to have broken ends, suggesting a detrital origin. Rod-shaped crystal (r) appears authigenic. Both are rich in Ca and P (apatite?). Mag: 1500X. (3-13-65-4W4).

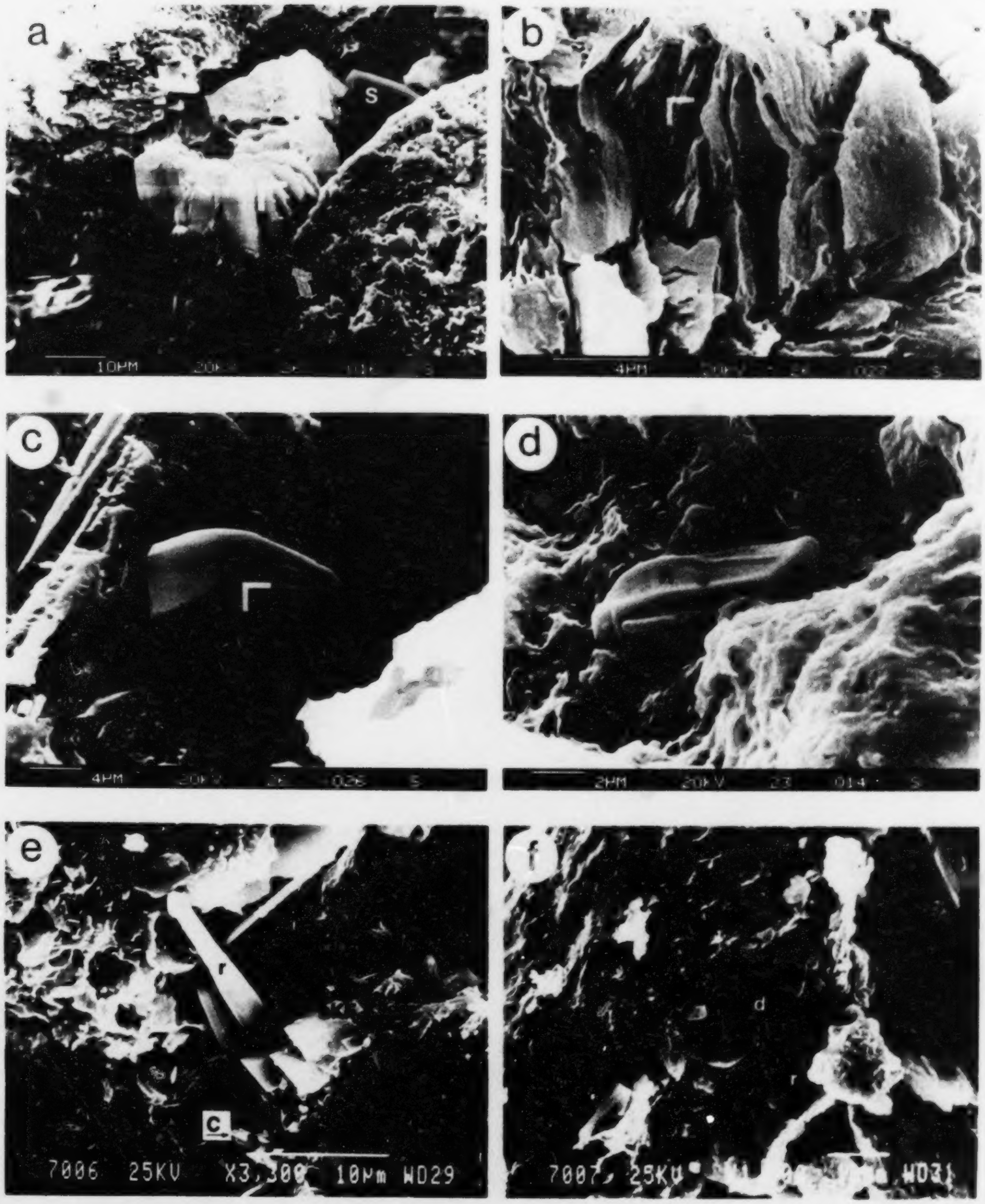
a
s
10PM
b
r
4PM
c
r
4PM 20KV 26 026 S
d
2PM 20KV 23 014 S
e
r
c
7006 25KV X3,300 10Pm WD29
f
d
r
7007 25KV WD31

CHAPTER 4:

A HYDROGEOLOGICAL STUDY OF THE COLD LAKE OIL SANDS AREA, EAST-CENTRAL ALBERTA

Influence on Clearwater Formation diagenesis

A. INTRODUCTION

The movement of groundwater in a regional system such as the Western Canadian Sedimentary Basin is capable of generating many physical and chemical changes in the subsurface. Water / rock interactions may result in mineral dissolution and the oxidation or hydration of organic or inorganic matter. Groundwater flow results in the transport of these chemical constituents as well as heat, and the propagation of pore pressure differences which may lead to the exchange of ionic constituents or precipitation of new mineral species. This process continues until equilibrium is achieved, as fluids are in constant contact with the rock framework.

Diagenesis includes all processes occurring during sediment burial from environments immediately below the sediment / water interface to environments transitional to metamorphism (Curtis, 1978). Diagenetic alteration is a function of sediment composition, fluid composition and burial depth. In clastic marine environments, detrital solids are the predominant source of reactive species, with ionic contributions from infiltrating pore fluids as a secondary source of solutes. An investigation of groundwater flow may therefore provide information that helps to differentiate changing chemical conditions associated with diagenesis in such a dynamic system.

The Cold Lake oil sands deposit, located 300km (187mi) northeast of Edmonton, Alberta, is Canada's second largest heavy oil deposit (Figure 4.1). It contains an estimated $3.5 \times 10^{10} m^3$ (2.2×10^{11}bbls) of high viscosity, low gravity bitumen within three formations of the Lower Cretaceous Mannville Group sediments: the McMurray; Clearwater; and Lower and Upper Grand Rapids Formations (A.E.R.C.B, 1985). The Clearwater Formation, the most prolific reservoir, is currently being produced by cyclic steam injection methods in the northern part of the deposit.

Mineralogical and geochemical variations within the formation were discussed in Chapter 3 of this thesis. The purpose of this study is to examine local groundwater flow patterns within the northern part of the Cold Lake oil sands area, to relate observed characteristics to known fluid flow patterns on a regional scale in the Western Canada

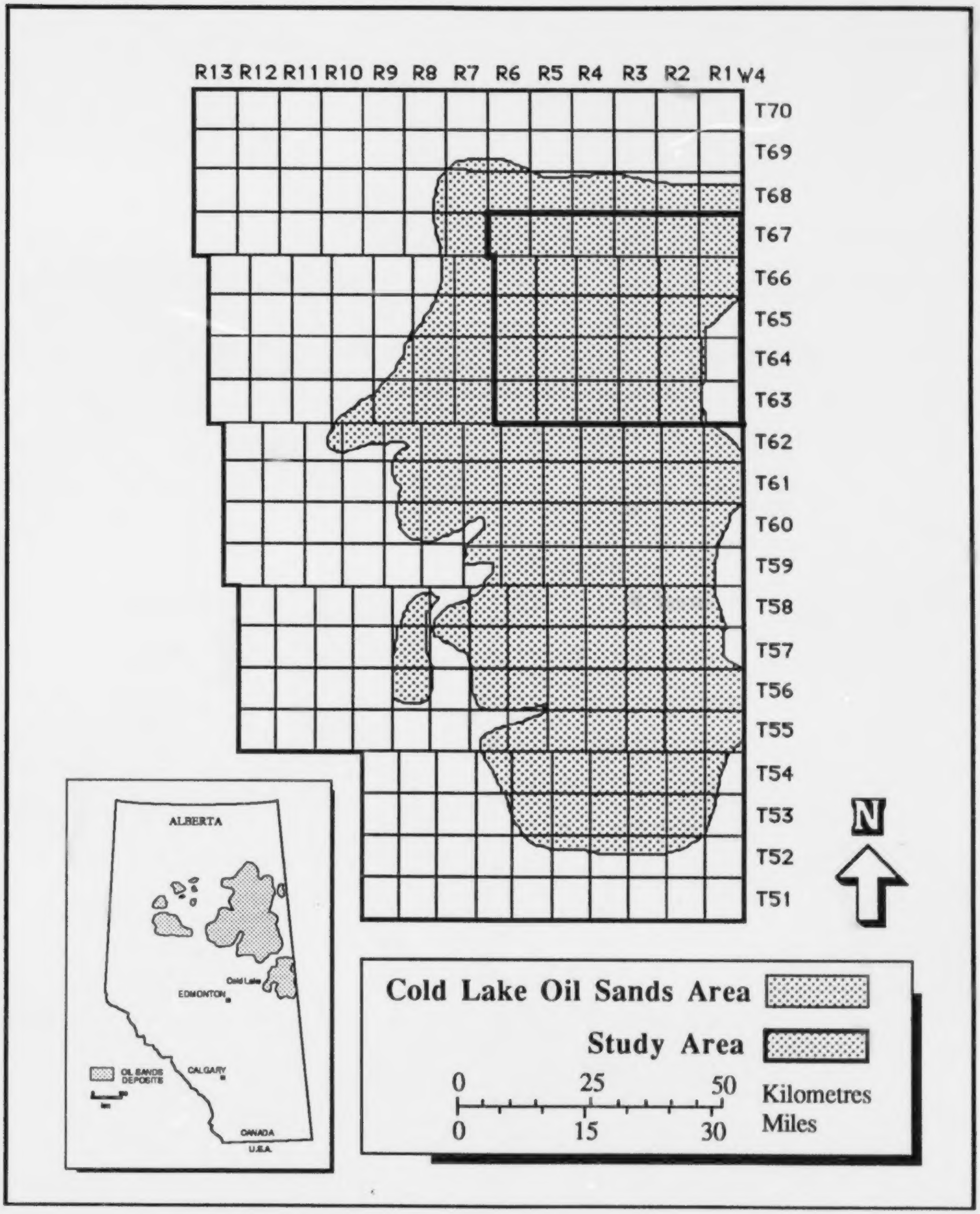
R13 R12 R11 R10 R9 R8 R7 R6 R5 R4 R3 R2 R1 W4
T70
T69
T68
T67
T66
T65
T64
T63
T62
T61
T60
T59
T58
T57
T56
T55
T54
T53
T52
T51
N
ALBERTA
Cold Lake
EDMONTON
CALGARY
OIL SANDS DEPOSITS
CANADA
U.S.A.
Cold Lake Oil Sands Area
Study Area
0 25 50 Kilometres
0 15 30 Miles

Figure 4.1: Location map of study area within the Cold Lake oil sands deposit.

Sedimentary Basin, and to propose general conclusions regarding the effect of moving groundwater on observed features of the Clearwater Formation.

Previously published hydrogeological work in the Cold Lake area consists of: a regional report on the hydrogeologic environment of the Cold Lake oil sands area by Yoon (1977); a hydrogeological report on the Sand River area by Ozoray *et al.* (1980); and a report on the influence of lithology and fluid flow on the temperature distribution in the Cold Lake oil sands area by Bachu (1985). The report by Yoon (1977) is a regional study of surficial groundwater flow in the Cold Lake area. The report by Ozoray *et al.* (1980) deals mainly with surficial geology and only briefly considers deeper subsurface conditions, and the report by Bachu (1985) considers the effect of fluid flow on temperature distributions. A recent study by Garven (1989) investigates fluid flow in the Western Canada Sedimentary Basin and proposes a hydrogeologic model for the formation of Alberta's heavy oil deposits, including the Cold Lake oil sands deposit.

B. STUDY AREA

The scope of study for this chapter is relatively narrow and as such the limits of the study were confined to the NTS Sand River area, townships 63 through 67, ranges 1 to 6 west of the fourth meridian in east-central Alberta (Figure 4.1). The majority of hydrogeological data collected within this study is from the Lower Cretaceous Mannville group, although there are selected analyses from carbonates in the Upper Devonian. All core samples used in the identification of mineralogic and geochemical characteristics of the Clearwater Formation are from a smaller area within townships 65 and 66, ranges 2 through 4 west of the fourth meridian.

PHYSIOGRAPHY

The northern Cold Lake oil sands area lies between the Eastern Alberta Plains and the Mostoos Hills Upland (Atlas of Alberta, 1969). The Eastern Alberta Plains are generally west of the study area, and the Mostoos Hills Upland lies in the northern part of the map area within which the highest elevation of 712.6m (2338ft) is located. The lowest elevation, approximately 512m (1680ft), is located in the southeast where the Beaver River exits the study area (Figure 4.2).

Topographically, the study area is flat to hummocky with rolling hills and undulating plains typical of glaciated terrain (Andriashek, 1985). Ground moraine forms

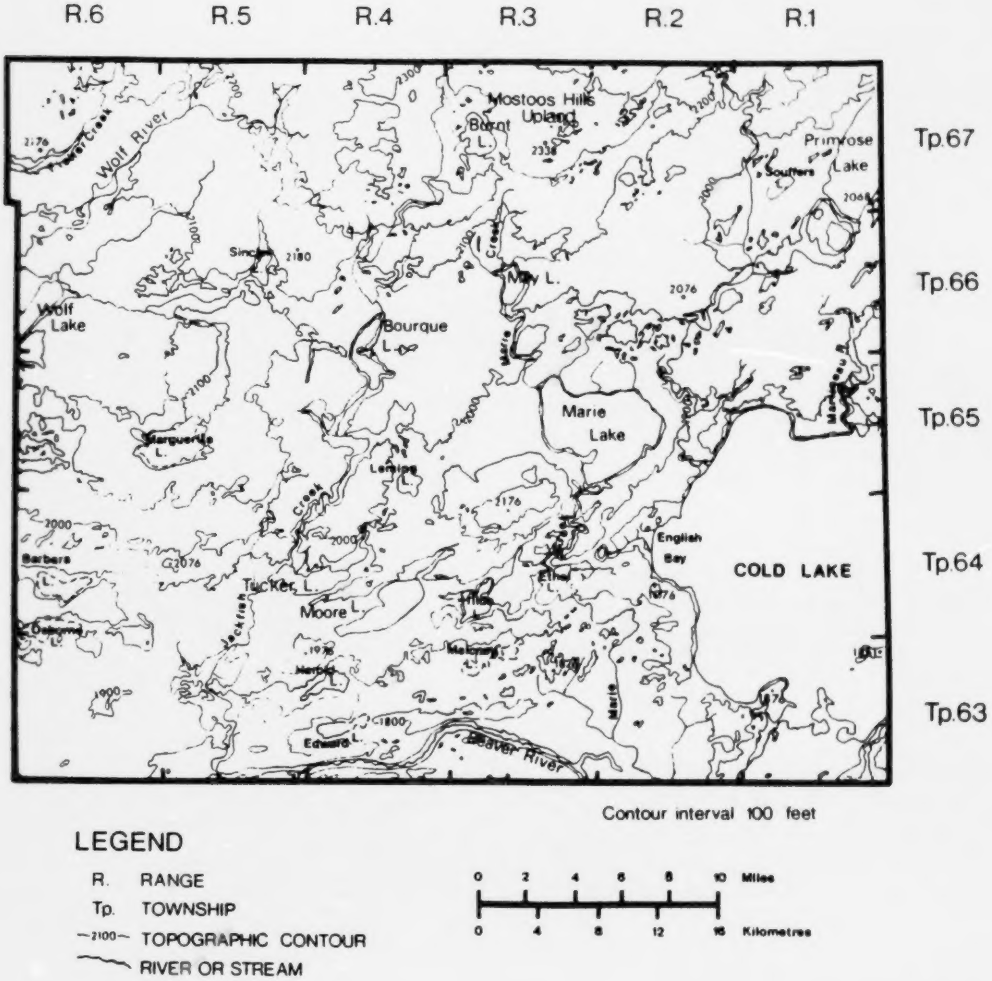
R.6
R.5
R.4
R.3
R.2
R.1
Tp.67
Tp.66
Tp.65
Tp.64
Tp.63
Mostoos Hills Upland
Burnt L.
Primrose Lake
Wolf River
Wolf Lake
Bourque L.
May L.
Marie Lake
Marguerite L.
Leming L.
English Bay
COLD LAKE
Barbara L.
Tucker L.
Moore L.
Ethel
Edward L.
Beaver River
Contour interval 100 feet
LEGEND
R. RANGE
Tp. TOWNSHIP
2100 TOPOGRAPHIC CONTOUR
RIVER OR STREAM
0 2 4 6 8 10 Miles
0 4 8 12 16 Kilometres

Figure 4.2: Physiographic map of the northern Cold Lake oil sands study area (modified from EMR, NTS Sand River Area 73L).

the hummocky surfaces, an alluvial terrace can be found along the Beaver River and a few eskers and glacio-fluvial surfaces have been identified in the area (Ozoray *et al.*, 1980).

A large number of lakes, most of glacial origin, are located within the study area (Figure 4.3). The largest of these are Cold Lake and Wolf Lake which extend to the east and west respectively out of the study area, and Marie, Moore, Bourque and Marguerite lakes which are located in the centre of the study area. Primrose Lake, which extends to the northeast, is located within the Department of National Defence Air Weapons Range which includes township 67, ranges 1 to 6 within the map area.

Surface water drains overall from the topographically high areas in the northern part of the study area south towards the Beaver River, the lowest topographic area. The Beaver River drains into the Hudson Bay via the Churchill River system (Ozoray *et al.*, 1980). The majority of the streams run from north to south, the exceptions being Wolf River, Fisher Creek and the stream which drains Fisher Lake. These streams drain to the southeast into Wolf Lake and the Sand River, which runs north to south just east of the study area. A number of smaller streams drain northwest to southeast or west to east into Cold Lake. The drainage pattern within the study area is shown in Figure 4.3.

CLIMATE

The climate of the Cold Lake area is characterized by long cold winters and short, cool summers. The area is within the climafrost zone in which soils may be frozen temporarily over the period of a year (Lindsay and Odynsky, 1965).

Mean annual temperatures for Medley, Alberta, located approximately 10km (6mi) southwest of the southwestern shore of Cold Lake, have been reported by Environment Canada for January, July and mean annual to be, -19.2, 17.1 and 1.1 (°C), respectively (Ozoray *et al.*, 1980).

Mean annual precipitation at Medley, Alberta is generally less than 433mm (17.1in), the largest portion of which falls between the months of May and September. The area is covered by snow from mid-October to mid-April. Snowfall is relatively consistent throughout the winter months and accounts for approximately thirty percent of the mean annual precipitation. The mean annual precipitation increases to approximately 560mm (22in) in the northeastern part of the study area (Environment Canada).

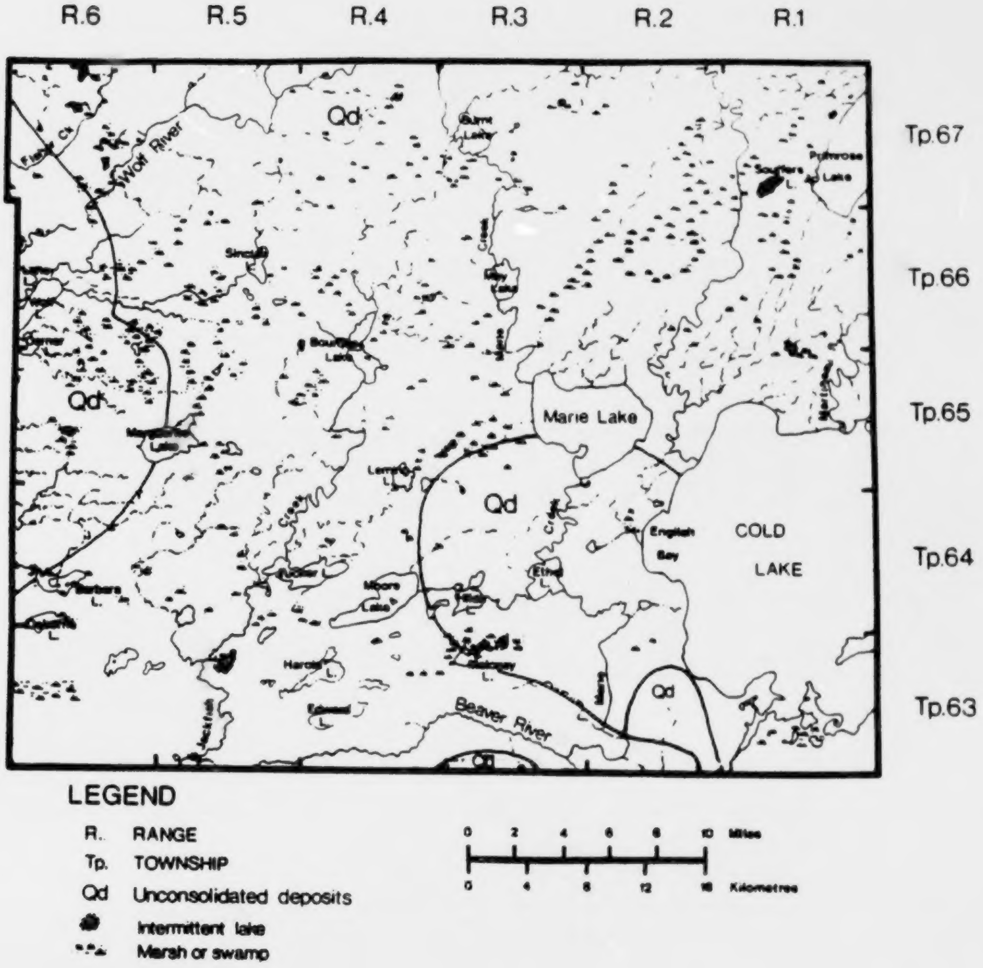
R.6
R.5
R.4
R.3
R.2
R.1
Tp.67
Tp.66
Tp.65
Tp.64
Tp.63
Qd
Wolf River
Marie Lake
COLD
LAKE
English Bay
Beaver River
Primrose Lake
LEGEND
R. RANGE
Tp. TOWNSHIP
Qd Unconsolidated deposits
Intermittent lake
Marsh or swamp
0 2 4 6 8 10 Miles
0 4 8 12 16 Kilometres

Figure 4.3: Drainage of the northern Cold Lake oil sands study area (modified from Ozoray *et al.*, 1980).

Mean monthly potential evapotranspiration reaches approximately 114mm (4.5in) during July and exceeds mean monthly precipitation from May to October at Medley, Alberta (Environment Canada).

C. GEOLOGY

WESTERN CANADA SEDIMENTARY BASIN

The Western Canada Sedimentary Basin is composed of thick sequences (up to 16 km) of Paleozoic to Tertiary strata which unconformably overlie the folded and faulted crystalline rocks of the Precambrian basement (Hitchon, 1969a). Paleozoic strata are predominantly calcareous and evaporitic within the basin; Cretaceous and Tertiary sediments are generally composed of clastic sedimentary rocks. The entire sequence is unconformably overlain by varying thicknesses of Quaternary sediments composed mainly of post-Pleistocene glacial drift (Andriashek, 1985). Tertiary sediments were eroded throughout much of the basin as the result of glacial erosion and tectonism.

The Western Canada Sedimentary Basin was subject to a number of tectonic events throughout deposition in addition to subsidence, resulting in its present configuration as an asymmetrical syncline. The basin is sharply defined on the east by the Precambrian rocks of the Canadian Shield which outcrop in northern Saskatchewan and Manitoba, and on the west by the folded and faulted rocks of the Canadian Cordillera. These rocks grade laterally into the deformed sediments of the disturbed belt on the steeply dipping west flank of the syncline. The eastern flank dips gently towards the southwest. This gradient increases downdip as the result of the increased thickness of Mesozoic and Paleozoic strata towards the centre of the syncline (Figure 4.4).

COLD LAKE STUDY AREA

Surficial Geology:

The Quaternary sediments of the northern Cold Lake oil sands area consists of Laurentide drift generally greater than 50m (165ft) thick. These sediments were studied in detail by L.D. Andriashek (1985) and results are reported in an unpublished M.Sc. thesis from the University of Alberta. Andriashek (1985) identified a total of eight Quaternary lithostratigraphic formations within the Sand River area (Figure 4.5), four of which are glacial (till) and four of which are non-glacial in origin. Quaternary stratigraphy was interpreted to consist predominantly of stratified and unstratified gravels, sands, silts and

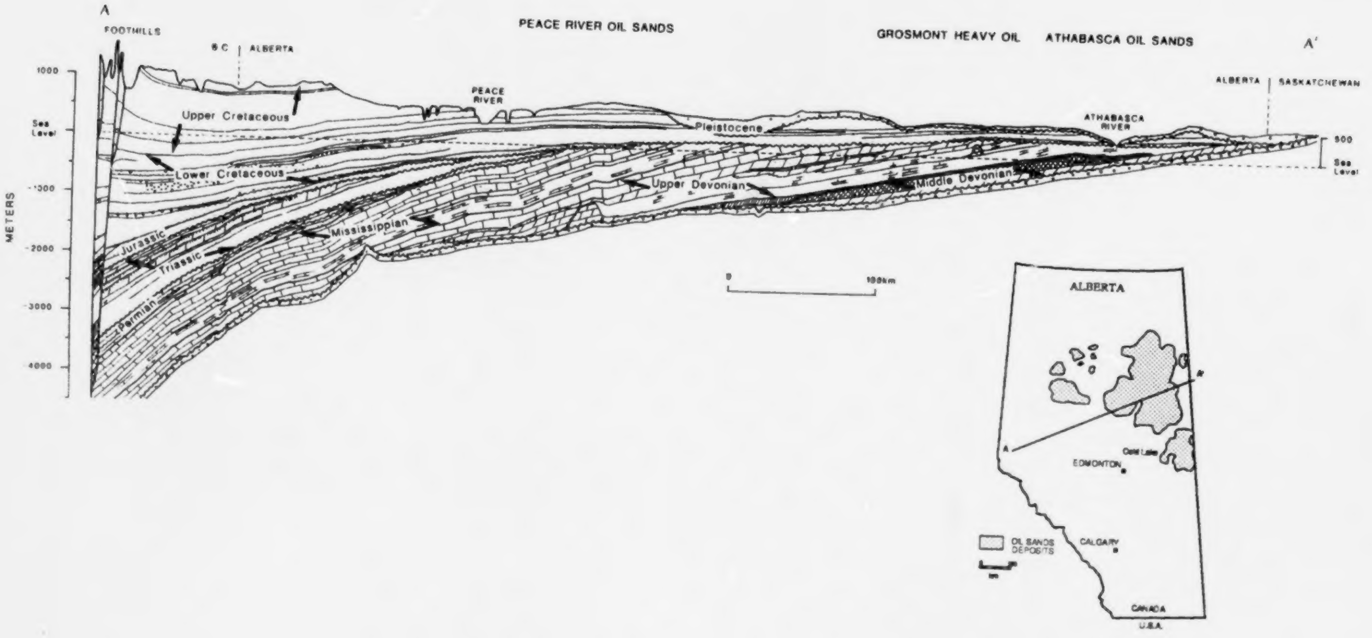
A
FOOTHILLS
B.C. | ALBERTA
PEACE RIVER OIL SANDS
GROSMONT HEAVY OIL
ATHABASCA OIL SANDS
A'
ALBERTA | SASKATCHEWAN
PEACE RIVER
ATHABASCA RIVER
Upper Cretaceous
Lower Cretaceous
Pleistocene
Upper Devonian
Middle Devonian
Mississippian
Jurassic
Triassic
Permian
METERS
1000
Sea Level
-1000
-2000
-3000
-4000
500
Sea Level
0
100km
ALBERTA
A
A'
Cold Lake
EDMONTON
CALGARY
OIL SANDS DEPOSITS
CANADA
U.S.A.

Figure 4.4: Geologic cross-section of the Western Canada Sedimentary Basin showing the major stratigraphic units, structural configuration, groundwater flow directions and present day topographic profile (modified from Garven, 1989).

LATE PLIOCENE & QUATERNARY SEDIMENTS IN THE SAND RIVER AREA

AGE	FORMATION	LITHOLOGY
QUATERNARY	Post glacial deposits	stratified sediments
	Grand Centre	till
	Sand River	stratified deposits
	Marie Creek	till
	Ethel Lake	stratified deposits
	Bonnyville	till & stratified deposits
	Muriel Lake	stratified deposits
	Bronson Lake	till & clay
TERTIARY	Empress Fm	glacial sand and gravel silt and clay

Figure 4.5: Summary of late Pliocene and Quarternary sediments in the Sand River map area (modified from Andriashek, 1985).

clays (till) corresponding to four glacial episodes of advance and retreat (Andriashek, 1985). All eight formations are present within the study area, although their distribution is somewhat sporatic and erosional because of their frequent presence within buried glacial valleys. Post glacial or recent sediments, which form the uppermost sediment layer in the northern Cold Lake area at the present time, are mainly stratified sand or gravel with some silt and clay of fluvial, lacustrine or aeolian origin (Andriashek, 1985). Figure 4.3 illustrates the position of possible groundwater yield probability in the study area estimated from pump and bailing tests (Ozoray *et al.*, 1980). Lower possible yields appear to be associated with the position of stratigraphically lower, buried valley deposits identified by Andriashek (1985), likely indicating the position of more clay to silt-rich facies.

Bedrock Geology:

The stratigraphic succession of post-Precambrian units within the Cold Lake study area consists of Lower to Upper Devonian limestones, dolomites and evaporites and Lower to Upper Cretaceous sands, silts and shales. Figure 4.6 is a stratigraphic table of formations for the Cold Lake area. For the most part, Beaverhill Lake and Woodbend Group (Cooking Lake Formation) carbonates subcrop at the pre-Cretaceous unconformity in the study area. The shales of the Ireton Formation subcrop to the west of the study area. Mannville Group sediments overlie the pre-Cretaceous unconformity. Sandstones of the Colony and McLaren formations, identified as distinct units from other Mannville formations in drill stem tests, have been laterally correlated to the Upper Grand Rapids Formation in the southern Lloydminster area by Putnam (1982), and elsewhere in eastern Alberta and Saskatchewan by other authors, and as such have been considered part of the Upper Mannville Group here. They have been placed stratigraphically overlying the Upper Grand Rapids Formation for this study, although they are quite possibly upper members of this formation. The marine shales of the Lea Park Formation subcrop at the Cretaceous / Quaternary unconformity in the southwestern portion of the Sand River Area (Ozoray *et al.*, 1980).

This study is concerned with the hydrogeologic characteristics of the Lower Cretaceous Mannville Group, focusing on their effect on the Clearwater Formation. Mannville sediments consist of interbedded sands, silts and clays whose origin is directly related to the encroachment of the epeiric Boreal sea during the Cretaceous (Badgley, 1952; Carrigy, 1959; Williams and Stelck, 1975; Mossop *et al.*, 1981; Jackson, 1984). Within the study area this encroachment resulted in fluvial to marginal marine conditions in the Aptian during deposition of the McMurray Formation (Carrigy, 1959; Harrison *et al.*,

STRATIGRAPHIC TABLE OF FORMATIONS – ALBERTA

PERIOD		STAGE	NORTHEAST PLAINS – Cold Lake Area		
				STRATIGRAPHIC UNIT	DOMINANT LITHOLOGY
QUATERNARY		PLEISTOCENE AND RECENT		Laurentide Drift	till, sand, silt and gravel
CRETACEOUS	UPPER	Campanian		Belly River Formation	sandstone
				Lea Park Formation	marine shale
		Santonian	COLORADO GROUP	First White Speckled Shale	marine shale
		Coniacian		Colorado Shale	
		Turonian		Second White Speckled Shale	
		Cenomanian		Colorado Shale	
				Fish Scale Zone	fish scale shale
	LOWER	Albian		Joli Fou Formation	marine shale
				Viking Formation	sandstone
				Joli Fou Formation	
			MANNVILLE GROUP	Colony Formation	sandstone
				McLaren Formation	
				Upper / Lower Grand Rapids Fm	brackish sands / silts / shales
				Clearwater Formation	marine sands / silts / shales
		Aptian		McMurray Formation	brackish sands / silts / shales
DEVONIAN	UPPER	Famennian	WOODBEND GROUP	Grosmont Formation	calcareous dolomite
		Frasnian		Ireton Formation	shale and shaly limestone
				Cooking Lake Fm.	limestone
			Beaverhill Lake Group	Waterways	limestone
	MIDDLE	Givetian		Slave Pt. Fm.	
				Fort Vermilion Fm.	anhydrite / gypsum
			ELKPOINT GROUP	Watt Mountain Fm.	shale and anhydrite
				Prairie Evaporite Fm.	salt
		Eifelian		Winnipegosis Fm.	calcareous dolomite
				Contact Rapids Fm.	anhydrite / gypsum
	LOWER	Exshaw		Cold Lake	salt
		Siegenian		Ernestina	anhydrite / gypsum
		Gedinnian		Lotsberg	salt
				Granite Wash	sandstone
PRECAMBRIAN			metasedimentary rocks and granite		

Figure 4.6: Stratigraphic succession in the northern Cold Lake oil sand area (modified from Mossop *et al.*, 1981; Western Atlas Int., 1988).

1981; Wightman*et al.*, 1990), predominantly marine conditions during Clearwater sediment deposition (Mellon, 1967; Jardine, 1973; Harrison *et al.*, 1981; Wightman*et al.*, 1990), and once again marginal marine, brackish water conditions during deposition of the Grand Rapids Formation and other Upper Mannville sediments (Wightman *et al.*, 1987). Mineralogic differences between Mannville Group sediments are a function of fluctuations in provenance during sediment deposition, variations related to depositional environment (continental to marine), and differences in post-depositional diagenesis.

The configuration of the Paleozoic surface (pre-Cretaceous unconformity) is the consequence of pre-Cretaceous erosion and pre-, syn- and post-Cretaceous tectonism resulting from the removal of Middle Devonian salts by dissolution activity (Jardine, 1973; Wightman and Berezniuk, 1986; Wightman*et al.*, 1990). Oil deposits on the eastern margin of the Alberta syncline are located in a broad, shallowly dipping anticline believed to be the result of such salt dissolution collapse (Mossop *et al.*, 1981). The topography of the upper Paleozoic surface was highly variable prior to deposition of the overlying McMurray Formation clastic sediments, and the configuration of this surface is believed to have influenced deposition considerably (Jardine, 1973; Mossop *et al.*, 1981; Harrison *et al.*, 1981; Wightman and Berezniuk, 1986; Wightman*et al.*, 1990). Depositional thicks in the McMurray sediments, and to a lesser degree in the other overlying Mannville sediments have been tied to topographic lows in the Paleozoic surface. This influence is believed to have decreased over time as the lows became filled with further sedimentation. Salt collapse of the Devonian evaporites is believed to have continued throughout the Cretaceous (Jardine, 1973; Mossop *et al.*, 1981) and is likely still occurring at the present time (Roberts, 1980), as suggested by the presence of salt springs along the Athabasca River where Upper Devonian sediments are exposed at the surface (M. Ranger[1], per. comm.). Areas of post-Cretaceous salt collapse can be identified by overlaying structure and isopach maps, and occur where structural lows in the Paleozoic surface cannot be correlated to depositional thicks in the Mannville Group. A sequential comparison of each formation within the Mannville Group in this way would help identify the timing of salt collapse.

The timing of oil accumulation into the Mannville Group formations has been the subject of controversy. Recent studies suggest oil emplacement occurred shortly after deposition (Harrison *et al.*, 1981; Garven, 1989). Oil has been identified by biomarker studies to be from a number of sources, namely the Jurassic, Devonian and Cretaceous organic-rich shales which lie west and topographically below the Mannville Group sediments, in the syncline of the Alberta basin (J. Allan[2] and S. Creaney[2], per. comm.). A number of migration processes have been hypothesized, although recent studies strongly suggest transient topographically-induced cross-formational flow as a likely mechanism (Tóth, 1978, 1980; Garven, 1989). Subsequent water washing by meteoric water and associated bacterial attack, has been proposed as the mechanism for the biodegradation of the once light oil to its current state as viscous, low gravity bitumen (Garven, 1989).

---

[1] Department of Geology, University of Alberta, Edmonton, Alberta, Canada.

Oil distribution or trapping within the Mannville sequence in the Cold Lake area is primarily stratigraphic within the broad, gently dipping flanks of the anticline, with structural control over Paleozoic highs (Mossop *et al.*, 1981). Bitumen is located in structurally high areas in each of the Mannville Group formations. The Clearwater Formation is the most highly saturated, usually only containing water saturated sands in the structurally lowest areas, while the Grand Rapids and McMurray formations commonly have thick water saturated intervals in their downdip sands. Isolated gas deposits have been identified in the updip sands of the Grand Rapids Formation, and the Colony and McLaren formations are generally gas bearing. The water saturated sands of all three formations therefore likely form good aquifers.

D. HYDROGEOLOGY

BACKGROUND

The flow of fluid through a porous media may be considered a transient or steady state phenomenon. In a small drainage area such as the study area considered in this report, steady state conditions are generally assumed (Hitchon, 1969a). This serves to simplify the problem and does not imply a static system, but one in which the amount of recharge to the system is equal to the amount of discharge, and any change in this balanced fluid volume is negligible.

General principles of regional groundwater flow have been thoroughly covered by other authors (Freeze and Cherry, 1979; Tóth, 1963, 1984) and therefore will not be discussed at length here. A classic paper by Hubbert (1940) was the first account that considered basin-wide groundwater flow in mathematical terms as a steady state phenomenon. Hubbert (1940) applied Darcy's Law (Appendix 5) to define flow on a macroscopic scale and developed an analytical method of defining fluid potential at any one point in a generalized flow region. Tóth (1963) applied this method to the characterization of fluid potential for an isotropic, homogeneous case which illustrated general flow patterns on regional, intermediate and local scales in a basin with appropriate boundary conditions (Figure 4.7). The upper surface of the system is the water table which in turn reflects topography. In general, topographically high areas are sites of groundwater recharge, topographically low areas are sites of groundwater discharge, and midline areas are characterized by lateral flow. Mathematically, steady state groundwater flow in such a case (basin) is expressed by the Laplace equation (Appendix 5). Such a steady state model is often applied to large, regional, sedimentary basins like the Western Canada Sedimentary Basin (Hitchon, 1969a, 1969b). In such an example, minor fluctuations in the water table resulting from local variations in topography are considered negligible.

---

[2] Esso Resources Ltd., Calgary, Alberta, Canada.

Chemical variations in groundwaters are linked to chemico-physical and biological processes operating in the subsurface. These processes are the result of the physical transport of dissolved ionic constituents and the interaction between the fluid and the surrounding rock framework (Carpenter, 1978; Freeze and Cherry, 1979). Dispersion and advection are the two most important mechanisms by which dissolved material is moved from one point to another in subsurface fluids (Schwartz, 1974). Advection or forced convection is the movement of dissolved constituents by the impulsion of groundwater flow, with rates equal to the average linear velocity of the water (Schwartz, 1974). Hydrodynamic dispersion is the dilution and spreading out of the solute as a result of mechanical mixing during advection (Freeze and Cherry, 1979). Diffusion is also an important process of solute transport in the subsurface, but only becomes dominant in the absence of a hydraulic gradient. Dissolved solutes are propelled in diffusion by their kinetic energy in the direction of a concentration gradient (from high to low concentration). The mass diffused is proportional to the concentration gradient and is also dependent on temperature (Freeze and Cherry, 1979). This process may be dominant in osmosis in shales because of their function as semi-permeable membranes and their very low flow rates.

Specific patterns and trends of dissolved constituents (anions and cations) in subsurface waters can be recognized which correspond to local, intermediate and regional flow systems, mainly because of changes corresponding with increasing depth, time and distance of flow. The evolution of groundwater and factors controlling regional groundwater composition and resulting flow patterns are discussed in detail in Tóth (1984). The dominant factors are:

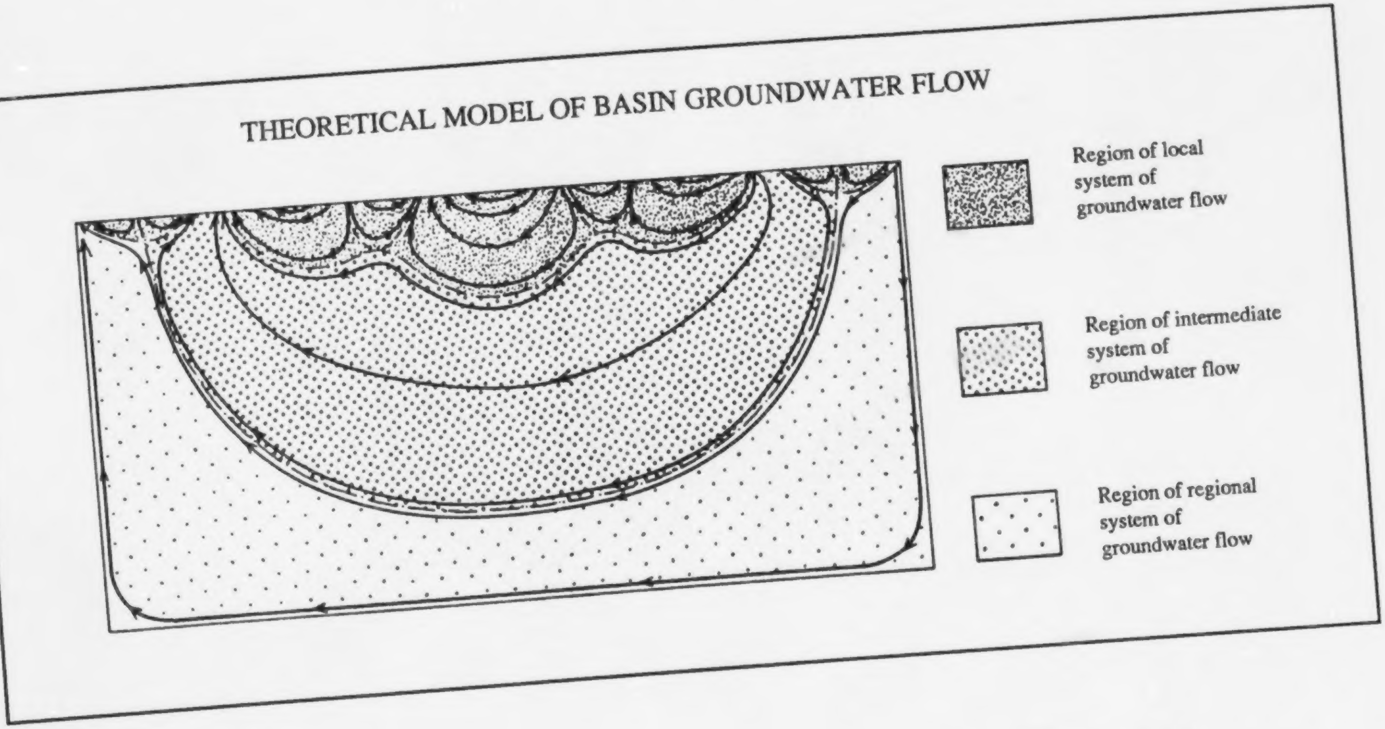
THEORETICAL MODEL OF BASIN GROUNDWATER FLOW
Region of local system of groundwater flow
Region of intermediate system of groundwater flow
Region of regional system of groundwater flow

Figure 4.7: Schematic of local, intermediate and regional systems of groundwater flow in a sedimentary basin. Similar to that believed to exist within the Western Canada Sedimentary Basin (modified after Tóth, 1963).

1) the mobility of an element;
2) temperature;
3) pressure;
4) the contact area between the water and rock;
5) the length of time of the contact;
6) the concentration of dissolved ions in the form of soluble salts; and
7) the former or antecedent water quality (Tóth, 1984).

In terms of anion composition, an empirical sequence of chemical evolution of groundwater was developed by Chebotarev (1955). It states that with increasing time and distance, total dissolved solids (TDS) will increase, and the predominant anion composition will shift from bicarbonate to sulphate and eventually to chloride with increased travel time and movement through flow systems (flowpath) (Figure 4.8) (Carpenter, 1978). In general, this chemical evolution of groundwaters can be explained by mineral availability and solubility in sedimentary basins. HCO_3^- is a common constituent in rainwaters and in the soil zone at shallow depths in most sedimentary basins. Such meteoric water therefore has a high CO_2 content, which aids in the dissolution of carbonate minerals (Freeze and Cherry, 1979). There are several sedimentary minerals which may result in the increase of SO_4^{2-} and Cl^- upon dissolution. Although gypsum ($CaSO_4.2H_2O$) and anhydrite ($CaSO_4$) are only present in trace amounts in most sedimentary basins, they are relatively soluble in water, and given time and increased flowpath increased SO_4^{2-} concentrations can be anticipated in solution (Freeze and Cherry, 1979). Halite (NaCl) and sylvite (KCl), although more readily soluble in water than gypsum or anhydrite, are generally only present deep in sedimentary basins. They formed in the past during restricted evaporitic periods, and do not contribute greatly to increased Cl^- contents in groundwater at shallow depths (Freeze and Cherry, 1979). Therefore, the increase in Cl^- concentration with time and flowpath as shown in the Chebotarev sequence results mainly from waters moving updip from more deeply buried rocks in most sedimentary basins. Hence, general trends such as the chemical evolution of anions, and overall increase in total dissolved solids with time, depth and flowpath are the function of anion mobility (solubility, kinetic effects, etc.), as well as the position and composition of basin lithologic units. Variations in the general trend of sedimentary basin lithologies can easily result in patterns that do not follow those projected by the Chebotarev sequence, and in fact water chemistry may fluctuate considerably from this trend or never progress beyond the SO_4^{2-} or HCO_3^- stage of evolution (Freeze and Cherry, 1979).

CHEBOTAREV SEQUENCE AND FLOW SYSTEM TYPES

$$HCO_3^- \rightarrow HCO_3^-,\ SO_4^{2-} \rightarrow SO_4^{2-} \rightarrow SO_4^{2-},\ Cl^- \rightarrow Cl^-,\ SO_4^{2-} \rightarrow Cl^-$$

$$\vert \longleftarrow 1 \longrightarrow \vert \longleftarrow 2 \longrightarrow \vert \longleftarrow 3 \longrightarrow \vert$$

FLOW SYSTEM TYPES:

1. **Local systems:** shallow depths; short flow paths; variable flow rates and flow directions; short residence time: low pressures and temperatures; homogeneous lithology

   Effects: thorough flushing; low TDS: HCO_3, Ca, Mg; seasonal variations

2. **Intermediate systems:**

   Effects: increase in TDS in variety of species: Na, SO_4, Cl; little or no seasonal variations

3. **Regional systems:** great depths; long flow paths; steady flow rates; long residence time; high pressures and temperatures

   Effects: high TDS: Na, Cl; depleted in CO_2 and O_2; independent of climate

Figure 4.8: The Chebotarev Sequence and flow system types of the chemical evolution of groundwater (modified after Tóth, 1984).

Variations in cation composition, resulting from water / rock interactions over time and flowpath, cannot be characterized in trends like those of anions in a sedimentary basin as there are so many exceptions to the rule (Freeze and Cherry, 1979). Generally, major cation data are grouped with anionic data and observed collectively by graphical means. There are a number of methods available, but a means of representing major ionic constituents described by Zaporozec (1972), will be used in this study.

METHODOLOGY

The hydrogeology of the northern Cold Lake area was examined in an effort to relate local groundwater flow to regional flow patterns that have been identified for surrounding areas and the Western Canada Sedimentary Basin as a whole. Two types of data were collected from available sources in the study area, undisturbed formation pressures and fluid analyses.

Undisturbed formation pressures of selected formations were obtained from drill stem tests for wells within the study area. Drill stem test data are available through the Energy Resources Conservation Board, in Calgary, Alberta. In general, the availability of formation pressures from drill stem tests in the Cold Lake area was poor for Mannville Group formations. Data was available from a number of intervals: the Colony, McLaren; Grand Rapids; Clearwater; McMurray; and Upper Devonian formations. In most cases however, only a few tests were available for each. The scarcity of data can likely be attributed to the nature of the high viscosity, low gravity (~12°API) bitumen located within most of the Mannville sediments. The bitumen does not flow under normal reservoir conditions, and must undergo steam injection to be produced at the surface. As a result, oil companies are reluctant to attempt drill stem tests except in the search for gas deposits. Substantial abundances of gas were rarely encountered in the tests.

Extrapolated (theoretically undisturbed) formation pressures were calculated from drill stem tests according the method of Horner (1951), and were subsequently expressed as freshwater hydraulic heads by the application of a modification of Darcy's Law:

$$h = z + \Psi = z + P/\rho \qquad (1)$$

where: h is the hydraulic head; Ψ is the pressure head or P/ρ; P is the undisturbed formation pressure; and ρ is the fluid density. Head values were then plotted on a map and contoured to form the potentiometric surface. The potentiometric surface is therefore a two-dimensional representation of hydraulic head distribution for a specific interval from which groundwater flow directions may be interpreted. Despite the scarcity of data, only pressures which were believed to represent true undisturbed formation pressures were used in the calculations of the potentiometric surface.

Formation pressures have also been studied by utilizing plots of 'pressure versus depth' and 'pressure versus elevation' (p(d) and p(z)) plots. Commonly used by the petroleum geologist in reservoir evaluation, these plots allow the examination of pressure gradients by plotting hydrostatic pressures against the altitude of the land surface (p(d)), and against that of a defined datum (usually sea level) (p(z)). The utilization of both of these plots with the same data will often unveil information regarding formation pressures and pressure relationships, such as confined versus unconfined aquifers, that would be difficult to recognize any other way.

Water analyses used in the study were available through the Energy Resources Conservation Board, Calgary, Canada. A total of 43 water analyses were examined in the study area for information regarding specific gravity, salinity (expressed as TDS or total dissolved solids), and the concentration of a number of ionic species (Ca^{2+}, Mg^{2+}, Cl^-, HCO_3^-, and SO_4^{2-}). Analyses were selected using specific criteria based on the site of the water sample and absence of contamination indicators such as high CO_3^{2-}. Criteria used in the selection of water quality data for the study are outlined in Appendix 6.

INFLUENCES ON HYDRAULIC HEAD

Three dominant factors have been identified to have a major influence on values of hydraulic head: topography; geology; and climate (Tóth, 1963). Topography-driven or gravity-driven fluid flow has been shown in many instances to be the major force behind groundwater flow in both regional and local systems, and in many cases is believed to be a major contributor to the accumulation of hydrocarbons (Tóth, 1978; 1984). Hitchon (1969b), Freeze and Witherspoon (1967), and Tóth and Corbett (1986) have illustrated the effect of geologic variation on groundwater flow patterns and phenomena. Results indicate that variable permeability (and hence hydraulic conductivity) can alter flowpaths substantially from those predicted ignoring geologic variation. Climate also has a significant effect on groundwater flow patterns and rates, but for the most part these effects are felt in sediments of continental origin that are or were at one time at relatively shallow depths for extended periods (Dutta and Suttner, 1986). Climate is not thought to be an important influence on hydraulic head within the Mannville Formation in this study area. Sediments were deposited in brackish to marine environments, deposition was believed to be quite rapid, and sediments currently range from 300 to 500m (950 to 1850ft) below surface.

Nine additional mechanisms have been identified by Bredehoeft and Hanshaw (1968), which may have an effect on the pressure head measured at any point in an aqueous system. These are:

1) tectonic compression;
2) loading and compaction;
3) fossil pressures corresponding to greater amounts of effective stress;
4) magmatic intrusions;
5) infiltration of gas;
6) solution or precipitation of minerals;
7) mineral phase change;
8) fluid volume change resulting from a temperature change; and
9) osmotic membrane phenomena (Hackbarth and Nastasa, 1979).

In terms of the effect of these mechanisms in the study area, the eastern margin of the Western Canada Sedimentary Basin is not actively subsiding and beyond salt dissolution collapse is not the site of significant tectonic activity. Magmatic intrusions are not a factor in this setting, the low geothermal gradient rules out fluid volume changes resulting from temperature differences and the effect of the infiltration of gas on hydraulic head is deemed insignificant (Hackbarth and Nastasa, 1979).

Mineral phase changes such as anhydrite to gypsum, which consume water, may have the effect of lowering hydraulic head if abundant quantities of the minerals were present. This would likely only be important in Middle Devonian evaporites in the study area, and their head distributions were not studied because of the lack of data.

The increased stress on a rock and its pore fluid because of sediment loading is one of the main causes of increased pore pressure in a clastic basin. Pore pressures will increase with depth until a point at which the fluid and grain matrix can no longer support the load from the overlying sediment, and compaction (including grain repacking, fluid escape and compression) begins to occur. Removal of the overburden by erosion, such as suggested in the Red Earth region of Alberta by Tóth (1978), will result in lowered hydraulic heads that have not yet had a chance to respond to the new elevation of the land surface. It is also possible that lowered hydraulic heads in such rocks remain low because they are currently expanding in response to the removal of ice in the Pleistocene (J. Tóth[3], per. comm.). The Mannville Group within the Cold Lake area consists of unlithified sediments presently buried at shallow depths. Tectonism and burial on the eastern margin of the basin, and additional loading resulting from to Pleistocene glaciation were not sufficient to result in lithification; very little evidence of compaction has been identified. Therefore, pore pressures would not have been significantly influenced by the effects of sediment loading in the study area.

---

[3] Department of Geology, University of Alberta, Edmonton, Alberta, Canada.

Osmotic membrane phenomena have been widely reported as creating high fluid pressures between two juxtaposed formations of differing salinity by the function of a clay membrane (Tóth, 1986). Clays also act as an ion filter, allowing the exchange and subsequent migration of cations, but retention of selected anions and anion-bound cations because of differences in electrochemical potential (Fritz, 1986).

Of the original twelve possible mechanisms, only four may have any significant effect on values of hydraulic head in the Cold Lake area: topography; geology; osmotic membrane phenomena; and the effect of dissolution or precipitation of minerals. The influence of these mechanisms will be examined later in this chapter.

GROUNDWATER FLOW

Western Canada Sedimentary Basin:

The main physiographic features that affect the fluid potential distribution in the Western Canada Sedimentary Basin (W.C.S.B.) are the Caribou Mountains, Clear Hills and Swan Hills of northern Alberta and the mountains of the disturbed belt stretching into southern Alberta (Hitchon, 1969a). In terms of geology, the fluid potential of a stratigraphic bed is a function of its permeability, with highly permeable units acting as fluid conduits. The regional study of the basin by Hitchon (1969a, 1969b) found that despite geological differences the dominant fluid potential corresponds closely to the fluid potential of the topographic surface in any one part of the basin. This follows the regional steady state model proposed by Tóth (1963, Figure 4.7). Groundwater recharge is concentrated in the elevated parts of the basin where fluids descend to great depth. Major aquifers such as the Devonian carbonates focus regional flow laterally to discharge areas near the eastern edge of the basin where the brines cool on ascending and mix with cooler, shallow circulating groundwater (Garven, 1989). Regional flow directions for the Western Canada Sedimentary Basin are illustrated in Figures 4.9 and 4.10. Fluid boundaries are

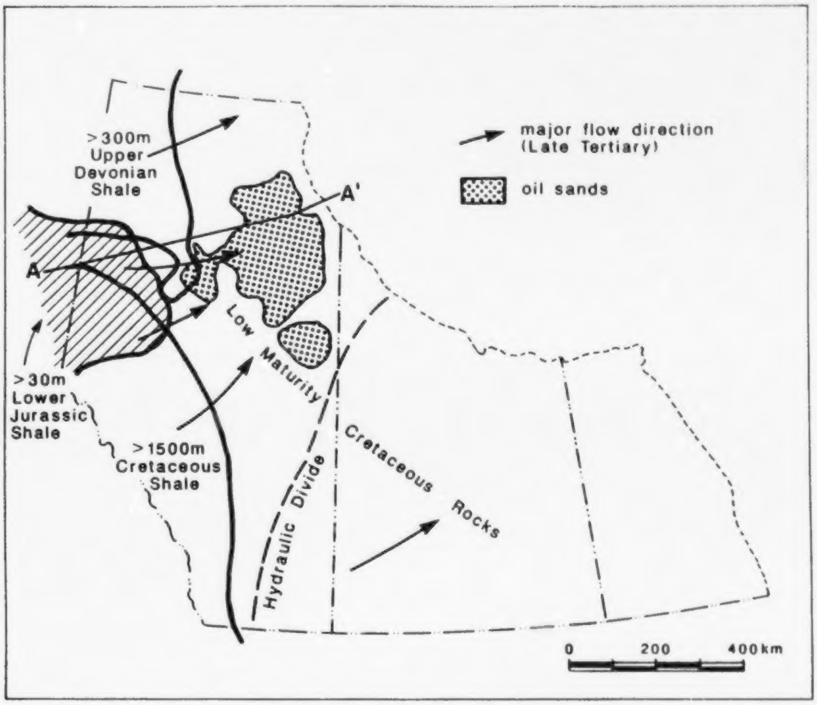
>300m Upper Devonian Shale
A
A'
>30m Lower Jurassic Shale
>1500m Cretaceous Shale
Low Maturity
Hydraulic Divide
Cretaceous Rocks
major flow direction (Late Tertiary)
oil sands
0
200
400km

Figure 4.9: Regional paleoflow and hydrocarbon accumulation for the oil sands deposits in Alberta, indicating possible source rocks in Devonian, Cretaceous and Jurassic (shaded area) shale (modified from Garven, 1989; Hitchon, 1984).

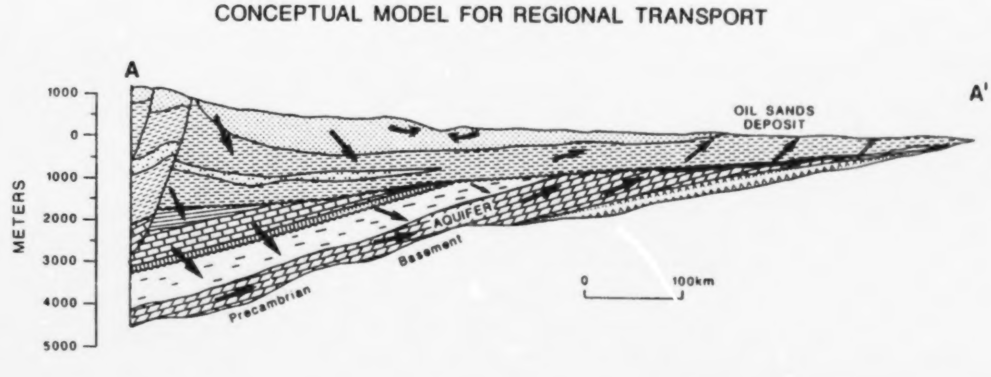
CONCEPTUAL MODEL FOR REGIONAL TRANSPORT
A
A'
OIL SANDS DEPOSIT
AQUIFER
Basement
Precambrian
METERS
1000
0
1000
2000
3000
4000
5000
0
100km

Figure 4.10: Conceptual model of gravity-driven groundwater flow and hydrocarbon accumulation on the eastern margin of the Western Canada Sedimentary Basin. Position of A to A' as illustrated in Figure 4.9 (modified from Garven, 1989).

considered to be the fold and thrust belt in the west and the erosional edge of sediments on the eastern margin of the basin. The maximum depth of regional flow was considered to be the Precambrian surface although hydrologically, fluids likely move through the fractures at the unconformity and mix with those from the Precambrian basement (Hitchon, 1969a).

The study of fluid flow in the W.C.S.B. by Garven (1989) found that the Upper Devonian aquifer with its high permeabilities acted as a drain, focusing moving fluids from upper and lower formations in the recharge areas. Fluids are transported laterally through the basin midline to where the carbonates subcrop at the pre-Cretaceous unconformity, and eventually to where they outcrop at the surface (Figure 4.10). This aquifer is believed to be a major conduit and one of the main flowpaths for hydrocarbon migration in the formation of Alberta's oil sands deposits. Regional groundwater flow would have had a major effect on heat flow within the basin, providing isothermal conditions for hydrocarbon transport (Garven, 1989). Cretaceous sands within the Western Canada Sedimentary Basin are also thought to have been involved as pathways in the migration of hydrocarbons from source areas at deeper depths. Indications of their participation are the numerous oil reservoirs found within the Cretaceous which were likely filled by migrating hydrocarbons enroute updip towards major accumulations in the Cretaceous oil sand deposits.

Cold Lake Study Area:

The effect of groundwater flow on subsurface heat distributions was considered for the Cold Lake area by Bachu (1985). Potentiometric surface maps of most aquifers within the eastern part of the Alberta basin were produced within his study area (townships 55 to 69; ranges 1 to 17W4). Bachu (1985) found that fluid flow in the Devonian aquifers was also of a basin-wide regional type, and identified vertical flow of a downward nature as predominant within the near-surface sediments in the Cold Lake area. Almost no flow was identified in the Upper Mannville units. He stated that the vertical downward flow originating from the water table as the result of recharge is turned laterally in the Lower Mannville aquifer by the flow of the Upper Devonian aquifers, and fluids are carried down and eastward along the pre-Cretaceous unconformity. Downward flow is reported as predominant flow direction in the Clearwater Formation (Bachu, 1985). The Grosmont Formation, located to the northeast beyond the study area of Bachu (1985) was identified as a drain. It is interesting to note that Bachu (1985) considered the Clearwater Formation to be an aquitard; no porosity values were reported, while all other Upper and Lower Mannville units have reported porosities and permeabilities of 33%, 34% and 1.0 and 2.0 darcys respectively (Bachu, 1985).

Potentiometric surface maps were created from calculated hydraulic head values within the northern Cold Lake study area. Potentiometric data used to create the maps is reported in Appendix 6. A number of isolated pressures for other formations are reported for reference although there were not enough values with which further potentiometric maps could be created. Hydraulic head values were calculated for equivalent freshwater head, which has a TDS value of about 10,000 mg/L. The average value of TDS for Mannville Group waters examined in the study is approximately 18,000 mg/L (Appendix 6).

The Grand Rapids Formation consists of fine grained sands, silts and shales which were deposited in brackish water, likely in an intertidal setting (Wightman *et al.*, 1987). Sediments are unconsolidated, and as such form a good aquifer with high porosities and permeabilities. The Clearwater and McMurray sediments differ lithologically from the sediments of the Grand Rapids Formation having been deposited under different sedimentological conditions, but are also unconsolidated and of approximately the same grain size. For these reasons, it is unlikely that the hydraulic parameters of the Clearwater Formation differ from that of Grand Rapids and McMurray units, contrary to what was reported by Bachu (1985). The Colony Formation is a continentally derived fluvial sand which unconformably overlies the McLaren Formation (Putnam, 1982). It was deposited near the edge of the Cretaceous shallow sea in possible brackish water conditions (Wightman *et al.*, 1987). Hackbarth and Nastasa (1979) examined the nature of fluid flow in the bitumen saturated sands of the Athabasca oil sands deposit, located north of the study area, and determined that flow conditions are a function of the degree of bitumen saturation. It was determined for the McMurray Formation that unless bitumen saturation was greater than 90% the formation still formed a good aquifer. Therefore, it is reasonable to assume that all three bitumen saturated formations of the Mannville Group form significant aquifers in the study area. Flow within the Clearwater Formation may be reduced in highly bitumen saturated areas, but would overall be comparable to the Grand Rapids and McMurray formations elsewhere in the deposit.

Initially, pressure data from the Colony and Grand Rapids formations were treated as two separate entities and potentiometric surface maps were created for each. Data were later consolidated, as evidence suggested that the two units were in hydraulic communication. Supporting evidence was:

1) the similarity and conformity of the hydraulic head data in the study area;
2) the similar values of relative density (Appendix 6) for both Colony and Grand Rapids formation waters resulting in analogous pressure gradients in p(d) and p(z) plots; and
3) similar results from p(d) and p(z) plots for both formations.

Henceforth, only one potentiometric surface map was created for the Upper Mannville sediments. Lack of data prevented the creation of a potentiometric surface map for other formations in the study area.

The potentiometric surface map for the Upper Mannville in the study area has an overall head drop of 102m (335ft) (Figure 4.11). Flow is predominantly from the northwest towards the southeast in the northern part of the map, with flow in the north and northeastern corner towards the southwest. Flow in the southwestern corner is towards the northeast where a local potentiometric high is located. Flow along the western boundary, where local potentiometric highs and lows are present, is highly uncertain as values differ greatly within a small areal extent. In general terms this pattern seems to loosely follow topography, which is essentially an exaggerated view of the topography of the water table. A plot of head versus topography was created to determine the extent of this relationship (Figure 4.12). Hydraulic head does not appear to correlate to any great degree with topographic elevation. This may suggest that topography has a small but variable effect depending upon depth, or that the relief observed in Figure 4.11 results from other factors, such as the influence of flow in the underlying Devonian aquifer. It is difficult to determine the vertical pattern of flow within the Cold Lake area because of the scarcity of data. Head values for the Clearwater Formation (Appendix 6) are generally lower that those for the overlying Grand Rapids and Colony Formations, suggesting downward flow within the Mannville sediments. Pressure versus depth and pressure versus elevation plots were generated for both the Colony (Figure 4.13) and Grand Rapids (Figure 4.14) formations in an effort to gather more information.

Figure 4.13a, a plot of formation pressure versus depth, shows the relationship of the hydrostatic pressure (P) gradient computed from formation salinity and pressure values from the Colony Formation. The data appeared to be randomly scattered upon initial observation, but a systematic deviation in pressure at various depths was associated with different ranges in topographic elevation. This staggered correlation may be the result of some influence by topography on the fluid potential, or pressure differences associated with the effect of flow in the formation. In general, values associated with topographic

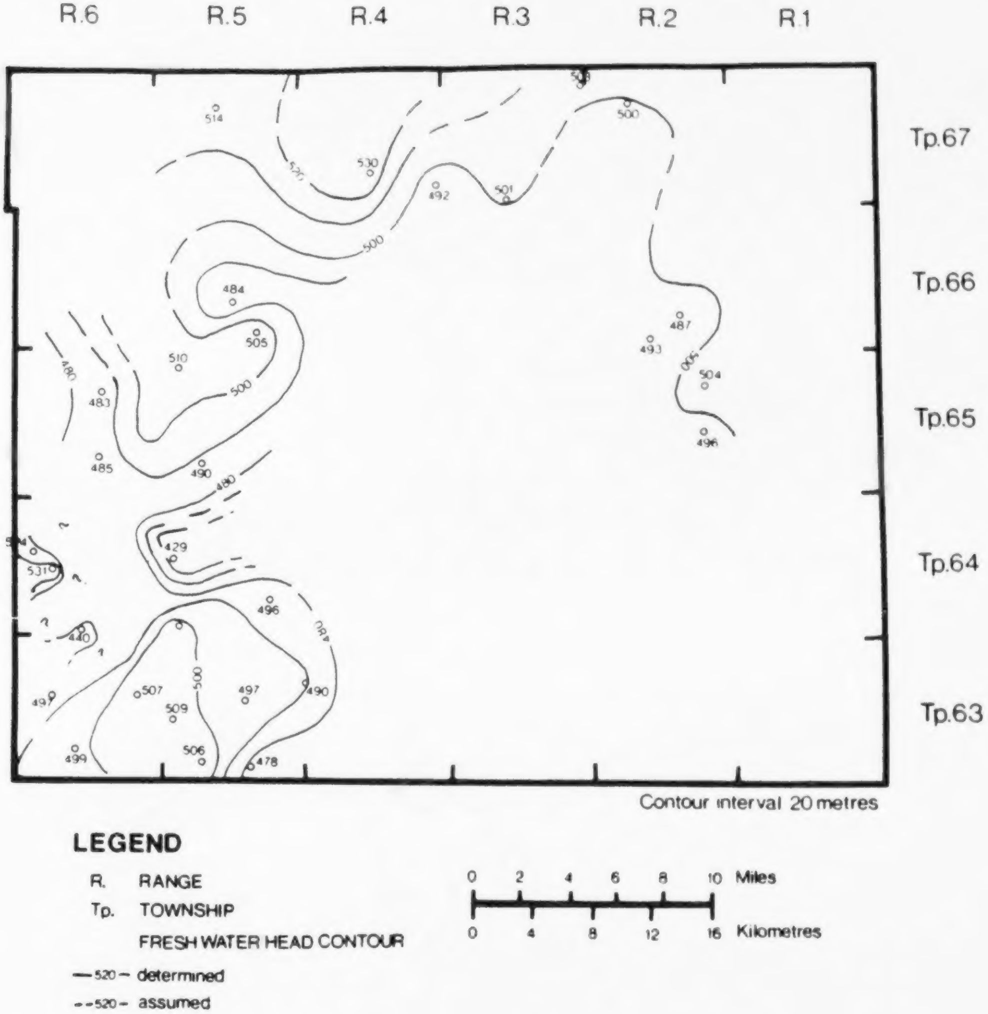
R.6
R.5
R.4
R.3
R.2
R.1
Tp.67
Tp.66
Tp.65
Tp.64
Tp.63
514
530
520
492
501
500
500
484
505
510
500
480
483
485
490
480
487
493
500
504
496
429
531
496
480
440
497
507
500
509
497
490
499
506
478
Contour interval 20 metres
LEGEND
R. RANGE
Tp. TOWNSHIP
FRESH WATER HEAD CONTOUR
—520— determined
--520-- assumed
0 2 4 6 8 10 Miles
0 4 8 12 16 Kilometres

Figure 4.11: Potentiometric surface map of the Upper Mannville Group (Colony and Grand Rapids formations) within the northern Cold Lake oil sands study area.

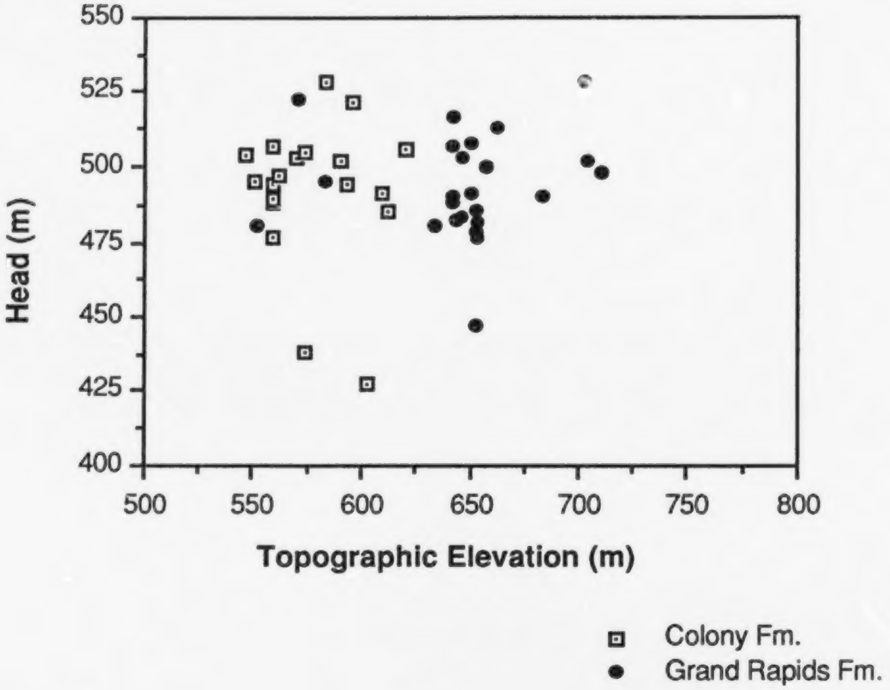

Figure 4.12: Plot of hydraulic head versus topography in the Colony and Grand Rapids formations of the Upper Mannville Group in the study area.

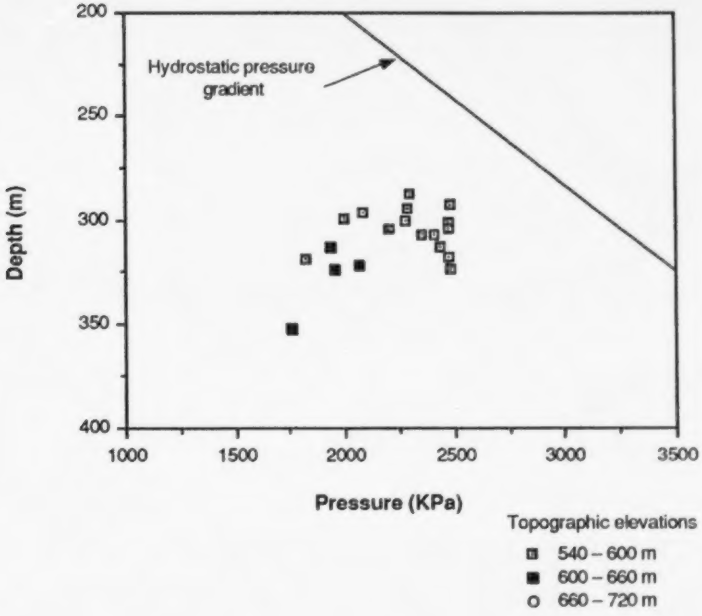

Figure 4.13a: Pressure versus depth (P(d) plot) for the Colony Formation.

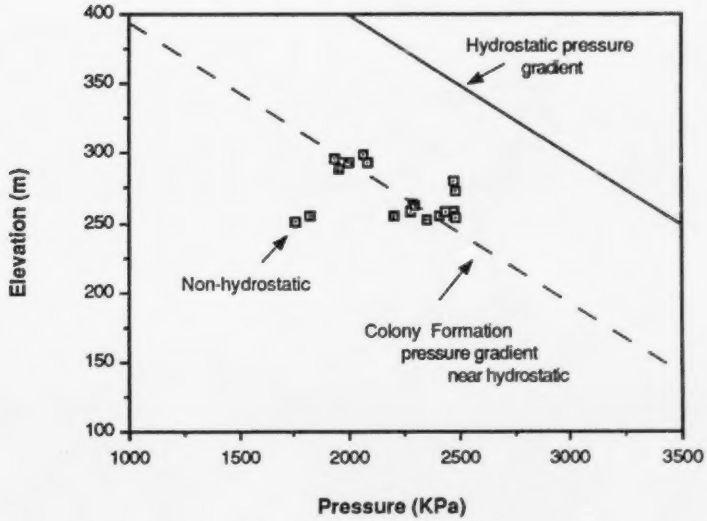

Figure 4.13b: Pressure versus elevation above sea level (datum) (P(z) plot) for the Colony Formation.

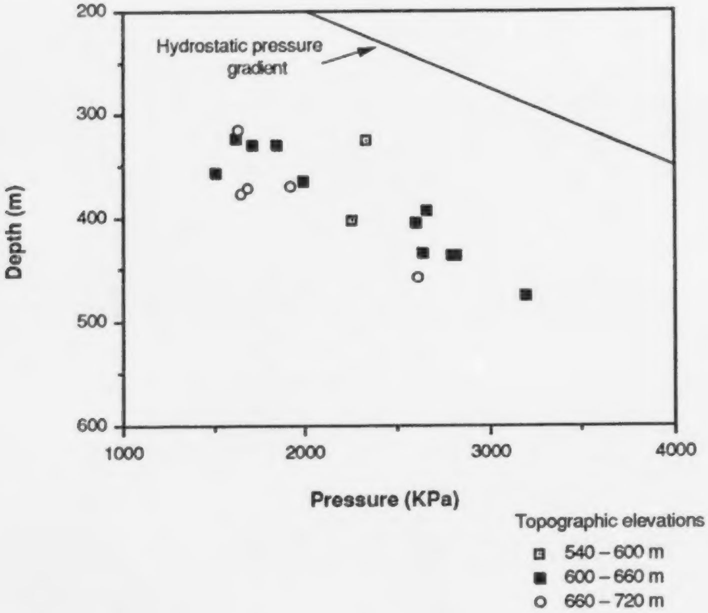

Figure 4.14a: Pressure versus depth (P(d) plot) for the Grand Rapids Formation.

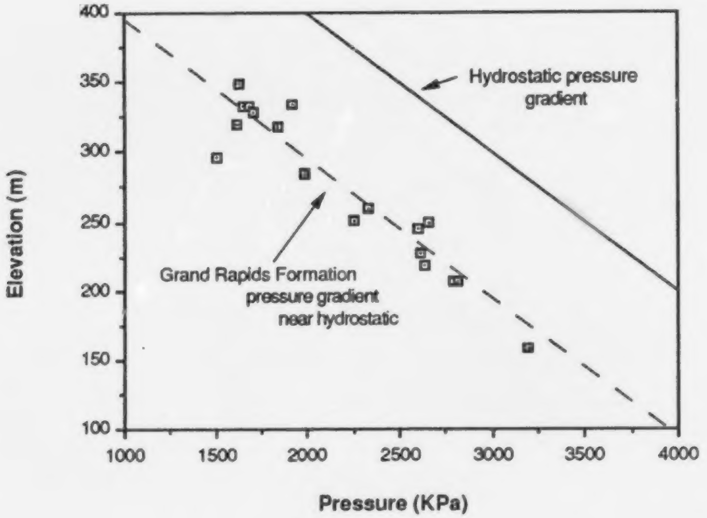

Figure 4.14b: Pressure versus elevation above sea level (datum) (P(z) plot) for the Grand Rapids Formation.

highs have lower pressures at the shallowest depths below the surface. A line drawn through each group of points would parallel the hydrostatic gradient for the area.

Figure 4.13b is a plot of formation pressure versus elevation (relative to sea level) for the Colony Formation. In this instance, data points are bunched together and for the most part lie on a line which approximates the hydrostatic pressure gradient for the formation. This shift from a number of lines of similar gradient in the p(d) plot to one line of an equal gradient in the p(z) plot is indicative of a confined hydrologic system.

Analogous p(d) and p(z) plots were made for the Grand Rapids Formation and comparable results were obtained. Figure 4.14a illustrates the same relationship of values in the pressure versus depth plot as in the Colony Formation, but better illustrates the spread of values with changing topographic elevation. Data points in the pressure versus elevation plot in Figure 4.14b also plot on a single line, indicating that confined conditions are predominant in the Grand Rapids Formation as well.

Overall, the four plots in Figures 4.13 and 4.14 suggest that the Colony and Grand Rapids formations of the Upper Mannville Group are hydraulically comparable and therefore likely continuous. Both have hydrostatic pressure gradients and show pressure deviations with depth below the surface that are likely associated with the dynamic effects of flow in a confined or semi-confined system. The overall pattern of flow within the study area seems to correspond with topographic elevation, with high heads located in upland areas and lows in discharge areas, but pressure data does not support topography-induced flow. The overlying Colorado shales are thick and laterally continuous and may form the barrier which results in confining conditions in the study area. The total amount of flow within the Upper Mannville Group in the study area has been shown to be relatively small (as indicated by small head differences), with major flow lateral towards the south and southeast, and to some degree down toward the pre-Cretaceous unconformity. A potentiometric surface map constructed for the Lower Mannville by Bachu (1985) suggested that flow had a higher velocity in the McMurray Formation and was also down towards the unconformity. Only one reliable head value was obtained from the Upper Devonian within the study area (Appendix 6). It had a substantially higher pressure than that of the overlying Cretaceous units, which fits well with the theory of higher velocity flow in the Upper Devonian units (Bachu, 1985; Garven, 1989).

GROUNDWATER CHEMISTRY

Western Canada Sedimentary Basin:

Formation fluids were studied in the Western Canada Sedimentary Basin by van Everdingen (1968a), who reported the existence of a number of major flow systems reflected by changes in formation chemistry. The flow systems he reported are essentially analogous to those discussed by Garven (1989). Van Everdingen (1968a) reported a number of anomalies or trends, the most prominent of which are:

1) an increase in TDS with depth and along the flowpath (as predicted by Tóth, 1963);
2) low TDS values in recharge areas;
3) the presence of brines (TDS>~50 000 mg/L) within the deeper parts of the basin and towards discharge areas;
4) low TDS values in outcropping Paleozoic formations in Manitoba resulting from mixing with fresh meteoric waters;
5) the presence of salt springs along the edge of the Canadian Shield, indicating salt dissolution of the Middle Devonian evaporites; and
6) low concentrations of sulphate (SO_4^{2-}) associated with high concentrations of bicarbonate (HCO_3^-) that may be related to sites of sulphate reduction.

He also discussed the importance of osmotic clay membranes and the ionic exchange of clays in the Western Canada Sedimentary Basin. Hitchon (1969a, 1969b) also discussed basin chemistry in regional terms and his views generally reflect those of van Everdingen (1968a).

In terms of water chemistry, meteoric waters that infiltrate the basin in topographically high (recharge) areas in the south and western portions of the Western Canada Sedimentary Basin gradually increase in TDS (salinity) as they mix with connate formation waters and react with the rock framework. Over time, as the distance through which the water has travelled increases, and through processes such as mineral precipitation, ionic exchange and osmosis, the chemistry of the moving groundwater changes in varying degrees depending on the flow system (local, intermediate or regional). Within the Western Canada Sedimentary Basin regional groundwater flow will move laterally and upward toward discharge areas along the eastern margin of the syncline (as discussed earlier). Mixing of upward moving basinal brines with downward moving meteoric water from local recharge systems may result in precipitation of mineral species, or merely lower the salinity of waters in discharge areas. In some cases the amount of infiltrating groundwater is volumetrically small compared to the amount of discharging groundwater, and salt springs result such as in northern Alberta and Saskatchewan. Regional flowpaths such as these are quite slow, with flow on the order of magnitude of 10^{-3}m/year (Garven, 1989).

Cold Lake Oil Sands Area:

Published studies of detailed formation fluid chemistry were not found for the Cold Lake (Sand River) area. Some mention of chemical variations in groundwater was made in Ozoray *et al.* (1980), but mainly in terms of surficial chemistry. In general, waters sampled from surficial wells are high in carbonate and bicarbonate and relatively high in calcium with isolated high values of potassium, sodium and sulphate. Formation waters sampled from deeper wells are generally higher in sodium, potassium and chloride with minor concentrations of calcium and magnesium (Ozoray *et al.*, 1980).

Chemical variations in the Cold Lake area were investigated in this study by observing ionic variations in water analyses from oil wells. Total dissolved solids (TDS), bicarbonate, sulphate and chloride concentrations were contoured for the Colony and Grand Rapids formations, and results are shown in Figures 4.15 through 4.22. Calcium and magnesium data were examined graphically (method of Zapozec, 1972). Sodium, potassium and carbonate ions were also reported in water analyses but were not used in this study because of possible contamination by drilling muds. Fluid data were reported for the Clearwater Formation (Appendix 6), but insufficient data was available to determine overall trends.

In the Colony Formation, the amount of total dissolved solids in formation waters varies significantly from a low of 3 261 mg/L in the northeastern corner of the study area to a high of 35 037 mg/L in the southwestern corner, with a number of high TDS values extending roughly to the north and northeast (Figure 4.15). In general, high TDS waters are concentrated along the southern boundary of the study area with a prominent central lobe extending towards the northeast. This trend corresponds to that of topographic elevation to some degree, with higher TDS values associated with lower elevations and local lows in the study area. Chloride concentrations show the same trends as those of TDS, with lows in the north and highs in the south, although values are smaller (Figure 4.16). This relationship is expected as chloride is the major contributor to the TDS content of the waters (Appendix 6). Sulphate concentration variations within the Colony Formation

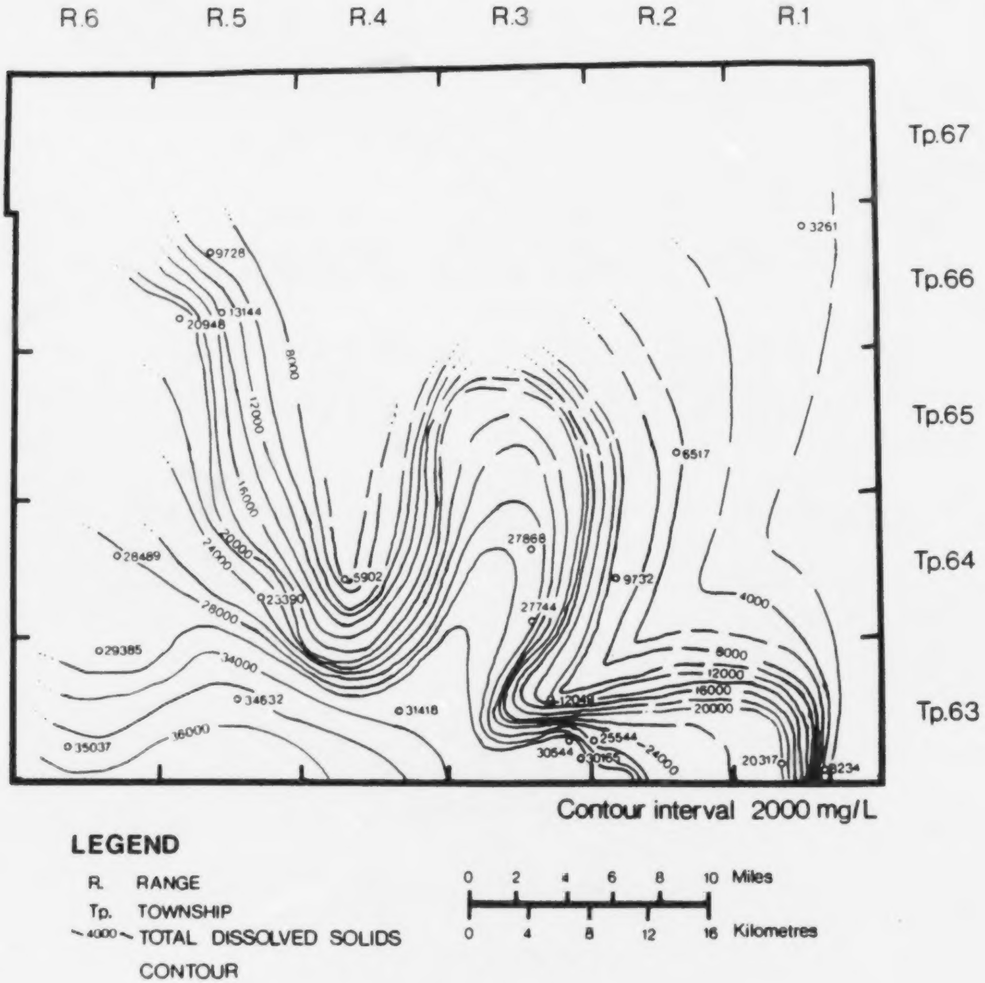
R.6
R.5
R.4
R.3
R.2
R.1
Tp.67
Tp.66
Tp.65
Tp.64
Tp.63
3261
9728
13144
20948
8000
12000
16000
20000
24000
28489
5902
23390
28000
6517
27868
9732
27744
4000
29385
34000
34632
31418
12049
8000
12000
16000
20000
35037
36000
25544
30544
30165
24000
20317
8234
Contour interval 2000 mg/L
LEGEND
R. RANGE
Tp. TOWNSHIP
4000 TOTAL DISSOLVED SOLIDS CONTOUR
0 2 4 6 8 10 Miles
0 4 8 12 16 Kilometres

Figure 4.15: Total dissolved solids (TDS) in the Colony Formation within the northern Cold Lake oil sands study area.

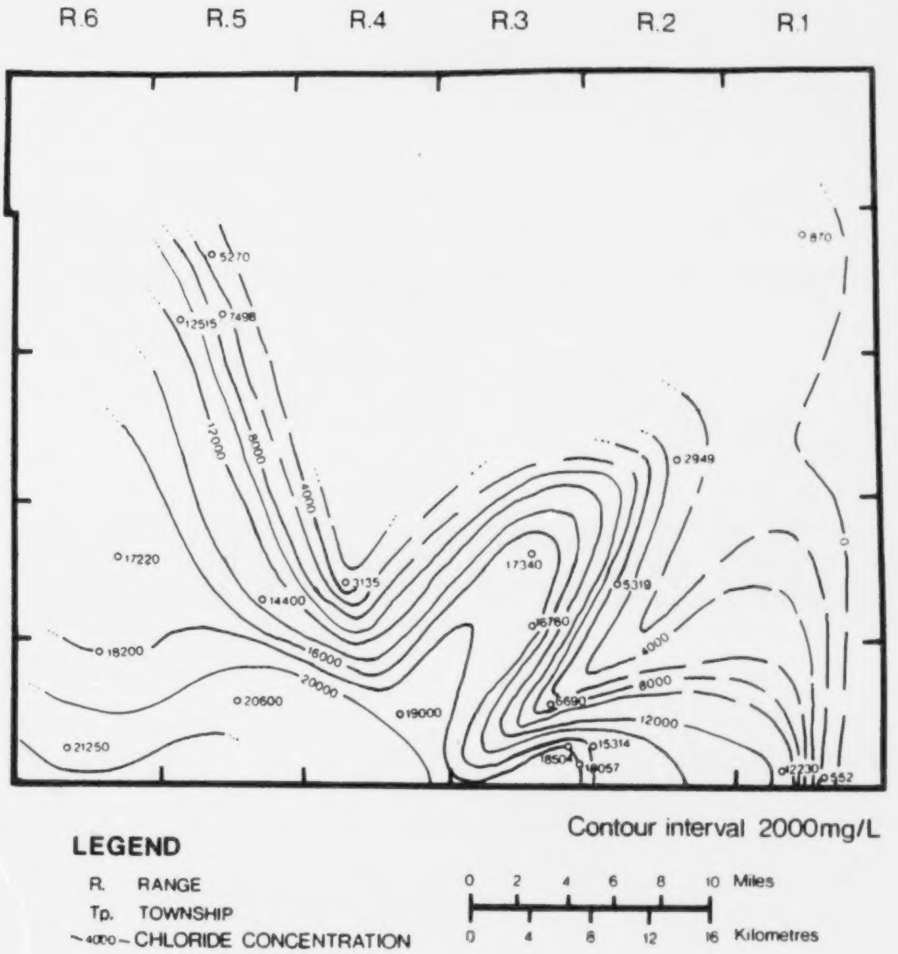
R.6
R.5
R.4
R.3
R.2
R.1
Tp.67
Tp.66
Tp.65
Tp.64
Tp.63
870
5270
12515
7498
12000
8000
4000
2949
17220
3135
17340
5319
14400
16760
18200
4000
16000
20000
8000
20600
6690
19000
12000
21250
15314
18504
18057
12230
552
0
Contour interval 2000mg/L
LEGEND
R. RANGE
Tp. TOWNSHIP
~4000~ CHLORIDE CONCENTRATION
0 2 4 6 8 10 Miles
0 4 8 12 16 Kilometres

Figure 4.16: Chloride (Cl⁻) concentration in the Colony Formation within the northern Cold Lake oil sands study area.

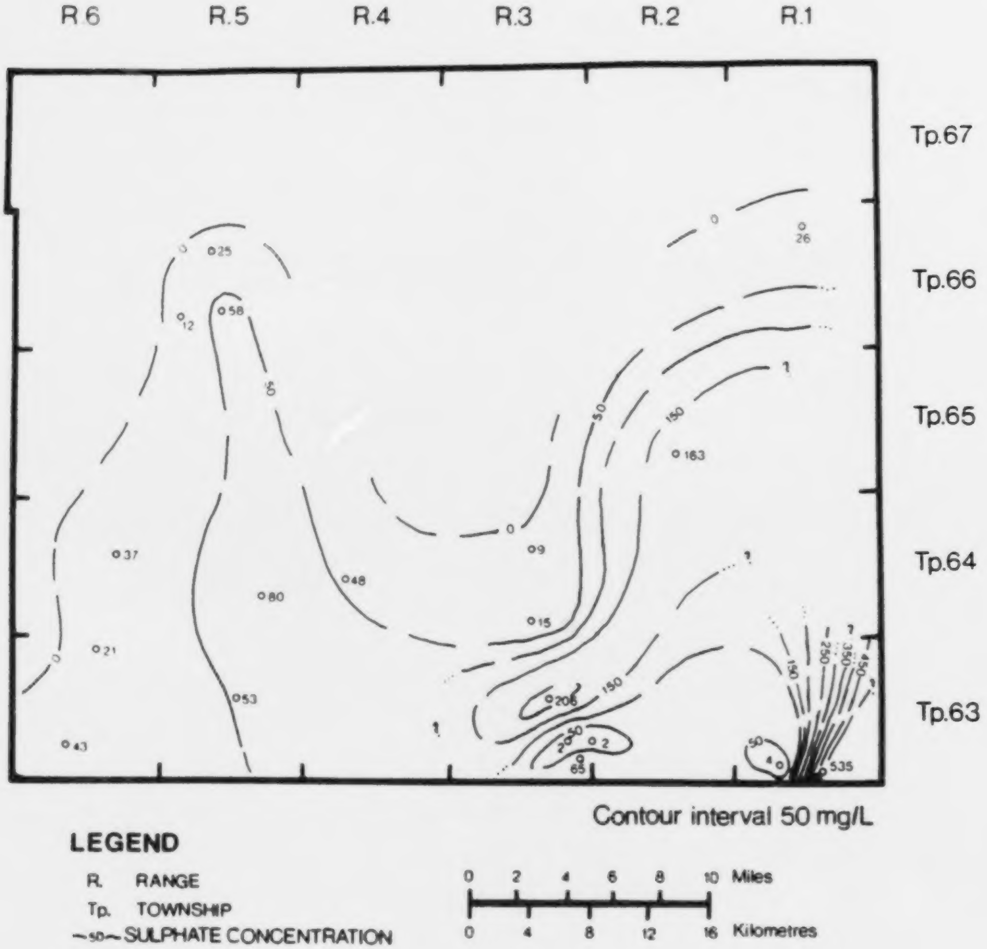
R.6
R.5
R.4
R.3
R.2
R.1
Tp.67
Tp.66
Tp.65
Tp.64
Tp.63
25
12
58
50
0
26
1
50
150
163
0
9
37
80
48
15
21
0
53
43
208
150
50
2
2
65
50
4
535
150
250
350
450
Contour interval 50 mg/L
LEGEND
R. RANGE
Tp. TOWNSHIP
~50~ SULPHATE CONCENTRATION
0 2 4 6 8 10 Miles
0 4 8 12 16 Kilometres

Figure 4.17: Sulphate (SO_4^{2-}) concentration in the Colony Formation within the northern Cold Lake oil sands study area.

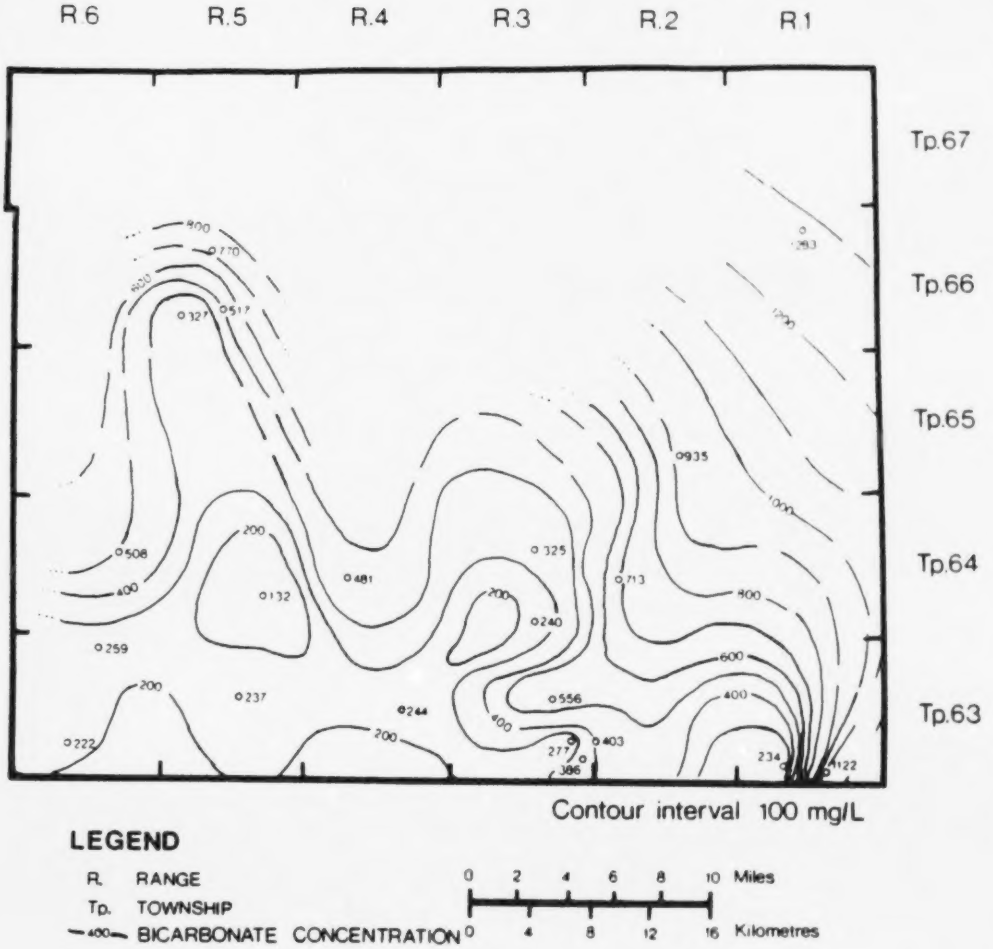
R.6
R.5
R.4
R.3
R.2
R.1
Tp.67
Tp.66
Tp.65
Tp.64
Tp.63
800
770
600
327
517
283
1200
935
1000
200
508
400
132
481
325
713
800
200
240
259
600
200
237
244
556
400
400
222
200
403
277
386
234
122
Contour interval 100 mg/L
LEGEND
R. RANGE
Tp. TOWNSHIP
400 BICARBONATE CONCENTRATION
0 2 4 6 8 10 Miles
0 4 8 12 16 Kilometres

Figure 4.18: Bicarbonate (HCO_3^-) concentration in the Colony Formation within the northern Cold Lake oil sands study area.

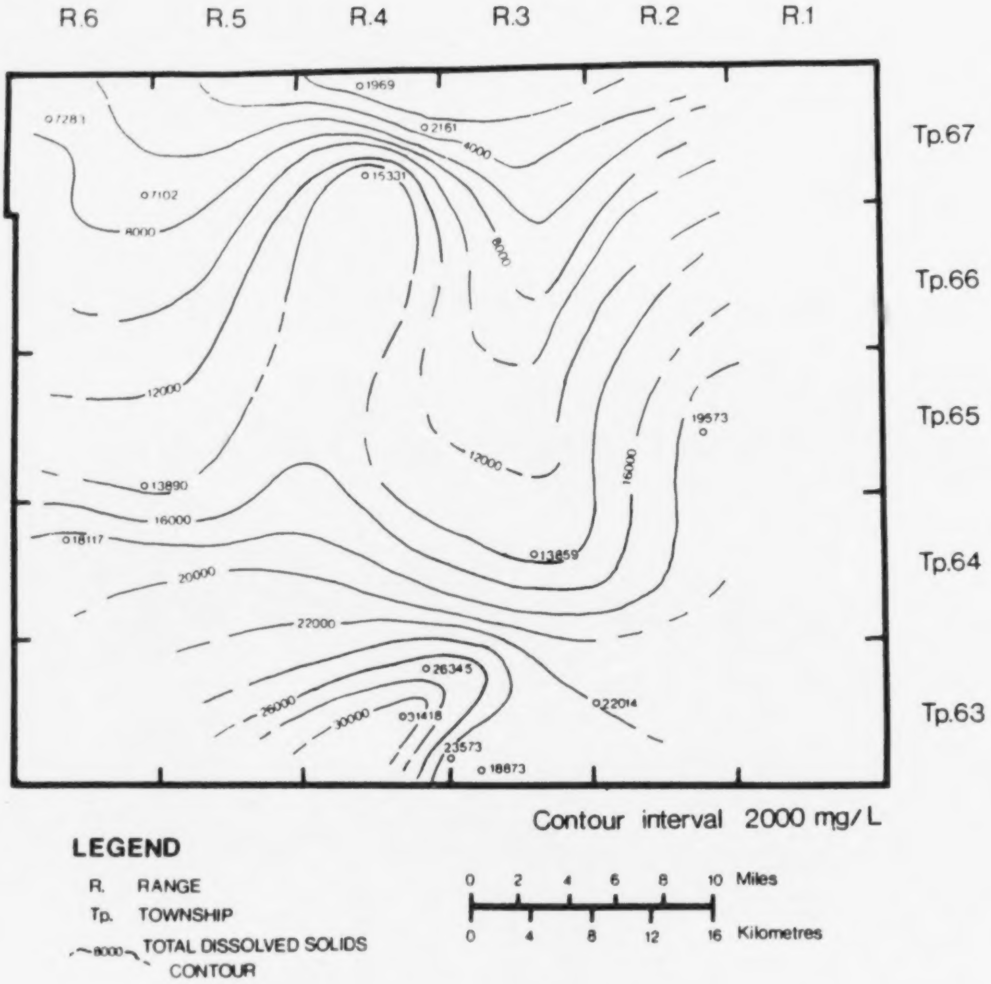
R.6
R.5
R.4
R.3
R.2
R.1
Tp.67
Tp.66
Tp.65
Tp.64
Tp.63
1969
2161
4000
7283
7102
8000
15331
8000
12000
19573
12000
16000
13890
16000
18117
13859
20000
22000
26345
26000
30000
31418
23573
18873
22014
Contour interval 2000 mg/L
LEGEND
R. RANGE
Tp. TOWNSHIP
8000 TOTAL DISSOLVED SOLIDS CONTOUR
0 2 4 6 8 10 Miles
0 4 8 12 16 Kilometres

Figure 4.19: Total dissolved solids (TDS) in the Grand Rapids Formation within the northern Cold Lake oil sands study area.

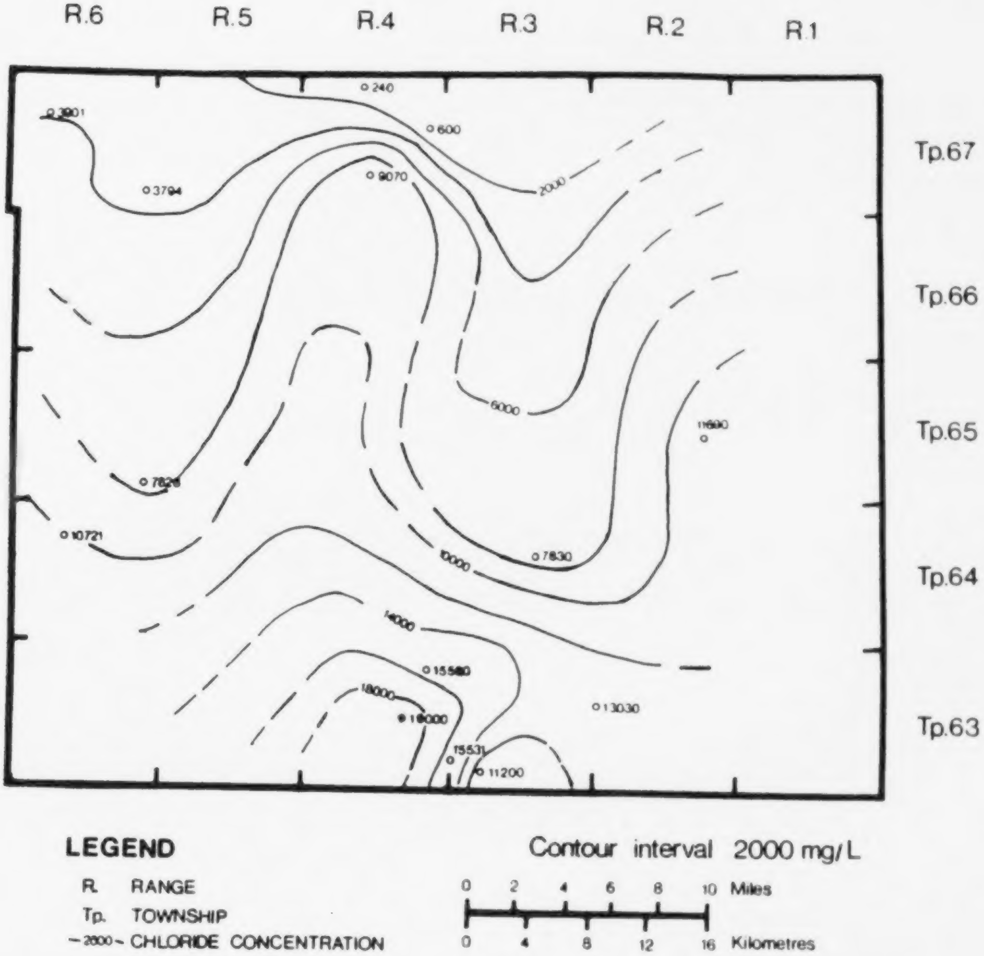
R.6
R.5
R.4
R.3
R.2
R.1
Tp.67
Tp.66
Tp.65
Tp.64
Tp.63
3901
240
600
9070
3794
2000
6000
11690
7828
10721
10000
7830
14000
15580
18000
19000
13030
15531
11200
LEGEND
R. RANGE
Tp. TOWNSHIP
-2000- CHLORIDE CONCENTRATION
Contour interval 2000 mg/L
0 2 4 6 8 10 Miles
0 4 8 12 16 Kilometres

Figure 4.20: Chloride (Cl^-) concentration in the Grand Rapids Formation within the northern Cold Lake oil sands study area.

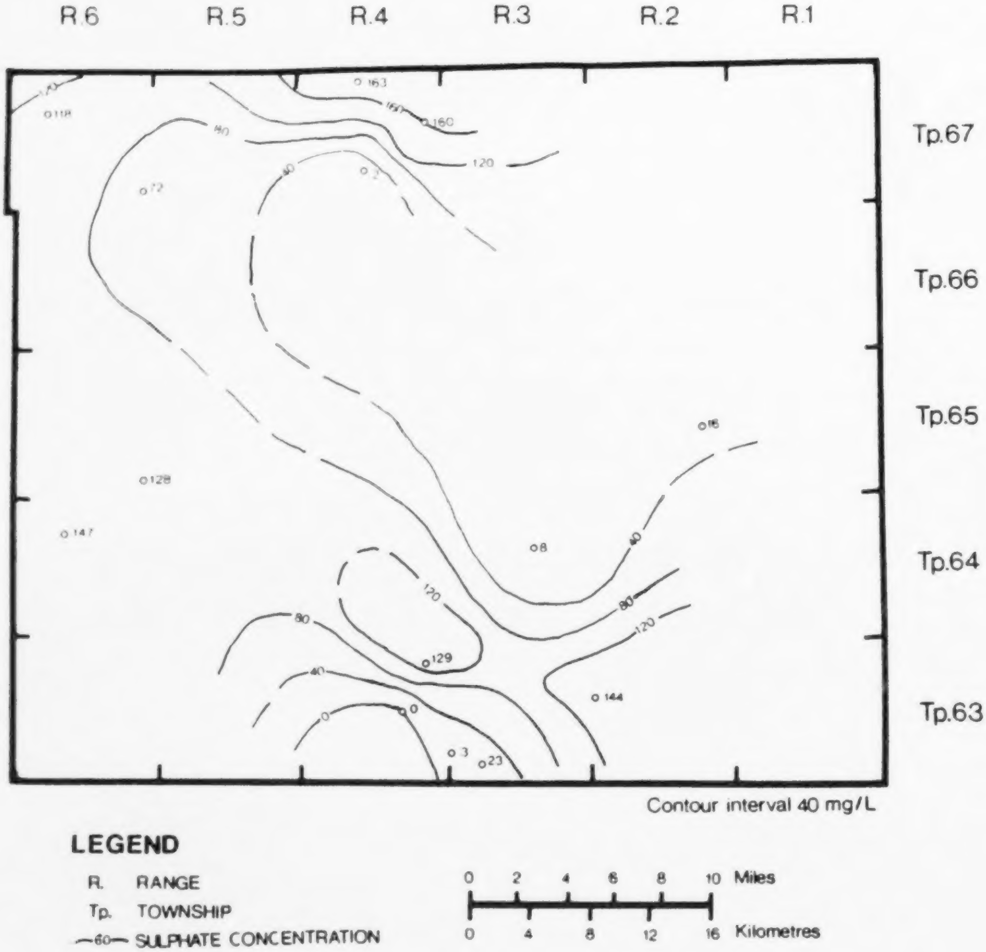
R.6
R.5
R.4
R.3
R.2
R.1
Tp.67
Tp.66
Tp.65
Tp.64
Tp.63
120
118
163
160
160
80
120
72
40
2
16
128
147
8
40
120
80
80
120
129
40
0
0
144
3
23
Contour interval 40 mg/L
LEGEND
R. RANGE
Tp. TOWNSHIP
—60— SULPHATE CONCENTRATION
0 2 4 6 8 10 Miles
0 4 8 12 16 Kilometres

Figure 4.21: Sulphate (SO_4^{2-}) concentration in the Grand Rapids Formation within the northern Cold Lake oil sands study area.

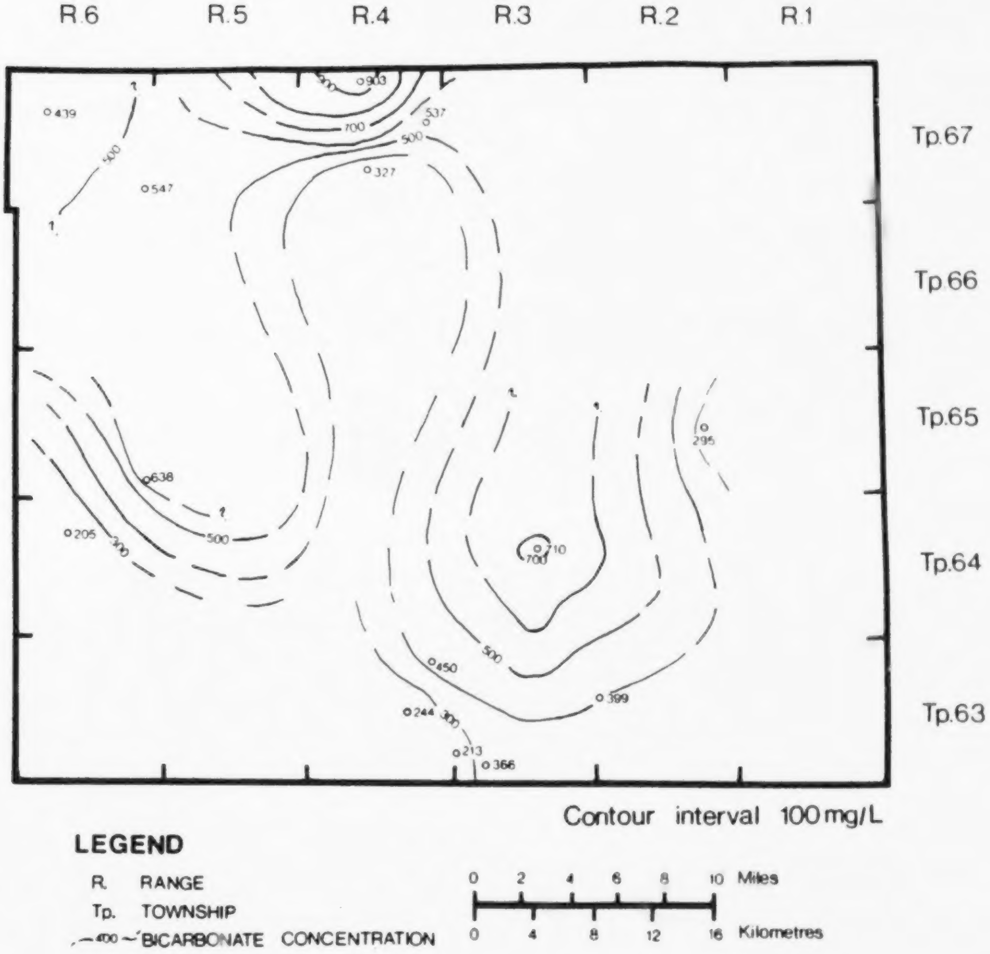
R.6
R.5
R.4
R.3
R.2
R.1
Tp.67
Tp.66
Tp.65
Tp.64
Tp.63
439
?
500
547
?
900
903
700
537
500
327
638
?
205
300
500
?
?
295
710
700
500
450
399
244
300
213
366
Contour interval 100 mg/L
LEGEND
R. RANGE
Tp. TOWNSHIP
—400— BICARBONATE CONCENTRATION
0 2 4 6 8 10 Miles
0 4 8 12 16 Kilometres

Figure 4.22: Bicarbonate (HCO_3^-) concentration in the Grand Rapids Formation within the northern Cold Lake oil sands study area.

are quite small, the range of values being within 200 mg/L with an isolated high value of 585 mg/L (Figure 4.17). In comparison to the other components this indicates a relatively constant sulphate concentration in Colony waters. Highs in sulphate concentration generally occur between highs and lows of other ionic species. Bicarbonate shows similar but opposite trends to that of TDS and chloride in Colony Formation waters, with high values associated with TDS and lows in Cl^- (Figure 4.18). The intermediate flow patterns of the Colony Formation appear to be affected by the elevation of the water table (reflected by surficial geometry). Recorded cation compositions of Colony Formation waters are generally quite low in the study area. Calcium ranges from a low of 16 to a high of 789 mg/L with a mean of 346 mg/L. Magnesium concentrations range from a low of 2 to a high of 379 mg/L with a mean of 168 mg/L (Appendix 6). The ratio of calcium to magnesium is approximately 2:1 in most samples. Calcium and magnesium concentrations in general show approximately the same trends as TDS and Cl^- in the Colony Formation.

The Grand Rapids Formation shows variations in TDS and chloride content similar to those of the Colony Formation (Figures 4.19 and 4.20). The highest TDS and chloride values are in the south and the lowest in the north, corresponding to highs and lows of topographic elevation, but the local, more detailed pattern of concentrations do not mimic topographic elevation to the same degree as in the Colony Formation. High concentrations in TDS and Cl^- occur as a large band across the southern part of the study area in the Grand Rapids Formation, with a central lobe of high values extending towards the north and a few high values along the eastern boundary. The variation in sulphate concentration is small in the Grand Rapids Formation (< 200 mg/L), and local highs and lows are scattered throughout the study area (Figure 4.21). Highs tend to occur between highs and lows of bicarbonate and chloride concentration. Bicarbonate concentrations show highs in the north and lows in the south and are opposite in trend to TDS and chloride in the Grand Rapids Formation (Figure 4.22). Low compositions of calcium and magnesium characterize the Grand Rapids Formation. Ranges in calcium content are from a high of 635 to a low of 22 mg/L with a mean of 225 mg/L. Magnesium values range from 15 to 313 mg/L with a mean value of 101 mg/L. As in the Colony Formation, Ca / Mg ratios tend to be approximately 2:1, and trends tend to mimic TDS and Cl^- patterns.

General trends in the concentration of anionic species in both the Colony and Grand Rapids Formation correspond to those of the empirical sequence proposed by Chebotarev (1955), for the chemical evolution of groundwaters. Bicarbonate and chloride-rich waters occur in different positions that correspond to some degree with topographic elevation, and sulphate highs generally occur between these two endmembers. Comparison between a structure map of the pre-Cretaceous unconformity (Paleozoic surface) and ionic trends in Figures 4.15 through 4.22 clearly indicates a relationship between structural lows and TDS highs (Figures 4.15, 4.19 and 4.23). In addition, the correlation between structural lows and the patterns of TDS compositions is more pronounced in the Grand Rapids Formation. This behaviour strongly suggests that the high concentration of total dissolved solids in Mannville Group waters are the result of infiltration of ionic constituents by such processes as ionic filtration or diffusion from the underlying Devonian units. Structural lows in the pre-Cretaceous unconformity can generally be correlated with areas of salt dissolution activity in Middle Devonian evaporites (M. Ranger[4], per. comm.). These evaporites and associated Upper Devonian carbonates are most likely sources of the higher than normal Cl^- values, as well as the presence of highs in the concentration patterns of Ca^{2+}, Mg^{2+} and to some degree $SO_4{}^{2-}$ in the study area. Transport of these ionic constituents is likely by diffusion processes, as large TDS differences between waters of Devonian and Mannville age generally rule out a hydraulic component of flow. This behavior suggests that flow by osmosis is associated with the pre-Cretaceous unconformity, which supports the presence of a semi-permeable shale-type membrane at or near the unconformity. Shales in the Lower Mannville Group are generally relatively thin and laterally discontinuous, but it is possible that shales in the lower part of the McMurray Formation are of sufficient thickness, and are acting as barriers to hydraulic flow. Although sulphate highs are associated to some degree with areas of dissolution activity in the Devonian, other factors appear to be influencing areal sulphate patterns in waters. It is possible that lows in sulphate associated with highs in bicarbonate may be related to areas of sulphate reduction as suggested by van Everdingen (1968a). High values of bicarbonate may be associated with areas of higher topographic relief, while lows correspond to positions of dissolution activity. This may suggest some percolation of bicarbonate from local recharge areas, despite confining conditions within the Mannville Group. This association of bicarbonate highs with topographic highs is more pronounced in the shallower Colony Formation. Overall, variation in the concentration of ionic constituents in the study area corresponds well to trends that have been predicted for the dissolution of lithologies found within the deeper areas of the Western Canada Sedimentary Basin. Regional waters from the basin discharging on the eastern margin contribute some solutes to the fresher waters of the intermediate to local system now present in the Mannville Group, which corresponds well to generalizations predicted by Chebotarev (1955) in his chemical evolution of sedimentary basin waters.

---

[4] Department of Geology, University of Alberta, Edmonton, Alberta, Canada.

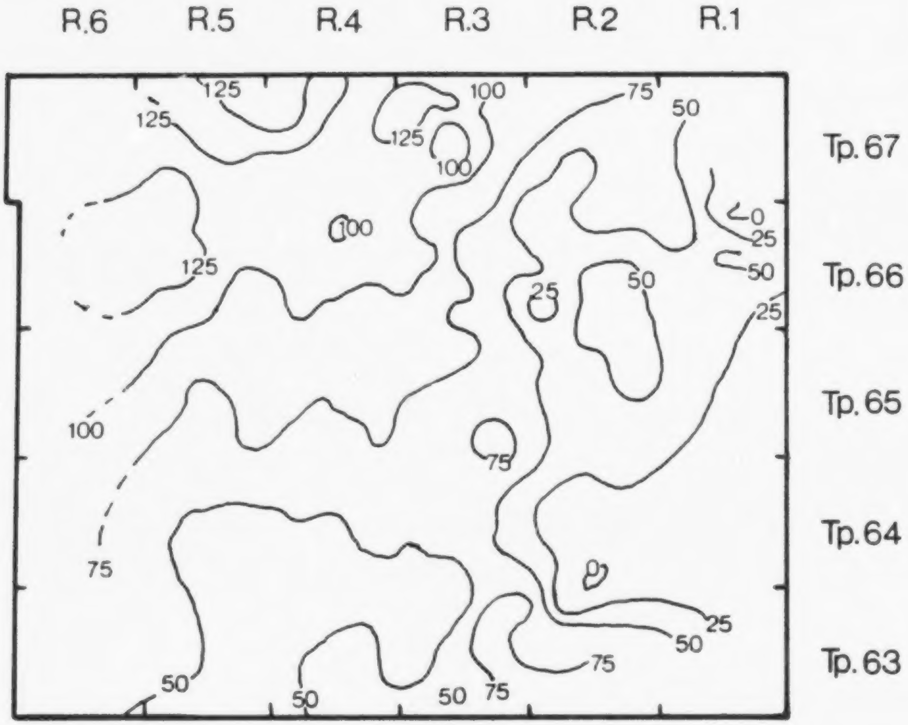
R.6
R.5
R.4
R.3
R.2
R.1
Tp. 67
Tp. 66
Tp. 65
Tp. 64
Tp. 63
125
125
125
125
100
100
100
75
50
0
25
50
25
50
25
100
75
75
50
50
50
25
50
75
75

0 10 miles

0 16 kilometres

LEGEND:

R. Range
Tp. Township

100 Structure contours
(relative to sea level)

Contour interval = 25m.

Figure 4.23: Structure map of the Devonian surface, Cold Lake study area.

Variations in ionic constituents within the study area were also investigated graphically by a method slightly altered from that presented by Zaporozec (1972). Major cations and anions from waters within the study area were plotted to determine if different water types were contributing to the system (Figure 4.24). The plot between calcium and magnesium clearly indicates a dominant Ca / Mg ratio of 2:1. The anionic ternary plot shows that the waters from the Mannville Group in this study are primarily of the chloride type, although there is some contribution from waters with higher abundances of sulphate and bicarbonate. The middle square, which intersects the Ca / Mg plot and the anion triangle, shows the variation in composition of Mannville Group waters based on dominant ionic composition. Both the middle square and the TDS portion of the diagram illustrate that although the total dissolved content between the waters is quite variable, there is a continuous gradation of TDS with respect to the major cations (as both calcium and magnesium show the same patterns). This suggests that waters of different composition within the study area are in fluid communication and that mechanical mixing of solutes is occurring.

The consistent Ca / Mg ratio found within the study area waters likely results from processes of cation exchange. Cations are generally less mobile as dissolved constituents in waters but are easily adsorbed by clays with exchange sites of strong negative charge (Fritz, 1986). The tightness of the bond between the cation and the clay is a function of the size of the cation and its valence. Monovalent cations (i.e. sodium) are not held as tightly as divalent ones, and are therefore more highly prone to replacement by divalent cations (van Everdingen, 1968b). This explains the often high abundances of sodium in basin formation waters. Magnesium is thought to have a higher replacing power than calcium in exchange sites of smectite-type clays found within the study area, which probably accounts for the higher abundance of calcium and the constituent ratio between calcium and magnesium in study area waters (van Everdingen, 1968b).

E. INFLUENCE OF HYDROGEOLOGY ON DIAGENESIS

CLEARWATER MINERALOGY

Clearwater sediments are composed of very fine to medium grained compositionally immature feldspathic litharenites, are mainly unlithified, and generally highly bitumen saturated (Putnam and Pedskalny, 1983; Prentice and Wightman, 1987). Five main lithologies were identified: 1) fine to medium grained (highly bitumen saturated)

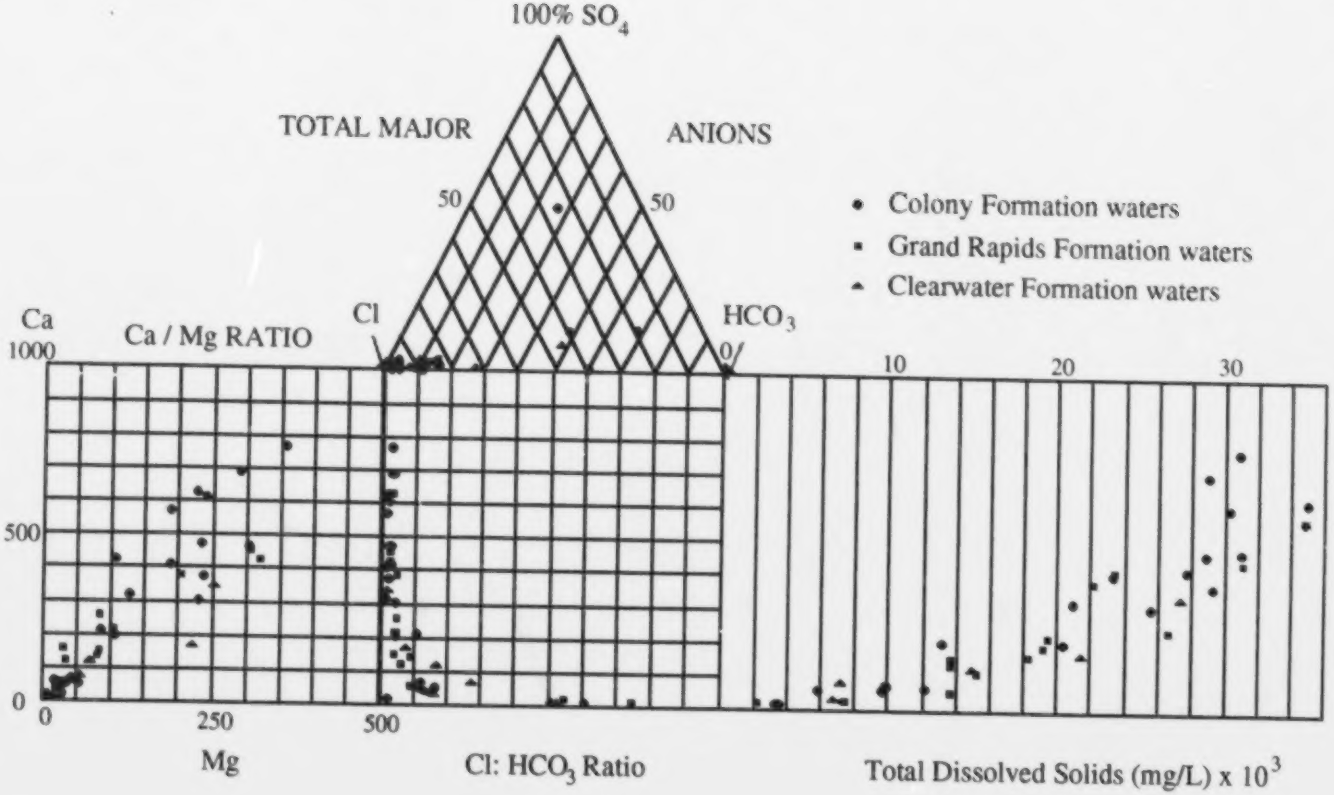

Figure 4.24: A graphical representation of Ca/Mg, the major anion and total dissolved solids for the study area (modified after Zaporozec, 1972).

'clean' sands deposited in upper delta front distributary channel and mouth-bar settings, as middle delta front transitional sands, or as isolated lenses in lower delta front sands; 2) fine to very fine grained (moderate to highly bitumen saturated) 'muddy' sands with interbedded silt or shale, deposited in middle and upper delta front settings, and in sandy areas of delta fringe sediments; 3) sandy silts or shales, which may be water saturated or contain low levels of bitumen, and typically occur in lower delta front and delta fringe sediments; 4) interstratified silts and shales (all water saturated), located in delta fringe sediments; and 5) carbonate cemented zones, containing calcite-rich sands or silts that may be located in any of the above lithologies, although they are concentrated primarily in middle to lower delta front and delta fringe sediments.

Detrital Minerals

Framework grains are dominated by rock fragments, quartz, feldspars, dolomite and detrital clays. Volcanic rock fragments are the most common, and occur in two types, acidic and porphyritic (Putnam and Pedskalny, 1983; Prentice and Wightman, 1987). Many altered grains are also present, most of which are thought to be former volcanic rock fragments and feldspars. Metamorphic and sedimentary rock fragments are relatively rare, the most common of which are polycrystalline quartz and chert.. The quartz is mainly from a volcanic source, although some may have originated from a plutonic or low-grade metamorphic environment. Plagioclase is the most common feldspar, followed by potassic feldspars (orthoclase and microcline). Pelitic grains of former silts and shales are generally rich in detrital clay minerals, primarily chlorite, and illitic and smectitic clays. Singular grains of detrital mica (likely muscovite) have also been identified. Accessory minerals are present at trace levels (generally <1%) and consist of amphiboles, ilmenite, magnetite, zircon, and tentatively olivine.

Diagenetic Mineralogy

Clearwater diagenetic minerals consist of: glauconite, pyrite, berthierine, diagenetic illite, illite / smectite (I/S), chlorite / smectite (C/S), siderite, calcite, quartz and feldspar overgrowths, zeolite, kaolinite, Fe oxides and phases of trace abundance (Chapter 3). Glauconite is a common phase and occurs as typical round to oval-shaped green grains, concentrated primarily in the sandy facies, and most prominent in the Wabiskaw Member.

Pyrite is relatively common, although volumetrically minor, and occurs as two different morphologies. Framboidal pyrite is an early pore-filling diagenetic phase with a spherical form (5–30μm), composed of smaller aggregates of many pyrite crystallites. Octahedral pyrite occurs as single crystals, in concentrations of individual crystals, or as 'knobby' framboids (<1–10μm), and is typical of late forming pyrite (Raiswell, 1982). Pyrite occurs most often in organic-rich, deeper water siltier and shaly facies, although its presence has been noted even in the thickest sands.

Diagenetic trioctahedral (7Å) berthierine occurs as abundant grain coating lath-shaped crystals on the surface of framework grains (~6μm thick), and is the most prominent in the thickest, most bitumen saturated sand facies. Other diagenetic clays include illite, mixed-layer I/S and C/S. Authigenic illite occurs as a grain coating clay, with laths very similar to those of berthierine, but with distinct prominent fuzzy edges. I/S occurs as a webby, slightly crenulated mass in silt or shale-rich facies in on the surface of grains, and as a pore-filling cement. Pore-filling clays were also observed intermixed, and are commonly difficult to differentiate.

Three types of calcite have been identified within calcite-cemented lenses or concretions in the study area: 1) Type 1 is a pervasive Fe-poor fibrous replacement cement; 2) Type 2 is an Fe-rich pore-filling crystalline mosaic that has replaced some grains, only the outer edges of others and left behind many grains of quartz; and 3) Type 3 is a vein-filling replacement cement which forms large euhedral to anhedral crystals. More than one generation may be present, and it typically changes in composition from Fe-rich to Fe-poor with progressive precipitation. The following stable isotope values were obtained for carbonate cemented zones in the study area: the $\delta^{18}O$ values for calcite range from 18.8‰ to 19.8‰, with an average of 19.4‰, and $\delta^{13}C$ values vary from -1.3 and 4.5‰. A few select stable isotope values were also obtained for detrital dolomite: $\delta^{18}O$ values of 21.5‰ and 24.1‰, and $\delta^{13}C$ values of 0.6 and 2.5‰. Results indicate that waters containing a proportion of meteoric water were involved in the formation of calcite during diagenesis. The source of the carbon ranges from an inorganic origin such as CO_2 resulting from the dissolution of detrital dolomite, to an origin partially affected by the presence of bacterially mediated CO_2, likely produced during bacterial fermentation.

Two generations of siderite are present. The first occurs as a siderite cement within mud-rich concretions within sandy facies, and the second as late, rhomb-shaped pore-filling crystals (20–50μm) which replaced framework grains, more commonly in sands.

Rhomb-shaped epitaxial overgrowths of K feldspar are relatively common in the formation, mainly within water saturated sands, and a few isolated examples of blocky plagioclase overgrowths were also noted. Quartz overgrowths are mainly syntaxial, although doubly terminated overgrowths interspersed with authigenic clays (likely smectitic) were also observed. Both quartz and feldspar overgrowths are more common in siltier, water saturated intervals, although authigenic K feldspars were also observed in thick, bitumen saturated sand facies.

Characteristic blocky, tabular, lath, and coffin-shaped crystals (5–30μm) of zeolite were also observed as a pore-filling phase, most often found in water saturated sands containing some silt or clay. The zeolite has been tentatively identified as clinoptilolite.

Only a few isolated occurrences of kaolinite were observed (7–15μm). The first as a replacement of another former grain, probably feldspar, and the second as typical kaolinite 'booklets'. Kaolinite, along with Fe oxides, is present only at trace levels within the Clearwater Formation in the study area. This contrasts with the much higher levels of kaolinite reported for the underlying McMurray Formation, overlying Grand Rapids Formation and surrounding study areas in the Clearwater Formation (Carrigy, 1971; Wightman *et al*., 1987; Hutcheon *et al*., 1989; Longstaffe *et al*., 1991a, 1992a).

DIAGENESIS

Three stages of diagenesis were identified within the study area (Chapter 3). Stage 1 incorporates early *shallow* diagenesis and early burial diagenesis. Processes varied from marine oxidation and the progressive alteration of parent substrates to form glauconite in a restricted open marine setting; to burial, reducing conditions and locally constrained sulphate reduction in the presence of sufficient organic matter in the formation of early framboidal pyrite; and with the depletion of available sulphate, a quick progression to bacterial fermentation and the development of Fe-rich berthierine, early Type 1 calcite, and siderite concretions.

Stage 2 involved intermediate to late burial diagenesis under conditions of bacterial fermentation, and resulted in extensive grain dissolution, the growth of illite and mixed layer clays, late pore-filling siderite, late pyrite, calcite, development of authigenic quartz and feldspar overgrowths, and zeolite. Bitumen emplacement is thought to have occurred progressively in the latter part of Stage 2 diagenesis, near maximum sediment burial.

The third stage of diagenesis is associated with the gradual uplift of the sediments, and their subsequent erosion on the eastern margin of the basin, which led to a change in porewater composition with the influx of meteoric water into the area. Water washing and the bacterial breakdown of the oil to bitumen, calcite cementation, and formation of kaolinite, and late Fe oxides are associated with this stage.

DISCUSSION

The hydrologic system present within the Clearwater Formation at each stage of diagenesis had an effect on the associated diagenetic events. At the time of initial burial, porewaters can be assumed to have been of the same composition as depositional porewaters. They are thought to have been mainly marine but with a brackish influence, especially in the more shoreline-proximal areas, closer to the outlet of sediment-laden fluvial waters into the deltaic system. More marine conditions would have been dominant further offshore, as indicated by the presence of abundant glauconite in the formation. Glauconite is characteristic of a semi-confined setting with a connection to open marine seawater (Odin and Matter, 1981). There is also the possibility, that the presence of meteoric water in the porewaters shortly after initial burial was influenced by meteoric incursion of fresh water arising from a change in the relative hydraulic head as suggested by Bloch (1990) for a comparable study area at the edge of the Boreal sea. Subsurface incursion of meteoric water is explained by a change (relative drop) in sea-level, resulting in a shift in the mixing zone for fresh and more saline basinal waters (Bloch, 1990).

Whether the source of the initial porewater composition reflects depositional waters or the early influx of fresh water, porewaters containing a sizeable fraction of meteoric water are thought to be typical of those present during the first stage of diagenetic activity, and during subsequent burial.

This early hydrogeologic setting is typical of a general local flow system type as proposed by Tóth (1984), with groundwater flow influenced primarily by topography. Porewaters within such a local system of groundwater flow are generally rich in bicarbonate, and increase in sulphate concentration with burial, in conjunction with the chemical evolution of groundwater (Figure 4.8)

The establishment of reducing conditions shortly after sediment burial, below the sediment / water interface, marks the beginning of early burial diagenesis. Processes of bacterial sulphate reduction are thought to have resulted in the development of early diagenetic pyrite in the study area, regulated by the presence of sufficient organic matter and dissolved sulphate. This resulted in local concentrations of pyrite within the study area; more abundant in siltier, organic-rich facies.

Processes of bacterial fermentation (methanogenesis) developed after the depletion of interstitial sulphate or in the absence of sulphate, shortly after burial. Fe-rich berthierine forms readily under low temperature reducing conditions, and abundant grain coating berthierine formed in the formation early in its diagenetic history, especially in sands. Iron was contributed from the dissolution of detrital phases incorporated in the sediment. The presence of marginal marine (brackish) porewaters favor the development of berthierine (Bhattacharyya, 1983). This formation of berthierine in the Clearwater Formation is addressed in more detail in Longstaffe *et al*. (1992b).

Other early burial diagenetic minerals are (Fe-poor) Type 1 calcite and early concretionary siderite. Stable isotope results for calcite from cemented zones indicates that it formed from an inorganic CO_2 source, such as the dissolution of detrital dolomite. Oxygen stable isotope results also indicate that a sizeable presence of meteoric water was present during its formation. The Fe-poor composition of the calcite is indicative of formation from iron depleted porewaters, with the majority of the iron likely being taken up by berthierine, pyrite and siderite. Berthierine is the most abundant phase, and it is likely that there is some formation relationship between berthierine and iron-poor calcite. Early siderite concretions formed within mud clasts under bacterial fermentation conditions. The presence of higher levels of bicarbonate in this first stage of diagenesis, contributed from more bicarbonate-rich surficial waters, may have contributed to the precipitation of early calcite and siderite in the study area.

Increased burial of Clearwater sediments can be assumed to have gradually resulted in a change to an intermediate flow system in the study area, with associated changes in porewater chemistry. Groundwater flow patterns would have been beyond the effect of topography, and mainly associated with lateral flow (Tóth, 1984). Intermediate flow systems are characterized by an increase in mineral dissolution, with associated increases in dissolved constituents to porewaters, also potentially from surrounding strata. Intermediate flow systems are characterized by higher levels of TDS, Na and Cl (Tóth, 1984).

Diagenetic conditions had progressed to those of microbial fermentation, and the increased dissolution and greater concentration of chemical species in solution resulted in the development of authigenic clays, including illite, I/S, and C/S. Late pore-filling siderite resulted from increased levels of Fe in the porewaters, and its replacement texture suggests this was locally controlled (grain replacement incorporating its dissolved Fe). The contribution of CO_2 for siderite may have resulted from a number of origins, including the dissolution of detrital dolomite, or as a by-product of methanogenesis.

Development of late octahedral pyrite is characteristic of slow growth from porewaters only slightly supersaturated with respect to iron (Raiswell, 1982). Contribution of sulphate had to have been from an external source, as all interstitial sulphate would have been depleted during earlier processes of sulphate reduction. The most likely source is sulphate-rich waters diffusing upward through the pre-Cretaceous unconformity, as the result of the ongoing dissolution of underlying Devonian (Elkpoint Group) evaporites. Sulphate may have also contributed to the formation of early pyrite, by extending the period of sulphate reduction, as evaporite dissolution was already occurring during Clearwater deposition. Transportation of the dissolved sulphate would have been significantly greater in the latter stages of diagenesis however, as it would have been aided by the development of the regional groundwater flow system in the basin.

Tectonic activity in the Tertiary resulted in the development of the asymmetrical shape, and the gravity-driven flow system in of the Western Canada Sedimentary Basin (Garven, 1989). According to the regional flow model proposed by Tóth (1963), fluids recharge in the western elevated portions of the basin, descend to great depths and flow laterally in various aquifers such as the Devonian carbonates, and discharge in the east where the basin meets the edge of the Precambrian shield. Fluids carried within this regional flow system would be elevated in TDS, and such constituents as Na and Cl (Tóth, 1984). The regional flow system is thought to have impacted the sediments in the study area at or near their maximum burial conditions. Gravity-driven flow resulted in the migration of hydrocarbons from their source rocks at depth up into Mannville Group sediments on the eastern margin of the basin (Garven, 1989). Under normal burial conditions such a flow system would not have led to the emplacement of hydrocarbons in a position such as the study area because of its relatively shallow burial. It developed only because of its position on the eastern margin of the basin, updip from the Devonian carbonates.

The increased dissolution and the elevated concentration of dissolved species associated with the regional flow system led to the development of overgrowths of feldspars and quartz. High levels of available silica favoured the formation of authigenic zeolites (clinoptilolite). Higher levels of Na from deeper porewaters may have led to the precipitation of salts such as halite in the formation (although they may also form from drilling fluids). An increase in the amount of bicarbonate carried up into the study area as the result of dissolution of the underlying Devonian carbonates may also have occurred. The isotopic composition of the carbon would be inorganic in origin, similar to that of dolomite in the formation . Influx of this bicarbonate into the study area may have led to more extensive precipitation of late carbonate minerals. They appear to be present at increased levels during the latter part of stage 2 diagenesis, having formed at or near the time of oil emplacement into the formation.The inorganically derived CO_2 from the Devonian fluids would have mixed with the bacterially mediated CO_2 arising from methanogenic processes, resulting in a mixed source of carbon.

The final change in the hydrologic system of the study area presumably arrived with gradual uplift and erosion to a local to intermediate flow system. Groundwater flow in the Mannville formations at the present day is predominantly lateral, towards the south and southeast, with some component of downward flow towards the pre-Cretaceous unconformity. There is a limited effect of topography on flow, and confined conditions predominate, although there is some seepage of dissolved solids upward from the underlying Devonian units present below the sub-Cretaceous unconformity. The greatest effect on diagenesis would have been the large change in the fluid chemistry from the regional flow system to that of the more surficial systems. This would have happened progressively over time however, and a return to the more meteoric water conditions likely resulted in increased dissolution of some minerals. Fresher water conditions and the associated changes in supersaturation likely led to the precipitation of kaolinite and Fe oxides. The influx of meteoric water also resulted in the development of biodegradation (and water washing) processes leading to the breakdown of the migrated oil into its present state as bitumen. This process may have also contributed to the development of late, low ^{13}C calcites via the oxidation of hydrocarbons, as noted in adjacent study areas (Dimitrakopoulos and Muehlenbachs, 1987; Hutcheon *et al*., 1989; Longstaffe *et al*., 1992b).

F. CONCLUSIONS

An examination of the present day hydrologic characteristics of the Cold Lake area, in conjunction with an investigation of diagenesis within the Clearwater Formation (Chapter 3) has resulted in a much clearer picture of the associated hydrogeologic and diagenetic history of the Clearwater Formation within the study area.

The movement of groundwater within various flow systems and associated changes in porewater chemistry influenced the diagenetic history of the Clearwater Formation in a number of ways.

Local Groundwater Flow System:

1) The initial Clearwater Formation porewater composition is believed to have been a mix of marine and meteoric (brackish). This is supported by the oxygen isotope values measured from early formed Type 1 calcite cements, which indicate the presence of a sizeable portion of meteoric water within porewaters shortly after burial.
2) Brackish porewaters contributed sufficient dissolved sulphate to sediments below the sediment / water interface shortly after burial and the onset of reducing conditions to develop early framboidal pyrite. It appears unlikely that diffusion of sulphate from underlying Devonian evaporites would have been of sufficient quantity to sustain sulphate reduction, and the quantity of pyrite observed.
3) The presence of brackish porewaters, and low temperatures in the formation during early diagenesis favoured the formation of Fe-rich berthierine-type clays.
4) Bicarbonate-rich waters present within the local flow system may have contributed to the development of early calcite and siderite. Dissolution of detrital dolomite by these fluids likely contributed to the inorganic source of carbon found in Type 1 calcite cements.

Intermediate Groundwater Flow System:

5) Increased dissolution and / or the influx of constituents from other areas resulted in higher concentrations of dissolved chemical species within formation porewaters, and in the development of an extensive suite of authigenic clays in burial diagenesis, including illite, illite / smectite and chlorite / smectite.
6) Increases in the amount of dissolved iron with dissolution likely led to the formation of late pore-filling siderite, with CO_2 contributed via a mix of bacterial mediated and inorganic source.

Regional Groundwater Flow System:

7) The development of the regional flow system in the basin led to further dissolution of detrital components in the formation, increasing the level of dissolved constituents, and leading to the formation of additional authigenic species, specifically feldspars, quartz, zeolites and late siderites.
8) Contribution of sulphate-rich waters from the ongoing dissolution of underlying Devonian evaporites through the pre-Cretaceous unconformity likely contributed to the formation of late pyrite by providing an external source of sulphate. Interstitial sulphate was depleted earlier during burial diagenesis. Transportation of the dissolved sulphate was likely aided by the development of gravity-driven flow, with fluids readily moving into the study area from below the unconformity.
7) Influx of carbonate-rich waters from the dissolution of underlying Devonian carbonates during the presence of the regional flow system may have contributed to a more extensive development of calcite cemented zones (inorganic source of CO_2). This is in addition to the presence of bacterially mediated CO_2 (^{13}C rich) evolving from microbial fermentation. The final CO_2 composition is likely a mix of the two sources of carbon.
8) Gravity-driven cross-formational flow resulted in the migration of oil from deeper within the basin, into the Clearwater Formation in the study area near maximum burial conditions.

Re-establishment of a Local to Intermediate Regional Groundwater Flow System:

9) The return to a local to intermediate flow system following processes of uplift and erosion, and associated influx of meteoric waters led to the development of fresher water phases such as kaolinite and Fe oxides in the formation.
10) The recharge of meteoric water in the last stage of diagenesis resulted in the eventual biodegradation of the oil to its present state as bitumen by processes of water washing and bacterial fermentation (Garven, 1989), and may have contributed CO_2 to the formation of late, low ^{13}C calcites (in adjacent study areas within the formation).

Present day porewater compositions are brackish (TDS ~18 000 mg/L). Groundwater flow is minor, and mainly lateral, with some aspect of downward flow towards the south and southeast under hydrostatic, semi-confined conditions. Recharge of some meteoric water from the local surficial, topography controlled, flow system percolates into the formation, as indicated by isolated high bicarbonate values. Some diffusion of ionic species is continuing through the pre-Cretaceous unconformity, and areas of high TDS content can be correlated with regions of salt solution in the Middle Devonian evaporites. The large chemical difference between the Devonian and Mannville waters does not support present day hydraulic flow through the unconformity. Cation variations are likely the result of processes of cation-exchange in the shales and shaly rocks in the Mannville Group, along with some contribution from dissolved Upper Devonian carbonates.

G. REFERENCES

Alberta Government and University. 1969. Atlas of Alberta. University of Alberta Press in association with University of Toronto Press, 158pp.

Alberta Resources Conservation Board, 1985. Atlas of Alberta's crude bitumen reserves.

Andriashek, L.D. 1985. Quaternary stratigraphy of the Sand River Area. Unpublished M.Sc thesis, University of Alberta, 368pp.

Bachu, S. 1985. Influence of lithology and fluid flow on the temperature distribution in a sedimentary basin: A case study from the Cold Lake area, Alberta, Canada. Tectonophysics, 120, p.257-284.

Badgley, P.C. 1952. Notes on the subsurface stratigraphy and oil and gas geology of the Lower Cretaceous series in central Alberta, Canada. Geological Survey Paper 52-11, 12pp.

Bhattacharyya, D.P. 1983. Origin of berthierine in ironstones. Clays and Clay Minerals, v. 31, no. 3, p. 173-182.

Bloch, J. 1990. Stable isotope composition of authigenic carbonates from the Albian Harmon Member (Peace River Formation): evidence of early diagenetic processes. Bulletin of Canadian Petroleum Geology, v. 38, no. 1, p. 39-52.

Bredehoeft, J.A. and Hanshaw, B.B. 1968. On the maintenance of anomalous fluid pressures: 1. Thick Sedimentary sequences. Geological Society of America Bulletin, v. 79, p. 1097-1106.

Carpenter, A. B. 1978. Origin and chemical evolution of brines in sedimentary basins. Oklahoma Geological Survey Circular, 79, p. 60-77.

Carrigy, M.A. 1959. Geology of the McMurray Formation, Pt. III. General geology of the McMurray area. Alberta Research Council, Geology Division, Memoir 1, 130pp.

Carrigy, M.A. 1971. Deltaic sedimentation in Athabasca tar sands. American Association of Petroleum Geologists Bulletin, v. 55, no. 8, p. 1155-1169.

Chebotarev. I.I. 1955. Metamorphism of natural water in the crust of weathering. Geochimica et Cosmochimica Acta, v. 8, p. 22-48, 137-170, 198-212.

Curtis, C.D. 1978. Possible links between sandstone diagenesis and depth-related geochemical reactions occurring in enclosing mudstones. Journal of the Geological Society of London, v. 135, p. 107-117.

Department of Energy, Mines and Resources. 1981. Topographic Map of the Sand River Area, NTS 73L, ed. 3., Surveys and Mapping Branch, Ottawa, Ont.

Dimitrakopoulos, R. and Muehlenbachs, K. 1987. Biodegradation of petroleum as a source of ^{13}C-enriched carbon dioxide in the formation of carbonate cement. Chemical Geology, v. 65, p. 283-291.

Dutta, P.K. and Suttner, L.J. 1986. Alluvial sandstone composition and paleoclimate. II. Authigenic mineralogy. Journal of Sedimentary Petrology, v. 56, no. 3, p. 346-358.

Environment Canada. Atmospheric Environment (undated). Temperature and precipitation 1941-1970, Prairie Provinces, Downsview, Ontario, 159pp.

Freeze, R.A. and Cherry, J.S. 1979. Groundwater. Prentice–Hall Inc. Englewood Cliffs, New Jersey, 604pp.

Freeze, R.A. and Witherspoon, P.A. 1967. Theoretical analysis of regional groundwater flow: 2. Effect of water table configuration and subsurface permeability variation. Water Resources Research, v. 3, no. 2, p. 623-634.

Fritz, S. J. 1986. Ideality of clay membranes in osmotic processes: A review. Clays and Clay Minerals, v. 34, no. 2, p. 214-223.

Garven, G. 1989. A hydrogeologic model for the formation of the giant oil sands deposits of the Western Canada Sedimentary Basin. American Journal of Science, v. 289, p. 105-166.

Hackbarth, D.A., and Nastasa, N. 1979. The hydrogeology of the Athabasca oil sands area. Alberta Research Council Bulletin, no. 38, 39pp.

Harrison, D.B., Glaister, R.P. and Nelson, H.W. 1981. Reservoir description of the Clearwater oil sand, Cold Lake, Alberta, Canada. *In:* Meyer, R.F. and Steele, C.T., eds., The Future of Heavy Crude and Tar Sands, Unitar, McGraw Hill, New York, ch. 30, p. 264-279.

Henderson, P. 1982. Inorganic Geochemistry. Permagon international library of science, technology, engineering, and social studies. Permagon Press, Oxford, 353pp.

Horner, D.R. 1951. Pressure build-up in wells. Proceedings of Third World Petroleum Congress, Section II, p. 503-521.

Hitchon, B. 1969a. Fluid flow in the Western Canada Sedimentary Basin. 1. Effect of topography. Water Resources Research, v. 5, no. 1, p. 186-195.

Hitchon, B. 1969b. Fluid flow in the Western Canada Sedimentary Basin. 2. Effect of geology. Water Resources Research, v. 5, no. 2, p. 460-469.

Hitchon, B. 1984. Geothermal gradients, hydrodynamics, and hydrocarbon occurrences, Alberta, Canada. American Association of Petroleum Geologists, v. 68, p. 713-743.

Hubbert, M.K. 1940. The theory of groundwater motion. Journal of Geology, v. 48, no. 8, p. 785-944.

Hutcheon, I., Abercrombie, H., Putnam, P., Gardner, R. and Krouse, R. 1989. Diagenesis and sedimentology of the Clearwater Formation at Tucker Lake. Bulletin of Canadian Petroleum Geology, v. 37, no. 1, p. 83-97.

Jardine, D. 1973. Cretaceous oil sands of Western Canada. *In:* Hills, L.W., ed., Oil Sands; Fuel of the Future, Canadian Society of Petroleum Geology, Memoir 3, p. 50-67.

Jackson, P.C. 1984. Paleogeography of the Lower Cretaceous Mannville Group of western Canada. *In:* Masters, J.C., ed., Elmworth–Case Study of a Deep Basin Gas Field, American Association of Petroleum Geologists Memoir 38, p. 49-77.

Lindsay, J.D. and Odynsky, W. 1965. Permafrost in organic soils of northern Alberta. Canadian Journal of Soil Science, v. 45, p. 265-269.

Longstaffe, F.J. 1984. The role of meteoric water in diagenesis of shallow sandstones: Stable isotope studies of the Milk River aquifer and gas pool, southeastern Alberta. *In:* McDonald, D.S., and Surdam, R.C., eds., Clastic Diagenesis, AAPG Memoir 37, p. 81-98.

Longstaffe, F.J., Racki, M.A. and Ayalon, A. 1991a. Diagenesis of Clearwater Formation Reservoirs in the Cold Lake Area, Alberta. AOSTRA-University Agreement #680, Final Report, AOSTRA, 223pp.

Longstaffe, F.J., McKay, J., Shier, W. and Colquhoun, I.M. 1992a. Regional mineralogical controls on reservoir performance in bitumen-saturated sands, northeastern Alberta. AOSTRA-Univeristy Agreement #868, Report #3 of 6 (January 1992), 86pp.

Longstaffe, F.J., Ayalon, A., and Racki, M.A. 1992b. Stable isotope studies of diagenesis in berthierine-bearing oil sands, Clearwater Formation, Alberta. *In:* Kharaka and Maest, eds., Proceedings of the Seventh International Symposium on Water-Rock Interaction. Balkema, Rotterdam, p. 955-958.

Mellon, G.B. 1967. Stratigraphy and petrology of the Lower Cretaceous Blairmore and Mannville groups, Alberta foothills and plains. Research Council of Alberta, Bulletin 21, 270pp.

Mossop, G.D., Kramers, J.W., Flach, P.D., and Rottenfusser, B.A. 1981. Geology of Alberta's oil sands and heavy oil deposits. *In:* Meyer, R.F. and Steele, C.T., eds., The Future of Heavy Crude Oils and Tar Sands, Unitar, McGraw Hill, New York, p. 197-207.

Odin, G.S. and Matter, A. 1981. De glauconiarum originae. Sedimentology, v. 28, p. 611-641.

Ozoray, G., Wallick, E.I. and Lytviak, A.T. 1980. Hydrogeology of the Sand River area, Alberta. Alberta Research Council Earth Sciences Report 79-1, 11pp.

Prentice, M.E. and Wightman, D.M. 1987. Mineralogy of the Clearwater Formation, Cold Lake oil sands area: Implications for enhanced oil recovery. Alberta Geological Survey Report, 41pp.

Putnam, P.E. and Pedskalny, M.A. 1983. Provenance of Clearwater sandstone, Cold Lake, Alberta, with comments on feldspar composition. Bulletin of Canadian Petroleum Geology, v. 31. p. 148-160.

Putnam, P.E. 1982. Aspects of the petroleum geology of the Lloydminster heavy oil fields, Alberta and Saskatchewan. Bulletin of Canadian Petroleum Geology, v. 30, no.2, p. 81-111.

Raiswell, R. 1982. Pyrite texture, isotopic composition and the availability of iron. American Journal of Science, v. 282, p. 1244-1263.

Roberts, W.H.III, 1980. Design and function of oil and gas traps. *In:* Roberts, W.H.III and Cordell, R.J., eds., Problems in Petroleum Migration. American Association of Petroleum Geologists, Studies in Geology 10, p. 217-240.

Schwartz, F.W. 1974. The origin of chemical variations in groundwaters from a small watershed in southwestern Ontario. Canadian Journal of Earth Sciences, v. 11, no. 7, p. 893-904.

Stelck, C.R. and Leckie, D. 1988. Foraminiferal inventory and lithologic description of the Lower Cretaceous (Albian) Hulcross Shale, Monkman area, northeastern British Columbia. Canadian Journal of Earth Science, v. 25, p. 793-798.

Tóth, J. 1963. A theoretical analysis of groundwater flow in small drainage basins. *In:* Benchmark Papers in Geology, v. 72: Physical Hydrogeology, Freeze, R.A. and Back, W., eds., Hutchinson Ross Pub. Co., 431pp.

Tóth, J. 1978. Gravity-induced cross-formational flow of formation fluids, Red Earth region, Alberta, Canada: Analysis, patterns, evolution. Water Resources Research, v. 14, no.5, p. 805-843.

Tóth, J. 1980. Cross-formational gravity flow of groundwater. A mechanism of the transport and accumulation of petroleum (The Generalized Hydraulic Theory of

Petroleum Migration). *In:* Roberts, W.H., III. and Cordell. R.J., eds., Problems of Petroleum Migration. American Association of Petroleum Geologists, Studies in Geology, no. 10, p. 121-167.

Tóth, J. 1984. The role of regional gravity flow in the chemical and thermal evolution of groundwater. Proceedings First Canadian / American Conference on Hydrogeology. Practical Applications of Groundwater Chemistry, Banff, Alberta, Canada, June 22-26. Hitchon, B. and Wallick, E.E., eds., National Water Well Association, Dublin, Ohio, 323pp.

Tóth, J. 1986. Models of subsurface hydrology of sedimentary basins. Proceedings Third Canadian / American Conference on Hydrology, Banff, Alberta, Canada, June 22-26. National Water Well Association, Dublin, Ohio.

Tóth, J. and Corbett. T. 1986. Post-Paleocene evolution of regional groundwater flow-systems and their relation to petroleum accumulations, Taber area, southern Alberta, Canada. Bulletin of Canadian Petroleum Geology, v. 34, no. 3, p. 339-363.

Western Atlas International. 1988. Stratigraphic correlation chart of the Western Canada Sedimentary Basin.Western Atlas Canada Ltd., Calgary, Alberta.

van Everdingen, R.O. 1968a. Studies of formation waters in western Canada: Geochemistry and hydrodynamics. Canadian Journal of Earth Sciences, v. 5, p. 523-543.

van Everdingen, R.O. 1968b. Mobility of main ion species in reverse osmosis and the modification of subsurface brines. Canadian Journal of Earth Sciences, v. 5, p. 1253-1260.

Wightman, D.M. and Berezniuk, T. 1986. Resource characterization and depositional modelling of the Clearwater Formation, Cold Lake oil sands deposit, east-central Alberta. *In:* Westhoff, J.D. and Marchart, L.C., eds., Proceedings of the 1986 Tar Sands Symposium, Jackson, Wyoming, July 7-10, p. 20-45.

Wightman, D.M., Pemberton, S.G. and Singh, C. 1987. Depositional modelling of the Upper Mannville (Lower Cretaceous), east-central Alberta: Implications for the recognition of brackish water deposits. Reservoir Sedimentology: Society of Economic Paleontologist and Mineralogists Special Publication No. 40, p. 189-220.

Wightman, D.M., MacGillivray, J.R., McPhee, D., Berhane, H. and Berezniuk, T. 1991. McMurray Formation and Wabiskaw Member (Clearwater Formation): Regional perspectives derived from the North Primrose area, Alberta, Canada, Fifth Unitar / UNDP International Conference on Heavy Crude & Tar Sands, p. 1-36.

Williams, G.D. and Stelck. 1973. Speculations on the Cretaceous paleography of North America. Geological Association of Canada Special Paper Number 13, p. 1-54.

Yoon, T.N., Goble, K.A. and Carlson, V.A. 1977. Groundwater resources in the Cold Lake oil sands area. *In:* Redford, D.A. and Winestock, A.G., eds., The Oil Sands of Canada-Venezuela, Canadian Institute of Mining Special Volume 17, p. 133-138.

Zaporozec, A. 1972. Graphical interpretation of water quality data. Groundwater, v. 10, p. 32-43.

CHAPTER 5:

GENERAL DISCUSSION AND CONCLUSIONS

A. INTRODUCTION

One of the main objectives of this thesis was to determine if there is a relationship between depositional and diagenetic characteristics of the Clearwater Formation in the Cold Lake oil sands deposit. Specifically, it was to ascertain if sequence boundaries could be characterized and thereby identified in another position by certain specific features and trends related to their depositional or diagenetic mineralogy or geochemistry. This investigation was approached on the premise that if unusual or important trends or features are to be recognized, it is first necessary to understand the basic processes well. Singular objectives were therefore:

1) to develop a model of the depositional history of the Clearwater Formation, based on sedimentologic and sequence stratigraphic features observed and inferred in the study area;
2) to utilize stratigraphic, geochemical and mineralogical data in the characterization of an unconformity / sequence boundary identified within the study area; and
3) to develop a basic understanding of diagenesis within the Clearwater Formation in the study area, including mineralogical variations, paragenetic trends, and their controls within the formation.

Secondary objectives were to develop a good understanding of factors which influenced the deposition of Clearwater sediments and led to their sedimentologic, ichnologic and mineralogic characteristics, and to determine local fluid flow and groundwater chemistry for the study area and its influence on diagenesis.

Diagenesis in the Clearwater Formation was influenced by the composition of its detrital mineralogy, shallow burial diagenetic processes and groundwater influx. The detrital mineralogy is a function of basin-wide processes, including the supply of detritus, its transport and eventual environment of deposition. Diagenesis was significantly influenced by depositional environment, as well as the only shallow burial of the formation (Hitchon, 1984). Fluid–rock interactions resulting from migrating groundwater, both basinal brines and meteoric water, also affected the final mineralogic assemblage. The relationships among these factors, and their influence on the overall pattern of Clearwater Formation diagenesis as it was inferred from the study area, are summarized in the following sections.

B. A MODEL OF DEPOSITION AND SEQUENCE STRATIGRAPHY IN THE CLEARWATER FORMATION

DEPOSITIONAL CONTROLS

Deposition of the Clearwater Formation within the Mannville Group on the eastern margin of the Western Canada Sedimentary Basin was the result of a number of events prior to and during the Early Cretaceous. Initially, development of the foreland basin began in the mid-Jurassic, the result of major tectonism in the west during the Columbian orogeny. This, combined with the downwarping of eroded sediments accumulating in a large wedge on the frontal ranges of the Rockies (now the Deep Basin), led to the basin's present asymmetrical configuration (Spencer, 1974; Garven, 1989). Erosion continued throughout the Cretaceous, with the greatest episode of uplift in the late Aptian / early Albian, providing the detritus deposited on the eastern basin margin as Clearwater sediments.

On the eastern margin of the basin, deposition was greatly influenced by the inundation of the northern Boreal sea from the north, resulting in the development of marine and transitional-marine conditions in east-central Alberta. Structural features prevalent at the time controlled the paleogeography of Mannville Group sediments. Of particular importance are:

1) the overall asymmetrical configuration of the Western Canada Sedimentary Basin with its foredeep trough and hingeline on the eastern flank;
2) an axial high (the Athabasca anticline), located on the eastern margin of the basin; and
3) development of an eastern regional low.

The relief of the Mannville Group depositional surface in east-central Alberta, and the eastern regional low was the function of:

1) variable deposition and erosion of Upper Devonian carbonates;
2) salt dissolution of underlying Middle Devonian evaporites; and
3) structural deformation associated with the Athabasca anticline (Jackson, 1984).

The axial high separated the southwestern and northeastern portions of the basin during the Early Cretaceous, and fluvial systems carrying eroded detritus from the west flowed from the axial high into structural lows in east-central Alberta. These systems are believed to have controlled drainage patterns during deposition of the McMurray Formation. Some McMurray sediments are also believed to have been contributed from the eastern Canadian Shield (Harrison *et al.*,1981).

Deposition of the Clearwater Formation in east-central Alberta was influenced primarily by the relief of its depositional surface, and periodic fluctuations in relative sea-level. Relief of the depositional surface greatly affected the morphology of Clearwater sediments, and was the result of:

1) the low (ramp-like) and variable slope of the eastern margin of the developing Western Canada Sedimentary Basin;
2) erosion and channel downcutting into McMurray Formation sediments overlying the pre-Cretaceous unconformity;
3) the structure of the pre-Cretaceous unconformity, resulting from depositional differences and erosion in the Devonian; and
4) pre-, syn-, and post-Devonian dissolution of underlying Paleozoic evaporites.

Fluctuation in relative sea-level resulted from several interrelated factors, but chiefly the effect of periodic dynamic tectonism and high sediment fluxes originating from the western Cordillera, and fluctuation in eustatic sea-level (Haq *et al.*, 1987). The effect of basin subsidence on the eastern margin of the Western Canada Sedimentary Basin is thought to have been low, and not of sufficient magnitude to affect accommodation.

CLEARWATER DEPOSITIONAL ENVIRONMENTS

Clearwater Formation sediments were deposited near the edge of the Boreal sea during its inundation into western Canada during the Cretaceous. They were deposited in a relatively thick deltaic complex and overall shallow marine environment. Sediment from the west was carried by eastward flowing streams from the axial high into east-central Alberta, and deposited sediment in a number of depositional environments, including:

1) upper delta front (distributary mouth-bar and channel sands);
2) middle delta front;
3) lower delta front;

4) delta fringe;
5) open marine / prodelta; and
6) shoreface (marine bar sands).

At the beginning of Clearwater deposition the coarsest sediment was dumped into various topographic lows during deltaic lobe development in the west and southwest. Finer sediments were carried further offshore into the more distal settings in the study area. This led to the presence of open marine–prodelta muds at the base of the formation.

A relative sea-level fall, and a basinward shift of the depositional centre of the deltaic complex led to a regressive depositional phase, shoreface conditions, and the deposition of coarser grained Wabiskaw Member sediments in the study area. The Wabiskaw Member has been interpreted as a marine bar sequence, and although its relative environments were not differentiated in detail, evidence of clean sands from a more central bar, and muddier sands from distal bar facies have been observed. Detailed characteristics of the Wabiskaw Member observed in the study area have been summarized in Table 5.1.

A relative rise in sea-level or short transgression of the shoreline, followed by a progradational period led to the deposition of sediments in the lower section of the remaining Clearwater Formation interval. Depositional patterns in the study area are quite random, and indicate the return of deltaic conditions, with a southwestern located shoreline. Sediments were deposited primarily in distal deltaic environments, ranging from interbedded sands and muds to thicker sands with some interbedded silts or muds in lower to middle delta front environments (Table 5.1). A short transgressive phase resulted in deposition of finer delta fringe and lower delta front sediments near the end of this sequence.

A thick sequence of sediments was deposited in lower to upper delta front environments following a second progradational phase initiated by a relative drop in sea-level and a basinward shift in the shoreline. This resulted in the formation of stacked fine to medium grained sands in the southwestern part of the study area, which have been interpreted as distributary channel and mouth-bar sands. The more distal facies are found towards the northeast, a direction believed to be close to the strike of sediment progradation and distribution during deposition of the sequence. The paleo-shoreline is believed to have been present to the east, in an approximate north / south to northwest / southeast orientation, similar to that of the orientation of the axial high at that time

Table 5.1 **Characteristics of Clearwater Formation Depositional Environments observed in the Study Area.**

			SEDIMENTARY FEATURES					SEQUENCE STRATIGRAPHY	
DEPOSITIONAL ENVIRONMENT	RELATIVE POSITION IN STUDY AREA	FACIES	Bedding & Other Physical Structures*	Organic Remains	Bioturbation	BITUMEN SATURATION	DIAGENETIC FEATURES	Sequence(s)	Cycle(s)
OPEN MARINE / PRODELTA	NE	marine silts and shales	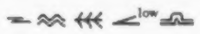	fine organic-rich detritus	low–high (churned)	water saturated to low	iron staining siderite	S_1	GR-marine muds
DELTA FRINGE	central–NE	marine muds and sands	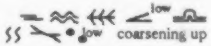	abundant coal & shell fragments	low / mod–high (churned)	water saturated to low	carbonate cements iron staining, pyrite	S_1;S_2	GR-marine muds; A,C
LOWER DELTA FRONT	SW–NE	vfg.–fg. sands and muds	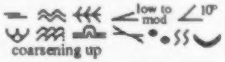	coal & shell fragments	(variable) low–mod	(variable) low to mod / high	carb. cem., clays siderite, iron staining, glauconite	S_1;S_2	A–D; A–C
MIDDLE DELTA FRONT	SW–NE	f.g. sands (and muds)	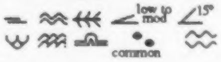	coal & wood fragments		(variable) water saturated to high	carbonate cements clays, siderite	S_1;S_2	B–D; B,C
UPPER DELTA FRONT	SW–central		coarsening up						
Distributary Channel	SW	f.g.–m.g. sands	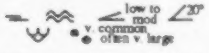	coal & shell fragments	none	high	carbonate cements siderite	S_1	C2
Distributary Mouth-Bar	SW–central	f.g.–m.g. sands, occ., muds	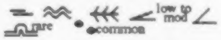	coal fragments	none–low	mod–high	carb. cem., siderite iron staining	S_1	B–D
Interdistributary Bay	SW–central	f.g. sands and muds	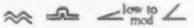	coal fragments	low–mod	low–mod	siderite	S_1	A, D2
WABISKAW - SHOREFACE	SW–NE	fg–mg marine sands & muds	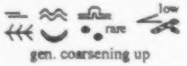	coal fragments	(variable) low–high (churned)	water saturated to moderate	glauconite carb. cem., siderite iron staining	S_2	Wab.Mbr.

* refer to Appendix 1 for legend.

(Maher, 1989). Characteristics of Clearwater facies identified in this sequence are also summarized in Table 5.1.

Ichnogenera observed in the study area indicate that the Clearwater Formation was deposited in a number of shallow marine environments, some of quite high organic matter content. A total of 13 different ichnogenera were identified in Clearwater sediments, most of which are deposit-feeders. Two ichnogenera in particular, *Skolithos* and *Chondrites*, exhibited opportunistic behavior and were present in nearly all facies. A summary of ichnological characteristics of the various depositional environments found in the study area is contained in Table 5.2. In general, biogenic abundance was fairly low, although could extend to moderate or high in particularly organic-rich facies. Biogenic diversity was also relatively low, which may suggest that there was an influence of brackish water conditions, especially in more shoreline proximal environments, resulting from the mixing of fresh and saline waters during sediment deposition. The predominant ichnofacies observed was that of Cruziana, but a mixed Cruziana / Zoophycos assemblage was interpreted for more open marine / prodelta settings, and a mixed Cruziana / Skolithos assemblage was found in more nearshore facies.

SEQUENCE STRATIGRAPHY

The Clearwater Formation has been subdivided into two sequences and various bounding surfaces, based on observations from the study area of this thesis. Sequence S_1 extends from the top of the formation at its contact with the Lower Grand Rapids marine shales to the base of the units lying above the last relative sea-level fall. The surface at this position is sequence boundary SB1. The top of the sequence is not bounded within the Clearwater Formation by a sequence boundary, but by a flooding surface, FS1, at the Clearwater / Grand Rapids contact. Internally the sequence has been subdivided into a number of genetic units or cycles, A to D. In the thick (stacked) distributary mouth-bar and channel sands in the southwestern part of the study area some of these cycles have been subdivided into sub-cycles.

Sequence S_2 extends from sequence boundary SB1 to the top of the open marine / prodelta muds at the base of the formation, the position of another relative sea-level fall, and sequence boundary SB2. S_2 contains a number of internal flooding surfaces. The first, FS2, occurs just below SB1, and fades laterally into SB1 in a shoreline or onlap direction. The second, FS3, marks the base of the transgressive interval at the top of the

Table 5.2: **Ichnological Characteristics of Clearwater Formation Depositional Environments in the Study Area**

DEPOSITIONAL ENVIRONMENT	FACIES	BIOGENIC ABUNDANCE	BIOGENIC DIVERSITY	ICHNOGENERA*	ICHNOFACIES ASSEMBLAGE
OPEN MARINE / PRODELTA	marine silts and shales	low–high	v. low	Ch,P	Mixed Cruziana / Zoophycos
DELTA FRINGE	marine muds and sands	low / mod –high	low–mod	Ch,P,Pa Z,A,Sk	Cruziana Ichnofacies
LOWER DELTA FRONT	vfg.–fg. sands and muds	(variable) low–mod	(variable) low-mod	Ch,Pa,P,B,A,R Cy,T,Th,D,Sk	Cruziana Ichnofacies – Mixed Cruziana / Skolithos
MIDDLE DELTA FRONT	f.g. sands (and muds)	none–low	low	Pa,Ch,P,A T,Sk,R,B	Cruziana Ichnofacies – Mixed Cruziana / Skolithos
UPPER DELTA FRONT					
Distributary Channel	f.g.–m.g. sands	none	none	none	none
Distributary Mouth-Bar	f.g.–m.g. sands, occ., muds	none–low	low	Ch,P,T,A	Mixed Cruziana / Skolithos Ichnofacies
Interdistributary Bay	f.g. sands and muds	low–mod	low–mod	P, Ch, A T, Pa, Sk	Cruziana Ichnofacies
WABISKAW - SHOREFACE	fg–mg marine sands & muds	(variable) low–high	low–mod	P,Ch,A,Pa,Z B,T,Sk,Rh,R,D	Mixed Cruziana / Skolithos Ichnofacies

* refer to Appendix 1 for legend.

Wabiskaw Member. Sequence S_2 has also been subdivided into a number of genetic units, cycles A to C as well as that of the Wabiskaw Member.

A model of Clearwater deposition relative to sequence stratigraphy, depositional environment and formation boundaries has been created for the study area (Figure 5.1). The model illustrates the relationship between the various divisions of the formation, and an interpretation of its genetic development and structure during deposition. As indicated, the slope of the *shelf* during Clearwater Formation was relatively shallow, with deposition into a continental basin. The lowermost units, the marine shale and Wabiskaw Member, are fairly continuous and were the most affected by the nonuniformity of the Clearwater depositional surface. A lateral and shoreward shift in depositional facies resulted in FS3, followed by the downlap of additional units from S_2. (This is not indicated because of the small size of the study area, but is prevalent in core and well logs). The shoreward shift in deposition of relative facies was repeated at FS2, in a periodic rise of relative sea-level. It has been indicated that FS2 grades out into SB1, although it is also probable that it continues within the more proximal facies in the southwestern part of the study area. Further evidence of it could not be distinguished in core or well logs. The units of sequence S_1 downlap during progradation and result in thicker units in the southwestern part of the study area and thinner units in the northeast, topped by FS1.

Sequence boundaries SB1 and SB2 are the surfaces which formally separate one sequence from another. They were characterized by a number of features in cores and well logs in the study area, which have been summarized as follows:

1) evidence of a relative sea-level fall, manifested by a shallowing of facies, (more pronounced in distal positions);
2) evidence of erosion, as indicated by features such as downcutting and mud clasts, (more evident in nearshore environments);
3) changes in the depositional environment, specifically in organic content, bioturbation, biogenic diversity and the ichnofossil assemblage;
4) changes in diagenetic features, such as the abundance of iron-bearing species, perhaps indicating a relationship between formation of the sequence boundary and early diagenesis; and
5) changes in bitumen saturation, useful as an aid in determining changes in grain-size and internal mineralization.

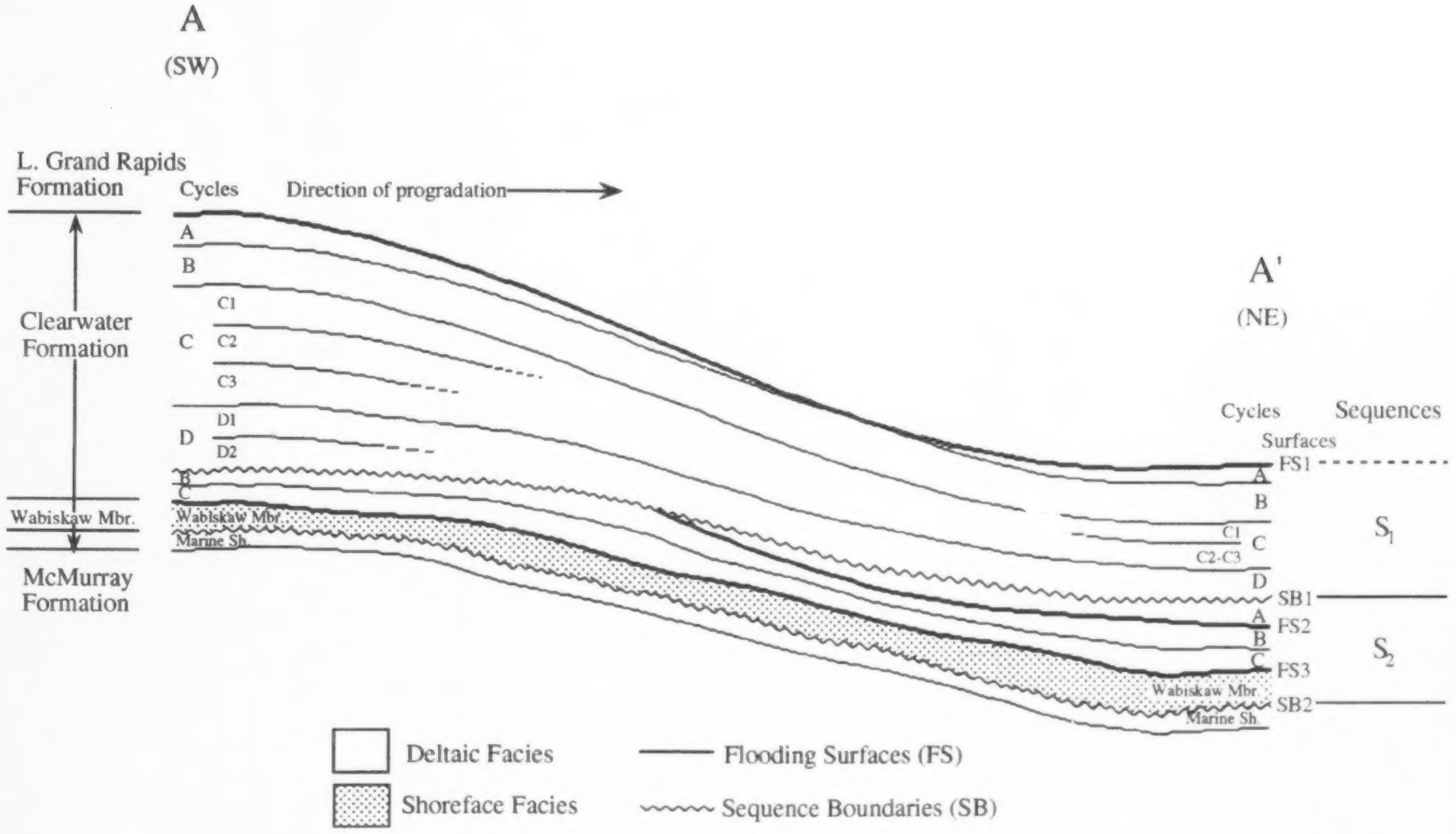
A
(SW)
L. Grand Rapids Formation
Clearwater Formation
Wabiskaw Mbr.
McMurray Formation
Cycles
Direction of progradation
A
B
C
C1
C2
C3
D
D1
D2
B
C
Wabiskaw Mbr.
Marine Sh.
A'
(NE)
Cycles
Surfaces
Sequences
FS1
A
B
C1
C
C2-C3
D
SB1
A
FS2
B
C
FS3
Wabiskaw Mbr.
SB2
Marine Sh.
S_1
S_2
Deltaic Facies
Shoreface Facies
Flooding Surfaces (FS)
Sequence Boundaries (SB)

Figure 5.1: Sequence Stratigraphic Model of Clearwater Formation deposition in the study area.

The sequence stratigraphic features observed in the study area are believed to extend some distance into the Clearwater Formation, but as only limited wells outside of the smaller study area were examined, it is not possible to ascertain if the interpretation put forward here may be correlated throughout the northern part of the Cold Lake oil sands deposit.

C. MINERALOGICAL AND GEOCHEMICAL CHARACTERIZATION OF SEQUENCE BOUNDARY SB1

Variations in mineralogical and geochemical composition over a sequence boundary such as SB1, are essentially the result of differences in detrital and diagenetic mineralogy in the sediment. Variations in geochemical composition are merely an elemental expression of the crystalline and noncrystalline components. For characteristic mineralogical features to occur at a sequence boundary, different mineralogical assemblages must develop either during deposition of the sediment or subsequently, during diagenesis. Therefore, the use of mineralogical and geochemical data, together with knowledge of the sedimentological and diagenetic characteristics of the deposit makes it possible to interpret the trends characteristic of the surface.

In general terms, differences in detrital mineralogy are the result of: 1) a change in the source area of the detritus; or 2) a change in the depositional setting. Variability in the diagenetic mineralogy of the sediment is a function of: 1) differences in original detrital mineralogy; and 2) differences in its diagenetic history. The composition of the detrital mineral assemblage accordingly has a direct influence on the resulting diagenetic composition. If the sediments above and below a sequence boundary are of the same detrital mineralogy, and subjected to the same depositional history, there would not be many features deemed characteristic. In contrast, if sediments are different in original detrital composition, despite being subjected to the same depositional history, many characteristic features will develop. This occurs because dissolution of the detrital minerals, amorphous compounds and any interspersed organic matter supplies the largest proportion of the basic components for diagenetic change (Pettijohn *et al.*, 1987). For most surfaces, the situation is somewhere in between these two end members. The challenge is to resolve which characteristics have resulted from the detrital mineralogy of a sediment and its diagenetic history, and which are associated with the development of the sequence boundary. It is clear that the only features related to the sequence boundary will be those which ensue because of processes which occur during the time of its development. By inference, the only geochemical features are therefore early diagenetic. Because of the dependence of at least *some* of the components which contribute to the diagenetic process on detrital mineralogy, all features which characterize a sequence boundary will be in some way related to the environment of deposition.

Mineralogical and geochemical trends which characterize the transition from the underlying facies of sequence S_2 into the overlying facies of S_1 are:

1) the presence of trace to minor levels of pyrite in all depositional settings, but diminishing in abundance in the overlying facies of S_1;
2) a strong decrease in sulphur (S) content;
3) a marked decrease in L.O.I.;
4) a moderate decrease in zirconium (Zr) content;
5) a slight decrease in quartz abundance;
6) a slight increase in SiO_2 content;
7) a minor increase in barium (Ba) content;
8) a slight decrease in the abundance of Fe_2O_3, MgO and TiO_2;
9) a substantial decrease in the abundance of smectitic mixed-layer clays;
10) a slight decrease in chromium (Cr) and yttrium (Y); and
11) a substantial increase in the proportion of 7Å clays within the clay assemblage of sequence S_1.

DISCUSSION

The same detrital mineral assemblage was found in all the sediments within the study area, which indicates that there was not a change in the source area(s) during deposition. Differences in detrital mineralogy are therefore a function of their position within the depositional environment in which they were deposited. In the study area, sediment segregation into coarser and finer units was primarily the function of its distance from the point at which fluvial waters released their sediment load into the delta. The above trends for Zr, quartz, SiO_2 and Ba have been interpreted to have resulted predominantly from differences in detrital mineralogy. The trends for Fe_2O_3, MgO, TiO_2, smectitic clays, Cr and Y are also thought to result mainly from differences in detrital mineralogy, although there may also be a diagenetic influence. All of these trends reflect higher levels of detrital clays in the facies underlying the sequence boundary. The majority of these clays, especially in the more distal wells, are smectitic. This is indicated by the comparable trend patterns between the major oxides (Fe_2O_3, MgO, and TiO_2) and the trend for the smectitic minerals (Figures 5.2 and 5.3).

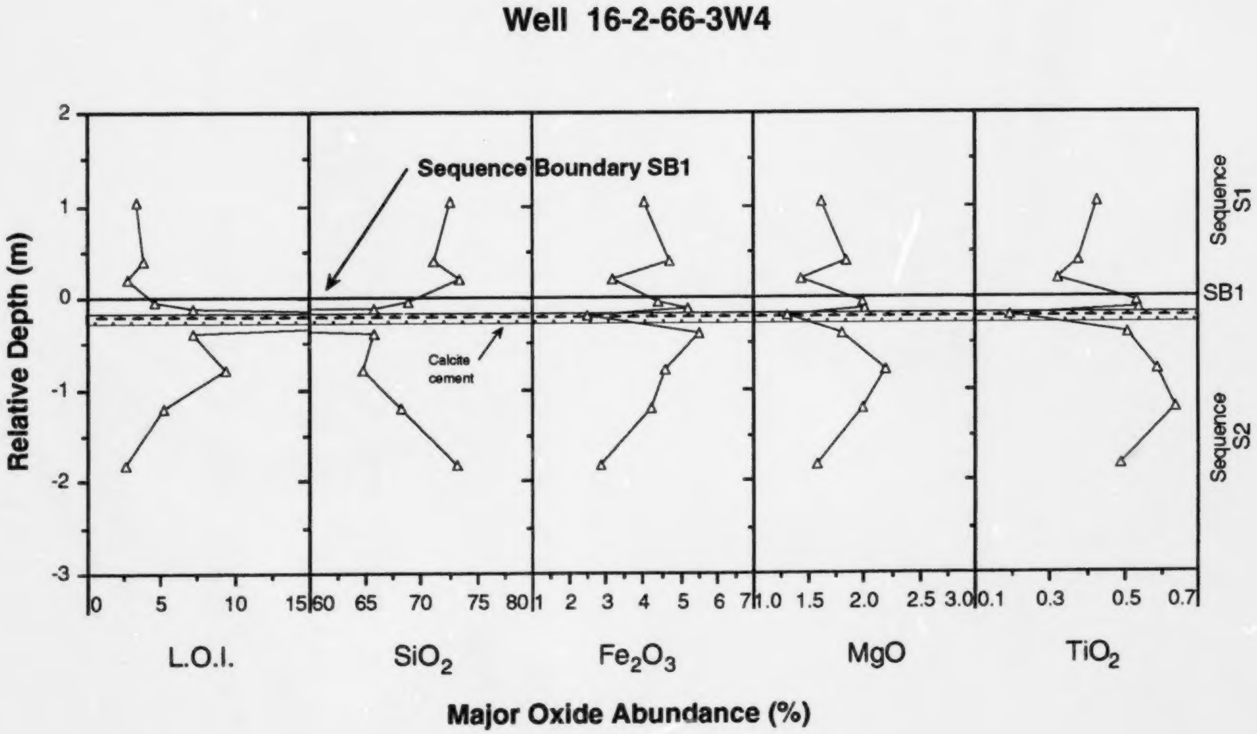

Figure 5.2: Distribution of the abundance (%) of various major oxides over sequence boundary SB1 in Well 16-2-66-3W4.

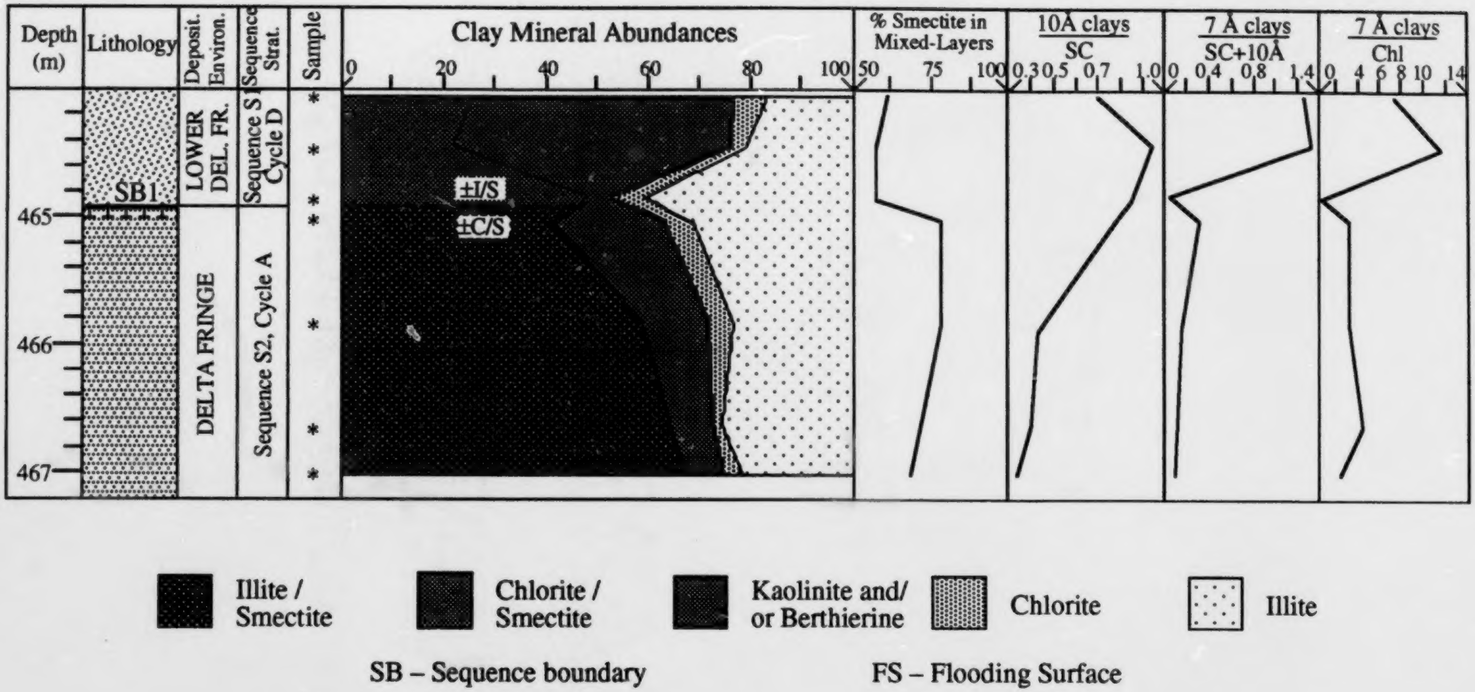

Figure 5.3: Detailed clay mineral succession over sequence boundary SB1, including details regarding sampling, lithology and depositional environment; Clearwater Formation, well 16-2-66-3W4 (legend for lithology as in Appendix 1).

The development of smectitic clays is highly dependent on contribution of ionic species from the dissolution of associated detrital minerals, and is characteristic of burial diagenesis. Therefore, the presence of smectitic clays is only indirectly related to the presence of the sequence boundary, dependent on detrital mineralogy.

The trends exhibited by pyrite, sulphur (S), L.O.I. and 7Å clay are thought to be diagenetic in origin. The 7Å clays are primarily berthierine, which occurs as a grain-coating clay in the coarsest sands, associated with the presence of bitumen. Many of these sands occur in the facies which overlies the sequence boundary, especially in the southwestern part of the study area. Reduced levels of 7Å clays have been recognized in the facies which underlies SB1. The reduced L.O.I. value for the facies overlying the sequence boundary is thought to be primarily a reflection of the reduction in organic content in the sediment. This value may also represent the loss of some S during heating. The high levels of sulphur in the underlying facies are believed to represent the S contained within pyrite. The evidence for this is the comparable trends between S and pyrite composition exhibited (Figures 5.4 and 5.5). Early formed pyrite found below the sequence boundary had a framboidal morphology.

Berthierine clays are characteristic of the coarser sands present above sequence boundary SB1 in the study area, but its dependence on unstable detrital components and presence at lower levels within the underlying facies (S_2) suggests that its development is unrelated to the development of the sequence boundary. However, the controls on its development within the study area have not been determined, only speculated, and if its development was shown to be related to depositional porewater conditions or another such factors this interpretation could change.

Framboidal pyrite is a mineral which typically forms in sediments as a by-product of bacterial sulphate reduction. This process mainly requires a source of organic matter, reducing conditions, and the presence of sufficient levels of sulphate to develop (Curtis, 1978). The Fe is generally supplied by the dissolution of detrital grains or amorphous Fe-rich compounds in most comparable settings (Pettijohn *et al.*, 1987). Pyrite is concentrated primarily below sequence boundary SB1, and is very abundant, especially in finer organic-rich sediments (Figure 5.5). However, it is present to some degree within all environments within the study area, even within organic-poor fine grained sands in some of the most bitumen saturated sediments. This prominent abundance is believed to be related to an extended time of formation during which pyrite could develop, resulting from the period of non-deposition associated with the

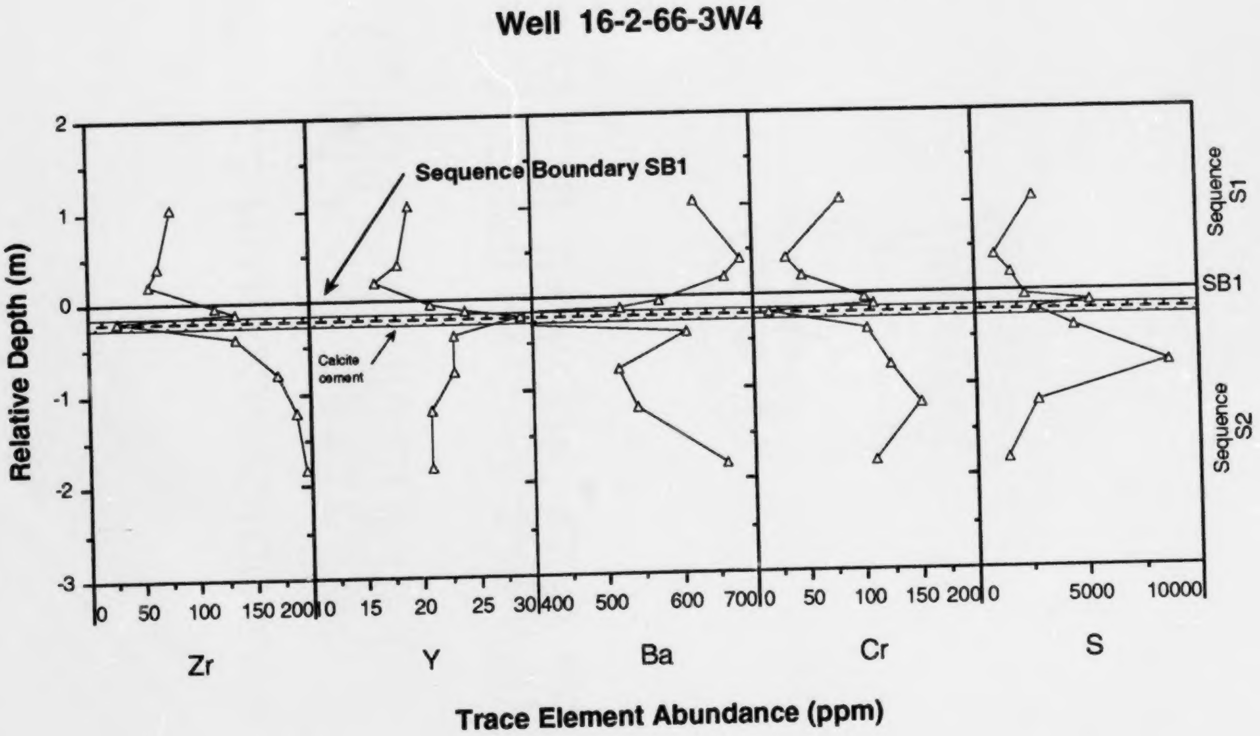

Figure 5.4: Distribution of the abundance (ppm) of various trace elements over sequence boundary SB1 in Well 16-2-66-3W4.

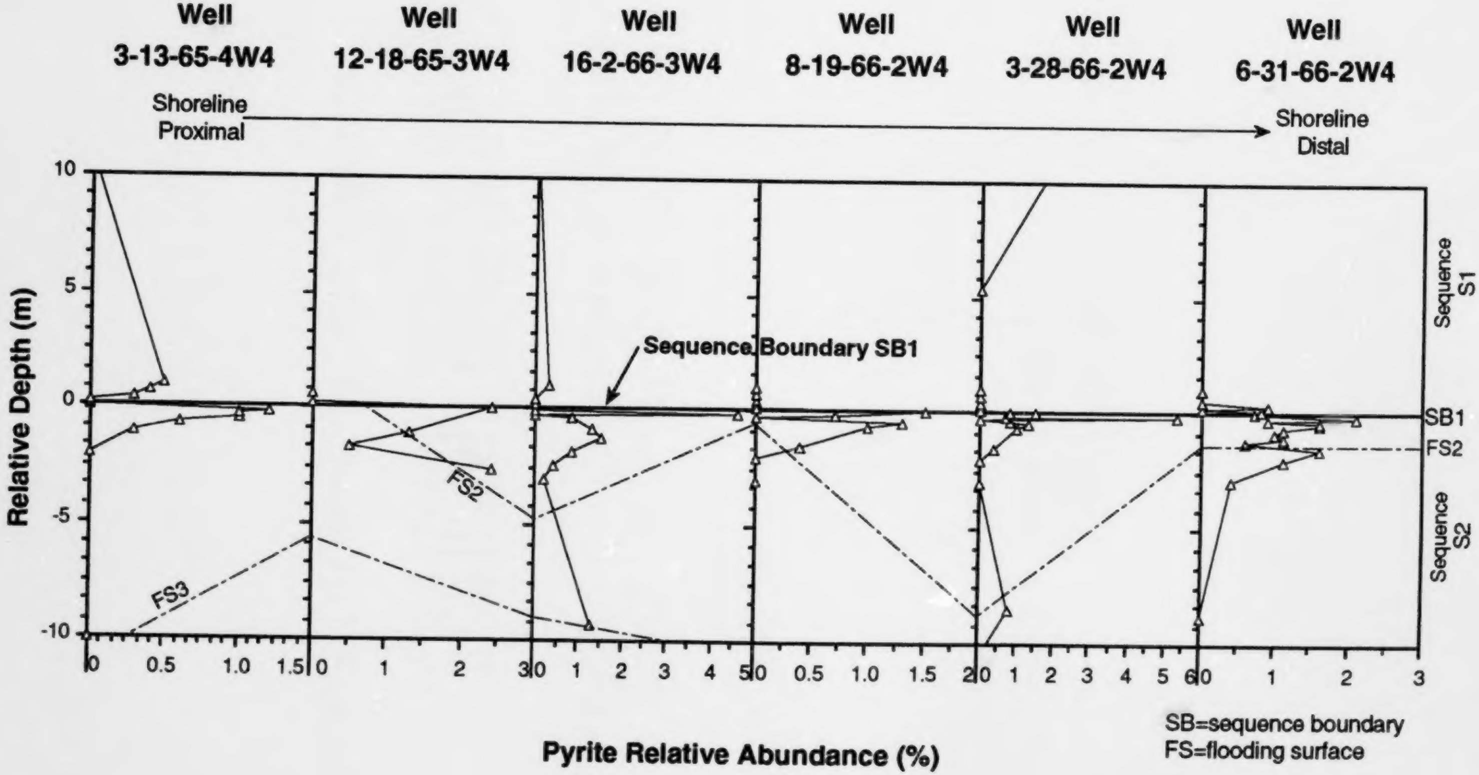

Figure 5.5: Distribution of pyrite relative abundance (%) over sequence boundary SB1 in wells located from proximal to distal positions relative to the paleo-shoreline during Clearwater deposition. Refer to Figure 3.3 for relative positions of wells in study area.

development of the sequence boundary. This implies that the diagenetic history of the facies over and under the sequence boundary SB1 were different.

A number of geochemical and mineralogical trends have been identified which appear to be associated with the development of sequence boundary SB1. However most of these trends are a function of, or highly dependent on, the original detrital mineralogy of the sediment. Therefore, they characterize the sequence boundary in this setting, but may not characterize other sequence boundaries developed during dissimilar geologic conditions with a different mineral assemblage. The presence of abundant pyrite below the sequence boundary may be an exception to this generalization however. The components required for its genesis are not restricted to this depositional setting. Therefore, pyrite has the best potential for use as a diagenetic sequence boundary marker based on the trends interpreted from the study area. There is the possibility that it has a limited application except within comparable geologic settings, but this hypothesis—that sequence boundaries are characterized by mineralogic and geochemical (diagenetic) variations that can be applied in other study areas, has yet to be tested.

D. MINERALOGY, DIAGENESIS AND HYDROGEOLOGY OF THE CLEARWATER FORMATION

CLEARWATER MINERALOGY AND PARAGENESIS

Clearwater sediments within the study area are compositionally immature, and composed predominantly of sandstones containing detritus derived from the west / southwest, which can be classified according to Folk's (1974) scheme as litharenites to feldspathic litharenites. Clay, calcite or viscous bitumen are the only matrix or cementing materials within the sands in the study area.

Clearwater lithologies identified in the study area are: fine to medium grained 'clean' sands; fine to very fine grained sands with interstratified silt or shale; sandy silts or shales; interstratified silt and shale; and carbonate cemented sands, silts or shales.

The following paragenetic sequence has been established:

1) olive to bright-yellowish-green round to oval glauconite pellets;
2) pore-filling spherical framboids of pyrite;
3) grain-coating intertwined, wormy-looking laths of berthierine in sands;
4) pore-filling fibrous, Type 1, Fe-poor, pore-filling, pervasive calcite;
5) pore-filling concretionary siderite in mud clasts within sands;

6) grain-coating fuzzy laths of diagenetic illite in silty units;
7) grain-coating and pore-filling, webby, crenulated crystals of illite / smectite (I/S) in silty units;
8) pore-filling? crystals of chlorite / smectite in sands;
9) pore-filling, rhomb-shaped replacements crystals of siderite in sandy facies;
10) pore-filling, epitaxial overgrowths of potassic feldspar (and minor overgrowths of plagioclase feldspar);
11) pore-filling prismatic overgrowths of quartz in silty units;
12) pore-filling blocky, tabular, rectangular, coffin and lath-shaped crystals of zeolite (clinoptilotite) in silty units;
13) pore-filling, crystalline mosaic of Type 2 calcite cement;
14) vein-filling, euhedral to anhedral crystals of Type 3 calcite (at least 2 generations);
15) pore-filling tabular book-like crystals of kaolinite (trace levels); and
16) late coating of amorphous Fe oxides on clays.

Fine to medium grained 'clean' sands are typically highly bitumen saturated and contain only a few diagenetic minerals, predominately berthierine, pyrite, K feldspar, trioctahedral C/S clays, and siderite. Water saturated 'clean' sands contain more diagenetic material and a much wider variety of diagenetic phases, including illite, I/S, feldspars, quartz, zeolite and kaolinite. Emplacement of bitumen into the formation probably halted further growth or development many diagenetic phases.

'Muddy' sands typically contain characteristic high values of 7 and 10Å clays, dioctahedral I/S, and most other phases common to 'clean' sands. As with 'clean' sands, most samples are bitumen saturated, and water sands contain the most clays and other diagenetic phases. The clay assemblage is mixed diagenetic–detrital.

Sandy silts or shales contain more pyrite and clays than 'muddy' sands, although overall they have the same approximate mineral suite, with more pyrite and siderite. The clay assemblage is mixed diagenetic and detrital, with more swelling clays and 10Å clays. Bitumen saturation is generally poor when present.

Interstratified silts and shales contain the most quartz and pyrite, and the most clays. The detrital clay assemblage was identified from these samples as 10Å illitic clays, swelling clays of dioctahedral I/S and minor detrital chlorite. All samples were water saturated.

Calcite cemented samples have high levels of diagenetic calcite, and reduced levels of framework grains because of *caustic* fluids which appear to precede cementation processes. The presence of diagenetic phases includes 7Å and 10Å clays, pyrite and siderite. For all samples, calcite cementation appears to precede bitumen emplacement.

HYDROGEOLOGY OF THE CLEARWATER FORMATION

Hydrogeological conditions for the Clearwater Formation are basically a function of their position on the eastern margin of the Western Canada Sedimentary Basin. Groundwater flow in the Western Canada Sedimentary Basin is dominated by a regional flow system, with recharge in the northern uplands and western Rocky mountains, lateral flow in the midline areas, and discharge on the eastern margin of the basin. Intermediate and local flow systems predominate in the central plains of Alberta, with recharge and downward flow in the uplands and discharge and upward flow in the lowlands (Hitchon, 1969a; Tóth, 1963, 1984). Upper Devonian carbonates are a major conduit for the movement of fluids laterally in the regional flow system, and act as a drain on the eastern margin of the basin, carrying fluids up to springs where sediments outcrop along the edge of the Precambrian Shield (Garven, 1989). Flow patterns are mainly influenced by topography and geology, and regional flow patterns in the basin are primarily the result of the structural deformation of the basin into an symmetrical syncline in the Tertiary (Hitchon, 1969a, 1969b; Garven, 1989). Hydrocarbons generated in deep basin source rocks are thought to have been carried in this regional system through the Devonian carbonates and emplaced into their current reservoirs on the eastern margin of the basin (in heavy oil deposits) (Garven, 1989).

Present day groundwater flow in the Mannville Group located at a depth of approximately 400m (1300ft) on the eastern margin is predominantly lateral and towards the southeast, with some component of downward flow towards the pre-Cretaceous unconformity. Hydrostatic pressures are present in the sediments, and flow appears to be influenced to some degree by topography, likely because of limited meteoric recharge, although the sediments appear to be confined, perhaps by the overlying Colorado shales.

Present day groundwaters in the Mannville Group formations contain fresh to brackish waters (~18 000 mg/L), resulting from a mix of former high salinity 'brines' during hydrocarbon emplacement, influx of meteoric waters, and infiltration of ionic constituents through the pre-Cretaceous unconformity from the underlying Devonian carbonate and evaporite units. Waters are generally high in TDS and chloride, contain moderate values of bicarbonate and low values of sulphate, calcium and magnesium. Lateral variability in water composition can be linked to areas of infiltration from the Devonian units, and potentially, areas of leakage of meteoric water through the overlying shales.

A DIAGENETIC / HYDROGEOLOGIC MODEL FOR THE LEMING AREA

The diagenetic history of the Clearwater Formation within the study area is believed to have progressed through 3 main stages, extending from early *shallow* diagenesis, through intermediate and late diagenesis to uplift and erosion. Groundwater flow and porewater compositions changed concurrently, and were affected substantially by events occurring on a regional scale in the Western Canada Sedimentary Basin. The diagenetic and hydrogeologic history for the study has been summarized and is depicted graphically within Figure 5.6.

Stage 1: Early *Shallow* Diagenesis and Early Burial Diagenesis–Local Groundwater Flow System:

Initial porewaters were brackish in composition, and were subsequently affected by the influx of small amounts of meteoric water ($\delta^{18}C \approx 19‰$ (SMOW),Type 1 calcite). Groundwater flow was controlled primarily by topography, and waters would have been rich in bicarbonate, with low levels of Ca, Mg, and TDS (Tóth, 1984).

Initial conditions were those of a continental sea, in which waters may have been layered, with little mixing, and somewhat anoxic conditions may have existed at deeper depths (Stelck and Leckie, 1988). This may have resulted more brackish–marine porewaters at distal shoreline positions, and meteoric–brackish waters at nearshore positions on the shelf. Grain dissolution would have been initiated shortly after burial.

Diagenetic History:

1) formation of syn-depositional glauconite pellets in oxygenated conditions above the sediment / water interface;
2) precipitation of framboidal pyrite by bacterial sulphate reduction processes;
3) development (neoformation) of Fe-rich berthierine;
4) precipitation of Fe-poor, Type 1 calcite ($\delta^{18}O \approx 19.1‰$ (SMOW), $\delta^{13}C \approx -0.3‰$ (PDB)); and
5) precipitation of concretionary siderite.

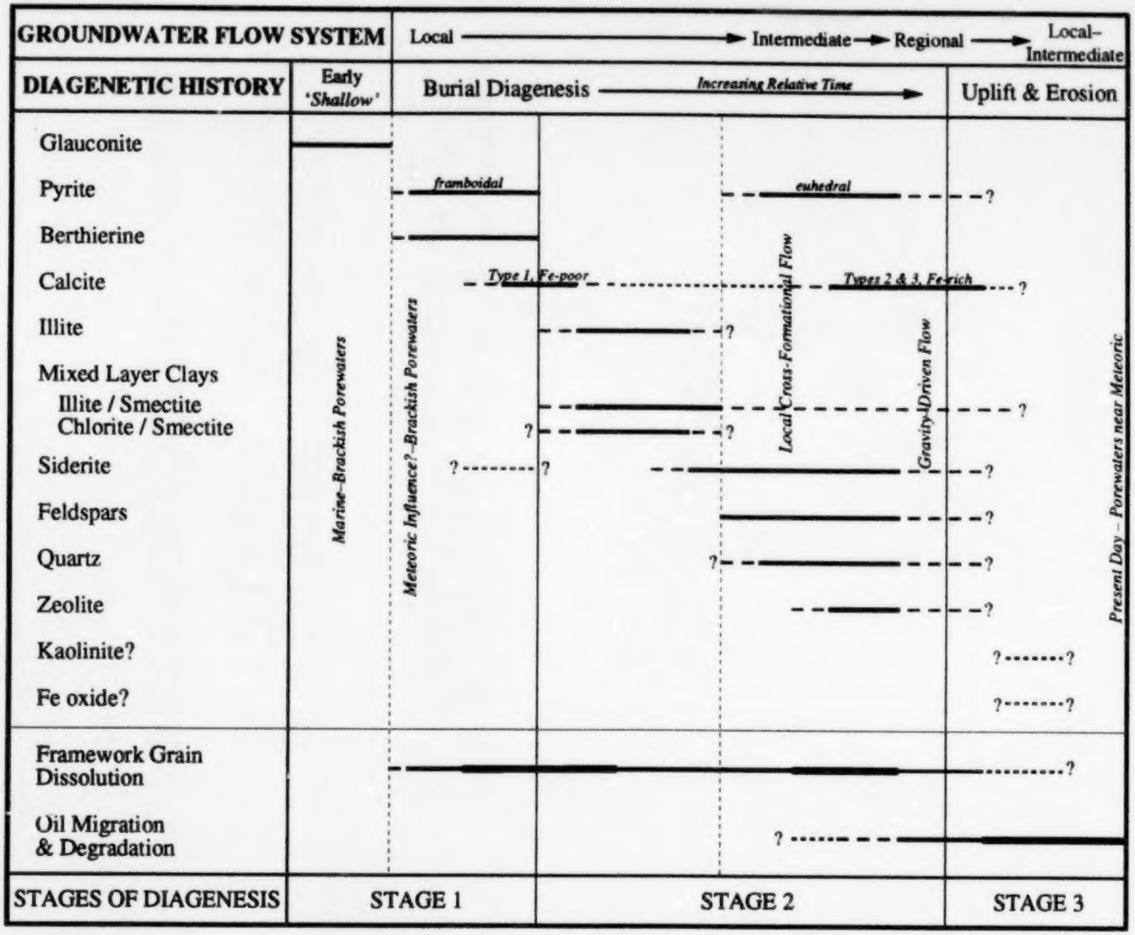
GROUNDWATER FLOW SYSTEM
Local
Intermediate
Regional
Local–Intermediate
DIAGENETIC HISTORY
Early 'Shallow'
Burial Diagenesis
Increasing Relative Time
Uplift & Erosion
Glauconite
Pyrite
Berthierine
Calcite
Illite
Mixed Layer Clays
Illite / Smectite
Chlorite / Smectite
Siderite
Feldspars
Quartz
Zeolite
Kaolinite?
Fe oxide?
Framework Grain Dissolution
Oil Migration & Degradation
framboidal
euhedral
Type 1, Fe-poor
Types 2 & 3, Fe-rich
Marine–Brackish Porewaters
Meteoric Influence?–Brackish Porewaters
Local Cross-Formational Flow
Gravity-Driven Flow
Present Day – Porewaters near Meteoric
STAGES OF DIAGENESIS
STAGE 1
STAGE 2
STAGE 3

Figure 5.6: A model of diagenetic and groundwater flow system history for the Leming study area in the Clearwater Formation.

Stage 2: Intermediate to Late Burial diagenesis–Progression from a Local to Intermediate Groundwater Flow System:

Porewater compositions developed shortly after burial would have persisted into this stage of diagenesis (continued meteoric influence). Groundwater flow patterns processed from that of local flow dominated by topography to intermediate predominately lateral flow (Tóth, 1963). Cross-formational flow, with constituents contributed from adjacent strata, would have started to develop (Tóth, 1984). In the latter part of Stage 2 diagenesis, a regional gravity-driven flow system developed, and eventually resulted in the migration and emplacement of hydrocarbons into the study area near maximum burial (Garven, 1989).

At the beginning of this second stage, porewater composition continued to increase in TDS, progressing to higher levels of Na and Cl in the local system, with an anionic composition dominated by sulphate (Tóth, 1984). Later establishment of the regional system would have increased the TDS content of the waters substantially, with considerable amounts of Na and Cl rich 'brines' mixing with previous brackish porewaters (Tóth, 1984).

Grain dissolution continued with increased burial, and became more pronounced with the increased temperatures at depth.

Diagenetic History:

1) formation of authigenic illite;
2) development of mixed-layer smectite clays (I/S, C/S);
3) precipitation of pore-filling, rhombic siderite;
4) precipitation of K feldspar overgrowths (with minor albite?);
5) precipitation of quartz overgrowths;
6) slow growth of euhedral pyrite;
7) precipitation of pore-filling zeolite;
8) precipitation of pore-filling, Fe-rich, Type 2 calcite;
9) precipitation of vein-filling, Fe-rich to Fe-poor, Type 3 calcite (mixture of Types 2 and 3: $\delta^{18}O \approx 19.2$‰ (SMOW), $\delta^{13}C \approx +4.2$‰ (PDB)); and
10) migration of oil into Clearwater sediments (near maximum burial).

Stage 3: Uplift and Erosion–Progression from a Regional Groundwater Flow System to the Present Local to Intermediate Flow System:

Buried Clearwater sediments were subjected to gradual uplift, with continued erosion of overlying basin sediments until its current position was reached (~400m depth). Groundwater flow within the study area progressed slowly from that of upward flow from the Devonian carbonates in the regional flow system, to that dominated by lateral and low levels of downward flow from the surface. Re-establishment of local to intermediate flow systems is associated with the infiltration of meteoric waters, which would have enhanced the biodegradation (bacterial oxidation) of the emplaced hydrocarbons by water washing (Garven, 1989).

Groundwater chemistry progressed from that dominated by Cl-rich brines to present conditions (~18,000 mg/L) which are slightly brackish, dominated by chloride anions, with moderate levels of bicarbonate, and low levels of sulphate, calcium and magnesium.

Mineral dissolution would have continued in this stage, resulting from the large change in porewater composition, although substantially reduced from that experienced in Stages 2 and 3.

Diagenetic History:

1) continued growth of calcite, pyrite, illite / smectite and other late diagenetic minerals within water saturated samples for a period of time;
2) water-washing and biodegradation of oil to bitumen (Garven, 1989);
3) potential formation of low ^{13}C calcites, with CO_2 contributed from the bacterial oxidation of oil to bitumen (observed in adjacent Clearwater study areas, Longstaffe *et al.*, 1992);
4) precipitation of kaolinite (only trace levels in study area, more prominent in nearby study areas, Hutcheon *et al.*, 1989);
5) late precipitation of Fe oxides, once oxygenated conditions developed in local areas, resulting from the infiltration of meteoric waters.

Overall, substantial diagenetic activity occurred within the Clearwater Formation during its depositional history. Diagenesis was also clearly affected by the progressive development of various groundwater flow systems, and changing porewater chemistry, despite the fact that neither significant compaction nor deep burial conditions were achieved (Hitchon, 1984).

E. RECOMMENDATIONS

The results from this study have indicated that the deposition of Clearwater sediments in the study area was controlled primarily by the structure of the eastern basin margin, with small scale variability of the depositional surface controlling local deposit morphology. Furthermore, variations in relative sea-level affected the stacking patterns and lateral variations in the type of sediment. Better prediction of the position of reservoir sands and internal barriers to steam injection fluids is crucial to the successful production of the reservoir. Therefore, further use of sequence stratigraphic concepts in the logging, interpretation and projection of Clearwater Formation depositional environments may prove to be economically rewarding in the future, as development of the Cold Lake oil sands deposit progresses.

Success or failure of current *in-situ* steam recovery processes in the Clearwater Formation will likely depend on a large extent on the better prediction of the type and amount of potential production problems associated with steam-induced authigenesis of many minerals. Completed work by Kirk *et al.*, (1987), and Abercrombie (1989), has indicated that significant permeability reduction occurs during steam injection by the precipitation of pore-filling smectitic (swelling) clays, calcite and zeolite. Prediction of potential problem areas, and typical reaction processes is dependent on a well delineated knowledge of the mineralogy and natural diagenetic assemblage within the Clearwater Formation. Characterization of the mineralogy and geochemistry of the Clearwater Formation within this study area contributes data to a large regional database for the Clearwater Formation, but it is clear that more work is required. Determination of the past diagenetic conditions for the formation requires more, further detailed carbon, oxygen and sulphur isotopic studies are required.

The groundwater flow system interpretation obtained here was almost solely based on information from the overlying Mannville units. They are comparable in their bulk properties (porosity, permeability, etc.) to those of the Clearwater Formation, therefore conclusions drawn are believed to be valid. However, in the future, more detailed knowledge of local controls on high permeability and porosity areas will be required for economic production by steam injection production to be realized. Substantial more hydrogeological data on the Clearwater Formation and surrounding units has to be collected before this information can be obtained.

E. REFERENCES

Abercrombie, H.J. 1989. Water-rock interaction during diagenesis and thermal recovery, Cold Lake Alberta. Ph.D. Thesis, University of Calgary, Calgary, Alberta.

Curtis, C.D. 1978. Possible links between sandstone diagenesis and depth-related geochemical reactions occurring in enclosing mudstones. Journal of the Geological Society of London, v. 135, p. 107-117.

Folk, R.L. 1974. Petrology of Sedimentary Rocks. Hemphill Publishing Co., Austin, Texas, 182pp.

Garven, G. 1989. A hydrogeologic model for the formation of the giant oil sands deposits of the Western Canada Sedimentary Basin. American Journal of Science, v. 289, p. 105-166.

Haq, B.U., Hardenbol, J. and Vail, P.R. 1987. Chronology of fluctuating sea-levels since the Triassic. Science, v. 235, p. 1156-1167.

Harrison, D.B., Glaister, R.P. and Nelson, H.W. 1981. Reservoir description of the Clearwater oil sand, Cold Lake, Alberta, Canada. *In:* Meyer, R.F. and Steele, C.T., eds., The Future of Heavy Crude and Tar Sands, McGraw Hill, New York, ch. 30, p. 264-279.

Hitchon, B. 1969a. Fluid flow in the Western Canada Sedimentary Basin. 1. Effect of topography. Water Resources Research, v. 5, no. 1, p. 186-195.

Hitchon, B. 1969b. Fluid flow in the Western Canada Sedimentary Basin. 2. Effect of geology. Water Resources Research, v. 5, no. 2, p. 460-469.

Hitchon, B. 1984. Geothermal gradients, hydrodynamics, and hydrocarbon occurrences, Alberta, Canada. American Association of Petroleum Geologists, v. 68, p. 713-743.

Hutcheon, I., Abercrombie, H., Putnam, P., Gardner, R. and Krouse, R. 1989. Diagenesis and sedimentology of the Clearwater Formation at Tucker Lake. Bulletin of Canadian Petroleum Geology, v. 37, no. 1, p. 83-97.

Jackson, P.C. 1984. Paleogeography of the Lower Cretaceous Mannville Group of western Canada. *In:* Masters, J.A., ed., Elmworth–Case Study of a Deep Basin Gas Field, American Association of Petroleum Geologists Memoir 38, p. 49-77.

Kirk, J.S., Bird, G.W. and Longstaffe, F.J. 1987. Laboratory study of the effects of steam-condensate flooding in the Clearwater Formation: High temperature flow experiments. Bulletin of Canadian Petroleum Geology, v. 35, no. 1, p. 34-47.

Longstaffe, F.J., Ayalon, A., and Racki, M.A. 1992. Stable isotope studies of diagenesis in berthierine-bearing oil sands, Clearwater Formation, Alberta. *In:* Kharaka and Maest, eds., Proceedings of the Seventh International Symposium on Water-Rock Interaction. Balkema, Rotterdam, p. 955-958.

Pettijohn, F.J., Potter, P.E., and Siever, R. 1987. Sand and Sandstone. Springer-Verlag, New York, N.Y., 553pp.

Spencer, A.M. (ed.). 1974. Mesozoic-Cenozoic orogenic belts: Data for orogenic studies. The Geological Society of London, Special Publication No. 4, p. 600-603.

Stelck, C.R. and Leckie, D. 1988. Foraminiferal inventory and lithologic description of the Lower Cretaceous (Albian) Hulcross Shale, Monkman area, northeastern British Columbia. Canadian Journal of Earth Science, v. 25, p. 793-798.

Tóth, J. 1963. A theoretical analysis of groundwater flow in small drainage basins. *In:* Benchmark Papers in Geology, v. 72: Physical Hydrogeology, Freeze, R.A. and Back, W., eds., Hutchinson Ross Pub. Co., 431pp.

Tóth, J. 1984. The role of regional gravity flow in the chemical and thermal evolution of groundwater. Proceedings First Canadian / American Conference on Hydrogeology. Practical Applications of Groundwater Chemistry, Banff, Alberta, Canada, June 22-26. Hitchon, B. and Wallick, E.E., eds., National Water Well Association, Dublin, Ohio, 323pp.

APPENDIX 1:

CORE LOG DATA

LEGEND:

LITHOLOGY

▦	med. – f.g. grained sand
▨	f.g.– v.f.g. sand
▤	interbedded sand and mud
≋	ripple bedded sand and mud
▥	interbedded mud and sand
☰	interbedded shale and silt
▩	carbonate cemented zone

PHYSICAL STRUCTURES

═	planar stratification
⥱	low angle stratification
⦣	high angle stratification
⁄10	stratification inclination
⌒⌒	ripple (current) stratification
⌇	ripple (climbing) stratification
⋙	herringbone x-stratification
◡◡◡	trough x-stratification
⋞	cross-bedding (general)
◡	mud flaser or drape
≈	wavy bedding
∿	lenticular bedding
⌓	load cast
⊔	scour and fill
⌂	soft sediment deformation
⟍	soft sediment faulting
●⁴⁰	mud clasts (%)

BEDDING CONTACTS

—	sharp
------	gradational
∿	erosional

ICHNOFAUNA

A	*Asterosoma*
Ar	*Arenicolites*
B	*Bergaueria*
Ch	*Chondrites*
Cy	*Cylindrichnus*
D	*Diplocraterion*
Pa	*Palaeophycus*
P	*Planolites*
Rh	*Rhizocorallium*
R	*Rosselia*
Sk	*Skolithos*
T	*Teichichnus*
Th	*Thalassinoides*
Z	*Zoophycos*

BIOGENIC STRUCTURES

⊍	burrowed
©	churned

Degree of bioturbation

1. low
2. moderate
3. high

ORGANIC REMAINS

⋏	rootlets
⌒	shell
∼	coal chips, lenses
w	wood fragments

DIAGENETIC FEATURES

C	Calcite
G	Glauconite
S	Siderite
Py	Pyrite
Fe	Fe oxides
Cl	Clay

CLASTIC LOGGING FORM

Well Location: 3-22-65-4W4 Esso 84 J3-13 Cold Lk.
K.B.: 612.0 m (2008 ft)
Core Interval: 431.0 - 510.85 m (1414.1 - 1676.1 ft)

Logged by: L.M. Wickert
Date: April 12, 1988
Page 1 of 4

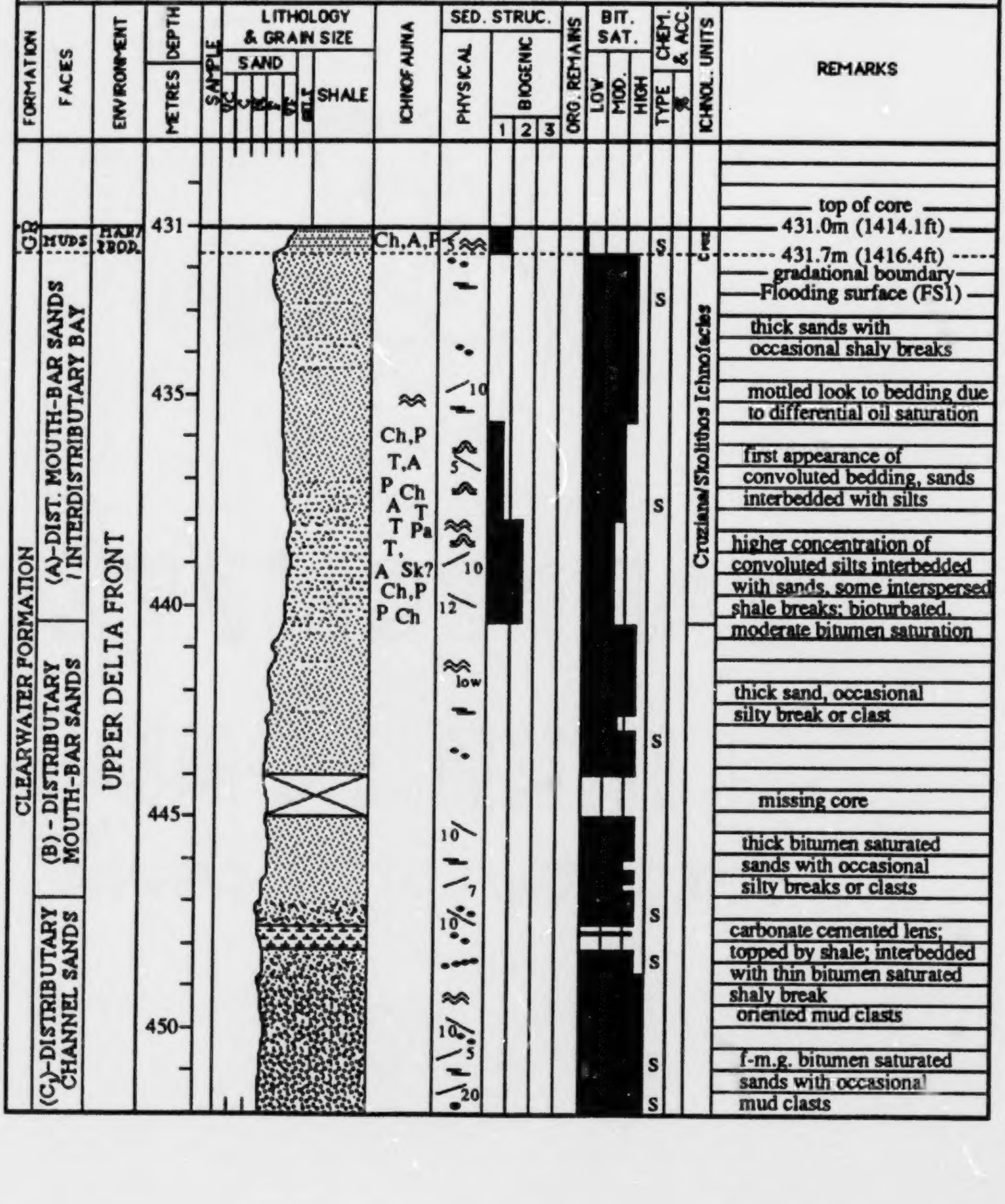
FORMATION
FACIES
ENVIRONMENT
DEPTH
METRES
SAMPLE
LITHOLOGY & GRAIN SIZE
SAND
SHALE
ICHNOFAUNA
SED. STRUC.
PHYSICAL
BIOGENIC
1
2
3
ORG. REMAINS
BIT. SAT.
LOW
MOD.
HIGH
CHEM. & ACC.
TYPE
ICHNOL. UNITS
REMARKS
431
435
440
445
450
GB
MUDS
CLEARWATER FORMATION
(A)-DIST. MOUTH-BAR SANDS / INTERDISTRIBUTARY BAY
(B) - DISTRIBUTARY MOUTH-BAR SANDS
(C1)-DISTRIBUTARY CHANNEL SANDS
UPPER DELTA FRONT
Ch,A,P
Ch,P
T,A
P Ch
A T
T Pa
T,
A Sk?
Ch,P
P Ch
10
5
10
12
low
10
7
10
10
5
20
S
Cruziana/Skolithos Ichnofacies

top of core
431.0m (1414.1ft)
431.7m (1416.4ft)
gradational boundary
Flooding surface (FS1)

thick sands with occasional shaly breaks

mottled look to bedding due to differential oil saturation

first appearance of convoluted bedding, sands interbedded with silts

higher concentration of convoluted silts interbedded with sands, some interspersed shale breaks; bioturbated, moderate bitumen saturation

thick sand, occasional silty break or clast

missing core

thick bitumen saturated sands with occasional silty breaks or clasts

carbonate cemented lens; topped by shale; interbedded with thin bitumen saturated shaly break

oriented mud clasts

f-m.g. bitumen saturated sands with occasional mud clasts

CLASTIC LOGGING FORM

Well Location: 3-22-65-4W4 Esso 84 J3-13 Cold Lk.
K.B.: 612.0 m (2008 ft)
Core Interval: 431.0 - 510.85 m (1414.1 - 1676.1 ft)

Logged by: L.M. Wickert
Date: April 12, 1988
Page 2 of 4

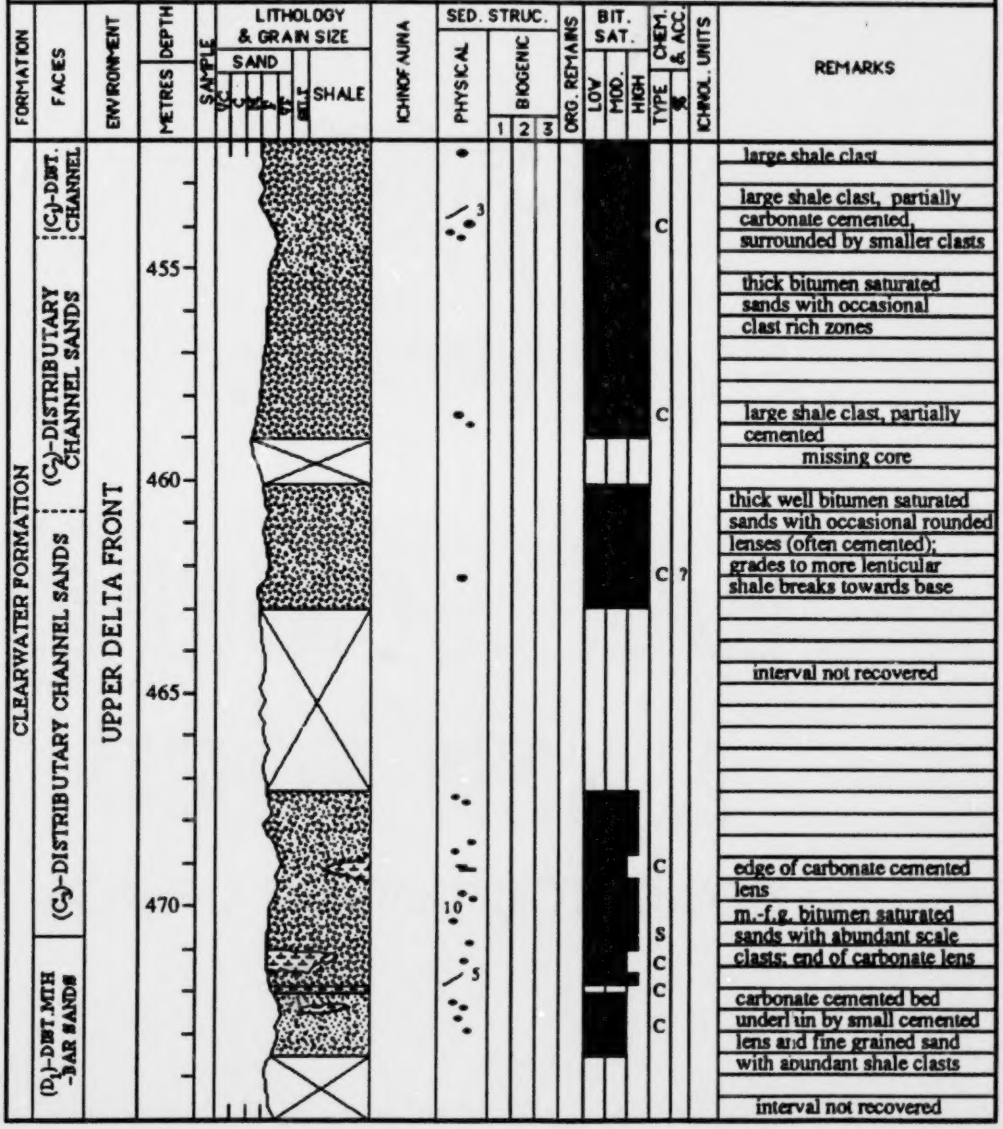
FORMATION
FACIES
ENVIRONMENT
DEPTH
METRES
SAMPLE
LITHOLOGY & GRAIN SIZE
SAND
SILT
SHALE
ICHNOFAUNA
SED. STRUC.
PHYSICAL
BIOGENIC
1
2
3
ORG. REMAINS
BIT. SAT.
LOW
MOD.
HIGH
CHEM. & ACC.
TYPE
ICHNOL. UNITS
REMARKS
CLEARWATER FORMATION
(C1)-DIST. CHANNEL
(C2)-DISTRIBUTARY CHANNEL SANDS
(C3)-DISTRIBUTARY CHANNEL SANDS
(D1)-DIST. MTH -BAR SANDS
UPPER DELTA FRONT
455
460
465
470
3
10
5
C
C
C
?
C
S
C
C
C

large shale clast

large shale clast, partially carbonate cemented, surrounded by smaller clasts

thick bitumen saturated sands with occasional clast rich zones

large shale clast, partially cemented

missing core

thick well bitumen saturated sands with occasional rounded lenses (often cemented); grades to more lenticular shale breaks towards base

interval not recovered

edge of carbonate cemented lens

m.-f.g. bitumen saturated sands with abundant scale clasts; end of carbonate lens

carbonate cemented bed underlain by small cemented lens and fine grained sand with abundant shale clasts

interval not recovered

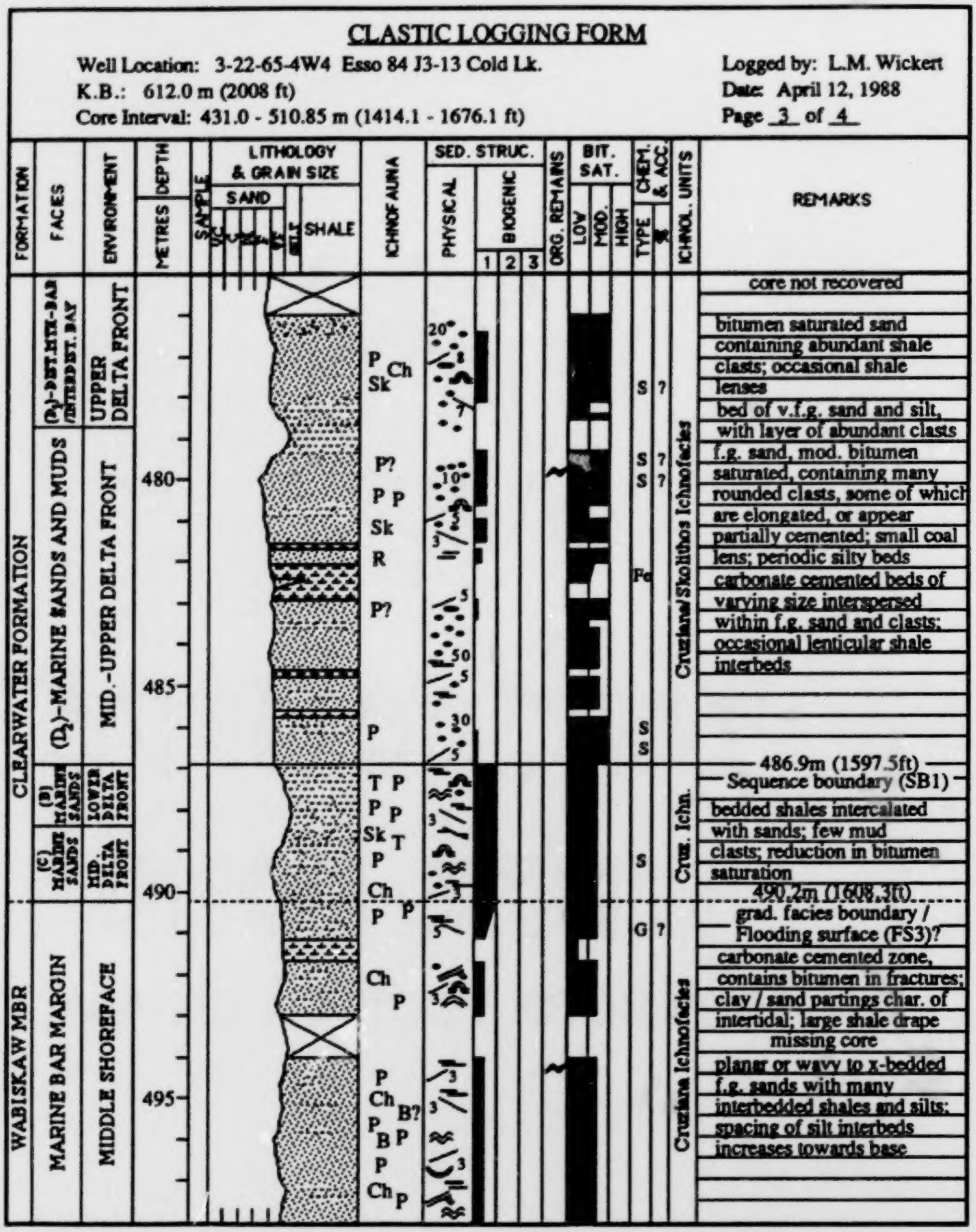

CLASTIC LOGGING FORM

Well Location: 3-22-65-4W4 Esso 84 J3-13 Cold Lk.
K.B.: 612.0 m (2008 ft)
Core Interval: 431.0 - 510.85 m (1414.1 - 1676.1 ft)

Logged by: L.M. Wickert
Date: April 12, 1988
Page 3 of 4

REMARKS

core not recovered

bitumen saturated sand containing abundant shale clasts; occasional shale lenses

bed of v.f.g. sand and silt, with layer of abundant clasts

f.g. sand, mod. bitumen saturated, containing many rounded clasts, some of which are elongated, or appear partially cemented; small coal lens; periodic silty beds

carbonate cemented beds of varying size interspersed within f.g. sand and clasts; occasional lenticular shale interbeds

486.9m (1597.5ft)
Sequence boundary (SB1)

bedded shales intercalated with sands; few mud clasts; reduction in bitumen saturation

490.2m (1608.3ft)
grad. facies boundary / Flooding surface (FS3)?

carbonate cemented zone, contains bitumen in fractures; clay / sand partings char. of intertidal; large shale drape

missing core

planar or wavy to x-bedded f.g. sands with many interbedded shales and silts; spacing of silt interbeds increases towards base

FORMATION
FACIES
ENVIRONMENT
DEPTH
METRES
SAMPLE
LITHOLOGY & GRAIN SIZE
SAND
SILT
SHALE
ICHNOFAUNA
SED. STRUC.
PHYSICAL
BIOGENIC
1
2
3
ORG. REMAINS
BIT. SAT.
LOW
MOD.
HIGH
CHEM. & ACC.
TYPE
%
ICHNOL. UNITS
CLEARWATER FORMATION
WABISKAW MBR
(D1)-DIST.INTR-BAR INTERDIST. BAY
(D2)-MARINE SANDS AND MUDS
(B) MARINE SANDS
(C) MARINE SANDS
MARINE BAR MARGIN
UPPER DELTA FRONT
MID.-UPPER DELTA FRONT
LOWER DELTA FRONT
MID. DELTA FRONT
MIDDLE SHOREFACE
480
485
490
495
P Ch
Sk
P?
P P
Sk
R
P?
P
T P
P P
Sk T
P
Ch
P P
Ch
P
P
Ch B?
P B P
P
Ch P
20°
8
7
10°
3
5
50
5
30
5
3
5
3
3
3
3
S ?
S ?
S ?
Fe
S
S
S
G ?
Cruziana/Skolithos Ichnofacies
Cruz. Ichn.
Cruziana Ichnofacies

CLASTIC LOGGING FORM

Well Location: 3-22-65-4W4 Esso 84 J3-13 Cold Lk.
K.B.: 612.0 m (2008 ft)
Core Interval: 431.0 - 510.85 m (1414.1 - 1676.1 ft)

Logged by: L.M. Wickert
Date: April 12, 1988
Page 4 of 4

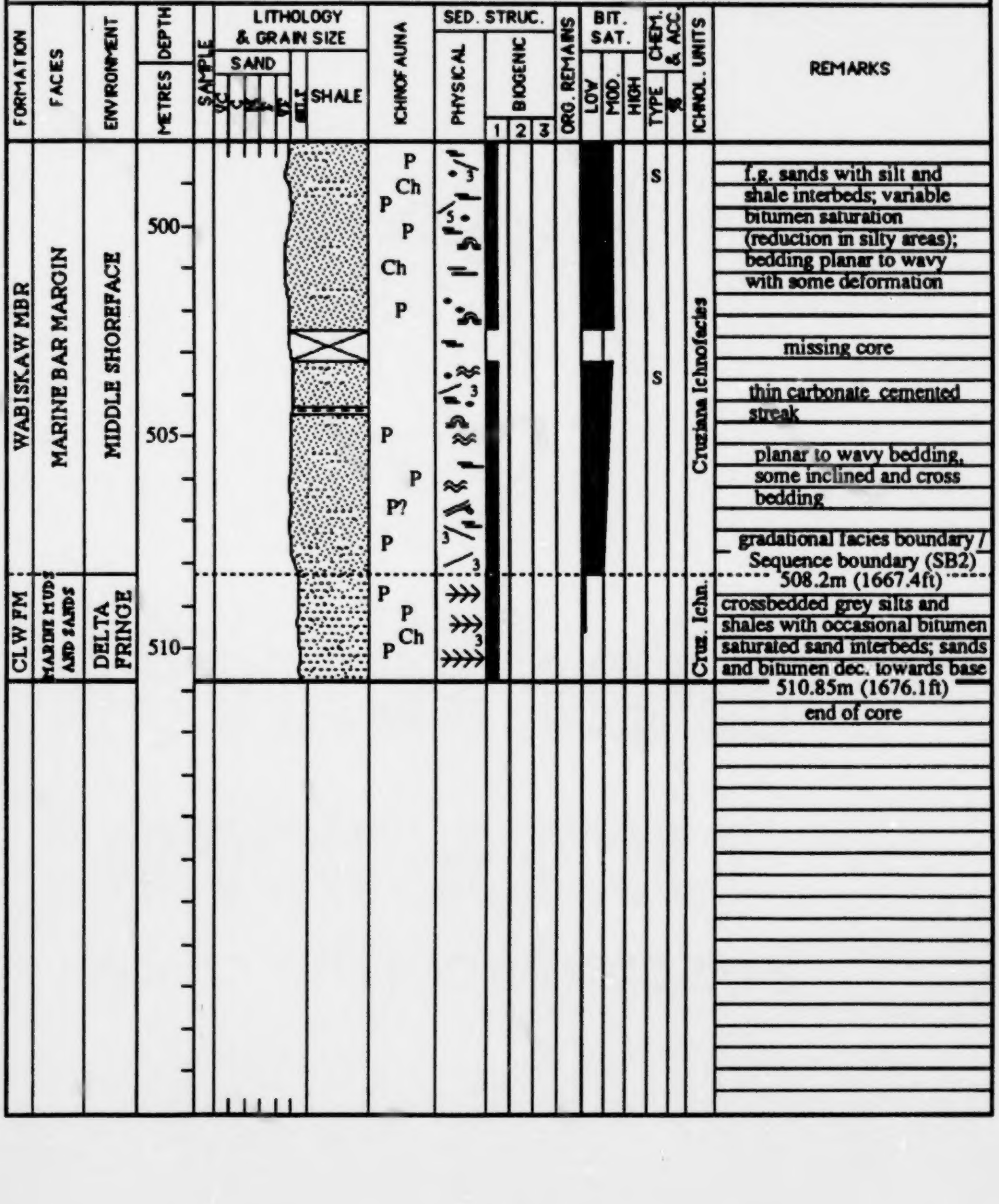
FORMATION
FACIES
ENVIRONMENT
METRES DEPTH
SAMPLE
LITHOLOGY & GRAIN SIZE
SAND
SILT
SHALE
ICHNOFAUNA
SED. STRUC.
PHYSICAL
BIOGENIC
1 2 3
ORG. REMAINS
BIT. SAT.
LOW
MOD.
HIGH
CHEM. & ACC.
TYPE
%
ICHNOL. UNITS
REMARKS
WABISKAW MBR
MARINE BAR MARGIN
MIDDLE SHOREFACE
CLW FM
MARINE MUDS AND SANDS
DELTA FRINGE
500
505
510
P
Ch
P
P
Ch
P
P
P
P?
P
P
P
Ch
P
S
S
Cruziana Ichnofacies
Cruz. Ichn.

f.g. sands with silt and shale interbeds; variable bitumen saturation (reduction in silty areas); bedding planar to wavy with some deformation

missing core

thin carbonate cemented streak

planar to wavy bedding, some inclined and cross bedding

gradational facies boundary / Sequence boundary (SB2) 508.2m (1667.4ft)

crossbedded grey silts and shales with occasional bitumen saturated sand interbeds; sands and bitumen dec. towards base

510.85m (1676.1ft)
end of core

CLASTIC LOGGING FORM

Well Location: 3-13-65-4W4 Esso 84 C1-12 Cold Lk. (oriented well)
K.B.: 609.4 m (2000 ft)
Core Interval: 451.0 – 500.0 m (1479.7 – 1640.5 ft)

Logged by: L.M. Wickert
Date: November 17, 1987
Page 1 of 3

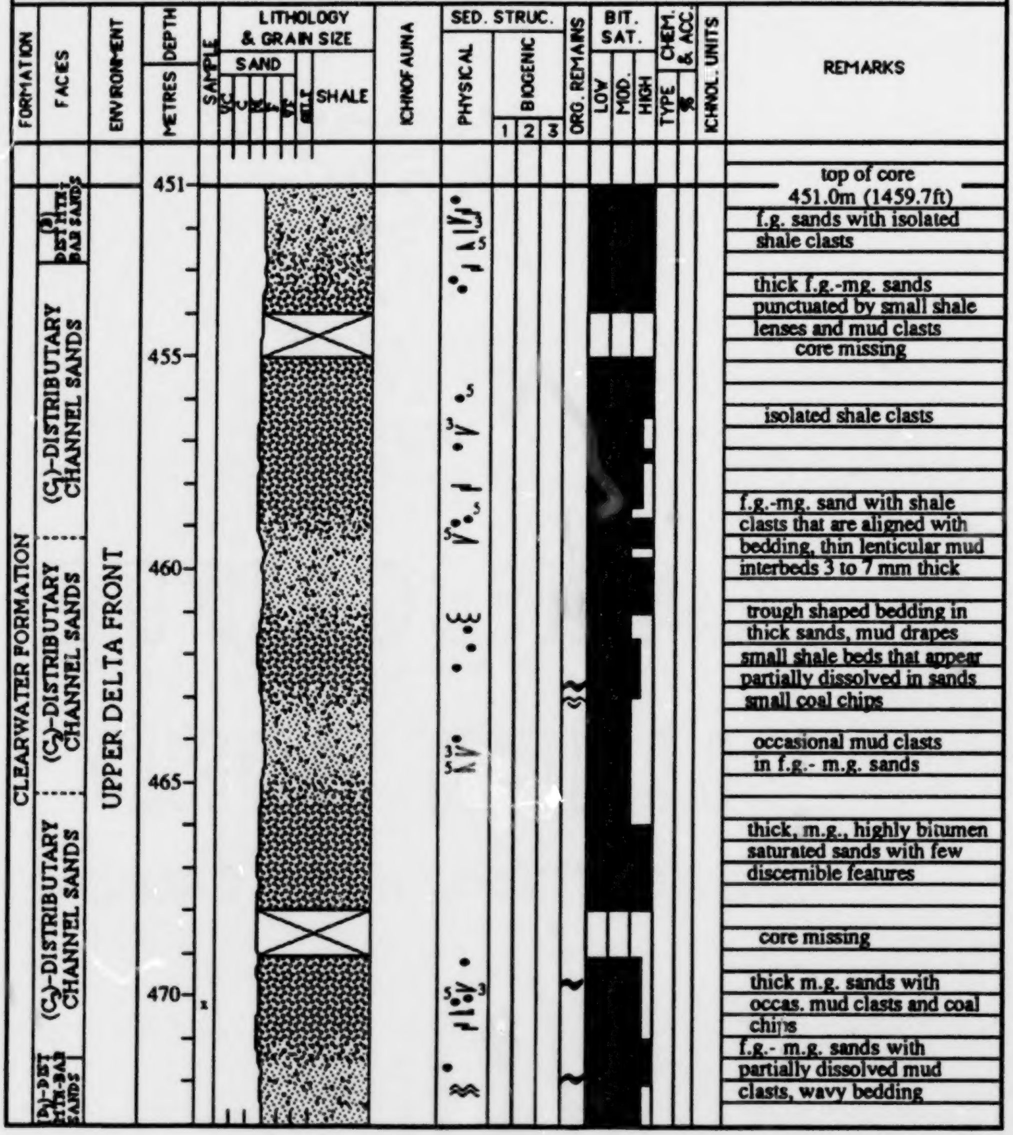
FORMATION
FACIES
ENVIRONMENT
METRES DEPTH
SAMPLE
LITHOLOGY & GRAIN SIZE
SAND
VC C M F VF SILT
SHALE
ICHNOFAUNA
SED. STRUC.
PHYSICAL
BIOGENIC
1 2 3
ORG. REMAINS
BIT. SAT.
LOW MOD. HIGH
CHEM. & ACC.
TYPE %
ICHNOL. UNITS
REMARKS
CLEARWATER FORMATION
(B)-DIST'RY-BAR SANDS
(C)-DISTRIBUTARY CHANNEL SANDS
(C)-DISTRIBUTARY CHANNEL SANDS
(C)-DISTRIBUTARY CHANNEL SANDS
(B)-DIST'RY-BAR SANDS
UPPER DELTA FRONT
451
455
460
465
470
3
5
top of core 451.0m (1459.7ft)
f.g. sands with isolated shale clasts
thick f.g.-mg. sands punctuated by small shale lenses and mud clasts
core missing
isolated shale clasts
f.g.-mg. sand with shale clasts that are aligned with bedding, thin lenticular mud interbeds 3 to 7 mm thick
trough shaped bedding in thick sands, mud drapes
small shale beds that appear partially dissolved in sands
small coal chips
occasional mud clasts in f.g.- m.g. sands
thick, m.g., highly bitumen saturated sands with few discernible features
core missing
thick m.g. sands with occas. mud clasts and coal chips
f.g.- m.g. sands with partially dissolved mud clasts, wavy bedding

CLASTIC LOGGING FORM

Well Location: 3-13-65-4W4 Esso 84 C1-12 Cold Lk. (oriented well)
K.B.: 609.4 m (2000 ft)
Core Interval: 451.0 – 500.0 m (1479.7 – 1640.5 ft)

Logged by: L.M. Wickert
Date: November 17, 1987
Page 2 of 3

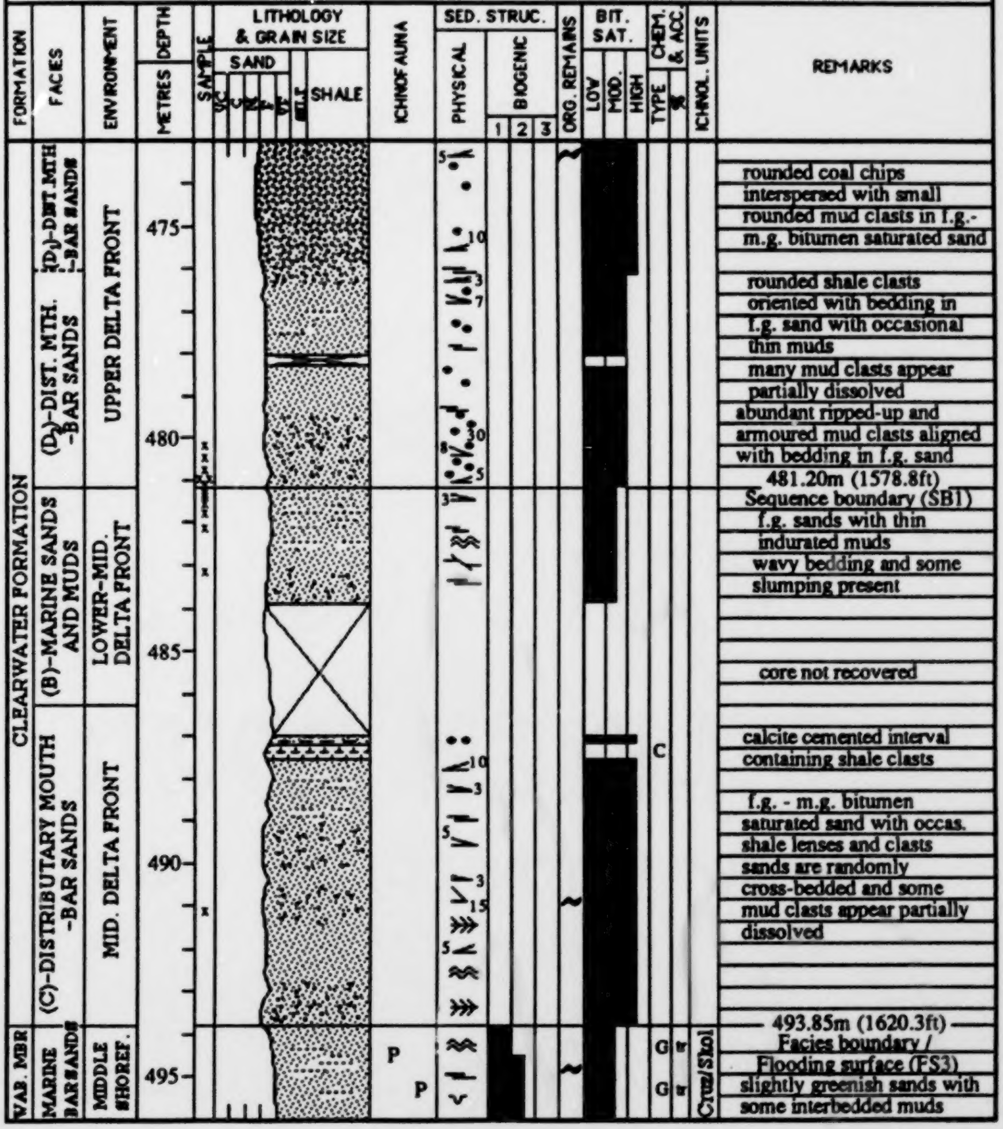
FORMATION
FACIES
ENVIRONMENT
DEPTH
METRES
SAMPLE
LITHOLOGY & GRAIN SIZE
SAND
SHALE
ICHNOFAUNA
SED. STRUC.
PHYSICAL
BIOGENIC
1 2 3
ORG. REMAINS
BIT. SAT.
LOW
MOD.
HIGH
CHEM. & ACC.
TYPE
%
ICHNOL. UNITS
REMARKS
CLEARWATER FORMATION
(D2)-DIST MTH -BAR SANDS
(D1)-DIST. MTH. -BAR SANDS
(B)-MARINE SANDS AND MUDS
(C)-DISTRIBUTARY MOUTH -BAR SANDS
VAB. MBR
MARINE BARSANDS
UPPER DELTA FRONT
LOWER-MID. DELTA FRONT
MID. DELTA FRONT
MIDDLE SHOREF.
475
480
485
490
495
5
10
3
7
30
8
5
3
10
3
5
3
15
5
C
G
tr
G
tr
P
P
Cruz/Skol

rounded coal chips interspersed with small rounded mud clasts in f.g.-m.g. bitumen saturated sand

rounded shale clasts oriented with bedding in f.g. sand with occasional thin muds

many mud clasts appear partially dissolved

abundant ripped-up and armoured mud clasts aligned with bedding in f.g. sand

481.20m (1578.8ft)
Sequence boundary (SB1)

f.g. sands with thin indurated muds

wavy bedding and some slumping present

core not recovered

calcite cemented interval containing shale clasts

f.g. - m.g. bitumen saturated sand with occas. shale lenses and clasts

sands are randomly cross-bedded and some mud clasts appear partially dissolved

493.85m (1620.3ft)
Facies boundary / Flooding surface (FS3)

slightly greenish sands with some interbedded muds

CLASTIC LOGGING FORM

Well Location: 3-13-65-4W4 Esso 84 C1-12 Cold Lk. (oriented well)
K.B.: 609.4 m (2000 ft)
Core Interval: 451.0 – 500.0 m (1479.7 – 1640.5 ft)

Logged by: L.M. Wickert
Date: November 17, 1987
Page 3 of 3

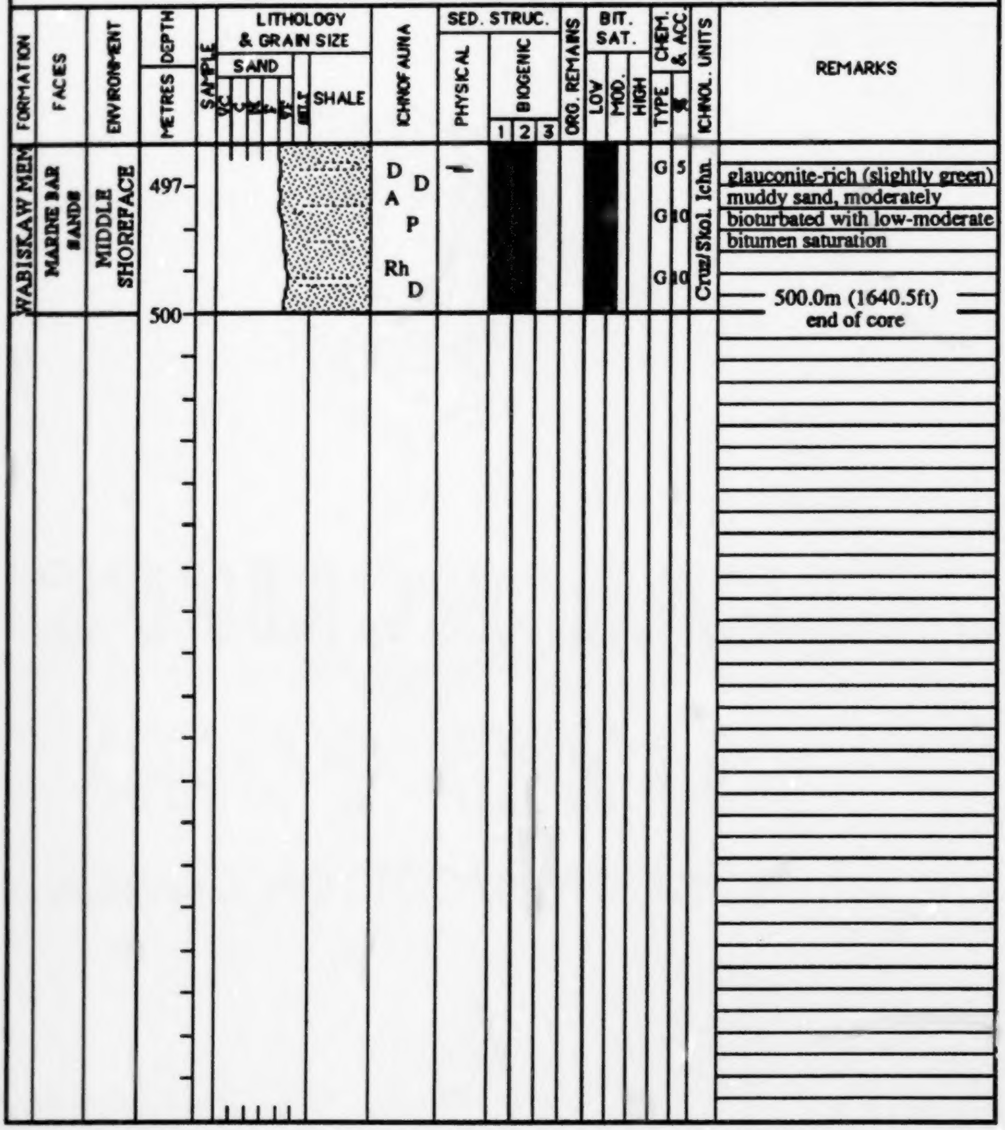
FORMATION
FACIES
ENVIRONMENT
DEPTH
METRES
SAMPLE
LITHOLOGY & GRAIN SIZE
SAND
VC
SILT
SHALE
ICHNOFAUNA
SED. STRUC.
PHYSICAL
BIOGENIC
1
2
3
ORG. REMAINS
BIT. SAT.
LOW
MOD.
HIGH
CHEM. & ACC.
TYPE
%
ICHNOL. UNITS
REMARKS
WABISKAW MEM
MARINE BAR SANDS
MIDDLE SHOREFACE
497
500
D
D
A
P
Rh
D
G
5
G
10
G
10
Cruz/Skol Ichn.

glauconite-rich (slightly green) muddy sand, moderately bioturbated with low-moderate bitumen saturation

500.0m (1640.5ft)
end of core

CLASTIC LOGGING FORM

Well Location: 12-18-65-3W4 Imp. 77 Medley O.V.
K.B.: 607.5 m (1993.2 ft)
Core Interval: 429.75 – 475.46 m (1410 – 1560 ft)

Logged by: L.M. Wickert
Date: April 12, 1988
Page 1 of 2

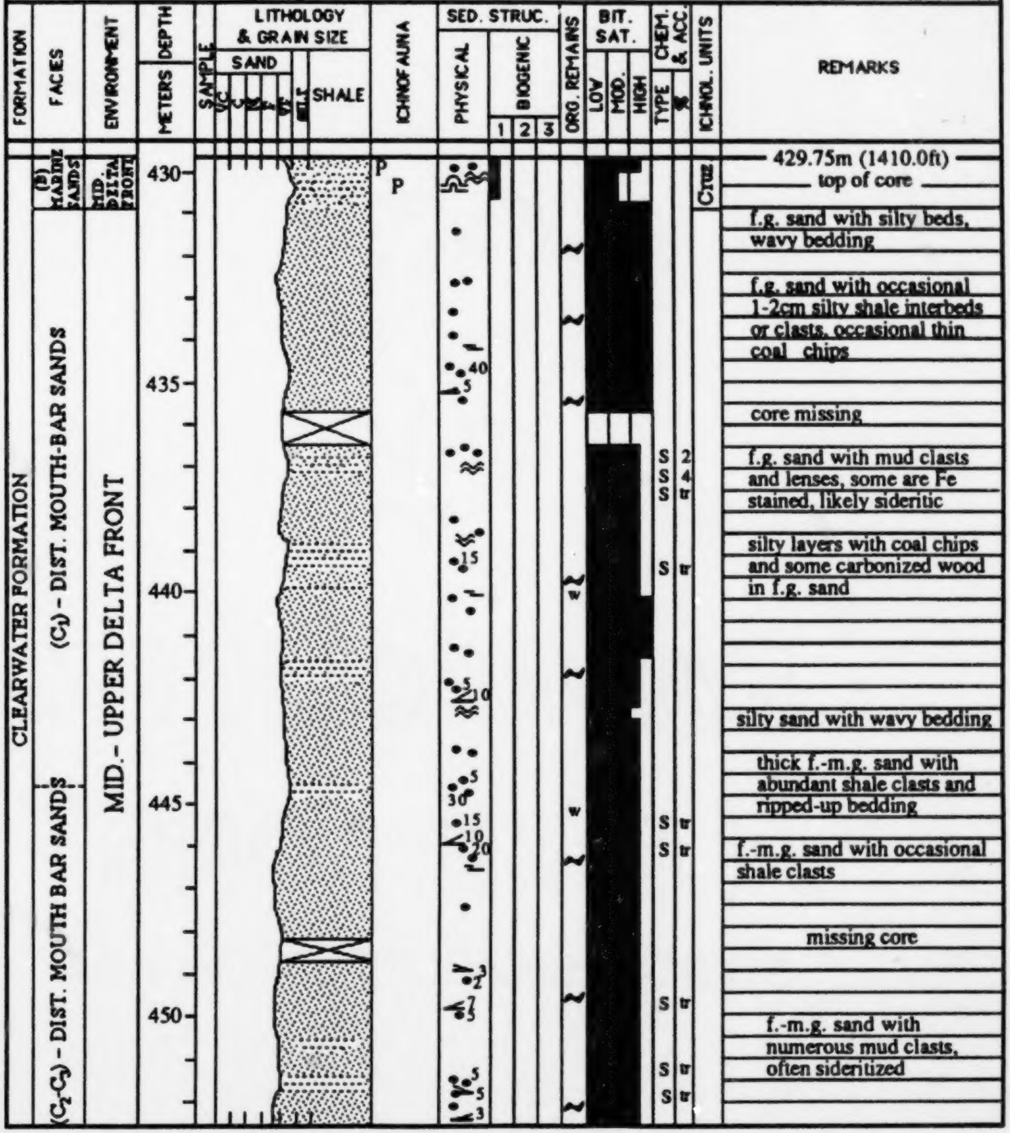
FORMATION
FACES
ENVIRONMENT
DEPTH
METERS
SAMPLE
LITHOLOGY & GRAIN SIZE
SAND
VC
C
M
F
VF
SILT
SHALE
ICHNOFAUNA
SED. STRUC.
PHYSICAL
BIOGENIC
1
2
3
ORG. REMAINS
BIT. SAT.
LOW
MOD.
HIGH
CHEM. & ACC.
TYPE
%
ICHNOL. UNITS
REMARKS
CLEARWATER FORMATION
(B) MARINE SANDS
(C1) - DIST. MOUTH-BAR SANDS
(C2-C3) - DIST. MOUTH BAR SANDS
MID DELTA FRONT
MID.- UPPER DELTA FRONT
430
435
440
445
450
P
P
40
5
15
5
10
5
30
15
10
20
3
2
7
5
5
5
3
w
w
S 2
S 4
S tr
S tr
S tr
S tr
S tr
S tr
S tr
Cruz

429.75m (1410.0ft)
top of core

f.g. sand with silty beds, wavy bedding

f.g. sand with occasional 1-2cm silty shale interbeds or clasts, occasional thin coal chips

core missing

f.g. sand with mud clasts and lenses, some are Fe stained, likely sideritic

silty layers with coal chips and some carbonized wood in f.g. sand

silty sand with wavy bedding

thick f.-m.g. sand with abundant shale clasts and ripped-up bedding

f.-m.g. sand with occasional shale clasts

missing core

f.-m.g. sand with numerous mud clasts, often sideritized

CLASTIC LOGGING FORM

Well Location: 12-18-65-3W4 Imp. 77 Medley O.V.
K.B.: 607.5 m (1993.2 ft)
Core Interval: 429.75 – 475.46 m (1410 – 1560 ft)

Logged by: L.M. Wickert
Date: April 12, 1988
Page 2 of 2

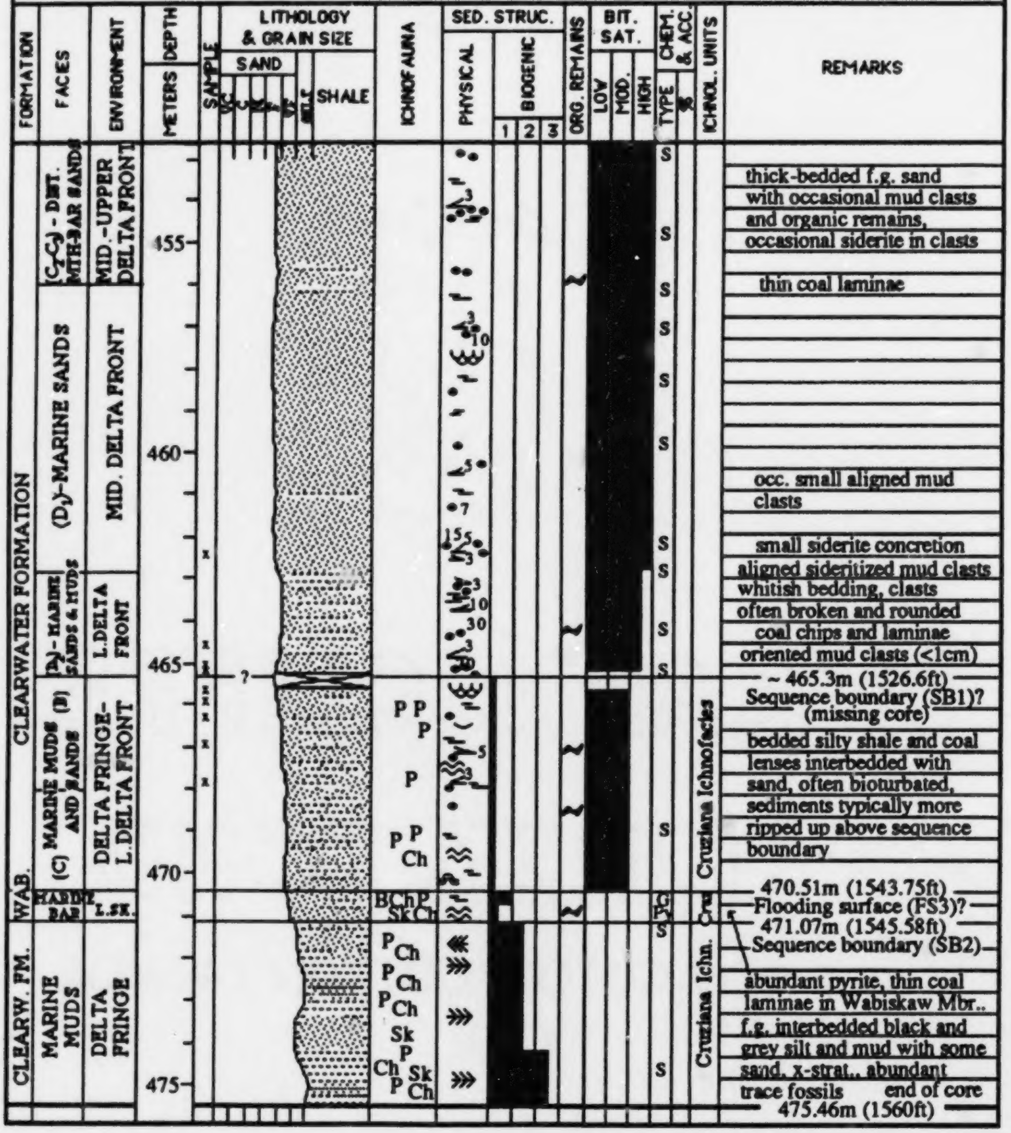
FORMATION
FACES
ENVIRONMENT
DEPTH
METERS
SAMPLE
LITHOLOGY & GRAIN SIZE
SAND
SILT
SHALE
ICHNOFAUNA
SED. STRUC.
PHYSICAL
BIOGENIC
1 2 3
ORG. REMAINS
BIT. SAT.
LOW
MOD.
HIGH
CHEM. & ACC.
TYPE
%
ICHNOL. UNITS
REMARKS
CLEARWATER FORMATION
WAB.
CLEARW. FM.
(C₂-C₃) - DIST. MTH-BAR SANDS
(D₁)-MARINE SANDS
(D₂)-MARINE SANDS & MUDS
(C) MARINE MUDS AND SANDS (B)
MARINE BAR
MARINE MUDS
MID.-UPPER DELTA FRONT
MID. DELTA FRONT
L.DELTA FRONT
DELTA FRINGE-L.DELTA FRONT
L.SX.
DELTA FRINGE
455
460
465
470
475
?
P P P
P
P P Ch
B Ch P Sk Ch
P Ch
P Ch
P Ch
Sk
P Ch Sk P Ch
3
10
5
7
15
3
10
30
S
G
Cruziana Ichnofacies
Cruziana Ichn.

thick-bedded f.g. sand with occasional mud clasts and organic remains, occasional siderite in clasts

thin coal laminae

occ. small aligned mud clasts

small siderite concretion

aligned sideritized mud clasts

whitish bedding, clasts often broken and rounded

coal chips and laminae

oriented mud clasts (<1cm)

~ 465.3m (1526.6ft)
Sequence boundary (SB1)?
(missing core)

bedded silty shale and coal lenses interbedded with sand, often bioturbated, sediments typically more ripped up above sequence boundary

470.51m (1543.75ft)
Flooding surface (FS3)?
471.07m (1545.58ft)
Sequence boundary (SB2)

abundant pyrite, thin coal laminae in Wabiskaw Mbr..

f.g. interbedded black and grey silt and mud with some sand, x-strat., abundant trace fossils

end of core
475.46m (1560ft)

CLASTIC LOGGING FORM

Well Location: 13-20-65-3W4
K.B.: approx. 602 m (1975 ft)
Core Interval: 410.0 - 464.0 m (1345.2 - 1522.4 ft)

Logged by: L.M. Wickert
Date: June 23, 1988
Page 1 of 3

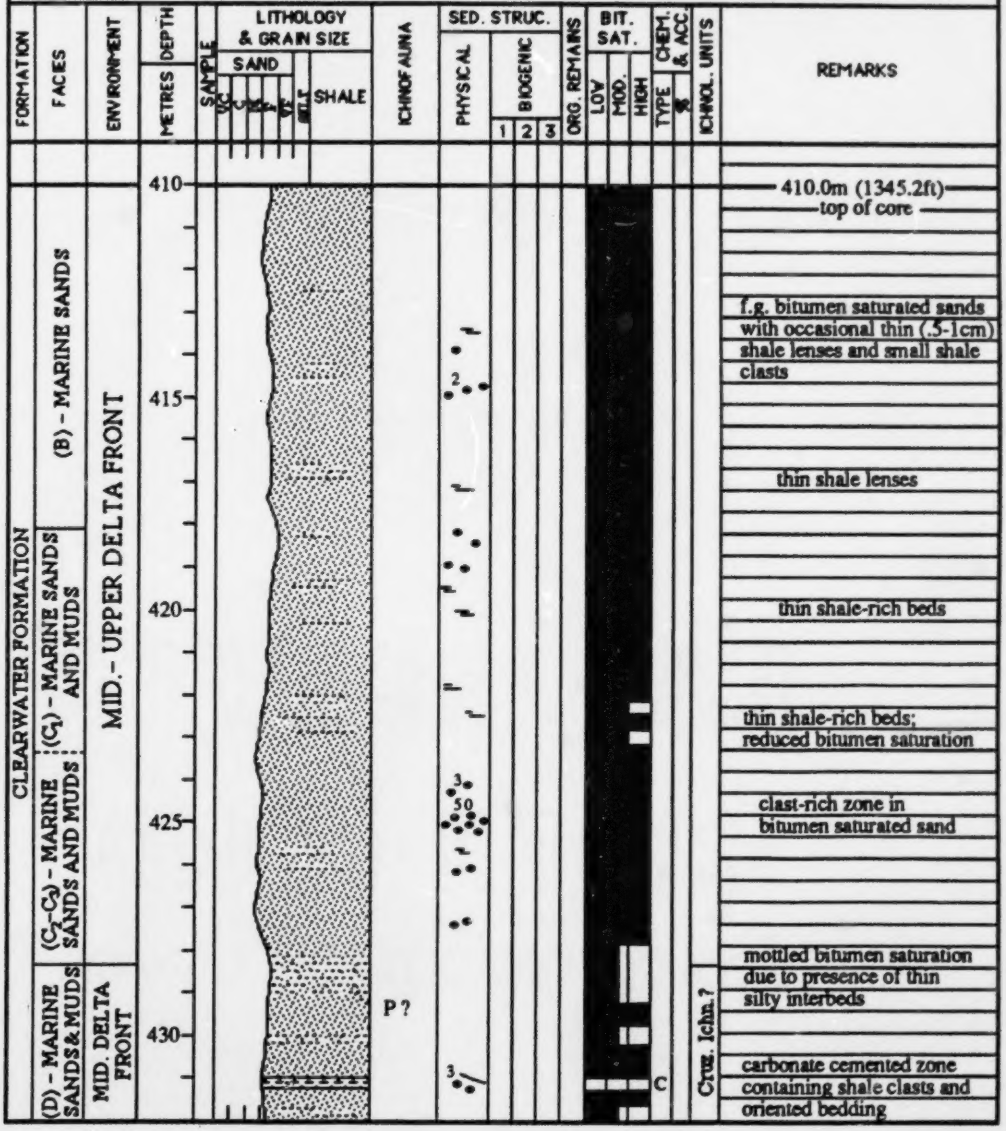
FORMATION
FACIES
ENVIRONMENT
DEPTH
METRES
SAMPLE
LITHOLOGY & GRAIN SIZE
SAND
VC
SILT
SHALE
ICHNOFAUNA
SED. STRUC.
PHYSICAL
BIOGENIC
1
2
3
ORG. REMAINS
BIT. SAT.
LOW
MOD.
HIGH
CHEM. & ACC.
TYPE
%
ICHNOL. UNITS
REMARKS
CLEARWATER FORMATION
(B) - MARINE SANDS
(C_1) - MARINE SANDS AND MUDS
(C_2-C_3) - MARINE SANDS AND MUDS
(D) - MARINE SANDS & MUDS
MID.- UPPER DELTA FRONT
MID. DELTA FRONT
410
415
420
425
430
2
3
50
3
P ?
C
Cruz. Ichn.?

410.0m (1345.2ft)
top of core

f.g. bitumen saturated sands with occasional thin (.5-1cm) shale lenses and small shale clasts

thin shale lenses

thin shale-rich beds

thin shale-rich beds; reduced bitumen saturation

clast-rich zone in bitumen saturated sand

mottled bitumen saturation due to presence of thin silty interbeds

carbonate cemented zone containing shale clasts and oriented bedding

CLASTIC LOGGING FORM

Well Location: 13-20-65-3W4
K.B.: approx. 602 m (1975 ft)
Core Interval: 410.0 - 464.0 m (1345.2 - 1522.4 ft)

Logged by: L.M. Wickert
Date: June 23, 1988
Page 2 of 3

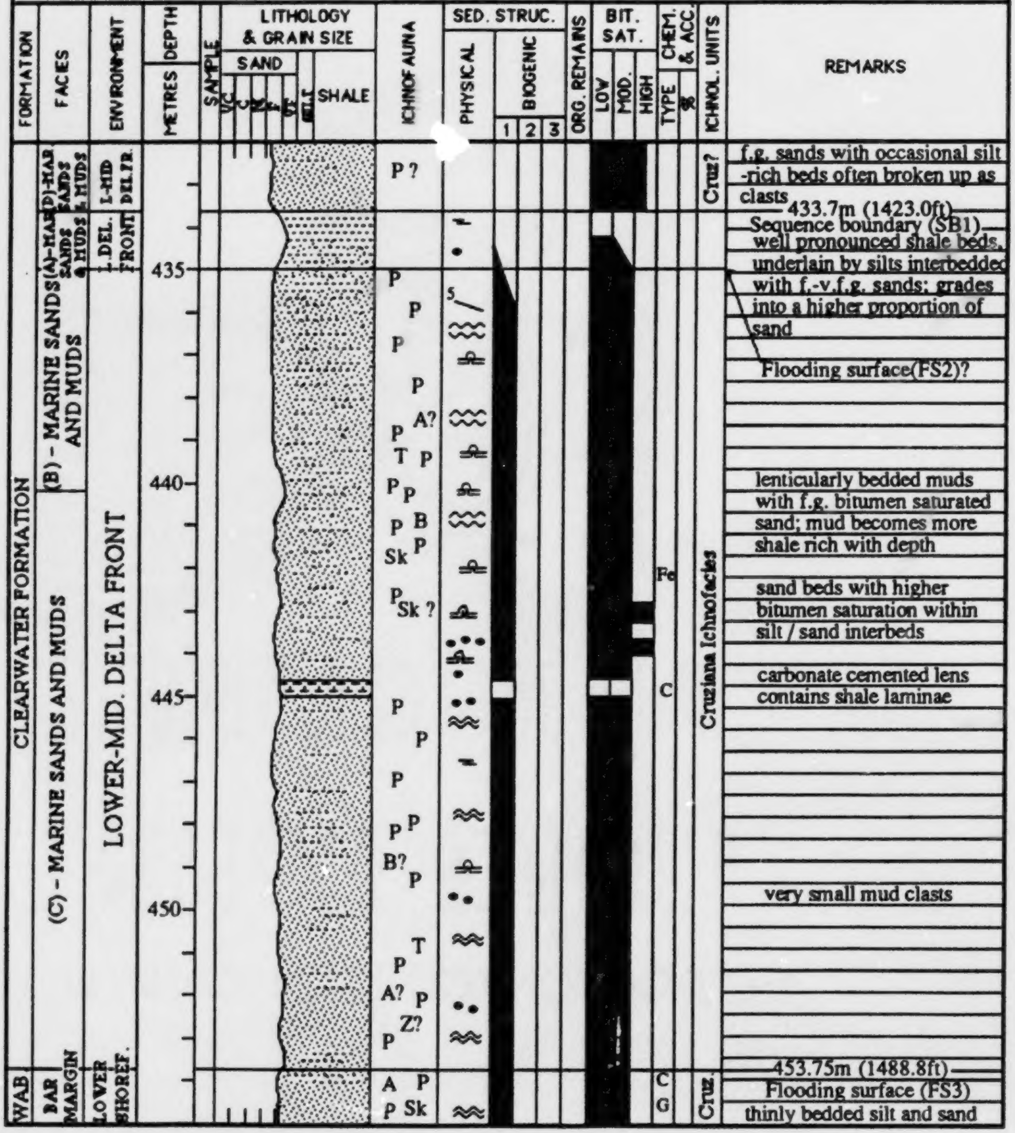
FORMATION
FACIES
ENVIRONMENT
METRES DEPTH
SAMPLE
LITHOLOGY & GRAIN SIZE
SAND
SILT
SHALE
ICHNOFAUNA
SED. STRUC.
PHYSICAL
BIOGENIC
1 2 3
ORG. REMAINS
BIT. SAT.
LOW MOD. HIGH
CHEM. & ACC.
TYPE
ICHNOL. UNITS
REMARKS
CLEARWATER FORMATION
WAB
(D)-MAR SANDS & MUDS
(A)-MAR SANDS & MUDS
(B) - MARINE SANDS AND MUDS
(C) - MARINE SANDS AND MUDS
BAR MARGIN
L-MID DEL.FR.
.DEL. FRONT
LOWER-MID. DELTA FRONT
LOWER SHOREF.
435
440
445
450
P ?
P
P
P
P
A?
P
T P
P P
P B
Sk P
P Sk ?
P
P
P
P P
B? P
T
P
A? P
P Z?
A P
P Sk
5
Fe
C
C
G
Cruz?
Cruziana Ichnofacies
Cruz.

f.g. sands with occasional silt -rich beds often broken up as clasts

433.7m (1423.0ft)

Sequence boundary (SB1)

well pronounced shale beds, underlain by silts interbedded with f.-v.f.g. sands; grades into a higher proportion of sand

Flooding surface(FS2)?

lenticularly bedded muds with f.g. bitumen saturated sand; mud becomes more shale rich with depth

sand beds with higher bitumen saturation within silt / sand interbeds

carbonate cemented lens contains shale laminae

very small mud clasts

453.75m (1488.8ft)

Flooding surface (FS3)

thinly bedded silt and sand

CLASTIC LOGGING FORM

Well Location: 13-20-65-3W4
K.B.: approx. 602 m (1975 ft)
Core Interval: 410.0 - 464.0 m (1345.2 - 1522.4 ft)

Logged by: L.M. Wickert
Date: June 23, 1988
Page 3 of 3

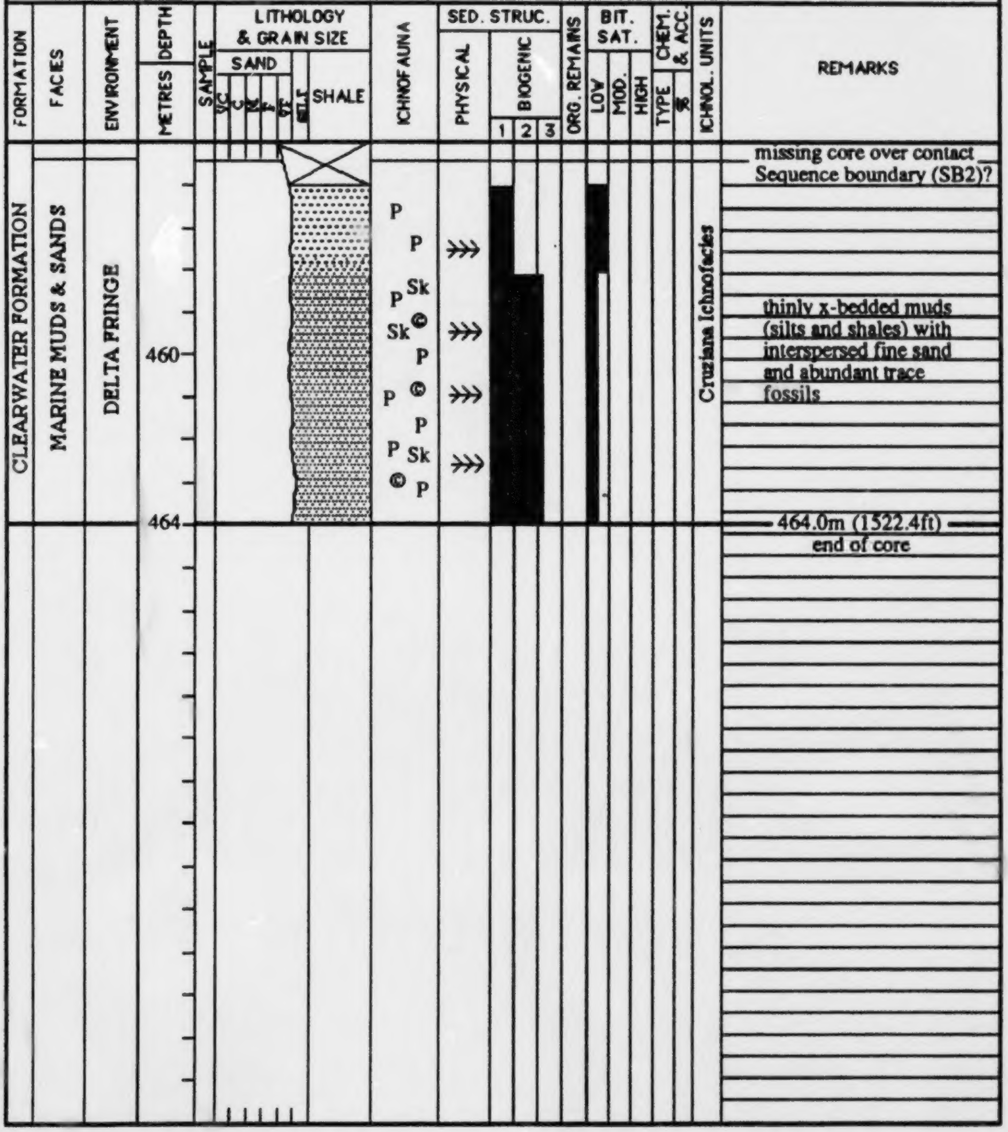
FORMATION
FACIES
ENVIRONMENT
METRES DEPTH
SAMPLE
LITHOLOGY & GRAIN SIZE
SAND
VC C M F VF
SILT
SHALE
ICHNOFAUNA
SED. STRUC.
PHYSICAL
BIOGENIC
1 2 3
ORG. REMAINS
BIT. SAT.
LOW
MOD.
HIGH
CHEM. & ACC.
TYPE
%
ICHNOL. UNITS
REMARKS
CLEARWATER FORMATION
MARINE MUDS & SANDS
DELTA FRINGE
460
464
P
P
P Sk
Sk ©
P
P ©
P
P Sk
© P
Cruziana Ichnofacies

missing core over contact
Sequence boundary (SB2)?

thinly x-bedded muds (silts and shales) with interspersed fine sand and abundant trace fossils

464.0m (1522.4ft)
end of core

CLASTIC LOGGING FORM

Well Location: 5-22-65-3W4 Imp. Marie O.V.
K.B.: 599.1 m (1965.65 ft)
Core Interval: 418.17 - 462.97 m (1372 - 1519 ft)

Logged by: L.M. Wickert
Date: April 11, 1988
Page 1 of 2

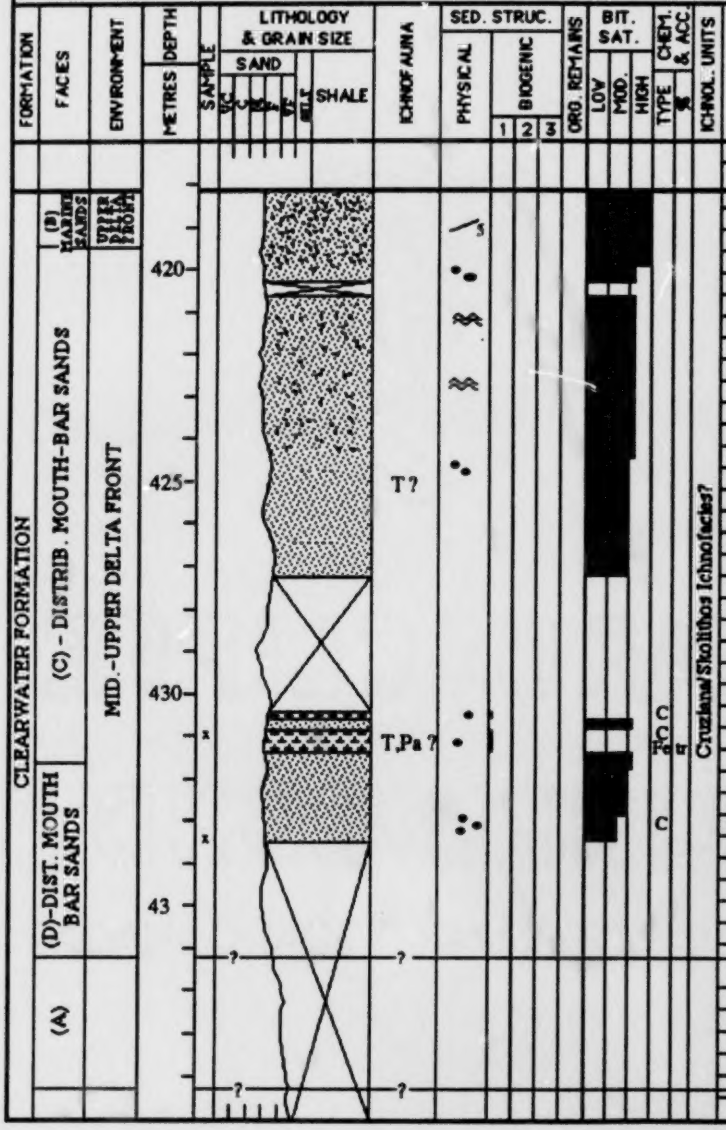
FORMATION
FACIES
ENVIRONMENT
METRES DEPTH
SAMPLE
LITHOLOGY & GRAIN SIZE
SAND
SILT
SHALE
ICHNOFAUNA
SED. STRUC.
PHYSICAL
BIOGENIC
1
2
3
ORG. REMAINS
BIT. SAT.
LOW
MOD.
HIGH
CHEM. & ACC.
TYPE
%
ICHNOL. UNITS
CLEARWATER FORMATION
(B) MARINE SANDS
UPPER DELTA FRONT
(C) - DISTRIB. MOUTH-BAR SANDS
MID.-UPPER DELTA FRONT
(D)-DIST. MOUTH BAR SANDS
(A)
420
425
430
43
s
T ?
T,Pa ?
x
x
C
C
C
Fe
tr
C
?
?
?
?
Cruziana/Skolithos Ichnofacies?

REMARKS

— 418.17m (1372ft) —
— top of core —

thick, f.-m.g. bitumen saturated sand with occasional shale clasts, some areas of lower bitumen saturation and f.g. sands

f.g. bitumen-rich sand with some siltier areas; some drilling debris present

missing core

carbonate cemented large fracture

carbonate cemented zone; some evidence of trace fossils

f.g. sand with areas of poorer bitumen saturation; small shale clasts preferentially carbonate cemented

?—436.3m (1431.5ft)—?
Sequence boundary (SB1)
approximate position
(interpreted from well logs)
core not recovered

— approx. position of FS2,-? —
interpret. from well logs

CLASTIC LOGGING FORM

Well Location: 5-22-65-3W4 Imp. Marie O.V.	Logged by: L.M. Wickert
K.B.: 599.1 m (1965.65 ft)	Date: April 11, 1988
Core Interval: 418.17 - 462.97 m (1372 - 1519 ft)	Page 2 of 2

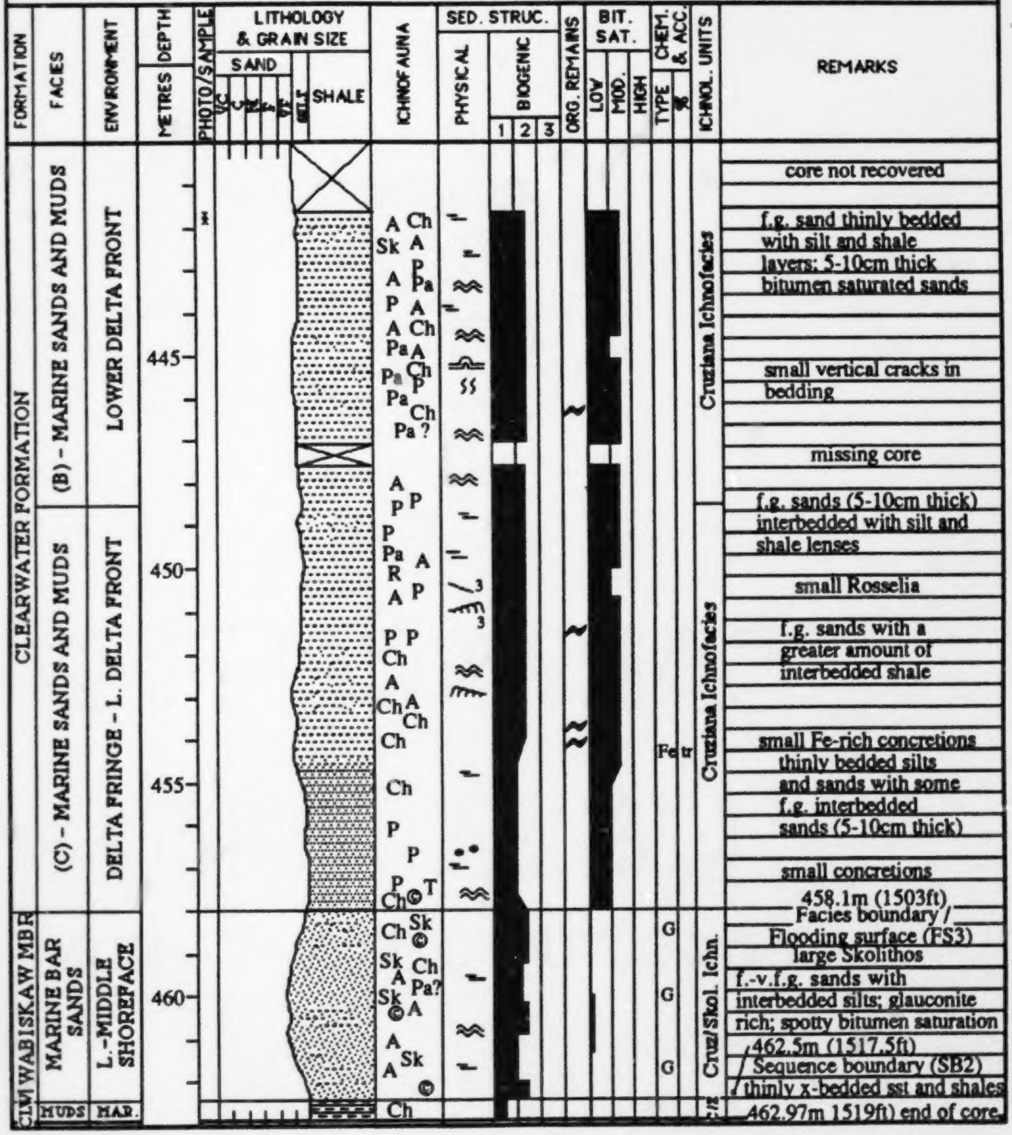
FORMATION
FACIES
ENVIRONMENT
METRES DEPTH
PHOTO/SAMPLE
LITHOLOGY & GRAIN SIZE
SAND
VC
SILT
SHALE
ICHNOFAUNA
SED. STRUC.
PHYSICAL
BIOGENIC
1
2
3
ORG. REMAINS
BIT. SAT.
LOW
MOD.
HIGH
CHEM. & ACC.
TYPE
%
ICHNOL. UNITS
REMARKS
CLEARWATER FORMATION
(B) - MARINE SANDS AND MUDS
LOWER DELTA FRONT
(C) - MARINE SANDS AND MUDS
DELTA FRINGE - L. DELTA FRONT
CLW
WABISKAW MBR
MARINE BAR SANDS
L.-MIDDLE SHOREFACE
MUDS
MAR.
445
450
455
460
A Ch
Sk A
P
A Pa
P A
A Ch
Pa A
Ch
Pa P
Pa Ch
Pa ?
A
P P
P
Pa A
R
A P
P P
Ch
A
Ch A
Ch
Ch
Ch
P
P
P
Ch © T
Ch Sk ©
Sk Ch
A Pa?
Sk
© A
A
A Sk
©
Ch
3
3
Fe tr
G
G
G
Cruziana Ichnofacies
Cruziana Ichnofacies
Cruz/Skol. Ichn.

core not recovered

f.g. sand thinly bedded with silt and shale layers: 5-10cm thick bitumen saturated sands

small vertical cracks in bedding

missing core

f.g. sands (5-10cm thick) interbedded with silt and shale lenses

small Rosselia

f.g. sands with a greater amount of interbedded shale

small Fe-rich concretions thinly bedded silts and sands with some f.g. interbedded sands (5-10cm thick)

small concretions

458.1m (1503ft) Facies boundary / Flooding surface (FS3)

large Skolithos

f.-v.f.g. sands with interbedded silts; glauconite rich; spotty bitumen saturation

462.5m (1517.5ft) Sequence boundary (SB2)

thinly x-bedded sst and shales

462.97m 1519ft) end of core

CLASTIC LOGGING FORM

Well Location: 16-28-65-3W4 Imp. 77 Marie O.V.
K.B.: 602.4 m (1976.47 ft)
Core Interval: 407.80 - 456.57 m (1338 - 1498 ft)

Logged by: L.M. Wickert
Date: April 29, 1988
Page 1 of 3

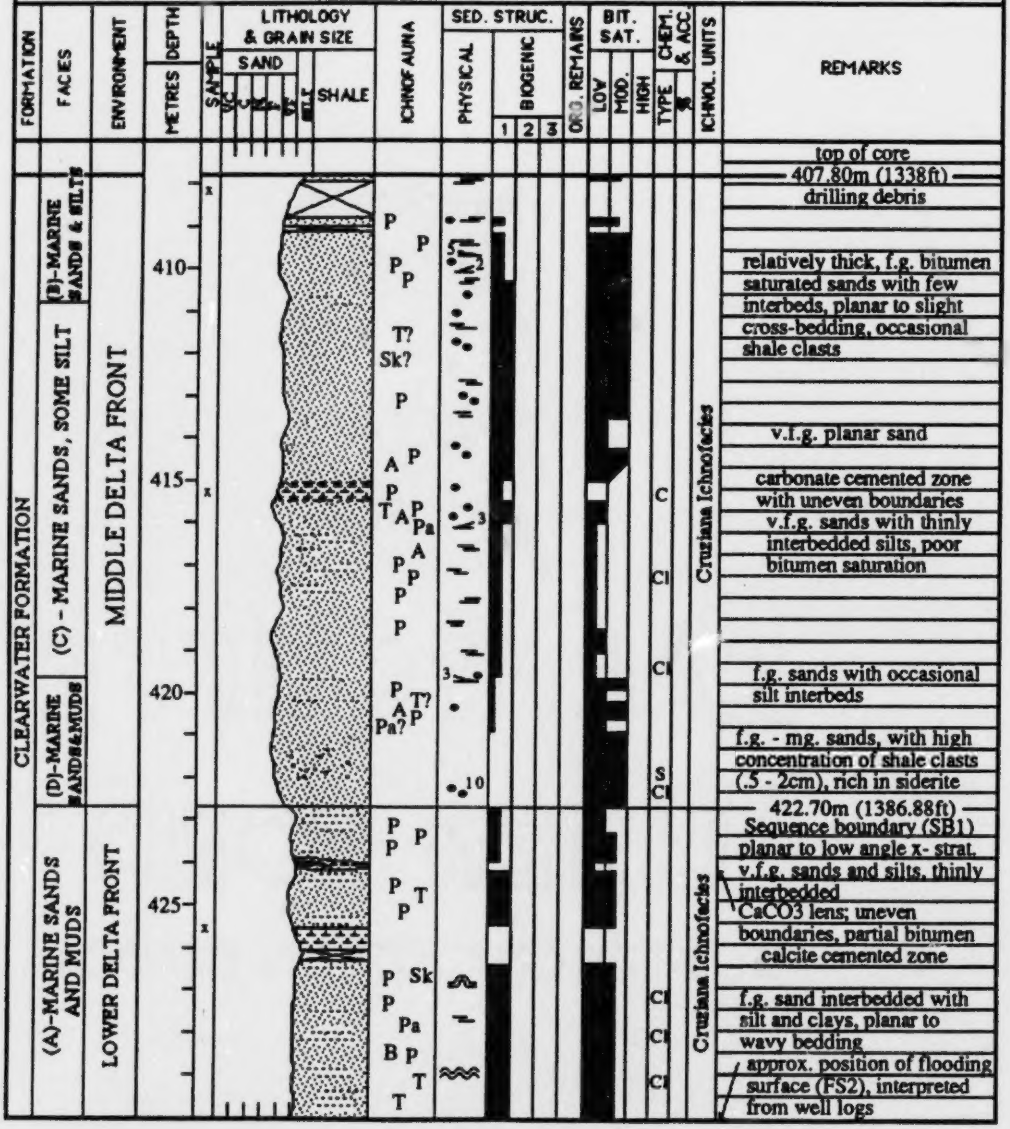
FORMATION
FACIES
ENVIRONMENT
DEPTH
METRES
SAMPLE
LITHOLOGY & GRAIN SIZE
SAND
SILT
SHALE
ICHNOFAUNA
SED. STRUC.
PHYSICAL
BIOGENIC
1
2
3
ORG. REMAINS
BIT. SAT.
LOW
MOD.
HIGH
CHEM. & ACC.
TYPE
%
ICHNOL. UNITS
REMARKS
CLEARWATER FORMATION
(B)-MARINE SANDS & SILTS
(C) - MARINE SANDS, SOME SILT
(D)-MARINE SANDS&MUDS
(A)-MARINE SANDS AND MUDS
MIDDLE DELTA FRONT
LOWER DELTA FRONT
410
415
420
425
x
x
x
P
P
P
P
T?
Sk?
P
A P
P
T A P Pa
A
P P
P
P
P T?
A P
Pa?
P P
P
P T
P
P Sk
P
Pa
B P
T
T
2
3
3
10
C
Cl
Cl
S
Cl
Cl
Cl
Cl
Cruziana Ichnofacies
Cruziana Ichnofacies

top of core
407.80m (1338ft)
drilling debris

relatively thick, f.g. bitumen saturated sands with few interbeds, planar to slight cross-bedding, occasional shale clasts

v.f.g. planar sand

carbonate cemented zone with uneven boundaries

v.f.g. sands with thinly interbedded silts, poor bitumen saturation

f.g. sands with occasional silt interbeds

f.g. - mg. sands, with high concentration of shale clasts (.5 - 2cm), rich in siderite

422.70m (1386.88ft)
Sequence boundary (SB1)

planar to low angle x- strat.

v.f.g. sands and silts, thinly interbedded

CaCO3 lens; uneven boundaries, partial bitumen

calcite cemented zone

f.g. sand interbedded with silt and clays, planar to wavy bedding

approx. position of flooding surface (FS2), interpreted from well logs

CLASTIC LOGGING FORM

Well Location: 16-28-65-3W4 Imp. 77 Marie O.V
K.B.: 602.4 m (1976.47 ft)
Core Interval: 407.80 - 456.57 m (1338 - 1498 ft)

Logged by: L.M. Wickert
Date: April 29, 1988
Page 2 of 3

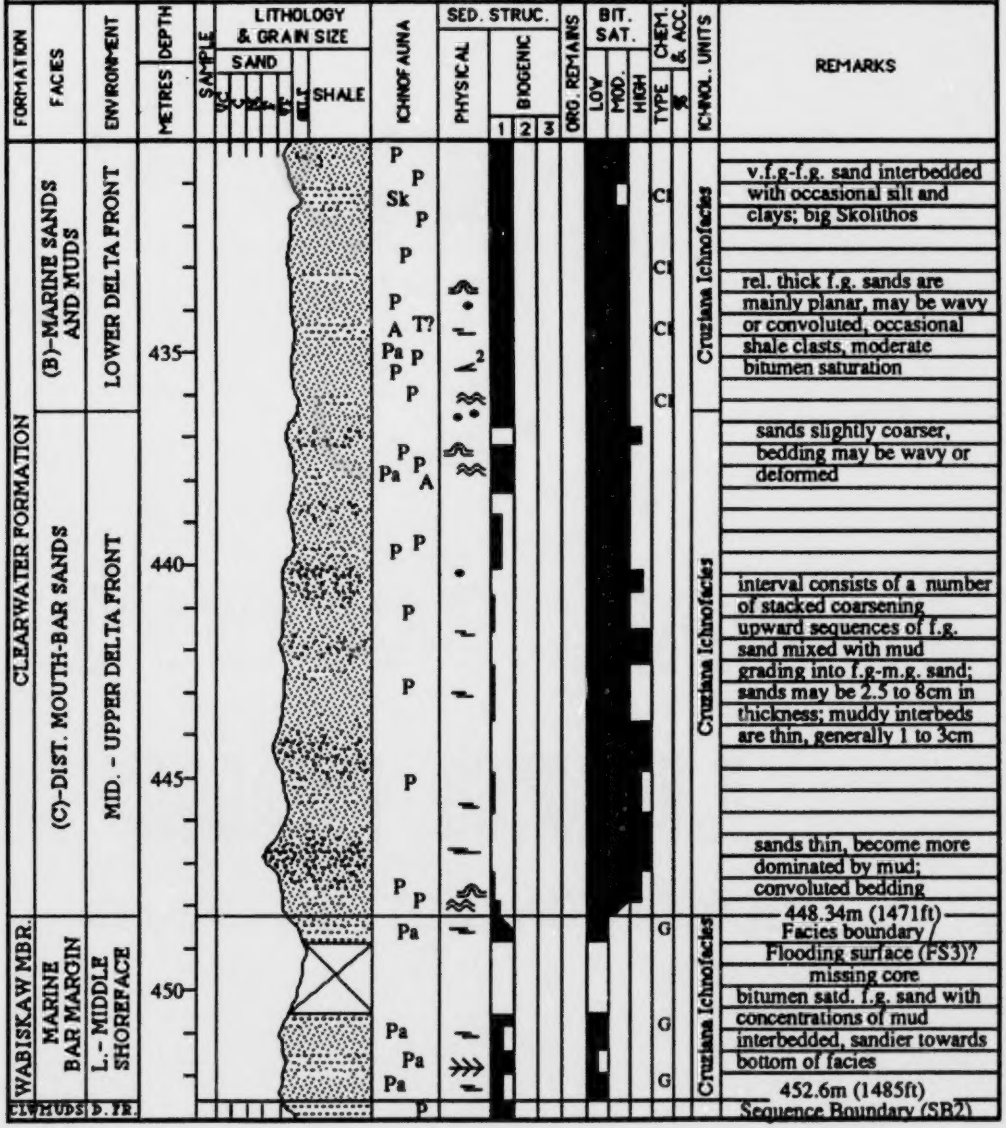
FORMATION
FACIES
ENVIRONMENT
METRES
DEPTH
SAMPLE
LITHOLOGY & GRAIN SIZE
SAND
VC
SILT
SHALE
ICHNOFAUNA
SED. STRUC.
PHYSICAL
BIOGENIC
1
2
3
ORG. REMAINS
BIT. SAT.
LOW
MOD.
HIGH
CHEM. & ACC.
TYPE
%
ICHNOL. UNITS
REMARKS
CLEARWATER FORMATION
(B)-MARINE SANDS AND MUDS
LOWER DELTA FRONT
(C)-DIST. MOUTH-BAR SANDS
MID. - UPPER DELTA FRONT
WABISKAW MBR.
MARINE BAR MARGIN
L.- MIDDLE SHOREFACE
CLWMUDS
D. FR.
435
440
445
450
P
Sk
A
T?
Pa
2
CI
G
Cruziana Ichnofacies

v.f.g-f.g. sand interbedded with occasional silt and clays; big Skolithos

rel. thick f.g. sands are mainly planar, may be wavy or convoluted, occasional shale clasts, moderate bitumen saturation

sands slightly coarser, bedding may be wavy or deformed

interval consists of a number of stacked coarsening upward sequences of f.g. sand mixed with mud grading into f.g-m.g. sand; sands may be 2.5 to 8cm in thickness; muddy interbeds are thin, generally 1 to 3cm

sands thin, become more dominated by mud; convoluted bedding

448.34m (1471ft)
Facies boundary / Flooding surface (FS3)?

missing core

bitumen satd. f.g. sand with concentrations of mud interbedded, sandier towards bottom of facies

452.6m (1485ft)
Sequence Boundary (SB2)

CLASTIC LOGGING FORM

Well Location: 16-28-65-3W4 Imp. 77 Marie O.V.
K.B.: 602.4 m (1976.47 ft)
Core Interval: 407.80 - 456.57 m (1338 - 1498 ft)

Logged by: L.M. Wickert
Date: April 29, 1988
Page 3 of 3

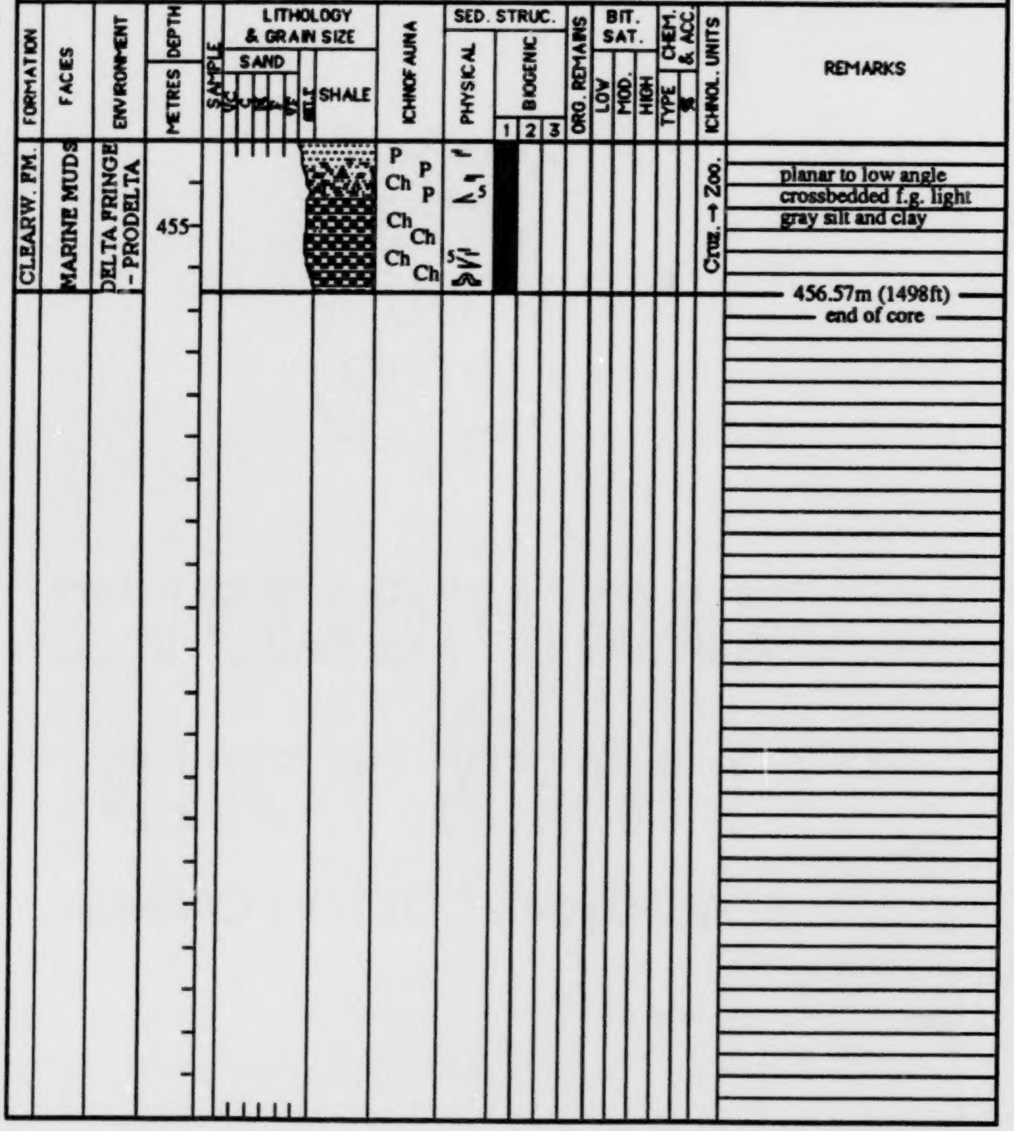
FORMATION
FACIES
ENVIRONMENT
DEPTH
METRES
SAMPLE
LITHOLOGY & GRAIN SIZE
SAND
SILT
SHALE
ICHNOFAUNA
SED. STRUC.
PHYSICAL
BIOGENIC
1
2
3
ORG. REMAINS
BIT. SAT.
LOW
MOD.
HIGH
CHEM. & ACC.
TYPE
ICHNOL. UNITS
REMARKS
CLEARW. FM.
MARINE MUDS
DELTA FRINGE - PRODELTA
455
P
Ch
P
P
Ch
Ch
Ch
Ch
5
5
Cruz. → Zoo.
planar to low angle crossbedded f.g. light gray silt and clay
456.57m (1498ft)
end of core

CLASTIC LOGGING FORM

Well Location: 16-2-66-3W4 Imp. 77 Medley O.V.
K.B.: 602.4 m (1976.5 ft)
Core Interval: 437.37 - 480.04 m (1435 - 1575 ft)

Logged by: L.M. Wickert
Date: November 27, 1987
Page 1 of 2

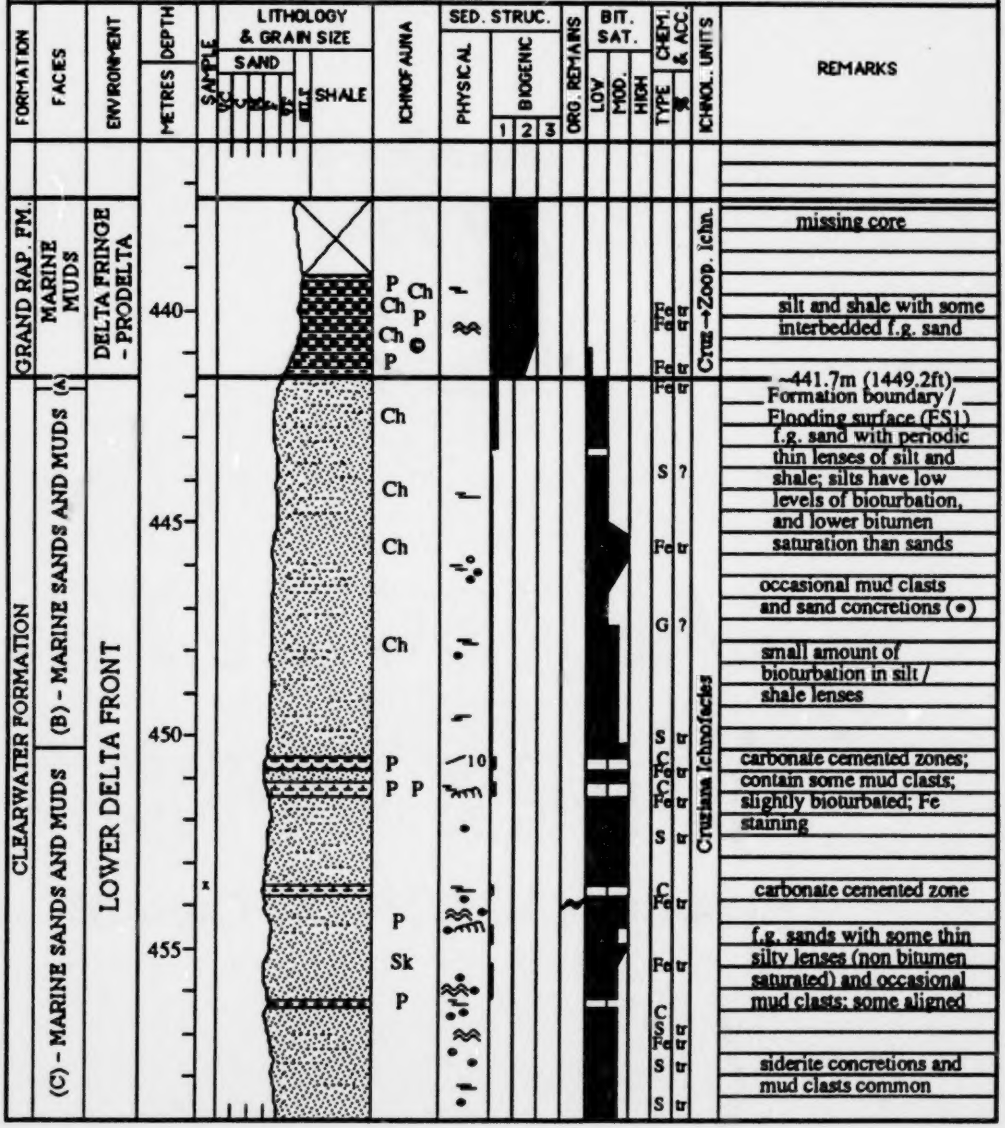
FORMATION
FACIES
ENVIRONMENT
METRES DEPTH
SAMPLE
LITHOLOGY & GRAIN SIZE
SAND
SILT
SHALE
ICHNOFAUNA
SED. STRUC.
PHYSICAL
BIOGENIC
1 2 3
ORG. REMAINS
BIT. SAT.
LOW
MOD.
HIGH
CHEM. & ACC.
TYPE
%
ICHNOL. UNITS
REMARKS
GRAND RAP. FM.
MARINE MUDS
DELTA FRINGE - PRODELTA
CLEARWATER FORMATION
(A)
(B) - MARINE SANDS AND MUDS
(C) - MARINE SANDS AND MUDS
LOWER DELTA FRONT
440
445
450
455
P
Ch
Ch
P
Ch
P
Ch
Ch
Ch
Ch
P
P P
P
Sk
P
10
Fe tr
Fe tr
Fe tr
Fe tr
S ?
Fe tr
G ?
S tr
C
Fe tr
C
Fe tr
S tr
C
Fe tr
Fe tr
C
S
Fe tr
S tr
S tr
Cruz→Zoop. Ichn.
Cruziana Ichnofacies

missing core

silt and shale with some interbedded f.g. sand

~441.7m (1449.2ft)
Formation boundary / Flooding surface (FS1)

f.g. sand with periodic thin lenses of silt and shale; silts have low levels of bioturbation, and lower bitumen saturation than sands

occasional mud clasts and sand concretions (•)

small amount of bioturbation in silt / shale lenses

carbonate cemented zones; contain some mud clasts; slightly bioturbated; Fe staining

carbonate cemented zone

f.g. sands with some thin silty lenses (non bitumen saturated) and occasional mud clasts; some aligned

siderite concretions and mud clasts common

CLASTIC LOGGING FORM

Well Location: 16-2-66-3W4 Imp. 77 Medley O.V.
K.B.: 602.4 m (1976.5 ft)
Core Interval: 437.37 - 480.04 m (1435 - 1575 ft)

Logged by: L.M. Wickert
Date: November 27, 1987
Page 2 of 2

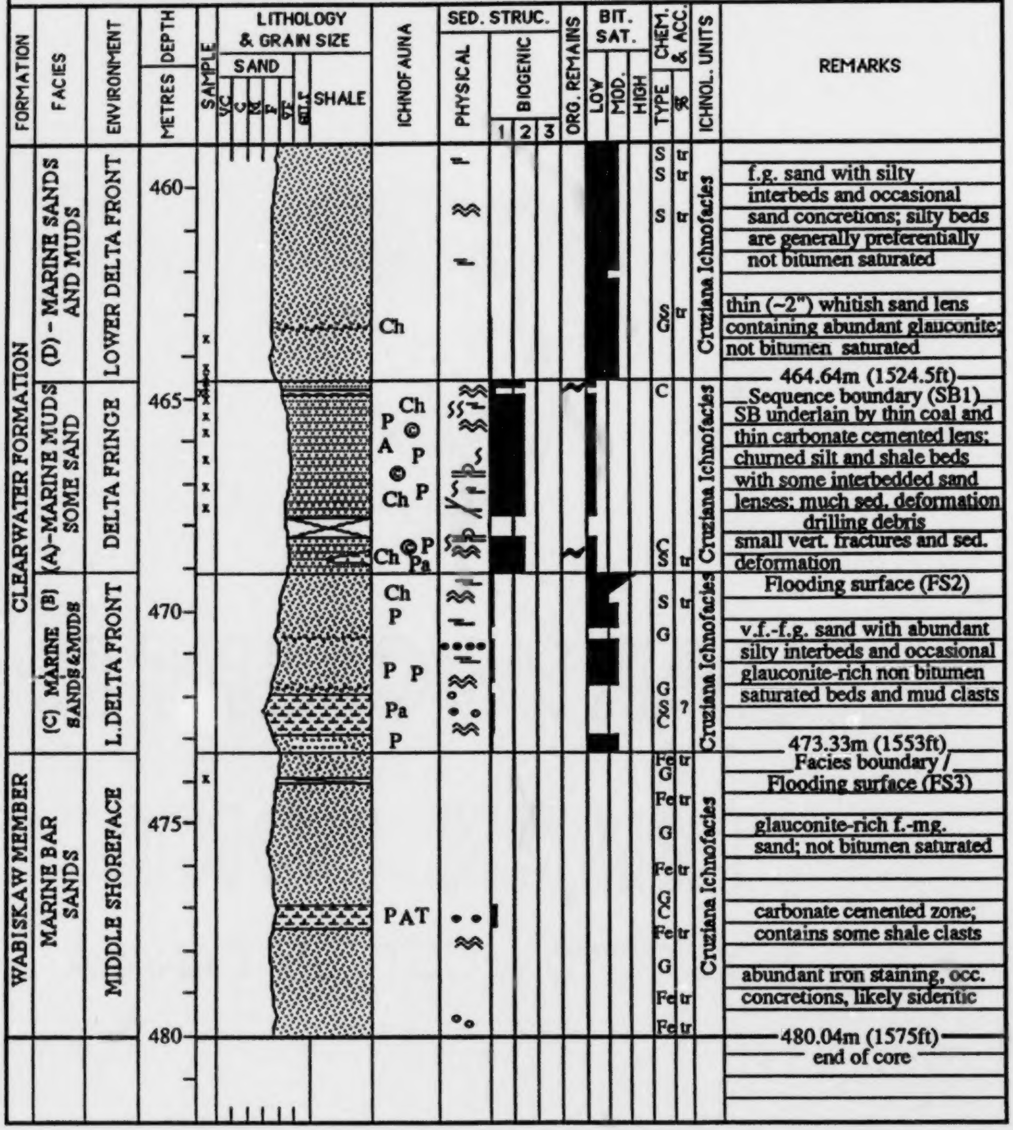
FORMATION
FACIES
ENVIRONMENT
METRES DEPTH
SAMPLE
LITHOLOGY & GRAIN SIZE
SAND
VC C M F VF
SILT
SHALE
ICHNOFAUNA
SED. STRUC.
PHYSICAL
BIOGENIC
1 2 3
ORG. REMAINS
BIT. SAT.
LOW
MOD.
HIGH
CHEM. & ACC.
TYPE
%
ICHNOL. UNITS
REMARKS
CLEARWATER FORMATION
WABISKAW MEMBER
(D) - MARINE SANDS AND MUDS
(A)-MARINE MUDS SOME SAND
(C) MARINE (B) SANDS & MUDS
MARINE BAR SANDS
LOWER DELTA FRONT
DELTA FRINGE
L.DELTA FRONT
MIDDLE SHOREFACE
460
465
470
475
480
Ch
P
A
Pa
PAT
S
G
C
Fe
tr
?
Cruziana Ichnofacies

f.g. sand with silty interbeds and occasional sand concretions; silty beds are generally preferentially not bitumen saturated

thin (~2") whitish sand lens containing abundant glauconite; not bitumen saturated

464.64m (1524.5ft)
Sequence boundary (SB1)
SB underlain by thin coal and thin carbonate cemented lens; churned silt and shale beds with some interbedded sand lenses; much sed. deformation

drilling debris

small vert. fractures and sed. deformation

Flooding surface (FS2)

v.f.-f.g. sand with abundant silty interbeds and occasional glauconite-rich non bitumen saturated beds and mud clasts

473.33m (1553ft)
Facies boundary / Flooding surface (FS3)

glauconite-rich f.-mg. sand; not bitumen saturated

carbonate cemented zone; contains some shale clasts

abundant iron staining, occ. concretions, likely sideritic

480.04m (1575ft)
end of core

CLASTIC LOGGING FORM

Well Location: 8-19-66-2W4 Esso 86 Marie O.V.
K.B.: 621.0 m (2037.50 ft)
Core Interval: 445.0 - 488.0 m (1460.05 - 1601.13 ft)

Logged by: L.M. Wickert
Date: November 17, 1987
Page 1 of 2

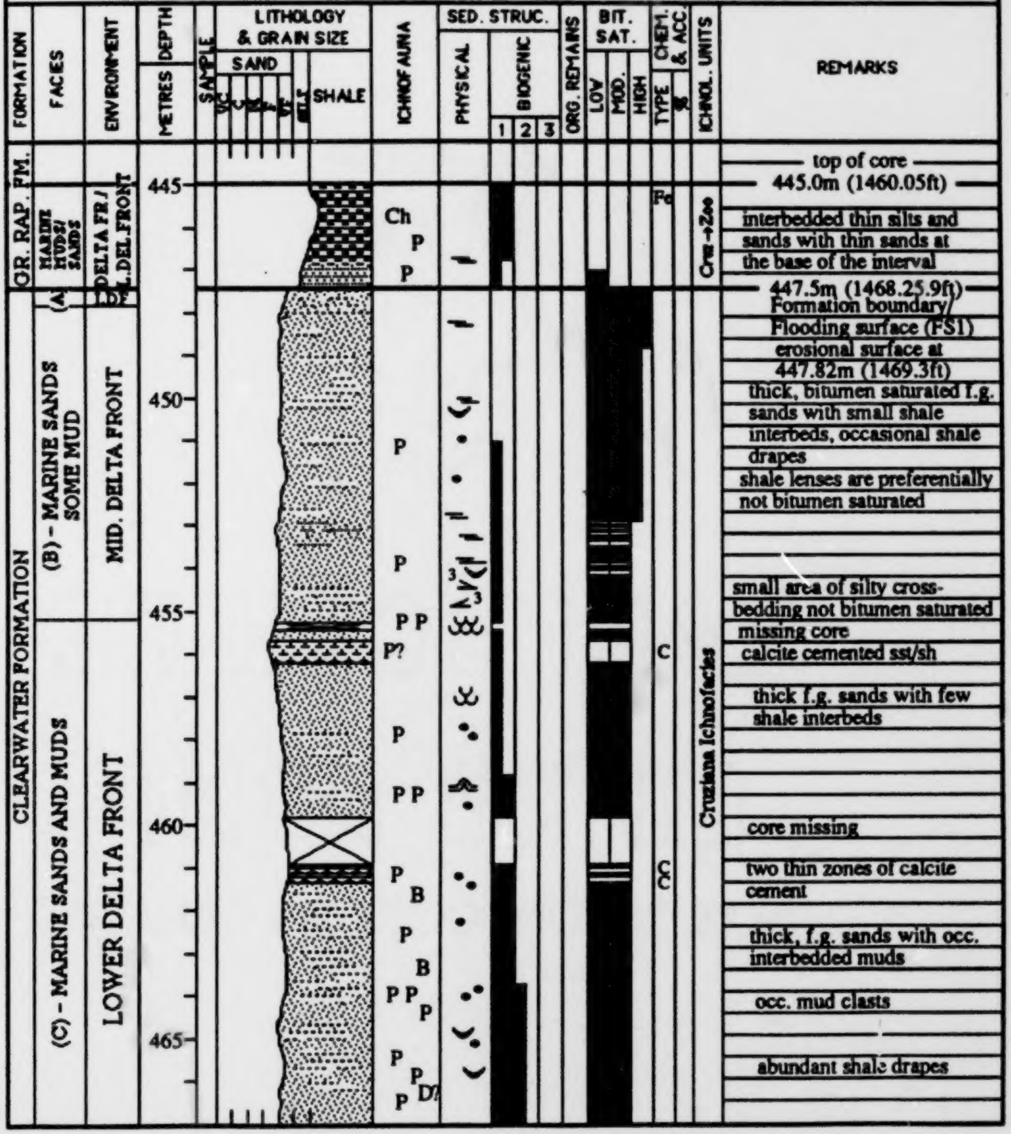
FORMATION
FACES
ENVIRONMENT
DEPTH
METRES
SAMPLE
LITHOLOGY & GRAIN SIZE
SAND
SILT
SHALE
ICHNOFAUNA
SED. STRUC.
PHYSICAL
BIOGENIC
1
2
3
ORG. REMAINS
BIT. SAT.
LOW
MOD.
HIGH
CHEM. & ACC.
TYPE
%
ICHNOL. UNITS
REMARKS
GR. RAP. FM.
MARINE MUDS/ SANDS
DELTA FR./ L. DEL. FRONT
(A)
LDF
CLEARWATER FORMATION
(B) - MARINE SANDS SOME MUD
MID. DELTA FRONT
(C) - MARINE SANDS AND MUDS
LOWER DELTA FRONT
445
450
455
460
465
Ch
P
P
P
P
P P
P?
P
P P
P
B
P
B
P P
P
P
P
P
D?
3
3
Fe
C
C
C
Cruz→Zoo
Cruziana Ichnofacies

top of core
445.0m (1460.05ft)
interbedded thin silts and sands with thin sands at the base of the interval
447.5m (1468.25.9ft)
Formation boundary/ Flooding surface (FS1)
erosional surface at 447.82m (1469.3ft)
thick, bitumen saturated f.g. sands with small shale interbeds, occasional shale drapes
shale lenses are preferentially not bitumen saturated
small area of silty cross-bedding not bitumen saturated
missing core
calcite cemented sst/sh
thick f.g. sands with few shale interbeds
core missing
two thin zones of calcite cement
thick, f.g. sands with occ. interbedded muds
occ. mud clasts
abundant shale drapes

CLASTIC LOGGING FORM

Well Location: 8-19-66-2W4 Esso 86 Marie O.V.
K.B.: 621.0 m (2037.50 ft)
Core Interval: 445.0 - 488.0 m (1460.5 - 1601.3 ft)

Logged by: L.M. Wickert
Date: November 17, 1987
Page 2 of 2

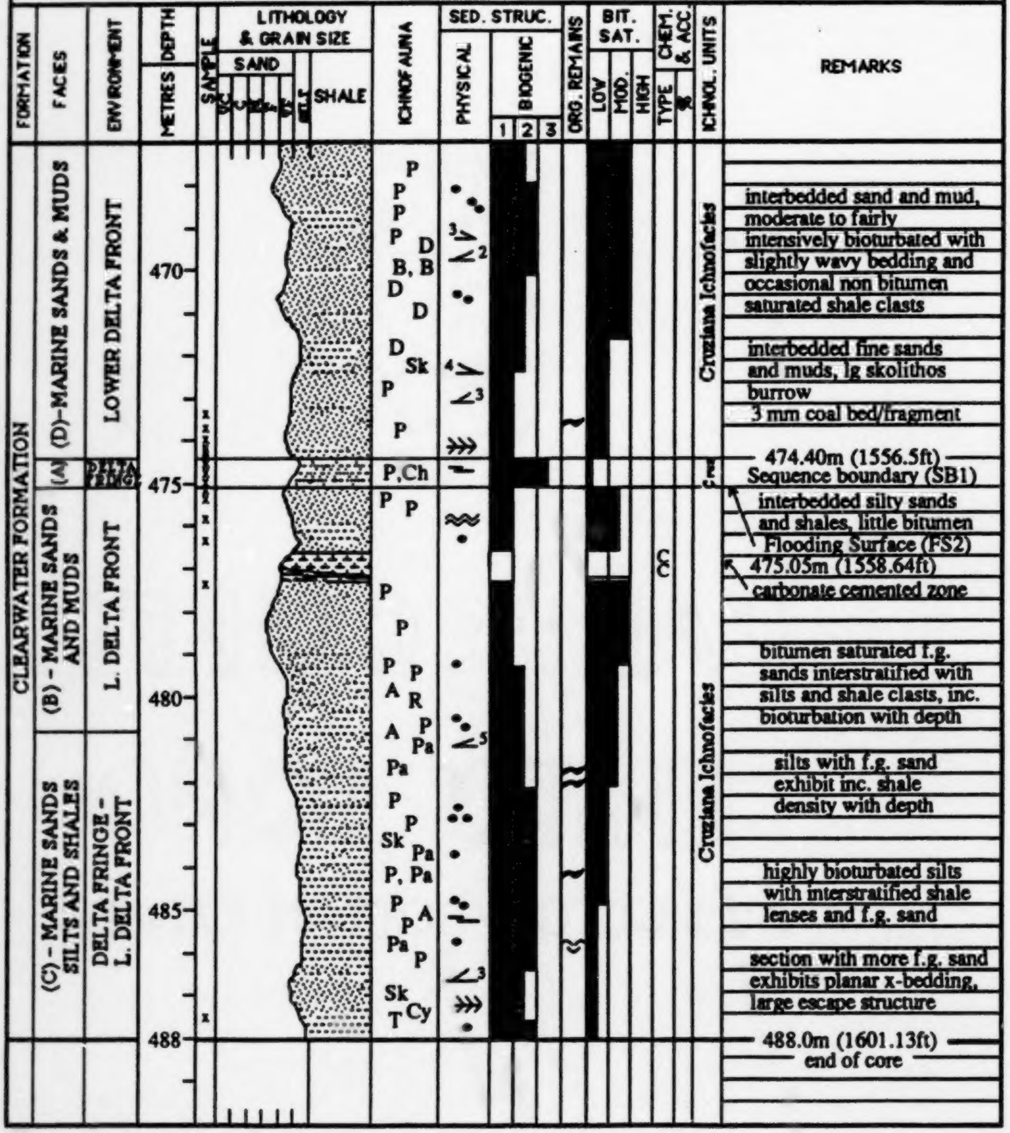
FORMATION
FACIES
ENVIRONMENT
DEPTH
METRES
SAMPLE
LITHOLOGY & GRAIN SIZE
SAND
SILT
SHALE
ICHNOFAUNA
SED. STRUC.
PHYSICAL
BIOGENIC
1
2
3
ORG. REMAINS
BIT. SAT.
LOW
MOD.
HIGH
CHEM. & ACC.
TYPE
%
ICHNOL. UNITS
REMARKS
CLEARWATER FORMATION
(D)-MARINE SANDS & MUDS
(A)
(B) - MARINE SANDS AND MUDS
(C) - MARINE SANDS SILTS AND SHALES
LOWER DELTA FRONT
DELTA FRINGE
L. DELTA FRONT
DELTA FRINGE - L. DELTA FRONT
470
475
480
485
488
P
P
P
P D
B, B
D
D
D
Sk
P
P
P,Ch
P P
P
P
P P
A R
A P
Pa
Pa
P
P
Sk Pa
P, Pa
P A
P
Pa P
Sk
T Cy
3
2
4
3
5
3
CC
Cruziana Ichnofacies
Cruziana Ichnofacies

interbedded sand and mud, moderate to fairly intensively bioturbated with slightly wavy bedding and occasional non bitumen saturated shale clasts

interbedded fine sands and muds, lg skolithos burrow

3 mm coal bed/fragment

474.40m (1556.5ft)
Sequence boundary (SB1)

interbedded silty sands and shales, little bitumen

Flooding Surface (FS2)
475.05m (1558.64ft)

carbonate cemented zone

bitumen saturated f.g. sands interstratified with silts and shale clasts, inc. bioturbation with depth

silts with f.g. sand exhibit inc. shale density with depth

highly bioturbated silts with interstratified shale lenses and f.g. sand

section with more f.g. sand exhibits planar x-bedding, large escape structure

488.0m (1601.13ft)
end of core

CLASTIC LOGGING FORM

Well Location: 3-28-66-2W4 Imp. 77 O.V.
K.B.: 619.4 m (2032.25 ft)
Core Interval: 451.7 – 499.54 m (1482 – 1639 ft)

Logged by: L.M. Wickert
Date: August 20, 1987
Page 1 of 3

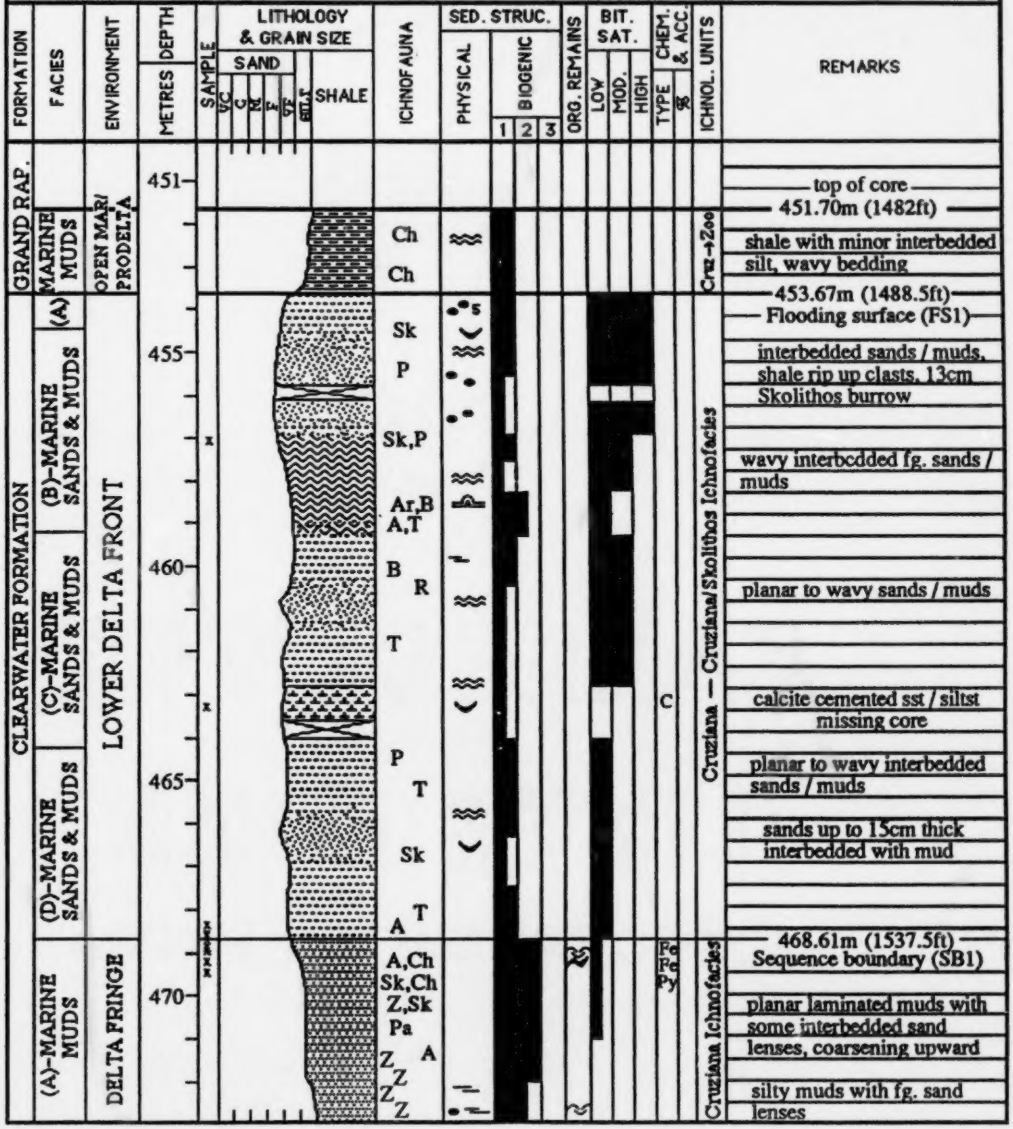
FORMATION
FACIES
ENVIRONMENT
DEPTH
METRES
SAMPLE
LITHOLOGY & GRAIN SIZE
SAND
VC
C
M
F
VF
SILT
SHALE
ICHNOFAUNA
SED. STRUC.
PHYSICAL
BIOGENIC
1
2
3
ORG. REMAINS
BIT. SAT.
LOW
MOD.
HIGH
CHEM. & ACC.
TYPE
%
ICHNOL. UNITS
REMARKS
GRAND RAP.
CLEARWATER FORMATION
MARINE MUDS
(A)
(B)-MARINE SANDS & MUDS
(C)-MARINE SANDS & MUDS
(D)-MARINE SANDS & MUDS
(A)-MARINE MUDS
OPEN MAR/ PRODELTA
LOWER DELTA FRONT
DELTA FRINGE
451
455
460
465
470
Ch
Ch
Sk
P
Sk,P
Ar,B
A,T
B
R
T
P
T
Sk
T
A
A,Ch
Sk,Ch
Z,Sk
Pa
Z
A
Z
Z
Z
s
C
Fe
Fe
Py
Cruz→Zoo
Cruziana — Cruziana/Skolithos Ichnofacies
Cruziana Ichnofacies

top of core
451.70m (1482ft)
shale with minor interbedded silt, wavy bedding
453.67m (1488.5ft)
Flooding surface (FS1)
interbedded sands / muds, shale rip up clasts, 13cm Skolithos burrow
wavy interbcdded fg. sands / muds
planar to wavy sands / muds
calcite cemented sst / siltst
missing core
planar to wavy interbedded sands / muds
sands up to 15cm thick interbedded with mud
468.61m (1537.5ft)
Sequence boundary (SB1)
planar laminated muds with some interbedded sand lenses, coarsening upward
silty muds with fg. sand lenses

CLASTIC LOGGING FORM

Well Location: 3-28-66-2W4 Imp. 77 O.V.
K.B.: 619.4 m (2032.25 ft)
Core Interval: 451.70 - 499.54 m (1482 - 1639 ft)

Logged by: L.M. Wickert
Date: August 20, 1987
Page 2 of 3

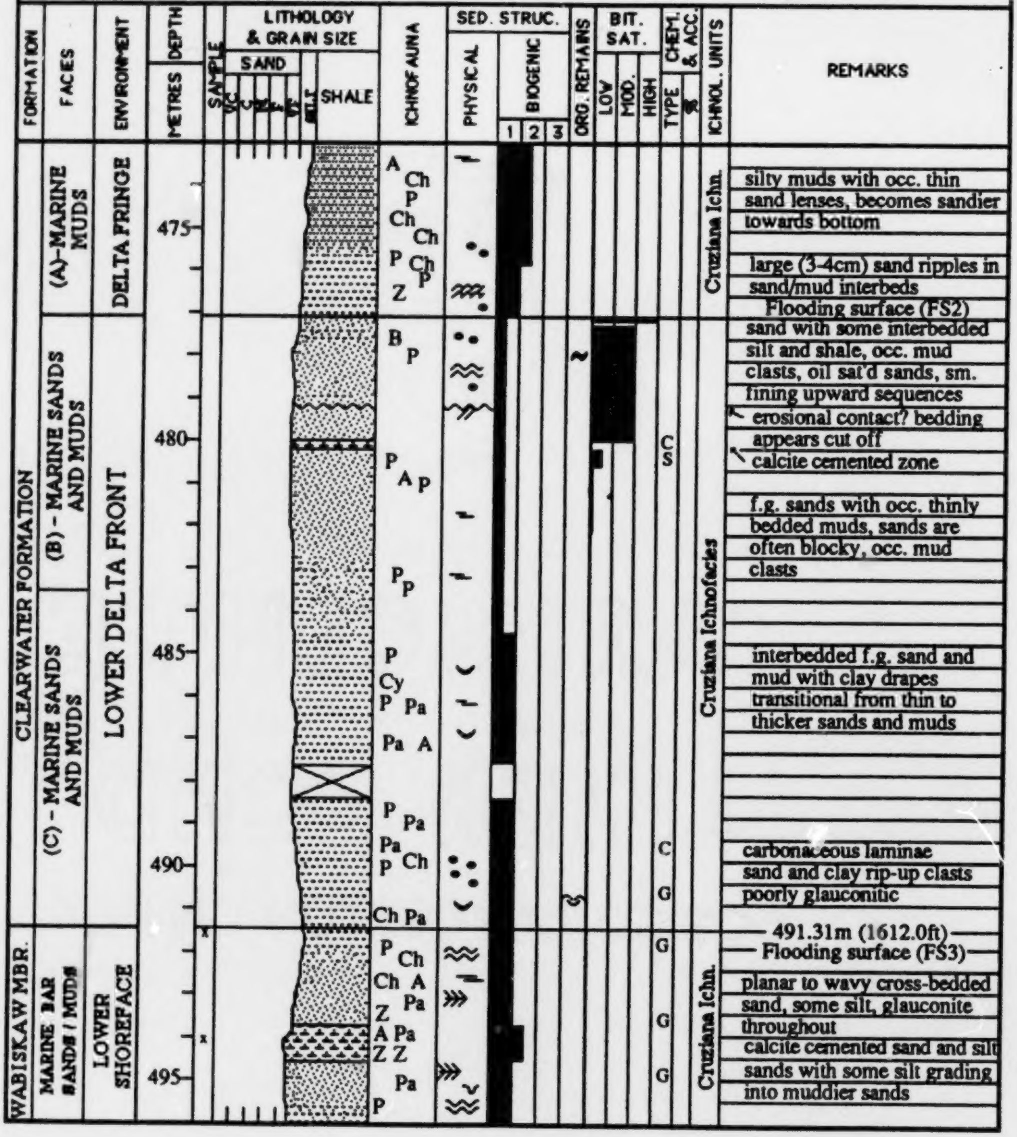
FORMATION
FACIES
ENVIRONMENT
DEPTH
METRES
SAMPLE
LITHOLOGY & GRAIN SIZE
SAND
SILT
SHALE
ICHNOFAUNA
SED. STRUC.
PHYSICAL
BIOGENIC
1
2
3
ORG. REMAINS
BIT. SAT.
LOW
MOD.
HIGH
CHEM. & ACC.
TYPE
%
ICHNOL. UNITS
REMARKS
CLEARWATER FORMATION
WABISKAW MBR.
(A)-MARINE MUDS
(B) - MARINE SANDS AND MUDS
(C) - MARINE SANDS AND MUDS
MARINE BAR SANDS / MUDS
DELTA FRINGE
LOWER DELTA FRONT
LOWER SHOREFACE
475
480
485
490
495
A Ch P Ch Ch P Ch P Z
B P
P A P
P P
P Cy P Pa Pa A
P Pa Pa P Ch Ch Pa
P Ch Ch A Z Pa A Pa Z Z Pa P
C S
C
G
G
G
G
Cruziana Ichn.
Cruziana Ichnofacies
Cruziana Ichn.

silty muds with occ. thin sand lenses, becomes sandier towards bottom

large (3-4cm) sand ripples in sand/mud interbeds

Flooding surface (FS2)

sand with some interbedded silt and shale, occ. mud clasts, oil sat'd sands, sm. fining upward sequences

erosional contact? bedding appears cut off

calcite cemented zone

f.g. sands with occ. thinly bedded muds, sands are often blocky, occ. mud clasts

interbedded f.g. sand and mud with clay drapes transitional from thin to thicker sands and muds

carbonaceous laminae

sand and clay rip-up clasts

poorly glauconitic

491.31m (1612.0ft)

Flooding surface (FS3)

planar to wavy cross-bedded sand, some silt, glauconite throughout

calcite cemented sand and silt

sands with some silt grading into muddier sands

CLASTIC LOGGING FORM

Well Location: 3-28-66-2W4 Imp. 77 O.V.
K.B.: 619.4 m (2032.25 ft)
Core Interval: 451.70 - 499.54 m (1482 – 1639 ft)

Logged by: L.M. Wickert
Date: August 20, 1987
Page 3 of 3

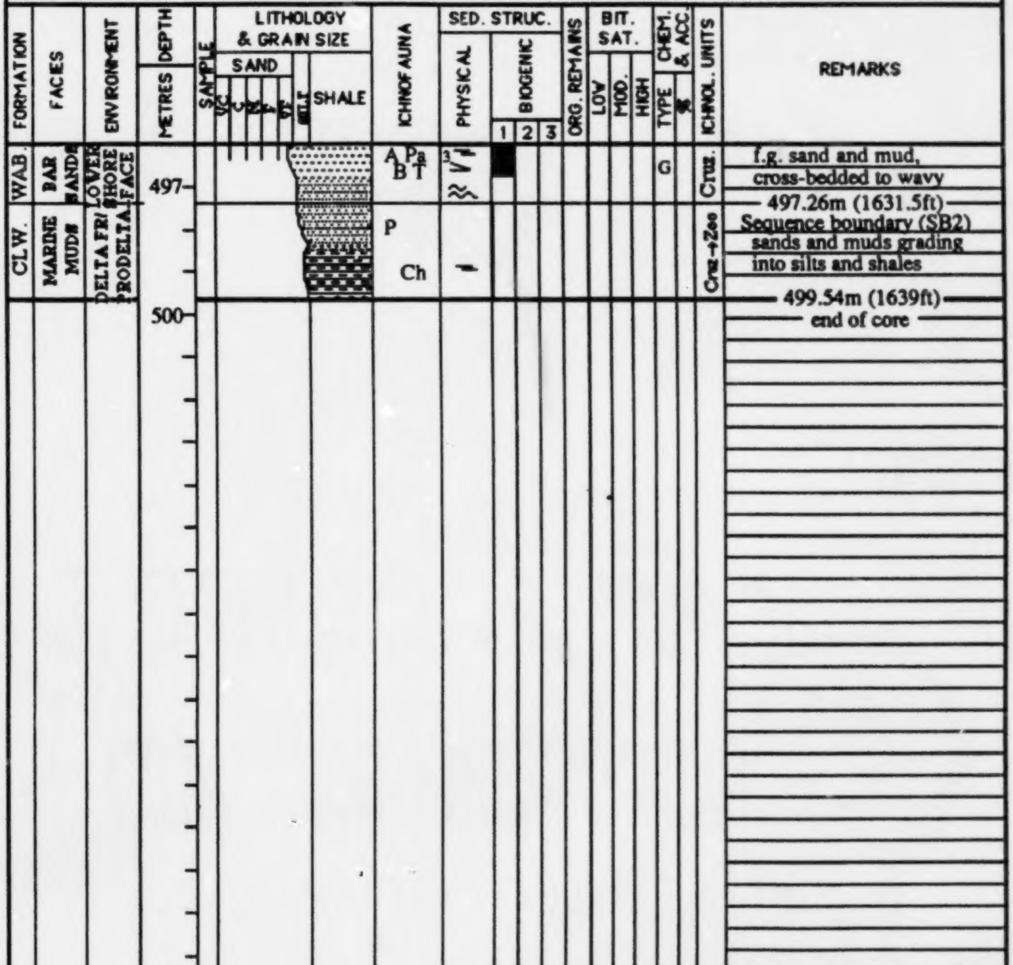
FORMATION
FACES
ENVIRONMENT
DEPTH
METRES
SAMPLE
LITHOLOGY & GRAIN SIZE
SAND
VC
C
M
F
VF
SILT
SHALE
ICHNOFAUNA
SED. STRUC.
PHYSICAL
BIOGENIC
1
2
3
ORG. REMAINS
BIT. SAT.
LOW
MOD.
HIGH
CHEM. & ACC.
TYPE
%
ICHNOL. UNITS
REMARKS
WAB.
BAR SANDS
LOWER SHORE FACE
CLW.
MARINE MUDS
DELTA FR/ PRODELTA
497
500
A Pa
B T
P
Ch
3
G
Cruz.
Cruz→Zoo

f.g. sand and mud,
cross-bedded to wavy
497.26m (1631.5ft)
Sequence boundary (SB2)
sands and muds grading
into silts and shales
499.54m (1639ft)
end of core

CLASTIC LOGGING FORM

Well Location: 6-31-66-2W4 Esso 86 Cold Lake O.V.
K.B.: 644.0 m (2113 ft)
Core Interval: 486.0 - 519.5 m (1594.57 - 1704.48 ft)

Logged by: L.M. Wickert
Date: October 21, 1987
Page 1 of 2

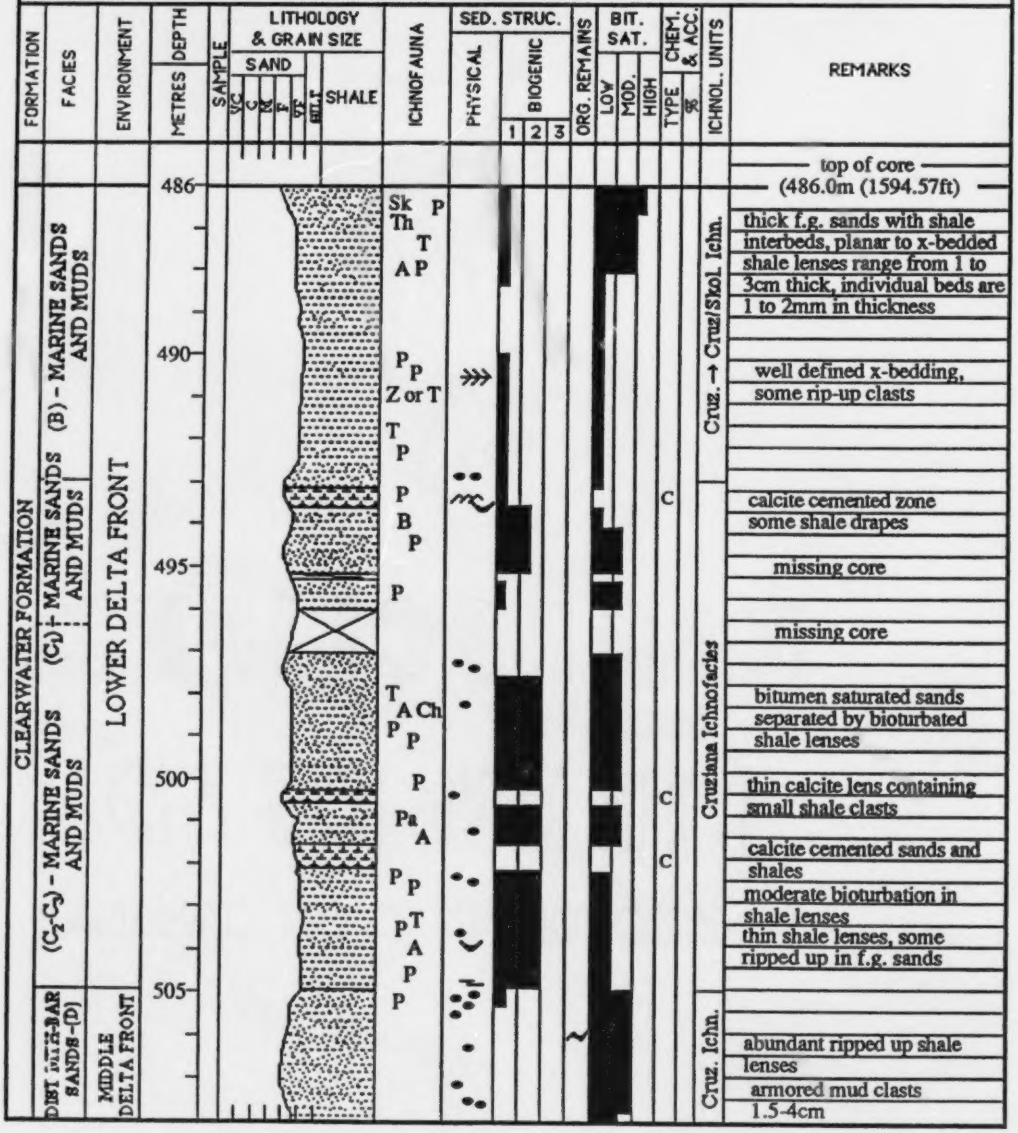
FORMATION
FACIES
ENVIRONMENT
DEPTH
METRES
SAMPLE
LITHOLOGY & GRAIN SIZE
SAND
VC C M F VF
SILT
SHALE
ICHNOFAUNA
SED. STRUC.
PHYSICAL
BIOGENIC
1 2 3
ORG. REMAINS
BIT. SAT.
LOW
MOD.
HIGH
CHEM. & ACC.
TYPE
%
ICHNOL. UNITS
REMARKS
CLEARWATER FORMATION
(B) - MARINE SANDS AND MUDS
(C1) - MARINE SANDS AND MUDS
(C2-C3) - MARINE SANDS AND MUDS
DIST. MTH-BAR SANDS - (D)
LOWER DELTA FRONT
MIDDLE DELTA FRONT
486
490
495
500
505
Sk P
Th
T
A P
P P
Z or T
T
P
P
B
P
P
T
A Ch
P P
P
Pa
A
P P
P T
A
P
P
C
C
C
Cruz. → Cruz/Skol. Ichn.
Cruziana Ichnofacies
Cruz. Ichn.
top of core
(486.0m (1594.57ft)
thick f.g. sands with shale interbeds, planar to x-bedded shale lenses range from 1 to 3cm thick, individual beds are 1 to 2mm in thickness
well defined x-bedding, some rip-up clasts
calcite cemented zone
some shale drapes
missing core
missing core
bitumen saturated sands separated by bioturbated shale lenses
thin calcite lens containing small shale clasts
calcite cemented sands and shales
moderate bioturbation in shale lenses
thin shale lenses, some ripped up in f.g. sands
abundant ripped up shale lenses
armored mud clasts 1.5-4cm

CLASTIC LOGGING FORM

Well Location: 6-31-66-2W4 Esso 86 Cold Lake O.V.
K.B.: 644.0 m (2113 ft)
Core Interval: 486.0 - 519.5 m (1594.57 - 1704.48 ft)

Logged by: L.M. Wickert
Date: October 21, 1987
Page 2 of 2

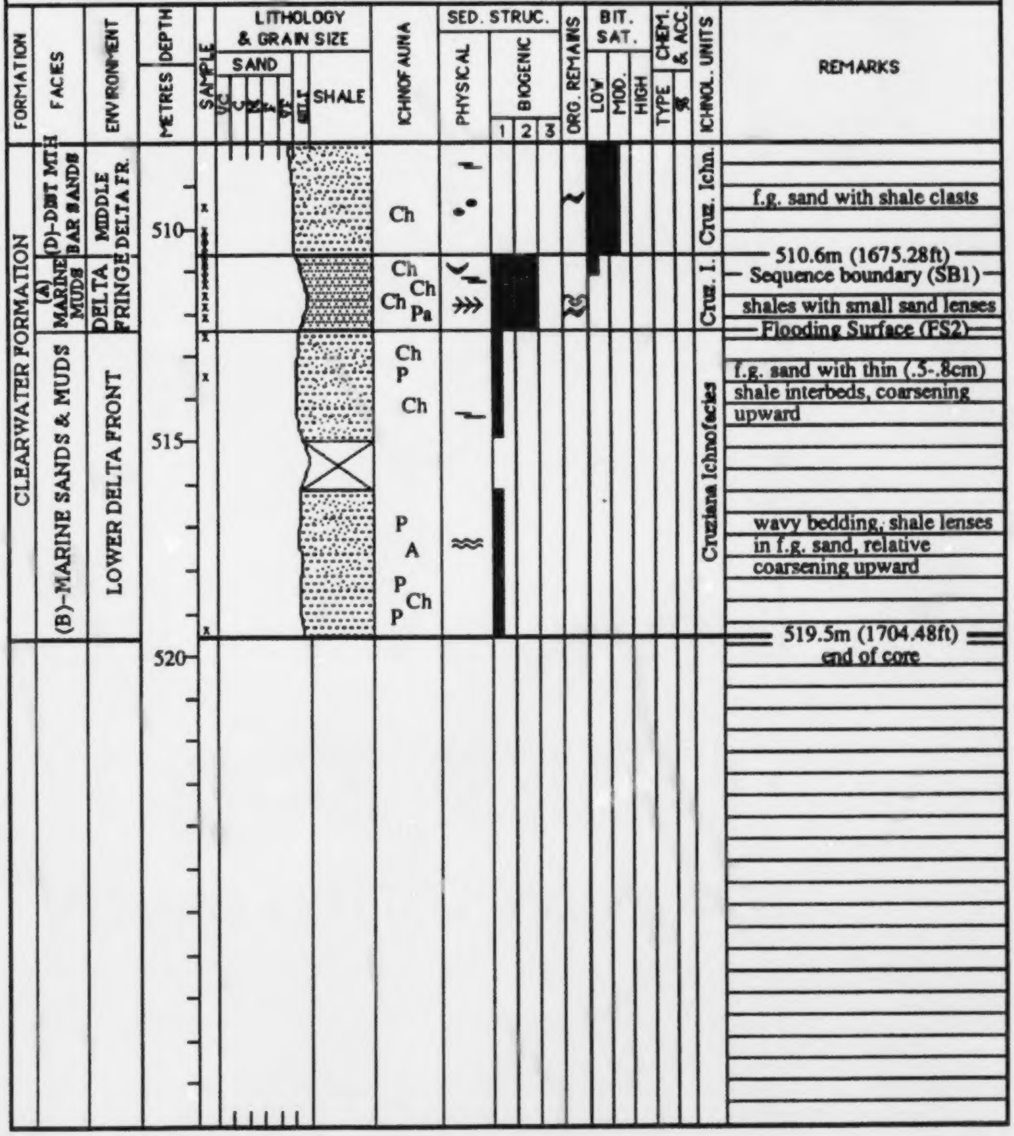
FORMATION
FACIES
ENVIRONMENT
DEPTH
METRES
SAMPLE
LITHOLOGY & GRAIN SIZE
SAND
VC
SILT
SHALE
ICHNOFAUNA
SED. STRUC.
PHYSICAL
BIOGENIC
1
2
3
ORG. REMAINS
BIT. SAT.
LOW
MOD.
HIGH
CHEM. & ACC.
TYPE
%
ICHNOL. UNITS
REMARKS
CLEARWATER FORMATION
(D)-DIST MTH BAR SANDS
(A) MARINE MUDS
(B)-MARINE SANDS & MUDS
MIDDLE DELTA FR.
DELTA FRINGE
LOWER DELTA FRONT
510
515
520
Ch
Ch
Ch
Ch
Pa
Ch
P
Ch
P
A
P
Ch
P
Cruz. Ichn.
Cruz. I.
Cruziana Ichnofacies
f.g. sand with shale clasts
510.6m (1675.28ft)
Sequence boundary (SB1)
shales with small sand lenses
Flooding Surface (FS2)
f.g. sand with thin (.5-.8cm) shale interbeds, coarsening upward
wavy bedding, shale lenses in f.g. sand, relative coarsening upward
519.5m (1704.48ft) end of core

APPENDIX 2:

CROSS-SECTION (A - A')

(contained within back pocket)

APPENDIX 3:

MINERALOGICAL DATA

List of Tables:

Point Count Data for Petrographic Classification of Clearwater Sands

Summary of Whole Rock XRD Data

Whole Rock XRD Mineral Data for Fine to Medium Grained Sands

Whole Rock XRD Mineral Data for Very Fine to Fine Grained Sands with Silt or Shale

Whole Rock XRD Mineral Data for Sandy Silts or Shales

Whole Rock XRD Mineral Data for Calcite Cemented Intervals

Summary of < 45µm XRD Data

< 45µm XRD Mineral Data for Fine to Medium Grained Sands

< 45µm XRD Mineral Data for Very Fine to Fine Grained Sands with Silt or Shale

<45 µm XRD Mineral Data for Sandy Silts or Shales

< 45µm XRD Mineral Data for Calcite Cemented Intervals

Summary of < 2µm XRD Data

Results from < 2µm Mineralogic Analysis - 3-13-65-4W4

Results from < 2µm Mineralogic Analysis - 16-2-66-3W4

Results from < 2µm Mineralogic Analysis - 8-19-66-2W4

POINT COUNT DATA FOR PETROGRAPHIC CLASSIFICATION OF CLEARWATER SANDS IN STUDY AREA

Sample*	% Quartz	% Feldspar	% Rock Fragments	Total
1	50.0	19.0	31.0	100
2	48.5	20.7	30.8	100
3	48.2	18.4	33.4	100
4	46.5	22.3	31.2	100
5	46.5	20.2	33.3	100
6	46.2	18.3	35.5	100
7	43.7	21.6	34.7	100
8	43.2	19.4	37.4	100
9	44.0	16.6	39.4	100
10	39.5	21.6	38.9	100

* 400 point grid counted per sample.

SUMMARY OF WHOLE ROCK XRD DATA – Clearwater Formation Study Area

SAMPLE NUMBER	LITHOLOGY	DEPTH (metres)	XRD RELATIVE ABUNDANCE (%)*														
			Qtz	Pl	KF	Chl	SC	10Å	7Å	Cal	Dol	Sid	Py	Amp	Ilm	Mag	Total
Well 3-28-66-2W4 Imp. 77 O.V.																	
LW3-90	si,f.g.sst,m	457.03	39.5	13.2	1.7	0.0	8.2	16.6	2.9	0.0	0.0	14.3	2.2	1.4	0.0	0.0	100
LW3-20	f.g.sst,m,c	463.21	29.6	7.3	4.6	1.2	0.0	5.8	1.8	45.1	1.4	1.2	0.0	2.0	0.0	0.0	100
LW3-36	f.g.sst,si	468.24	32.3	36.4	12.8	1.2	0.0	4.9	5.4	0.0	2.4	1.0	0.0	3.5	0.0	0.0	100
LW-87-CW-58	f.g.sst,si	468.51	53.0	29.3	3.0	0.8	0.4	3.0	4.8	0.0	4.4	1.1	0.0	0.3	0.0	0.0	100
LW-87-CW-59	f.g.sst,si	468.61	54.9	12.3	3.8	2.2	2.7	10.0	7.6	0.0	3.5	2.3	0.8	0.0	0.0	0.0	100
LW3-38	f.g.sst,si,m,c	468.76	29.0	30.6	9.7	1.8	0.7	7.4	5.9	6.8	0.0	2.0	5.3	0.9	0.0	0.0	100
LW3-39	f.g.sst,si	468.91	53.5	14.9	1.5	2.8	3.0	12.0	2.3	0.0	7.7	1.2	0.8	0.4	0.0	0.0	100
LW3-66	sh,tr.sst,si	477.14	46.0	5.8	3.1	7.1	7.5	15.9	0.6	0.0	2.9	10.4	0.8	0.0	0.0	0.0	100
LW3-73	f.g.sst	479.27	49.6	25.4	11.5	1.2	0.8	4.6	4.2	0.0	0.0	2.2	0.0	0.6	0.0	0.0	100
LW3-13	sh,tr.sst,si	491.62	65.9	7.1	3.6	3.1	3.7	9.0	3.7	0.0	2.6	0.0	1.3	0.0	0.0	0.0	100
LW3-21	f.g.sst,si,c	494.15	32.6	1.2	1.2	0.7	0.5	4.3	1.7	29.2	17.8	9.3	0.5	0.8	0.0	0.0	100
Well 6-31-66-2W4 Esso 86 Cold Lake O.V.																	
LW-87-CW-10	f.g.sst,tr.sh	509.60	41.7	31.2	4.0	1.0	0.0	12.5	5.4	0.0	2.6	1.0	0.0	0.8	0.0	0.0	100
LW-87-CW-11	f.g.sst,si	510.10	53.5	8.8	9.5	1.9	2.2	16.2	5.0	0.0	1.6	0.0	0.0	1.3	0.0	0.0	100
LW-87-CW-12	f.g.sst,tr.sh	510.30	51.7	15.7	9.0	1.8	1.4	9.4	7.6	0.0	0.0	0.0	0.9	0.0	0.0	2.6	100
LW-87-CW-13	f.g.sst,tr.sh	510.40	60.5	15.0	9.6	1.1	0.9	8.5	3.8	0.0	0.0	0.0	0.0	0.7	0.0	0.0	100
LW-87-CW-14	f.g.sst,tr.sh	510.50	62.9	15.5	4.7	1.5	0.0	9.3	5.3	0.0	0.0	0.0	0.8	0.0	0.0	0.0	100
LW-87-CW-15	f.g.sst,tr.sh	510.60	56.1	20.1	6.5	1.4	1.1	8.6	4.8	0.0	0.0	0.0	0.7	0.8	0.0	0.0	100
LW-87-CW-16	f.g.sst,si	510.70	59.4	9.2	4.6	1.8	8.7	8.2	4.5	0.0	0.0	0.0	2.1	1.5	0.0	0.0	100
LW-87-CW-17	sh,tr.sst,si	510.80	42.4	17.8	6.2	1.9	12.7	11.6	4.4	0.0	0.0	0.0	0.9	2.0	0.0	0.0	100
LW-87-CW-18	sh,tr.sst,si	510.90	49.3	7.0	4.1	1.9	11.8	13.0	6.4	0.0	3.7	0.0	1.6	1.1	0.0	0.0	100
LW-87-CW-19	sh,tr.sst,si	511.00	43.2	10.9	5.4	3.3	16.9	12.5	1.3	0.0	3.2	0.0	1.6	1.7	0.0	0.0	100
LW-87-CW-20	v.f.g.sst,si,sh	511.20	57.4	9.3	5.2	1.9	7.5	8.6	4.8	0.0	3.3	0.0	1.1	1.0	0.0	0.0	100

SUMMARY OF WHOLE ROCK XRD DATA – Clearwater Formation Study Area (cont'd)

SAMPLE NUMBER	LITHOLOGY	DEPTH (metres)	XRD RELATIVE ABUNDANCE (%)*													
			Qtz	Pl	KF	Chl	SC	10Å	7Å	Cal	Dol	Sid	Py	Amp	Ilm	Mag	Total
Well 6-31-66-2W4 Esso 86 Cold Lake O.V.																	
LW-87-CW-21	v.f.g.sst,tr.sh	511.40	58.7	5.0	1.8	1.8	2.6	9.4	5.0	0.0	13.9	0.0	1.0	0.8	0.0	0.0	100
LW-87-CW-22	v.f.g.sst,si,sh	511.65	63.3	10.7	2.9	2.0	4.2	7.9	3.4	0.0	4.5	0.0	1.1	0.0	0.0	0.0	100
LW-87-CW-23	v.f.g.sst,tr.sh	511.80	59.9	11.6	3.9	1.4	5.2	7.8	3.8	0.0	4.7	0.0	0.6	1.2	0.0	0.0	100
LW-87-CW-24	v.f.g.sst,sh	512.10	59.4	8.8	4.3	2.2	7.7	8.6	5.4	0.0	2.1	0.0	1.6	0.0	0.0	0.0	100
LW-87-CW-25	sh,tr.si,sst	512.60	53.0	6.2	11.8	2.1	9.5	13.4	2.9	0.0	0.0	0.0	1.1	0.0	0.0	0.0	100
LW-87-CW-26	f.g.sst	513.55	59.7	17.2	2.9	1.2	0.0	6.1	6.5	0.0	0.0	5.4	0.4	0.7	0.0	0.0	100
LW-87-CW-27	f.g.sst	519.40	48.8	29.5	3.2	1.9	1.0	3.5	6.8	0.0	0.0	1.7	0.0	0.0	3.6	0.0	100
Well 3-13-65-4W4 Esso 84 (C1-12) Cold Lk.																	
LW-87-CW-28	f.-m.g.sst	470.25	40.1	47.6	1.4	1.0	0.9	3.1	3.9	0.0	0.0	1.3	0.0	0.0	0.7	0.0	100
LW-87-CW-29	f.-m.g.sst	480.20	66.8	19.2	1.2	1.0	0.0	2.8	3.2	0.0	0.0	2.4	0.5	0.7	0.0	2.2	100
LW-87-CW-30	f.g.sst,tr.m	480.50	44.1	15.7	22.6	1.4	2.2	7.7	2.9	0.0	0.0	2.4	0.4	0.6	0.0	0.0	100
LW-87-CW-31	f.-m.g.sst	480.80	43.2	37.6	2.0	1.3	0.9	5.5	4.7	0.0	0.0	3.1	0.3	0.0	0.0	1.4	100
LW-87-CW-32	f.g.sst	481.00	50.0	18.3	19.4	1.1	0.0	4.0	3.1	0.0	0.0	3.3	0.0	0.0	0.0	0.8	100
LW-87-CW-33	sh,sst,si	481.10	55.9	9.4	2.8	1.7	2.0	15.9	6.4	0.0	3.4	2.6	0.0	0.0	0.0	0.0	100
LW-87-CW-34	f.g.sst,m	481.20	57.6	17.6	3.1	1.9	2.4	7.9	6.0	0.0	0.0	2.5	0.0	0.0	0.0	1.1	100
LW-87-CW-35	f.g.sst,tr.sh	481.30	54.7	20.8	10.1	1.1	1.4	6.1	3.9	0.0	0.0	0.0	1.2	0.7	0.0	0.0	100
LW-87-CW-36	f.g.sst	481.40	55.4	20.3	5.9	1.6	0.8	5.8	5.5	0.0	0.0	2.3	1.0	0.3	0.0	1.2	100
LW-87-CW-37	f.g.sst,m	481.60	54.1	25.2	3.0	1.5	1.3	6.5	4.1	0.0	0.0	2.7	1.0	0.6	0.0	0.0	100
LW-87-CW-38	f.g.sst	481.80	51.1	24.1	10.8	1.1	0.0	4.0	4.9	0.0	0.0	2.3	0.6	0.0	0.0	1.0	100
LW-87-CW-39	f.g.sst,si	482.20	51.2	28.5	2.3	1.4	0.9	6.3	5.6	0.0	2.2	0.0	0.3	0.0	0.0	1.2	100
LW-87-CW-40	f.g.sst	483.20	62.3	17.4	3.7	1.4	0.0	6.4	4.3	0.0	0.0	3.2	0.0	0.0	0.0	1.4	100
LW-87-CW-41	f.g.sst	491.20	54.9	15.0	9.8	1.5	0.0	5.7	4.8	0.0	0.0	7.7	0.0	0.0	0.0	0.7	100
LW-87-CW-41	> 45 µm§	491.20	27.9	66.0	2.7	0.6	0.0	1.9	0.0	0.0	0.0	0.9	0.0	0.0	0.0	0.0	100
LW-87-CC-01	concretion	481.00	37.1	8.7	3.2	2.2	6.4	7.2	7.3	0.0	0.0	26.6	0.0	0.0	0.0	1.3	100

SUMMARY OF WHOLE ROCK XRD DATA – Clearwater Formation Study Area (cont'd)

SAMPLE NUMBER	LITHOLOGY	DEPTH (metres)	XRD RELATIVE ABUNDANCE (%)* Qtz	Pl	KF	Chl	SC	10Å	7Å	Cal	Dol	Sid	Py	Amp	Ilm	Mag	Total
Well 8-19-66-2W4 Esso 86 Marie O.V.																	
LW-87-CW-42	si,f.g.sst	473.40	44.0	27.1	3.6	1.6	2.4	9.2	3.8	0.0	5.7	1.0	0.0	0.0	0.0	1.5	100
LW-87-CW-43	f.g.sst,m	473.70	62.1	9.8	4.8	2.3	3.7	10.1	6.3	0.0	0.0	0.0	0.0	0.9	0.0	0.0	100
LW-87-CW-44	f.g.sst	474.00	53.6	21.9	3.0	0.9	1.0	8.4	7.8	0.0	1.9	0.9	0.0	0.7	0.0	0.0	100
LW-87-CW-45	f.-m.g.sst,sh	474.20	37.3	21.3	16.4	1.2	0.8	5.7	5.9	0.0	7.4	0.0	0.0	0.0	0.0	4.1	100
LW-87-CW-46	f.g.sst,si	474.30	69.0	4.4	5.1	1.7	2.1	9.1	7.7	0.0	0.0	0.0	0.0	0.9	0.0	0.0	100
LW-87-CW-47	si,sh	474.40	59.0	6.1	2.5	2.3	11.0	13.2	4.4	0.0	0.0	0.0	1.5	0.0	0.0	0.0	100
LW-87-CW-48	sh,si	474.50	52.6	15.1	4.2	2.3	6.3	10.0	8.1	0.0	0.0	0.0	0.7	0.6	0.0	0.0	100
LW-87-CW-49	f.g.sst,sh	474.60	63.3	17.7	3.9	1.6	1.7	6.7	5.0	0.0	0.0	0.0	0.0	0.0	0.0	0.0	100
LW-87-CW-50	sh,si	474.80	57.9	10.7	4.0	1.4	8.8	9.5	6.5	0.0	0.0	0.0	1.3	0.0	0.0	0.0	100
LW-87-CW-51	sh,f.g.sst	475.00	55.3	17.9	3.6	1.3	6.6	6.0	3.3	4.1	0.0	0.0	1.0	0.8	0.0	0.0	100
LW-87-CW-54	f.g.sst,si	475.90	63.4	16.5	4.8	1.4	8.5	2.6	1.6	0.0	0.0	0.0	0.4	0.8	0.0	0.0	100
LW-87-CW-55	f.g.sst,sh	476.40	46.4	19.4	12.2	1.6	1.6	7.1	6.4	0.0	0.0	3.9	0.0	0.0	0.0	1.4	100
LW-87-CW-56	sh,si,c	477.40	6.5	2.0	0.0	1.4	2.4	5.8	0.9	79.3	0.0	1.7	0.0	0.0	0.0	0.0	100
LW-87-CW-57	f.g.sst,si	487.53	48.1	27.2	2.5	1.7	6.9	3.8	3.3	0.0	6.5	0.0	0.0	0.0	0.0	0.0	100
Well 16-2-66-3W4 Imp. 77 Medley O.V.																	
LW-87-CW-92	si,f.g.sst,c	453.57	24.7	5.2	0.8	0.5	0.5	1.3	1.0	65.3	0.0	0.7	0.0	0.0	0.0	0.0	100
LW-87-CW-61	f.g.sst	463.60	61.7	23.7	5.2	0.7	0.0	2.9	2.2	0.0	2.2	1.1	0.3	0.0	0.0	0.0	100
LW-87-CW-62	f.g.sst,si	464.24	51.7	18.3	14.9	1.5	1.2	5.2	4.3	0.0	0.0	2.2	0.0	0.6	0.0	0.0	100
LW-87-CW-63	f.g.sst	464.44	39.0	42.5	8.7	0.9	0.4	3.2	2.2	0.0	2.5	0.7	0.0	0.0	0.0	0.0	100
LW-87-CW-64	f.g.sst,sh	464.68	44.1	8.9	16.1	1.3	0.0	1.1	7.9	0.0	19.1	0.0	0.0	0.0	0.0	1.6	100
LW-87-CW-65	f.g.sst,si	464.75	60.0	11.4	2.4	1.1	0.9	9.3	4.0	0.0	6.3	0.0	4.6	0.0	0.0	0.0	100
LW-87-CW-66	f.g.sst,sh,c	464.84	35.0	8.5	0.8	1.0	1.5	3.5	0.5	47.1	0.0	1.2	0.0	0.9	0.0	0.0	100

SUMMARY OF WHOLE ROCK XRD DATA – Clearwater Formation Study Area (cont'd)

SAMPLE NUMBER	LITHOLOGY	DEPTH (metres)	XRD RELATIVE ABUNDANCE (%)*														
			Qtz	Pl	KF	Chl	SC	10Å	7Å	Cal	Dol	Sid	Py	Amp	Ilm	Mag	Total
Well 16-2-66-3W4 Imp. 77 Medley O.V.																	
LW-87-CW-67	f.g.sst	465.03	44.3	17.0	18.4	1.2	0.9	4.9	5.5	0.0	3.2	3.8	0.8	0.0	0.0	0.0	100
LW-87-CW-68	f.g.sst,si	465.43	56.9	16.9	4.5	1.3	2.7	4.8	0.0	3.3	3.9	2.3	1.3	0.7	0.0	1.5	100
LW-87-CW-69	f.g.sst,si	465.85	50.0	19.8	3.5	1.1	1.2	7.1	4.2	0.0	4.6	5.7	1.5	0.0	0.0	1.3	100
LW-87-CW-70	f.g.sst,si,sh	466.45	44.5	25.8	9.7	1.5	3.0	5.7	5.7	0.0	0.0	1.7	0.8	0.9	0.9	0.0	100
LW-87-CW-71	f.g.sst	467.07	56.0	9.7	3.1	1.0	1.2	3.5	2.8	0.0	4.9	11.2	0.4	0.4	4.0	1.9	100
LW-87-CW-72	f.g.sst,sh	467.64	30.8	51.7	4.0	0.8	3.8	2.9	1.8	0.0	2.4	0.4	0.2	0.0	0.0	1.3	100
LW-87-CW-73	f.g.sst,sh	473.94	50.4	25.0	1.9	1.5	5.2	6.4	5.8	0.0	2.6	0.0	1.3	0.0	0.0	0.0	100
Well 12-18-65-3W4 Imp. 77 Medley O.V.																	
LW-87-CW-75	f.g.sst	464.64	67.2	8.9	15.4	1.0	0.0	3.8	2.0	0.0	0.0	1.7	0.0	0.0	0.0	0.0	100
LW-87-CW-76	f.g.sst	465.05	66.4	18.3	0.0	1.4	0.0	3.4	4.5	0.0	0.0	6.0	0.0	0.0	0.0	0.0	100
LW-87-CW-77	f.g.sst	465.27	47.3	25.5	9.0	0.8	0.0	3.5	3.8	0.0	0.0	0.7	2.4	0.0	0.6	6.4	100
LW-87-CW-80	f.g.sst	466.32	52.8	23.9	4.1	1.1	1.0	5.3	2.3	0.0	0.0	5.8	1.3	0.0	0.0	2.5	100
LW-87-CW-81	f.g.sst,sh	466.93	50.8	18.6	2.3	1.5	5.5	8.1	7.6	0.0	0.0	2.9	0.5	0.9	0.0	1.3	100
LW-87-CW-82	f.g.sst,sh	467.88	50.5	21.5	0.0	1.6	1.6	10.7	6.0	0.0	4.5	0.9	2.4	0.0	0.0	0.0	100
Well 5-22-65-3W4 Imp. Marie O.V.																	
LW-87-CW-93	f.g.sst,sh,c	430.97	27.7	8.9	2.8	0.6	0.0	3.6	2.8	51.3	0.0	1.5	0.0	0.7	0.0	0.0	100
LW-87-CW-83	f.g.sst.	433.40	41.3	19.0	25.1	1.0	0.7	4.7	6.3	0.0	0.0	1.9	0.0	0.0	0.0	0.0	100
LW-87-CW-84	f.g.sst,si,sh	440.75	57.8	19.7	3.4	1.8	1.5	8.5	5.8	0.0	0.0	0.0	0.0	0.0	0.0	1.4	100
LW-87-CW-85	f.g.sst	441.69	53.2	33.4	1.2	1.7	2.6	3.9	2.4	0.0	0.0	0.0	0.4	0.0	0.0	1.3	100

SUMMARY OF WHOLE ROCK XRD DATA – Clearwater Formation Study Area (cont'd)

SAMPLE NUMBER	LITHOLOGY	DEPTH (metres)	XRD RELATIVE ABUNDANCE (%)*														
			Qtz	Pl	KF	Chl	SC	10Å	7Å	Cal	Dol	Sid	Py	Amp	Ilm	Mag	Total
Well 16-28-66-3W4 Imp. 77 Marie O.V.																	
LW-87-CW-91	f.g.sst,si,c	415.26	23.0	8.3	15.7	0.0	0.0	12.0	2.9	36.1	0.0	0.0	0.0	0.0	0.0	2.0	100
LW-87-CW-90	f.g.sst,si,sh,c	425.58	24.9	8.5	2.5	1.0	0.0	3.8	2.8	52.9	0.0	2.2	0.9	0.6	0.0	0.0	100
LW-87-CW-94	drilling mud†	408.20	46.6	22.5	6.4	1.0	17.1	4.8	1.6	0.0	0.0	0.0	0.0	0.0	0.0	0.0	100

* Results expressed as normalized relative abundances based on peak heights, not weight percent;
sst=sand, si=silt, sh=shale, m=mud, c=carbonate cemented, d.m.=drilling mud;
v.f.g=very fine grained, f.g.=fine grained, m.g.=medium grained;
Qtz=quartz, Pl=plagioclase, KF=K feldspar, Chl=14Å chlorite, SC=swelling clays (~12Å), 10Å=mica / illite group clays;
7Å=kaolinite and / or berthierine clays, Cal=calcite, Dol=dolomite, Sid=siderite, Py=pyrite, Amp=amphiboles, Ilm=ilmenite, Mag=magnetite;
§ > 45µm portion of sample LW-87-CW-41, included here for comparison purposes;
† drilling mud sample also contains some of the surrounding core material.

WHOLE ROCK XRD MINERAL DATA FOR FINE TO MEDIUM GRAINED SANDS – Clearwater Formation Study Area

SAMPLE NUMBER	DEPTH (metres)	DEPOSITIONAL CHARACTERISTICS			XRD RELATIVE ABUNDANCE (%)*														
		Lithology	Environment	Sequence	Qtz	Pl	KF	Chl	SC	10Å	7Å	Cal	Dol	Sid	Py	Amp	Ilm	Mag	Total
Oil (Bitumen) Saturated Sands																			
LW-87-CW-28	470.25	f.-m.g.sst	UDF-DC	S1, C3	40.1	47.6	1.4	1.0	0.9	3.1	3.9	0.0	0.0	1.3	0.0	0.0	0.7	0.0	100
LW-87-CW-44	474.00	f.g.sst	LDF	S1, D1	53.6	21.9	3.0	0.9	1.0	8.4	7.8	0.0	1.9	0.9	0.0	0.7	0.0	0.0	100
LW-87-CW-75	464.64	f.g.sst	MDF	S1, D2	67.2	8.9	15.4	1.0	0.0	3.8	2.0	0.0	0.0	1.7	0.0	0.0	0.0	0.0	100
LW-87-CW-29	480.20	f.-m.g.sst	UDF-DMB	S1, D2	66.8	19.2	1.2	1.0	0.0	2.8	3.2	0.0	0.0	2.4	0.5	0.7	0.0	2.2	100
LW-87-CW-31	480.80	f.-m.g.sst	UDF-DMB	S1, D2	43.2	37.6	2.0	1.3	0.9	5.5	4.7	0.0	0.0	3.1	0.3	0.0	0.0	1.4	100
LW-87-CW-32	481.00	f.g.sst	UDF-DMB	S1, D2	50.0	18.3	19.4	1.1	0.0	4.0	3.1	0.0	0.0	3.3	0.0	0.0	0.0	0.8	100
LW-87-CW-76	465.05	f.g.sst	MDF	S1, D2	66.4	18.3	0.0	1.4	0.0	3.4	4.5	0.0	0.0	6.0	0.0	0.0	0.0	0.0	100
LW-87-CW-77	465.27	f.g.sst	MDF	S1, D2	47.3	25.5	9.0	0.8	0.0	3.5	3.8	0.0	0.0	0.7	2.4	0.0	0.6	6.4	100
LW-87-CW-61	463.60	f.g.sst	LDF	S1, D	61.7	23.7	5.2	0.7	0.0	2.9	2.2	0.0	2.2	1.1	0.3	0.0	0.0	0.0	100
LW-87-CW-63	464.44	f.g.sst	LDF	S1, D	39.0	42.5	8.7	0.9	0.4	3.2	2.2	0.0	2.5	0.7	0.0	0.0	0.0	0.0	100
LW-87-CW-83	433.40	f.g.sst.	M/UDF	S1, D	41.3	19.0	25.1	1.0	0.7	4.7	6.3	0.0	0.0	1.9	0.0	0.0	0.0	0.0	100
Average (S1):					52.4	25.7	8.2	1.0	0.4	4.1	4.0	0.0	0.6	2.1	0.3	0.1	0.1	1.0	
LW-87-CW-67	465.03	f.g.sst	DF	S2, A	44.3	17.0	18.4	1.2	0.9	4.9	5.5	0.0	3.2	3.8	0.8	0.0	0.0	0.0	100
LW-87-CW-71	467.07	f.g.sst	DF	S2, A	56.0	9.7	3.1	1.0	1.2	3.5	2.8	0.0	4.9	11.2	0.4	0.4	4.0	1.9	100
LW3-73	479.27	f.g.sst	LDF	S2, B	49.6	25.4	11.5	1.2	0.8	4.6	4.2	0.0	0.0	2.2	0.0	0.6	0.0	0.0	100
LW-87-CW-36	481.40	f.g.sst	L/MDF	S2, B	55.4	20.3	5.9	1.6	0.8	5.8	5.5	0.0	0.0	2.3	1.0	0.3	0.0	1.2	100
LW-87-CW-38	481.80	f.g.sst	L/MDF	S2, B	51.1	24.1	10.8	1.1	0.0	4.0	4.9	0.0	0.0	2.3	0.6	0.0	0.0	1.0	100
LW-87-CW-40	483.20	f.g.sst	L/MDF	S2, B	62.3	17.4	3.7	1.4	0.0	6.4	4.3	0.0	0.0	3.2	0.0	0.0	0.0	1.4	100
LW-87-CW-80	466.32	f.g.sst	DF/LDF	S2, B	52.8	23.9	4.1	1.1	1.0	5.3	2.3	0.0	0.0	5.8	1.3	0.0	0.0	2.5	100
LW-87-CW-85	441.69	f.g.sst	LDF	S2, B	53.2	33.4	1.2	1.7	2.6	3.9	2.4	0.0	0.0	0.0	0.4	0.0	0.0	1.3	100
LW-87-CW-41	491.20	f.g.sst	MDF-DMB	S2, C	54.9	15.0	9.8	1.5	0.0	5.7	4.8	0.0	0.0	7.7	0.0	0.0	0.0	0.7	100
Average (S2):					53.3	20.7	7.6	1.3	0.8	4.9	4.1	0.0	0.9	4.3	0.5	0.1	0.4	1.1	
Average (Oil Sands):					52.8	23.4	7.9	1.1	0.6	4.5	4.0	0.0	0.7	3.1	0.4	0.1	0.3	1.0	
Water Saturated Sands																			
LW-87-CW-26	513.55	f.g.sst	LDF	S2, B	59.7	17.2	2.9	1.2	0.0	6.1	6.5	0.0	0.0	5.4	0.4	0.7	0.0	0.0	100
LW-87-CW-27	519.40	f.g.sst	LDF	S2, B	48.8	29.5	3.2	1.9	1.0	3.5	6.8	0.0	0.0	1.7	0.0	0.0	3.6	0.0	100
Average (Water Sands):					54.2	23.3	3.1	1.5	0.5	4.8	6.7	0.0	0.0	3.5	0.2	0.4	1.8	0.0	

WHOLE ROCK XRD MINERAL DATA FOR FINE TO MEDIUM GRAINED SANDS (cont'd) – Clearwater Formation Study Area

SAMPLE	DEPTH	DEPOSITIONAL CHARACTERISTICS			XRD RELATIVE ABUNDANCE (%)*														
NUMBER	(metres)	Lithology	Environment	Sequence	Qtz	Pl	KF	Chl	SC	10Å	7Å	Cal	Dol	Sid	Py	Amp	Ilm	Mag	Total
Overall Averages:																			
Average (S1):					52.4	25.7	8.2	1.0	0.4	4.1	4.0	0.0	0.6	2.1	0.3	0.1	0.1	1.0	
Average (S2):					53.5	21.2	6.8	1.3	0.7	4.9	4.5	0.0	0.7	4.1	0.4	0.2	0.7	0.9	
Average for all sands:					52.9	23.4	7.5	1.2	0.6	4.5	4.2	0.0	0.7	3.1	0.4	0.2	0.4	0.9	
Standard Deviation					8.6	9.7	6.8	0.3	0.6	1.4	1.7	0.0	1.4	2.7	0.6	0.3	1.1	1.5	
Minimum Value					39.0	8.9	0.0	0.7	0.0	2.8	2.0	0.0	0.0	0.0	0.0	0.0	0.0	0.0	
Maximum value					67.2	47.6	25.1	1.9	2.6	8.4	7.8	0.0	4.9	11.2	2.4	0.7	4.0	6.4	

* Results expressed as normalized relative abundances based on peak heights, not weight percent;
sst=sand, f.g.=fine grained, m.g.=medium grained;
UDF=Upper Delta Front, DC=Distributary Channel, DMB=Distributary Mouth Bar, MDF=Middle Delta Front, LDF=Lower Delta Front, DF=Delta Fringe;
Qtz=quartz, Pl=plagioclase, KF=K feldspar, Chl=14Å chlorite, SC=swelling clays (~12Å), 10Å=mica / illite group clays;
7Å=kaolinite and / or berthierine clays, Cal=calcite, Dol=dolomite, Sid=siderite, Py=pyrite, Amp=amphiboles, Ilm=ilmenite, Mag=magnetite.

WHOLE ROCK XRD MINERAL DATA FOR VERY FINE TO FINE GRAINED SANDS WITH SILT OR SHALE
Clearwater Formation Study Area

SAMPLE	DEPTH	DEPOSITIONAL CHARACTERISTICS			XRD RELATIVE ABUNDANCE (%)*														
NUMBER	(metres)	Lithology	Environment	Sequence	Qtz	Pl	KF	Chl	SC	10Å	7Å	Cal	Dol	Sid	Py	Amp	Ilm	Mag	Total
Oil (Bitumen) Saturated Sands																			
LW-87-CW-43	473.70	f.g.sst,m	LDF	S1, D1	62.1	9.8	4.8	2.3	3.7	10.1	6.3	0.0	0.0	0.0	0.0	0.9	0.0	0.0	100
LW-87-CW-45	474.20	f.-m.g.sst,sh	LDF	S1, D1	37.3	21.3	16.4	1.2	0.8	5.7	5.9	0.0	7.4	0.0	0.0	0.0	0.0	4.1	100
LW-87-CW-46	474.30	f.g.sst,si	LDF	S1, D1	69.0	4.4	5.1	1.7	2.1	9.1	7.7	0.0	0.0	0.0	0.0	0.9	0.0	0.0	100
LW-87-CW-30	480.50	f.g.sst,tr.m	UDF-DMB	S1, D2	44.1	15.7	22.6	1.4	2.2	7.7	2.9	0.0	0.0	2.4	0.4	0.6	0.0	0.0	100
LW-87-CW-58	468.51	f.g.sst,si	LDF	S1, D	53.0	29.3	3.0	0.8	0.4	3.0	4.8	0.0	4.4	1.1	0.0	0.3	0.0	0.0	100
LW-87-CW-10	509.60	f.g.sst,tr.sh	MDF	S1, D	41.7	31.2	4.0	1.0	0.0	12.5	5.4	0.0	2.6	1.0	0.0	0.8	0.0	0.0	100
LW-87-CW-11	510.10	f.g.sst,si	MDF	S1, D	53.5	8.8	9.5	1.9	2.2	16.2	5.0	0.0	1.6	0.0	0.0	1.3	0.0	0.0	100
LW-87-CW-12	510.30	f.g.sst,tr.sh	MDF	S1, D	51.7	15.7	9.0	1.8	1.4	9.4	7.6	0.0	0.0	0.0	0.9	0.0	0.0	2.6	100
LW-87-CW-13	510.40	f.g.sst,tr.sh	MDF	S1, D	60.5	15.0	9.6	1.1	0.9	8.5	3.8	0.0	0.0	0.0	0.0	0.7	0.0	0.0	100
LW-87-CW-14	510.50	f.g.sst,tr.sh	MDF	S1, D	62.9	15.5	4.7	1.5	0.0	9.3	5.3	0.0	0.0	0.0	0.8	0.0	0.0	0.0	100
LW-87-CW-62	464.24	f.g.sst,si	LDF	S1, D	51.7	18.3	14.9	1.5	1.2	5.2	4.3	0.0	0.0	2.2	0.0	0.6	0.0	0.0	100
Average (S1):					53.4	16.8	9.4	1.5	1.4	8.8	5.4	0.0	1.5	0.6	0.2	0.5	0.0	0.6	
LW-87-CW-59	468.61	f.g.sst,si	DF	S2, A	54.9	12.3	3.8	2.2	2.7	10.0	7.6	0.0	3.5	2.3	0.8	0.0	0.0	0.0	100
LW-87-CW-15	510.60	f.g.sst,tr.sh	DF	S2, A	56.1	20.1	6.5	1.4	1.1	8.6	4.8	0.0	0.0	0.0	0.7	0.8	0.0	0.0	100
LW-87-CW-16	510.70	f.g.sst,si	DF	S2, A	59.4	9.2	4.6	1.8	8.7	8.2	4.5	0.0	0.0	0.0	2.1	1.5	0.0	0.0	100
LW-87-CW-49	474.60	f.g.sst,sh	DF	S2, A	63.3	17.7	3.9	1.6	1.7	6.7	5.0	0.0	0.0	0.0	0.0	0.0	0.0	0.0	100
LW-87-CW-64	464.68	f.g.sst,sh	DF	S2, A	44.1	8.9	16.1	1.3	0.0	1.1	7.9	0.0	19.1	0.0	0.0	0.0	0.0	1.6	100
LW-87-CW-65	464.75	f.g.sst,si	DF	S2, A	60.0	11.4	2.4	1.1	0.9	9.3	4.0	0.0	6.3	0.0	4.6	0.0	0.0	0.0	100
LW-87-CW-68	465.43	f.g.sst,si	DF	S2, A	56.9	16.9	4.5	1.3	2.7	4.8	0.0	3.3	3.9	2.3	1.3	0.7	0.0	1.5	100
LW-87-CW-69	465.85	f.g.sst,si	DF	S2, A	50.0	19.8	3.5	1.1	1.2	7.1	4.2	0.0	4.6	5.7	1.5	0.0	0.0	1.3	100
LW-87-CW-70	466.45	f.g.sst,si,sh	DF	S2, A	44.5	25.8	9.7	1.5	3.0	5.7	5.7	0.0	0.0	1.7	0.8	0.9	0.9	0.0	100
LW-87-CW-72	467.64	f.g.sst,sh	DF	S2, A	30.8	51.7	4.0	0.8	3.8	2.9	1.8	0.0	2.4	0.4	0.2	0.0	0.0	1.3	100
LW-87-CW-34	481.20	f.g.sst,m	L/MDF	S2, B	57.6	17.6	3.1	1.9	2.4	7.9	6.0	0.0	0.0	2.5	0.0	0.0	0.0	1.1	100
LW-87-CW-35	481.30	f.g.sst,tr.sh	L/MDF	S2, B	54.7	20.8	10.1	1.1	1.4	6.1	3.9	0.0	0.0	0.0	1.2	0.7	0.0	0.0	100
LW-87-CW-37	481.60	f.g.sst,m	L/MDF	S2, B	54.1	25.2	3.0	1.5	1.3	6.5	4.1	0.0	0.0	2.7	1.0	0.6	0.0	0.0	100
LW-87-CW-39	482.20	f.g.sst,si	L/MDF	S2, B	51.2	28.5	2.3	1.4	0.9	6.3	5.6	0.0	2.2	0.0	0.3	0.0	0.0	1.2	100
LW-87-CW-54	475.90	f.g.sst,si	LDF	S2, B	63.4	16.5	4.8	1.4	8.5	2.6	1.6	0.0	0.0	0.0	0.4	0.8	0.0	0.0	100
LW-87-CW-55	476.40	f.g.sst,sh	LDF	S2, B	46.4	19.4	12.2	1.6	1.6	7.1	6.4	0.0	0.0	3.9	0.0	0.0	0.0	1.4	100
LW-87-CW-81	466.93	f.g.sst,sh	DF/LDF	S2, B	50.8	18.6	2.3	1.5	5.5	8.1	7.6	0.0	0.0	2.9	0.5	0.9	0.0	1.3	100
LW-87-CW-82	467.88	f.g.sst,sh	DF/LDF	S2, B	50.5	21.5	0.0	1.6	1.6	10.7	6.0	0.0	4.5	0.9	2.4	0.0	0.0	0.0	100
LW-87-CW-84	440.75	f.g.sst,si,sh	LDF	S2, B	57.8	19.7	3.4	1.8	1.5	8.5	5.8	0.0	0.0	0.0	0.0	0.0	0.0	1.4	100

WHOLE ROCK XRD MINERAL DATA FOR VERY FINE TO FINE GRAINED SANDS WITH SILT OR SHALE (cont'd)
Clearwater Formation Study Area

SAMPLE NUMBER	DEPTH (metres)	DEPOSITIONAL CHARACTERISTICS Lithology	Environment	Sequence	XRD RELATIVE ABUNDANCE (%)* Qtz	Pl	KF	Chl	SC	10Å	7Å	Cal	Dol	Sid	Py	Amp	Ilm	Mag	Total
Oil (Bitumen) Saturated Sands																			
LW-87-CW-57	487.53	f.g.sst,si	DF/LDF	S2, C	48.1	27.2	2.5	1.7	6.9	3.8	3.3	0.0	6.5	0.0	0.0	0.0	0.0	0.0	100
LW-87-CW-73	473.94	f.g.sst,sh	MS	S2, WAB	50.4	25.0	1.9	1.5	5.2	6.4	5.8	0.0	2.6	0.0	1.3	0.0	0.0	0.0	100
Average (S2):					52.6	20.7	5.0	1.5	3.0	6.6	4.8	0.2	2.6	1.2	0.9	0.3	0.0	0.6	
Average (Oil Sands):					52.9	19.3	6.5	1.5	2.4	7.3	5.0	0.1	2.2	1.0	0.7	0.4	0.0	0.6	
Water Saturated Sands																			
LW3-36	468.24	f.g.sst,si	LDF	S1, D	32.3	36.4	12.8	1.2	0.0	4.9	5.4	0.0	2.4	1.0	0.0	3.5	0.0	0.0	100
LW3-39	468.91	f.g.sst,si	DF	S2, A	53.5	14.9	1.5	2.8	3.0	12.0	2.3	0.0	7.7	1.2	0.8	0.4	0.0	0.0	100
LW-87-CW-20	511.20	v.f.g.sst,si,sh	DF	S2, A	57.4	9.3	5.2	1.9	7.5	8.6	4.8	0.0	3.3	0.0	1.1	1.0	0.0	0.0	100
LW-87-CW-21	511.40	v.f.g.sst,tr.sh	DF	S2, A	58.7	5.0	1.8	1.8	2.6	9.4	5.0	0.0	13.9	0.0	1.0	0.8	0.0	0.0	100
LW-87-CW-22	511.65	v.f.g.sst,si,sh	DF	S2, A	63.3	10.7	2.9	2.0	4.2	7.9	3.4	0.0	4.5	0.0	1.1	0.0	0.0	0.0	100
LW-87-CW-23	511.80	v.f.g.sst,tr.sh	DF	S2, A	59.9	11.6	3.9	1.4	5.2	7.8	3.8	0.0	4.7	0.0	0.6	1.2	0.0	0.0	100
LW-87-CW-24	512.10	v.f.g.sst,sh	DF	S2, A	59.4	8.8	4.3	2.2	7.7	8.6	5.4	0.0	2.1	0.0	1.6	0.0	0.0	0.0	100
Average (S2):					58.7	10.1	3.2	2.0	5.0	9.0	4.1	0.0	6.0	0.2	1.0	0.6	0.0	0.0	
Average (Water Sands):					54.9	13.8	4.6	1.9	4.3	8.5	4.3	0.0	5.5	0.3	0.9	1.0	0.0	0.0	
Overall Averages:																			
Average (S1):					51.6	18.5	9.7	1.4	1.2	8.5	5.4	0.0	1.5	0.6	0.2	0.8	0.0	0.6	
Average (S2):					54.0	18.3	4.6	1.6	3.4	7.1	4.7	0.1	3.4	1.0	0.9	0.4	0.0	0.4	
Average for all sands:					53.3	18.3	6.2	1.5	2.8	7.5	4.9	0.1	2.8	0.9	0.7	0.5	0.0	0.5	
Standard Deviation					8.5	9.2	5.0	0.4	2.4	2.9	1.7	0.5	4.0	1.3	0.9	0.7	0.1	0.9	
Minimum Value					30.8	4.4	0.0	0.8	0.0	1.1	0.0	0.0	0.0	0.0	0.0	0.0	0.0	0.0	
Maximum Value					69.0	51.7	22.6	2.8	8.7	16.2	7.9	3.3	19.1	5.7	4.6	3.5	0.9	4.1	

* Results expressed as normalized relative abundances based on peak heights, not weight percent;
sst=sand, si=silt, sh=shale, m=mud, v.f.g=very fine grained, f.g.=fine grained, UDF=Upper Delta Front, DMB=Distributary Mouth Bar;
MDF=Middle Delta Front, LDF=Lower Delta Front, DF=Delta Fringe, MS=Middle Shoreface, WAB= Wabiskaw Member;
Qtz=quartz, Pl=plagioclase, KF=K feldspar, Chl=14Å chlorite, SC=swelling clays (~12Å), 10Å=mica / illite group clays;
7Å=kaolinite and / or berthierine clays, Cal=calcite, Dol=dolomite, Sid=siderite, Py=pyrite, Amp=amphiboles, Ilm=ilmenite, Mag=magnetite.

WHOLE ROCK XRD MINERAL DATA FOR SANDY SILTS OR SHALES – Clearwater Formation Study Area

SAMPLE	DEPTH	DEPOSITIONAL CHARACTERISTICS			XRD RELATIVE ABUNDANCE (%)*														
NUMBER	(metres)	Lithology	Environment	Sequence	Qtz	Pl	KF	Chl	SC	10Å	7Å	Cal	Dol	Sid	Py	Amp	Ilm	Mag	Total
Oil (Bitumen) Saturated Silts or Shales																			
LW3-90	457.03	si,f.g.sst,m	LDF	S1, B	39.5	13.2	1.7	0.0	8.2	16.6	2.9	0.0	0.0	14.3	2.2	1.4	0.0	0.0	100
LW-87-CW-42	473.40	si,f.g.sst	LDF	S1, D1	44.0	27.1	3.6	1.6	2.4	9.2	3.8	0.0	5.7	1.0	0.0	0.0	0.0	1.5	100
LW-87-CW-33	481.10	sh,sst,si	UDF-DMB	S1, D2	55.9	9.4	2.8	1.7	2.0	15.9	6.4	0.0	3.4	2.6	0.0	0.0	0.0	0.0	100
Average (S1):					46.5	16.6	2.7	1.1	4.2	13.9	4.4	0.0	3.0	5.9	0.7	0.5	0.0	0.5	
LW-87-CW-17	510.80	sh,tr.sst,si	DF	S2, A	42.4	17.8	6.2	1.9	12.7	11.6	4.4	0.0	0.0	0.0	0.9	2.0	0.0	0.0	100
LW-87-CW-51	475.00	sh,f.g.sst	DF	S2, A	55.3	17.9	3.6	1.3	6.6	6.0	3.3	4.1	0.0	0.0	1.0	0.8	0.0	0.0	100
LW3-13	491.62	sh,tr.sst,si	LS	S2, WAB	65.9	7.1	3.6	3.1	3.7	9.0	3.7	0.0	2.6	0.0	1.3	0.0	0.0	0.0	100
Average (S2):					54.6	14.3	4.5	2.1	7.7	8.9	3.8	1.4	0.9	0.0	1.1	0.9	0.0	0.0	
Average (Oil Silts/Shales):					50.5	15.4	3.6	1.6	5.9	11.4	4.1	0.7	1.9	3.0	0.9	0.7	0.0	0.3	
Water Saturated Silts or Shales																			
LW-87-CW-18	510.90	sh,tr.sst,si	DF	S2, A	49.3	7.0	4.1	1.9	11.8	13.0	6.4	0.0	3.7	0.0	1.6	1.1	0.0	0.0	100
LW-87-CW-19	511.00	sh,tr.sst,si	DF	S2, A	43.2	10.9	5.4	3.3	16.9	12.5	1.3	0.0	3.2	0.0	1.6	1.7	0.0	0.0	100
LW3-66	477.14	sh,tr.sst,si	LDF	S2, B	46.0	5.8	3.1	7.1	7.5	15.9	0.6	0.0	2.9	10.4	0.8	0.0	0.0	0.0	100
LW-87-CW-25	512.60	sh,tr.si,sst	LDF	S2, B	53.0	6.2	11.8	2.1	9.5	13.4	2.9	0.0	0.0	0.0	1.1	0.0	0.0	0.0	100
Average (S2/Water Silts/Shales):					47.8	7.5	6.1	3.6	11.4	13.7	2.8	0.0	2.5	2.6	1.3	0.7	0.0	0.0	
Overall Averages:																			
Average (S1):					46.5	16.6	2.7	1.1	4.2	13.9	4.4	0.0	3.0	5.9	0.7	0.5	0.0	0.5	
Average (S2):					50.7	10.4	5.4	3.0	9.8	11.6	3.2	0.6	1.8	1.5	1.2	0.8	0.0	0.0	
Average for all silts or shales:					49.4	12.2	4.6	2.4	8.1	12.3	3.6	0.4	2.2	2.8	1.1	0.7	0.0	0.2	
Standard Deviation					8.1	6.9	2.8	1.9	4.8	3.4	1.9	1.3	2.0	5.2	0.7	0.8	0.0	0.5	
Minimum Value					39.5	5.8	1.7	0.0	2.0	6.0	0.6	0.0	0.0	0.0	0.0	0.0	0.0	0.0	
Maximum Value					65.9	27.1	11.8	7.1	16.9	16.6	6.4	4.1	5.7	14.3	2.2	2.0	0.0	1.5	

* Results expressed as normalized relative abundances based on peak heights, not weight percent;
sst=sand, si=silt, sh=shale, m=mud, f.g.=fine grained;
UDF=Upper Delta Front, DMB=Distributary Mouth Bar, LDF=Lower Delta Front, DF=Delta Fringe, LS=Lower Shoreface, WAB=Wabiskaw Member;
Qtz=quartz, Pl=plagioclase, KF=K feldspar, Chl=14Å chlorite, SC=swelling clays (~12Å), 10Å=mica / illite group clays;
7Å=kaolinite and / or berthierine clays, Cal=calcite, Dol=dolomite, Sid=siderite, Py=pyrite, Amp=amphiboles, Ilm=ilmenite, Mag=magnetite.

WHOLE ROCK XRD MINERAL DATA FOR SILTS AND SHALES – Clearwater Formation Study Area

SAMPLE	DEPTH	DEPOSITIONAL CHARACTERISTICS			XRD RELATIVE ABUNDANCE (%)*														
NUMBER	(metres)	Lithology	Environment	Sequence	Qtz	Pl	KF	Chl	SC	10Å	7Å	Cal	Dol	Sid	Py	Amp	Ilm	Mag	Total
Water Saturated Silts and Shales																			
LW-87-CW-47	474.40	si,sh	DF	S2, A	59.0	6.1	2.5	2.3	11.0	13.2	4.4	0.0	0.0	0.0	1.5	0.0	0.0	0.0	100
LW-87-CW-48	474.50	sh,si	DF	S2, A	52.6	15.1	4.2	2.3	6.3	10.0	8.1	0.0	0.0	0.0	0.7	0.6	0.0	0.0	100
LW-87-CW-50	474.80	sh,si	DF	S2, A	57.9	10.7	4.0	1.4	8.8	9.5	6.5	0.0	0.0	0.0	1.3	0.0	0.0	0.0	100
Overall Average (S2/Water Silts/Shales):					56.5	10.6	3.6	2.0	8.7	10.9	6.3	0.0	0.0	0.0	1.2	0.2	0.0	0.0	
Standard Deviation					3.4	4.5	0.9	0.5	2.4	2.0	1.9	0.0	0.0	0.0	0.4	0.4	0.0	0.0	
Minimum Value					52.6	6.1	2.5	1.4	6.3	9.5	4.4	0.0	0.0	0.0	0.7	0.0	0.0	0.0	
Maximum Value					59.0	15.1	4.2	2.3	11.0	13.2	8.1	0.0	0.0	0.0	1.5	0.6	0.0	0.0	

* Results expressed as normalized relative abundances based on peak heights, not weight percent;
si=silt, sh=shale, DF=Delta Fringe;
Qtz=quartz, Pl=plagioclase, KF=K feldspar, Chl=14Å chlorite, SC=swelling clays (~12Å), 10Å=mica / illite group clays;
7A=kaolinite and / or berthierine clays, Cal=calcite, Dol=dolomite, Sid=siderite, Py=pyrite, Amp=amphiboles, Ilm=ilmenite, Mag=magnetite.

WHOLE ROCK XRD MINERAL DATA FOR CALCITE CEMENTED INTERVALS – Clearwater Formation Study Area

SAMPLE NUMBER	DEPTH (metres)	DEPOSITIONAL CHARACTERISTICS Lithology	Environment	Sequence	XRD RELATIVE ABUNDANCE (%)* Qtz	Pl	KF	Chl	SC	10Å	7Å	Cal	Dol	Sid	Py	Amp	Ilm	Mag	Total
Calcite Cemented Samples																			
LW3-20	463.21	f.g.sst,m,c	LDF	S1, C	29.6	7.3	4.6	1.2	0.0	5.8	1.8	45.1	1.4	1.2	0.0	2.0	0.0	0.0	100
LW-87-CW-92	453.57	si,f.g.sst,c	LDF	S1, C	24.7	5.2	0.8	0.5	0.5	1.3	1.0	65.3	0.0	0.7	0.0	0.0	0.0	0.0	100
LW-87-CW-93	430.97	f.g.sst,sh,c	M/UDF	S1, C	27.7	8.9	2.3	0.6	0.0	3.6	2.8	51.3	0.0	1.5	0.0	0.7	0.0	0.0	100
LW-87-CW-91	415.26	f.g.sst,si,c	MDF	S1, C	23.0	8.3	15.7	0.0	0.0	12.0	2.9	36.1	0.0	0.0	0.0	0.0	0.0	2.0	100
Average (S1):					26.2	7.4	6.0	0.6	0.1	5.7	2.1	49.4	0.3	0.8	0.0	0.7	0.0	0.5	
LW3-38	468.76	f.g.sst,si,m,c	DF	S2, A	29.0	30.6	9.7	1.8	0.7	7.4	5.9	6.8	0.0	2.0	5.3	0.9	0.0	0.0	100
LW-87-CW-66	464.84	f.g.sst,sh,c	DF	S2, A	35.0	8.5	0.8	1.0	1.5	3.5	0.5	47.1	0.0	1.2	0.0	0.9	0.0	0.0	100
LW-87-CW-90	425.58	f.g.sst,si,sh,c	LDF	S2, A	24.9	8.5	2.5	1.0	0.0	3.8	2.8	52.9	0.0	2.2	0.9	0.6	0.0	0.0	100
LW-87-CW-56	477.40	sh,si,c	LDF	S2, B	6.5	2.0	0.0	1.4	2.4	5.8	0.9	79.3	0.0	1.7	0.0	0.0	0.0	0.0	100
LW3-21	494.15	f.g.sst,si,c	LS	S2, WAB	32.6	1.2	1.2	0.7	0.5	4.3	1.7	29.2	17.8	9.3	0.5	0.8	0.0	0.0	100
Average (S2):					25.6	10.2	2.8	1.2	1.0	5.0	2.4	43.1	3.6	3.3	1.3	0.6	0.0	0.0	
Overall Average:					25.9	9.0	4.2	0.9	0.6	5.3	2.3	45.9	2.1	2.2	0.7	0.7	0.0	0.2	
Standard Deviation					8.2	8.6	5.2	0.5	0.8	3.1	1.6	20.8	5.9	2.7	1.7	0.6	0.0	0.7	
Minimum Value					6.5	1.2	0.0	0.0	0.0	1.3	0.5	6.8	0.0	0.0	0.0	0.0	0.0	0.0	
Maximum Value					35.0	30.6	15.7	1.8	2.4	12.0	5.9	79.3	17.8	9.3	5.3	2.0	0.0	2.0	
Average, recalculated to 0% calcite basis:					47.8	16.5	7.8	1.7	1.2	9.8	4.2	0.0	3.9	4.1	1.4	1.2	0.0	0.4	100

* Results expressed as normalized relative abundances based on peak heights, not weight percent;
sst=sand, si=silt, sh=shale, m=mud, c=carbonate cemented, f.g.=fine grained;
UDF=Upper Delta Front, MDF=Middle Delta Front, LDF=Lower Delta Front, DF=Delta Fringe, LS=Lower Shoreface, WAB=Wabiskaw Member;
Qtz=quartz, Pl=plagioclase, KF=K feldspar, Chl=14Å chlorite, SC=swelling clays (~12Å), 10Å=mica / illite group clays;
7Å=kaolinite and / or berthierine clays, Cal=calcite, Dol=dolomite, Sid=siderite, Py=pyrite, Amp=amphiboles, Ilm=ilmenite, Mag=magnetite.

SUMMARY OF < 45µm XRD DATA – Clearwater Formation Study Area

SAMPLE NUMBER	LITHOLOGY	DEPTH (metres)	XRD RELATIVE ABUNDANCE (%)* Qtz	Pl	KF	Chl	SC	10Å	7Å	Cal	Dol	Sid	Py	Amp	Ilm	Mag	Total
Well 3-28-66-2W4 Imp. 77 O.V.																	
LW3-90	si,f.g.sst,m	457.03	36.1	4.5	3.5	3.1	9.1	19.3	4.6	0.0	0.0	15.8	1.4	2.7	0.0	0.0	100
LW3-20	f.g.sst,m,c	463.21	27.4	9.4	1.8	1.0	0.0	6.2	3.1	45.0	3.2	1.6	0.0	1.4	0.0	0.0	100
LW3-36	f.g.sst,si	468.24	33.0	22.5	8.2	2.2	1.5	9.1	11.1	0.0	5.2	5.0	0.0	2.3	0.0	0.0	100
LW-87-CW-58	f.g.sst,si	468.51	43.9	21.8	5.6	1.8	0.8	6.5	12.4	0.0	0.0	6.2	1.1	0.0	0.0	0.0	100
LW-87-CW-59	f.g.sst,si	468.61	46.4	10.5	4.5	3.0	3.8	13.5	8.1	0.0	3.7	4.3	0.9	1.4	0.0	0.0	100
LW-87-CW-60	si,f.g.sst,m	468.73	47.6	10.5	4.0	3.1	1.4	7.5	5.3	8.6	7.8	0.0	3.4	0.9	0.0	0.0	100
LW3-38	f.g.sst,si,m,c	468.76	37.6	10.1	4.3	2.2	1.8	7.6	5.2	11.8	0.0	5.5	12.9	1.0	0.0	0.0	100
LW3-39	f.g.sst,si	468.91	49.8	7.4	3.8	2.1	4.2	12.4	5.9	0.0	9.3	2.0	2.1	0.9	0.0	0.0	100
LW3-66	sh,tr.sst,si	477.14	48.7	6.5	3.3	2.5	7.3	15.3	5.6	0.0	0.0	10.8	0.0	0.0	0.0	0.0	100
LW3-73	f.g.sst	479.27	50.8	20.8	6.2	1.8	1.2	5.0	7.0	0.0	0.0	7.3	0.0	0.0	0.0	0.0	100
LW3-13	sh,tr.sst,si	491.62	61.1	6.1	2.2	2.4	3.6	10.5	4.9	0.0	7.6	0.0	0.9	0.7	0.0	0.0	100
LW3-21	f.g.sst,si,c	494.15	32.1	1.3	0.6	0.7	0.5	4.7	1.4	38.3	9.6	10.6	0.0	0.4	0.0	0.0	100
Well 6-31-66-2W4 Esso 86 Cold Lake O.V.																	
LW-87-CW-10	f.g.sst,tr.sh	509.60	37.5	22.5	8.8	2.3	0.9	9.4	9.2	0.0	3.6	4.3	0.8	0.8	0.0	0.0	100
LW-87-CW-11	f.g.sst,si	510.10	52.6	10.1	4.6	2.1	2.7	20.4	6.2	0.0	0.0	0.0	0.0	1.2	0.0	0.0	100
LW-87-CW-12	f.g.sst,tr.sh	510.30	43.8	22.6	5.9	3.3	1.9	12.5	4.7	0.0	0.0	2.6	0.5	0.9	0.0	1.3	100
LW-87-CW-13	f.g.sst,tr.sh	510.40	47.2	15.4	6.6	1.5	2.0	15.9	8.5	0.0	0.0	1.1	0.4	1.4	0.0	0.0	100
LW-87-CW-14	f.g.sst,tr.sh	510.50	51.7	17.2	7.7	1.9	1.4	10.7	8.1	0.0	0.0	0.0	0.5	0.8	0.0	0.0	100
LW-87-CW-15	f.g.sst,tr.sh	510.60	50.1	14.8	7.5	2.1	3.3	13.2	7.0	0.0	0.0	0.0	1.1	1.0	0.0	0.0	100
LW-87-CW-16	f.g.sst,si	510.70	50.2	12.6	5.2	3.2	8.6	11.9	3.1	0.0	0.0	0.0	4.0	1.1	0.0	0.0	100
LW-87-CW-17	sh,tr.sst,si	510.80	51.3	8.2	4.7	2.4	13.7	10.0	2.8	0.0	3.6	0.0	2.4	0.9	0.0	0.0	100
LW-87-CW-18	sh,tr.sst,si	510.90	46.9	7.4	6.2	2.2	13.8	11.7	4.4	0.0	2.5	0.0	2.8	2.0	0.0	0.0	100
LW-87-CW-19	sh,tr.sst,si	511.00	48.4	9.3	5.3	2.5	16.6	10.0	2.9	0.0	2.2	0.0	2.8	0.0	0.0	0.0	100
LW-87-CW-20	v.f.g.sst,si,sh	511.20	65.0	7.6	4.3	1.9	7.1	7.5	3.6	0.0	0.0	0.0	1.8	1.2	0.0	0.0	100

SUMMARY OF < 45μm XRD DATA – Clearwater Formation Study Area (cont'd)

SAMPLE NUMBER	LITHOLOGY	DEPTH	XRD RELATIVE ABUNDANCE (%)*														
		(metres)	Qtz	Pl	KF	Chl	SC	10Å	7Å	Cal	Dol	Sid	Py	Amp	Ilm	Mag	Total
Well 6-31-66-2W4 Esso 86 Cold Lake O.V.																	
LW-87-CW-21	v.f.g.sst,tr.sh	511.40	55.4	6.3	3.4	1.5	2.9	6.9	5.8	0.0	15.5	0.0	1.2	1.2	0.0	0.0	100
LW-87-CW-22	v.f.g.sst,si,sh	511.65	48.5	11.1	4.1	1.7	5.7	8.7	5.2	0.0	10.9	0.0	2.7	1.5	0.0	0.0	100
LW-87-CW-23	v.f.g.sst,tr.sh	511.80	60.9	8.3	4.2	2.0	6.6	9.2	5.2	0.0	2.7	0.0	1.0	0.0	0.0	0.0	100
LW-87-CW-24	v.f.g.sst,sh	512.10	55.0	10.4	4.0	2.4	9.1	10.1	4.6	0.0	2.6	0.0	1.8	0.0	0.0	0.0	100
LW-87-CW-25	sh,tr.si,sst	512.60	56.0	8.0	5.3	2.2	8.5	8.5	3.6	0.0	3.7	0.0	1.2	1.5	1.5	0.0	100
LW-87-CW-26	f.g.sst	513.55	35.4	20.0	3.2	2.4	1.2	9.5	10.7	0.0	0.0	15.6	1.5	0.6	0.0	0.0	100
LW-87-CW-27	f.g.sst	519.40	40.3	15.2	5.4	2.4	1.5	10.6	14.8	0.0	0.0	3.7	1.0	0.0	5.0	0.0	100
Well 3-13-65-4W4 Esso 84 (C1-12) Cold Lk.																	
LW-87-CW-28	f.-m.g.sst	470.25	47.3	24.5	2.6	1.4	1.7	6.8	8.7	0.0	0.0	2.8	0.7	0.0	0.0	3.6	100
LW-87-CW-29	f.-m.g.sst	480.20	35.2	30.0	4.8	2.3	0.0	8.0	13.2	0.0	0.0	5.3	1.2	0.0	0.0	0.0	100
LW-87-CW-30	f.g.sst,tr.m	480.50	52.9	12.2	2.4	2.4	6.2	13.6	5.2	0.0	0.0	5.1	0.0	0.0	0.0	0.0	100
LW-87-CW-31	f.-m.g.sst	480.80	42.6	19.6	5.5	2.0	2.1	8.3	11.4	0.0	0.0	6.3	1.3	0.9	0.0	0.0	100
LW-87-CW-32	f.g.sst	481.00	51.7	20.2	3.2	1.3	0.9	4.5	8.0	0.0	0.0	7.2	1.0	1.0	0.0	1.2	100
LW-87-CW-33	sh,sst,si	481.10	46.5	16.1	1.8	1.8	3.8	14.2	5.9	2.7	3.0	2.6	0.7	0.9	0.0	0.0	100
LW-87-CW-34	f.g.sst,m	481.20	53.4	17.4	4.4	2.2	3.0	9.0	6.6	0.0	0.0	2.9	1.0	0.0	0.0	0.0	100
LW-87-CW-35	f.g.sst,tr.sh	481.30	46.3	15.2	5.0	2.5	2.4	11.7	5.7	0.0	0.0	8.3	0.9	0.0	0.0	2.0	100
LW-87-CW-36	f.g.sst	481.40	48.9	18.2	6.5	1.9	1.5	5.0	7.6	0.0	0.0	3.1	3.2	0.0	0.0	4.0	100
LW-87-CW-37	f.g.sst,m	481.60	44.9	17.1	8.1	3.6	2.0	8.5	8.5	0.0	0.0	4.6	1.0	0.0	0.0	1.8	100
LW-87-CW-38	f.g.sst	481.80	38.7	17.8	7.5	1.9	5.6	3.5	8.7	0.0	0.0	11.2	2.6	0.0	0.0	2.5	100
LW-87-CW-39	f.g.sst,si	482.20	44.6	24.1	5.9	1.8	2.1	5.9	7.4	0.0	1.5	4.7	0.9	0.0	0.0	1.2	100
LW-87-CW-40	f.g.sst	483.20	44.2	17.3	6.5	2.6	5.7	4.2	6.2	0.0	2.7	6.8	1.6	0.0	0.0	2.1	100
LW-87-CW-41	f.g.sst	491.20	46.9	24.2	2.5	2.9	3.4	4.9	5.6	0.0	3.9	4.9	0.9	0.0	0.0	0.0	100

SUMMARY OF < 45µm XRD DATA – Clearwater Formation Study Area (cont'd)

SAMPLE NUMBER	LITHOLOGY	DEPTH (metres)	XRD RELATIVE ABUNDANCE (%)* Qtz	Pl	KF	Chl	SC	10Å	7Å	Cal	Dol	Sid	Py	Amp	Ilm	Mag	Total
Well 8-19-66-2W4 Esso 86 Marie O.V.																	
LW-87-CW-42	si,f.g.sst	473.40	49.4	18.0	3.0	2.5	4.3	15.7	7.2	0.0	0.0	0.0	0.0	0.0	0.0	0.0	100
LW-87-CW-43	f.g.sst,m	473.70	48.3	13.7	4.7	1.8	4.1	11.5	8.2	0.0	2.2	3.5	0.7	1.3	0.0	0.0	100
LW-87-CW-44	f.g.sst	474.00	42.8	19.5	2.4	2.2	1.2	8.0	11.6	0.0	3.9	5.0	0.0	0.9	0.0	2.6	100
LW-87-CW-45	f.-m.g.sst,sh	474.20	44.1	17.4	5.0	1.9	2.2	10.5	11.1	0.0	0.0	7.2	0.6	0.0	0.0	0.0	100
LW-87-CW-46	f.g.sst,si	474.30	51.6	18.8	3.0	1.5	1.9	7.4	6.2	0.0	0.0	1.8	6.0	0.8	0.0	1.2	100
LW-87-CW-47	si,sh	474.40	60.2	6.2	4.1	1.9	11.0	10.0	3.7	0.0	0.0	0.0	2.0	0.9	0.0	0.0	100
LW-87-CW-48	sh,si	474.50	57.7	10.4	5.5	1.9	7.5	9.6	5.2	0.0	0.0	0.0	1.2	1.1	0.0	0.0	100
LW-87-CW-49	f.g.sst,sh	474.60	64.9	10.0	3.2	1.4	4.9	7.1	5.6	0.0	0.0	0.0	1.0	0.0	0.0	2.0	100
LW-87-CW-50	sh,si	474.80	62.0	6.1	2.8	1.7	8.2	10.5	4.7	0.0	2.3	0.0	1.8	0.0	0.0	0.0	100
LW-87-CW-51	sh,f.g.sst	475.00	59.5	8.6	3.1	1.9	9.6	10.1	3.7	2.3	0.0	0.0	1.2	0.0	0.0	0.0	100
LW-87-CW-54	f.g.sst,si	475.90	51.9	17.0	3.5	2.1	12.6	5.8	1.0	0.0	0.0	4.2	2.0	0.0	0.0	0.0	100
LW-87-CW-55	f.g.sst,sh	476.40	52.3	15.0	1.3	1.9	2.2	9.4	8.1	0.0	4.3	3.3	0.0	0.9	1.4	0.0	100
LW-87-CW-56	sh,si,c	477.40	9.5	0.0	0.0	1.2	0.0	4.9	0.4	82.0	0.0	2.1	0.0	0.0	0.0	0.0	100
LW-87-CW-57	f.g.sst,si	487.53	47.7	14.3	3.2	1.6	11.1	1.4	5.9	0.0	5.2	5.8	0.0	1.0	0.0	3.0	100
Well 16-2-66-3W4 Imp. 77 Medley O.V.																	
LW-87-CW-61	f.g.sst	463.60	40.7	25.4	1.4	1.8	6.0	2.9	4.3	0.0	9.6	4.3	0.0	0.0	0.0	3.6	100
LW-87-CW-62	f.g.sst,si	464.24	17.9	52.6	1.3	3.1	1.9	5.6	7.0	0.0	0.0	5.3	1.4	1.2	0.0	2.6	100
LW-87-CW-63	f.g.sst	464.44	20.5	62.2	7.2	1.6	0.0	3.3	2.7	0.0	0.0	2.6	0.0	0.0	0.0	0.0	100
LW-87-CW-64	f.g.sst,sh	464.68	37.9	26.9	1.9	1.7	2.4	1.8	15.5	0.0	0.0	7.2	1.3	0.7	0.0	2.6	100
LW-87-CW-65	f.g.sst,si	464.75	49.0	12.3	3.2	2.1	2.6	10.2	5.9	0.0	10.2	0.0	1.8	1.0	0.0	1.8	100
LW-87-CW-66	f.g.sst,sh,c	464.84	11.6	2.4	1.0	1.1	2.4	5.6	2.1	69.9	1.3	1.9	0.0	0.9	0.0	0.0	100
LW-87-CW-67	f.g.sst	465.03	38.6	26.5	2.4	2.2	3.2	8.4	9.5	0.0	0.0	5.7	2.4	1.2	0.0	0.0	100
LW-87-CW-68	f.g.sst,si	465.43	53.1	11.1	4.3	1.4	4.3	8.2	4.5	0.0	7.1	2.1	2.4	1.3	0.0	0.0	100
LW-87-CW-69	f.g.sst,si	465.85	50.0	12.7	5.2	1.3	1.1	5.6	7.2	0.0	6.9	7.3	1.1	0.0	0.0	1.7	100

SUMMARY OF < 45µm XRD DATA – Clearwater Formation Study Area (cont'd)

SAMPLE	LITHOLOGY	DEPTH	XRD RELATIVE ABUNDANCE (%)*														
NUMBER		(metres)	Qtz	Pl	KF	Chl	SC	10Å	7Å	Cal	Dol	Sid	Py	Amp	Ilm	Mag	Total
Well 16-2-66-3W4 Imp. 77 Medley O.V.																	
LW-87-CW-70	f.g.sst,si,sh	466.45	51.5	14.7	2.9	5.4	6.8	7.0	3.0	0.0	0.0	6.4	1.1	0.0	0.0	1.4	100
LW-87-CW-71	f.g.sst	467.07	41.6	15.2	7.9	2.4	4.6	10.4	7.6	0.0	5.7	3.4	1.3	0.0	0.0	0.0	100
LW-87-CW-72	f.g.sst,sh	467.64	46.2	13.1	5.5	1.6	10.8	3.7	3.8	0.0	5.5	3.4	1.1	1.1	0.0	4.4	100
LW-87-CW-73	f.g.sst,sh	473.94	55.9	9.6	3.6	2.1	6.9	9.3	5.9	0.0	4.5	0.0	2.1	0.0	0.0	0.0	100
Well 12-18-65-3W4 Imp. 77 Medley O.V.																	
LW-87-CW-74	f.g.sst,d.m.?	462.47	52.7	12.9	4.4	1.9	7.3	11.2	5.8	0.0	0.0	3.8	0.0	0.0	0.0	0.0	100
LW-87-CW-75	f.g.sst	464.64	44.4	30.8	0.0	1.2	0.9	4.9	7.8	0.0	0.0	9.0	1.1	0.0	0.0	0.0	100
LW-87-CW-76	f.g.sst	465.05	37.5	15.2	1.6	1.8	0.0	4.4	15.0	0.0	0.0	23.5	1.0	0.0	0.0	0.0	100
LW-87-CW-77	f.g.sst	465.27	32.4	15.8	1.7	2.2	0.0	4.7	27.9	0.0	0.0	9.3	1.5	0.0	0.0	4.4	100
LW-87-CW-80	f.g.sst	466.32	35.4	28.0	2.6	1.5	1.7	7.3	4.0	0.0	0.0	13.6	2.2	0.0	0.0	3.6	100
LW-87-CW-81	f.g.sst,sh	466.93	41.7	14.7	5.5	3.9	3.4	18.9	2.4	0.0	0.0	6.1	1.6	1.8	0.0	0.0	100
LW-87-CW-82	f.g.sst,sh	467.88	43.6	14.7	2.8	2.3	2.3	14.9	8.4	0.0	6.4	1.3	3.4	0.0	0.0	0.0	100
Well 5-22-65-3W4 Imp. Marie O.V.																	
LW-87-CW-83	f.g.sst.	433.4	36.6	22.7	2.6	2.3	1.5	6.0	11.7	1.8	0.0	9.2	0.0	1.2	0.0	4.4	100
LW-87-CW-84	f.g.sst,si,sh	440.75	41.0	16.5	3.1	2.9	3.2	14.3	11.3	0.0	5.8	0.0	0.8	0.0	0.0	1.1	100
LW-87-CW-85	f.g.sst	441.69	43.2	21.2	4.3	1.9	13.1	6.3	5.1	0.0	0.0	2.1	0.6	0.0	0.0	2.3	100

* Results expressed as normalized relative abundances based on peak heights, not weight percent;
sst=sand, si=silt, sh=shale, m=mud, c=carbonate cemented, d.m.=drilling mud;
v.f.g=very fine grained, f.g.=fine grained, m.g.=medium grained;
Qtz=quartz, Pl=plagioclase, KF=K feldspar, Chl=14Å chlorite, SC=swelling clays (~12Å), 10Å=mica / illite group clays;
7Å=kaolinite and / or berthierine clays, Cal=calcite, Dol=dolomite, Sid=siderite, Py=pyrite, Amp=amphiboles, Ilm=ilmenite, Mag=magnetite.

< 45µm XRD MINERAL DATA FOR FINE TO MEDIUM GRAINED SANDS – Clearwater Formation Study Area

SAMPLE NUMBER	DEPTH (metres)	DEPOSITIONAL CHARACTERISTICS			XRD RELATIVE ABUNDANCE (%)*														
		Lithology	Environment	Sequence	Qtz	Pl	KF	Chl	SC	10Å	7Å	Cal	Dol	Sid	Py	Amp	Ilm	Mag	Total
Oil (Bitumen) Saturated Sands																			
LW-87-CW-28	470.25	f.-m.g.sst	UDF-DC	S1, C3	47.3	24.5	2.6	1.4	1.7	6.8	8.7	0.0	0.0	2.8	0.7	0.0	0.0	3.6	100
LW-87-CW-44	474.00	f.g.sst	LDF	S1, D1	42.8	19.5	2.4	2.2	1.2	8.0	11.6	0.0	3.9	5.0	0.0	0.9	0.0	2.6	100
LW-87-CW-75	464.64	f.g.sst	MDF	S1, D2	44.4	30.8	0.0	1.2	0.9	4.9	7.8	0.0	0.0	9.0	1.1	0.0	0.0	0.0	100
LW-87-CW-29	480.20	f.-m.g.sst	UDF-DMB	S1, D2	35.2	30.0	4.8	2.3	0.0	8.0	13.2	0.0	0.0	5.3	1.2	0.0	0.0	0.0	100
LW-87-CW-31	480.80	f.-m.g.sst	UDF-DMB	S1, D2	42.6	19.6	5.5	2.0	2.1	8.3	11.4	0.0	0.0	6.3	1.3	0.9	0.0	0.0	100
LW-87-CW-32	481.00	f.g.sst	UDF-DMB	S1, D2	51.7	20.2	3.2	1.3	0.9	4.5	8.0	0.0	0.0	7.2	1.0	1.0	0.0	1.2	100
LW-87-CW-76	465.05	f.g.sst	MDF	S1, D2	37.5	15.2	1.6	1.8	0.0	4.4	15.0	0.0	0.0	23.5	1.0	0.0	0.0	0.0	100
LW-87-CW-77	465.27	f.g.sst	MDF	S1, D2	32.4	15.8	1.7	2.2	0.0	4.7	27.9	0.0	0.0	9.3	1.5	0.0	0.0	4.4	100
LW-87-CW-61	463.60	f.g.sst	LDF	S1, D	40.7	25.4	1.4	1.8	6.0	2.9	4.3	0.0	9.6	4.3	0.0	0.0	0.0	3.6	100
LW-87-CW-63	464.44	f.g.sst	LDF	S1, D	20.5	62.2	7.2	1.6	0.0	3.3	2.7	0.0	0.0	2.6	0.0	0.0	0.0	0.0	100
LW-87-CW-83	433.4	f.g.sst	M/UDF	S1, D	36.6	22.7	2.6	2.3	1.5	6.0	11.7	1.8	0.0	9.2	0.0	1.2	0.0	4.4	100
Average (S1):					39.2	26.0	3.0	1.8	1.3	5.6	11.1	0.2	1.2	7.7	0.7	0.4	0.0	1.8	
LW-87-CW-67	465.03	f.g.sst	DF	S2, A	38.6	26.5	2.4	2.2	3.2	8.4	9.5	0.0	0.0	5.7	2.4	1.2	0.0	0.0	100
LW-87-CW-71	467.07	f.g.sst	DF	S2, A	41.6	15.2	7.9	2.4	4.6	10.4	7.6	0.0	5.7	3.4	1.3	0.0	0.0	0.0	100
LW3-73	479.27	f.g.sst	LDF	S2, B	50.8	20.8	6.2	1.8	1.2	5.0	7.0	0.0	0.0	7.3	0.0	0.0	0.0	0.0	100
LW-87-CW-36	481.40	f.g.sst	L/MDF	S2, B	48.9	18.2	6.5	1.9	1.5	5.0	7.6	0.0	0.0	3.1	3.2	0.0	0.0	4.0	100
LW-87-CW-38	481.80	f.g.sst	L/MDF	S2, B	38.7	17.8	7.5	1.9	5.6	3.5	8.7	0.0	0.0	11.2	2.6	0.0	0.0	2.5	100
LW-87-CW-40	483.20	f.g.sst	L/MDF	S2, B	44.2	17.3	6.5	2.6	5.7	4.2	6.2	0.0	2.7	6.8	1.6	0.0	0.0	2.1	100
LW-87-CW-80	466.32	f.g.sst	DF/LDF	S2, B	35.4	28.0	2.6	1.5	1.7	7.3	4.0	0.0	0.0	13.6	2.2	0.0	0.0	3.6	100
LW-87-CW-85	441.69	f.g.sst	LDF	S2, B	43.2	21.2	4.3	1.9	13.1	6.3	5.1	0.0	0.0	2.1	0.6	0.0	0.0	2.3	100
LW-87-CW-41	491.20	f.g.sst	MDF-DMB	S2, C	46.9	24.2	2.5	2.9	3.4	4.9	5.6	0.0	3.9	4.9	0.9	0.0	0.0	0.0	100
Average (S2):					43.1	21.0	5.2	2.1	4.4	6.1	6.8	0.0	1.4	6.5	1.6	0.1	0.0	1.6	
Average (Oil Sands):					41.0	23.7	4.0	2.0	2.7	5.8	9.2	0.1	1.3	7.1	1.1	0.3	0.0	1.7	
Water Saturated Sands																			
LW-87-CW-26	513.55	f.g.sst	LDF	S2, B	35.4	20.0	3.2	2.4	1.2	9.5	10.7	0.0	0.0	15.6	1.5	0.6	0.0	0.0	100
LW-87-CW-27	519.40	f.g.sst	LDF	S2, B	40.3	15.2	5.4	2.4	1.5	10.6	14.8	0.0	0.0	3.7	1.0	0.0	5.0	0.0	100
Average (Water Sands):					37.8	17.6	4.3	2.4	1.3	10.1	12.7	0.0	0.0	9.7	1.3	0.3	2.5	0.0	

< 45µm XRD MINERAL DATA FOR FINE TO MEDIUM GRAINED SANDS (cont'd) – Clearwater Formation Study Area

SAMPLE NUMBER	DEPTH (metres)	DEPOSITIONAL CHARACTERISTICS			XRD RELATIVE ABUNDANCE (%)*														
		Lithology	Environment	Sequence	Qtz	Pl	KF	Chl	SC	10Å	7Å	Cal	Dol	Sid	Py	Amp	Ilm	Mag	Total
Overall Averages:																			
Average (S1):					39.2	26.0	3.0	1.8	1.3	5.6	11.1	0.2	1.2	7.7	0.7	0.4	0.0	1.8	
Average (S2):					42.2	20.4	5.0	2.2	3.9	6.8	7.9	0.0	1.1	7.0	1.6	0.2	0.5	1.3	
Average for all sands:					40.7	23.2	4.0	2.0	2.6	6.2	9.5	0.1	1.2	7.4	1.1	0.3	0.2	1.6	
Standard Deviation					6.9	9.9	2.3	0.4	3.0	2.3	5.3	0.4	2.5	5.1	0.9	0.4	1.1	1.8	
Minimum Value					20.5	15.2	0.0	1.2	0.0	2.9	2.7	0.0	0.0	2.1	0.0	0.0	0.0	0.0	
Maximum Value					51.7	62.2	7.9	2.9	13.1	10.6	27.9	1.8	9.6	23.5	3.2	1.2	5.0	4.4	

* Results expressed as normalized relative abundances based on peak heights, not weight percent;
sst=sand, f.g.=fine grained, m.g.=medium grained;
UDF=Upper Delta Front, DC=Distributary Channel, DMB=Distributary Mouth Bar, MDF=Middle Delta Front, LDF=Lower Delta Front, DF=Delta Fringe;
Qtz=quartz, Pl=plagioclase, KF=K feldspar, Chl=14Å chlorite, SC=swelling clays (~12Å), 10Å=mica / illite group clays;
7Å=kaolinite and / or berthierine clays, Cal=calcite, Dol=dolomite, Sid=siderite, Py=pyrite, Amp=amphiboles, Ilm=ilmenite, Mag=magnetite.

<45μm XRD MINERAL DATA FOR VERY FINE TO FINE GRAINED SANDS WITH SILT OR SHALE
Clearwater Formation Study Area

SAMPLE NUMBER	DEPTH (metres)	DEPOSITIONAL CHARACTERISTICS Lithology	Environment	Sequence	XRD RELATIVE ABUNDANCE (%)* Qtz	Pl	KF	Chl	SC	10Å	7Å	Cal	Dol	Sid	Py	Amp	Ilm	Mag	Total
Oil (Bitumen) Saturated Sands																			
LW-87-CW-43	473.70	f.g.sst,m	LDF	S1, D1	48.3	13.7	4.7	1.8	4.1	11.5	8.2	0.0	2.2	3.5	0.7	1.3	0.0	0.0	100
LW-87-CW-45	474.20	f.-m.g.sst,sh	LDF	S1, D1	44.1	17.4	5.0	1.9	2.2	10.5	11.1	0.0	0.0	7.2	0.6	0.0	0.0	0.0	100
LW-87-CW-46	474.30	f.g.sst,si	LDF	S1, D1	51.6	18.8	3.0	1.5	1.9	7.4	6.2	0.0	0.0	1.8	6.0	0.8	0.0	1.2	100
LW-87-CW-30	480.50	f.g.sst,tr.m	UDF-DMB	S1, D2	52.9	12.2	2.4	2.4	6.2	13.6	5.2	0.0	0.0	5.1	0.0	0.0	0.0	0.0	100
LW-87-CW-58	468.51	f.g.sst,si	LDF	S1, D	43.9	21.8	5.6	1.8	0.8	6.5	12.4	0.0	0.0	6.2	1.1	0.0	0.0	0.0	100
LW-87-CW-10	509.60	f.g.sst,tr.sh	MDF	S1, D	37.5	22.5	8.8	2.3	0.9	9.4	9.2	0.0	3.6	4.3	0.8	0.8	0.0	0.0	100
LW-87-CW-11	510.10	f.g.sst,si	MDF	S1, D	52.6	10.1	4.6	2.1	2.7	20.4	6.2	0.0	0.0	0.0	0.0	1.2	0.0	0.0	100
LW-87-CW-12	510.30	f.g.sst,tr.sh	MDF	S1, D	43.8	22.6	5.9	3.3	1.9	12.5	4.7	0.0	0.0	2.6	0.5	0.9	0.0	1.3	100
LW-87-CW-13	510.40	f.g.sst,tr.sh	MDF	S1, D	47.2	15.4	6.6	1.5	2.0	15.9	8.5	0.0	0.0	1.1	0.4	1.4	0.0	0.0	100
LW-87-CW-14	510.50	f.g.sst,tr.sh	MDF	S1, D	51.7	17.2	7.7	1.9	1.4	10.7	8.1	0.0	0.0	0.0	0.5	0.8	0.0	0.0	100
LW-87-CW-62	464.24	f.g.sst,si	LDF	S1, D	17.9	52.6	1.3	3.1	1.9	5.6	7.0	0.0	0.0	5.3	1.4	1.2	0.0	2.6	100
Average (S1):					44.7	20.4	5.1	2.1	2.4	11.3	7.9	0.0	0.5	3.4	1.1	0.8	0.0	0.5	
LW-87-CW-59	468.61	f.g.sst,si	DF	S2, A	46.4	10.5	4.5	3.0	3.8	13.5	8.1	0.0	3.7	4.3	0.9	1.4	0.0	0.0	100
LW-87-CW-15	510.60	f.g.sst,tr.sh	DF	S2, A	50.1	14.8	7.5	2.1	3.3	13.2	7.0	0.0	0.0	0.0	1.1	1.0	0.0	0.0	100
LW-87-CW-16	510.70	f.g.sst,si	DF	S2, A	50.2	12.6	5.2	3.2	8.6	11.9	3.1	0.0	0.0	0.0	4.0	1.1	0.0	0.0	100
LW-87-CW-49	474.60	f.g.sst,sh	DF	S2, A	64.9	10.0	3.2	1.4	4.9	7.1	5.6	0.0	0.0	0.0	1.0	0.0	0.0	2.0	100
LW-87-CW-64	464.68	f.g.sst,sh	DF	S2, A	37.9	26.9	1.9	1.7	2.4	1.8	15.5	0.0	0.0	7.2	1.3	0.7	0.0	2.6	100
LW-87-CW-65	464.75	f.g.sst,si	DF	S2, A	49.0	12.3	3.2	2.1	2.6	10.2	5.9	0.0	10.2	0.0	1.8	1.0	0.0	1.8	100
LW-87-CW-68	465.43	f.g.sst,si	DF	S2, A	53.1	11.1	4.3	1.4	4.3	8.2	4.5	0.0	7.1	2.1	2.4	1.3	0.0	0.0	100
LW-87-CW-69	465.85	f.g.sst,si	DF	S2, A	50.0	12.7	5.2	1.3	1.1	5.6	7.2	0.0	6.9	7.3	1.1	0.0	0.0	1.7	100
LW-87-CW-70	466.45	f.g.sst,si,sh	DF	S2, A	51.5	14.7	2.9	5.4	6.8	7.0	3.0	0.0	0.0	6.4	1.1	0.0	0.0	1.4	100
LW-87-CW-72	467.64	f.g.sst,sh	DF	S2, A	46.2	13.1	5.5	1.6	10.8	3.7	3.8	0.0	5.5	3.4	1.1	1.1	0.0	4.4	100
LW-87-CW-34	481.20	f.g.sst,m	L/MDF	S2, B	53.4	17.4	4.4	2.2	3.0	9.0	6.6	0.0	0.0	2.9	1.0	0.0	0.0	0.0	100
LW-87-CW-35	481.30	f.g.sst,tr.sh	L/MDF	S2, B	46.3	15.2	5.0	2.5	2.4	11.7	5.7	0.0	0.0	8.3	0.9	0.0	0.0	2.0	100
LW-87-CW-37	481.60	f.g.sst,m	L/MDF	S2, B	44.9	17.1	8.1	3.6	2.0	8.5	8.5	0.0	0.0	4.6	1.0	0.0	0.0	1.8	100
LW-87-CW-39	482.20	f.g.sst,si	L/MDF	S2, B	44.6	24.1	5.9	1.8	2.1	5.9	7.4	0.0	1.5	4.7	0.9	0.0	0.0	1.2	100
LW-87-CW-54	475.90	f.g.sst,si	LDF	S2, B	51.9	17.0	3.5	2.1	12.6	5.8	1.0	0.0	0.0	4.2	2.0	0.0	0.0	0.0	100
LW-87-CW-55	476.40	f.g.sst,sh	LDF	S2, B	52.3	15.0	1.3	1.9	2.2	9.4	8.1	0.0	4.3	3.3	0.0	0.9	1.4	0.0	100
LW-87-CW-81	466.93	f.g.sst,sh	DF/LDF	S2, B	41.7	14.7	5.5	3.9	3.4	18.9	2.4	0.0	0.0	6.1	1.6	1.8	0.0	0.0	100
LW-87-CW-82	467.88	f.g.sst,sh	DF/LDF	S2, B	43.6	14.7	2.8	2.3	2.3	14.9	8.4	0.0	6.4	1.3	3.4	0.0	0.0	0.0	100
LW-87-CW-84	440.75	f.g.sst,si,sh	LDF	S2, B	41.0	16.5	3.1	2.9	3.2	14.3	11.3	0.0	5.8	0.0	0.8	0.0	0.0	1.1	100

<45µm XRD MINERAL DATA FOR VERY FINE TO FINE GRAINED SANDS WITH SILT OR SHALE (cont'd)
Clearwater Formation Study Area

SAMPLE NUMBER	DEPTH (metres)	DEPOSITIONAL CHARACTERISTICS			XRD RELATIVE ABUNDANCE (%)*														
		Lithology	Environment	Sequence	Qtz	Pl	KF	Chl	SC	10Å	7Å	Cal	Dol	Sid	Py	Amp	Ilm	Mag	Total
Oil (Bitumen) Saturated Sands																			
LW-87-CW-74	462.47	f.g.sst,d.m.?	MDF	S1, D1	52.7	12.9	4.4	1.9	7.3	11.2	5.8	0.0	0.0	3.8	0.0	0.0	0.0	0.0	100
LW-87-CW-57	487.53	f.g.sst,si	DF/LDF	S2, C	47.7	14.3	3.2	1.6	11.1	1.4	5.9	0.0	5.2	5.8	0.0	1.0	0.0	3.0	100
LW-87-CW-73	473.94	f.g.sst,sh	MS	S2, WAB	55.9	9.6	3.6	2.1	6.9	9.3	5.9	0.0	4.5	0.0	2.1	0.0	0.0	0.0	100
Average (S2):					48.9	14.9	4.3	2.4	4.9	9.2	6.4	0.0	2.8	3.4	1.3	0.5	0.1	1.0	
Average (Oil Sands):					47.5	16.7	4.5	2.3	4.0	9.9	6.9	0.0	2.0	3.4	1.3	0.6	0.0	0.8	
Water Saturated Sands																			
LW3-36	468.24	f.g.sst,si	LDF	S1, D	33.0	22.5	8.2	2.2	1.5	9.1	11.1	0.0	5.2	5.0	0.0	2.3	0.0	0.0	100
LW3-39	468.91	f.g.sst,si	DF	S2, A	49.8	7.4	3.8	2.1	4.2	12.4	5.9	0.0	9.3	2.0	2.1	0.9	0.0	0.0	100
LW-87-CW-20	511.20	v.f.g.sst,si,sh	DF	S2, A	65.0	7.6	4.3	1.9	7.1	7.5	3.6	0.0	0.0	0.0	1.8	1.2	0.0	0.0	100
LW-87-CW-21	511.40	v.f.g.sst,tr.sh	DF	S2, A	55.4	6.3	3.4	1.5	2.9	6.9	5.8	0.0	15.5	0.0	1.2	1.2	0.0	0.0	100
LW-87-CW-22	511.65	v.f.g.sst,si,sh	DF	S2, A	48.5	11.1	4.1	1.7	5.7	8.7	5.2	0.0	10.9	0.0	2.7	1.5	0.0	0.0	100
LW-87-CW-23	511.80	v.f.g.sst,tr.sh	DF	S2, A	60.9	8.3	4.2	2.0	6.6	9.2	5.2	0.0	2.7	0.0	1.0	0.0	0.0	0.0	100
LW-87-CW-24	512.10	v.f.g.sst,sh	DF	S2, A	55.0	10.4	4.0	2.4	9.1	10.1	4.6	0.0	2.6	0.0	1.8	0.0	0.0	0.0	100
Average (S2):					55.7	8.5	4.0	1.9	5.9	9.1	5.1	0.0	6.8	0.3	1.8	0.8	0.0	0.0	
Average (Water Sands):					52.5	10.5	4.6	2.0	5.3	9.1	5.9	0.0	6.6	1.0	1.5	1.0	0.0	0.0	
Overall Averages:																			
Average (S1):					43.7	20.6	5.3	2.2	2.3	11.1	8.1	0.0	0.9	3.5	1.0	0.9	0.0	0.4	
Average (S2):					50.3	13.5	4.2	2.3	5.1	9.2	6.1	0.0	3.6	2.8	1.4	0.6	0.1	0.8	
Average for all sands:					48.4	15.6	4.5	2.2	4.2	9.8	6.7	0.0	2.8	3.0	1.3	0.7	0.0	0.7	
Standard Deviation					8.2	7.7	1.8	0.8	3.0	4.0	2.9	0.0	3.8	2.6	1.2	0.6	0.2	1.1	
Minimum Value					17.9	6.3	1.3	1.3	0.8	1.4	1.0	0.0	0.0	0.0	0.0	0.0	0.0	0.0	
Maximum Value					65.0	52.6	8.8	5.4	12.6	20.4	15.5	0.0	15.5	8.3	6.0	2.3	1.4	4.4	

* Results expressed as normalized relative abundances based on peak heights, not weight percent;
sst=sand, si=silt, sh=shale, m=mud, v.f.g=very fine grained, f.g.=fine grained, UDF=Upper Delta Front;
MDF=Middle Delta Front, LDF=Lower Delta Front, DF=Delta Fringe, MS=Middle Shoreface, WAB= Wabiskaw Member;
Qtz=quartz, Pl=plagioclase, KF=K feldspar, Chl=14Å chlorite, SC=swelling clays (~12Å), 10Å=mica / illite group clays;
7Å=kaolinite and / or berthierine clays, Cal=calcite, Dol=dolomite, Sid=siderite, Py=pyrite, Amp=amphiboles, Ilm=ilmenite, Mag=magnetite.

< 45μm XRD MINERAL DATA FOR SANDY SILTS OR SHALES – Clearwater Formation Study Area

SAMPLE	DEPTH	DEPOSITIONAL CHARACTERISTICS			XRD RELATIVE ABUNDANCE (%)*														
NUMBER	(metres)	Lithology	Environment	Sequence	Qtz	Pl	KF	Chl	SC	10Å	7Å	Cal	Dol	Sid	Py	Amp	Ilm	Mag	Total
Oil (Bitumen) Saturated Silts or Shales																			
LW3-90	457.03	si,f.g.sst,m	LDF	S1, B	36.1	4.5	3.5	3.1	9.1	19.3	4.6	0.0	0.0	15.8	1.4	2.7	0.0	0.0	100
LW-87-CW-42	473.40	si,f.g.sst	LDF	S1, D1	49.4	18.0	3.0	2.5	4.3	15.7	7.2	0.0	0.0	0.0	0.0	0.0	0.0	0.0	100
LW-87-CW-33	481.10	sh,sst,si	UDF-DMB	S1, D2	46.5	16.1	1.8	1.8	3.8	14.2	5.9	2.7	3.0	2.6	0.7	0.9	0.0	0.0	100
Average (S1):					44.0	12.9	2.8	2.5	5.7	16.4	5.9	0.9	1.0	6.1	0.7	1.2	0.0	0.0	
LW-87-CW-17	510.80	sh,tr.sst,si	DF	S2, A	51.3	8.2	4.7	2.4	13.7	10.0	2.8	0.0	3.6	0.0	2.4	0.9	0.0	0.0	100
LW-87-CW-51	475.00	sh,f.g.sst	DF	S2, A	59.5	8.6	3.1	1.9	9.6	10.1	3.7	2.3	0.0	0.0	1.2	0.0	0.0	0.0	100
LW3-13	491.62	sh,tr.sst,si	LS	S2, WAB	61.1	6.1	2.2	2.4	3.6	10.5	4.9	0.0	7.6	0.0	0.9	0.7	0.0	0.0	100
Average (S2):					57.3	7.6	3.3	2.2	8.9	10.2	3.8	0.8	3.7	0.0	1.5	0.5	0.0	0.0	
Average (Oil Silts/Shales):					50.7	10.2	3.0	2.3	7.3	13.3	4.9	0.8	2.4	3.1	1.1	0.9	0.0	0.0	
Water Saturated Silts or Shales																			
LW-87-CW-18	510.90	sh,tr.sst,si	DF	S2, A	46.9	7.4	6.2	2.2	13.8	11.7	4.4	0.0	2.5	0.0	2.8	2.0	0.0	0.0	100
LW-87-CW-19	511.00	sh,tr.sst,si	DF	S2, A	48.4	9.3	5.3	2.5	16.6	10.0	2.9	0.0	2.2	0.0	2.8	0.0	0.0	0.0	100
LW-87-CW-60	468.73	si,f.g.sst,m	DF	S2, A	47.6	10.5	4.0	3.1	1.4	7.5	5.3	8.6	7.8	0.0	3.4	0.9	0.0	0.0	100
LW3-66	477.14	sh,tr.sst,si	LDF	S2, B	48.7	6.5	3.3	2.5	7.3	15.3	5.6	0.0	0.0	10.8	0.0	0.0	0.0	0.0	100
LW-87-CW-25	512.60	sh,tr.si,sst	LDF	S2, B	56.0	8.0	5.3	2.2	8.5	8.5	3.6	0.0	3.7	0.0	1.2	1.5	1.5	0.0	100
Average (S2/Water Silts/Shales):					49.5	8.3	4.8	2.5	9.5	10.6	4.4	1.7	3.2	2.2	2.0	0.9	0.3	0.0	
Overall Averages:																			
Average (S1):					44.0	12.9	2.8	2.5	5.7	16.4	5.9	0.9	1.0	6.1	0.7	1.2	0.0	0.0	
Average (S2):					52.4	8.1	4.3	2.4	9.3	10.4	4.2	1.4	3.4	1.3	1.8	0.8	0.2	0.0	
Average for all silts or shales:					50.1	9.4	3.9	2.4	8.3	12.1	4.6	1.2	2.8	2.6	1.5	0.9	0.1	0.0	
Standard Deviation					6.9	4.1	1.4	0.4	4.9	3.6	1.3	2.6	2.8	5.4	1.2	0.9	0.5	0.0	
Minimum Value					36.1	4.5	1.8	1.8	1.4	7.5	2.8	0.0	0.0	0.0	0.0	0.0	0.0	0.0	
Maximum Value					61.1	18.0	6.2	3.1	16.6	19.3	7.2	8.6	7.8	15.8	3.4	2.7	1.5	0.0	

* Results expressed as normalized relative abundances based on peak heights, not weight percent; sst=sand, si=silt, sh=shale, m=mud, f.g.=fine grained; UDF=Upper Delta Front, DMB=Distributary Mouth Bar, LDF=Lower Delta Front, DF=Delta Fringe, LS=Lower Shoreface, WAB=Wabiskaw Member; Qtz=quartz, Pl=plagioclase, KF=K feldspar, Chl=14Å chlorite, SC=swelling clays (~12Å), 10Å=mica / illite group clays; 7Å=kaolinite and / or berthierine clays, Cal=calcite, Dol=dolomite, Sid=siderite, Py=pyrite, Amp=amphiboles, Ilm=ilmenite, Mag=magnetite.

< 45µm XRD MINERAL DATA FOR SILTS AND SHALES – Clearwater Formation Study Area

SAMPLE	DEPTH	DEPOSITIONAL CHARACTERISTICS			XRD RELATIVE ABUNDANCE (%)*														
NUMBER	(metres)	Lithology	Environment	Sequence	Qtz	Pl	KF	Chl	SC	10Å	7Å	Cal	Dol	Sid	Py	Amp	Ilm	Mag	Total
Water Saturated Silts and Shales																			
LW-87-CW-47	474.40	si,sh	DF	S2, A	60.2	6.2	4.1	1.9	11.0	10.0	3.7	0.0	0.0	0.0	2.0	0.9	0.0	0.0	100
LW-87-CW-48	474.50	sh,si	DF	S2, A	57.7	10.4	5.5	1.9	7.5	9.6	5.2	0.0	0.0	0.0	1.2	1.1	0.0	0.0	100
LW-87-CW-50	474.80	sh,si	DF	S2, A	62.0	6.1	2.8	1.7	8.2	10.5	4.7	0.0	2.3	0.0	1.8	0.0	0.0	0.0	100
Overall Average (S2/Water Silts/Shales):					59.9	7.6	4.1	1.8	8.9	10.0	4.5	0.0	0.8	0.0	1.7	0.7	0.0	0.0	
Standard Deviation					2.2	2.5	1.4	0.1	1.9	0.5	0.8	0.0	1.3	0.0	0.4	0.6	0.0	0.0	
Minimum Value					57.7	6.1	2.8	1.7	7.5	9.6	3.7	0.0	0.0	0.0	1.2	0.0	0.0	0.0	
Maximum Value					62.0	10.4	5.5	1.9	11.0	10.5	5.2	0.0	2.3	0.0	2.0	1.1	0.0	0.0	

* Results expressed as normalized relative abundances based on peak heights, not weight percent;
si=silt, sh=shale, DF=Delta Fringe;
Qtz=quartz, Pl=plagioclase, KF=K feldspar, Chl=14Å chlorite, SC=swelling clays (~12Å), 10Å=mica / illite group clays;
7Å=kaolinite and / or berthierine clays, Cal=calcite, Dol=dolomite, Sid=siderite, Py=pyrite, Amp=amphiboles, Ilm=ilmenite, Mag=magnetite.

< 45µm XRD MINERAL DATA FOR CALCITE CEMENTED INTERVALS – Clearwater Formation Study Area

SAMPLE NUMBER	DEPTH (metres)	DEPOSITIONAL CHARACTERISTICS Lithology	Environment	Sequence	Qtz	Pl	KF	XRD RELATIVE ABUNDANCE (%)* Chl	SC	10Å	7Å	Cal	Dol	Sid	Py	Amp	Ilm	Mag	Total
Calcite Cemented Samples																			
LW3-20	463.21	f.g.sst,m,c	LDF	S1, C	27.4	9.4	1.8	1.0	0.0	6.2	3.1	45.0	3.2	1.6	0.0	1.4	0.0	0.0	100
LW3-38	468.76	f.g.sst,si,m,c	DF	S2, A	37.6	10.1	4.3	2.2	1.8	7.6	5.2	11.8	0.0	5.5	12.9	1.0	0.0	0.0	100
LW-87-CW-66	464.84	f.g.sst,sh,c	DF	S2, A	11.6	2.4	1.0	1.1	2.4	5.6	2.1	69.9	1.3	1.9	0.0	0.9	0.0	0.0	100
LW-87-CW-56	477.40	sh,si,c	LDF	S2, B	9.5	0.0	0.0	1.2	0.0	4.9	0.4	82.0	0.0	2.1	0.0	0.0	0.0	0.0	100
LW3-21	494.15	f.g.sst,si,c	LS	S2, WAB	32.1	1.3	0.6	0.7	0.5	4.7	1.4	38.3	9.6	10.6	0.0	0.4	0.0	0.0	100
Average (S2):					22.7	3.4	1.5	1.3	1.2	5.7	2.3	50.5	2.7	5.0	3.2	0.6	0.0	0.0	
Overall Average:					23.6	4.6	1.5	1.3	0.9	5.8	2.4	49.4	2.8	4.3	2.6	0.7	0.0	0.0	
Standard Deviation					12.5	4.8	1.7	0.6	1.1	1.2	1.8	27.6	4.0	3.8	5.8	0.5	0.0	0.0	
Minimum Value					9.5	0.0	0.0	0.7	0.0	4.7	0.4	11.8	0.0	1.6	0.0	0.0	0.0	0.0	
Maximum Value					37.6	10.1	4.3	2.2	2.4	7.6	5.2	82.0	9.6	10.6	12.9	1.4	0.0	0.0	
Average, recalculated to 0% calcite basis:					46.7	9.1	3.0	2.5	1.8	11.5	4.8	0.0	5.5	8.5	5.1	1.4	0.0	0.0	100

* Results expressed as normalized relative abundances based on peak heights, not weight percent;
sst=sand, si=silt, sh=shale, m=mud, c=carbonate cemented, f.g.=fine grained;
LDF=Lower Delta Front, DF=Delta Fringe, LS=Lower Shoreface, WAB=Wabiskaw Member;
Qtz=quartz, Pl=plagioclase, KF=K feldspar, Chl=14Å chlorite, SC=swelling clays (~12Å), 10Å=mica / illite group clays;
Qtz=quartz, Pl=plagioclase, KF=K feldspar, Chl=14Å chlorite, SC=swelling clays (~12Å), 10Å=mica / illite group clays; Sid=siderite, Py=pyrite, Amp=amphiboles, Ilm=ilmenite, Mag=magnetite.
7Å=kaolinite and / or berthierine clays, Cal=calcite, Dol=dolomite, Sid=siderite, Py=pyrite, Amp=amphiboles, Ilm=ilmenite, Mag=magnetite.

SUMMARY OF < 2μm XRD DATA – Clearwater Formation Study Area

SAMPLE NUMBER	LITHOLOGY	DEPTH (metres)	CLAY ABUNDANCE (XRD)* SC¥	Chl	10Å	7Å	% Sm	COMMENTS
Well 3-13-65-4W4 Esso 84 (C1-12) Cold Lk.								
LW-87-CW-28	f.-m.g.sst	470.25	11	7	7	76	79†	SC=dioct. I/S (octa.sub.)±C/S; 7Å=Be
LW-87-CW-29	f.-m.g.sst	480.20	12	6	19	63	61†	SC=dioct. I/S ± C/S; 7Å=Be
LW-87-CW-31	f.-m.g.sst	480.80	19	3	10	68	60	SC=I/S; 7Å=Be ± Ka
LW-87-CW-32	f.g.sst	481.00	15	5	2	77	55	SC=dioct. I/S; 7Å=Be
LW-87-CW-33	sh,sst,si	481.10	24	1	52	23	72†	SC=I/S; 7Å=Be
LW-87-CW-34	f.g.sst,m	481.20	34	4	41	22	69	SC=I/S; 7Å=Be
LW-87-CW-35	f.g.sst,tr.sh	481.30	25	5	38	32	61†	SC=dioct. (octa.sub.) I/S; 7Å=Be
LW-87-CW-36	f.g.sst	481.40	20	7	24	49	57	SC=I/S; 7Å=Be ± Ka
LW-87-CW-37	f.g.sst,m	481.60	23	3	25	49	58	SC=I/S; 7Å=Be ± Ka
LW-87-CW-39	f.g.sst,si	482.20	29	4	32	36	62†	SC=I/S; 7Å=Be ± Ka
LW-87-CW-40	f.g.sst	483.20	12	6	26	56	53	SC=dioct. I/S ± C/S; 7Å=Be ± Ka
LW-87-CW-41	f.g.sst	491.20	17	10	24	49	61†	SC=I/S ± C/S; 7Å=Be ± Ka
Well 8-19-66-2W4 Esso 86 Marie O.V.								
LW-87-CW-43	f.g.sst,m	473.70	39	4	38	19	75	SC=I/S; 7Å=Be ± Ka
LW-87-CW-44	f.g.sst	474.00	12	6	16	66	73	SC=dioct. (octa.sub.) I/S; 7Å=Be
LW-87-CW-46	f.g.sst,si	474.30	35	3	31	31	62	SC=I/S; 7Å=Be ± Ka
LW-87-CW-47	si,sh	474.40	52	3	43	2	80†	SC=I/S; 7Å=Be ± Ka
LW-87-CW-48	sh,si	474.50	47	1	43	8	76†	SC=I/S; 7Å=Be ± Ka
LW-87-CW-49	f.g.sst,sh	474.60	66	1	28	5	70	SC=I/S; 7Å=Be ± Ka
LW-87-CW-50	sh,si	474.80	64	2	31	3	69	SC=I/S; 7Å=Be ± Ka
LW-87-CW-51	sh,f.g.sst	475.00	63	3	32	2	76†	SC=I/S; 7Å=Be ± Ka
LW-87-CW-54	f.g.sst,si	475.90	39	5	32	25	71†	SC=I/S; 7Å=Be ± Ka
LW-87-CW-56	sh,si,c	477.40	52	7	38	3	58	SC=C/S ± Sm; 7Å=Be ± Ka

SUMMARY OF < 2µm XRD DATA (cont'd) – Clearwater Formation Study Area

SAMPLE NUMBER	LITHOLOGY	DEPTH (metres)	CLAY ABUNDANCE (XRD)*					COMMENTS
			SC¥	Chl	10Å	7Å	% Sm	
Well 16-2-66-3W4 Imp. 77 Medley O.V.								
LW-87-CW-62	f.g.sst,si	464.24	25	7	17	51	61	SC=Trioct. C/S ± dioct. I/S; 7Å=Be
LW-87-CW-63	f.g.sst	464.44	21	4	20	54	56	SC=Trioct.C/S ± dioct.I/S; 7Å=Be±Ka
LW-87-CW-66	f.g.sst,sh,c	464.84	48	8	40	5	56	SC=C/S ± I/S; 7Å=Be ± Ka
LW-87-CW-67	f.g.sst	465.03	40	7	31	22	78	SC=Dioct. I/S ± C/S; 7Å=Be
LW-87-CW-69	f.g.sst,si	465.85	58	4	24	14	78†	SC=I/S; 7Å=Be ± Ka
LW-87-CW-70	f.g.sst,si,sh	466.65	63	2	26	9	69†	SC=I/S; 7Å=Be ± Ka
LW-87-CW-71	f.g.sst	467.07	67	3	22	8	66	SC=I/S; 7Å=Be ± Ka

* Results expressed as normalized relative abundances based on peak heights, not weight percent;
Chl=chlorite, 10Å=illite / mica and other 10Å clays, Be=berthierine, Ka=kaolinite;
¥ SC = smectitic clay; including smectite, and mixed layer illite/smectite (I/S) or chlorite/smectite (C/S);
† questionable value; due to poor form of saddle on Ca glycol chart;
sst=sand, si=silt, sh=shale, m=mud, c=carbonate cemented, d.m.=drilling mud;
v.f.g=very fine grained, f.g.=fine grained, m.g.=medium grained;
trioct.=trioctahedral, dioct.=dioctahedral, octa.sub.=octahedrally substituted.

RESULTS FROM <2µm MINERALOGIC ANALYSIS
WELL: *3-13-65-4W4 Esso 84 (C1-12) Cold Lk.*

SAMPLE LOCATION	DEPTH	DEPOSITIONAL CHARACTERISTICS			SC¥	CLAY ABUNDANCE (XRD)*			% Sm
		Lithology	Environment	Sequence		Chl	10Å	7Å	
LW-87-CW-28	470.25	f.-m.g.sst	UDF-Dist.Chl	S1, C3	11	7	7	76	79†
LW-87-CW-29	480.20	f.-m.g.sst	UDF-Dist.MB	S1, D2	12	6	19	63	61†
LW-87-CW-31	480.80	f.-m.g.sst	UDF-Dist.MB	S1, D2	19	3	10	68	60
LW-87-CW-32	481.00	f.g.sst	UDF-Dist.MB	S1, D2	15	5	2	77	55
LW-87-CW-33	481.10	sh,sst,si	UDF-Dist.MB	S1, D2	24	1	52	23	72†
LW-87-CW-34	481.20	f.g.sst,m	L/MDF	S2, B	34	4	41	22	69
LW-87-CW-35	481.30	f.g.sst,tr.sh	L/MDF	S2, B	25	5	38	32	61†
LW-87-CW-36	481.40	f.g.sst	L/MDF	S2, B	20	7	24	49	57
LW-87-CW-37	481.60	f.g.sst,m	L/MDF	S2, B	23	3	25	49	58
LW-87-CW-39	482.20	f.g.sst,si	L/MDF	S2, B	29	4	32	36	62†
LW-87-CW-40	483.20	f.g.sst	L/MDF	S2, B	12	6	26	56	53
LW-87-CW-41	491.20	f.g.sst	MDF-Dist.MB	S1, C	17	10	24	49	61†

CLAY MINERAL RATIOS:

SAMPLE LOCATION	DEPTH	10Å / SC	10Å / Chl	SC / Chl	7Å / 10Å	7Å / SC	7Å /SC+10Å	7Å / Chl	10Å+SC / Chl
LW-87-CW-28	470.25	0.66	1.02	1.55	10.79	7.09	4.28	11.02	2.58
LW-87-CW-29	480.20	1.69	3.46	2.05	3.26	5.50	2.05	11.26	5.50
LW-87-CW-31	480.80	0.51	3.05	5.98	6.83	3.48	2.31	20.83	9.03
LW-87-CW-32	481.00	0.15	0.43	2.94	34.29	5.02	4.38	14.75	3.37
LW-87-CW-33	481.10	2.14	42.59	19.87	0.43	0.93	0.30	18.51	62.46
LW-87-CW-34	481.20	1.20	11.52	9.61	0.55	0.65	0.30	6.28	21.13
LW-87-CW-35	481.30	1.54	7.76	5.03	0.84	1.30	0.51	6.53	12.79
LW-87-CW-36	481.40	1.18	3.33	2.83	2.09	2.46	1.13	6.98	6.17
LW-87-CW-37	481.60	1.07	7.26	6.80	1.98	2.11	1.02	14.35	14.06
LW-87-CW-39	482.20	1.09	8.29	7.59	1.14	1.24	0.59	9.44	15.88

RESULTS FROM <2µm MINERALOGIC ANALYSIS (cont'd)
CLAY MINERAL RATIOS: WELL: *3-13-65-4W4 Esso 84 (C1-12) Cold Lk.*

SAMPLE LOCATION	DEPTH	10Å / SC	10Å / Chl	SC / Chl	7Å / 10Å	7Å / SC	7Å /SC+10Å	7Å / Chl	10Å+SC / Chl
LW-87-CW-40	483.20	2.09	4.10	1.96	2.16	4.51	1.46	8.84	6.06
LW-87-CW-41	491.20	1.45	2.51	1.72	2.04	2.97	1.21	5.12	4.23

* all values are expressed as percent relative abundances calculated from normalized XRD data;
¥ SC = Smectitic clay; including smectite, and mixed layer illite/smectite (I/S) or chlorite/smectite (C/S);
† questionable value; due to poor form of saddle on Ca glycol chart; c=carbonate cement;
sst=sand, si=silt, sh=shale, m=mud, c=carbonate cemented; v.f.g=very fine grained, f.g.=fine grained, m.g.=medium grained;
UDF=Upper Delta Front, MDF=Middle Delta Front, LDF=Lower Delta Front; Dist.Chl.=Distributary Channel, Dist.MB=Distributary Mouth Bar;
S1=Sequence S1, S2=Sequence S2, A1–D4=respective cycle designations (see Appendix 1).

RESULTS FROM <2µm MINERALOGIC ANALYSIS
WELL: *16-2-66-3W4 Imp. 77 Medley O.V.*

SAMPLE LOCATION	DEPTH	DEPOSITIONAL CHARACTERISTICS				CLAY ABUNDANCE (XRD)*			
		Lithology	Environment	Sequence	SC¥	Chl	10Å	7Å	% Sm
LW-87-CW-62	464.24	f.g.sst,si	LDF	S1, D	25	7	17	51	61
LW-87-CW-63	464.44	f.g.sst	LDF	S1, D	21	4	20	54	56
LW-87-CW-66	464.84	f.g.sst,sh,c	DF	S2, A	48	8	40	5	56
LW-87-CW-67	465.03	f.g.sst	DF	S2, A	40	7	31	22	78
LW-87-CW-69	465.85	f.g.sst,si	DF	S2, A	58	4	24	14	78†
LW-87-CW-70	466.65	f.g.sst,si,sh	DF	S2, A	63	2	26	9	69†
LW-87-CW-71	467.07	f.g.sst	DF	S2, A	67	3	22	8	66

CLAY MINERAL RATIOS:

SAMPLE LOCATION	DEPTH	Ill / SC	10Å / Chl	SC / Chl	7Å / 10Å	7Å / SC	7Å /SC+10Å	7Å / Chl	10Å+SC / Chl
LW-87-CW-62	464.24	0.70	2.58	3.70	2.99	2.08	1.23	7.71	6.28
LW-87-CW-63	464.44	0.94	5.04	5.34	2.70	2.55	1.31	13.62	10.38
LW-87-CW-66	464.84	0.85	5.33	6.30	0.11	0.10	0.05	0.61	11.63
LW-87-CW-67	465.03	0.78	4.67	6.00	0.69	0.54	0.30	3.21	10.67
LW-87-CW-69	465.85	0.42	5.52	13.24	0.56	0.24	0.17	3.11	18.77
LW-87-CW-70	466.65	0.40	12.42	30.76	0.35	0.14	0.10	4.36	43.18
LW-87-CW-71	467.07	0.33	6.81	20.70	0.34	0.11	0.09	2.35	27.52

* all values are expressed as percent relative abundances calculated from normalized XRD data;
¥ SC = Smectitic clay; including smectite, and mixed layer illite/smectite (I/S) or chlorite/smectite (C/S);
† questionable value; due to poor form of saddle on Ca glycol chart; c=carbonate cement;
sst=sand, si=silt, sh=shale, m=mud, c=carbonate cemented; v.f.g=very fine grained, f.g.=fine grained, m.g.=medium grained;
LDF=Lower Delta Front, DF=Delta Fringe; S1=Sequence S1, S2=Sequence S2, A1–D4=respective cycle designations (see Appendix 1).

RESULTS FROM <2µm MINERALOGIC ANALYSIS
WELL: *8-19-66-2W4 Esso 86 Marie O.V.*

SAMPLE LOCATION	DEPTH	DEPOSITIONAL CHARACTERISTICS			SC¥	CLAY ABUNDANCE (XRD)*			
		Lithology	Environment	Sequence		Chl	10Å	7Å	% Sm
LW-87-CW-43	473.70	f.g.sst,m	LDF	S1, D	39	4	38	19	75
LW-87-CW-44	474.00	f.g.sst	LDF	S1, D	12	6	16	66	73
LW-87-CW-46	474.30	f.g.sst,si	LDF	S1, D	35	3	31	31	62
LW-87-CW-47	474.40	si,sh	DF	S2, A	52	3	43	2	80†
LW-87-CW-48	474.50	sh,si	DF	S2, A	47	1	43	8	76†
LW-87-CW-49	474.60	f.g.sst,sh	DF	S2, A	66	1	28	5	70
LW-87-CW-50	474.80	sh,si	DF	S2, A	64	2	31	3	69
LW-87-CW-51	475.00	sh,f.g.sst	DF	S2, A	63	3	32	2	76†
LW-87-CW-54	475.90	f.g.sst,si	LDF	S2, B	39	5	32	25	71†
LW-87-CW-56	477.40	sh,si,c	LDF	S2, B	52	7	38	3	58

CLAY MINERAL RATIOS:

SAMPLE LOCATION	DEPTH	10Å / SC	10Å / Chl	SC / Chl	7Å / 10Å	7Å / SC	7Å /SC+10Å	7Å / Chl	10Å+SC / Chl
LW-87-CW-43	473.70	0.99	9.13	9.22	0.50	0.50	0.25	4.57	18.36
LW-87-CW-44	474.00	1.36	2.51	1.85	4.08	5.54	2.35	10.24	4.36
LW-87-CW-46	474.30	0.89	10.69	11.95	1.00	0.90	0.47	10.73	22.64
LW-87-CW-47	474.40	0.82	12.60	15.36	0.04	0.03	0.02	0.45	27.96
LW-87-CW-48	474.50	0.91	35.27	38.60	0.18	0.17	0.09	6.43	73.87
LW-87-CW-49	474.60	0.42	47.49	112.02	0.19	0.08	0.06	8.97	159.51
LW-87-CW-50	474.80	0.49	17.19	35.40	0.10	0.05	0.03	1.65	52.60
LW-87-CW-51	475.00	0.51	9.14	18.00	0.07	0.03	0.02	0.59	27.14
LW-87-CW-54	475.90	0.83	7.01	8.47	0.79	0.65	0.36	5.51	15.47
LW-87-CW-56	477.40	0.74	5.56	7.54	0.08	0.06	0.03	0.43	13.10

abbreviations / footnotes as expressed for <2µm data in well 3-13-65-4W4.

APPENDIX 4:

ELEMENTAL DATA

SUMMARY OF XRF MAJOR OXIDE ELEMENTAL DATA – Clearwater Formation Study Area

SAMPLE NUMBER	DEPTH (metres)	DEPOSITIONAL CHARACTERISTICS			XRF ELEMENTAL ANALYSIS (%) – Raw Data											
		Lithology	Environment	Sequence	LOI	SiO2	Al2O3	Fe2O3	Na2O	K2O	CaO	MgO	TiO2	P2O5	MnO	Total
Well 6-31-66-2W4 Esso 86 Cold Lake O.V.																
LW-87-CW-10	509.60	f.g.sst,tr.sh	MDF	S1, D	4.1	72.9	12.1	3.46	2.03	2.08	1.65	1.35	0.39	0.14	0.03	100.1
LW-87-CW-11	510.10	f.g.sst,si	MDF	S1, D	8.8	63.9	14.7	4.84	2.26	2.26	0.91	1.76	0.53	0.11	0.04	100.1
LW-87-CW-12	510.30	f.g.sst,tr.sh	MDF	S1, D	5.4	69.6	13.0	4.35	2.58	2.05	1.38	1.53	0.40	0.11	0.06	100.4
LW-87-CW-13	510.40	f.g.sst,tr.sh	MDF	S1, D	6.3	69.0	13.2	3.95	2.47	2.24	1.18	1.31	0.44	0.12	0.04	100.3
LW-87-CW-14	510.50	f.g.sst,tr.sh	MDF	S1, D	4.7	72.6	12.3	2.95	2.59	2.07	1.45	1.16	0.36	0.13	0.02	100.2
LW-87-CW-15	510.60	f.g.sst,tr.sh	DF	S2, A	4.7	71.1	12.7	3.43	2.14	2.09	1.48	1.49	0.46	0.14	0.02	99.8
LW-87-CW-16	510.70	f.g.sst,si	DF	S2, A	13.2	59.5	14.7	5.55	1.64	2.05	0.65	2.16	0.63	0.08	0.03	100.2
LW-87-CW-17	510.80	sh,tr.sst,si	DF	S2, A	13.1	58.2	15.9	5.62	1.55	1.98	0.52	2.17	0.62	0.07	0.03	99.7
LW-87-CW-18	510.90	sh,tr.sst,si	DF	S2, A	12.6	58.9	15.6	5.67	1.29	2.07	0.64	2.32	0.64	0.09	0.02	99.8
LW-87-CW-19	511.00	sh,tr.sst,si	DF	S2, A	13.5	57.4	16.2	5.76	2.06	2.05	0.55	2.28	0.63	0.07	0.03	100.5
LW-87-CW-20	511.20	v.f.g.sst,si,sh	DF	S2, A	11.2	62.3	14.5	4.87	1.44	1.97	0.72	2.17	0.59	0.10	0.03	99.9
LW-87-CW-21	511.40	v.f.g.sst,tr.sh	DF	S2, A	9.1	67.6	12.0	4.20	0.90	2.01	1.27	2.32	0.53	0.16	0.02	100.1
LW-87-CW-22	511.65	v.f.g.sst,si,sh	DF	S2, A	9.5	64.7	13.8	4.35	2.09	2.04	0.94	2.09	0.56	0.12	0.03	100.2
LW-87-CW-23	511.80	v.f.g.sst,tr.sh	DF	S2, A	10.8	61.7	15.0	5.36	1.59	2.22	0.65	2.27	0.69	0.11	0.02	100.3
LW-87-CW-24	512.10	v.f.g.sst,sh	DF	S2, A	11.9	60.0	15.5	5.62	1.61	2.27	0.64	1.98	0.70	0.12	0.03	100.3
LW-87-CW-25	512.60	sh,tr.si,sst	LDF	S2, B	12.5	58.5	16.2	5.60	1.44	2.36	0.47	2.22	0.68	0.07	0.02	100.0
Average S1:					5.9	69.6	13.0	3.9	2.4	2.1	1.3	1.4	0.4	0.1	0.0	100.2
Average S2:					11.1	61.8	14.7	5.1	1.6	2.1	0.8	2.1	0.6	0.1	0.0	100.1
Average 6-31-66-2W4					9.4	64.2	14.2	4.7	1.9	2.1	0.9	1.9	0.6	0.1	0.0	100.1
Well 16-2-66-3W4 Imp. 77 Medley O.V.																
LW-87-CW-61	463.60	f.g.sst	LDF	S1, D	3.4	72.6	11.9	4.04	1.68	2.02	1.70	1.61	0.43	0.14	0.03	99.6
LW-87-CW-62	464.24	f.g.sst,si	LDF	S1, D	3.9	71.1	12.3	4.72	2.27	2.17	1.47	1.84	0.38	0.12	0.02	100.3
LW-87-CW-63	464.44	f.g.sst	LDF	S1, D	2.8	73.4	12.1	3.19	2.74	2.21	1.32	1.44	0.32	0.10	0.02	99.6
LW-87-CW-64	464.68	f.g.sst,sh	DF	S2, A	4.7	68.8	13.3	4.40	2.45	2.16	1.55	2.00	0.53	0.16	0.02	100.0
LW-87-CW-65	464.75	f.g.sst,si	DF	S2, A	7.3	65.7	12.5	5.21	2.76	2.07	1.72	2.02	0.54	0.21	0.03	100.1
LW-87-CW-66	464.84	f.g.sst,sh,c	DF	S2, A	34.2	16.1	3.4	2.49	0.00	0.51	41.13	1.30	0.19	0.10	0.91	100.3

SUMMARY OF XRF MAJOR OXIDE ELEMENTAL DATA (cont'd) – Clearwater Formation Study Area

SAMPLE	DEPTH	DEPOSITIONAL CHARACTERISTICS			XRF ELEMENTAL ANALYSIS (%) – Raw Data											
NUMBER	(metres)	Lithology	Environment	Sequence	LOI	SiO2	Al2O3	Fe2O3	Na2O	K2O	CaO	MgO	TiO2	P2O5	MnO	Total
Well 16-2-66-3W4 Imp. 77 Medley O.V.																
LW-87-CW-67	465.03	f.g.sst	DF	S2, A	7.3	65.8	12.3	5.53	2.56	2.09	1.67	1.80	0.51	0.18	0.06	99.7
LW-87-CW-68	465.43	f.g.sst,si	DF	S2, A	9.4	64.8	12.8	4.56	2.35	2.08	1.56	2.19	0.59	0.16	0.02	100.4
LW-87-CW-69	465.85	f.g.sst,si	DF	S2, A	5.2	68.3	13.7	4.23	2.16	2.07	1.59	2.00	0.64	0.17	0.03	100.0
LW-87-CW-70	466.45	f.g.sst,si,sh	DF	S2, A	2.6	73.1	12.3	2.84	2.81	2.07	1.73	1.57	0.49	0.16	0.03	99.7
Average S1:					3.4	72.4	12.1	4.0	2.2	2.1	1.5	1.6	0.4	0.1	0.0	99.8
Average S2:					10.1	60.4	11.5	4.2	2.2	1.9	7.3	1.8	0.5	0.2	0.2	100.0
Average 16-2-66-3W4					8.1	64.0	11.7	4.1	2.2	1.9	5.5	1.8	0.5	0.2	0.1	100.0
Overall average:					8.9	64.1	13.2	4.5	2.0	2.0	2.7	1.9	0.5	0.1	0.1	100.1

sst=sand, si=silt, sh=shale, m=mud, c=carbonate cemented, v.f.g=very fine grained, f.g.=fine grained, m.g.=medium grained;
MDF=Middle Delta Front, LDF=Lower Delta Front, DF=Delta Fringe.

SUMMARY OF XRF TRACE ELEMENT DATA - Clearwater Formation Study Area

SAMPLE NUMBER	DEPTH (metres)	DEPOSITIONAL CHARACTERISTICS			XRF ELEMENTAL ANALYSIS (ppm) - Raw Data															
		Lithology	Environment	Sequence	Nb	Zr	Y	Sr	Rb	Ba	Ga	La	Pb	Zn	Cu	Ni	Co	Cr	V	S
Well 6-31-66-2W4 Esso 86 Cold Lake O.V.																				
LW-87-CW-10	509.60	f.g.sst,tr.sh	MDF	S1, D	6	76	19	328	52	626	9	16	14	68	13	18	75	48	99	1298
LW-87-CW-11	510.10	f.g.sst,si	MDF	S1, D	9	107	22	258	90	445	20	32	20	71	21	30	55	73	169	1382
LW-87-CW-12	510.30	f.g.sst,tr.sh	MDF	S1, D	6	75	20	322	63	580	13	19	9	63	13	16	50	61	121	1316
LW-87-CW-13	510.40	f.g.sst,tr.sh	MDF	S1, D	7	96	22	311	75	578	15	32	16	69	17	24	67	45	136	1791
LW-87-CW-14	510.50	f.g.sst,tr.sh	MDF	S1, D	6	75	18	327	57	653	12	<1	15	70	16	21	71	42	121	1810
LW-87-CW-15	510.60	f.g.sst,tr.sh	DF	S2, A	7	110	21	308	63	583	13	19	22	73	17	22	59	47	131	2328
LW-87-CW-16	510.70	f.g.sst,si	DF	S2, A	9	199	22	245	91	326	22	18	25	72	22	26	34	73	185	9499
LW-87-CW-17	510.80	sh,tr.sst,si	DF	S2, A	12	187	24	250	99	241	25	16	20	63	21	20	24	48	149	5178
LW-87-CW-18	510.90	sh,tr.sst,si	DF	S2, A	10	194	23	248	98	260	25	26	20	68	26	19	27	53	142	6309
LW-87-CW-19	511.00	sh,tr.sst,si	DF	S2, A	11	184	24	244	105	241	27	26	20	62	24	19	24	41	149	5271
LW-87-CW-20	511.20	v.f.g.sst,si,sh	DF	S2, A	9	216	27	252	93	343	22	26	19	68	20	23	37	81	157	5116
LW-87-CW-21	511.40	v.f.g.sst,tr.sh	DF	S2, A	10	219	29	200	80	427	16	27	67	83	24	25	37	77	154	5359
LW-87-CW-22	511.65	v.f.g.sst,si,sh	DF	S2, A	8	188	23	251	80	408	20	25	22	75	20	25	53	103	162	4529
LW-87-CW-23	511.80	v.f.g.sst,tr.sh	DF	S2, A	12	201	28	232	115	350	22	38	26	74	27	26	47	66	177	3348
LW-87-CW-24	512.10	v.f.g.sst,sh	DF	S2, A	12	174	27	241	111	317	25	28	31	75	23	27	31	77	151	3814
LW-87-CW-25	512.60	sh,tr.si,sst	LDF	S2, B	12	166	26	245	119	300	28	28	17	66	23	29	28	81	180	2582
Average S1:					7	86	20	309	67	576	14	25	15	68	16	22	64	54	129	1519
Average S2:					10	185	25	247	96	345	22	25	26	71	22	24	36	68	158	4848
Average 6-31-66-2W4:					9	154	23	266	87	417	20	25	23	70	20	23	45	64	149	3808
Well 16-2-66-3W4 Imp. 77 Medley O.V.																				
LW-87-CW-61	463.60	f.g.sst	LDF	S1, D	6	76	19	329	51	623	11	24	10	63	8	25	77	80	109	2709
LW-87-CW-62	464.24	f.g.sst,si	LDF	S1, D	6	63	18	331	57	685	11	26	10	60	15	18	206	31	96	890
LW-87-CW-63	464.44	f.g.sst	LDF	S1, D	4	55	16	329	55	663	7	24	13	65	10	22	146	46	101	1608
LW-87-CW-64	464.68	f.g.sst,sh	DF	S2, A	5	115	21	345	60	574	13	24	9	68	6	25	57	101	132	2273
LW-87-CW-65	464.75	f.g.sst,si	DF	S2, A	6	134	24	309	65	520	17	20	13	76	11	26	54	109	145	5117
LW-87-CW-66	464.84	f.g.sst,sh,c	DF	S2, A	3	27	29	650	19	162	<1	12	11	40	10	17	44	14	43	2637
LW-87-CW-67	465.03	f.g.sst	DF	S2, A	6	135	23	323	59	609	12	20	14	71	10	25	252	104	123	4414
LW-87-CW-68	465.43	f.g.sst,si	DF	S2, A	8	172	23	313	63	516	12	12	16	71	13	29	46	124	153	8702

SUMMARY OF XRF TRACE ELEMENT DATA – Clearwater Formation Study Area

SAMPLE NUMBER	DEPTH (metres)	DEPOSITIONAL CHARACTERISTICS Lithology	Environment	Sequence	Nb	Zr	Y	Sr	Rb	Ba	Ga	La	Pb	Zn	Cu	Ni	Co	Cr	V	S
					XRF ELEMENTAL ANALYSIS (ppm) – Raw Data															
Well 16-2-66-3W4 Imp. 77 Medley O.V.																				
LW-87-CW-69	465.85	f.g.sst,si	DF	S2, A	8	187	21	339	60	543	18	21	7	63	6	20	63	150	130	2799
LW-87-CW-70	466.45	f.g.sst,si,sh	DF	S2, A	7	196	21	378	52	663	13	13	11	67	8	20	102	109	98	1418
Average S1:					5	65	18	330	54	657	10	25	11	63	11	22	143	52	102	1736
Average S2:					6	138	23	380	54	512	14	17	12	65	9	23	88	102	118	3909
Average 16-2-66-3W4					6	116	22	365	54	556	13	20	11	64	10	23	105	87	113	3257
Overall Average:					8	140	23	304	74	471	17	23	18	68	16	23	68	72	135	3596
Detection Limit:					1	1	1	1	1	1	1	1	3	1	1	1	1	1	1	261
Analysis of Standards																				
UWO-1					16	273	32	205	220	498	28	49	34	52	8	8	38	<1	75	666
GSP-1					24	549	19	239	282	1133	29	123	53	76	35	11	8	<1	76	627
Literature values:					26	530	29	234	254	1310	22	185	54	103	34	10	7	13	53	350
G-2					11	321	10	457	181	1578	27	82	31	71	10	5	<1	<1	52	<261
Literature values:					13	300	11	478	170	1880	22	90	31	85	11	5	46	9	36	-

sst=sand, si=silt, sh=shale, m=mud, c=carbonate cemented, v.f.g=very fine grained, f.g.=fine grained, m.g.=medium grained;
MDF=Middle Delta Front, LDF=Lower Delta Front, DF=Delta Fringe,

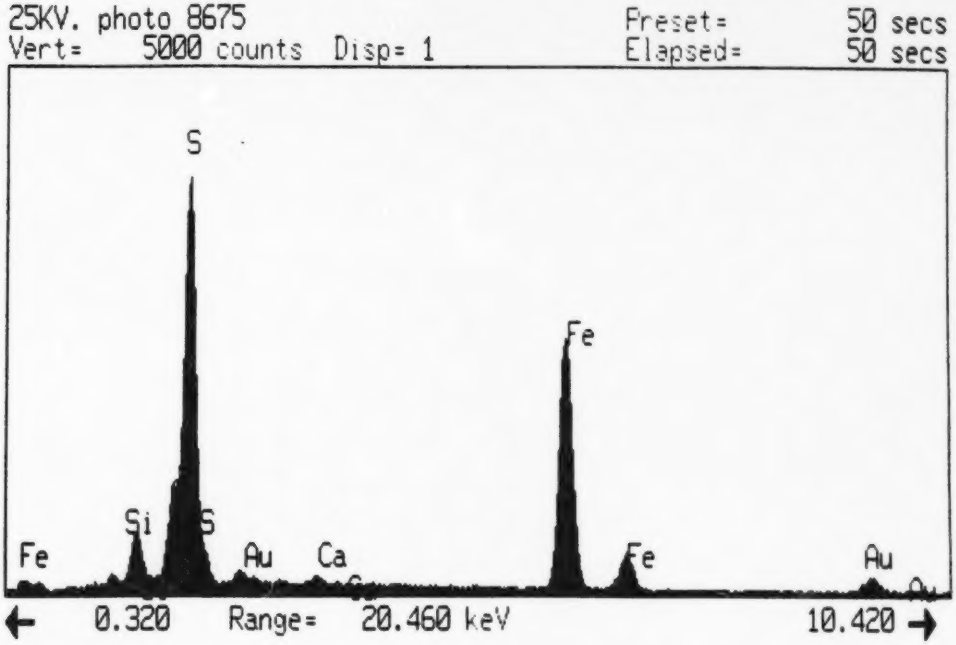

EDX analysis of pyrite (FeS_2) at arrow in Plate 3.7d.

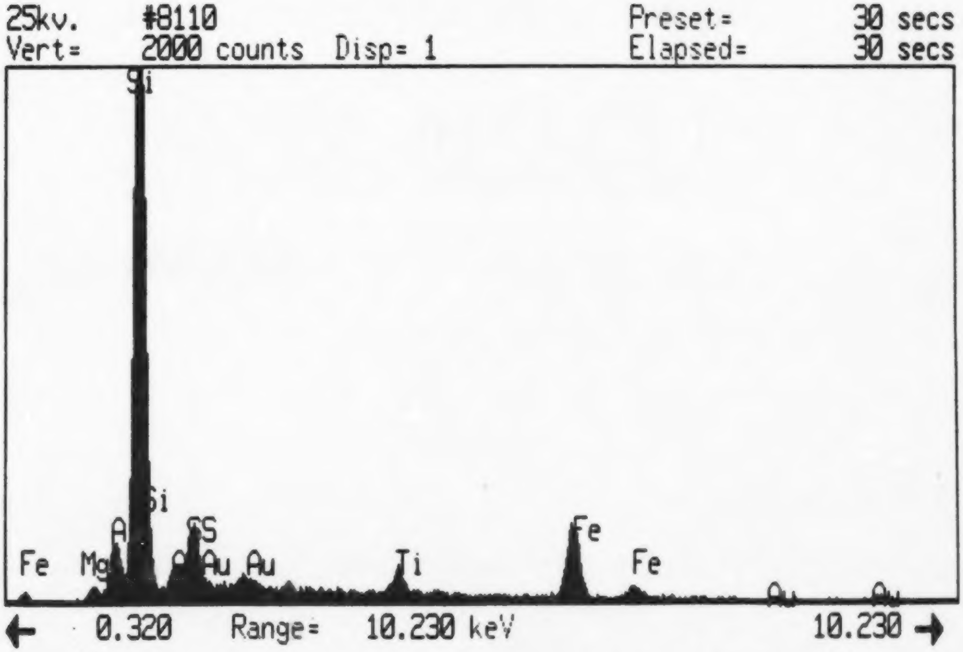

EDX analysis of berthierine ($\sim(Fe^{2+},Mn^{2+},Mg)_{3-x}(Fe^{3+},Al)_x(Si_{2-x},Al_x)O_5(OH)_4$) at arrow in Plate 3.8f.

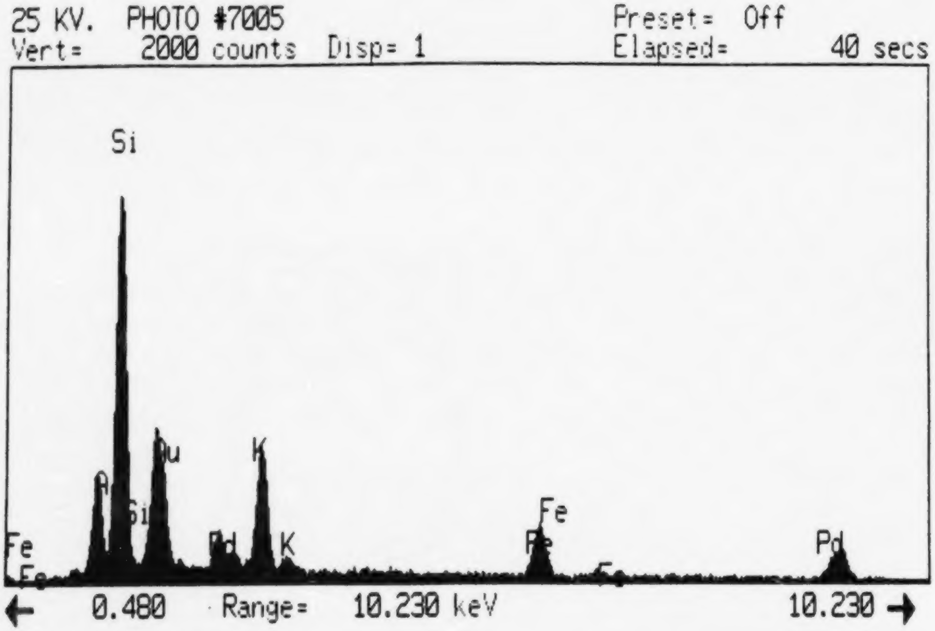

EDX analysis of illite (~$K_{1-1.5}$,Al_4($Si_{7-6.5}$,$Al_{1-1.5}$,O_{20}) $(OH)_4$) at arrow in Plate 3.10b.

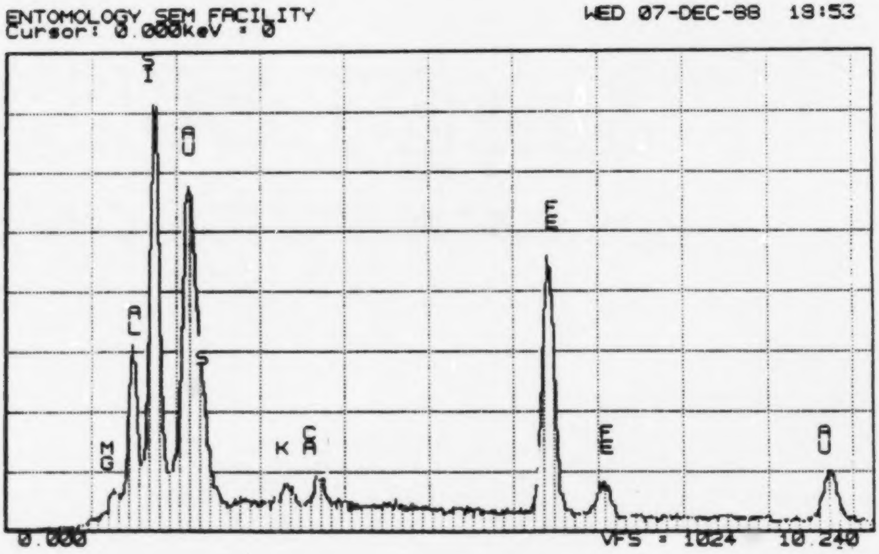

EDX analysis of mixed-layer illite / smectite (K, Ca, Mg and Fe-rich aluminum silicate), at ◤ in Plate 3.8f.

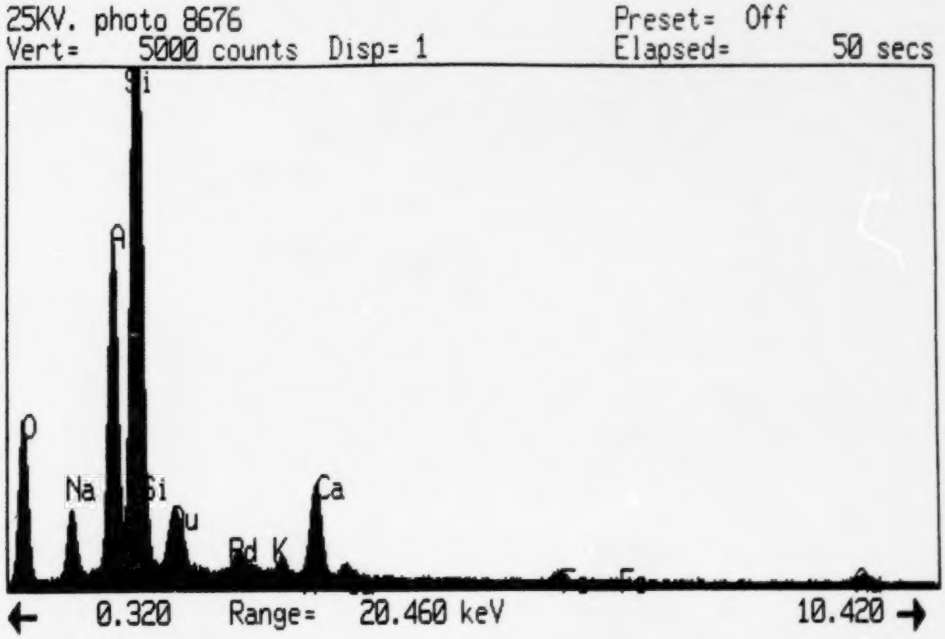

EDX analysis of zeolite (clinoptilolite)(~$Na_{1.3}$,$K_{1.2}$,$Ca_{1.55}$,$Al_{6.2}$,$Si_{29.8}$,O_{72}.23H_2O) at arrow in Plate 3.13e.

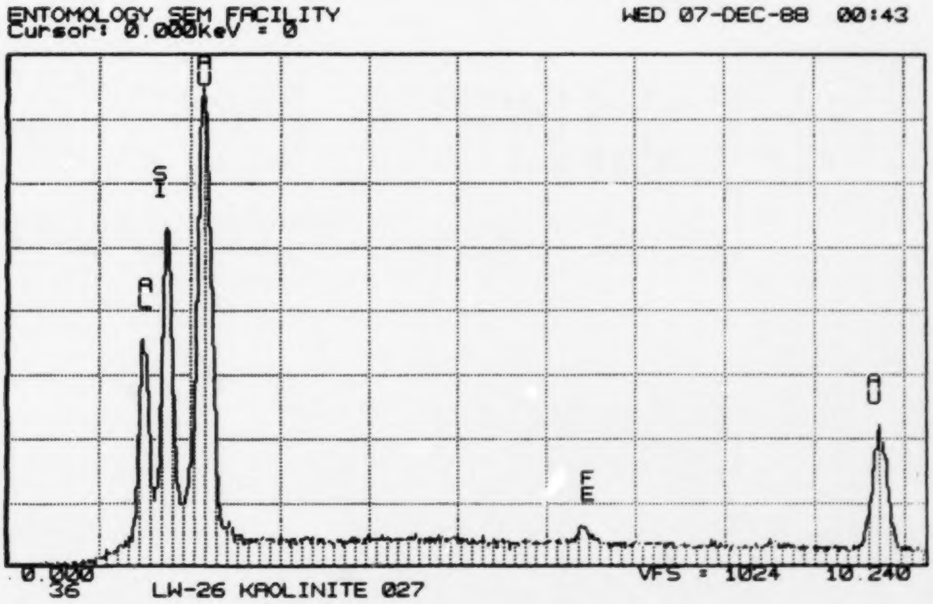

EDX analysis of kaolinite ($Al_4(Si_4O_{10})(OH)_8$) at ┏ in Plate 3.14b.

APPENDIX 5:

HYDROGEOLOGICAL EQUATIONS

EQUATIONS OF GROUNDWATER FLOW:

DARCY'S LAW:

An empirical equation which mathematically expresses fluid flow on a macroscopic scale.

(Freeze and Cherry, 1979) $$q = -K \frac{dh}{dl} \quad \text{or} \quad q = -K \text{ grad } h = -K \, \Delta \, h \qquad (1)$$

where, q is the specific discharge, K is the hydraulic conductivity, h is the hydraulic head and dh / dl is the hydraulic gradient.

FLUID POTENTIAL:

The mechanical energy per unit mass of fluid:

(Freeze and Cherry, 1979) $$\Phi = gz + \frac{p - p_o}{\rho} = gh \qquad (2)$$

where, Φ is the fluid potential, z is the elevation above a datum, p is pore pressure, p_o is atmospheric pore pressure and ρ is the relative fluid density.

LAW OF MASS CONSERVATION:

A law which mathematically states that a change in the rate of mass flow through a unit volume would result in a corresponding change in the mass stored within that unit volume. Also known as the continuity equation:

(Tóth, 1984) $$\text{div}\,(\rho q) = (\rho q) = \frac{\partial\,(\rho n)}{\partial t} \qquad (3)$$

where, $\rho(x,y,z,t)$ is fluid density and n (x,y,x,t) is porosity, for the flow of a compressible liquid through a compressible porous medium.

LAPLACE EQUATION:

A combination of both Darcy's Law and the Law of Mass Conservation. The general equation for steady-state groundwater flow in an isotopic, homogeneous medium:

(Tóth, 1984) $$\nabla^2 h = \frac{\partial^2 h}{\partial x^2} + \frac{\partial^2 h}{\partial y^2} + \frac{\partial^2 h}{\partial z^2} \qquad (4)$$

where, h is the hydraulic head and x, y, and z are directions. This equation mathematically expresses the movement of water in regional groundwater flow systems.

APPENDIX 6:

FLUID DATA AND METHODOLOGY

List of Contents:

Procedure for Selecting Chemical Fluid Analyses Data

Pressure Data: Cold Lake Study Area, Colony Formation

Pressure Data: Cold Lake Study Area, Grand Rapids Formation

Pressure Data: Cold Lake Study Area, Clearwater Formation

Pressure Data: Cold Lake Study Area, other formations

Water Analyses: Cold Lake Study Area, Colony Formation

Water Analyses: Cold Lake Study Area, Colony Formation, normalized to major anions and cations

Water Analyses: Cold Lake Study Area, Grand Rapids Formation

Water Analyses: Cold Lake Study Area, Grand Rapids Formation, normalized to major anions and cations

Water Analyses: Cold Lake Study Area, Clearwater Formation

Water Analyses: Cold Lake Study Area, Clearwater Formation, normalized to major anions and cations

PROCEDURE FOR SELECTING CHEMICAL FLUID ANALYSES DATA: (For Hydrocarbon Wells)

1. A listing of all wells with fluid analyses in the study area, and their complete analysis was obtained from the ERCB fluid analysis index for non-confidential wells.

2. Water analysis data were generally rejected if they did not correspond to the following criteria:

   a) pH (if available) between 6 and 9 (for Cretaceous waters);
   b) K^+ (if present), less than ~50 mg/L (high values may indicate KCl contamination);
   c) CO_3^{2-} (if present), less than 100 mg/L (for Cretaceous waters; much higher values will be obtained for Paleozoic waters);
   d) SO_4^{2-}, was discarded if erroneously high values were encountered, higher than the average for the area (may indicate gypsum-based drilling mud contamination);
   e) OH^- (if available), less than 600 mg/L;
   f) data rejected if value for Cl^- was very different than that of Na^+.

3. The sampling site for each well was also examined as this may affect the fluid composition greatly. Samples obtained downhole from drill stem tests are the most valuable. Analyses with high mud or sediment content were generally rejected, as were samples from a holding tank or a battery (multi-well samples). Samples from the separator or flare glassete, or swabbed, bailed or pumped through the drillpipe are not of the best quality and an effort was made to use other wells if possible.

4. Samples were also checked for their ionic balance, and that a long period of time had not elapsed between sampling and analysis.

5. In some cases, wells with slightly less than ideal fluid analyses were kept for this study because of the low number of analyses available for the study area.

PRESSURE DATA: COLD LAKE STUDY AREA
COLONY FORMATION

LSD	SEC	TWP	RGE	KB	P.R. DEPTH	FM. PRESS.	HEAD
10	14	65	2	592.81	299.30	1994.80	494.39
10	26	65	2	589.76	296.56	2077.55	502.41
11	4	66	2	609.90	313.26	1936.00	491.60
10	10	66	2	612.62	324.29	1954.86	485.19
6	22	66	2	620.15	321.55	2060.32	506.08
10	3	63	5	558.60	304.00	2199.10	476.05
15	5	63	5	546.80	293.00	2482.00	503.74
11	18	63	5	558.80	301.00	2469.30	506.46
6	22	63	5	550.90	288.00	2301.00	494.62
1	25	63	5	559.30	300.82	2280.14	488.09
11	6	64	5	570.50	312.90	2436.00	502.91
11	11	64	5	558.70	295.00	2284.13	493.72
6	19	64	5	603.00	351.90	1754.00	427.73
6	9	63	6	561.50	306.90	2409.00	497.19
11	20	63	6	559.55	307.00	2348.76	489.07
9	23	63	6	573.80	318.00	2476.20	505.16
7	4	64	6	574.30	318.86	1819.00	438.62
14	17	64	6	583.40	304.00	2473.00	528.44
10	19	64	6	596.10	324.00	2482.00	522.04

LSD – legal subdivision
SEC – section
TWP – township
RGE – range
KB – kelly bushing
FM – formation
PR. DEPTH – pressure depth
PRESS.– pressure

PRESSURE DATA: COLD LAKE STUDY AREA
GRAND RAPIDS FORMATION

LSD	SEC	TWP	RGE	KB	PRD	PRESS	HEAD
10	29	63	6	571.20	303.00	2527.00	522.67
6	5	64	2	552.40	382.00	3082.80	480.84
15	17	64	6	584.20	324.00	2334.20	495.26
7	8	65	5	643.10	394.00	2659.56	516.92
7	8	65	5	643.10	408.00	2694.57	506.45
7	8	65	5	643.10	436.00	2792.00	488.26
7	8	65	5	643.10	436.00	2810.00	490.07
7	31	65	5	650.50	405.22	2606.00	507.71
7	31	65	5	650.50	388.82	2278.00	491.08
11	1	65	6	654.00	434.82	2638.00	484.83
11	1	65	6	654.00	403.00	2254.00	477.98
11	1	65	6	654.00	426.82	2471.00	476.01
11	1	65	6	654.00	414.00	2394.60	481.14
11	10	65	6	647.00	363.22	1986.00	483.77
6	27	65	6	634.10	476.00	3197.20	480.06
16	3	66	5	646.20	328.50	1840.90	503.08
1	16	66	5	643.44	323.80	1617.00	482.48
10	29	67	2	710.76	378.40	1646.00	498.12
11	4	67	3	657.50	329.00	1700.00	499.69
9	16	67	3	653.00	357.00	1500.00	447.05
7	36	67	3	704.30	371.90	1682.00	501.78
9	9	67	4	703.40	368.90	1922.49	528.10
2	12	67	4	683.60	456.90	2612.94	489.83
6	28	67	5	663.60	314.96	1632.00	512.99

PRESSURE DATA: COLD LAKE STUDY AREA
CLEARWATER FORMATION

LSD	SEC	TWP	RGE	KB	P.R. DEPTH	FM. PRESS.	HEAD
14	17	64	6	583.40	412.00	3060.00	479.55
6	18	66	5	638.88	432.00	2678.00	476.56
2	12	67	4	683.60	456.90	2612.94	489.83
11	1	65	6	654.00	426.82	2471.00	476.01
11	1	65	6	654.00	434.82	2638.00	484.83
11	1	65	6	646.20	328.50	1840.90	503.08

PRESSURE DATA: COLD LAKE STUDY AREA
OTHER FORMATIONS

LSD	SEC	TWP	RGE	KB	P.R. DEPTH	FM. PRESS.	HEAD	SAMPLE
10	10	66	6	633.3	911.00	8556.6	583.97	1
2	20	64	4	588.1	293.5	1549.8	450.67	2

SAMPLE 1: DEVONIAN
SAMPLE 2: U. MANNVILLE?

WATER ANALYSES: COLD LAKE STUDY AREA
COLONY FORMATION

LSD	SEC	TWP	RGE	TDS	Ca	Mg	Cl	HCO3	SO4	Sp. Grav.	Comments
7	3	63	1	3234	16	11	552	1122	535	1.00	dst
1	33	66	1	3261	16	2	870	1283	26	1.00	dst
9	5	63	1	20317	219	101	12230	234	4	1.01	high K+
12	7	63	2	25546	312	236	15314	403	2	1.02	high K+
15	1	63	3	30165	628	241	18057	386	65	1.02	tubing sample
12	12	63	3	30544	789	357	18504	277	2	1.02	tubing sample
6	23	63	3	12049	80	45	6690	556	206	1.01	tubing sample
10	3	64	3	27744	423	103	16760	240	15	1.02	drillpipe sample
5	17	64	2	9732	78	36	5319	713	0	1.01	drillpipe sample
10	22	64	3	28768	480	234	17340	325	9	1.02	drillpipe sample
8	17	64	4	5902	74	16	3135	481	48	1.01	high sand %
10	9	66	5	13144	227	85	7498	517	58	1.01	CO3: 53
13	14	63	4	31418	460	304	19000	244	0	1.03	CO3:60
9	22	64	3	37815	649	260	22840	330	30	1.03	tubing sample
8	7	66	5	20948	320	119	12515	327	12	1.01	sampled above tool
4	28	66	5	9728	79	50	5270	770	25	1.01	145ft above tool
6	22	63	5	34632	581	379	20600	237	53	1.02	bottom sample
6	9	63	6	35037	641	416	21250	222	43	1.02	bottom sample K+:35
7	34	63	6	29385	388	224	18200	259	21	1.02	bottom sampl K+:35
11	11	64	5	23390	412	180	14400	132	80	1.02	downhole sample K+:36
6	23	64	6	28459	709	284	17220	508	37	1.02	bottom sample K+:71
10	10	65	2	6517	35	9	2949	935	163	1.01	top of recovery K+:18
Average compositions:				21260.68	346.18	167.82	12568.77	477.32	65.18	1.02	

TDS=Total dissolved solids
-anions, cations and TDS in mg/L

WATER ANALYSES: COLD LAKE STUDY AREA
COLONY FORMATION
Percent compositions normalized to major anions and cations

LSD	SEC	TWP	RGE	TDS	% Ca	% Mg	% Cl	% HCO3	% SO4	Ca/Mg
7	3	63	1	3234	59.26	40.74	24.99	50.79	24.22	1.45
1	33	66	1	3261	88.89	11.11	39.93	58.88	1.19	8.00
9	5	63	1	20317	68.44	31.56	98.09	1.88	0.03	2.17
12	7	63	2	25546	56.93	43.07	97.42	2.56	0.01	1.32
15	1	63	3	30165	72.27	27.73	97.56	2.09	0.35	2.61
12	12	63	3	30544	68.85	31.15	98.51	1.47	0.01	2.21
6	23	63	3	12049	64.00	36.00	89.77	7.46	2.76	1.78
10	3	64	3	27744	80.42	19.58	98.50	1.41	0.09	4.11
5	17	64	2	9732	68.42	31.58	88.18	11.82	0.00	2.17
10	22	64	3	28768	67.23	32.77	98.11	1.84	0.05	2.05
8	17	64	4	5902	82.22	17.78	85.56	13.13	1.31	4.63
10	9	66	5	13144	72.76	27.24	92.88	6.40	0.72	2.67
13	14	63	4	31418	60.21	39.79	98.73	1.27	0.00	1.51
9	22	64	3	37815	71.40	28.60	98.45	1.42	0.13	2.50
8	7	66	5	20948	72.89	27.11	97.36	2.54	0.09	2.69
4	28	66	5	9728	61.24	38.76	86.89	12.70	0.41	1.58
6	22	63	5	34632	60.52	39.48	98.61	1.13	0.25	1.53
6	9	63	6	35037	60.64	39.36	98.77	1.03	0.20	1.54
7	34	63	6	29385	63.40	36.60	98.48	1.40	0.11	1.73
11	11	64	5	23390	69.59	30.41	98.55	0.90	0.55	2.29
6	23	64	6	28459	71.40	28.60	96.93	2.86	0.21	2.50
10	10	65	2	6517	79.55	20.45	72.87	23.10	4.03	3.89

WATER ANALYSES: COLD LAKE STUDY AREA
GRAND RAPIDS FORMATION

LSD	SEC	TWP	RGE	TDS	Ca	Mg	Cl	HCO3	SO4	Sp. Grav.	Comments
5	19	63	2	22014	393	209	13030	399	144	1.02	sample extracted from mud -high K+:46
11	5	63	3	18873	223	104	11200	366	23	1.01	bottom sample
4	7	63	3	23573	441	313	15531	213	3	1.02	Sparky Mbr - dst
5	28	64	6	30966	635	97	18633	315	0	1.02	swabbed sample
10	22	64	3	13859	83	27	7830	710	8	1.01	wellhead: Na & K are high
13	14	63	4	31418	460	304	19000	244	0	1.03	dst
13	25	63	4	26345	276	90	15500	450	129	1.03	drillpipe; CO3:60
10	14	65	2	19573	220	104	11690	295	16	1.02	bottom sample
5	28	64	6	18117	175	31	10721	205	147	1.02	swabbed sample
11	1	65	6	13890	168	78	7826	638	128	1.01	dst
9	9	67	4	15331	144	73	9070	327	2	1.01	bottom sample K+:35
11	24	67	4	2161	36	33	600	537	160	1.00	bottom sample K+:16
7	33	67	4	1969	22	26	240	903	163	1.00	bottom sample K+:20
15	1	67	6	7102	51	15	3794	547	72	1.01	RFT K+:20
2	29	67	6	7283	55	15	3901	439	118	1.00	RFT K+:21; CO3:48
Average compositions:				16831.60	225.47	101.27	9904.40	439.20	74.20	1.01	

TDS=Total dissolved solids
-anions, cations and TDS in mg/L

WATER ANALYSES: COLD LAKE STUDY AREA
GRAND RAPIDS FORMATION
Percent compositions normalized to major cations and anions

LSD	SEC	TWP	RGE	TDS	% Ca	% Mg	% Cl	% HCO3	% SO4	Ca/Mg
5	19	63	2	22014	65.28	34.72	96.00	2.94	1.06	1.88
11	5	63	3	18873	68.20	31.80	96.64	3.16	0.20	2.14
4	7	63	3	23573	58.49	41.51	98.63	1.35	0.02	1.41
5	28	64	6	30966	86.75	13.25	98.34	1.66	0.00	6.55
10	22	64	3	13859	75.45	24.55	91.60	8.31	0.09	3.07
13	14	63	4	31418	60.21	39.79	98.73	1.27	0.00	1.51
13	25	63	4	26345	75.41	24.59	96.40	2.80	0.80	3.07
10	14	65	2	19573	67.90	32.10	97.41	2.46	0.13	2.12
5	28	64	6	18117	84.95	15.05	96.82	1.85	1.33	5.65
11	1	65	6	13890	68.29	31.71	91.08	7.43	1.49	2.15
9	9	67	4	15331	66.36	33.64	96.50	3.48	0.02	1.97
11	24	67	4	2161	52.17	47.83	46.26	41.40	12.34	1.09
7	33	67	4	1969	45.83	54.17	18.38	69.14	12.48	0.85
15	1	67	6	7102	77.27	22.73	85.97	12.40	1.63	3.40
2	29	67	6	7283	78.57	21.43	87.51	9.85	2.65	3.67

WATER ANALYSES: COLD LAKE AREA
CLEARWATER FORMATION

LSD	SEC	TWP	RGE	TDS	Ca	Mg	Cl	HCO3	SO4	Sp. Grav.	Comments
11	25	63	3	21282	192	219	12380	765	21	1.01	high K+:35
8	26	63	3	14494	133	70	7856	1129	78	1.01	high K+:27
9	22	64	3	30103	39	547	18330	204	17	1.02	drillpipe sample
14	7	64	6	27422	364	250	16950	246	21	1.02	dst K+:61
2	12	67	4	7097	92	51	3310	1208	14	1.00	bottom sample K+:33
2	29	67	6	6588	47	11	3404	532	112	1.01	RFT CO3:48
7	29	66	1	3517	28	17	1225	903	185	1.01	dst
Average compositions:				15786.14	127.86	166.43	9065.00	712.43	64.00	1.01	

TDS=Total dissolved solids
-anions, cations and TDS in mg/L

WATER ANALYSES: COLD LAKE AREA
CLEARWATER FORMATION
Percent compositions normalized to major cations and anions:

LSD	SEC	TWP	RGE	TDS	% Ca	% Mg	% Cl	% HCO3	%SO4	Ca/Mg
11	25	63	3	21282	46.72	53.28	94.03	5.81	0.16	0.88
8	26	63	3	14494	65.52	34.48	86.68	12.46	0.86	1.90
9	22	64	3	30103	6.66	93.34	98.81	1.10	0.09	0.07
14	7	64	6	27422	59.28	40.72	98.45	1.43	0.12	1.46
2	12	67	4	7097	64.34	35.66	73.04	26.65	0.31	1.80
2	29	67	6	6588	81.03	18.97	84.09	13.14	2.77	4.27
7	29	66	1	3517	62.22	37.78	52.96	39.04	8.00	1.65